FORMERLY ACTA CHIMICA ACADEMIAE SCIENTIARUM HUNGARICAE

Acta Chimica Hungarica

VOLUME 114, NUMBER 1, SEPTEMBER 1983

EDITOR-IN-CHIEF
F. MÁRTA

MANAGING EDITOR
GY. DEÁK

ASSISTANT EDITOR
L. HAZAI

EDITORIAL BOARD
M. T. BECK, R. BOGNÁR, GY. HARDY, K. LEMPERT,
B. LENGYEL, K. POLINSZKY, E. PUNGOR, G. SCHAY,
Z. G. SZABÓ, P. TÉTÉNYI

Akadémiai Kiadó, Budapest
ACTA CHIM. HUNG. ACASA2 114 (1) 1–102 (1983) HU ISSN0231-3146

ACTA CHIMICA HUNGARICA

A JOURNAL OF THE HUNGARIAN ACADEMY OF SCIENCES

Acta Chimica publishes original reports on all aspects of chemistry in English.

Acta Chimica is published in three volumes per year, each volume consisting of four issues, by

AKADÉMIAI KIADÓ

Publishing House of the Hungarian Academy of Sciences
H-1054 Budapest, Alkotmány u. 21.

Manuscripts and editorial correspondence should be addressed to

Acta Chimica
H-1450 Budapest P.O. Box 67

Subscription information

Orders should be addressed to

KULTURA Foreign Trading Company
H-1389 Budapest P.O. Box 149

or to its representatives abroad

Acta Chimica is indexed in Current Contents.

NOTICE TO AUTHORS

Acta Chimica publishes original papers on all aspects of chemistry in English. Before preparing a manuscript for submission to this journal authors are advised to consult recent issues.

Form of manuscript

Manuscripts, tables and illustrations should be submitted in triplicate. Manuscripts should be typewritten double spaced (25 lines, 50 characters per line including spaces). The *title page* should include (1) the title of the paper, (2) the full names of the author(s) in the sequence to be published; apply an asterisk to designate the name of the author to whom correspondence should be addressed, (3) name and address of the institution where the work was done. If the paper is part of a series, reference to the previous communication must be given as a footnote.

Abstract

A summary is printed at the head of each paper. This should not exceed 200 words and should state briefly the principal results and major conclusions of the work. It should be suitable for use by abstracting services.

ACTA CHIMICA HUNGARICA

EDITORIAL BOARD

M. T. BECK, R. BOGNÁR, GY. HARDY,
K. LEMPERT, B. LENGYEL, K. POLINSZKY,
E. PUNGOR, G. SCHAY,
Z. G. SZABÓ, P. TÉTÉNYI

EDITOR-IN-CHIEF

F. MÁRTA

MANAGING EDITOR

GY. DEÁK

ASSISTANT EDITOR

L. HAZAI

VOLUME 114

AKADÉMIAI KIADÓ, BUDAPEST

1983

Abou-Sekkina, M. M., El-Dissouky, A., El-Sonbati, A. Z.: Metal chelates of heterocyclic nitrogen containing ketones, VII. Magnetic and spectral studies on nickel(II) and copper(II) complexes of 2,6-lutidyl-2-phenyl ketone thiosemicarbazone 29
Aglietto, M. s. **Panchenko, Yu. N.**
Ahluwalia, V. K., Arora, K. K., Jolly, R. S.: Acid-catalyzed condensation of isoprene and 2-methylbut-3-en-2-ol with phloroacetophenon, new synthesis of alloevodionol and franklinone 117
Albright, L. F. s. **Siklós, P.**
Arora, K. K. s. **Ahluwalia, V. K.**
Arya, R. S. s. **Sharma, C. L.**
Attia, A., Michael, M.: Azachalcones, III. Reactions of azachalcones with amines and hydrazines 337

Bálint, Á. s. **Siklós, P.**
Bartók-Bozóki, G. s. **Bartók, M.**
Bartók, M., Molnár, Á., Bartók-Bozóki, G.: Decomposition of carbonate esters of 1,3-diols. The chemistry of 1,3-bifunctional systems, XXVI..... 375
Basha, D. M. s. **Shafiullah**
Benedetti, F. s. **Panchenko, Yu. N.**
Borbély, J. s. **Borda, J.**
Borda, J., Szabó, V., Borbély, J.: Reactions of 4-thionochromones and 4-thionoisoflavones with hydroxylamine (Preliminary communication) 103
Bresińska, I. s. **Kowalek, S.**

Cherneva, A., Cser, F., Nyitrai, K., Kiss, K., Hardy, Gy.: Studies on copolymerizations of hexadecyl acrylamide 235
Cooper, S. s. **Jákli, Gy.**
Császár, P. s. **Panchenko, Yu. N.**
Cser, F. s. **Cherneva, A.**
Cser, F. s. **Nyitrai, K.**
Csobod, É. M. s. **Szabó, K.**
Csobod, É. M. s. **Szabó, K.**

Deák, Gy. s. **Tikk, I.**
Deák, Gy. s. **Tikk, I.**
Dékány, I., Szántó, F., Rudzinski, W.: Effect of surface modification on immersional wetting of organophilic kaolinite and illite derivatives..... 283
Dvortsák, P. s. **Somorai, T.**

El-Asmy, A. A. s. **Shallaby, A. M.**
El-Dissouky, A. s. **Abou-Sekkina, M. M.**
El-Sonbati, A. Z. s. **Abou-Sekkina, M. M.**

Garg, J. K., Jain, D. S., Verma, P. S.: Polarographic study of mixed ligand complexes of Pb(II) with some diamines and malonic acid..... 125
Gergely, A. s. **Kiss, T.**
Göndör, M. s. **Lipták, A.**
Gupta, S. R. s. **Sharma, V. K.**

Hardy, Gy. s. **Cherneva, A.**
Hardy, Gy. s. **Nyitrai, K.**
Hargittai, I. s. **Mayer, I.**
Horkay, F., Zrínyi, M.: Comparative study of polymer gels based on theories of critical phenomena and classical thermodynamics 261
Horváth, Gy. s. **Kőrösi, J.**
Horváth, L. I. s. **Szabó-Plánka, T.**
Hosztafi, S., Makleit, S., Miskolczi, Zs.: *N*-Demethylation of morphine alkaloids, II. Codeine isomers 63
Husain, S. s. **Shafiullah**
Hutchings, R. S. s. **Jákli, Gy.**

Jain, D. S. s. **Garg, J. K.**
Jákli, Gy., Cooper, S., Hutchings, R. S., Van Hook, W. A.: H_2O-D_2O solvent isotope effects on apparent and partial molar volumes of $CaCl_2$ and $BaCl_2$ solutions..... 365
Jákli, Gy., Juhász, P., Jancsó, G.: Deuterium vapour pressure isotope effect in bromoform 133
Jancsó, G. s. **Jákli, Gy.**
Jolly, R. S. s. **Ahluwalia, V. K.**
Juhász, P. s. **Jákli, Gy.**
Juhász, Z. A.: Chemical reaction of substances under mechanical load 199

Kaushik, N. K. s. **Sharma, A. K.**
Kaushik, N. K. s. **Sodhi, G. S.**
Kiss, K. s. **Cherneva, A.**
Kiss, T., Gergely, A.: Complexes of 3,4-dihydroxyphenyl derivatives, V. Ambidentate character of L-dopa in manganese(II) and cobalt(II) complexes..... 249
Kowalak, S., Bresińska, I.: Catalytic activity of the $Al_2O_3-AlF_3$ system for the Claus reaction..... 255
Kőrösi, J., Láng, T., Neszmélyi, A., Horváth, Gy.: Heterocyclic compounds, V. The preparation and characterization of 1-(3,4-dimethoxyphenyl)-6,7-dimethoxy-4-ethyl-3-methyl-isoquinoline-*N*-imine salts 301
Kőrösi, J. s. **Neszmélyi, A.**
Kumar, S. s. **Sodhi, G. S.**

Langó, J. s. **Somorai, T.**
Láng, T. s. **Kőrösi. J.**
Láng, T. s. **Neszmélyi, A.**
Lipták, A., Göndör, M.: Synthesis of (1 → 1)-bonded rhamnopyranosyl-rhamnopyranosides containing L,L and L,D building-stones. High-field ^1H- and ^{13}C-NMR spectroscopic studies on the conformation of the interglycosidic bonds..... 309
Litkei, Gy., Patonay, T.: Flavonoids, XXXVII. Ring contraction and ring enlargement reactions with trimethylsilyl azide in the field of flavonoids..... 47

Mahapatra, B. B., Patel, B., Satyanarayana, D., Pujari, S. K.: Polymetallic complexes, II. Schiff base complexes of cobalt(II) nickel(II), copper(II), zinc(II), cadmium(II) and mercury(II) 217
Makleit, S. s. **Hosztafi, D.**
Mayer, I., Révész, M., Hargittai, I.: On the C—S bond length variations and d-orbital participation in some sulphonyl chloride derivatives..... 159
Michael, M. s. **Attia, A.**
Mishra, V. P. s. **Sharma, C. L.**
Miskolczi, Zs. s. **Hosztafi, S.**
Mochalov, V. I. s. **Panchenko, Yu. N.**
Molnár, Á. s. **Bartók. M.**
Mostafa, M. M. s. **Shallaby, A. M.**

Naidu, P. R. s. **Sastry, G. S.**
Narvi, S. S. s. **Sharma, C. L.**
Neszmélyi, A., Láng, T., Kőrösi. J.: Heterocyclic compounds, IV. Structure of the salts of 1-(3,4-dimethoxyphenyl)-7,8-dimethoxy-5-ethyl-4-methyl-5*H*-2,3-benzodiazepine 293
Neszmélyi, A. s. **Kőrösi, J.**

Nyitrai, J., Cser, F., Parragh, L., Hardy, Gy.: Copolymerization of cholesterol-based mesogenic monomers 223
Nyitrai, K. s. **Cherneva, A.**

Panchenko, Yu, N., Mochalov, V. I., Császár, P., Török, F., Benedetti, F., Aglietto, M.: Theoretical interpretation of the vibrational spectra of *trans-* and *cis*-penta-1,3--dienes and 2,3-dimethylbutadiene 149
Pandey, A. K., Singh, R., Verma, V. K.: Synthesis of some 3,5-diarylimino-2-phenyl--1,2,4-thiadiazolidines. Oxidative debenzylation and cyclization of 1-(*N,N'*--diarylamidino)-3-aryl-2-benzylisothioureas 107
Parragh, L. s. **Nyitrai, K.**
Patel, B. s. **Mahapatra, B. B.**
Patonay, T. s. **Litkei, Gy.**
Pujari, S. K. s. **Mahapatra, B. B.**

Ramamurthy, M. s. **Sastry, G. S.**
Reiter, J. s. **Somorai, T.**
Révész, M. s. **Mayer, I.**
Rudzinski, W. s. **Dékány, I.**

Sastry, G. S., Ramamurthy, M., Naidu, P. R.: Excess volumes of binary mixtures of di-*n*--butylamine with normal alcohols at 303.15 K 113
Satyanarayana, D. s. **Mahapatra, B. B.**
Shafiullah, Husain, S., Basha, D. M.: Reaction of lead(IV) acetate with steroidal nitro-olefins (Short communication) 121
Shallaby, A. M., Mostafa, M. M., El-Asmy, A. A.: Complexes of 1-benzoyl-4-phenyl-3-thio-semicarbazide with Co(II), Ni(II), Cu(II), Cd(II) and Hg(II) 9
Sharma, A. K., Kaushik, N. K.: Halides and complex halogeno anions as salts of benzoylacetonato bis-cyclopentadienyl zirconium(IV) chelates 41
Sharma, C. L., Mishra, V. P.: Characterisation of the complexes of some biologically active *N*-aryl-*N'*-benzoylthiocarbamides with metal(II) phthalimides 3
Sharma, C. L., Narvi, S. S., Arya, R. S.: Characterisation of Cu(II), Ni(II), Co(II), Pd(II) and Fe(III) complexes of anilic acids 349
Sharma, V. K., Gupta, S. R.: Synthesis of Agecorynin-A 361
Sengupta, S. K.: Preparation and characterization of complexes of uranium(VI), vanadium(IV), titanium(IV), zirconium(IV) and hafnium(IV) with mercapto triazoles 323
Siklós, P., Bálint, Á., Albright, L. F.: A kinetic-mathematical model of ethane pyrolysis 79
Singh, C. P.: Synthesis and antimalarial activity of N^1-isonicotinoyl-3-methyl-5-phenyl-4--(sulfamoylphenylazo)-1,2-diazoles 57
Singh, R. s. **Pandey, A. K.**
Sodhi, G. S., Kumar, S., Kaushik, N. K.: Dithiocarbamate anions as salts of oxinate chelates of zirconium(IV) 329
Somorai, T., Dvortsák, P., Langó, J., Reiter, J.: Structure investigations on some diphenyl-triazoles 23
Szabó, K., Csobod, É. M.: pH-Dependence of the catalytic effect of thiourea and *N,N'*--dimethylthiourea on hydrogen overvoltage at the dropping gallium electrode 173
Szabó, K., Csobod, É. M., Takács, M.: Changing of the catalytic effect of thiourea with temperature at the dropping gallium electrode 187
Szabó, V. s. **Borda, J.**
Szabó-Plánka, T., Horváth, L. I.: EPR study on copper(II) complexes pf *l*-α-amino acids in frozen solutions 15
Szántó, F. s. **Dékány, I.**
Szebényi, N. s. **Wittmann, Zs.**

Takács, M. s. **Szabó, K.**
Tikk, I., Deák, Gy., Tóth, G.: (Hydroxyimino)-3(2*H*)-isoquinolinones, II. A convenient method for the preparation of 4-(hydroxyimino)-1,4-dihydro-3(2*H*)-isoquinolinones and their *O*-alkyl and *O*-acyl derivatives 69
Tikk, I., Tóth, G., Deák, Gy.: (Hydroxyimino)-3(2*H*)-isoquinolinones, III. Determination of the structure of phenyl-substituted 1,4-dihydro-3(2*H*)-isoquinolinone obtained in the cyclization reaction of 3-biphenyl-*N*-methyl-acetamide by ^{1}H-NMR spectroscopic study of the 4-(hydroxyimino)-derivative 355

Tóth, G. s. **Tikk, I.**
Tóth, G. s. **Tikk, I.**
Török, F. s. **Panchenko, Yu. N.**

Van Hook, W. A. s. **Jákli, Gy.**
Verma, P. S. s. **Garg, J. K.**
Verma, V. K. s. **Pandey, A. K.**
Wittmann, Zs., Szebényi, N.: Simple methods for the determination of phosphonates 89

Zrínyi, M. s. **Horkay, F.**

CONTENTS

PHYSICAL AND INORGANIC CHEMISTRY

Complexes of 1-benzoyl-4-phenyl-4-thiosemicarbazide with Co(II), Ni(II), Cu(II), Cd(II) and Hg(II), **A. M. Shallaby, N. M. Mostafa, A. A. El-Asmy** 9

EPR study on copper(II) complexes of *l*-α-amino acids in frozen solutions, **T. Szabó-Plánka, L. I. Horváth** 15

Metal chelates of heterocyclic nitrogen containing ketones, VII. Magnetic and spectral studies on nickel(II) and copper(II) complexes of 2,6-lutidyl-2-phenyl ketone thiosemicarbazone, **M. M. Abou-Sekkina, A. El-Dissouky, A. Z. El-Sonbati** 29

Halides and complex halogeno anions as salts of benzoylacetonato bis-cyclopentadienyl zirconium(IV) chelates, **A. K. Sharma, N. K. Kaushik** 41

ORGANIC CHEMISTRY

Characterization of the complexes of some biologically active *N*-aryl-*N*'-benzoylthiocarbamides with metal(II) phthalimides, **C. L. Sharma, V. P. Mishra** 3

Structure investigations on some diphenyltriazoles, **T. Somorai, P. Dvortsák, J. Langó, J. Reiter** 23

Flavonoids, XXXVII. Ring contraction and ring enlargement reactions with trimethylsilyl azide in the field of flavonoids, **Gy. Litkei, T. Patonay** 47

Synthesis and antimalarial activity of N^1-isonicotinoyl-3-methyl-5-phenyl-4 (sulfamoylphenylazo)-1,2-diazoles, **C. P. Singh** 57

N-Demethylation of morphine alkaloids, II. Codeine isomers, **S. Hosztafi, S. Makleit, Zs. Miskolczi** 63

Hydroxyimino-3(2*H*)-isoquinolinones, II. A convenient method for the preparation of 4-hydroxyimino-1,4-dihydro-3(2*H*)-isoquinolinones and their *O*-alkyl and *O*-acyl derivatives, **I. Tikk, Gy. Deák, G. Tóth** 69

ANALITICAL CHEMISTRY

Simple methods for the determination of phosphonates **Zs. Wittmann, N. Szebényi** 89

CHEMICAL TECHNOLOGY

A kinetic-mathematical model of ethane pyrolysis, **P. Siklós, Á. Bálint, L. F. Albright** 79

BOOK REVIEWS 95

Acta Chimica Hungarica 114 (1), pp. 3—8 (1983)

CHARACTERIZATION OF THE COMPLEXES OF SOME BIOLOGICALLY ACTIVE *N*-ARYL-*N'*-BENZOYLTHIOCARBAMIDES WITH METAL(II) PHTHALIMIDES

C. L. SHARMA* and V. P. MISHRA

(Chemistry Department, University of Roorkee, Roorkee-247672, India)

Received May 26, 1982
Accepted for publication August 25, 1982**

The mixed ligand complexes of Cu(II), Pd(II), Pt(II), Co(II) and Ni(II) with phthalimide as primary and *N*-aryl-*N'*-benzoylthiocarbamides as secondary ligands have been prepared and characterized on the basis of chemical analysis, conductance, magnetic measurements, IR and electronic spectral studies. The Cu(II), Pd(II) and Pt(II) complexes were planar, Co(II) complexes were tetrahedral and Ni(II) complexes had a tetragonal distortion of *Oh* symmetry.

The pharmacological activity of thiocarbamides [1—5], antipolio activity [6] and industrial importance [7, 8] of metal-phthalimides have been reported in the literature. The chelates containing metal-sulphir bonds are also very important because of their versalite use as antifungal and antibacterial agents [9, 10]. Hence it was considered worthwhile to carry out the preparation and characterization of mixed ligand complexes of Cu(II), Ni(II), Pd(II), Pt(II) and Co(II) using phthalimide as primary and *N*-aryl-*N'*-benzoylthiocarbamides as secondary ligands.

Experimental

Physical measurements

The conductances were measured on a conductivity bridge type CL01/0 using an Elico type CC-03 cell. Magnetic measurements were done on a vibrating sample magnetometer, model VSM-155 at room temperature using a magnetic field of 4200 gauss. The IR spectra were run on a Beckmann IR-20 spectrophotometer. The UV and visible spectra were recorded on Carl-Ziess SPECORD u.v.-viz. spectrophotometer.

Reagents and solutions

The solvents used were doubly distilled and all the reagents were of BDH(AR) quality.

* Correspondence to be made at Vikash Nagar, 134/3, University of Roorkee, Roorkee (U.P.) — 247667, India.

** In final form accepted December 29, 1982.

Metal(II) phthalimides

The solutions of metal ion [chlorides of Cu(II), Pd(II), Pt(II), Co(II) and sulphate of Ni(II) and potassium phthalimide were mixed in the ratio 1 : 2 and the green, chocolate, light brown, blue and yellow precipitates formed in the case of Ni(II), Cu(II), Pd(II), Co(II) and Pt(II) respectively were filtered, washed several times with distilled water and then dried in the oven at 70 °C.

***N*-Phenyl-*N*'-benzoylthiocarbamide (A)**

A warm solution (0.05 mol) of benzoylisothiocyanate in acetone was added dropwise with stirring to a solution (0.05 mol) of aniline in acetone over a period of about ten minutes. An exothermic reaction took place and the reaction mixture deposited a pale yellow crystalline product which was collected, washed with water and dried. It was recrystallized into beautiful colourless shining needles from 70% ethanol. The structure was confirmed from its carbon-hydrogen analysis, IR studies and m.p. (139 °C).

Similarly other *N*-aryl-*N*'-benzoylthiocarbamide derivatives were prepared by the reaction of benzoylisothiocyanate with different phenyl amines according to the following reaction.

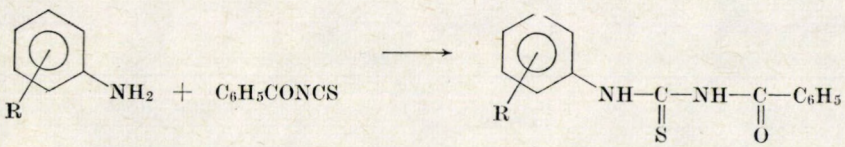

R = 3-CH_3; 3-Cl; 2,5-$(Cl)_2$; 2-Cl

Thus the compounds formed were B = *N*-(*m*-tolyl)-*N*'-benzoylthiocarbamide (m.p. = = 121 °C); C = *N*-(*m*-chlorophenyl)-*N*'-benzoylthiocarbamide (m.p. = 125 °C); D = *N*-(2,5--dichlorophenyl)-*N*'-benzoylthiocarbamide (m.p. = 147 °C) and E = *N*-(*o*-chlorophenyl)-*N*'--benzoylthiocarbamide (m.p. = 150 °C).

Mixed ligand complexes

The methanolic solutions of metalphthalimide and the thiocarbamide derivative were mixed in the ratio of 1 : 1. The mixture was refluxed on waterbath for half an hour and then allowed to stand for five or six hours. The light green, dark green, yellowish green, greenish blue and yellowish brown precipitates formed in the case of Ni(II), Cu(II), Pd(II), Co(II) and Pt(II) respectively were filtered, washed several times with methanol and finally with acetone and then dried in a dessiccator over anhydrous sulphuric acid.

The results of micro-analysis for the metal, carbon, nitrogen, and hydrogen and magnetic moments are in Table I. The values of molar conductances in dioxane ($\approx$5.0 ohm^{-1} cm^2 mol^{-1}) indicated their non-electrolytic nature.

Results and Discussion

IR studies

The carbonyl stretching frequency shifted from 1740 cm^{-1} to 1660 cm^{-1} in the spectra of metal phthalimides. This shifting has been reported earlier due to the mass effect of heavy metal ions linked to nitrogen [11, 12]. Further the band obtained at 1470 cm^{-1} in the spectrum of phthalimide due to —C—N shifted to about 1485 cm^{-1} in the spectra of metal phthalimides.

Table I

Analytical data

S. N.	Complexes	Percentage calculated (found)				μ_{eff} (B.M.)
		Metal	C	H	N	
1.	$[Ni(P)_2(A)(H_2O)_2]$	9.12 (9.21)	55.93 (56.54)	3.72 (3.69)	8.70 (8.77)	2.80
2.	$[Ni(P)_2(B)(H_2O)_2]$	8.93 (8.99)	56.56 (57.05)	3.95 (3.91)	8.51 (8.59)	2.84
3.	$[Ni(P)_2(C)(H_2O)_2]$	8.65 (8.72)	53.04 (53.48)	3.39 (3.36)	8.25 (8.32)	2.82
4.	$[Ni(P)_2(D)(H_2O)_2]$	8.24 (8.31)	50.51 (51.00)	3.09 (3.05)	7.86 (7.94)	2.80
5.	$[Ni(P)_2(E)(H_2O)_2]$	8.65 (8.73)	53.04 (53.50)	3.39 (3.34)	8.25 (8.34)	2.84
6.	$[Cu(P)_2A]$	10.37 (10.30)	58.78 (59.27)	3.27 (3.24)	9.14 (9.24)	2.12
7.	$[Cu(P)_2B]$	10.14 (10.03)	59.38 (59.96)	3.51(3.47)	8.99 (9.08)	2.14
8.	$[Cu(P)_2C]$	9.79 (9.74)	55.60 (56.14)	2.93 (2.90)	8.65 (8.72)	2.10
9.	$[Cu(P)_2D]$	9.32 (9.38)	52.82 (53.41)	2.64 (2.62)	8.22 (8.31)	2.14
10.	$[Cu(P)_2E]$	9.79 (9.72)	55.60 (56.12)	2.93 (2.90)	8.65 (8.74)	2.11
11.	$[Pd(P)_2A]$	16.23 (16.18)	54.92 (55.37)	3.05 (3.02)	8.54 (8.61)	0.00
12.	$[Pd(P)_2B]$	15.89 (15.77)	55.57 (55.99)	3.29 (3.26)	8.37 (8.44)	0.00
13.	$[Pd(P)_2C]$	15.42 (15.30)	52.18 (52.69)	2.75 (2.73)	8.12 (8.21)	0.00
14.	$[Pd(P)_2D]$	14.69 (14.56)	49.69 (50.00)	2.48 (2.46)	7.37 (7.80)	0.00
15.	$[Pd(P)_2E]$	15.42 (15.29)	52.18 (52.71)	2.75 (2.72)	8.12 (8.20)	0.00
16.	$[Pt(P)_2A]$	26.24 (26.46)	48.43 (48.91)	2.69 (2.66)	7.53 (7.47)	0.00
17.	$[Pt(P)_2B]$	25.76 (26.00)	49.12 (49.63)	2.90 (2.88)	7.39 (7.32)	0.00
18.	$[Pt(P)_2C]$	25.08 (25.33)	46.28 (46.75)	2.44 (2.41)	7.20 (7.12)	0.00
19.	$[Pt(P)_2D]$	24.01 (24.26)	44.31 (44.74)	2.22 (2.20)	6.89 (6.82)	0.00
20.	$[Pt(P)_2E]$	25.08 (25.35)	46.28 (46.75)	2.44 (2.41)	7.20 (7.13)	0.00
21.	$[Co(P)_2A]$	9.70 (9.61)	59.29 (59.90)	3.29 (3.25)	9.22 (9.13)	4.50
22.	$[Co(P)_2B]$	9.49 (9.41)	59.88 (59.50)	3.54 (3.50)	9.01 (8.90)	4.49
23.	$[Co(P)_2D]$	9.18 (9.10)	56.10 (56.68)	2.96 (2.93)	8.73 (8.65)	4.51
24.	$[Co(P)_2D]$	8.71 (8.62)	53.24 (53.80)	2.66 (2.64)	8.28 (8.20)	4.50
25.	$[Co(P)_{28}E]$	9.18 (9.10)	56.10 (56.68)	2.96 (2.93)	8.73 (8.66)	4.49

P = $C_8H_4O_2N$ (deprotonated phthalimide)
A = $C_{14}H_{12}N_2OS$
B = $C_{15}H_{14}N_2OS$
C = $C_{14}H_{11}N_2OSCl$
D = $C_{14}H_{10}N_2OSCl_2$
E = $C_{14}H_{11}N_2OSCl$

The nature of coordination of thiocarbamide and its derivatives has been debated by many workers [13—18]. The main bands characterizing the coordination were found at ~1600 cm^{-1} due to —NH, ~1450 cm^{-1} due to —C—N sym. and —C=S stretching and at 750—800 cm^{-1} due to N—C—N and C—S stretching. The thiocarbamide derivatives gave —NH deformation

bands in the range from 1590—1620 cm^{-1} which remained unaffected on complex formation. The position and intensity of —NH band appeared at ~3300 cm^{-1} in the spectra of these ligands also remained unchanged even after the interaction with metals indicating the absence of coordination through nitrogen of thiocarbamides [19]. There was no band in the region 2600—2900 cm^{-1} in the spectra of ligands and of complexes which indicated the absence of S—H bond i.e. no appreciable amount of enolic form of the ligands, as theoretically expected, was present in the complexes. The bands appeared in the region 1650—1680 cm^{-1} in the spectra of thiocarbamide derivatives due to —C=O shifted to 1620 cm^{-1} in the spectra of complexes indicating thereby the coordination through carbonyl oxygen [20]. Secondly the band obtained at ~1450 cm^{-1} in the spectra of ligands due to C=S stretch and C—N symmetric stretch also shifted to lower frequency side i.e. 1400 cm^{-1} on complex formation which is assigned due to the coordination through sulphur [21—24]. An intense band was obtained at around 500 cm^{-1} which may be due to the combined effect of M—N anD M—O bond [25]. A weak band due to M—S was observed at 350 cm^{-1} [26, 27]. The presence of coordinated water in the case of nickel(II) complexes gave an extra band at 825 cm^{-1} [28].

Electronic spectra and magnetic studies

The diamagnetic behaviour of Pd(II) and Pt(II) complexes indicated their square planar structure. The electronic spectra of Pd(II) complexes in dioxane gave four bands at 38,000, 30,000, 28,500 and 22,500 cm^{-1} corresponding to the transitions $^1A_{1g} \rightarrow {}^1E_u$, $^1A_{1g} \rightarrow {}^1E_g$, $^1A_{1g} \rightarrow {}^1B_{1g}$ and $^1A_{1g} \rightarrow {}^1A_{2g}$ respectively and of Pt(II) complexes in methanol gave three bands at 40,000, 39,000 and 35,000 cm^{-1} corresponding to the transitions $^1A_{1g} \rightarrow {}^1A_{2u}$, $^1A_{1g} \rightarrow {}^1E_u$ and $^1A_{1g} \rightarrow {}^1B_{1u}$ respectively. The orbital energy differences Δ_1, Δ_2 and Δ_3 for $F_2 = 10$, $F_4 = 700$ cm^{-1} were found to be 24,950, 7400 and 1150 cm^{-1} respectively for the complexes of Pd(II) and Δ_2 and Δ_3 for the complexes of Pt(II) were found to be 12,500 and —2700 cm^{-1} respectively. The separation Δ_1 for Pd(II) complexes was the largest of the three orbital parameters which indicated that the $d_{x^2-y^2}$ was much more antibonding than any of the other d, orbitals. The separation Δ_3 for Pt(II) complexes is less than Pd(II) complexes which indicated that the dii was much more unstable than di-, di- in the complexes of Pd(II) and d_{z^2} was much more stable than d_{xz}, d_{yz} in the complexes of Pd(II) and d_{z^2} was much more stable than d_{xz}, d_{yz} in the complexes of Pt(II). This was compatible with the idea that the axial interaction of the solvent molecules is lesser in Pt(II) complexes.

The copper(II) complexes were paramangetic having the value of magnetic moment around 2.10 B.M., close enough to those predicted for spin

only value. The electronic spectra in dioxane gave three bands at 34,800, 15,000 and 14,000 cm^{-1} corresponding to the charge transfer, $^2B_{1g} \rightarrow {}^2E_g$ and $^2B_{1g} \rightarrow {}^2A_{1g}$ transitions respectively.

The values of magnetic moments obtained around 2.80 B.M. in the case of Ni(II) complexes are lower than predicted for octahedral or tetrahedral complexes which may be due to a mixture of paramagnetic octahedral molecules and diamagnetic planar molecules [29]. This distortion of *Oh* symmetry was further confirmed from their electronic spectra. The four bands at 12,000 (ν_1), 21,500 (ν_2), 31,000 (ν_3) and 13,000 cm^{-1} were obtained in each case which gave the value of $B = 1100$ cm^{-1} calculated from $15B = \nu_2 + \nu_3 - 3\nu_1$. This value is sufficiently higher than the free ion value and hence suggests the distortion of *Oh* symmetry. Using the value of first spin allowed band (ν_1) as 10 D_q, the energies of bands were calculated from the equations:

$$\nu_2 = \frac{15}{2} B + \frac{3}{2}(10Dq) - \frac{1}{2}\left[(9B - 10\,Dq)^2 + 144\,B^2\right]^{1/2}$$

$$\nu_2 = \frac{15}{2} B + \frac{3}{2}(10Dq) + \frac{1}{2}\left[(9B - 10\,Dq)^2 + 144\,B^2\right]^{1/2}$$

which were found to be 19,567 cm^{-1} and 32,933 cm^{-1} respectively. They are not in good agreement with the experimental values hence suggest a tetragonal distortion of *Oh* symmetry Secondly the ratio of ν_2/ν_1 comes out to be 1.79 which is greater than the usual range for octahedral complexes. Thus it was concluded that the band appeared at 13,000 cm^{-1} is a low symmetry component. Hence all the four bands may be assigned to $B_1 \rightarrow E^a$ (12,000 cm^{-1}) $B_1 \rightarrow B_2$; A_2 (13,000 cm^{-1}); $B_1 \rightarrow E^b$ (21,500 cm^{-1}) and $B_1 \rightarrow A_1$ (31,000 cm^{-1}) transitions.

In the case of bluish green complexes of Co(II), the values of magnetic moment were found near about 4.50 B.M. which are usually encountered in tetrahedral cobalt(II) complexes [30] Their electronic spectra in methanol gave two bands at 7618 (ν_2) and 17,910 (ν_3) correcponding to the transition $^4A_2 \rightarrow {}^4T_1(F)$ and $^4A_2 \rightarrow {}^4T_1(P)$ respectively. Using numerical procedure, the value of 10 *Dq* has been theoretically calculated to occur at 4455 cm^{-1} which is in fair agreement with the predicted value for tetrahedral complexes. The value of *B* and β were thus found to be 811 cm^{-1} and 0.83 respectively.

REFERENCES

[1] Astwood, E. B.: J. Pharmacol., **78,** 79 (1943); CA., **37,** 4471[8]
[2] Campbell, D. et al.: Lancet., **I,** 630 (1944); CA., **38,** 6389[5]
[3] Astwood, E. B. Bissell, A., Hughes, A. M.: Endocrinology, **37,** 456 (1945); CA., **40,** 3827[5]
[4] Pitt-Rivers, R., Tata, R. J.: in The Thyroid Hormones, Pergamon Press, London 1959
[5] May, J. D., Mc Naughton, J. L.: Poult. Sci., **59,** 893 (1980); CA., **92,** 196874e

[6] Hollinshead, A. C., Smith, P. K.: Antibiotics Ann., **1959—60,** 313 (1960); CA., **54,** 17561a
[7] Okuhashi, T., Shimizu, I., Shimizu, A. (Teijin Ltd.) Japan 7017, 549 (Cl 25 H 62) 17 June 1970; CA., **73,** 121466x
[8] Bairamora, A. G., Mamedov., F. N. (USSR) Prisadki K. Samazoch. Maslam 4, 111 (1976); CA., **87,** 202499b
[9] Horsfall, J. G., Rich, S.: Contribs. Boyce Thompson Inst., **16,** 313 (1951); CA., **46,** 11543f
[10] Akbar Ali, M., Livingstone, S. E.: Coord. Chem. Rev., **13,** 101 (1974)
[11] Narain, G.: J. Inorg. Nucl. Chem., **28,** 2403, 2703 (1966)
[12] Narain G., Shukla, P., Srivastava, L. N.: J. Prakt. Chem. **31,** 123 (1966)
[13] Yamaguchi, A., Penland, R. B., Mizushima, S., Lane, T. J., Curran, C., Quagliano, J. V.: J. Am. Chem. Soc., **80,** 527 (1958)
[14] Lane, T. J., C. S. C., Yamaguchi, A., Quagliano, J. V., Ryan, J. A., Mizushima, S.: J. Am. Chem., Soc., **81,** 3824 (1959)
[15] Gosavi R. K., Rao, C. N. R.: J. Inorg. Nucl. Chem., **29,** 1937 (1957)
[16] Swaminathan, K., Irwing, H. M. N. H.: J. Inorg. Nucl. Chem., **26,** 1291 (1964)
[17] Dwarikanath, K., Sathyanarayana, D. N.: Ind. J. Chem., **18A,** 302 (1979)
[18] Satpathy, K. C., Mishra, H. P., Mahana, T. D.: J. Indian Chem. Soc., **56,** 248 (1979); ibid., **59,** 40 (1982)
[19] Marneotrigiano, G., Battistuzzi, R.: J. Inorg. Nucl. Chem., **35,** 2265 (1973)
[20] Giesbrecht, E., Kawashita, M.: J. Inorg. Nucl. Chem., **32,** 246 (1970)
[21] Dwivedi, J. S., Agrawal, U.: Indian J. Chem., **10,** 657 (1972)
[22] Gajendragad, M. R., Agrawal, U.: J. Inorg. Nucl. Chem., **37,** 2429 (1975)
[23] Mahadevappa, D. S., Gowda, B. T., Murthy, A. S. A.: Indian J. Chem., **14A,** 985 (1976)
[24] Preti, C., Tosi, G.: Canad. J. Chem., **54,** 1588 (1976)
[25] Nakamura, A., Tatsuno, Y., Yamamoto, M., Otsuka, S.: J. Am. Chem. Soc., **93,** 6052 (1971)
[26] Watt, G. W., McCormick, B. J.: Spectrochim. Acta, **21,** 753 (1965)
[27] Bradley, D. C., Gitilitz, M. H.: J. Chem. Soc. A, **1969,** 1152
[28] Nakagawa, I., Shimanouchi, T.: Spectrochim. Acta, **20,** 429 (1964)
[29] Bull, W. E., Moore, L. E.: J. Inorg. Nucl. Chem., **27,** 1341 (1965)
[30] Carlin, R. L.: Transition Metal Chemistry p. 20 Marcel-Dekker N. Y. Vol. **I,** Chap. *i* 1965

Acta Chimica Hungarica 114 (1), pp. 9 – 13 (1983)

COMPLEXES OF 1-BENZOYL-4-PHENYL-3--THIOSEMICARBAZIDE WITH Co(II), Ni(II), Cu(II), Cd(II) AND Hg(II)

A. M. SHALLABY, M. M. MOSTAFA* and A. A. EL-ASMY

(Chemistry Department, Faculty of Science, Mansoura University, Egypt)

Received May 27, 1982
In revised form August 5, 1982
Accepted for publication September 30, 1982

The complexes of 1-benzoyl-4-phenyl-3-thiosemicarbazide (BPTS) with some bipositive metal ions have been prepared and characterized on the basis of elemental analyses, conductivity, spectra (visible and IR) and magnetic measurements. IR spectral data indicate that the ligand acts as a bidentate and coordinating via carbonyl oxygen and NH and/or thioenol and NH groups.

Introduction

Our studies on thiosemicarbazide derivatives as ligands [1—4] are extended to 1-benzoyl-4-phenyl-3-thiosemicarbazide. The complexes of BPTS have recently been described by Aggarval and his co-workers [5]. This work reports the preparation and characterization of some complexes of BPTS with Co(II), Ni(II), Cu(II), Cd(II) and Hg(II). According to Ref. [5], this ligand acts as a tridentate with transition metal ions. Under the conditions used in this work, the ligand behaves as a bidentate. Our results showed a considerable disagreement between Aggarwal and our findings regarding the locations of some infrared bands, coordination sites and the stereochemistry of the isolated solid complexes.

Experimental

BPTS was prepared as described earlier [5]. The complexes of Co(II), Ni(II) and Cu(II) [other than Cu(II) sulphate] were prepared by adding equimolar amounts of the hydrated metal salt and the ligand and then heating the reaction mixture under reflux for 10 min. The complexes were filtered off on hot, washed with ethanol and dried in a vacuum desiccator over anhydrous calcium chloride. The same procedure was used in case of Cu(II) sulphate and Hg(II) chloride but on cold. The elemental analyses and physical measurements were carried out as described in our previous work [1 – 4]. The analytical data are shown in Table I.

* To whom all correspondence should be addressed.

Table I

Analytical and physical data for the complexes

Compound	M.P. °C	Colour	Found (Calc.) %				Λ_m in DMF
			C	H	M	X	
[Cu((BPTS—H)Cl]	212	grey	45.78 (45.53)	3.45 (3.27)	17 46 (17.20)	9.81 (9.60)	26.0
[Cu(BPTS—H)Br]	178	grey	41.00 (40.68)	3.34 (3.92)	15.03 (15.36)	19.54 (18.31)	35.0
[Cu(BPTS—H)Ac]3H_2O	156	green	42.89 (42.89)	3.98 (4.72)	14.13 (14.18)	—	19.6
[Co(BPTS—$H)_2 \cdot 2H_2O$]	360	orange	55.63 (52.91)	4.32 (4.44)	9.42 (9.27)	—	12.3
[Ni(BPTS—$H)_2$]	360	brown	57.04 (56.11)	4.22 (4.04)	9.71 (9.80)	—	3.2
[Cd(BPTS—$H)_2$]H_2O	187	yellow	49.51 (50.11)	4.04 (3.90)	17.40 (16.75)	—	6.8
[Cu$(BPTS)_2SO_4$]	202	black	47.64 (47.89)	3.24 (3.73)	9.61 (9.05)	—	37.4
[Hg(BPTS)Cl_2]	360	white	31.11 (30.97)	1.99 (2.41)	—	13.18 (13.06)	—

Table II

Important IR spectral bands and assignments

Compound	$^4\nu$NH	$^2\nu$NH	$^1\nu$NH	ν(C=O)	ν(C=N)	ν(C=S)	ν(N—N)	ν(C—S)	ν(M—S)	ν(M—N)
BPTS	3300 s	3220 s	3190 m	1670 s (1698)*	—	1325 s, 725m (1332)*	918 m (904)*	—	—	—
[Cu(BPTS—H)Cl]	3260 m		3150 m	1670 s	1570 s		925 m	635 w	430 m	
[Cu(BPTS—H)Br]	3270 m		3150 m	1665 s	1580 s		930 m	625 w	425 m	
[Cu(BPTS—H)Ac]3H_2O	3280 s		3180 m	1665 m	1560 m		930 m	625 w	410 m	
[Co(BPTS—$H)_2 \cdot 2H_2O$]	3280 s		3170 s	1665 sh	1550 s		935 m	630 w	430 m	
[Ni(BPTS—$H)_2$]	3290 s		3170 s	1660 m	1550 s		930 m	630 w	430 m	
[Cd(BPTS—$H)_2$]H_2O	3270 s		3170 s	1660 m	15 60s		930 m	625 w	425 m	
[Cu$(BPTS)_2SO_4$]	3260 s	3120 m	3160 m	1650 sh		1325 m, 720 m	945 m	—	—	360 w
[Hg(BPTS)Cl_2]	3280 s	3140 m	3120 m	1645 s		1320 m, 730 m	440 m	—	—	350 w

* Assignments by Aggarwal.

Results and Discussion

The infrared spectrum of BPTS shows that the ligand exists mainly in the keto form (**I**); it show respectively, the νCO and νCS at 1670 and 1325 cm^{-1}. No bands are observed above 3340 cm^{-1} and in the region 2600—2550 cm^{-1} which could be expected for the enol forms (structures **II** and **III**).

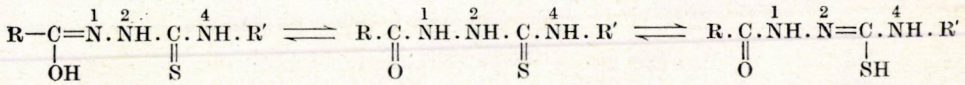

(II) (I) (III)

R and R' = phenyl groups

The observation of two weak broad bands at 2030 and 1840 cm^{-1} due to O...H—N stretching and bending vibrations [6, 7] suggests the presence of intramolecular hydrogen bonding which is presumed to be formed between carbonyl oxygen and NH as shown in structure **IV**.

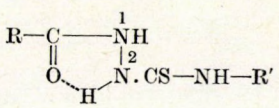

(IV)

The complexes of BPTS which have been isolated from ethanolic solution are given in Table I. They are insoluble in non-polar solvents but easily soluble in DMF and DMSO. Molar conductivities in DMF at 25 °C indicate [8] that these complexes are non-electrolytes in this solvent.

Infrared spectra for all complexes are more or less the same except the $CuSO_4$ and $HgCl_2$ complexes. The bands at 1325 and 725 cm^{-1} due to ν(C=S) in the spectrum of the ligand disappear on complexation with Co(II), Ni(II) and Cu(II) ions, while remains existing in case of $CuSO_4$ and $HgCl_2$ complexes. This may suggest the enolization of thioketo group and the involvement of the thioenol group in bonding to the Co(II), Ni(II) and Cu(II) (other than $CuSO_4$) complexes. The appearance of a new band in the region 615—635 cm^{-1} attributed to ν(C—S) [9] can be taken as evidence for the destruction of the thioketo group via enolization and the involvement of thioenolic sulphur in bonding. Strong evidence for the involvement of thioenol sulphur in bonding comes from the appearance of new bands in the region 1580—1550 cm^{-1} and 430—410 cm^{-1} attributable to ν(C=N) and ν(M—S) [10] respectively. Also, the replacement of HX (X=Cl, Br, Ac) during complex formation is detected qualitatively by spot test techniques and support the enolization of thioketo group. The three bands at 3300, 3220 and 3190 cm^{-1} in the spectrum

of the ligand are assigned, respectively, to N^4H, N^2H and N^1H. The negative shifts of the first and the third bands with the disappearance of the second band in case of Co(II), Ni(II) and Cu(II) complexes suggest that the enolization takes place through N^2H. Aggarwal and co-workers pointed out that the carbonyl band exists at 1698 cm^{-1} (nujol mull) which disappeared on complexation due to the involvement of ν(C—O) in bonding. Contrary to this observation, we found the carbonyl band at 1670 cm^{-1} (nujol mull) which remained existing in the spectra of all complexes while shifted to lower wave-number in case of copper sulphate and mercury (II) chloride complexes. This shows that the carbonyl oxygen does not take part in coordination in case of Co(II), Ni(II) and Cu(II) while has been considered as a potential site in case of $CuSO_4$ and $HgCl_2$ complexes.

The spectrum of $[Cu(BPTS)_2SO_4]$ shows ν_3 at 1205, 1170 and 1010 cm^{-1} and ν_1 at 925 cm^{-1} for the sulphate group which indicates the presence of a chelating sulphato group [11] The large negative shift of the band at 3220 cm^{-1} (N^2H), in the spectra of $CuSO_4$ and $HgCl_2$ complexes, with the appearance of a new band at $\sim$360 cm^{-1} assigned to ν(M—N) [12] can be taken as evidence that the NH group is taking part in coordination. The most important assignments of the ligand and its metal complexes are given in Table II.

The room temperature magnetic moments and the reflectance spectra of the complexes are given in Table III, the spectrum of [Cu(BPTS—H)Cl] exhibits four bands at 18,300, 15,200, 13,100 and 9400 cm^{-1}. In addition, a weak shoulder at about 12,700 cm^{-1} was observed. This spectrum is similar to those reported for distorted tetrahedral by Sacconi and Ciamolini [13]. Also, the effective magnetic moment of [Cu(BPTS—H)Cl] was found to be 1.95 B.M., which is in line with the values for tetrahedral copper(II) [14]. Cu(II) bromide complex [Cu(BPTS—H)Br] is isostructural with Cu(II) chloride complex but has lower magnetic moment (1.48 B.M.). This behaviour has

Table III

Spectral and magnetic properties of BPTS complexes

Compound	Magnetic moment μ_{eff} (B.M.)	Electronic spectra (in $cm^{-1} \times 10^3$)	
		Ligand field bands	Charge transfer
[Cu(BPTS – H)Cl]	1.95	9.4, 12.7, 13.1, 15.2, 18.3	22.1, 27.8, 36.1
[Cu(BPTS – H)Br]	1.48	8.9, 12.5, 13.3, 15.4, 18.5	22.8, 27.8, 36.2
[Cu(BPTS – H)Ac]3 H_2O	1.04	8.9, 13.3, 15.1, 18.2	23.1, 28.0, 36.7
[Co(BPTS – $H)_2 \cdot 2\ H_2O$]	4.85	8.2, 14.6, 15.6, 18.8	23.2, 28.1, 36.5
[Ni(BPTS – $H)_2$]	3.38	6.5, 9.8, 14.1, 16.2, 18.8	21.5, 27.5, 36.6
[$Cu(BPTS)_2SO_4$]	1.69	9.1, 12.9	22.2, 27.9, 36.3

been reported in which Cu(II) complexes containing the bromide ion have magnetic moments lower than those of the corresponding chloride [15]. The subnormal magnetic moment of the acetate complex is accounted for by assuming the existence of dimeric or polymeric structure in the solid state and considerable interaction between Cu(II) due to spin exchange phenomena [15]. Both the spectra of copper(II) bromide and acetate complexes are similar to that observed for Cu(II) chloride indicating a tetrahedral geometry around the Cu(II) ion. The band at 12,900 cm^{-1} in the spectrum of $[Cu(BPTS)_2SO_4]$ due to the $^2E_{2g} \rightarrow {}^2T_{2g}$ transition together with a magnetic moment of 1.69 B.M., suggest a distorted octahedral structure [16].

The spectrum of $[Ni(BPTS-H)_2]$ exhibits the bands at 6500, 9800, 14,100, 16,200 and 18,800 cm^{-1} which is similar to those of tetrahedral complexes reported earlier [17]. The band observed at 6500 cm^{-1} is attributed to $\nu_3[^3T_1(F) \rightarrow {}^3A_2(F)]$ transition while the band at 9800 cm^{-1} may be assigned to a spin forbidden one. The three bands at 14,100, 16,200 and 18,800 cm^{-1} are assigned to the $\nu_3[^3T_1(F) \rightarrow {}^3T_1(P)]$ transition [18]. According to the observed magnetic moment ($\mu_{eff} = 3.38$ B.M.), tetrahedral symmetry [17] around Ni(II) is proposed. It is interesting to note that the more bulky the ligand, the more likely the adoption of the tetrahedral configuration becomes. The magnetic moment and reflectance spectrum of $[Co(BPTS-H)_2 2H_2O]$ as well as the colour of the complex indicate that around Co(II) the geometry is octahedral [19]. The more intense bands in the region of 22,000, 27,000 and 36,000 cm^{-1} are assumed to arise from the M → L charge transfer and could be due to transitions from bonding to antibonding π level [20].

REFERENCES

[1] Mostafa, M. M., Shallaby, A. M., El-Asmy, A. A.: Trans. Met. Chem., **6,** 303 (1981)
[2] Mostafa, M. M., Shallaby, A. M., El-Asmy, A. A.: J. Inorg. Nucl. Chem., **43,** 2998 (1981)
[3] Mostafa, M. M., Shallaby, A. M., El-Asmy, A. A.: J. Ind. Chem. Soc. (in press)
[4] Mostafa, M. M., Shallaby, A. M., El-Asmy, A. A.: Egypt J. Chem. (in press)
[5] Aggarwal, R. C., Yadava, R. B. S.: Trans. Met. Chem., **1,** 139 (1976)
[6] Hamilton, W. C.: Acta Crystallogr., **14,** 95 (1961)
[7] Hall, D.: Acta Crystallogr., **18,** 955 (1965)
[8] Geary, W. J.: Coord. Chem. Rev., **7,** 81 (1971)
[9] Bellamy, L. J.: The Infrared Spectra of Complex Molecules p. 220 Methuen, London 1966
[10] Browall, K. W., Interranta, L. V.: J. Coord. Chem., **3,** 27 (1973)
[11] Nakamoto, K.: Infrared Spectra of Inorganic and Coordination Compounds, p. 161 Wiley, Interscience, New York 1963
[12] Lever, A. B. P., Mantovani, E.: Inorg. Chim. Acta, **5,** 429 (1971)
[13] Sacconi, L., Ciamolini, M.: J. Chem. Soc., **1964,** 276
[14] Hathaway, B. J., Billing, G.: Coord. Chem. Rev., **5,** 143 (1970)
[15] Kato, M., Jonassen, H. B., Fanning, J. C.: Chem. Rev. **64,** 99 (1964)
[16] Campbell, M. J., Grzeskowiak, R.: J. Chem. Soc., A, **1967,** 396
[17] Sacconi, L.: Coord. Chem. Rev. **1,** 126 (1966)
[18] Liehr, D., Ballhausen, C. J.: Ann. Physik., **6,** 1341 (1959)
[19] Cotton, F. A., Wilkinson, G.: Advanced Inorganic Chemistry, p. 880 3 rd. Interscience, 1972,
[20] Bosnich, B.: J. Am. Chem. Soc., **90,** 627 (1968)

Acta Chimica Hungarica 114 (1), pp. 15–22 (1983)

EPR STUDY ON COPPER(II) COMPLEXES OF *l*-α-AMINO ACIDS IN FROZEN SOLUTIONS

T. SZABÓ-PLÁNKA[1]* and L. I. HORVÁTH[2]

([1]Department of General and Physical Chemistry, József Attila University, H-6701 Szeged, P.O. Box 105 and [2]Department of Biophysics, Biological Research Center of the Hungarian Academy of Sciences, H-6701 Szeged, P.O. Box 521.)

Received June 24, 1982
Accepted for publication September 30, 1982

Molecular orbital coefficients of coordinative bonds in copper(II) complexes of eight *l*-α-amino acids were determined from EPR spectra taken in frozen glycerine–water mixtures. It has been obtained that (a) in-plane σ, in-plane π, and, in contrast to previous data, out-of-plane π bond as well, are of fairly covalent character, (b) the covalency of the in- and out-of-plane π bond varies parallel, (c) there is a competition between the σ bonds of different symmetry in the series, and, (d) in solutions the effect of the substituents on the metal–ligand bonds is relatively small.

We investigated the coordinative bonds of Cu(II) complexes of α-amino acids. One one hand, the molecular orbital coefficients of the metal-ligand bonds were obtained by evaluating the EPR spectra of the polycrystalline copper(II)- doped zinc(II) complexes [1]. This work deals with the coordinative bonds of the copper(II) complexes in frozen glycerine–water mixtures.

Experimental

Complexes of glycine, *l*-alanine, *l*-valine, *l*-serine, *l*-proline, *l*-threonine, *l*-arginine, and *l*-lysine (Gly, *l*-Ala, *l*-Val, *l*-Ser, *l*-Pro, *l*-Thr, *l*-Arg, *l*-Lys) were prepared according to a literature method [2]. Compositions of the polycrystalline compounds are shown in Table I.

The EPR spectra were recorded on a JEOL JES-PE-1X X-band spectrometer using diphenyl-picryl-hydrazyl free radical and Mn(II)-doped MgO as standards. Spectra were taken in glycerine–water mixtures of 1 : 3 or 3 : 2 volume ratio at 77 K and in water at room temperature, with $\sim$1 mole m^{-3} concentration.

Electronic spectra of the Cu(II) chelates were taken with a BECKMAN DU spectrometer in glycerine–water solutions at room temperature.

Theoretical

Antibonding molecular orbitals of copper(II) ions under D_{4h} symmetry (tetragonally distorted octahedral geometry) can be written as [3]:

$$\Psi_{b_{1g}} = \alpha d_{x^2-y^2} - \alpha' \varphi_L(x^2 - y^2) \qquad (1)$$

* To whom correspondence should be addressed.

$$\Psi_{a_{1g}} = \alpha_1 \mathrm{d}_{z^2} - \alpha_1' \varphi_L(z^2) \tag{2}$$

$$\Psi_{b_{2g}} = \beta_1 \mathrm{d}_{xy} - \beta_1' \varphi_L(xy) \tag{3}$$

$$\left.\begin{aligned} \Psi_{e_g} &= \beta \mathrm{d}_{xz} - \beta' \varphi_L(xz) \\ \Psi_{e_g} &= \beta \mathrm{d}_{xy}\, \beta' \varphi_L(xy) \end{aligned}\right\} \tag{4}$$

The x and y axes are directed towards the donor atoms of the ligands. The d and φ_L functions represent copper(II) 3d orbitals and ligand group orbitals of appropriate symmetry, respectively. In the case of elongated octahedral structure unpaired electron occupies the $\Psi_{b_{1g}}$ antibonding orbital. Then the MO coefficients can be related to the parallel and perpendicular components of the g and A tensors as follows [3—5]:

$$g_{\|} - g_e = -\frac{8\lambda_0}{\Delta E_{xy}} (\alpha^2 \beta_1^2 - f_1) \tag{5}$$

$$g_{\perp} - g_e = -\frac{2\lambda_0}{\Delta E_{xz,yz}} (\alpha^2 \beta^2 - f_2) \tag{6}$$

$$A_{\|} = -K + P\left[-\frac{4}{7}\alpha^2 + (g_{\|} - g_e)(1 + f_3) + \frac{3}{7}(g_{\perp} - g_e)(1 + f_4)\right] \tag{7}$$

$$A_{\perp} = -K + P\left[\frac{2}{7}\alpha^2 + \frac{11}{14}(g_{\perp} - g_e)(1 + f_4)\right]. \tag{8}$$

$g_e = 2.0023$ is the free electron g-factor, λ_0 is the spin-orbit coupling constant of the free copper(II) ion (-828 cm^{-1}). K is the Fermi hyperfine contact term. $P = 0.036$ cm^{-1} is the dipole coefficient of the free ion. ΔE_{xy} and $\Delta E_{xz,yz}$ are the energies of the $B_{2g} \leftarrow B_{1g}$ and $E_g \leftarrow B_{1g}$ transitions, respectively. f_1, f_2, f_3 and f_4 are small correction terms:

$$f_1 = \alpha\beta_1\left[\alpha' \beta_1 S + \alpha' \beta_1' \frac{T(n)}{2}\right], \tag{9}$$

$$f_2 = \alpha\beta\left[\alpha' \beta S + \alpha' \beta' \frac{T(n)}{\sqrt{2}}\right], \tag{10}$$

$$f_3 = \frac{f_1}{\alpha^2 \beta_1^2 - f_1}, \tag{11}$$

$$f_4 = \frac{f_2}{\alpha^2 \beta^2 - f_2}, \tag{12}$$

where α', β_1', and β' can be obtained from Eqs (13—14):

$$\alpha^2 + \alpha'^2 - \alpha\alpha' S - 1 = 0 \tag{13}$$

$$\beta_1' = \sqrt{1 - \beta_1^2},\ \beta' = \sqrt{1 - \beta^2}\,. \tag{14}$$

According to the calculations of Kivelson and Neiman [4], the value of the overlap integral (S) is 0.076 and $T(n) = 0.22$ for oxygen, whereas for nitrogen donor atoms $S = 0.093$, $T(n) = 0.33$ at a metal-donor atom distance of $\sim$1.9 Å.

The MO coefficients α, β_1, and β characterizing the covalency of the in-plane σ, in-plane π, and out-of-plane π bonds, respectively, can be calculated from Eqs (5—7). Their first approximate values are obtained by neglecting the correction terms. From Eq. (7)

$$\alpha^2 = \frac{1}{8}\left[-14(A_{\parallel} + K)/P + 11(g_{\parallel} - g_e) + 9(g_0 - g_e)\right] + F, \tag{15}$$

where F is composed from that part of Eq. (7), which contains the small correction terms. If we compute F, using approximate values of α, β_1, β, and α' obtained from Eq. (13), we get refined value of α^2, that can be used for calculating refined values of α', β_1, and β.

This iteration procedure is analogous to that described by Misra and Sharma [6]. The only difference is that the assumption regarding proportionality of K to α^2 was rejected. K was determined from isotropic EPR spectra. From Eqs (7—8), neglecting the correction terms we obtain:

$$K = -A_0 + P(g_0 - g_e), \tag{16}$$

where

$$A_0 = \frac{1}{3}(A_{\parallel} + 2A_{\perp}) \text{ and } g_0 = \frac{1}{3}(g_{\parallel} + 2g_{\perp})\,. \tag{17}$$

The variation of K with α^2 is explained on the basis of the spin polarization of the partially occupied 4s orbitals through a σ bond and a competition between this σ and the in-plane σ bond [7]. The bonding orbital between the metal 4s and ligand orbitals is

$$\Psi'_{a_{1g}} = \varepsilon' 4s + \varepsilon\varphi_L(a_{1g}). \tag{18}$$

The total Fermi term can be written as follows:

$$K = \alpha^2(K_{\text{core}} + \varepsilon'^2 K_{4s}), \tag{19}$$

where $K_{core} = K_{1s} + K_{2s} + K_{3s}$ and K_{4s} represent the respective spin polarizations, their values are given as 0.0185 cm^{-1} and -0.015 cm^{-1}, respectively. On the basis of this model of competing σ bonds, a linear relationship between ε'^2 and α^2 is expected, and observed [7]. A rhombic distortion of the tetragonal ligand field can lead to 3d—4s orbital mixing and consequently to the overestimation of ε'^2 from Eq. (19), while in the case of tetrahedral distortion (3d—4p hibridization) the understimation of α^2 and so of ε'^2 can be expected [7]

Results and Discussion

In glycerine–water glasses the EPR spectra of the complexes are of axial character, and so may reflect tetragonally distorted octahedral or compressed tetrahedral geometry. Crystal structures of the complexes of Gly, *l*-Ala, and *l*-Ser are known [8—10], there is no significant tetrahedral distortion in these compounds. Neither in the glass spectra of the former three chelates, nor those of the other five complexes notable decrease in $A_{||}$ and increase in $g_{||}$, characteristic of tetrahedral distortion [7, 11], is observed.

Table I

EPR spectral parameters of copper(II) complexes of l-α-amino acids

Compound	Solvent ratio[a]	$g_{||}$[b]	$g\perp$[b]	$-A_{||} \cdot 10^4$ cm^{-1}	$-A_0 \cdot 10^4$[c] cm^{-1}
$Cu(Gly)_2 \cdot H_2O$	1/3	2.248	2.053	156.2[b] 152.1[d]	64.3
$Cu(l\text{-Ala})_2$	1/3	2.240	2.051	160.2[b] 154.6[d]	65.8
$Cu(l\text{-Val})_2$	1/3	2.240	2.051	159.7[b]	66.2
$Cu(l\text{-Ser})_2$	3/2	2.237	2.050	158.4[b] 170.9[d]	66.3
$Cu(l\text{-Pro})_2 \cdot 2H_2.O$	3/2	2.235	2.050	163.6[b] 172.2[d]	68.7
$Cu(l\text{-Thr})_2 \cdot H_2O$	3/2	2.235	2.049	158.9[b]	67.5
$Cu(l\text{-Arg})_2 \cdot 6H_2O$	3/2	2.239	2.050	158.2[b]	66.2
$Cu(l\text{-Lys})_2 \cdot 2H_2O$	3/2	2.239	2.050	158.9[b]	66.3

[a] Glycerine/water volume ratio; [b] from the spectra taken in glycerine–water mixtures at 77 °K; [c] from isotropic spectra recorded in water at laboratory temperature and [d] from the spectra of the copper(II)-doped Zn(II) complexes [1]

Table II

Absorption spectral data of copper(II) complexes of l-α-amino acids in glycerine–water mixtures[a] *at room temperature*

$c = 6 \cdot 10^{-4} \div 3 \cdot 10^{-3}$ mol dm^{-3}

Ligand	$\nu^*_{max} \cdot 10^{-3}$ cm^{-1}	lg ε_{max}	Energies of Gaussian components in 10^3 cm^{-1}		
			1	2	3
Gly	15.95	1.72	14.75	16.04	17.54
l-Ala	15.90	1.81	14.93	16.08	17.32
l-Val	16.40	1.74	15.18	16.20	17.59
l-Ser	15.80	1.85	15.43	16.00	16.70
l-Pro	16.10	1.83	15.27	16.24	17.37
l-Thr	15.50	1.72	14.80	15.99	17.30
l-Arg	12.95	1.19	12.91	16.17	18.22
	16.70	1.31			
l-Lys	12.95	1.50	13.04	16.46	18.17
	16.60	1.69			

[a] The volume ratios of the two solvents see in Table I

Thus, it seems to be reasonable to evaluate EPR spectral data (Table I) according to D_{4h} symmetry.

The electronic spectra up to 25,000 cm^{-1} consist of one or two absorption bands at about 16,000 and 13,000 cm^{-1} (Table II). Considering that (a) the bis-(*l*-amino acidato) Cu(II) chelates have two or three CD bands below 22,000 cm^{-1} [12], (b) there are three bands in the single-crystal polarized electronic spectra of bis-(*l*-tyrosinato) copper(II) [13] below 18,000 cm^{-1}, and (c) a significant splitting of E_g level occurs with a notable rhombic distortion, which would be manifested in rhombic EPR spectra, we assumed that these compounds have three overlapping d—d bands, each below 20,000 cm^{-1}. The absorption spectrum was resolved into three Gaussian components by a FORTRAN IV program[a] (Table II). The component bands were assigned according to the orbital energy sequence in bis-(*l*-tyrosinato) copper(II) [13, 1] as follows

$$A_{1g} \leftarrow B_{1g} < B_{2g} \leftarrow B_{1g} < E_g \leftarrow B_{1g}.$$

[a] The program was kindly offered by Dr. L. Zalotai.

The molecular orbital coefficients of the different metal-ligand bonds were calculated by the iteration procedure described in the Theoretical (Table III). The in-plane σ bond is rather covalent for each member of the series. It is striking that not only the in-, but also the out-of-plane π bond is fairly covalent in contrast with a previous assumption [14]. The differences between literature [14, 6, 15] and our data (Table III) are, in our opinion, mostly caused by the uncertainties in d—d transition energies, especially in $\Delta E_{xz,yz}$, though Misra and Sharma [6] did not supply any information about excitation energies used in their calculations. Another source of inequalities is — besides the different experimental circumstances and errors — that we used a Fermi hyperfine contact term computed from isotropic spectral data, while in Refs [14, 6] $K = 0.43\ \alpha^2$ was applied.

It is interesting that the covalency of the in-plane π bond varies parallel to that of the out-of-plane π bond in the series (Fig. 1). The differences in α^2 and β_1^2 for 7 members of the series are too small relative to the experimental errors, to allow of recognizing competition between the in-plane bonds, observed with copper(II) complexes of tridentate Schiff-bases in solutions [16, 17] and with the complexes of the type discussed in crystalline state [1]. However, the most covalent in-plane π bond is observed in the Cu(II) complex of *l*-Val with the greatest α^2 value (Table III).

Table III

Molecular orbital coefficients of copper(II) complexes of l-α-amico acids in glycerine–water glasses

Ligand	α^2	β_1^2	β^2	ε'^2
Gly	0.74	0.88	0.83	0.28
	0.83[a]	0.69[a]	0.91[a]	
	0.75[b]	0.90[b]	0.97[b]	
l-Ala	0.74	0.86	0.78	0.28
l-Val	0.78	0.83	0.76	0.32
l-Ser	0.73	0.86	0.76	0.27
l-Pro	0.74	0.85	0.78	0.26
l-Thr	0.72	0.86	0.78	0.25
l-Lys	0.73	0.88	0.81	0.26
	0.81[b]	0.69[b]	0.88[b]	
l-Arg	0.73	0.87	0.82	0.26

[a] In frozen 3/2 glycerine–water mixture [10] and [b] in frozen ethylene glycol [9]

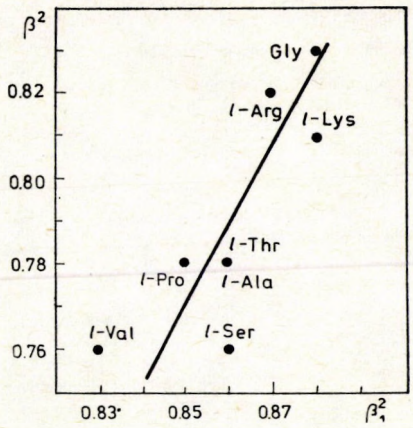

Fig. 1. The β^2 vs. β_1^2 plot for Cu(II) complexes of *l*-α-amino acids in glycerine–water glasses

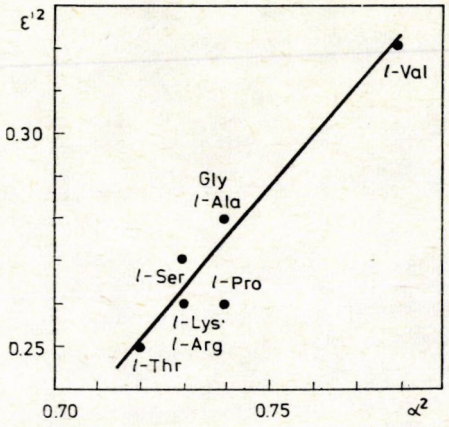

Fig. 2. The ε'^2 vs. α^2 plot for bis(*l*-α-amino acidato) copper(II) complexes

The ε'^2 values computed from K and α^2 (see Theoretical) are somewhat larger (Table III) than those obtained for Cu(II) complexes of other type [7]. Since K_{core} and K_{4s} are arbitrarily chosen and particularly the value of the former is uncertain, ε'^2 is rather tentative [7]. However, there is a linear relationship between ε'^2 and α^2 with our complexes as well (Fig. 2). The slope of the straight line (1.16) is close to the literature value (1.06) [7]. This correlation reflects a competition between the different σ bonds: a more ionic in-plane σ bond is compensated by a more covalent 4s σ bond and vice versa. The fact that all the points lie very close to the line support the D_{4h} symmetry, providing no proof for either 3d—4s, or 3d—4p orbital mixing.

The complexes of *l*-Lys and *l*-Arg in some respect differ from the other members of the series. The most striking is that their ΔE_{z^2} energies are about 2,000 cm^{-1} lower than those of the other compounds (Table II). This fact is

attributed to a change in axial coordination, since it is the d_{z^2} orbital, energy of which is the most sensitive to interactions of such type. We think that besides the solvent molecules the amino groups of the side chains may take part in the *axial* coordination with these complexes.

The above discussed differences in the covalency of the coordinative bonds within the series are small as compared to the crystalline complexes of this type [1]. This fact reflects that in solutions the effect of substituents on metal — ligand bonds is small.

REFERENCES

[1] Szabó-Plánka, T., Horváth, L. I.: To be published
[2] Jung, C., Ottnad, M., Bohnenkamp, W., Bremser, W., Weser, U.: Biochim. Biophys. Acta, **295,** 77 (1973)
[3] Maki, A. H., McGarvey, B. R.: J. Chem. Phys., **29,** 31, 35 (1958)
[4] Kivelson, D., Neiman, R.: J. Chem. Phys., **35,** 149 (1961)
[5] Gersmann, H. R., Swalen, J. D.: J. Chem. Phys., **36,** 3221 (1962)
[6] Misra, B. N., Sharma, S. D.: J. Chem. Phys., **63,** 5322 (1975)
[7] Rockenbauer, A.: J. Magn. Reson., **35,** 429 (1979)
[8] Freeman, H. C., Snow, M. R., Nitta, I., Tomita, K.: Acta Cryst., **17,** 1463 (1964)
[9] Dijkstra, A.: Acta Cryst., **20,** 588 (1966)
[10] van der Helm, D., Franks, W. A.: Acta Cryst., **25,** 451 (1969)
[11] Sharnoff, M.: J. Phys. Chem., **41,** 2203 (1964); **42,** 3383 (1965)
[12] Tsangaris, J. M.: Chim. Chron., **1,** 124 (1972)
[13] Brown, D. H., Mangrio, N. G., Smith, W. E.: Spectrochim. Acta, **35A,** 123 (1979)
[14] Jezowska-Trzebiatowska, B., Antonów, A., Kozlowski, H.: Bull. Acad. Pol. Sci., Ser. Sci. Chim., **22,** 399 (1974)
[15] Misra, B. N., Kripal, R.: Acta Chim. Acad. Sic. Hung. **107,** 101 (1981)
[16] Rockenbauer, A., Casella, L., Gullotti, M., Pasini, A.: XXth AMPERE Congress Tallin, 1978
[17] Casella, L., Gullotti, M., Pasini, A., Rockenbauer, A.: Inorg. Chem., **18,** 2825 (1979)

Acta Chimica Hungarica 114 (1), pp. 23–27 (1983)

STRUCTURE INVESTIGATIONS ON SOME DIPHENYLTRIAZOLES

T. SOMORAI[1]*, P. DVORTSÁK[1], J. LANGÓ[1] and J. REITER[2]

([1]Institute for Drug Research, H-1325 Budapest, P.O. Box 82. and [2]EGYT Pharmacochemical Works, H-1106 Budapest, Keresztúri u. 30–38.)

Received July 16, 1982
In revised form October 4, 1982
Accepted for publication November 4, 1982

Syntheses of 1,3-diphenyl-4*H*-1,2,4-triazolin-5-thione (**1**) and 1,5-diphenyl-2*H*-1,2,4-triazolin-3-thione (**2**) have been reinvestigated and the structures proposed in the literature corrected. ^{1}H-NMR, ^{13}C-NMR, UV and MS studies of these compounds and their *S*-methyl derivatives have been carried out and are discussed.

Studying the reaction of benzoyl isothiocyanate with phenylhydrazine in benzene Pohloudek-Fabini and Schröpl [1] isolated two isomeric triazole derivatives. One of them melted at 255—257 °C and was claimed to be 1,5-diphenyl-1,2,4-triazol-3-thiol on the basis of its metal mercaptide forming behaviour. The other product that melted at 179—182 °C was dethiolated and the resulting compound of m.p. 93 °C was identified as 1,3-diphenyl-1,2,4-triazole (m.p. 91 °C [2]) although its measured m.p. may also correspond to 1,5-diphenyl-1,2,4-triazole (m.p. 96—97 °C [2]).

When preparing 1,3-diphenyl-5-methylthio-1,2,4-triazole (**3**) and 1,5-diphenyl-3-methylthio-1,2,4-triazole (**4**) via the corresponding thiols mentioned above (Fig. 1) we have found that methylation of the thiol melting at 255—258 °C (*lit.* [1] m.p. 255—257 °C) leads to 1,3-diphenyl-5-methylthio-1,2,4-triazole (**3**, m.p. 50—51 °C; *lit.* [3] m.p. 48 °C), while the isomer **2** melting at 191—193 °C (*lit.* [1] m.p. 179—182 °C) gives 1,5-diphenyl-3-methylthio-1,2,4-triazole (**4**, m.p. 102—103 °C; *lit.* m.p. 102—104 °C [4]; 103—105 °C [5]), showing that the correct structures of the thiones** **1** and **2** are just the reverse of those stated in the literature [1].

We have also succeeded in isolating an open-chain intermediate, 4-benzoyl-1-phenyl-thiosemicarbazide, Ph—CO—NH—CS—NH—NH—Ph (**5**), as a by-product of the reaction carried out according to Pohloudek-Fabini and Schröpl [1] and identified it with the compound prepared by Chinese authors [6]; we also proved the correctness of its structure by spectroscopic methods. However, our attempts to recrystallize it from acetic acid, which

* To whom correspondence should be addressed.
** The thione rather the thiol forms are present on the basis of spectroscopic properties.

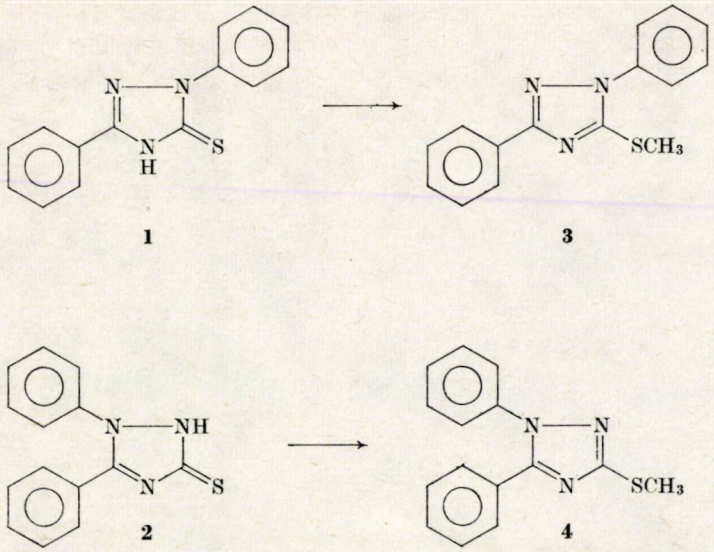

1 3

2 4

Fig. 1

had been reported [6] as a suitable recrystallization solvent, failed because of ring closure to **2**. This experience is in agreement with those mentioned above.

We have supported the structures of these compounds by their spectroscopic properties. Both of the adjacent phenyl groups are perpendicular to the triazole ring in **2** and **4**, giving rise to a singlet at 7.45 and 7.35 ppm, respectively, in the ^{1}H-NMR spectrum. In **1** and **3**, separation of the *C*-phenyl *ortho* protons from the others by about 0.5 ppm downfield indicates the coplanarity of the *C*-phenyl and triazole rings (cf. phenyltetrazoles [7, 8]). The *N*-phenyl *ortho* protons in **1** also separate indicating preference of the thione to thiol form in DMSO (this signal overlaps that of the *C*-phenyl *ortho* protons at 8.1 ppm) due to the anisotropic effect of the C=S group [9]. Only the *C*-phenyl *ortho* proton signals are split in **3**, showing that the *N*-phenyl cannot be coplanar with the triazole ring, presumably owing to the presence of the methylthio group.

The ^{13}C-NMR spectra confirm the ring positions deduced from the ^{1}H-NMR data and have been interpreted in view of experiences with phenyltetrazoles. ^{13}C-NMR chemical shifts and the differences between the *ortho*- and *meta*-carbon shifts in **1**—**4** are collected in Table I.

The chemical shifts differences for the *N*-phenyl carbons are in good agreement with those of phenyltetrazoles having no interannular conjugation (the corresponding $\Delta\delta$ values are 9—10 ppm for coplanar and 3.3 – 4.6 ppm for non-coplanar *N*-phenyltetrazoles). However, the *C*-phenyl ring in **1** and **3** seems to be coplanar with the triazole ring (the corresponding differences

Table I

^{13}C-NMR *data*[a]

Carbon atom		Chemical shifts (in $CDCl_3$) ppm							
		1		**2**		**3**		**4**	
	1	139.4		139.0		137.5		138.1	
N-Phenyl	2.6	125.5	$\Delta\delta$=4.8*	127.0	$\Delta\delta$=3.9*	123.7	$\Delta\delta$=5.6*	125.2	$\Delta\delta$=4.0*
group	3.5	130.3		130.9		129.3		129.2	
	4	129.4		130.1		128.3+		128.4+	
	1	126.4		131.8		130.9		127.6	
C-Phenyl	2.6	127.7	$\Delta\delta$=3.0**	130.0	$\Delta\delta$=0.9*	126.5	$\Delta\delta$=2.8**	128.7	$\Delta\delta$=0.5*
group	3.5	130.7		130.9		129.3		129.2	
	4	132.7		130.1		128.5+		129.9+	
Triazole	C – S	168.0		163.5		154.1		161.7	
carbon	C – Ph	159.9		158.0		162.1		154.7	
atoms	CH_3 – S					15.8		14.3	

[a] These assignments are confirmed by ^{1}H-coupled spectra
+ These assignments may be reversed
* Non-coplanar with the triazole ring
** Coplanar, or nearly so, with the triazole ring

for *C*-phenyl-tetrazoles are 3.2—3.8 ppm), but non-coplanar in **2** and **4** (cf. 0.0—0.7 ppm for tetrazoles [10]).

These results are in good agreement with Könnecke's statement [11] that "even a methine group in heterocycles" in an adjacent position can force a phenyl group to turn from the plane of the azole ring (compare the *C*-phenyl groups in **1** and **3**) and only the absence of substituents in its neighbourhood allows it to be coplanar (compare the *C*-phenyl rings in **2** and **4** and the *N*--phenyl rings).

To decide on the tautomeric structure of **1** we have investigated a non-tautomeric compound, 3,4-bis-(4-chlorophenyl)-1*H*-1,2,4-triazolin-5-thione [12], and found that the chemical shifts of the triazoline carbons are comparable and differ from those of **2**, showing that in DMSO solution **1** exists mainly as 1,3-diphenyl-4*H*-1,2,4-triazol n-5-thione.

Experimental

M.p.-s were determined on a Kofler Boetius hot stage and are uncorrected. The spectra were recorded on IR (Perkin-Elmer 557), ^{1}H-NMR (Varian EM-390 and JEOL C-60 HL), ^{13}C-NMR (Varian XL-100) and UV (Varian Cary 118) instruments. Mass spectrometric investigations were carried out on a Varian MAT SM 1 spectrometer (T_v = 100 °C). Elemental analyses were satisfactory within 0.3%.

1,3-Diphenyl-4*H*-1,2,4-triazolin-5-thione (1) and 1,5-diphenyl-2*H*-1,2,4-triazolin-3-thione (2)

These were prepared according to the procedure of Pohloudek-Fabini and Schröpl [1].
Compound **1**, m.p. 255–258 °C (*lit.* [1] m.p. 255–257 °C).
IR (KBr): 1605, 1590, 1500, 776, 762, 685 cm^{-1} (ν_{Ar}).
^{1}H-NMR (DMSO-d_6): δ 7.9–8.2 ppm (m, 4H, *o*-aryl), 7.5–7.8 (m, 6H, aryl).
MS: 253 (M^+, 100%), 252 (66), 150 (1), 104 (2), 91 (23), 77 (3).
Compound **2**, m.p. 191–193 °C (*lit.* [1] m.p. 179–182 °C).
IR (KBr): 1605, 1595, 1500, 778, 762, 695, 690 cm^{-1} (ν_{Ar}).
^{1}H-NMR (DMSO-d_6): δ 7.45 ppm (br, s, aryl).
MS: 253 (M^+, 100%), 252 (1), 150 (19), 104 (6), 91 (11), 77 (4).

4-Benzoyl-1-phenyl-thiosemicarbazide (5), (9%) was isolated from the mother liquor of **1** and **2** by column chromatography; m.p. 135–137 °C (*lit.* [6] m.p. 138–139 °C).
IR (KBr): 3200, 3160 cm^{-1} (ν_{NH}), 1675 (ν_{CO}), 1600 (ν_{Ar}).
^{1}H-NMR ($CDCl_3$): δ 12.2 and 7.2 ppm (NH–NH, J = 6 Hz), 9.2 (NH), 6.8–7.9 (m, 10H, aryl).
MS: 271 (M^+, 59%), 150 (21), 108 (17), 107 (6), 105 (100), 92 (10), 77 (42).

1,5-Diphenyl-2*H*-1,2,4-triazolin-3-thione (2) by ring closure of 5

Compound **5** (1.36 g; 5 mmol) was refluxed in 5 mL of acetic acid for 10 min. After cooling, the crystals were collected to yield 1.14 g (90%) of **2**, m.p. 190–193 °C; mixed m.p. 190–193 °C.

1,3-Diphenyl-5-methylthio-1,2,4-triazole (3)

To a stirred solution of 6.33 g (25 mmol) **1** and 5 mL 5*N* NaOH in 100 mL MeOH was added 3.15 g (25 mmol) dimethylsulfate. After standing overnight, the crystals were separated to obtain 5.0 g (75%) of **3**, m.p. 45–47 °C; recrystallization from *n*-hexane gave an analytical sample of m.p. 51–53 °C (*lit.* [3] m.p. 48 °C).
IR (KBr): 1605, 1505, 760, 690 cm^{-1} (ν_{Ar}).
^{1}H-NMR ($CDCl_3$): δ 7.4–7.6 ppm (m, 2H, *o*-aryl), 6.8–7.2 (m, 8H, aryl), 2.53 (s, 3H, CH_3).
MS: 267 (M^+, 100%), 266 (11), 194 (30), 158 (11, M^+-*PhS.*), 91 (80), 77 (5).
UV: 239 nm (20.0), 258 (15.7 sh) (EtOH); no change in HCl and NaOH.

1,5-Diphenyl-3-methylthio-1,2,4-triazole (4)

It was prepared similarly, yielding 89% of **4**, m.p. 95–96 °C; recrystallization from ethanol–water gave an analytical sample of m.p. 102–103 °C (*lit.* m.p. 102–104 °C [4]; 103–105 °C [5]).
IR (KBr): 1595, 1500, 775, 770, 700, 695 cm^{-1} (ν_{Ar}).
^{1}H-NMR ($CDCl_3$): δ 7.4 ppm (br, s, 10H, aryl), 2.65 (s, 3H, CH_3).
MS: 267 (M^+, 100%), 266 (14), 164 (20), 91 (95), 77 (12).
UV: 226 nm (21.1), 270 (6.47) (EtOH); no change in HCl and NaOH.

*

The authors' thanks are due to Mrs. G. Bodrogai and her co-workers for the microanalyses, to Dr. A. Szabó and Mr. L. Lőwinger for the recording of the UV spectra, and to Prof. Á. Kiss (Technical University, Budapest) for the helpful discussion of these spectra.

REFERENCES

[1] Pohloudek-Fabini, R., Schröpl, E.: Pharm. Zentralhalle, **107,** 736 (1968)
[2] Beilsteins Handbuch d. Organischen Chemie, **26,** 68
[3] Conde, S., Corral, C., Madronero, R.: Synthesis, **1974,** 28

[4] Augustin, M., Richter, M., Salas, S.: J. Prakt. Chem., **322,** 55 (1980)
[5] Masuda, K., Adachi, J., Shibata, T., Nomura, K.: Chem. Pharm. Bull., **27,** 1683 (1979)
[6] Ch'en, Y.-T., Chang, T.-I.: K'o Hsueh T'ung Pao, **1962,** 37; Chem. Abstr., **58,** 13937 (1963)
[7] Begtrup, M.: Acta Chem. Scand. Ser. B, **28,** 61 (1974)
[8] Könnecke, A., Kleinpeter, E.: Org. Magn. Res., **12,** 667 (1979)
[9] Könnecke, A., Lippmann, E., Kleinpeter, E.: Z. Chem., **15,** 402 (1975)
[10] Begtrup, M.: Acta Chem. Scand. Ser. B, **27,** 3101 (1973)
[11] Könnecke, A.: Tetrahedron, **32,** 499 (1976)
[12] Mhasalkar, M. Y., Shah, M. H., Nikam, S. T., Anantanarayanan, K. G., Deliwala, C. V.: J. Med. Chem., **14,** 260 (1971)

Acta Chimica Hungarica 114 (1), pp. 29–39 (1983)

METAL CHELATES OF HETEROCYCLIC NITROGEN CONTAINING KETONES, VII

MAGNETIC AND SPECTRAL STUDIES ON NICKEL(II) AND COPPER(II) COMPLEXES OF 2,6-LUTIDYL-2-PHENYL KETONE THIOSEMICARBAZONE

M. M. ABOU-SEKKINA[1], A. EL-DISSOUKY[2]* and A. Z. EL-SONBATI[1]

([1]Chemistry Department, Faculty of Science, Tanta University, Tanta, Egypt. [2]Chemistry Department, Faculty of Science, Alexandria University, Alexandria, Egypt)

Received September 16, 1982
Accepted for publication November 4, 1982

The reaction products of 2,6-lutidyl-2-phenyl ketone thiosemicarbazone, LPKTS, with NiX_2 and CuX_2 salts (X = Cl^-, Br^- or I^-) were investigated by IR and electronic spectroscopy, molar conductivity and variable temperature magnetic susceptibility.The room temperature ESR spectra were used for complete investigation of copper(II) complexes. Nickel(II) complexes were found to have the stoichiometry $[(LPKTS\ H)Ni]_nX_n$, (X = Cl^-, Br^- or I^-; $n = 2, 3$ or 4) with magnetic moments 1.23, 1.21 and 1.24 B.M., respectively. These complexes follow the Curie-Weiss law in the 298-77 K temperature range. In solution, these complexes appear to be dimers. However, in the solid state they appear to be polymeric. Based on the spectral and magnetic data, these complexes appear to have both square planar diamagnetic sites and paramagnetic sites in which the nickel (II) ion has a coordination number more than four. The copper(II) complexes were found to have the stoichiometry $[(LPKTS\text{-}H)CuX]_2$ (X = = Cl^- or Br^-). Both complexes exhibit antiferromagnetic behaviour typical of binuclear copper(II) complexes. ESR, electronic and IR spectra together with magnetic data showed that both complexes are of square pyramidal structure.

Introduction

The coordination chemistry of metallo-sulfur compounds is a source of stimulation to many research workers, due to the fact that it possesses unique stereochemical, magnetic and spectral properties. Metal complexes of ligands containing sulfur as donor atoms were studied by many authors [1—3]. The biological and carcinogenic activities of metallo-sulfur compounds have been surveyed [4, 5]. The chelation properties of Schiff base derivatives thiosemicarbazone have been reported by many authors [6—9]. We report herein the preparation and characterization of 2,6-lutidyl-2-phenyl ketone thiosemicarbazone, LPKTS, complexes with nickel(II) and copper(II) halides. The solid complexes prepared were investigated using electronic, IR and ESR spectra. Magnetic data in the temperature range 340—77 K and molar conductivities are also given.

* To whom correspondence should be addressed.

Experimental

Preparation of the ligand

2,6-Lutidyl-2-phenyl ketone was prepared according to the method given in a previous publication [3]. The Schiff base was prepared by refluxing equimolar amounts of the ketone and thiosemicarbazide in EtOH for 30 min. The pale yellow crystals separated were recrystallized from benzene; M.P. 118 °C.

Preparation of the metal complexes

The metal complexes were prepared by the general method, viz., to an ethanolic solution of the metal(II) halide (0.015 mol), 0.01 mol of the Schiff base in EtOH was added. The reaction mixture was stirred for two hours at room temperature and the separated crystals were filtered, recrystallized from benzene–chloroform mixture and dried in vacuum over P_2O_5.

Table I

Analytical and molar conductivity data*

Compound	%C	%H	%N	%S	%M	%X	Λ_M^{**}
LPKTS	63.38 (63.29)	5.63 (5.66)	19.27 (19.69)	11.27 (11.30)	—	—	—
1. $[(LPKTS-H)Ni]_2Cl_2$	—	—	14.84 (14.86)	8.48 (8.46)	15.56 (15.55)	9.41 (9.39)	162
2. $[(LPKTS-H)Ni]_2Br_2$	—	—	13.27 (13.28)	7.58 (7.55)	13.92 (13.93)	18.97 (18.95)	172
3. $[(LPKTS-H)Ni]_2I_2$	—	—	11.94 (11.92)	6.82 (6.85)	12.52 (12.51)	27.09 (27.11)	176
4. $[(LPKTS-H)CuCl]_2$	—	—	14.61 (14.63)	8.35 (8.38)	16.58 (16.56)	9.25 (9.25)	—
5. $[(LPKTS-H)CuBr]_2$	—	—	13.09 (13.11)	7.48 (7.46)	14.86 (14.85)	18.71 (18.69)	—

* Values given first are the calculated percentages; Values in parentheses are the percentages found.

** Molar conductivity values of 10^{-3} *M* solution in CH_3NO_2 ($ohm^{-1}\,cm^2\,mol^{-1}$).

The metal, sulfur and halogen contents were determined according to the method given in our previous paper [3]. Carbon and hydrogen contents were deterdetermined at Microanalysis Laboratory, Cairo University, Cairo, Egypt. The analytical data are collected in Table I.

Physical measurements

The electronic spectra were recorded using a UNICAM S.P. 800 spectrophotometer. IR spectra were recorded in KBr discs using a UNICAM S.P. 2000 spectrophotometer. The molar conductances of the complexes in CH_3NO_2 were determined at 25 °C with a Siemens conductivity bridge using platinum electrodes. Magnetic susceptibility values were determined in the 340—77 K temperature range by the Gouy method and the diamagnetic corrections were calculated by the use of Pascal's constants [10]. The ESR data were obtained in the X-band (9 GHz) using 1000 Hz field modulation at room temperature. DPPH ($g = 2.0036$) was used as internal refrence.

Results and Discussion

2,6-Lutidyl-2-phenyl ketone thiosemicarbazone, LPKTS, has a proton adjacent to the thione group. The thione group is relatively unstable in the monomeric form and tends to give the more stable C—S bond by enethiolization [11], therefore, two tautomeric forms can be given (**1a** and **b**). Compounds similar to that under study here were shown to be mainly in the thione form in the solid state [12].

The most characteristic IR bands of the ligand and its metal chelates are listed in Table II. The bands at 3380—3180 cm^{-1} in the free ligand are due to ν(NH) while the bands around 1620, 1515, 1490 and 1320 cm^{-1} are due to the thione group [13]. The bands at 1620—1515 cm^{-1} are due to νN—C=S, which results from coupling of C—N stretching and N—H deformation vibrations. The band at 800 cm^{-1} is attributed to νC=S [12]. Thus it may be concluded that **1a** is the predominant form in the solid.

Complexation affects the spectrum of the ligand in a similar manner regardless of the metal ions. The bands in the region 3380—3180 cm^{-1} due to ν(NH) are not greatly affected on complexation. The most markedly affected bands are those at 800 cm^{-1} and 1620—1515 cm^{-1}, which shifted to lower frequencies with a decrease in their intensities. This may be due to the increased charge delocalization on sulfur atom upon chelation, i.e. the decrease in the

Table II

Major IR *bands* (cm^{-1}) *for* LPKTS *and its metal(II) chelates*

Compound	ν(NH)	amide II δNH	νC=H δNH	νC=S C=N δNH	νC=S
LPKTS	3380m 3285m 3195m	1620s 1650s	1515sh 1535s	1490m 1320m	800vs
1.	3363m 3282m 3190m	1605s 1640s	1505sh 1510m	1440m 1315s	705m
2.	3365m 3275m 3185m	1600s 1635s	1505sh 1515m	1435s 1310m	705m
3.	3360m 3272w 3190w	1610s 1640m	1510w 1525m	1440s 1315m	700m
4.	3370m 3275w 3185w	1600vs 1645vs	1500m 1515sh	1455s 1310s	700m
5.	3375m 3275w 3188w	1600vs 1635s	1505sh 1515sh	1455m 1310s	700m

s = strong, vs = very strong, m = medium, w = weak and sh = shoulder

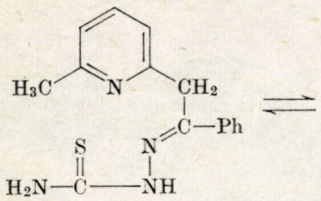

1a

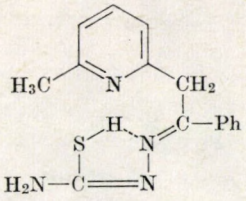

1b

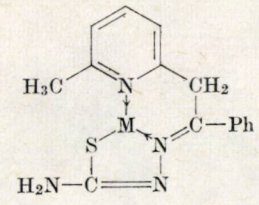

2

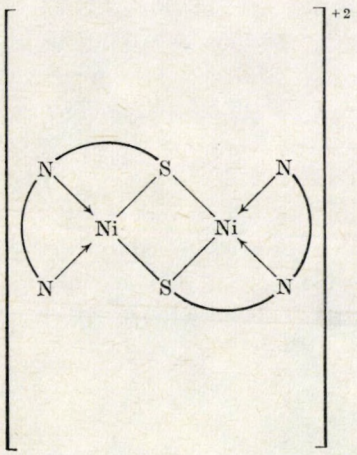

3

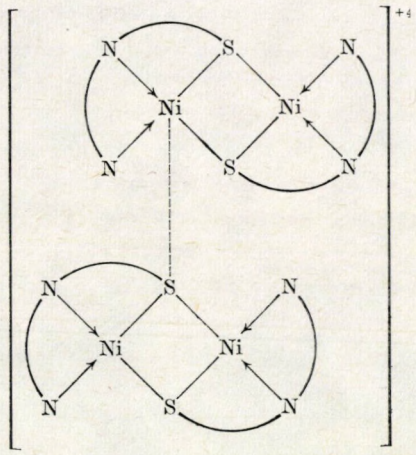

4

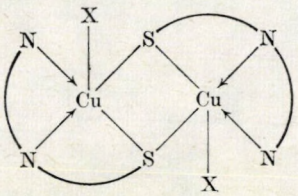

5

X = Cl^- or Br^-

C=S bond order. Also the bands at 1580, 630 and 400 cm^{-1}, which are due to the pyridine moiety, exhibit positive shift upon complex formation. Consequently the ligand coordinate through the thiole sulfur atom and azomethine and pyridine nitrogen atoms acting as monobasic tridentate ligand giving chelates of type 2.

Nickel(II) complexes

The reaction of LPKTS with nickel(II) halides gave dark brown crystals. The elemental analyses showed that the complexes have the stoichiometry [(LPKTS—H)Ni]X. The effective magnetic moments at room temperature are 1.23, 1.21 and 1.24 B.M. for chloride, bromide and iodide containing complexes, respectively (Table III). The subnormal magnetic moments can be explained on the basis of the presence of diamagnetic species together with paramagnetic species. The reflectance spectra of these complexes at room temperature indicate that the nickel ion is in a square planar environment [14] (Table III).

The molar conductivities (Table I), display values of 163, 172 and 176 $ohm^{-1}\,cm^2\,mol^{-1}$ for 10^{-3} *M* solutions of chloride, bromide and iodide containing complexes respectively (CH_3NO_2 is used as solvent). These values indicate that the complexes are 1 : 2 electrolytes [15]. Because of the low solubility of these complexes in most organic solvents, the molecular weights could not be determined.

The magnetic susceptibilities of the nickel(II) complexes in the 298—77 K temperature range are given in Table IV. Since the magnetic data fit the Curie—Weiss law [16], the low magnetic moments could be due to the coexistence of high and low spin nickel(II) ions in a constant ratio over the entire experimental temperature range. These paramagnetic nickel(II) ions are likely to have a coordination number of five and six. The electronic spectra showed no bands in the near IR region indicative of six-coordinate nickel(II) ions at room temperature and there is no spectral evidence for tetrahedral nickel(II). However, at 77 K a weak band is observed at ca. 11,100 cm^{-1} for all complexes. This band is characteristic of high spin nickel(II) ions therefore, both magnetic and low temperature spectral data suggest that these nickel(II) complexes have two different stereochemical nickel(II) sites. Similar observations were

Table III

Magnetic and reflectance spectral data for Ni(II) complexes

Compound	$\mu_{eff.}$ (B.M.)	State	cm^{-1} (εL mol^{-1} cm^{-1})			
			ν_3	ν_2	ν_1	M—L
1.	1.23	Solid		19 995		27 680
		CH_3NO_4	19 860 (250)	16 300 (49)	14 484 (15)	27 753 (3000)
2.	1.21	Solid		19 990		27 486
		CH_3NO_2	19 828 (242)	16 315 (53)	14 495 (17)	27 552 (3215)
3.	1.24	Solid		19 890		27 685
		CH_3NO_2	19 905 (258)	16 285 (50)	14 490 (16)	28 000 (3189)

Table IV

Temperature dependence of the magnetic moments of Ni(II) complexes

Temperature (K)	Effective magnetic moments (μ_{eff} B.M.)		
	1	2	3
298	1.23	1.21	1.24
280	1.22	1.22	1.23
240	1.23	1.22	1.24
200	1.25	1.24	1.25
180	1.27	1.26	1.27
160	1.28	1.28	1.29
120	1.30	1.31	1.31
95	1.33	1.34	1.33
77	1.34	1.34	1.35

made with nickel(II) complexes containing the tridentate Schiff ligand *N*-salicylidenargine [17, 18].

There are several different ways in which the nickel(II) ion could achieve the coordination number five in these complexes. A possibility is that several $[(LPKTS—H)Ni]_2^{2+}$ units may interact via bridging sulfur atoms. Such a structure would require some thiol groups to be bonded to three nickel(II) ions. Such interaction have been demonstrated for analogous complexes [19]. The basic interacting unit is likely to be a dimer, $[(LPKTS—H)Ni]_2^{2+}$, based on our conductivity data. One model consistent with magnetic and electronic spectral data is that dimer (**3**) and a tetramer (**4**) coexist in a one to one ratio in the solid unit cell. The two nickel(II) in structure (**3**) are square planar and diamagnetic and three of the four nickel(II) in structure (**4**) would be in square planar stereochemistry and diamagnetic. Therefore, only one nickel(II) per six would be paramagnetic.

In relatively polar solvents such as CH_3NO_2, structure (**4**) should break down into the basic $[(LPKTS—H)Ni]_2^{2+}$. This would explain why the conductivities indicate that these complexes appear to be 2 : 1 electrolytes in CH_3NO_2. Since $[(LPKTS—H)Ni]_2^{2+}$ and $[(LPKTS—H)Ni]_4^{4+}$ coexist in a 1 : 1 ratio, an equilibrium between these species should not alter adhering to the Beer—Lambert law. The Beer—Lambert law does hold over a wide concentration range for the complexes under investigation in benzene at 20,000 cm^{-1}. However, at 28,571 cm^{-1}, the Beer—Lambert law is valid at low concentrations. At a concentration of 5×10^{-4} *M* there is peak maximum at 28,571 cm^{-1}, however, upon increasing the concentration to 5×10^{-3} *M*, the peak maximum moves steadly to 28,609 cm^{-1}. Apparently, the higher energy band is influenced by solute-solute interactions but the lower energy band is not.

Copper(II) complexes

The interaction of LPKTS with $CuCl_2$ and $CuBr_2$ salts gave olive green and black crystals, respectively. The elemental analyses show that these complexes have the stoichiometry, $[(LPKTS—H)CuX]_2$, X=Cl^- or Br^-.

The room temperature reflectance spectra of these complexes exhibit a broad band with a maximum at ca. 14,500 and 14,380 cm^{-1} beside shoulders

Table V

Magnetic and reflectance spectral data for Cu(II) complexes

Compound	$\mu_{eff.}$ (B.M.)	State	cm^{-1}, (ε L mol^{-1} cm^{-1})	
			d-d transitions	M-L
4.	1.49	Solid	14,500, 12,100sh	28,230
		CH_3NO_2	14,565 (285), 12,080 (42),	28,300 (6500)
5.	0.79	Solid	14,278, 12,120sh	27,936
		CH_3NO_2	14,365 (300), 12,100 (40)	28.010 (5885)

Table VI

Temperature dependence of magnetic susceptibility of Cu(II) complexes

Temperature (K)	Magnetic data for the complexes			
	4		5	
	$\chi_M^{corr} \times 10^6$	$\mu_{eff.}$ (B.M.)	$\chi_M^{corr} \times 10^6$	$\mu_{eff.}$ (B.M.)
340	858.37	1.53	254.45	0.83
320	892.86	1.51	257.73	0.81
300	925.93	1.49	261.09	0.79
280	961.54	1.47	264.20	0.77
260	1000.00	1.44	267.38	0.75
240	1036.27	1.41	271.37	0.72
220	1086.96	1.38	274.73	0.69
200	1129.95	1.35	278.16	0.67
180	1190.48	1.31	281.69	0.64
160	1242.24	1.26	285.31	0.60
140	1315.79	1.22	289.44	0.57
120	1388.89	1.16	293.26	0.53
100	1492.54	1.09	297.62	0.49
80	1562.50	1.00	301.66	0.44
	$2J = -398$ cm^{-1}		$2J = -403$ cm^{-1}	
	$\theta = -$ 39 K		$\theta = -$ 54 K	
	$g =$ 2.19		$g =$ 2.20	

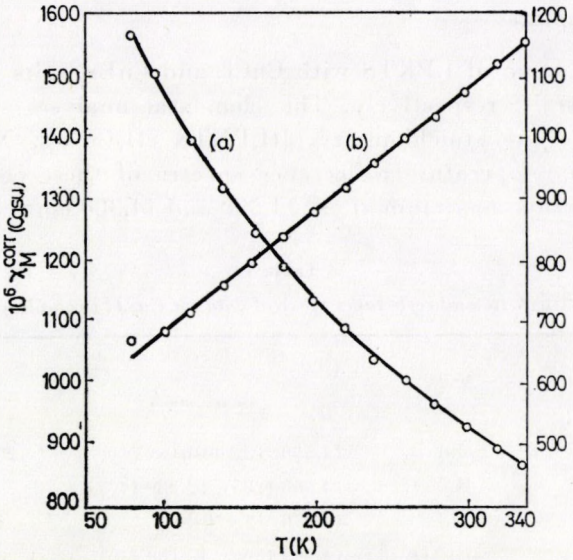

Fig. 1. Magnetic susceptibility data for (LPKTS-H)$CuCl_2$; (a) molar magnetic susceptibility, (b) reciprocal molar magnetic susceptibility

at ca 12,100 and 12,120 cm^{-1} for chloro and bromo complexes, respectively (Table V). The spectral ranges of these ligand field bands are characteristic of distorted five-coordinate copper(II) complexes in square pyramidal environments [20, 21]. The dependence of the band position on the nature of the halide ion may be attributed to the fact that they are coordinated to the copper-(II) ions. This is confirmed by the molar conductivity measurement,s which show that these complexes are non-electrolytes in CH_3NO_2 or $C_6H_5NO_2$ as 10^{-3} *M* solutions.

The far IR bands at 340, 370, 350, 356 and 282 and 210 cm^{-1} for chloro and bromo complexes could be assigned to ν(Cu—N), ν(Cu—S) and ν(Cu—X); X=Cl^- or Br^-, respectively. The latter one could be taken as a criterion for terminal coordinating halides [22, 23].

The room temperature magnetic moments are 1.49 and 0.79 B.M. for $[$(LPKTS—H)CuCl$]_2$ and $[$(LPKTS—H)CuBr$]_2$ respectively. The low effective magnetic moments can be attributed to spin–spin interaction between two copper(II) ions [24].

The variation of the magnetic susceptibility of both complexes with temperature (340—80 K) is shown in Table VI and in Fig. 1. Such behaviour is characteristic of a strong antiferromagnetic coupling between the copper(II) ions. The magnetic curves are perfectly described by Eq. (1), giving the temperature dependence of χ_M^{corr} for copper(II) binuclear complexes [25],

$$\chi_M^{corr} = N\beta^2 g^2 / 3K(T - \theta) \left[1 + 1/3 \exp^{-2J/KT}\right]^{-1} \qquad (1)$$

where J is the spin–spin coupling constant for the magnetic interaction occurring within the dimer, θ is a constant which takes into account any additional effects in the lattice. A computer program in Fortran IV was used in conjunction with Eq. (1) to obtain the best fit parameters, $2J = -398$ cm^{-1}, $g = 2.19$ and $\theta = -39.6$ K for $[(LPKTS—H)CuCl]_2$ and $2J = -403$ cm^{-1}, $g = 2.20$ and $\theta = -54$ K for $[(LPKTS—H)CuBr]_2$ (Table VI). The high values of the $2J$ parameter show that the halide ion is not acting as a bridge between copper centers, which would have been accompanied by low $2J$ value ($\simeq$200 cm^{-1})[26].

The lowering of magnetic moment to 1.00 and 0.44 B.M. at 80 K for chloro and bromo complexes, respectively, may be probably caused by a σ-type superexchange interaction between $d_{x^2-y^2}$ orbitals of the two copper(II) ions via $P\sigma$-orbitals of the bridging thiolic sulfur atom, $Cu(3d_{x^2-y^2})$—$-S\ (2P\sigma)-Cu(3d_{x^2-y^2})$.

In addition, a π-type superexchange interaction in the plane between d_{xz} and d_{yz} orbitals of the two copper(II) ions via the sulfur $P\pi$-orbitals, $Cu(3d_{xz})—S(P\pi)—Cu(3d_{yz})$ is present in the binuclear copper(II) complexes. Accordingly, both σ and π type interactions could be responsible for the observed magnetic behaviour of these complexes.

According to the magnetic and spectral data, structure (**5**) can be assumed involving a sulfur bridge between copper(II) ions similar to those reported before [3].

The X-band ESR spectra for the pure powdered solids at room temperature exhibit a very strong unsymmetrical absorption near 3165 and 3180 G

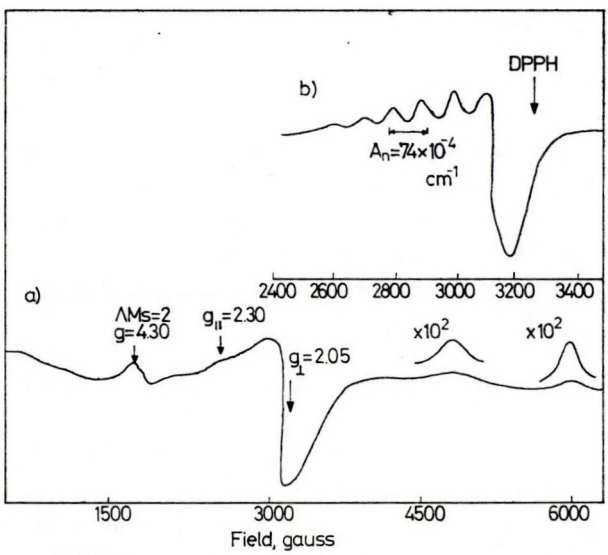

Fig. 2. X-band ESR spectrum of $(LPKTS\text{-}H)CuCl_2$; (a) polycrystalinne sample at room temperature, (b) 77 K CH_2Cl_2 glass spectrum

Table VII

Electron spin resonance data for Cu(II) complexes

Compound	g_{11}	$g_{\perp}$	$g_{av.}$	$A_{11}\times10^{4*}$ cm^{-1}	D cm^{-1}	D_{d_1} cm^{-1}	$D_{exch.}$ cm^{-1}	$M_s^2=\pm2$
4.	2.30	2.05	2.21	74	0.026	0.00200	0.0240	4.30
5.	2.31	2.08	2.23	76	0.025	0.00165	0.0235	4.38

* Electron spin resonance data obtained from 77K CH_2Cl_2 glass spectra

with absorptions at 1600, 1590, 4700, 4680 and 5900 and 6000 G for chloro and bromo complexes, respectively. The two high field features (4700, 4680 and 5900, 6000 G) in the pure samples were tentatively assigned as the parallel and perpendicular components of a singlet ($S'=0$, $M_s=0$) to triplet ($S'=1$, $M_s=1$) transitions. A representative spectrum is shown in Fig. 2a. We concur that the weak absorption at 1600 and 1590 G can be assigned to $\Delta M_s = \pm2$ transition for copper(II) dimer. The analysis of the ESR spectra of both complexes gave $g_{11} = 2.30$, 2.31, $g_{\perp} = 2.05$, 2.08 and $g_{av} = 2.21$, 2.23 in $\Delta M_s = \pm1$ for chloro and bromo complexes, respectively. In the $M_s = 2$, the g-value was found to be 4.30 and 4.38, respectively. The ESR spectra indicate axial type structure with $g_{11} > g_{\perp}$ in agreement with a $d_{x^2-y^2}$ ground state for a distorted square pyramidal configuration. Table VII lists the g values for these copper(II) complexes.

A 77 K CH_2Cl_2 glass spectra were obtained for our samples and a representative curve is shown in Fig. 2b. Six peaks can be seen in the CH_2Cl_2 glass spectra at the low field side of the perpendicular region, the separation between each peak is 74×10^{-4} and 76×10^{-4} cm^{-1} for $([LPKTS-H)CuCl]_2$ and $[(LPKTS-H)\ CuBr]_2$, respectively. The magnetic susceptibility and $M_s = 2$ ESR transitions indicate the presence of an intermolecular electron exchange in these complexes. It is important to note that this assignment gives $A_{11} = 74\times10^{-4}$ and 76×10^{-4} cm^{-1} for these two complexes, respectively, which are as expected for copper dimers with magnetic exchange [27].

From the low field parallel sequences and the use of Eq. (2), it was found that $D = 0.026$ and 0.025 cm^{-1} for both complexes;

$$W_0 = h\nu = g_{11}\beta H + 2D\,(M_s - 1/2) + (A/N)M_I \qquad (2)$$

where $h\nu$ is the quantum energy = 0.3063 cm^{-1}, $g_{11} = 2.30$ and 2.31 for the two complexes as obtained from the ESR spectra, N is the number of interacting ions (two in this case), A is the nuclear hyperfine splitting constant obtained from the splitting pattern in the low field parallel lines (74×10^{-4} and 76×10^{-4} cm^{-1}), M_s and M_I are the electronic and nuclear spins which have

values of 1,0 and +3, +2, +1, −1, −2 and −3, respectively. The exchange coupling constant, $D_{\text{exch.}}$, can be calculated using the expression (3),

$$D_{\text{exch.}} = -1/8\,(2J\,(g_{11} - 2)/4 - 2J(g - 2)^2) \tag{3}$$

It was found to have values of 0.024 and 0.0235 cm^{-1} for the two complexes, respectively. On using the expression (4) [3].

$$D = D_{dd} + D_{\text{exch.}} \tag{4}$$

the dipole–dipole exchange, D_{dd}, could be estimated and was found to be 0.002 and 0.000165 cm^{-1} for $[(LPKTS—H)CuCl]_2$ and $[(LPKTS—H)CuBr]_2$, respectively. Consequently, the D_{dd} values are very small compared to $D_{\text{exch.}}$, indicating that the direct copper–copper interaction can be neglected in these copper(II) dimers.

The X-ray structural study of these complexes is in progress.

REFERENCES

[1] Livingstone, S. E.: Quart. Rev., **19,** 386 (1965)
[2] Akbar, A., Livingstone, S. E.: Coord. Chem. Rev., **13,** 10 (1974)
[3] El-Dissouky, A., Refaat, L. S., Kenawey, I. M.: Gazz. Chim. Ital., **8,** 112 (1982)
[4] Mihich, E., Nichol, C. A.: Cancer Res., **25,** 1410 (1965)
[5] French, F. A., Blanz, E. J.: J. Med. Chem., **9,** 585 (1966)
[6] Ablov, N. A., Belichuk, N. I.: Russ. J. Chem., **14,** 93 (1969)
[7] Bovykin, B. A., Barba, N. A.: Russ. J. Chem., **16,** 90 (1971)
[8] Gerbleu, N. V., Bodyu, V. G.: Russ. J. Chem., **16,** 716 (1971)
[9] Beecroft, B., Campbell, M. J. M., Grzeskowiak : J. Inorg. Nucl. Chem., **36,** 55 (1974)
[10] Figgis, B. N., Lewis, J.: in Modern Coordination Chemistry, Ed., J. Lewis and Wilkins, p. 403, New York, Interscience 1967
[11] Mayer, R.: in Organosulfur Chemistry, Ed. M. Jansen, p. 219, Wiley-Interscience 1967
[12] Colthup, N. B., Daly, L. H., Wiberly, S. E.: in Introduction to Infrared and Raman Spectroscopy, p. 305, Academic Press, New York 1964
[13] Rao, C. N.: in Chemical Application of Infrared Spectroscopy, Academic Press, New York 1963
[14] El-Shazly, M. F., Salem, T. M., El-Dissouky, A., Hindawey, A. M.: Inorg. Chim. Acta, **25,** 55 (1977)
[15] Feltman, R. D., Hyter, R.: J. Chem. Soc., **1964,** 4587
[16] Barefield, F. K., Busch, D. H., Nelson, S. M.: Quart, Rev., **22,** 457 (1968)
[17] Chow Shui-Tse, Jhons, D. M., McAuliffe, C. A., Machin, D. J.: Inorg. Chim. Acta., **25,** 1 (1977)
[18] Mockler, G. M., Chaffey, G. W., Einn, E., Wong, H.: Inorg. Chem., **11,** 1308 (1972)
[19] Lane, R. H., Pantaleo, N. S., Fair, J. K., Coney, W. M., Newton, M. G.: J. Amer. Chem. Soc., **100,** 1610 (1978)
[20] Barbucci, R., Mastroinni, A., Campbell, M. J. M.: Inorg. Chem. Acta, **27,** 109 (1978)
[21] Miskowski, V. M., Tich, J. A., Solomon, R.,Schugar, H. J.: J. Amer. Chem. Soc., **98,** 8344 (1976)
[22] Canhan, W. R., Lever, A. B. P.: Can. J. Chem., **50,** 3866 (1972)
[23] Ferraro, J. R.: Low Frequency Vibrations of Inorganic and Coordination Compounds, p. 248, Plenum Press, New York 1965
[24] Kato, M., Jonassen, H. B., Fannings, J. C.: Chem. Rev., **64,** 99 (1964)
[25] Kokoszka, G. F., Duer, R. W.: Coord. Chem. Rev., **5,** 209 (1970)
[26] Tokii, T., Muto, Y., Kato, M., Imai, K., Jonassen, H. B.: J. Inorg. Nucl. Chem., **34,** 3377 (1972)
[27] Hasty, E. F., Wilson, L. J., Hendrickson, D. N.: Inorg. Chem., **17,** 183 (1978)

Acta Chimica Hungarica 114 (1), pp. 41—45 (1983)

HALIDES AND COMPLEX HALOGENO ANIONS AS SALTS OF BENZOYLACETONATO BIS-CYCLOPENTADIENYL ZIRCONIUM(IV) CHELATES

A. K. SHARMA and N. K. KAUSHIK*

(Department of Chemistry, University of Delhi, Delhi-110 007, India)

Received September 17, 1982
Accepted for publication November 10, 1982

A series of $[Cp_2Zr(bzac)]^+X^-$ compounds where $X^- = Br^-$, I^-, $CuCl_3^-$, $ZnCl_3(H_2O)^-$, $CdCl_4^{2-}$, $HgCl_3^-$, $SnCl_3^-$, $FeCl_4^-$ and Hbzac = benzoylacetone, have been synthesised. Conductivity measurements in nitrobenzene indicate that all these complexes are electrolytes. IR and ^{1}H-NMR studies carried out for these complexes indicate that ligand benzoylacetone is chelating in all these complexes and the zirconium atom is essentially tetrahedrally coordinated with two π-cyclopentadienyl groups and two oxygens of benzoylacetone ligand.

Introduction

In earlier communications [1, 2] we have reported the preparation of $[RR'TiL]^+X^-$ compounds where $R = R' = C_5H_5$; $R = C_5H_5$, $R' = C_9H_7$; $R = C_5H_5$, $R' = C_4H_4N$; HL = benzoylacetone or 8-hydroxyquinoline and X^- is a large number of uninegative anions. We observed that coordination of four oxygen atoms or two oxygen and two nitrogen atoms to $RR'Ti^{2+}$ moiety leads to a weakening of the metal-ring bond. Hence it is not possible to isolate bis-chelate complexes. However, the ionic complexes of the type $[RR'TiL]^+Cl^-$ are readily obtained in water by the reaction of $RR'TiCl_2$ with HL. The present communication describes the preparation of some ionic complexes of zirconium(IV) of the type $[Cp_2Zr(bzac)]^+X^-$. Conductance IR and ^{1}H NMR studies have been carried out for these complexes.

Materials and Methods

Reagents and general techniques

All the solvents and reagents used were of AnalaR grade. Conductance measurements were performed in nitrobenzene at 30 ± 0.05° with Systronic Digital Direct Reading Conductivity Meter Type 304. Infrared spectra were recorded in the solid state in KBr pellets in the 4000—200 cm^{-1} region with a Perkin Elmer-621 grating spectrophotometer. ^{1}H-NMR spectra

* To whom correspondence should be addressed.

were recorded in deuterated acetone at a sweep width of 900 Hz with a Perkin Elmer R-32 spectrophotometer. Chemical shifts are expressed relative to an internal reference of TMS (1% by volume).

Preparation of the complexes

To a concentrated aqueous solution of bis-cyclopentadienyl zirconium dichloride (1 g in 40 mL water) solid benzoylacetone (0.6 g) was added in excess and the mixture was stirred for 2 h. This solution was added dropwise under shaking to a concentrated hot aqueous solution containing an excess of KI, KBr, $CuCl_2$, $ZnCl_2$, $CdCl_2$, $HgCl_2$, $SnCl_2$ or $FeCl_3$, until no more precipitate was formed. The precipitate was digested on a water bath for 2 h, collected on a glass frit and washed several times with diethylether. Recrystallization from methanol gave the desired salt (65%).

Results and Discussion

The reaction of bis-cyclopentadienyl zirconium dichloride with benzoylacetone in aqueous solution is the following:

$$Cp_2ZrCl_2 + H_2O \longrightarrow Cp_2ZrOH^+ + Cl^- + HCl$$

$$Cp_2ZrOH^+ + Cl + Hbzac \xrightarrow{\text{water}} \underset{\text{(in solution)}}{[Cp_2Zr(bzac)]^+Cl^-} + H_2O$$

Adding other mononegative anions to the solution of $[Cp_2Zr(bzac)]^+Cl^-$ insoluble $[Cp_2Zr(bzac)]^+X^-$ compounds precipitated.

$$[Cp_2Zr(bzac)]^+Cl^- + X^- \rightarrow [Cp_2Zr(bzac)]^+X^- + Cl^-$$

where

$$X^- = I^-,\ Br^-\ CuCl_3^-,\ ZnCl_3^-(H_2O)^-,\ CdCl_4^{2-},\ HgCl_3^-,\ SnCl_3^-\ \text{or}\ FeCl_4^-.$$

Efforts were made to prepare analogous chelates using CNS^-, F^- and azide ions but compounds of the type Cp_2ZrX_2 precipitated, where $X = CNS^-$, F^- and N_3^-.

Even when employing a high concentration of chelating agent bis-chelate could not be isolated, because the free ligand concentration in the solution remained low due to the decomposition of Cp_2Zr^{2+} moiety with breaking of $Zr—C_5H_5$ moiety above pH 2.8.

Table I lists the analytical data and physical characteristics of the complexes. The complexes are thermally stable and decompose at higher temperatures without melting. They are moderately soluble in acetone, methanol, THF, nitrobenzene and partially soluble in halogenated hydrocarbons. With zinc chloride an aquotrichlorozincate(II) anion, $[Cp_2Zr(bzac)]^+ZnCl_3(H_2O^-)$ is precipitated. Conductivity measurements show that all the complexes except the Cd(II) derivatives are 1 : 1 electrolytes in nitrobenzene. However,

Table I

Analytical and physical data

Comopund	Colour	Dec. temp.[a] (°C)	Conductance[b] $M \times 10^3 = 0.5$	Found (Calc.)%		
				C	H	Halogen
$[Cp_2Zr(bzac)]^+Br^-$	Pale yellow	208	28.6	51.82 (51.95)	4.20 (4.11)	17.28 (17.32)
$[Cp_2Zr(bzac)]^+I^-$	Yellow	228	30.0	47.22 (47.15)	3.82 (3.73)	24.90 (24.95)
$[Cp_2Zr(bzac)]^+CuCl_3^-$	Light yellow	188	28.8	43.54 (43.48)	3.50 (3.44)	19.32 (19.29)
$[Cp_2Zr(bzac)]^+ZnCl_3(H_2O)^-$	Greenish white	194—196	30.4	42.02 (42.97)	3.70 (3.67)	(18.58) (18.62)
$[Cp_2Zr(bzac)_2^+CdCl_4^{2-}$	Light brown	204	59.6	47.22 (47.13)	3.78 (3.73)	13.88 (13.94)
$[Cp_2Zr(bzac)]^+HgCl_3^-$	Greenish brown	188—190	30.4	34.80 (34.83)	2.82 (2.76)	15.49 (15.45)
$[Cp_2Zr(bzac)]^+SnCl_3^-$	Green	158—160	30.0	39.72 (39.53)	3.18 (3.13)	17.59 (17.54)
$[Cp_2Zr(bzac)]^+FeCl_4^-$	Brown	168—170	29.2	41.51 (41.39)	3.32 (3.28)	24.54 (24.49)

[a] Uncorrected values, [b] in ohm^{-1} cm^2 mole^{-1}

in case of Cd(II) derivatives the results are consistent with those of 1 : 2 electrolytes, indicating that the binegative anion is precipitated.

The assignment of IR bands have been done on the basis of published work. The bands occurring around 1570 cm^{-1}, 1530 cm^{-1} and 470 cm^{-1} in $[Cp_2Zr(bzac)]^+X^-$ complexes may be assigned to ν(C⋯O), ν(C⋯C) and ν(Zr—O) vibrations [3]. The bands occurring consistently around 3080 cm^{-1} (C—H stretching band), 1430 cm^{-1} (asymmetric ring breathing), 1030 cm^{-1} (C—H deformation of C_5H_5 ring) and 815 cm^{-1} (C—H bending out of plane deformation) in all the chelates suggest the presence of π-bonded cyclopentadienyl ring [4]. An additional band near 440 cm^{-1} may be assigned to Zr—C_5H_5 vibration [5]. In case of $[Cp_2Zr(bzac)]^+ZnCl_3(H_2O)^-$, the presence of coordinated water is identified by its intense infrared absorption at 3450 cm^{-1}. The metal chlorine stretching frequencies (Table II) in the infrared spectra of the complex halogeno chelates are in accord with the presence of complex chloro anions [2, 6—9].

Since the complexes are electrolytes, a solvent of relatively high dielectric constant such as $(CD_3)_2CO$ was used as a solvent for taking ^1H NMR spectra. All compounds gave four resonance signals (i) the C_5H_5 ring protons signal at δ6.60 ppm, (ii) the methyl group protons of benzoylacetone group at δ 2.48 ppm, (iii) the phenyl group of benzoylacetonate group at δ 7.1—8.2 ppm and (iv) the signal due to γ-proton (—CH=) of benzoylacetonate group at δ 6.1 ppm.

The signal integrals obtained as a result of these four resonances were in the 10 : 3 : 5 : 1 ratio, respectively. In the spectra of $[Cp_2Zr(bzac)]^+ZnCl_3(H_2O)^-$ an additional signal is present at δ 6.40 ppm corresponding to the coordinated water and integral ratio of signals in this case is 10 : 3 : 5 : 1 : 2. Table II lists the ^1H NMR data obtained for the complexes.

The resonance signals due to CH_3, C_6H_5 groups and γ-proton of the benzoyl acetonate moiety in the chelates occur at lower fields than expected for benzoylacetonato chelates. This is probably due to at least in part to the net positive charge on the complex ion [3].

Both the IR and ^1H NMR spectral studies carried out for the present complexes indicate that the ligand benzoylacetone is chelating and the Cp_2Zr^{2+} moiety possesses a wedge like sandwich structure with essentially tetrahedral coordination around the metal atom similar to that of dichlorides [10]. Typical vibrational frequencies assigned to the X^- ion in the benzoylacetonato chelates fully supports the view that the X^- is a free anion. Therefore the general formula

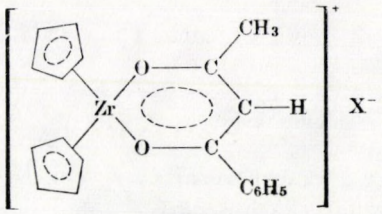

may be assigned to these complexes where X = I^-, Br^-, $CuCl_3^-$, $ZnCl_3(H_2O)^-$, $CdCl_4^{2-}$, $HgCl_3^-$, $SnCl_3^-$ or $FeCl_4^-$.

Table II

Spectral data of the complexes

Compound	IR (cm^{-1})[1] (M'-Cl)	^1H NMR (δ ppm)[2]				
		C_5H_5	CH_3 in benzoyl-acetone	C_6H_5 in benzoylacetone	νH(—CH=) in benzoyl-acetone	H_2O of coordi-nation
$[Cp_2Zr(bzac)]^+ Br^-$		6.62s	2.48s	7.10 – 8.20m	6.12s	
$[Cp_2Zr(bzac)]^+ I^-$		6.62s	2.46s	7.10 – 8.10m	6.10s	
$[Cp_2Zr)bzc)]^+ CuCl_3^-$	292m, 318s	6.60s	2.50s	7.10 – 8.00m	6.08s	
$[Cp_2Zr(bzac)]^+ ZnCl_3(H_2O)$	296s, 315s	6.64s	2.46s	7.18 – 8.08m	6.06s	6.40s
$[Cp_2Zr(bzac)]_2^+ CdCl_4^{2-}$	305m, 320s	6.60s	2.56s	7.22 – 8.10m	6.08s	
$[Cp_2Zr(bzac]^+ HgCl_3^-$	286m	6.64s	2.45s	7.20 – 8.10m	6.10s	
$[Cp_2Zr(bzac)]^+ SnCl_3^-$	250s, 300s	6.62s	2.50s	7.12 – 8.12m	6.10s	
$[Cp_2Zr(bzac)]^+ FeCl_4^-$	320w, 370s	6.66s	2.48s	7.16 – 8.12m	6.16s	

[1] s = strong, m = medium, w = weak; [2] s = singlet, m = multiplet

The possibility of benzoylacetonato ligand bonding with simple hard sphere coulombic interaction to the Cp_2Zr^{2+} moiety is ruled out because in such case a bis-benzoylacetonato complex in contrast to present observations, with four oxygen atoms in the *xy* plane and parallel cyclopentadienyl rings could be isolated. Such a structure would maximize the coordination number for the metal atom and simultaneously maximize the total metal-cyclopentadienyl ring overlap. Since the π-cloud of C_5H_5 ring are used in the formation of Zr—C_5H_5 ring bonds and would exert less steric effect on *equatorial* ligands this configuration cannot be described, as unstable on the steric grounds. Further according to Ballahausen and Dahl's theory [11], the coordination of four oxygen atoms in the *xy* plane by strong covalent bonds would result in the weakening of Zr—C_5H_5 bonds and would be energetically unfavourable. As the Zr—O bond has appreciable covalent character only one benzoylacetone ligand can interact.

*

One of the authors (AKS) is grateful to CSIR, New Delhi, for the award of a Senior Research Fellowship.

REFERENCES

[1] Sodhi, G. S., Sharma, A. K., Kaushik, N. K.: J. Organometal. Chem., **238,** 177 (1982)
[2] Sharma, A. K., Kaushik, N. K.: Indian J. Chem. Sec. A (in Press); Bull. Soc. Chim. France **1983,** 1—52; Monatschefte für chemie (in Press)
[3] Fackler, J. P. Jr.: Prog. Inorg. Chem., **7,** 631 (1966)
[4] Fritz, H. P.: Advance in Organometallic Chemistry, Academic Press, New York, **1,** 279 1964
[5] Coutts, R. S. P., Wailes, P. C.: J. Organometal. Chem., **84,** 47 (1975)
[6] Woodward, L. A., Tayler, M. J.: J. Chem. Soc., **1962,** 407
[7] Woodward, L. A., Tayler, M. J.: J. Chem. Soc., **1960,** 4473
[8] Morris, D. F. C., Short, E. L., Waters, D. N.: J. Inorg. Nucl. Chem., **25,** 975 (1963)
[9] Jang, G. J., James, D. W.: J. Chem. Phys., **38,** 905 (1963)
[10] Alekseev, N. V., Ronova, I. A.: Zh. Strukt. Khim., **7,** 103 (1966)
[11] Ballhausen, C. J., Dehl, J. P.: Acta Chem. Scand., **15,** 1333 (1961)

Acta Chimica Hungarica 114 (1), pp. 47—56 (1983)

FLAVONOIDS, XXXVII[+]

RING CONTRACTION AND RING ENLARGEMENT REACTIONS WITH TRIMETHYLSILYL AZIDE IN THE FIELD OF FLAVONOIDS[++*]

GY. LITKEI[**] and T. PATONAY

(Institute of Organic Chemistry, Kossuth Lajos University, H-4010 Debrecen, P.O. Box 20)

Received August 30, 1982
Accepted for publication November 10, 1982

The reaction of flavanone with trimethylsilyl azide (TMSA) in trifluoroacetic acid (TFA) afforded by ring expansion, 2,3-dihydro-2-phenyl-1,4-benzoxazepin-5(4*H*)-one or 2,3-dihydro-2-phenyl-4*H*-tetrazolo[1,5*d*]-1,4-benzoxazepine. The same products could be isolated using sodium azide in TFA. An unknown intermediate of the Schmidt reaction was also isolated.

Treatment of 2'-hydroxychalcone with TMSA or sodium azide in TFA resulted in isoflavone and *trans*-3-aminoflavanone.

The reaction of 4-substituted 2'-hydroxychalcones with TMSA in dimethylformamide gave, with ring contraction, aurones and flavones.

Recently a great number of silicon compounds have been successfully utilized in achieving a number of chemical transformations in high yields and under mild conditions [1, 2]. It is known that carbonyl compounds give enol ethers with trimethylsilyl derivatives in basic medium [3], whereas addition on the carbonyl group occurs in the presence of Lewis acids [4, 5].

To our knowledge such reactions of flavonoid compounds have not been studied in detail. In this paper we report the reaction of trimethylsilyl azide (TMSA) and sodium azide with flavanone and 2'-hydroxychalcone.

Reaction of flavanone with trimethylsilyl azide

When flavanone (**1**) was treated with trimethylsilyl chloride in boiling *abs.* acetonitrile no reaction was observed and the starting material was recovered even when the reaction was continued for 24 hours and catalyzed by

[+] Part XXVI: T. Patonay, Gy. Litkei, R. Bognár: Acta Chim. Acad. Sci. Hung., **108**, 135 (1981).

[++] A part of this work was presented at the International Bioflavonoid Symposium, Munich, 6 - 9 September, 1981: "Flavonoids and Bioflavonoids — 1981. Proceedings of the International Bioflavonoid Symposium" (Ed. L. Farkas, M. Gábor, F. Kállay and H. Wagner), p. 11. Akadémiai Kiadó, Budapest and Elsevier, Amsterdam 1982.

* Dedicated to Prof. R. Bognár on the occassion of his 70th birthday.

** To whom correspondence should be addressed.

either potassium cyanide, sodium azide, KCN. 18-crown-6- or by NaN_3. 18--crown-6 ethers [5].

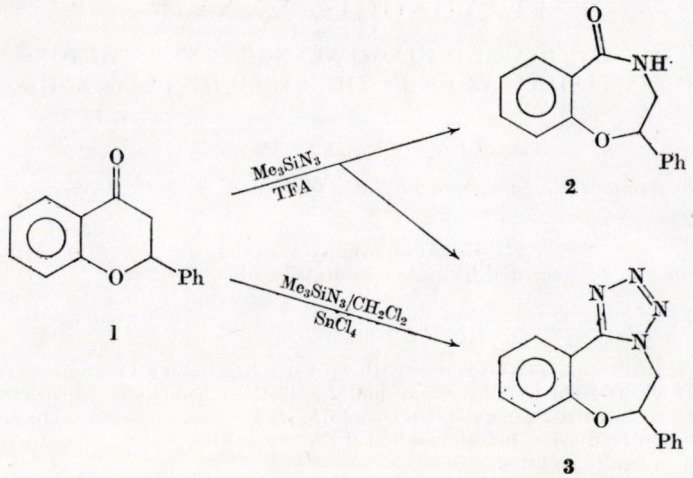

Fig. 1

However, the reaction of flavanone (**1**) with trimethylsilyl azide (TMSA) in the presence of trifluoroacetic acid (TFA) resulted in ring enlargement to

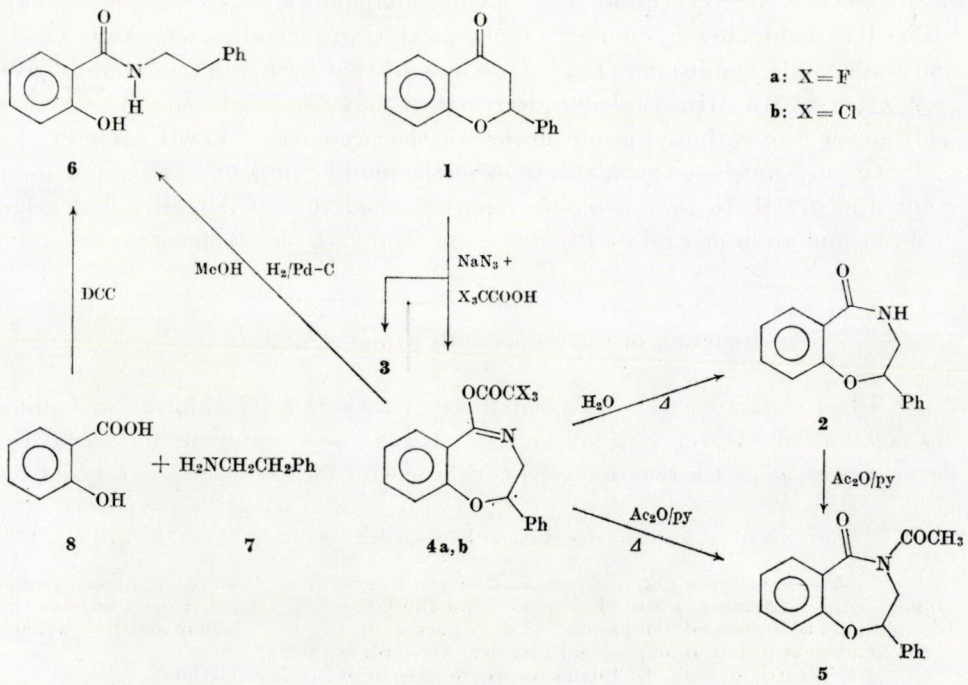

Fig. 2

afford 60% of 2,3-dihydro-2-phenyl-1,4-benzoxazepin-5(4*H*)-one (**2**) and 20% of the tetrazole analogue (**3**) of **2**. When this reaction performed in dichloromethane and in the presence of stannic chloride, the tetrazole **3** was isolated as the sole product (Fig. 1).

According to Krapcho and Turk [6] and Misiti and Rimatori [7] the Schmidt reaction of flavanone (with sodium azide in acetic acid in the presence of concentrated sulfuric acid) led to the oxazepinone (**2**) and cca. 5% of the tetrazole (**3**). When the same reaction was carried out in either trifluoroacetic acid or trichloroacetic acid, cca. 5% of the tetrazole **3** was formed, and as the main product the intermediate of the Schmidt reaction, i.e. the iminoester **4a** and **4b**, could be isolated in 90% yield. The structures **4a** and **4b** are based on elemental analysis*, IR and MS data, and chemical transformations (Fig. 2).

The assignment of the structure of **4a, b** by ^{1}H-NMR measurements was unsuccessful since the compounds transformed into the oxazepinone (**2**) in DMSO-d_6 or in pyridine-d_5. The decomposition of **4b** was monitored with ^{13}C-NMR and the formation of $CHCl_3$ was detected. The characteristic mass spectral peaks of **4b** were *m/e* 266 $(M—CCl_3)^+$, *m/e* 238 $(M—CCl_3—CO)^+$ and *m/e* 222 $(M—CCl_3—CO_2)^+$ (Fig. 3).

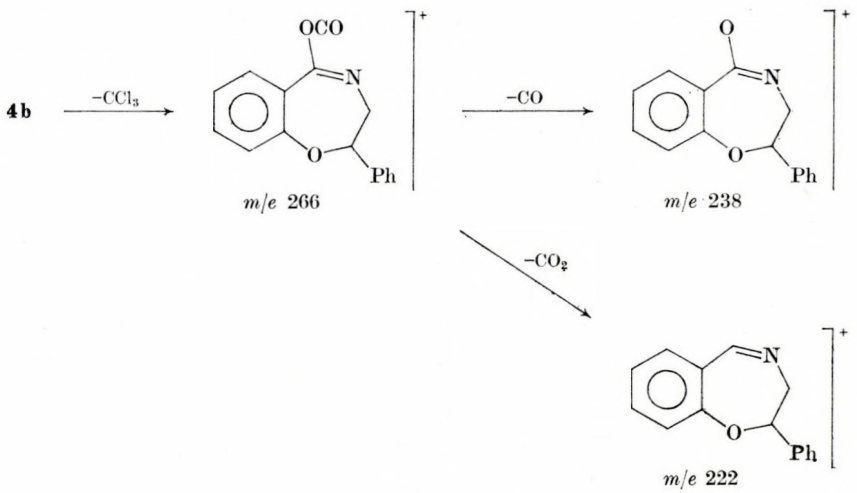

Fig. 3

Recrystallization of **4a, b** from water or alcohol/water mixture resulted in decomposition into the oxazepine (**2**), again, but **4a** was found to be stable in heating in a nonpolar solvent (xylene). Upon treatment with acetic anhydride

* No unambiguous analytical data could be obtained for **4a** because of the presence of the CF_3 group which yields CHF_3 on decomposition interfering with the C, H, N measurements [9].

in pyridine **4a, b** gave the *N*-acetate **5** and this latter compound was obtained also from the oxazepinone (**2**) by acetylation. On hydrogenation in the presence of Pd/C **4a** consumed one molecular equivalent of hydrogen and the salicylamide (**6**) was isolated. The structure of this latter was substantiated by a definitive synthesis; the reaction of **7** with **8** in the presence of DCC resulted in compound **6**.

When flavanone (**1**) was treated with sodium azide in an acetic anhydride–acetic acid mixture, no reaction was observed.

The isolation of the intermediates **4a** and **4b** in the above reactions gives further support to the supposed mechanism of the Schmidt reaction [8].

Reaction of 2'-hydroxychalcone (9) with $(CH_3)_3SiN_3$

The reaction of 2'-hydroxychalcone (**9**) with TMSA in the presence of TFA resulted in two products which were assigned, after separation, as the trifluoroacetic acid salt of *trans*-3-aminoflavanone (**10**) and isoflavone (**11**) (Fig. 4).

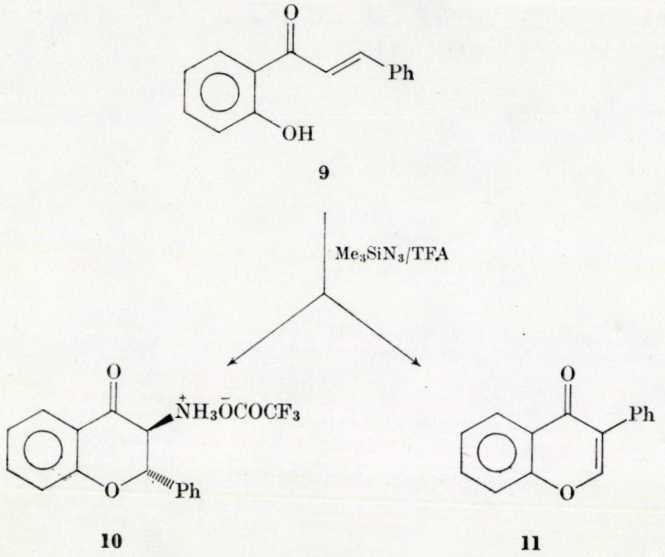

Fig. 4

The formation of flavanone (**1**) during this reaction can be excluded, since if it had been formed it would have been transformed into the oxazepin-5(4*H*)-one (**2**). Misiti and co-workers [10] isolated also **10** and **11** among other products when the reaction was performed with sodium azide either in TFA or in a mixture of sulfuric and acetic acids [11]. We propose that no silylation occurred, and **10** and **11** were presumably produced by 1,2- or 1,4-addition of HN_3 followed by rearrangement via the aziridines **12** and **13** in

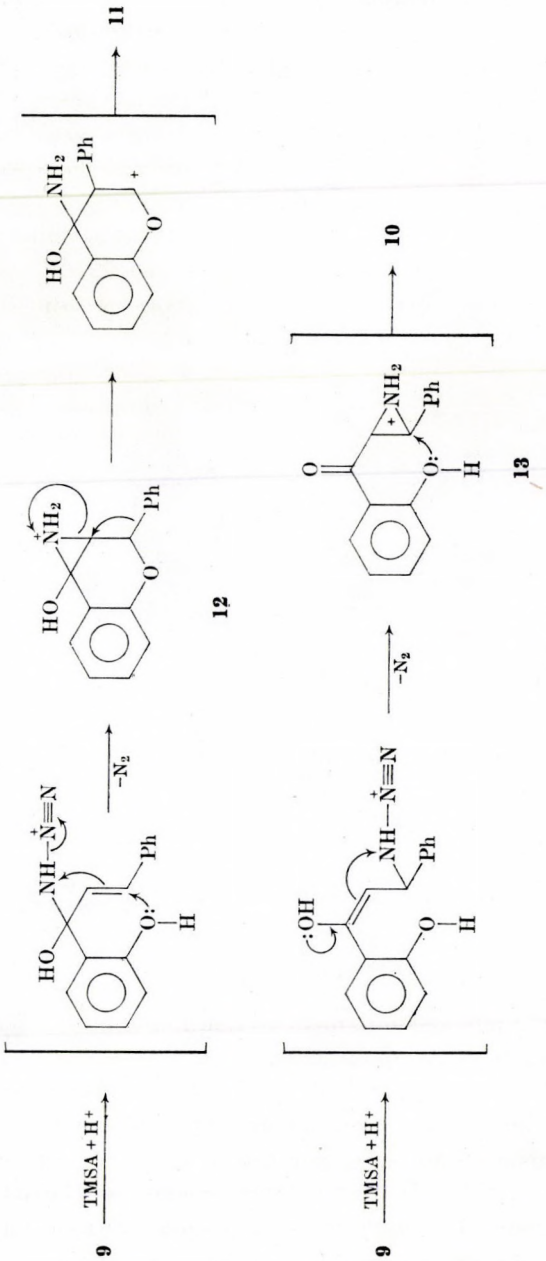

Fig. 5

both cases, in agreement with the results of Misiti et al. [10] (Fig. 5). We have shown earlier [12] that *trans*-3-aminoflavanone is formed from *trans*-aziridines (**13**) by acid-catalyzed cyclization.

The 3,4-addition of HN_3 on α,β-unsaturated ketones to give β-azides is well-known [13, 14]. In the case of chalcone, however, such a reaction is improbable, otherwise either aurone or 3-hydroxyflavanone would have been formed by the decomposition of the β-azide or via an intermediary 1,2-diketone [14], respectively. In fact, we found that no reaction occurs with sodium azide in acetic acid even after a longer reaction time, demonstrating that HN_3 addition and the rearrangement proceed only in the presence of strong acids.

When the 4-substituted 2'-hydroxychalcones (**9a—f**) were reacted with TMSA in *N*,*N*-dimethylformamide, *Z*-aurones (**14a—f**) and flavones (**15a—f**)

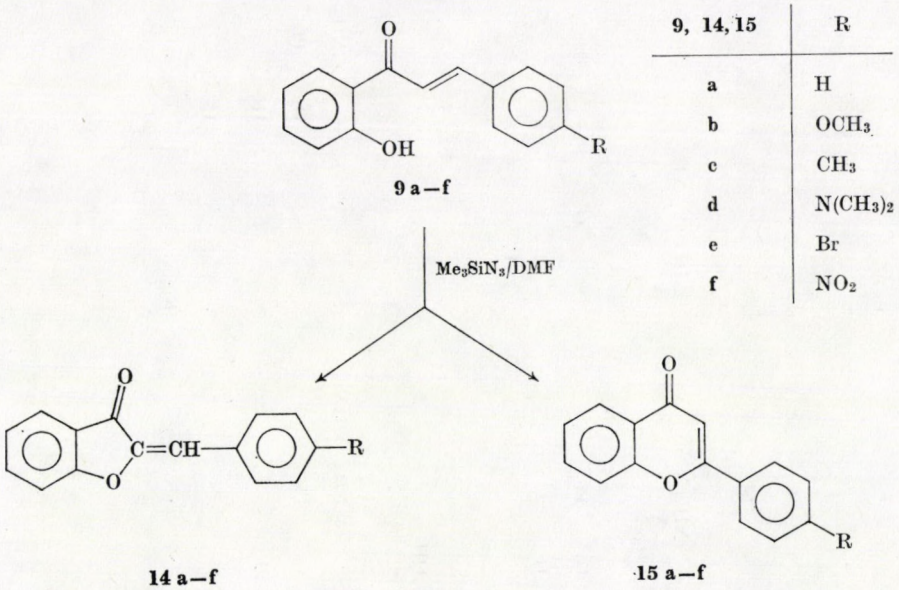

Fig. 6

were the major products accompained by small amounts of flavanones (**1a—f**) and other, unidentified, compounds (Fig. 6).

The product ratio is controlled by the Hammett-σ value of the R substituent (Table I) and no reaction occurs in the absence of TMSA.

The mechanism of aurone formation may involve an initial enol ether **16**, as suggested by Miller and McKean [15], which, on the attack of phenolate anion at the α-carbon gives α-azido-2-benzyl-coumaran-3-one (**17**). This latter compound may easily transform [16] into aurone **14** (Fig. 7). The explanation of the mechanism of the formation of flavones (**15a—f**) during the reactions requires further work.

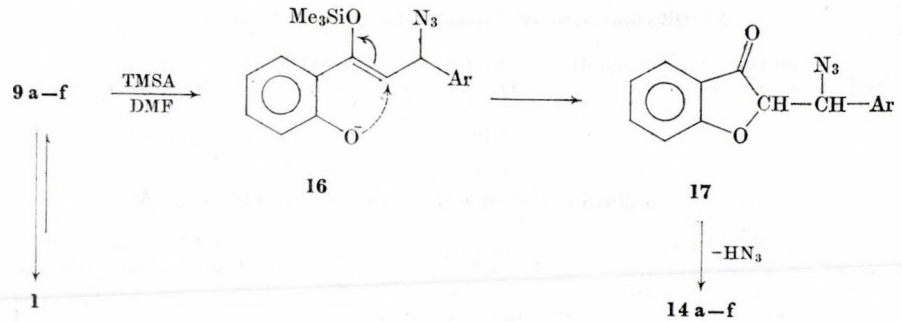

Fig. 7

Experimental

M.p.' were determined on a Kofler hot-stage and are uncorrected. IR spectra were recorded with Unicam SP-200 G and Perkin-Elmer 283 instruments: NMR spectra were obtained with a Jeol MH-100 instrument (tetramethylsilane internal standard). Mass spectra were obtained with a VG-7035 GC-MS instrument.

Reaction of flavanone (1) with trimethylsilyl azide

(*a*) To a stirred solution of flavanone (**1**) (1 mmol) in trifluoroacetic acid (10 mL), trimethylsilyl azide (1.5 mmol) was added at room temperature under nitrogen atmosphere. After three days the reaction was complete; the solution was evaporated and the products were separated by column chromatography with 4 : 1 ethyl acetate–*n*-hexane as the eluent to give first **2,3-dihydro-2-phenyl-4*H*-tetrazolo[1,5-*d*]-1,4-benzoxazepine (3)**, (0.55 g; 19.65%), m.p. 136–137 °C, *lit.* [7] m.p. 137–138 °C, and **2,3-dihydro-2-phenyl-1,4-benzoxazepin-5(4*H*)-one (2)** (1.45 g; 60.6%), m.p. 126–128 °C, *lit.* [7] m.p. 125–126 °C, both identified by comparison with authentic samples.

(*b*) To a stirred solution of flavanone (**1**) (1 mmol) and $SnCl_4$ (1.1 mmol) in dry dichloromethane (50 mL), trimethylsilyl azide (2.2 mmol) was added in small portions at room temperature under nitrogen atmosphere. After 5 days only traces of **1** and **9** could be detected by TLC. The precipitated product was filtered off, washed with water and crystallized from ethanol to give **3**. The yield after processing the mother liquor was 1.60 g (67%); m.p. 137–138 °C.

Reaction of flavanone (1) with sodium azide

(*a*) To a solution of flavanone (**1**) (1 mmol) in trifluoroacetic acid (10 mL) sodium azide (1.3 mmol) was added in small portions at room temperature under nitrogen atmosphere. After 2 days ether (150 mL) was added and the separated product was filtered off to obtain 3.1 g of **2,3-dihydro-2-phenyl-5-trifluoroacetoxy-1,4-benzoxazepine (4a)** (95%), m.p 190–192 °C (abs. EtOH–hexane).

IR (KBr): 1670, 1639 ($\nu_{C=O} + \nu_{C=N}$), 1262 ($\nu_{as}C-O-C$), 1131 (ν_{C-F})cm^{-1}.

$C_{17}H_{12}O_3F_3N$ (335.28). Calcd. C 60.89; H 3.57; F 16.99; N 4.17. Found C 60.11; H 3.59; F 16.36; N 8.18 (Dumas), 3.95% (Kjeldahl).

The filtrate was washed with sodium carbonate solution, dried (Na_2SO_4) and concentrated. The oily residue was chromatographed on a silica gel column with 1 : 4 ethyl acetate–*n*-hexane as the eluent to obtain **3** in 5% yield, m.p. 135–137 °C.

(*b*) A mixture of flavanone (**1**) (1 mmol), trichloroacetic acid (10 g) and sodium azide (1.3 mmol) was heated at 50 °C for 3 days. After the addition of ether (150 mL) the precipitated **2,3-dihydro-2-phenyl-5-trichloroacetoxy-1,4-benzoxazepine (4b)** (3.5 g; 90%) was filtered off, m.p. 177–178 °C.

IR (KBr): 1677, 1648 ($\nu_{C=O} + \nu_{C=N}$); 1220 ($\nu_{as}C-O-C$), 832 (ν_{C-Cl}) cm^{-1}.

Mass spectrum *m/e* (*I*%): 266 (17.5) $M-CCl_3^+$; 238 (14.9); 224 (55.9); 223 (40.7); 222 (20.1); 207 (5.6); 194 (7.5); 163 (5.4); 147 (39.4); 121 (63.8); 120 (100); 118 (33.6); 85 (10.0); 83 (16.1).

2,3-Dihydro-2-phenyl-1,4-benzoxazepin-5(4*H*)-one (2)

(*a*) A mixture of **4a** (1 mmol) and water (25 mL) was refluxed for 0.5 h and then allowed to stand at room temperature for 16 h. The separated product **2** was filtered off (yield 90%), m.p. 125—126 °C.

(*b*) Similar treatment of **4b** as described above gave 85% of **2**, m.p. 124—126 °C.

N-Acetyl-2,3-dihydro-2-phenyl-1,4-benzoxazepin-5(4*H*)-one (5)

(*a*) A mixture of **4a** (1.5 mmol), acetic anhydride (15 mL) and abs. pyridine (1.5 mL) was heated on a steam bath for 2 h. The mixture was then poured onto ice and the product was crystallized from ethanol; yield: 80%, m.p. 92—94 °C.

(*b*) A similar treatment of **2** (1 mmol) gave **5** in 80% yield, m.p. 93—94 °C.

IR (KBr): 1699, 1688 ($\nu_{C=O}$); 1257, 1274 sh (amide III); 1224, 1215 ($\nu_{as}C-O-C$); 1033 ($\nu_{s}C-O-C$).

^{1}H-NMR ($CDCl_3$): δ 6.9—8.0 (m, 9H, Ar—*H*); 5.47 (AMX, 1H, *H*-2); 4.58 (AMX, 1H, *H*-3*a*); 3.95 (AMX, 1H, *H*-3*e*); 2.57 (s, 3H, Me); (J_{AM} = 4 Hz, J_{AX} = 8 Hz, J_{MX} = 16 Hz).

$C_{17}H_{15}O_3N$ (281.3). Calcd. N 4.97. Found N 4.90%.

2-Hydroxy-*N*-(2-phenylethyl)benzamide (6)

(*a*) A mixture of **4a** (3 mmol), *abs.* methanol (30 mL) and 0.2 g 10% Pd/C was hydrogenated until the consumption of 1 molar equivalent of hydrogen. The catalyst was then filtered off, the filtrate evaporated to dryness and the residue was crystallized from aqueous ethanol, yield 45%, m.p. 95—96 °C.

(*b*) A mixture of *β*-phenylethylamine (**7**) (1.2 g; 10 mmol), salicylic acid (**8**) (1.4 g; 10 mmol) and DCC (2.1 g;10 mmol) in abs. THF was allowed to stand at room temperature for 6 h and then in a refrigerator for further 24 h. The precipitated dicyclohexylurea was filtered off, the filtrate was evaporated and the residue crystallized from aqueous ethanol; yield 64%, m.p. 92—94 °C.

IR (KBr): 3370 (ν_{NH}); 1637 (Amide-I); 1545 (Amide-II); 1227 ($\nu_{C-O(H)}$).

^{1}H-NMR ($CDCl_3$): δ 12.45 (s, 1H, O*H*); 6.75—7.50 (m, 9H, Ar—*H*); 6.4 (broad s, 1H, N*H*); 3.75 (m, 2H, NH—C*H*); 2.95 (t, 2H, CH_2—Ph).

$C_{15}H_{15}O_2N$ (241.3). Calcd. N 5.80. Found 5.55%.

Reaction of 2'-hydroxychalcone (9) with TMSA in TFA

A mixture of 2'-hydroxychalcone **9** (2.14 g; 10 mmol), trifluoroacetic acid (10 mL) and trimethylsilyl azide (2 mL) was kept at room temperature for 56 h. The addition of ether (50 mL) to the reaction mixture resulted in the separation of ***trans*-3-aminoflavanone trifluoroacetate (10)**, yield 40%, m.p. 194—195 °C, *lit.* [10] m.p. 177—179 °C.

IR (KBr): 3300—2300 (max: 2907, 2647, 2470; $\nu_{NH_3^+}$); 1709 ($\nu_{C=O}$); 1650 ($\nu_{as}COO^-$), 1300 ($\nu_{Ar-C(=O)}$); 1016 ($\nu_{s}C-O-C$); 995 (*trans*-dihydropyranone skeleton).

^{1}H-NMR (pyridine-d_5): 9.48 (s, 3H, NH_3); 6.9—8.10 (m, 9H, Ar—*H*); 5.94 (d, 1H, *H*-2); 4.98 (d, 1H, *H*-3); ($J_{2,3}$ = 12 Hz).

$C_{17}H_{14}F_3O_4$ (353.28). Calcd. C 57.80; H 3.96; N 3.96. Found C 57.75; H 3.86; N 3.89%.

The residue obtained from the etheral solution on evaporation was chromatographed on a Kieselgel Woelm (Activity I) column with 1 : 4 ethyl acetate–petroleum ether as the eluent to obtain 0.6 g (30%) of isoflavone **11** m.p. 132—133 °C, *lit.* [17] m.p. 131 °C.

Reactions of 2'-hydroxychalcones (9a—f) with TMSA in DMF

A mixture of the 2'-hydroxychalcone (**9a—f**) (5 mmol), *abs.* DMF (10 mL) and trimethylsilyl azide (1 mL) was heated at 150—160 °C for 24 h. The cold reaction mixture was diluted with hexane (50 mL) and then washed with 5% aqueous sodium hydrogen carbonate and dried. After evaporation the residue was chromatographed on a Kieselgel 40 column.

The physical data of the products are indicated in Table I.

*

Table I

Products of the reaction of 2'-hydroxychalcones (9a – f) with TMSA in DMF

	R	Aurones (14)			Flavones (15)			Flavanones (1)			Unchanged 9 (%)
		Yield (%)	M.p. (°C)	*Lit.* m.p. (°C)	Yield (%)	M.p. (°C)	*Lit.* m.p. (°C)	Yield	M.p. (°C)	*Lit.* m.p. (°C)	
a	H	45.9	107 – 109	108 [18]	5.7	94 – 95	97 [19]	1.8	72 – 73	76 [20]	1.8
b	MeO	40.4	137 – 138	138 139 [21]	3.2	154 – 157	157 – 158 [22]	3.5	90 – 92	91 – 92 [23] 97 [24]	4.3
c	Me	39.2	98.5 – 100	—	5.8	111 – 112	113 [25] 116 [26]	+			3.1
d	NMe_2	18.9	173 – 174	171 [27]	2.3	160 – 163	—	6.7	116 – 119	116 – 117 [28]	35.6
e	Br	32.7	172	—	10.9	180	176 [29]	0.0	—	—	0.0
f	NO_2	2.8	206 – 208	207 – 208 [30]	42.7	241 – 243	244 – 246 [30]	0.0	—	—	0.0

14c Anal. $C_{16}H_{12}O_2$ (236.27). Calcd. C 81.33; H 5.12. Found C 81.19; H 5.23%
IR (CCl_4): 1713 ($\nu_{C=O}$), 1655 ($\nu_{C=C}$); 1299 (νAr – C(=O)), 884 dihydrofuranone skeleton)

14e Anal. $C_{15}H_9BrO_2$ (301.35) Calcd. Br 26.52; Found Br 26.39%
IR (CCl_4): 1717 ($\nu_{C=O}$); 1660 ($\nu_{C=C}$); 1298 (νAr – C(=O)), 885 (dihydrofuranone skeleton)

15d Anal. $C_{17}H_{15}NO_2$ (265.31) Calcd. N 5.28; Found N 5.10%
IR (KBr): 2825 (ν_{NMe}), 1631 ($\nu_{C=O} + \nu_{C=C}$), 1370 (flavone skeleton)

+ Not isolated

The authors thank G. Janzsó (Research Institute for Organic Chemical Industry, Budapest) and L. Szilágyi for the ^{13}C-NMR spectra and Z. Dinya for the IR and mass spectroscopic investigations.

REFERENCES

[1] Fleming, I.: Chimia, **34,** 265 (1980)
[2] Croutas, W. C., Felker, D.: Synthesis, **1980,** 861
[3] Rasmussen, J. K., Heilman, S. M.: Synthesis, **1978,** 219 and references cited therein
[4] Birkofer, L., Muller, F., Kaiser, W.: Tetrahedron Lett., **1967,** 2781
[5] Evans, D. A., Truesdale, L. K.: Tetrahedron Lett., **1973,** 4923
[6] Krapcho, J., Turk, C. F.: J. Med. Chem., **9,** 191 (1966)
[7] Misiti, D., Rimatori, V.: Tetrahedron Lett., **1970,** 947; Ann. Ist. Super. Sanita, **9,** 150 (1973)
[8] Fikes, L. E., Shechter, H.: J. Org. Chem., **44,** 741 (1979)
[9] Hegedűs J.: Microchim. Acta, **1977,** 441; Magy. Kém. Foly., **84,** 90 (1978)
[10] Cacchi, S., Palmieri, G., Misiti, D.: J. Chem. Soc., **1976,** 2371
[11] Misiti, D.: Ann. Ist. Super. Sanita, **9,** 174 (1973); Chem. Abstr. **81,** 63599 (1974)
[12] Litkei Gy., Mester, T., Patonay, T., Bognár, R.: Acta Chim. Acad. Sci. Hung., **101,** 53 (1979)
[13] Boyer, J. H.: J. Am. Chem. Soc., **73,** 5248 (1951)
[14] Davis, A. J., Donald, A. S. R., Mark, R. E.: J. Chem. Soc. (C), **1967,** 2109
[15] Miller, R. D., McKean, D. R.: Tetrahedron Lett., **1979,** 2305
[16] Wong, E.: Chem. Ind. (London), **1966,** 598
[17] Baker, W., Chadderton, J., Harborne, J., Ollis, W. D.: J. Chem. Soc., **1953,** 1852
[18] Friedlander, P., Neudorfer, J.: Ber. Dtsch. Chem. Ges., **30,** 1082 (1897)
[19] Feurstein, W., Kostanecki, S.: Ber. Dtsch. Chem. Ges., **31,** 1760 (1898)
[20] Löwenbein, A.: Ber., **57,** 1515 (1924)
[21] Gowan, J. E., Hayden, P. M., Wheeler, T. S.: J. Chem. Soc., **1955,** 862
[22] Auwers, K., Anschutz, L.: Ber., **54,** 1543 (1921)
[23] Hattori, S.: Acta Phytochim., **2,** 99 (1925)
[24] Edelstein, A. Kostanecki, S.: Ber. Dtsch. Chem. Ges., **38,** 1507 (1905)
[25] Meyer-Dayan, M., Bodo, B., Deschamps-Vallet, C., Molho, D.: Tetrahedron Lett., **1978,** 3359
[26] Cramer, F., Elschnig, G. H.: Chem. Ber., **89,** 1 (1956)
[27] Nagy, E.: Thesis, Debrecen 1980
[28] Fujise, S., Ohtoho, Y.: Nippon Kagaku Zasshi, **74,** 899 (1953); Chem. Abstr., **49,** 3952 (1955)
[29] Chen, F. C., Yang, C. H.: Taiwan Pharm. Assoc., **3,** 39 (1951); Chem. Abstr., **49,** 2432 (1955)
[30] Reichel, L., Hempel, G.: Justus Liebigs Ann. Chem., **625,** 184 (1959)

Acta Chimica Hungarica 114 (1), pp. 57—61 (1983)

SYNTHESIS AND ANTIMALARIAL ACTIVITY OF N^1-ISONICOTINOYL-3-METHYL-5-PHENYL-4--(SULFAMOYLPHENYLAZO)-1,2-DIAZOLES

C. P. SINGH

(Chemical Laboratories Sahu Jain College, Najibabad-246763, U.P., India)

Received June 10, 1982
In revised form November 8, 1982
Accepted for publication November 17, 1982

A novel series of N^1-isonicotinoyl-3-methyl-5-phenyl-4-(sulfamoylphenylazo)--1,2-diazoles have been synthesized by the condensation of sulfamoylphenylazo-1--phenyl-1,3-butanedione with isonicotinic acid hydrazide, using glacial acetic acid as condensing agent. Some of the products showed significant antimalarial activity against *Plasmodium berghei* KBG 173 in swiss mice.

Introduction

A survey of the literature reveals that diazole derivatives possess various types of biological activities, viz., potential anti-inflammatory [1, 2], tranquillizing, muscle relaxant, psychoanaleptic, hypnotic, anticonvulsant [3—7], antituberculous [8], antineoplastic [9], antidiabetic [10], antifertility [11] and antitumor [12, 13] actions etc. Isonicotinic acid hydrazide (INH) is used as an antituberculous [14] and antitumor [15] agent. In view of these observations, it was thought desirable to synthesize some new diazole derivatives having the sulfonamide moiety attached through an azo linkage at position 4 and an isonicotinoyl moiety at position 1, in the hope that the resulting compounds may prove to possess valuable pharmacological properties.

The present communication described the synthesis of N^1-isonicotinoyl-3-methyl-5-phenyl-4-(sulfamoylphenylazo)-1,2-diazoles of type (**A**) by the condensation of sulfamoylphenylazo-1-phenyl-1,3-butanediones [16] with INH, using glacial acetic acid as the condensing agent, and the study of the biological activity of the products. The homogeneity and purity of the compounds were checked by TLC and their structures established by IR, NMR spectral studies and element analyses.

Experimental

All the chemicals used were BDH or E. Merck products.

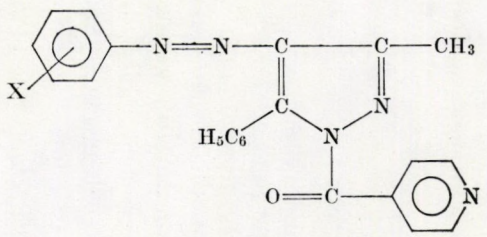

(A)

where: $-X = -Cl, -Br, -NO_2, -CH_3, -OH, -CO_2H, -OCH_3, -NHCOCH_3,$ 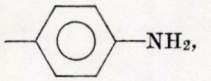 $-NH_2,$

$-SO_2NH_2, -SO_2NHCOCH_3, -SO_2NH-C(=NH)-NH_2,$ 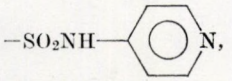

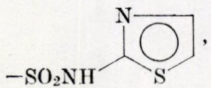, 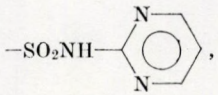, 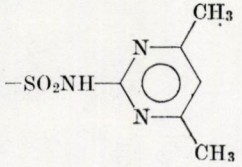 and 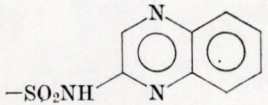

Table I

Characteristics of N^1-isonicotinoyl-3-methyl-5-phenyl-4-(X)-azo-1,2-diazoles

S	X	M.p., °C	Colour	Molecular formula	Nitrogen		R_f value
					Found	Calcd.	
1.	2.	3.	4.	5.	6.	7.	8.
1.	Phenyl	115	Pale yellow	$C_{22}H_{17}N_5O$	19.01	19.07	0.61
2.	2-Chlorophenyl	130	Shining pale yellow	$C_{22}H_{16}N_5OCl$	17.40	17.46	0.91
3.	3-Chlorophenyl	126	Shining yellow orange	$C_{22}H_{16}N_5OCl$	17.42	17.46	0.54
4.	4-Chlorophenyl	199	Pale yellow	$C_{22}H_{16}N_5OCl$	17.41	17.46	0.76
5.	2,4,6-Tribromophenyl	285	Light yellow	$C_{22}H_{14}N_5OBr_3$	11.51	11.59	0.69
6.	3-Fluorophenyl	295	Shining pale yellow	$C_{22}N_{16}N_5OF$	18.12	18.18	0.79
7.	2-Chloro-4-nitrophenyl	240	Light brown	$C_{22}H_{15}N_6O_3Cl$	18.69	18.84	0.65
8.	2-Nitrophenyl	138	Shining orange yellow	$C_{22}H_{16}N_6O_3$	20.29	20.39	0.88
9.	3-Nitrophenyl	120	Dirty yellow	$C_{22}H_{16}N_6O_3$	20.30	20.39	0.67
10.	4-Nitrophenyl	117	Yellow	$C_{22}H_{16}N_6O_3$	20.30	20.39	0.86
11.	3-Nitro-4-methylphenyl	190	Orange	$C_{23}H_{18}N_6O_3$	19.62	19.72	0.71
12.	2-Methylphenyl	178	Shining dark yellow needles	$C_{23}H_{19}N_5O$	18.30	18.38	0.81
13.	4-Methylphenyl	115	Dark yellow	$C_{23}N_{19}N_5O$	18.32	18.38	0.90
14.	2-Methoxyphenyl	181	Pale yellow	$C_{23}H_{19}N_5O_2$	17.60	17.63	0.54
15.	4-Methoxyphenyl	189	Yellow	$C_{23}H_{19}N_5O_2$	17.60	17.63	0.96
16.	4-Aminodiphenyl	175	Red	$C_{28}H_{22}N_6O$	18.31	18.34	0.85
17.	1-Naphthyl	110	Brown	$C_{26}H_{19}N_5O$	16.76	16.79	0.93
18.	2-Naphthyl	105	Dirty yellow	$C_{26}H_{19}N_5O$	16.74	16.79	0.91
19.	4-Carboxyphenyl	185	Yellow	$C_{23}H_{17}N_5O_3$	17.01	17.03	0.78
20.	4-Hydroxyphenyl	163	Yellow needles	$C_{22}H_{17}N_5O_2$	18.21	18.28	0.95
21.	2,3-Dimethyl-1-phenyl-pyrazolone	213	Shining brown	$C_{27}H_{23}N_7O_2$	20.51	20.54	0.49
22.	2-Sulfonamidobenzene	225	Pale yellow	$C_{22}H_{18}N_6O_3S$	18.80	18.84	0.90
23.	N^1-2-pyridylsulfonamido-benzene	256	Dark yellow	$C_{27}H_{21}N_7O_3S$	18.7 2	18.74	0.60
24.	N^1-2-pyrimidylsulfonami-dobenzene	245	Yellow	$C_{26}H_{20}N_8O_3S$	21.30	21.37	0.50
25.	N^1-2-thiazolylsulfonami-dobenzene	213	Shining yellow	$C_{25}H_{19}N_7O_3S_2$	18.48	18.52	0.85
26.	N^1-2-guanylsulfonamido-benzene	276	Light orange	$C_{23}H_{20}N_8O_3S$	22.91	22.95	0.73
27.	N^1-2(4,6-dimethyl)-pyri-midylsulfonamido-benzene	261	Dirty yellow	$C_{28}H_{24}N_8O_3S$	20.24	20.29	0.82
28.	N^1-2-acetylsulfonamido-benzene	249	Pale yellow	$C_{24}H_{20}N_6O_4S$	17.19	17.22	0.99
29.	N^1-2-quinoxalylsulfon-amidobenzene	289	Shining yellow flakes	$C_{30}H_{22}N_8O_3S$	19.42	19.51	0.79

* The R_f values for all the compounds: on silica gel plates (thickness 0.5 mm), developing solvent acetone/dimethylformamide (3 : 1), non-saturated chambers at room temperature (20 ± 1 °C)

Synthesis of N^1-isonicotinoyl-3-methyl-5-phenyl-4-(X)-azo-1,2-diazoles

A mixture of the appropriate sulfamoylphenylazo-1-phenyl-1,3-butanedione (0.1 g) and isonicotinic acid hydrazide (0.05 g) in glacial acetic acid was refluxed on an oil bath at 120—130 °C for 4 h and then allowed to stand overnight. The coloured compound which separated was filtered off, washed well with water, dried and recrystallized from a mixture of glacial acetic acid and DMF.

By analogous procedures, several substituted-1,2-diazoles have been synthesized; their characteristics are recorded in Table I. The yields were between 75 and 85%.

IR and NMR spectra

IR spectra in KBr were recorded on a Perkin Elmer grating IR spectrophotometer. The spectra had characteristic peaks at 780 cm^{-1} —; aromatic ring); 1580 cm^{-1} (—N=N—); 1638 cm^{-1} (C=N); 1750 cm^{-1} (C=O of *tert.* amide having N in diazole ring), which helped in establishing the structures of the compounds.

The structures of the substituted diazoles were also confirmed by ^{1}H-NMR spectral studies. In $CDCl_3$ solution, the following δ (ppm) values were obtained: 2.46 (2s, 3, CH_3); 6.9 (dd, 2, Ar*H*, *ortho* to X, J = 10 and 2 Hz); 7.18 – 7.40 (m, 4,4-pyridinecarbonyl, *meta* to C=O); 7.46 (bs, 5, Ar*H*, $C_1 - C_6H_5$); 7.70 – 7.79 (2dd, 2,4-pyridinecarbonyl, *ortho* to C=O, J = 8 and 3 Hz). (X denotes the substituent group.)

Biological assay

All the compounds were screened for their antimalarial activity against *Plasmodium berghei* KBG173 malaria in swiss mice by the Osdene and Russell method [17]. The antimalarial results were obtained from the Medicinal Chemistry Division, W.A.R.I., Washington

Table II

Antimalarial activity data, MTS[c] (days), C (cures)[d,e]

S. No.	Name of the compound	Dose, mg/kg					
		20	40	80	160	320	640
1.	N^1-isonicotinoyl-3-methyl-5-phenyl-4-(N^1-2-thiazolylsulfonamidobenzeneazo)-1,2-diazole	1.3	5.3	13.7	1c	4c	4c
2.	N^1-isonicotinoyl-3-methyl-5-phenyl-4-(N^1-2-quinoxalylsulfonamidobenzeneazo)-1,2-diazole	2c	3c	5c	5c	5c	5c
3.	N^1-isonicotinoyl-3-methyl-5-phenyl-4-(N^1-2-acetylsulfonamidobenzeneazo)-1,2-diazole	13.9	3c	5c	5c	5c	5c

c — Mean survivial times in days; a compound is considered active when MST is doubled or more

[d]*C* — Number of cures (mice surviving to 60 days) out of test group of five mice

e — 15 test groups were ten mice

(D.C.). Some of the products, namely, N^1-isonicotinoyl-3-methyl-5-phenyl-4-(N^1-2-thiazolylsulfonamidobenzeneazo)-, -4-(N^1-2-quinoxalylsulfonamidobenzeneazo)-, and -4-(N^1-2-acetylsulfonamidobenzeneazo)-1,2-diazoles showed significant antimalarial activity and their results are given in Table II.

*

The author wishes to express his sincere thanks to Prof. M. K. Jain (Principal), Prof. A. C. Ojha, Sahu Jain College, Nijababad, for necessary laboratory facilities and pertinent discussions. The author is also indebted to Dr. T. R. Sweeny, Director, W.A.R.I. Washington (D.C.) for testing the compounds as antimalarial agents, and to CSIR, New Delhi, for financial assistance.

REFERENCES

[1] Kato, K., Hori, M., Ohatani, O., Izumi, K., Kitumikado, T., Asai, H. and Sugiura, S.: J. Med. Chem. **20,** 80 (1977)
[2] Sugiura, S., Kato, K., Ohno, S., Ohtani, O., Wakayama, T.: J. Pharm. Soc., **97,** 719 (1977)
[3] Polevoi, L. G.: Tr. Nauchn. Konf. Aspir. i Ord. 1-yi (Pervyi) Mosk. Med. Inst., Moscow **1964,** 159; Chem. Abstr., **65,** 19147 (1966)
[4] Avakumov, V. M., Batulin, Yu. M.: Farmakol. Toksikol., **31,** 402 (1968); Chem. Abstr., **69,** 75439 (1938)
[5] Polevoi, L. G., Kudrin, A. N., Grandberg, I. I., Kost, A. N.: Izv. Timiryazev. Sel'skokhoz. Akad. **1968,** 192; Chem. Abstr., **69,** 1557 (1968)
[6] Batulin, Y. M.: Farmakol. Toksikol., **31,** 533 (1968); Chem. Abstr., **70,** 2236 (1969)
[7] Parmar, S. S., Pandey, B. R., Dwivedi, C., Harbison, R. D.: J. Pharm. Sci., **63,** 1152 (1974)
[8] Behnischi, R., Mietzch, F , Schmidt, H.: Am. Rev. Tuber., **61,** 1 (1950)
[9] Garg, H. G., Sharma, R. A.: J. Pharm. Sci., **59,** 350 (1970)
[10] Garg, H. G., Singh, P. P. J. Med. Chem., **13,** 1250 (1970)
[11] Tiwari, S. S., Sharma, A.: J. Indian Chem. Soc., **52,** 153 (1975)
[12] Wilson, W., Bottigliere, N.: Cancer Chemotherapy, **21,** 137 (1962)
[13] Noell, C. W., Cheng, C. C.: J. Med. Chem., **12,** 545 (1969)
[14] Dictionary of Organic Compounds, Vol. **5,** p. 2317. Oxford, New York 1965
[15] Woodburg, E. C., Koppaka, V.: Cancer Chemotherapy Rept., **6,** 58 (1974)
[16] Singh, C. P.: Ph. D. Thesis, Synthesis and Studies of 1,2-Diazoles and Diazolones, Rohilkhand University, Bareilly 1980
[17] Osdene, T. S., Russell, P. B., Rane, L.: J. Med. Chem., **10,** 431 (1967)

Acta Chimica Hungarica 114 (1), pp. 63–68 (1983)

N-DEMETHYLATION OF MORPHINE ALKALOIDS, II*

CODEINE ISOMERS

S. HOSZTAFI, S. MAKLEIT** and ZS. MISKOLCZI

(Institute of Organic Chemistry, Kossuth Lajos University ,H-4010 Debrecen, P.O.Box 20)

Received September 14, 1982
Accepted for publication November 18, 1982

New *N*-demethyl derivatives of codeine isomers (isocodeine, pseudocodeine and allopseudocodeine) are described. *N*-Demethylation has been effected with cyanogen bromide or diethyl azodicarboxylate starting from the acetyl derivatives of the isomers. The *N*-demethyl derivatives afford a possibility for the preparation of new *N*-alkyl *N*-demethyl derivatives. In the course of these studies several new morphine derivatives have hitherto been prepared (see Scheme 1: compounds **Ic–f**, **IIc–f** and **IIIc–f**).

Codeine and codeine isomers (pseudocodeine, **Ia**, allopseudocodeine, **IIa** and isocodeine, **IIIa**) have equivalent analgetic activity [1, 2]. *N*-Demethyl and *N*-alkyl *N*-demethyl derivatives of these compounds are, however, unknown so far. Reaction of the methyl and phenyl ethers of pseudocodeine with cyanogen bromide is described in a German Patent [2] but the hydrolysis of the cyanamide derivatives formed is not mentioned.

As a continuation of our former work [4], preparation of the *N*-demethyl derivatives*** of codeine isomers [5] has been studied.

Several methods are available for the synthesis of codeine isomers [5, 6]. Pseudocodeine and allopseudocodeine were prepared by using the method of Speyer and Krauss [7]. Isocodeine was obtained by our own procedure [8], Later, another method was also published [9] for the synthesis of isocodeine.

Acetyl derivatives of codeine isomers (**Ib**, **IIb** and **IIIb**) are known compounds. The ^{1}H-NMR spectral properties measured by us for these compounds are in accordance with the literature data [10, 11, 12, 13].

If the reactions were performed by von Braun's method, the expected cyanamide derivatives (**Ic**, **IIc** and **IIIc**) were formed. Compound **Ic** could not be crystallized.

Only compound **Id** was obtained as a crystalline product on deacetylation with hydrochloric acid. Compound **IId** was prepared by alkaline hydroly-

* For Part I, see Ref. [4].

** To whom correspondence should be addressed.

*** The designation "nor" used frequently in the alkaloid literature is not unambiguous in the case of some groups of compounds (e.g. steroids), therefore, it is more expedient to use the "*N*-nor" or "*N*-demethyl" designations accepted by Chemical Abstracts.

sis. The ^{1}H-NMR spectral properties of compounds **Ic—d** and **IIc—d** (see Experimental) are in accordance with the literature data [10, 11, 12]. Compound **IIId** could not be prepared as a pure product either by acid or alkaline hydrolysis. For this reason, in the case of this compound the acetyl group and the cyanamide moiety were simultaneously hydrolized like the cyanamide group of compounds **Id** and **IId**. The structures of the *N*-demethyl derivatives obtained (**Ie**, **IIe** and **IIIe**) were elucidated, besides the microanalyses, IR and ^{1}H-NMR data, by their methylation with a mixture of formaldehyde and formic acid to yield compounds **Ia**, **IIa** and **IIIa**.

Compounds **If**, **IIf** and **IIIf** were prepared by the *N*-demethylation of compounds **Ib**, **IIb** and **IIIb** with diethyl azodicarboxylate (ADDE). Besides the IR and ^{1}H-NMR data, the structures were corroborated by deacetylation to afford compounds **Ie**, **IIe** and **IIIe**.

No spontaneous [14] or thermally induced [15] O→N acyl migration was observed on the *N*-demethylation of compound **If** with ADDE, indicating that the known conformation of ring C [11] in this compound does not make possible the formation of the intermediate [14] of the acyl migration.

Pharmacological assay of the new compounds prepared is scheduled.

Experimental

M. p.'s were meassured on a Koffler hot-stage apparatus and are uncorrected. Thin-layer chromatography was performed on Silica gel $60F_{254}$ (Merck 5554) layer using benzene : methanol (8 : 2) or 1 : 1 *v/v*) and chloroform : acetone : diethylamine (5 : 4 : 1 *v/v*) developing mixtures. The spots were visaulized with Dragendorff reagent. ^{1}H-NMR spectra were recorded on a Bruker spectrometer at 200 MHz ($\delta_{TMS} = 0.0$ ppm). IR spectra were measured in KBr discs with a Perkin-Elmer 283B instrument.

O-Acetylpseudocodeine (Ib)

Prepared by the method of Knorr and Horlein [16]: yield 69%. M.p. of the hydroiodide was 282—285 °C, *lit.* m.p. 285 °C. The base is a colourless oil.

IR: $\nu_{C=O}$ 1740 cm^{-1}.

^{1}H-NMR ($CDCl_3$): 6.72 dd (H-1,2, 2H), 5.7—5.8 m (H-6,7, 2H), 5.0 m (8αH, 1H), 4.95 (5βH, 1H), 3.8 s (OMe, 3H), 2.45 s (N—Me, 3H), 2.05 s (OAc, 3H).

O-Acetylallopseudocodeine (IIb)

Prepared by the method of Knorr et al. [17]: yield 84%. M.p. 194—195 °C (crystallized from ethanol), *lit.* m.p. 194—195 °C.

IR: $\nu_{C=O}$ 1735 cm^{-1}.

^{1}H-NMR ($CDCl_3$): 6.6 dd (H-1,2, 2H), 6.0—5.9 (6-H, 7-H, 2H), 5.3 m (8βH, 1H), 4.95 s (6βH, 1H), 3.85 s (OMe, 3H), 2.3 s (N—Me, 3H), 1.65 s (OAc, 3H)

O-Acetylisocodeine (IIIb)

Made according to the procedure of Sargent et al. [18]: yield 70.2%. M.p. 88—90 °C, *lit.* m.p. 88—89 °C.

IR: $\nu_{C=O}$ 1740 cm^{-1}.

^{1}H-NMR ($CDCl_3$): 6.67 dd (H-1,2, 2H), 6 m (H-7, 1H), 5.55 m (H-8, 1H), 5.3 m (6αH, 1H), 4.8 m (5βm, 1H), 3.85 s (OMe, 1H), 2.35 s (N—Me, 3H), 2.1 s (OAc, 3H).

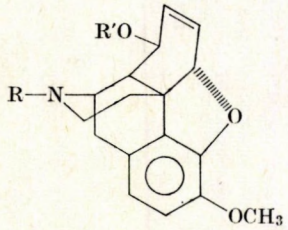

Ia: R = CH_3, R' = H

Ib: R = CH_3, R' = $-C(=O)-CH_3$

Ic: R = CN, R' = $-C(=O)-CH_3$

Id: R = CN, R' = H

Ie: R = H, R' = H

If: R = H, R' = $-C(=O)-CH_3$

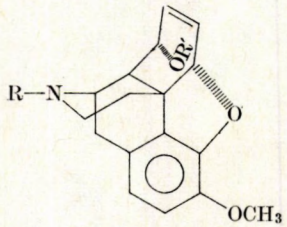

IIa: R = CH_3, R' = H

IIb: R = CH_3, R' = $-C(=O)-CH_3$

IIc: R = CN, R' = $-C(=O)-CH_3$

IId: R = CN, R' = H

IIe: R = H, R' = H

IIf: R = H, R' = $-C(=O)-CH_3$

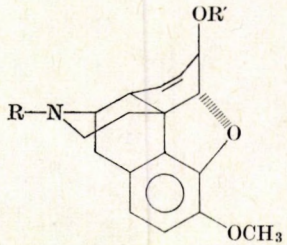

IIIa: R = CH_3, R' = H

IIIb: R = CH_3, R' = $-C(=O)-CH_3$

IIIc: R = CN, R' = $-C(=O)-CH_3$

IIId: R = CN, R' = H

IIIe: R = H, R' = H

IIIf: R = H, R' = $-C(=O)-CH_3$

Scheme 1

O-Acetyl-*N*-cyano-*N*-demethylpseudocodeine (Ic)

O-Acetylpseudocodeine (**Ib**, 2.4 g; 7.0 mmol) was dissolved in anhydrous choroform (15 mL), cyanogen bromide (1.1 g; 10.5 mmol) in chloroform (10 mL) was added, and the mixture refluxed for 8 h. The solvent was removed in vacuum, the residue dissolved in chloroform (30 mL), washed with water, with 10% hydrochloric acid and again with water. The solution was dried over $MgSO_4$ and the solvent evaporated to yield 2.43 g (98%) of a colourless oil which was homogeneous according to TLC.

IR: $\nu_{C=O}$ 1745 cm^{-1}, $\nu_{C\equiv N}$ 2200 cm^{-1}.

^{1}H-NMR ($CDCl_3$): 6.75 dd (H-1,2, 2H), 5.75 m (H-6,7, 2H), 5.0 s (5βH, 1H), 4.85 d (8αH, 1H), 3.8 s (OMe, 3H), 2.1 s (OAc, 3H).

O-Acetyl-*N*-cyano-*N*-demethylallopseudocodeine (IIc)

O-Acetylallopseudocodeine (**IIb**, 1.7 g; 5 mmol) was dissolved in anhydrous chloroform (15 mL) and cyanogen bromide (0.69 g; 6.5 mmol) in chloroform (10 mL) was added, and the mixture was refluxed for 4 h. The solvent was evaporated, ethanol was added to the residue and the mixture was then evaporated to dryness. The solid residue was triturated with water (40 mL) and allowed to stand overnight. The white crystalline product was filtered off and washed with ethanol to obtain 1.58 g (90%), m.p. 242 °C, of **IIc** which was crystallized from a mixture of chloroform and ethanol; m.p. 246 – 248 °C.

IR: $\nu_{C=O}$1730cm^{-1}, $\nu_{C\equiv N}$ 2200 cm^{-1}.

^{1}H-NMR ($CDCl_3$): 6.75 dd (H-1,2, 2H), 6.0 m (6-H, 7-H, 2H), 5.3 m (8βH, 1H), 4.95 (5βH, 1H), 3.85 s (OMe, 3H), 1.75 s (OAc, 3H).

$C_{20}H_{20}N_2O_4$ (352.38). Calcd. C 68.16; H 5.86; N 7.95. Found C 68.65; H 5.82; N 7.78%.

O-Acetyl-*N*-cyano-*N*-demethylisocodeine (IIIc)

O-Acetylisocodeine (**IIIb**, 2.0 g; 5.85 mmol) was dissolved in anhydrous chloroform (20 mL), cyanogen bromide (0.95 g; 8 mmol) in chloroform (10 mL) was added, and the mixture was refluxed for 4 h. The solvent was evaporated, ethanol was added to the residue and then evaporated to dryness. The oily residue was dissolved in ethanol (8—10 mL) and water was added to precipitate a solid material on standing at 0 °C for several hours. The solid material was filtered off, washed with water to afford 1.8 g (87.4%), m.p. 144—147 °C, of a substance which was crystallized from ethanol; m.p. 150—153 °C.

IR: $\nu_{C=O}$ 1735 cm^{-1}, $\nu_{C\equiv N}$ 2200 cm^{1-}.

^{1}H-NMR ($CDCl_3$): 6.7 dd (H-1,2, 2H), 5.95 s (H-7, 1H), 5.6 s (H-8, 1H), 5.25 s (6αH, 1H), 4.75 s (5βH, 1H), 3.85 s (OMe, 3H), 2.05 s (OAc, 3H).

$C_{20}H_{20}N_2O_4$ (352.38). Calcd. C 68.16; H 5.68; N 7.95. Found C 68.35; H 5.70; N 8.0%.

N-Cyano-*N*-demethylpseudocodeine (Id)

Conc. hydrochloric acid (15 mL) was added to *O*-acetyl-*N*-cyano-*N*-demethylpseudocodeine (**Ic**, 1.85 g; 5.96 mmol) and the solution was heated on a steam-bath for 5 min. The mixture was cooled down, diluted with water (40 mL) and let to stand at 0 °C for one day. The precipitated crystalline material was filtered off and washed with water to yield 1.32 g (81%) of the product, m.p. 94 °C.

IR: $\nu_{C\equiv N}$ 2200 cm^{-1}.

^{1}H-NMR ($CDCl_3$): 6.7 dd (H-1,2, 2H), 6.75—6.9 (H-6, H-7, 2H), 5.0 s (5βH, 1H), 3.6 m (8αH, 1H).

$C_{18}H_{18}N_2O_3$ (310.34). Calcd. C 69.68; H 5.8; N 9.02. Found C 69.40; H 5.7; N 9.10%.

N-Cyano-*N*-demethylallopseudocodeine (IId)

O-Acetyl-*N*-cyano-*N*-demethylallopseudocodeine (**IIc**, 0.6 g) was dissolved in methanol (20 mL), 10% potassium carbonate solution (10 mL) was added and the mixture stirred at room temperature for 2 h. The methanol was evaporated and the residue extracted with chloroform (2×40 mL). The solution was washed with brine and dried with $MgSO_4$. The chloroform was evaporated to obtain 0.4 g (77%) of a colourless oil which was pure according to TLC.

IR: $\nu_{C\equiv N}$ 2200 cm^{-1}.

^{1}H-NMR ($CDCl_3$): 6.7 dd (H-1,2, 2H), 6.0 m (H-7, 1H), 5.8 (H-6, 1H), 5.0 s (5βH, 1H), 4.0 m (8βH, 1H), 3.85 s (OMe, 3H).

Hydrolysis of cyanamides Id, IId, and IIIc

The substance (1.0 g) was refluxed on 6% hydrochloric acid (30 mL) for 16 h. ***N*-Demethylpseudocodeine (Ie)** hydrochloride precipitated on cooling and the crystals were filtered off. The hydrochlorides of ***N*-demethylallopseudocodeine (IIe)** and ***N*-demethylisocodeine (IIIe)** remained in solution. Solutions of **IIe** and **IIIe** were made alkaline with *conc.* ammonium hydroxide and extracted with chloroform (4×25 mL). The combined organic phase was washed with brine (2×30 mL) and dried. Base **Ie** was obtained from its hydrochloride in the same manner.

N-Demethylpseudocodeine (Ie)

The hydrochloride obtained (0.83 g; 80%) had m.p. 329 °C (decomp.). The m.p. of the base was 196 °C (from ethyl acetate).

IR: ν_{OH} 3250 cm^{-1}

^{1}H-NMR ($CDCl_3$): 6.7 dd (H-1,2, 2H), 5.85 and 5.7 m (H-6, H-7, 2H), 4.95 m (5βH, 1H), 3.85 s (OMe, 3H), 3.55 d (8αH, 1H).

$C_{17}H_{19}NO_3$ (295.33). Calcd. C 71.55; H 6.71; N 4.91. Found C 71.45; H6.42; N 4.8%.

N-Demethylallopseudocodeine (IIe)

The slowly crystallizing crude product (0.83 g; 80%) was homogeneous according to TLC, m.p. 151—153 °C (from ethanol).

IR: ν_{OH} 3300 cm^{-1}.

^{1}H-NMR ($CDCl_3$): 6.75 dd (H-1,2, 2H), 6.0 m (H-7, 1H), 5.75 m (H-6, 1H), 5.05 s (5βH, 1H), 4.0 m (H-8, 1H), 3.9 s (OMe, 3H).

$C_{17}H_{19}NO_3$ (285. 33). Calcd. C 71.55; H 6.71; N 4.91. Found C 71.35; H 6.65; N 4.85%.

The base was dissolved in ethanol and ethanol saturated with hydrogen chloride was added to obtain the crystalline hydrochloride, m.p. 310—314 °C (decomp.).

N-Demethylisocodeine (IIIe)

Hydrolysis of **IIIc** (1.0 g) gave crude *N*-demethylisocodeine (0.4 g; 50%) as a colourless gum which was homogeneous according to TLC. It was crystallized from ethyl acetate and dried in vacuum (20 mbar) at 60 °C to afford a crystalline product, m.p. 186—188 °C.

IR: ν_{OH} 3250 cm^{-1}.

^{1}H-NMR ($CDCl_3$): 6.7 dd (H-1,2, 2H), 6.05 s (H-7, 1H), 5.7 s (H-8, 1H), 4.8 s (5βH, 1H), 4.25 d (6αH, 1H), 3.85 s (OMe, 3H).

$C_{17}H_{19}NO_3$ (285.33). Calcd. 71.55; H 6.71; N 4.91. Found C 71.40; H 6.55; N 5.1%.

N-Demethylation with diethyl azodicarboxylate

Compound **Ib**, **IIb** or **IIIb** (2.05 g; 6 mmol) was dissolved in anhydrous benzene diethyl azodicarboxylate (1.57 g; 9 mmol) was added and the mixture refluxed for 5 h. The solvent was evaporated and the residue dissolved in ethanol (20 mL); saturated ammonium chloride solution (10 mL) was added and the solution refluxed for 6 h. The mixture was allowed to stand overnight, the ethanol removed in vacuum and 5% hydrochloric acid (10 mL) was added to the residue. The acidic solution was extracted with ether (3×15 mL), then made alkaline with *conc.* ammonium hydroxide (pH ~10) at 0 °C, and the *O*-acetyl-*N*-demethyl derivative was extracted with chloroform (4×20 mL). The organic phase was washed with brine, dried and the solvent evaporated. Further purification was performed via salification.

O-Acetyl-*N*-demethylpseudocodeine (If)

The crude product was allowed to react with an equimolar amount of tartaric acid in ethanol; the acidic tartrate crystallized slowly to afford 1.2 g (41%), m.p. 131—134 °C, of the crystalline product. The base was a colourless oil.

IR: $\nu_{C=O}$ 1745 cm^{-1}.

^{1}H-NMR ($CDCl_3$): 6.7 dd (H-1,2, 2H), 6.75—6.8 m (6-H, 7-H, 2H), 5.1 m (8αH, 1H), 5.0 s (5βH, 1H), 3.85 s (OMe, 3H), 2.0 s (OAc, 3H).

$C_{23}H_{27}NO_{10}$ (477.47). Calcd. C 57.85. H 5.7; N 2.93. Found C 58.2; H 5.92; N 2.75%.

O-Acetyl-*N*-demethylallopseudocodeine (IIf)

O-Acetyl-*N*-demethylallopseudocodeine hydrochloride (1.7 g; 78%), m.p. 310 °C was precipitated from ethanolic solution by acidification (pH ~3—4) with ethanol saturated with hydrogen chloride. M.p. 143—145 °C.

IR: $\nu_{C=O}$ 1722 cm^{-1}.

^{1}H-NMR ($CDCl_3$): 6.65 dd (H-1,2, 2H), 6.0—5.85 m (H-6, H-7, 2H), 5.3 s (8βH, 1H), 4.95 s (5βH, 1H), 3.85 s (OMe, 3H), 1.7 s (OAc, 3H).

$C_{19}H_{21}NO_4$ (327.38). Calcd. C 69.70; H 6.46; N 4.27. Found C 69.90; H 6.41; N 4.2%

O-Acetyl-*N*-demethylisocodeine (IIIf)

This compound was purified as the hydrochloride to yield 0.55 g (25%), m.p. 272—278 °C of the crystalline product. The base was a colourless oil.

IR: $\nu_{C=O}$ 1735 cm^{-1}, ν_{OH} 3320 cm^{-1}.

^{1}H-NMR ($CDCl_3$): 6.7 dd (H-1,2, 3H), 6.05 s (H-7, 1H), 5.7 s (H-8, 1H), 5.2 d (6αH, 1H), 4.75 s (5βH, 1H), 3.85 s (OMe, 3H), 2.05 s (OAc, 3H).

$C_{19}H_{22}NO_4Cl$ (363.82). Calcd. C 62.72; H 6.09; N 3.85. Found C 62.80; H 5.85; N 3.62%.

Hydrolysis of the *O*-acetyl-*N*-demethyl derivatives If, IIf and IIIf

An ethanolic solution of compound **If** or **IIIf** was refluxed with 10% potassium hydroxide for 10 min to afford compounds **Ie** and **IIIe**, respectively. Compound **IIf** in methanolic solution was allowed to stand with 10% potassium carbonate at room temperature for 8 h to yield compound **IIe**. Yields of the reactions were 90—95%.

*

The authors' thanks are due to the Alkaloid Chemical Works, Tiszavasvári, Hungary, and to the Hungarian Academy of Sciences for financial support of these studies; to Drs. L. Szilágyi, and Z. Dinya for the ^{1}H-NMR and IR spectra.

REFERENCES

[1] Burger, A.: Medicinal Chemistry, Vol. **1**, pp. 164—165. Intersci. Publ., New York 1951
[2] Eddy, N. B., Halbach, H., Braenden, O. J.: Bull. World Health Org., **14**, 353 (1956)
[3] Hoffmann—La Roche and Co.: Ger. Pat. 286.743 (1914); Frdl., **12**, 741; Houben, **4**, 588
[4] Hosztafi, S., Makleit, S., Bognár, T.: Magy. Kém. Foly., **86**, 15 (1980); Acta Chim. Acad. Sci. Hung., **103**, 371 (1980)
[5] Bentley, K. W.: The Chemistry of the Morphine Alkaloids, pp. 74—80, Clanderon Press, Oxford 1954
[6] Small, L. F.: Chemistry of the Opium Alkaloids, p. 221, Washington 1932
[7] Speyer, E., Krauss, W.: Justus Liebigs. Ann. Chem., **432**, 233 (1923)
[8] Makleit, S., Bognár, R.: Magy. Kém. Foly., **75**, 235 (1969); Acta Chim. Acad. Sci. Hung., **59**, 387 (1969)
[9] Barber, R. B., Rapoport, H.: J. Med. Chem., **18**, 1074 (1975)
[10] Okuda, S., Yamaguchi, S., Kawazoe, Y., Tsuda, K.: Chem. Pharm. Bull., **12**, 104 (1964)
[11] Batterham, T. J., Bell, K. H., Weiss, U.: Aust. J. Chem., **18**, 1799 (1965)
[12] Jacobson, A. E., Yeh, H. J. C., Sargent, L. J.: Org. Magn. Reson., **4**, 875 (1972)
[13] Brine, G. A., Prakash, D., Hart, C. G., Kotchmar, D. J., Moreland, C. G., Carrol, F. I.: J. Org. Chem., **41**, 3445 (1976)
[14] Fodor, G.: in Recent Developments in the Chemistry of Natural Carbon Compounds, Vol. **1**, pp. 75—160. Akadémiai Kiadó, Budapest 1965
[15] Saucier, M., Daris, J. P., Lambert, Y. Monkovic, I., Pircio, A. W.: J. Med. Chem., **20**, 676 (1977)
[16] Knorr, L., Horlein, H.: Ber., **39**, 4409 (1906)
[17] Knorr, L., Horlein, H., Grimme, C.: Ber., **40**, 3844 (1907)
[18] Sargent, L. J., Schwartzman, L. H., Small, L. F.: J. Org. Chem., **23**, 1247 (1958)

Acta Chimica Hungarica 114 (1), pp. 69–77 (1983)

HYDROXYIMINO-3(2*H*)-ISOQUINOLINONES, II*

A CONVENIENT METHOD FOR THE PREPARATION OF 4-(HYDROXYIMINO)-1,4-DIHYDRO-3(2*H*)-ISOQUINOLINONES AND THEIR *O*-ALKYL AND *O*-ACYL DERIVATIVES

I. TIKK[1], GY. DEÁK[1]** and G. TÓTH[2]

([1]Institute of Experimental Medicine, Hungarian Academy of Sciences, H-1450 Budapest, P.O. Box 67, and [2]Institute for General and Analytical Chemistry, Technical University, H-1521 Budapest, Gellért tér 4.)

Received August 31, 1982
Accepted for publication November 21, 1982

Several 4-(hydroxyimino)-1,4-dihydro-3(2*H*)-isoquinolinones were synthesized by the isonitrosation of the corresponding 1,4-dihydro-3(2*H*)-isoquinolinones. The hydrogen bond formed between the hydroxyl and oxo groups gives rise to a characteristic change in the IR and ^{1}H-MNR spectra, furthermore in the physical and chemical properties of the compounds.

We have previously reported [2] that the methylene group in position 4 of 1-aryl-1,4-dihydro-3(2*H*)-isoquinolinones, synthesized first by us, has CH-acid character in the presence of a strong base, and in its reaction with an aromatic aldehyde in the first step the 4-arylidene derivative is produced, which then undergoes rearrangement into the 4-arylmethyl-3-isoquinolinol. Following our work also the synthesis of 4-formyl-1,4-dihydro-3(2*H*)-isoquinolinones by the Vilsmeier reaction has been reported [3].

In continuation of the study of the reactions of 1,4-dihydro-3(2*H*)--isoquinolinones we investigated whether the selective nitration of the methylene group in position 4 is practicable. It was found that only the aromatic rings were nitrated, mostly accompanied by some degradation of the isoquinoline skeleton.

It is well known that some methylene groups adjacent to an oxo or lactam carbonyl group can be isonitrosated under suitable conditions and thus hydroxyimino derivatives can be prepared [4, 5].

In accordance with this observations we have found that when allowing 1,4-dihydro-3(2*H*)-isoquinolinones to react with *n*-butyl nitrite in the presence of potassium *t*-butoxide a rapid isonitrosation takes place even at 0 °C, as soon as the base is added. We as soon as also established that in the absence of steric factors the production of the *E* isomer was favoured, and the *Z* isomer could be detected in a quantity less than 10%. For instance starting from benzo [f] isoquinolinone only the *Z* oxime could be prepared, but from the

* Part I see Ref. [1].
** To whom correspondence should be addressed.

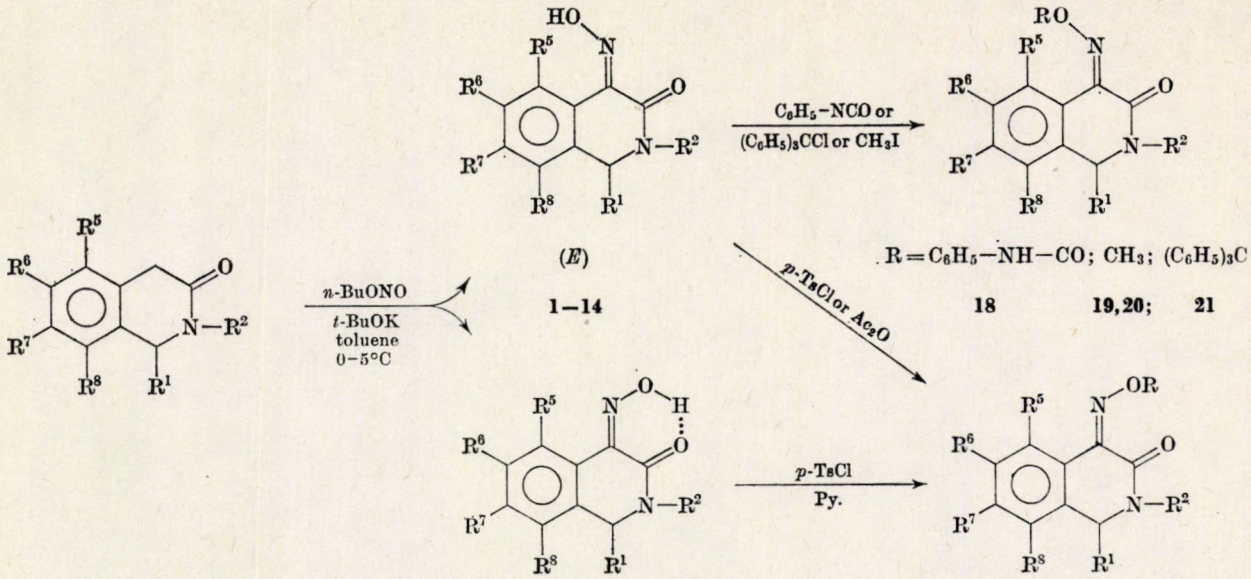
n-BuONO
t-BuOK
toluene
0–5°C
(E)
(Z)
1–14
C6H5–NCO or
(C6H5)3CCl or CH3I
p-TsCl or Ac2O
p-TsCl
Py.
R = C6H5–NH–CO; CH3; (C6H5)3C
18 19,20; 21
R = Ac; p-Ts
15; 16; 17

Scheme 1

benzo [h] isoquinolinone a mixture of the *E* and *Z* isomers was obtained. It is interesting to mention that the 5-methyl (**6**) derivative afforded only the *E* hydroxyimino derivative.

On increasing the temperature of the reaction a decrease in the yield was observed; the increasing of the reaction time favoured the production of the *Z* isomer. For example, at 0 °C after 1 hour a significant decrease in the proportion of the *E* and *Z* isomers was found.

The presence and quantity of the two isomers can be detected and estimated by observed the νO=C—N band in the IR spectra: this appears for the *Z* oxime always at a lower wavenumber than for the corresponding *E* oxime. In the *Z* isomers a hydrogen bond can be formed between the hydroxyl and oxo groups, and this facilitates the distinction and also the separation of the isomers; the solubility and reactivity of the chelated *Z* oximes significantly differ from those of the *E* isomers and this difference in some cases makes possible the separation of the isomers. Such differences are as follows: *a)* a difference in the solubility which is greater for the *Z* oximes in apolar or weakly polar aprotic solvents; *b)* difference in the chemical reactivity e.g. the *Z* isomer cannot be alkylated or deoximated under normal conditions.

Table I shows some physical data of the new 4-(hydroxyimino) derivatives.

Further on some *O*-alkyl and *O*-acyl derivatives of the hydroxyiminoisoquinolinones have been prepared.

We have found that the *E* isomers can be transformed into the corresponding *O*-alkyl derivatives with retention of the configuration. In the course of the esterification, however, when it was performed by acyl chloride or anhydride we obtained always, the esters, of *Z* configuration, which is indicated in their ^{1}H-NMR spectra by the H-5 shift (Table II).

In the determination of the *Z* or *E* configuration of the different 4-hydroxyimino derivatives we could rely, besides the IR spectra, also on the ^{1}H-NMR spectra. If the compounds were soluble in $CDCl_3$, the chemical shift of the OH proton in the *Z* isomer was extremely high 15 ppm, in accordance with the inner hydrogen bond. In DMSO-d_6 solution, however, the chemical shift of the OH signal alone was insufficient to decide between the *Z* and *E* configurations. Independently of the solvent, characteristic differences could be observed in the H-5 signal of the *Z* and *E* isomers, as in the spectrum of the *E* isomer the expected [6] downfield shift (0.5 ppm) appeared. When the formation of only one isomer was experienced, its configuration could be concluded from the H-5 chemical shift only with great caution, e.g. in the knowledge of the experience [7] that the R^6=R^7=OMe substituents give rise to a 0.57 ppm upfield effect. In consideration of this it is obvious that the chemical shifts H-5=8.12 ppm for **7** and 8.09 ppm for **18** (R=CONHPh) prove the *E* configuration.

Table I

4-(Hydroxyimino)-1,4-dihydro-3 (2H)-isoquinoli

Product	R^1	R^2	R^5	R^6	R^7	R^8	Yield, %
1	H	Me	H	H	H	H	56
2	H	Et	H	H	H	H	47
3	H	Et	H	MeO	MeO	H	48
4	C_6H_5	H	H	H	H	H	68
5	C_6H_5	Me	H	H	H	H	87
6	C_6H_5	H	Me	H	H	H	25
7	C_6H_5	H	H	MeO	MeO	H	40
8	C_6H_5	Me	H	MeO	MeO	H	82
9	C_6H_5	H	H	H	CH=CH–CH=CH		10

nones (2) *from 1,4-dihydro-3(2H)-isoquinolinones* (1)

	m.p.[a] (solv.) °C	Molecular[b] formula	IR (KBr)[c] νO=C—N cm^{-1}		^{1}H-NMR[d] δ ppm
Z	126–128 (MeOH)	$C_{10}H_{10}N_2O_2$ (190.2)	1642	A	3.15 (s, 3H, N—Me); 3.63 (s, 2H, N—CH_2) 7.0–7.5 (m, 3H, H_{arom}); 8.02 (m, 1H_{arom}, H-5); 15.82 (s, 1H, OH)
E	171–173 (EtAc)		1670	A/B (9:1)	3.16 (s, 3H, N—Me); 4.53 (s, 2H, N—CH_2) 7.1–7.5 (m, 4H, H_{arom} + OH); 8.65 (m, 1H_{arom}, H-5)
Z	110–111 (EtOH)	$C_{11}H_{12}N_2O_2$ (204.2)	1628	A	1.25 (t, 3H, CH_3); 3.54 (q, 2H, N—CH_2); 7.0–7.4 (m, 3H, H_{arom}); 7.88 (dd, 1H, H-5); 15.98 (s, 1H, OH)
E	143–145 (Acetone)		1650		
E	173–175 (MeOH)	$C_{13}H_{16}N_2O_4$ (264.3)	1650		
Z	167–168 (EtAc)	$C_{15}H_{12}N_2O_2$ (252.3)	1660	B	5.91 (d, 1H, H-1); 7.1–7.5 (m, 8H, H_{arom}); 7.90 (m, 1H, H-5); 9.75 (d, 1H, NH); 15.65 (s, 1H, OH)
E	194–195 (MeOH)		1680	B	5.80 (d, 1H, H-1); 7.2–7.6 (m, 8H, H_{arom}); 8.42 (m, 1H, H-5); 9.00 (d, 1H, NH); 12.47 (s, 1H, OH)
Z	118–119 (MeOH)	$C_{16}H_{14}N_2O_2$ (266.3)	1630	A	3.93 (s, 3H, N—Me); 5.53 (s, 1H, H-1); 6.9–7.5 (m, 8H, H_{arom}); 8.08 (m, 1H, H-5); 16.02 (s, 1H, OH)
E	173–176 (MeOH)		1670	A	3.06 (s, 3H, N—Me); 5.48 (s, 1H, H-1); 7.1—7.4 (m, 9, H_{arom} + NH); 9.05 (s, 1H, OH)
E	214–215 (MeOH)	$C_{16}H_{14}N_2O_2$ (266.3)	1670	B	2.25 (s, 3H, 5-CH_3); 5.57 (s, 1H, He-1); 7.1–7.4 (m, 9H, H_{arom} + NH); 8.05 (s, 1H, OH)
E	198–199 (MeOH)	$C_{17}H_{16}N_2O_4$ (312.3)	1660	B	3.86 (s, 3H, MeO); 3.88 (s, 3H, MeO); 5.66 (d, 1H, He-1); 7.10 (s, 1H, H_{arom}); 8.12 (s, 1H, H_{arom}); 7.30 (s, 5H, H_{arom}); 9.02 (d, 1H, NH); 12.48 (s, 1H, OH)
E	209–210 (EtOH)	$C_{18}H_{18}N_2O_4$ (326.3)	1665	A	3.79 (s, 3H, MeO); 3.91 (s, 3H, MeO); 3.03 (s, 3H, N—Me); 5.40 (s, 1H, He-1); 6.50 (s, 1H, H-8); 8.61 (s, 61 (s, H, H-3); 7.1—8.4 (m, 5H, H_{arom})
Z	238–239 (MeOH)	$C_{19}H_{14}N_2O_2$ (302.3)	1650	B	6.50 (d, 1H, He-1); 7.25 (s, 5H, H_a'$_{om}$); 7.4–7.6 (m, 2H, H_{arom}); 7.8—8.15 (m, 4H, H_{arom}); 10.07 (d, 1H, NH); 15.79 s, 1H, OH
E	206–208 (MeOH)		1665		

Table I (continued)

Product	R^1	R^5	R^6	R^7	R^8	Yield, %
10	C_6H_5	H	CH=CH–CH=CH	H	H	10
11	4'-Cl–C_6H_4	H	H	H	H	57
12	4'-Cl–C_6H_4	Me	H	H	H	72
13	2',6'-diCl–C_6H_3	H	H	H	H	16
14	3'-NO_2–C_6H_4	Me	H	H	H	36

[a] Non-corrected
[b] The microanalyses were in good agreement with the calculated values
[c] All IR spectra were recorded with a Perkin-Elmer Model 457 spectrometer

Table II

H-5 shift for the Z and E isomers in the ^{1}H-NMR *spectra of 4-(hydroxyimino)-1,4-dihydro-3(2H)-isoquinolinones*[a,b]

	R^1	R^2	R^6	R^7	R	δ (ppm)	
						Z	*E* (solvent)
1	H	H	H	H	H	8.02 (c)	8.65 (c+d; 9;1)
2	H	Et	H	H	H	7.88 (c)	
4	C_6H_5	H	H	H	H	7.90 (c)	8.42 (c)
5	C_6H_5	Me	H	H	H	8.06 (c)	8.95 (c)
7	C_6H_5	H	MeO	MeO	H		8.12 (d)[e]
8	C_6H_5	Me	MeO	MeO	H	7.44 (c)	8.57 (c)[e]
15	C_6H_5	H	H	H	Ac	8.24 (c)	
16	H	Et	H	H	tosyl	8.12 (c)	
18	C_6H_5	Me	MeO	MeO	CO–NH–C_6H_5		8.09 (c)[e]
19	H	Me	H	H	Me		8.38 (c)
21	C_6H_5	H	H	H	trityl		8.60 (c)

[a] All ^{1}H-NMR spectra were recorded with a JEOL-FX-100 spectrometer using TMS as internal standard; [b] Reference [7]; [c] Solvent c=$CDCl_3$; [d] Solvent d=DMSO-d_6; [e] 6,7-OMe groups cause the upfield effect

	m.p.[a] (solv.) °C	Molecular[b] formula	IR (KBr)[c] νO=C—N cm^{-1}	^{1}H-NMR[d] δ ppm
Z	196—198 ($CHCl_3$)	$C_{19}H_{14}N_2O_2$ (302.3)	1662	A/B 5.75 (d, 1H, H-1); 7.1—7.8 (m, 10H, (9:1) H_{arom}); 9.20 (d, 1H, H-5); 9.55 (d, 1H, NH);, 15.42 (s, 1H, OH)
E	175—180 (MeOH)	$C_{15}H_{11}N_2O_2Cl$ (286.7)	1655	
E	180—182 ($CHCl_3$—Et_2O)	$C_{16}H_{13}N_2O_2Cl$ (300.7)	1650	
E	239—241 (Dioxan)	$C_{15}H_{10}N_2O_2Cl_2$ (321.2)	1685	
Z	189—193 (MeOH)	$C_{16}H_{13}N_3O_4$ (311.3)	1630	
E	221—222 (MeOH)		1678	

[d] All ^{1}H-NMR spectra were recorded with a JEOL-100 spectrometer with tetramethylsilane as internal standard, Solvent A: $CDCl_3$; Solvent B: DMSO-d_6

Chemical shifts of the H-1 signal of the R^1=Ph derivatives greater than 5.37 ppm are indicative, on the basis of our earlier studies [8], also in this case of a *quasi-axial* position of the Ph group in the dominant conformer.

Experimental

4-(Hydroxyimino)-1,4-dihydro-3(2*H*)-isoquinolines

General procedure

1,4-Dihydro-3(2*H*)-isoquinolinone (0.19 mol) was dissolved or suspended in 900 mL of dry toluene, and butyl nitrite (1.15 mol) was added in one portion. Under vigorous stirring and bubbling of dry N_2 the mixture was cooled to 0°—2 °C, then potassium *t*-butoxide (0.36 mol; 40.4 g) was added at such a rate that the temperature did not exceed 5 °C. After having finished the addition, the toluene solution was immediately poured into water, the aqueous phase was acidified to pH 2 with 2*N* HCl, the precipitate was filtered off and washed with water. The still wet material was washed, depending on its solubility, with cold or warm ethanol; the 4-hydroxyimino-1,4-dihydro-3(2*H*)-isoquinoline was thus obtained in a satisfactory purity. When the crude product is a mixture of isomers, the pure *E* isomer can be isolated from the *Z* oxime by fractional crystallization. The *Z* isomer can be recovered from the oily residue obtained after evaporation of the toluene by trituration with diethyl ether and by recrystallizing the solidified material. Table I shows the data of these new compounds.

4-(Acetoxyimino)-1-phenyl-1,4-dihydro-3(2*H*)-isoquinolinone (15)

4-(Hydroxyimino)-1-phenyl-1,4-dihydro-3(2*H*)-isoquinolinone (0.09 mol; 0.2 g) was dissolved in acetic anhydride (3.0 mL) and heated for 10 min at 60—70 °C. On cooling the acetoxyimino derivative (0.15 g; 65%), precipitated m.p. 170—171 °C.

$C_{17}H_{14}N_2O_3$. (294.32). Calcd. C 69.38; H 4.79; N 9.52. Found 69.09; 4.65; 9.45%.

IR (KBr): 3290, 1768, 1688, 1600, 1452, 1372, 1225, 1192, 1015, 925, 875, 790, 730, 695 cm^{-1}.

^{1}H-NMR ($CDCl_3$): δ (ppm) 2.43 (s, 3H, CH_3CO); 5.70 (d, 1H, C_1-H); 7.0 – 7.6 (m, 8H, ArH); 8.32 (dd, 1H, C_5-H).

2-Ethyl-4-(tosyloxyimino)-1,3-dihydro-3(2*H*)-isoquinolinone (16)

2-Ethyl-4-(hydroxyimino)-1,4-dihydro-3(2*H*)-isoqiunolinone (4.0 g; 19.6 mol) was dissolved at room temperature in dry pyridine (50 mL), and to the stirred solution *p*-toluenesulfonyl chloride (4.0 g; 21 mmol) was added. The mixture was stirred for 2 h, poured onto ice, and acidified with 2*N* HCl to pH 2. The precipitated crystals were filtered off and washed with cold methanol to obtain 5.6 g (80%) of the product; m.p. 134 °C.

$C_{18}H_{18}N_2O_4S$ (358.42). Calcd. C 60.32; H 5.06; N 7.81; S 8.95. Found 60.47; 5.17; 8.01; 9.01%.

IR (KBr): 2970, 2920, 1655, 1587, 1480, 1450, 1370, 1292, 1192, 1174, 1095, 830, 810, 785, 688, 658, 548 cm^{-1}.

^{1}H-NMR ($CDCl_3$): δ (ppm) 1.2 (t, 3H); 3.58 (q, 2H, N – Et); 4.48 (broad s, 2H, N – CH_2); 2.41 (s, 3H); 7.91 (d, 2H, ArH); 7.1—7.5 (m, 5H, ArH); 8.12 (dd, 1H, C_5-H).

1-Phenyl-2-methyl-4-(tosyloxyimino)-1,4-dihydro-3(2*H*)-isoquinolinone (17)

1-Phenyl-4-(hydroxyimino)-2-methyl-1,4-dihydro-3(2*H*)-isoquinolinone (2.0 g; 7.5 mmol) was dissolved in dry pyridine (20 mL) tosyl chloride (2.0 g; 10 mmol) was added to the solution, and it was stirred at room temperature for 2 h. After pouring onto ice, the precipitated crystals were filtered off, washed with cold ethanol and dried to obtain 2.3 g (79%) of the product, m.p. 156 – 157 °C.

$C_{23}H_{20}N_2O_4S$ (420.50). Calcd. C 65.70; H 4.79; N 6.66; S 7.63. Found 65.66; 4.80; 6.90; 7.51%.

IR (KBr): 2918, 1672, 1598, 1450, 1438, 1400, 1375, 1325, 1190, 1180, 1090, 856, 820, 788, 738, 687, 575, 552, 548 cm^{-1}.

2-Methyl-6,7-dimethoxy-1-phenyl-4-[*O*-(*N*-phenylcarbamoyl)-hydroxyimino]--1,4-dihydro-3(2*H*)-isoquinolinone (18)

4-(Hydroxyimino)-2-methyl-6,7-dimethoxy-1-phenyl-1,4-dihydro-3(2*H*)-isoquinolinone (1.0 g; 3 mmol) was dissolved in toluene (20 mL), phenyl isocyanate (0.8 mL; 0.86 g; 7.4 mmol) was added to the solution, and it was refluxed for 50 min. On cooling the product (0.8 g) separated in crystalline form. Recrystallization from ethyl acetate gave 0.5 g (36.7%), of the pure product, m.p. 160 – 161 °C.

$C_{25}H_{23}N_3O_5$ (445.48). Calcd. C 66.30; H 5.50; N 8.60. Found 66.27; 5.68; 9.00%.

IR (KBr): 3380, 3000, 2930, 1475, 1655, 1575, 1528, 1508, 1440, 1372, 1318, 1190, 1130, 1050, 955, 922, 870 cm^{-1}.

^{1}H-NMR ($CDCl_3$): δ (ppm) 3.08 (s, 3H, NMe); 3.81 (s, 3H); 3.92 (s, 3H, OMe); 5.37 (s, 1H, C_1-H); 6.59 (s, 1H, C_8-H); 8.09 (s, 1H, C_5-H); 7.0 – 7.4 (m, 8H, ArH); 7.59 (mdd, 2H, $J_o = 9$ Hz, $J_m = 2$ Hz, ArH); 8.35 (s, 1H, NH).

4-(Methoxyimino)-2-methyl-1,4-dihydro-3(2*H*)-isoquinolinone (19)

4-(Hydroxyimino)-2-methyl-1,4-dihydro-3(2*H*)-isoquinolinone (3.0 g; 15 mmol) was dissolved in chloroform (30 mL) and then methyl iodide (4.0 mL; 9.12 g; 64 mmol) and silver oxide (10.0 g; 44 mmol) were added to the solution at room temperature. The mixture was stirred for 2 h filtered and evaporated in vacuum. On trituration with diethyl ether the oily residue (4.65 g) solidified to give 2.25 g (70%), of the product m.p. 118 – 120 °C. It can be recrystallized from methanol.

$C_{11}H_{12}N_2O_2$ (204.23). Calcd. C 64.69; H 5.92; N 13.72. Found 64.88; 6.14; 13.78%.

IR (KBr): 2930, 1658, 1560, 1342, 1260, 1055, 972, 865, 782, 752, 735, 705 cm^{-1}.

^{1}H-NMR ($CDCl_3$): δ (ppm) 3.20 (s, 3H); 4.18 (s, 3H, OMe); 4.56 (s, 2H, N—CH_2); 7.1—7.55 (m, 3H, ArH); 8.38 (m, 1H, C_5-H).

4-(Methoxyimino)-1-phenyl-1,4-dihydro-3(2*H*)-isoquinolinone (20)

The reaction of 4-(hydroxyimino)-1-phenyl-1,4-dihydro-3(2*H*)-isoquinolinone as described above yielded 1.6 g (50.6%) of the product which decomposed at 150 °C.

$C_{16}H_{14}N_2O_2$ (266.30). Calcd. C 72.17; H 5.30; N 10.51. Found 71.78; 5.69; 10.11%.

IR (KBr): 3050, 3010, 1622, 1538, 1482, 1430, 1395, 1320, 1245, 1222, 1050, 970, 960, 845, 758, 740, 695 cm^{-1}.

1-Phenyl-4-(trityloxyimino)-1,4-dihydro-3(2*H*)-isoquinolinone (21)

4-(Hydroxyimino)-1-phenyl-1,4-dihydro-3(2*H*)-isoquinolinone (0.4 g; 1.6 mmol) was dissolved in dry pyridine (10 mL) and triphenylmethyl chloride (0.44 g; 1.6 mmol) was added to the stirred solution. It was refluxed for 12 h, evaporated, the residue was dissolved in water and extracted with $CHCl_3$. The organic layer was dried over Na_2SO_4, clarified with charcoal and concentrated; the crystalline product (0.15 g; 20%), separated on cooling, m.p. 222 – 224 °C.

$C_{34}H_{26}N_2O_2$ (494.60). Calcd. C 82.56; H 5.30; N 5.66. Found 82.41; 5.18; 5.71%.

IR (KBr): 3080, 3050, 1678, 1585, 1572, 1488, 1442, 1405, 978, 945, 900, 755, 728, 695 cm^{-1}.

^{1}H-NMR ($CDCl_3$): δ (ppm) 5.58 (d, 1H, C_1-H, $J_{CH, NH} = 3$ Hz); 6.50 (broad, 1H, NH); 7.0 – 7.5 (m, 23H, ArH); 8.60 (m, 1H, C_5-H).

The authors express their thanks to Mrs. J. Haskó – Breuer for recording the infrared spectra, to Miss M. Fodor for the microanalyses, and to Miss J. Hamar and Mrs. I. Kovács for technical assistance.

REFERENCES

[1] Tikk, I., Deák, Gy., Tóth, G.: Acta Chim. Acad. Sci. Hung., **106**, 83 (1981)
[2] Deák, Gy., Hazai, L., Tóth, G.: J. Heterocycl. Chem., **14**, 583 (1977)
[3] Bartmann, W., Konz, E., Kruse, H.: Ger. Offen 2,811,361 (1970); Chem. Abstr., **92**, 6431n (1980)
[4] Touster, O.: The Nitrosation of Aliphatic Carbon Atoms, in Org. Reactions, Vol. **7**, pp. 327 – 377. John. Wiley and Sons Inc., London 1953
[5] Warhant, J., Farcilli, A., Toromnoff, E.: Ger. Offen 2,115,718 (1971); Chem. Abstr., **76**, 34462m (1953)
[6] Martin, G. J., Martin, M. L.: The stereochemistry of double bonds p. 198, in Progress in NMR Spectroscopy, Vol. **8**, Pergamon Press, Oxford 1972
[7] Pretsch, E., Clerc, T., Siebl, J., Simon, W.: Tabellen zur Strukturaufklärung organischer Verbindunger mit spektroskopischen Methoden, p. 4255, Springer-Verlag, Berlin 2nd Ed. 1981
[8] Tóth, G., Hazai, L., Deák, Gy., Duddeck, H.: Liebigs Ann. Chem. **1978**, 1103

Acta Chimica Hungarica 114 (1), pp. 79–87 (1983)

A KINETIC-MATHEMATICAL MODEL OF ETHANE PYROLYSIS

P. SIKLÓS[1]*, Á. BÁLINT[1] and L. F. ALBRIGHT[2]

([1]Technical University, Department of Chemical Technology, H-1521 Budapest, Budafoki u. 8. and [2]Purdue University, West Lafayette, Indiana, U.S.A.)

Received May 19, 1982
Accepted for publication November 23, 1982

A kinetic-mathematical model based on a free radical chain mechanism is described. The model can predict ethane pyrolysis data under non-isothermal, non-isobaric industrial conditions. The concentration changes of the components are represented by a system of differential equations. It was solved using the numerical integration method of Gear. (Thus the steady-state principle was not applied, that is, changes in the concentrations of free radicals could also be accounted for.) Due to the increased number of molecules, a chemical expansion factor, and due to temperature rise and pressure decrease, a physical expansion factor was taken into consideration in the integration procedure. The temperature and pressure profiles of the tubular reactor were described by regression polynomials. The steps of ethane pyrolysis are summarized in a reaction matrix. The constants of the Arrhenius equations were taken from the literature. Twenty reactions, most of them reversible, are involved in the model.

Product gas composition was determined experimentally under different conditions in a commercial pyrolysis unit. Compositions predicted by the model are in very good agreement with the experimental data and with data from the literature.

According to our present knowledge, hydrocarbon pyrolysis proceeds by a free-radical chain mechanism (known as the Rice—Herzfeld mechanism).

The models proposed by Snow [1], Herriot, Eckert and Albright [2], Edelson and Allara [3] and Dunkleman and Albright [4] involve free-radical reactions. These models were, however, developed and used for pyrolysis data only at essentially isothermal and isobaric conditions.

To model non-isothermal, non-isobaric pyrolysis processes, empirical models, that is, such involving molecular reactions were applied, thereby simplifying the numerical integration procedure; Froment et al. [5], Shah [6]. Recently Sundaram and Froment [7] have proposed a model based on free-radical reactions which is suitable for describing non-isothermal, non-isobaric conditions. The model consists of 133 free-radical and molecular reactions, being — with one exception — homogeneous gas-phase reactions. The authors recommend various combination of the 133 reactions to describe the pyrolysis process of different hydrocarbons. Good agreement was found between the predicted data and product gas composition determined in a pilot plant. According to their earlier paper [5], product composition in the pilot plant is similar to that in a commercial tubular reactor.

* To whom correspondence should be addressed.

Independent of Sundaram and Froment, we have developed a kinetic-mathematical model based on free-radical chain reactions, for the prediction of ethane pyrolysis data under non-isothermal, non-isobaric conditions [8, 9]. Our objective is to establish a model for industrial tubular reactors.

The kinetic model

Most of the 20 reactions utilized in our model are reversible; they contain a total of 12 components (Table I).

Table 1

Reaction schemes and rate constants used in the calculations

(frequency factor A, s^{-1}; $cm^3\ mol^{-1}\ s^{-1}$, and activation energy A, kcal mol^{-1})

No.	Reaction	Forward reaction		Reverse reaction	
		A	ΔE	A	ΔE
1.	$C_2H_6 \rightleftarrows 2CH_3^{\cdot}$	4×10^{16}	86.0	3.8×10^{13}	0
2.	$CH_3^{\cdot} + C_2H_6 \rightleftarrows CH_4 + C_2H_5^{\cdot}$	1×10^{12}	10.6	1.0×10^{11}	11.0
3.	$CH_3^{\cdot} + H_2 \rightleftarrows CH_4 + H^{\cdot}$	3.2×10^{12}	10.2	1.3×10^{14}	12.6
4.	$C_2H_5^{\cdot} \rightleftarrows C_2H_4 + H^{\cdot}$	3.8×10^{13}	38.0	4.0×10^{13}	1.6
5.	$H^{\cdot} + C_2H_6 \rightleftarrows C_2H_5^{\cdot} + H_2$	1.3×10^{14}	9.7	3.0×10^{11}	10.8
6.	$H^{\cdot} + C_2H_5^{\cdot} \rightarrow C_2H_6$	2.1×10^{14}	0		
7.	$CH_3^{\cdot} + C_2H_5^{\cdot} \rightarrow CH_4 + C_2H_4$	1.5×10^{11}	0		
8.	$2C_2H_5^{\cdot} \rightleftarrows C_4H_{10}$	1.7×10^{13}	0	7.9×10^{17}	86.0
9.	$2C_2H_5^{\cdot} \rightarrow C_2H_4 + C_2H_6$	2.6×10^{12}	0		
10.	$C_3H_8 \rightleftarrows C_2H_5^{\cdot} + CH_3^{\cdot}$	1.2×10^{17}	86.0	4.2×10^{12}	0
11.	$C_2H_5^{\cdot} + C_3H_8 \rightarrow C_2H_6 + C_3H_7^{\cdot}$	7.5×10^{10}	10.0		
12.	$CH_3^{\cdot} + C_3H_8 \rightleftarrows CH_4 + C_3H_7^{\cdot}$	8.1×10^{11}	10.3	2.5×10^{11}	19.5
13.	$H^{\cdot} + C_3H_8 \rightleftarrows H_2 + C_3H_7^{\cdot}$	3.2×10^{13}	7.8	6.3×10^{12}	14.6
14.	$C_3H_7^{\cdot} \rightleftarrows C_2H_4 + CH_3^{\cdot}$	2.0×10^{12}	34.5	3.3×10^{11}	7.8
15.	$C_3H_7^{\cdot} \rightleftarrows C_3H_6 + H^{\cdot}$	1.0×10^{14}	37.0	2.5×10^{14}	3.8
16.	$CH_3^{\cdot} + C_3H_6 \rightarrow C_2H_4 + C_2H_5^{\cdot}$	3.2×10^{10}	7.5		
17.	$C_3H_7^{\cdot} + C_3H_7^{\cdot} \rightarrow C_3H_6 + C_3H_8$	6.3×10^{13}	0		
18.	$CH_3^{\cdot} + C_3H_7^{\cdot} \rightarrow C_4H_{10}$	4.0×10^{12}	0		
19.	$CH_3^{\cdot} + C_2H_5^{\cdot} \rightarrow XCH_4 + \left(\frac{1}{2} - \frac{X}{6}\right)C_6H_6 + \left(\frac{5}{2} - \frac{3X}{2}\right)H_2$	1.3×10^{13}	0	—	
20.	$2\,C_2H_5^{\cdot} \rightarrow 2XCH_4 + \left(\frac{2}{3} - \frac{X}{3}\right)C_6H_6 + 3(1-X)H_2$	2.0×10^{13}	0		

This list of reactions is similar to those utilized in the model of Dunkleman and Albright [4]. We omitted seven secondary reactions, e.g. $H^{\cdot} + C_2H_4 \rightleftharpoons C_2H_3^{\cdot} + H_2$, and changed the values of several rate parameters. Also, we added two additional reactions (Nos 19 and 20) which, among other products, yield benzene. All high-molecular aromatic compounds occurring in the product gas were assumed to be as benzene.

The stoichiometric coefficients of the reactions are given by a stoichiometric matrix in which each row and each column corresponds to a reaction and component, respectively. Values of the stoichiometric coefficient X for the last two reactions Nos 19 and 20 are temperature-dependent. Snow et al. [1] reported the values for three temperatures:

X	0.5	0.85	0.95
T (K)	863	1089	1255

A polynomial of the second degree was fitted to the three pairs of points X—T, and X was calculated for the given temperatures. The two rows of the stoichiometric matrix containing X as stoichiometric coefficient were corrected after each integration step.

The constants of the Arrhenius equations A and ΔE were taken from the literature [4, 7, 10, 11].

The mathematical model

The principle of our mathematical calculation was suggested by Snow et al. [1]. After solving the rate equations, the system of differential equations representing the changes in the concentration of the components with time are solved. The principle of the calculations is

$$\frac{dc_j}{dt} = \sum_{i=1}^{n} \gamma_{ij} w_i$$

where γ_{ij} is the stoichiometric coefficient of component j in reaction i

$$w_i = \vec{k}_i \prod_j^{-} c_j^{|\gamma_{ij}|} + \overleftarrow{k}_i \prod_j^{+} c_j^{|\gamma_{ij}|} = \text{the rate of reaction } i$$

$\vec{k}_i$ and $\overleftarrow{k}_i$ are the rate constants of the forward reaction i and the reverse reaction i, respectively; c_j is the actual concentration of component j; t is time and n is the number of reactions considered in the model.

Snow employed the numerical technique of Runge—Kutta to solve the system of differential equations. He applied the steady-state principle, that is, he neglected, after a short period of initiation, the rates of changes on free radical concentrations beside the rates of changes in molecule concentrations.

To calculate the steady state radical concentrations, Newton's iteration procedure was applied by Snow. Against this simplification Edelson and Allara [3] recommended the numerical integrating technique of Gear, which takes into account concentration changes of free radicals too. Their calculations demonstrated that the concentrations of the radicals, $H^{\cdot}$, $CH_3^{\cdot}$ and $C_2H_5^{\cdot}$ — playing an important part in Snow's model — are not constant. We therefore also applied Gear's numerical integrating technique to solve the system of differential equations representing changes in the concentration of the components. For each integration step, we assumed isothermal and isobaric conditions. The concentrations calculated were then corrected after each step for the temperature and pressure changes along the tubular reactor occurring as the reaction progresses. The temperature and pressure profiles of the reactor were described by polynomials;

$$T_k = T_0 + T_1\frac{l_k}{l_t} + T_2\left(\frac{l_k}{l_t}\right)^2 + \ldots + T_n\left(\frac{l_k}{l_t}\right)^n$$

$$p_k = p_0 + p_1\frac{l_k}{l_t} + p_2\left(\frac{l_k}{l_t}\right)^2 + \ldots + p_m\left(\frac{l_k}{l_t}\right)^m$$

where T_k, p_k are the temperature and pressure after integration step k; T_0, T_1, $T_2 \ldots T_n$ and p_0, p_1, $p_2 \ldots p_m$ are constants, l_t is the total length of the tubular reactor and l_k is the length coordinate. The constants of the polynomials for a given tubular reactor were calculated from experimental results using regression analysis.

The effects of the varying parameters temperature and pressure were accounted for by means of a coefficient termed physical expansion factor:

$$\mathrm{Exp}_{\mathrm{phys},k} = \frac{T_k\, p_0}{T_0\, p_k}$$

where $\mathrm{Exp}_{\mathrm{phys},k}$ is the physical expansion factor after integration step k; T_0 and p_0 are temperature and pressure, respectively, at the inlet of the reactor. The value of this factor always exceeds 1, since temperature increases and pressure decreases along the tubular reactor as the reaction progresses.

A further correction was necessary due to the expansion of the gas mixture caused by the increased number of molecules. A coefficient termed chemical expansion factor was introduced for this purpose:

$$\mathrm{Exp}_{\mathrm{chem},k} = \frac{n_{tk}}{n_t^0}$$

where $\mathrm{Exp}_{\mathrm{chem},k}$ is the chemical expansion factor after integration step k; n_{tk} is the number of molecules after integration step k, and n_t^0 is the initial number of molecules.

The corrected actual concentration is hence expressed by

$$c'_{jk} = c_{jk} \frac{(\mathrm{Exp_{chem}}\,\mathrm{Exp_{phys}})_{k-1}}{(\mathrm{Exp_{chem}}\,\mathrm{Exp_{phys}})_k}$$

where c'_{jk} is the corrected concentration of the component j after integration step k, and c_{jk} is the corresponding calculated concentration. The corrected concentration is lower than calculated, due to the expansion of the gas mixture.

It should, however, be noted that the calculation of the length coordinate and of the expansion factors is not as simple as shown above. On the one hand,

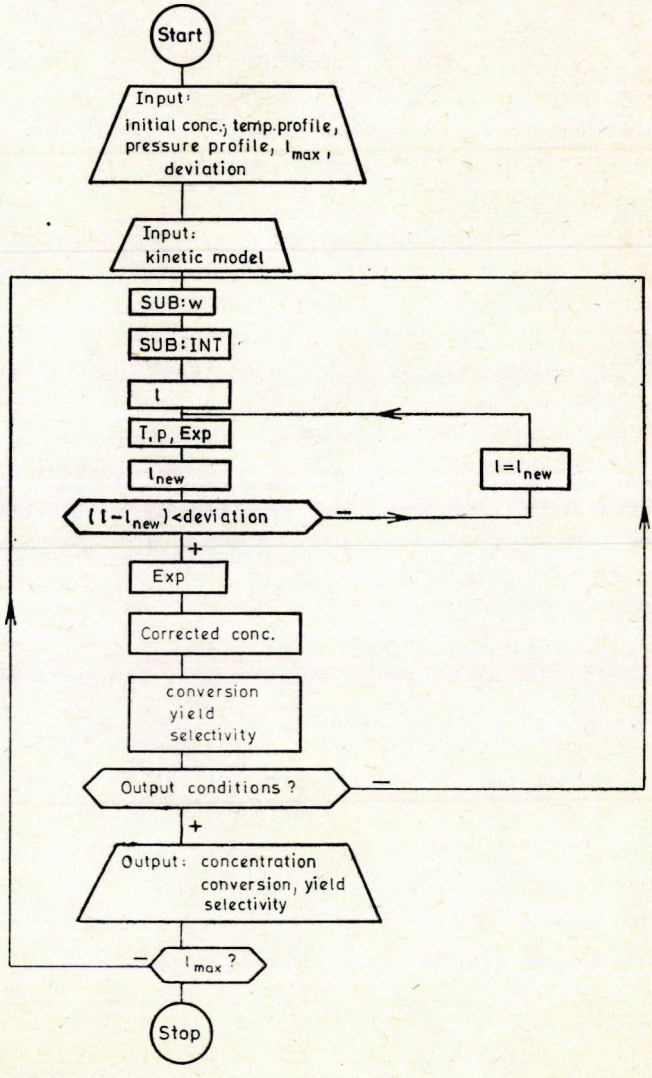

Fig. 1. Simplified flow-chart of the computer program

the length coordinate is calculated using the expansion coefficients. On the other hand, the knowledge of the length coordinate is required to calculate the expansion factors (to calculate actual temperature and pressure values). For this reason an iteration technique was needed to calculate these values.

Rate constants are also temperature-dependent, and must therefore be recalculated after each integration step for the new temperature, using the Arrhenius equation.

In addition to the concentrations of the reactants, conversion, yield and selectivity were also calculated. A simplified flow chart of calculations is presented in Fig. 1.

Results of calculations

The values calculated with our model and program were compared with the experimental values measured in a commercial pyrolysis unit, and also with data from the literature.

The conditions in the commercial unit were as follows: the ethane-steam mixture preheated in a convection zone entered the radiation zone at a temperature of 600—650 °C. Decomposition proceeding in the convection zone was neglected and only the pyrolysis reactions in the radiation zone were considered in the model. The internal diameter of the tubular reactor was 108 mm. The volumes of the collector and transfer tubes to the quench cooler were neglected. Temperature was measured at four points and the temperature profile was represented by a third-degree equation. Pressure was measured at the inlet and outlet only. Nonetheless, we assigned a polynomial of the second degree to the pressure profile. The samples for analysis were taken after the quench cooler.

The comparison of measured and calculated values is presented in Table II.

Product gas compositions calculated with the model are in very good agreement with the measured compositions. This is particularly the case for the main components ethane, ethylene, hydrogen and methane. Agreement for propane and propylene is also good. More important differences between measured and calculated values are observed in the cases of C_4 hydrocarbons and benzene. It should, however, be noted that in our program the term "benzene" includes all aromatics and heavy hydrocarbons formed in secondary reactions. Hence coke, and carbon oxides from coke and steam could be taken into considertion to some extent, and this might then serve as an explanation for the high values of the calculated "benzene" content.

Froment and al. [5] have published some results based on industrial data where detailed reaction conditions and the concentrations of the main components in the product gas are given. We hence checked the validity of our model and program with Froment's experimental data. The results are

Table II

Measured and calculated product compositions for threee sets of pyrolysis conditions

	Conditions of pyrolysis		
Ethane feed ($Nm^3\ h^{-1}$)	1570	1541	1661
Steam dilutions (mol%)	50.8	51.2	63.0
Inlet pressure (Pa)	4.40×10^5	4.40×10^5	4.50×10^5
Outlet pressure (Pa)	1.60×10^5	1.60×10^5	1.54×10^5
Temperature			
inlet (°C)	638	649	673
at 0.56 rel.length	780	790	795
at 0.78 rel.length	800	812	813
outlet	815	822	825

Composition (mol %)

Component	Feed	Product gas					
		measured	calcd.	measured	calcd.	measured	calcd.
H_2		29.44	30.02	31.70	32.15	30.68	31.19
CH_4		2.51	2.75	2.94	3.18	3.54	3.32
C_2H_2		0.01		0.03		0.02	
C_2H_4		28.99	28.10	29.30	29.87	32.50	32.26
C_2H_6	99.8	37.51	37.79	34.20	33.28	30.52	31.67
C_3H_6	0.2	0.29	0.32	0.32	0.36	0.36	0.36
C_3H_8		0.03	0.04	0.05	0.05	0.08	0.05
C_4 hydrocarbons		0.31	0.57	0.35	0.63	0.34	0.64
benzene		0.03	0.40	0.04	0.48	0.04	0.51
CO		0.90		0.97		1.89	

presented in Table III indicating very good agreement between our values and the values experimentally measured by Froment.

Sundaram and Froment have more recently [7] described the process of ethane pyrolysis with a model involving 49 reactions of a total of 20 components (11 molecules and 9 free radicals). Our model comprises 31 reactions of a total of 12 components (8 molecules and 4 free radicals). 16 reactions are common in both models but in these reactions the two models use significantly different A and ΔE values. As mentioned earlier, even empirical models consisting of only molecular reactions can correctly predict the results of ethane pyrolysis. This finding that three distinctly different models could all effec-

Table III

Product compositions measured experimentally by Froment et al. [5], calculated by Froment and in this work

	Parameters of pyrolysis
Ethane feed	68.68 kg m^{-2} s^{-1}
Steam dilution	0.4 mass%
Length of radiation zone	95 m
Internal diam. of tube	0.108 m
Inlet pressure	3.09×10^5 Pa
Outlet pressure	2.06×10^5 Pa
Temperature	
inlet	680 °C
at 0.4 rel.length	770 °C
at 0.8 rel.length	820 °C
outlet	835 °C

Composition (mol%)

Component	Feed	Product gas		
		measured	calcd. by Froment	calcd. in this work
H_2		3.71	3.75	3.64
CH_4		3.35	3.45	3.60
C_2H_6	98.2	39.27		38.65
C_2H_4	1.0	48.68	48.00	48.00
C_3H_8		0.21		0.21
C_3H_6	0.8	1.07		1.17
C_2H_2		0.20		
C_4 hydrocarb.		1.63		2.14
benzene				2.40

tively predict data of ethane pyrolysis suggested the following ideas. If no reliable experimental data exist for individual A and ΔE values (and apparently they do not exist, since the different authors calculate with significantly different values) how many reactions should be incorporated in the model? Presumably, any desired product composition data can be calculated by increasing the number of reactions involved and modifying the rate parameters. The model of Sundaram and Froment contains, for instance, many C_4 and C_5 free-radical reactions. Yet it does not consider the reaction $C_3H_8 \rightleftharpoons C_2H_5^{\cdot} + CH_3^{\cdot}$,

which in our opinion is at least as important as C_4 and C_5 free-radical reactions are, and strongly affects the composition of the product gas.

Reliable measurement of A and ΔE values for the pressure and temperature conditions of commercial pyrolysis processes should therefore be the most important objective in this field for further progress. Heterogeneous reactions like e.g. coke formation should also be investigated more closely.

REFERENCES

[1] Snow, R. H., Peck, R. E., Fredersdorff, C. G.: AICHE Journal, **5,** 304 (1959)
[2] Herriott, E. G., Eckert, R. E., Albright, L. F.: AICHE Journal, **18,** 184 (1972)
[3] Edelson, D., Allara, D. L.: AICHE Journal, **19,** 638 (1973)
[4] Dunkleman, J. J., Albright, L. F.: Industrial and Laboratory Pyrolyses, pp. 141—260. Amer. Chem. Soc., Washington, D. C. 1976
[5] Froment, G. F., Van de Steene, B. O., Van Damme, P. S.: Ind. Eng. Chem. Proc. Des. Dev., **15,** 495 (1976)
[6] Shah, N. J.: Ind. Eng. Chem., **59,** 70 (1967)
[7] Sundaram, K. F., Froment, G. F.: Ind. Eng. Chem. Fundam., **17,** 174 (1978)
[8] Németh, T.: Thesis, Technical University, Budapest 1977
[9] Bálint, Á.: Thesis, Technical University, Budapest 1978
[10] Snow, R. H.: J. Phys. Chem., **70,** 2780 (1966)
[11] Benson, S. W.: The Foundations of Chemical Kinetics, pp. 50—54. Mc Graw-Hill, New York 1960

Acta Chimica Hungarica 114 (1), pp. 89—93 (1983)

SIMPLE METHODS FOR THE DETERMINATION OF PHOSPHONATES

Zs. WITTMANN* and N. SZEBÉNYI

(Hungarian Oil and Gas Research Institute ,H-8201 Veszprém, József A. u. 34.)

Received July 5, 1982
In revised from October 25, 1982
Accepted for publication November 23, 1982

Two simple titrimetric methods are described and checked by NMR spectrometry for determining the phosphonate content in inorganic phosphorus containing phosphonate products and solutions.

Corrosion and scale in cooling tower waters is often eliminated by phosphorus-containing organic compounds, phosphonates such as nitrilotrismethylenetriphosphonic acid (NTMP) and hydroxyethylenediphosphonic acid (HEDPA). These phosphonates in cooling tower waters are determined by titrimetric [1, 2] and colorimetric methods [3, 4, 5].

Sloat and Buck [6] examined these five methods and established their defects. Their new method [6], an iron chelation method, eliminates the interferences. Sample after total complexation of the phosphonate in the presence of excess iron(III) is passed through a cation exchange column to remove excess iron and other metal ions. The phosphonate in the chelate is determined after addition of a strong reducing agent and 1,10-phenanthroline indicator by colorimetric method on the basis of iron content in the complex. The above mentioned methods are suitable to determine phosphonates in cooling tower waters at very low concentrations. To follow phosphonate production, one needs less sensitive but simple and rapid methods.

In this apper methods are described for following the production of phosphonates. They are modified methods of Sloat's. After removing the iron chelated by the phosphonate from the cation exchange column the excess iron(III) ions are eluted from the resin and titrated by a complexometric method for HEDPA and NTMP and a direct complexometric method for HEDPA. These methods were checked by NMR spectrometry.

Phosphonates in the presence of excess iron(III) at a pH between 2.5 and 2.6 form complexes. Then samples are passed through a cation exchange column. The iron complex passes through and the excess iron remains on the

* To whom correspondence should be addressed.

resin. This excess iron is eluted with 4 *M* hydrochloric acid solution and measured by a complexometric method. The amount of phosphonate is determined from the difference of the total and excess iron concentrations. The ion exchange resin is Amberlite IR-120 (H^+-form) as recommended by Sloat and Buck [6].

The other simple possibility is to determine the excess of iron(III) ions by a complexometric method directly from the solution containing the iron complex and excess iron(III) ions. But the excess of iron(III) ions from the solution of iron NTMP complex cannot be determined because of the poor indication in the opalescent solution. Presence of phosphate does not disturb the methods.

According to the data Sloat and Buck [6], iron is combined with NTMP in a 3/1 and HEDPA in a 1/1 molar ratios. Our experiments show the same results. The effect of the raw materials, intermediates (acetic acid, acetyl chloride, phosphonic acid, phosphorus trichloride) are checked in the solution of phosphonates. Neither substance causes an interference.

Determination of HEDPA and NTMP

The sample containing about 0.2—0.6 mmol phosphonate is diluted by 10 cm^3 demineralized water and the pH is adjusted to pH = 3 ± 0.2 with 1 *M* sodium hydroxide. 25.0 cm^3 of 0.02 *M* iron(III) solution (pH not less than 2.0) is added. After mixing, the solution is loaded into the ion exchange column (15 cm long, 1 cm i.d. tube, filled with Amberlite IR — 120 resin washed with demineralized water). The resin is washed with 50 cm^3 demineralized water. 5 cm^3 4 *M* hydrochloric acid solution is added to elute the iron(III) ions from the resin, then the resin is washed with demineralized water until the solution dropping from the resin is neutral. The iron(III) ion content of the solution is titrated with 0.02 *M* ethylenediamine-*N*,*N*,*N*,'*N*'-tetraacetic acid (EDTA) using sulfosalycilic acid indicator [7].

HEDPA determination by a direct method

The sample containing about 0.2— 0.6 mmol phosphonate is diluted with 50 cm^3 demineralized water and 25.0 cm^3 0.02 *M* iron(III) solution is added to the sample. The pH of the solution is adjusted as described above and the solution is titrated with EDTA using sulfosalycilic acid as indicator.

^{1}H-NMR was chosen as a suitable analytcial method to study and control phosphonate production where an inorganic phosphorus compound as phosphonic acid is converted to an organic phosphonate compound. The phosphonic acid in its stable predominant form has a proton bound to phos-

phorus. Therefore, the spectrum of phosphonic acid in the mixture is a doublet in both (^{1}H and ^{31}P) NMR spectra with a large coupling constant I_{P-H} 780 Hz with peaks at ca. —19 and +7 ppm in ^{31}P NMR spectrum and at ca. 1.4 and 14.4 ppm is proton NMR spectrum.

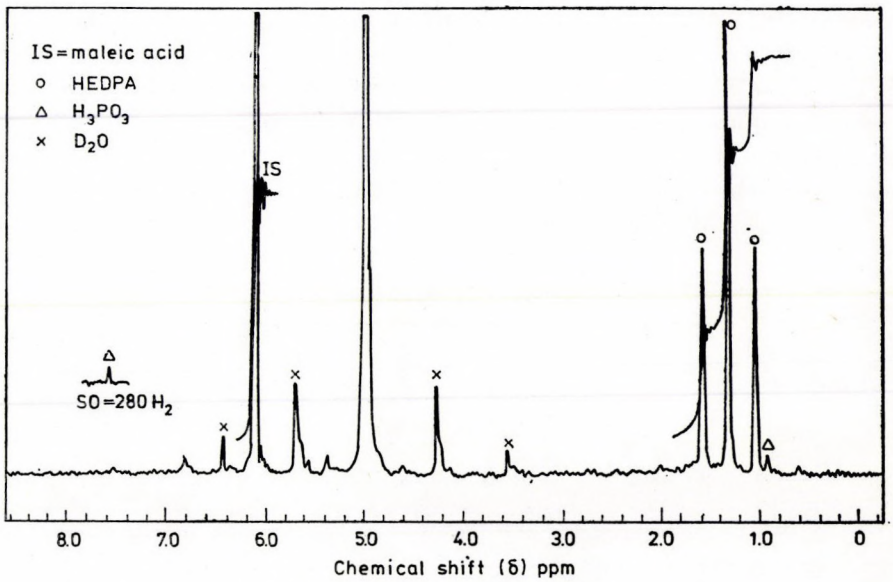

Fig. 1. NMR spectra of NTMP

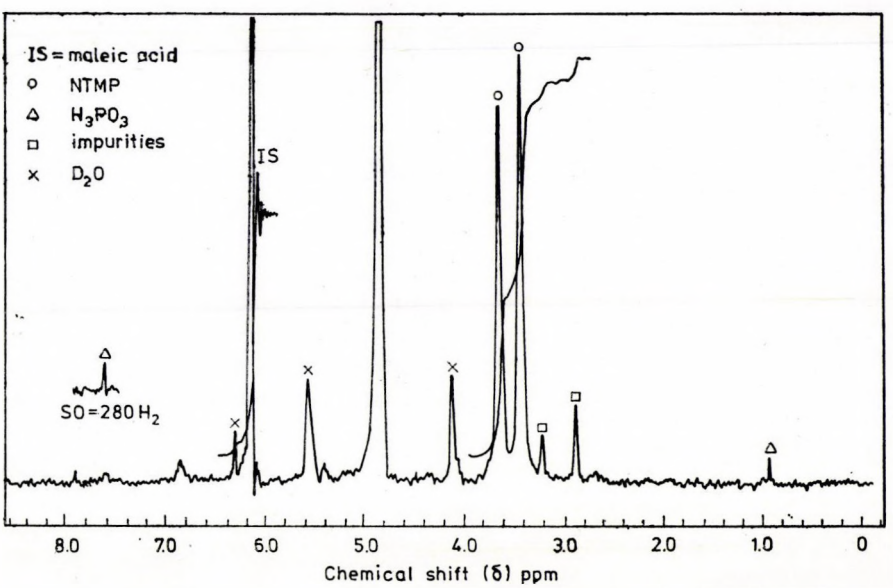

Fig. 2. NMR spectra of HEDPA

The mixtures containing NTMP were prepared by evaporating the volatile parts and dissolving the residue in deuterated water for proton NMR measurements. NTMP was shown by the appearance of the doublet at ca. 4.1 ppm [8].

In the case of HEDPA the sample was diluted, without evaporating, with deuterated water for the ^{1}H-NMR measurements. The method is fast but is disturbed by the large amount of intermediate present. In addition to this the organic phosphonate is present mostly in a complex form containing the dimerized and acetylated form of HEDPA [9]. In this case the method is less adequate. The decrease and disappearance of the resonance signal of phosphonic acid permits to measure HEDPA formation.

Table I

Reproducibility of phosphonate

Sample	Mean ± SD (g/100 g)		
	Modified Sloat's method	Direct method	NMR spectrometry
HEDPA	74.2 ± 3.0	76.1 ± 3.8	75.2 ± 3.0
	16.6 ± 0.7	16.6 ± 0.8	17.1 ± 0.7
NTMP	61.8 ± 2.5	—	60.2 ± 2.4
	14.6 ± 0.6	—	14.2 ± 0.6

Table II

Some data of phosphonates determined by different methods

Phosphonate		Phosphonate content determined by		
		titrimetric methods		NMR spectrometry
		modified Sloat's method	direct method	
		(g/100 g)		
HEDPA	1	63.0	62.7	64.5
	2	74.2	76.1	75.2
	3	48.5	49.3	47.4
	4	16.6	15.4	17.1
NTMP	1	14.6	—	14.2
	2	34.5	—	36.3
	3	61.8	—	60.2
	4	75.1	—	74.7

Determination of phosphonates by NMR spectrometry

In both cases the quantitative evolution of NMR spectra obtained during the reaction help establish the preferred reaction conditions. To determine the phosphonate content, maleic acid is used as internal standard in both cases. NMR spectra of NTMP and HEDPA containing samples can be seen in Figs 1 and 2.

To test the reproducibility of the analysis, two samples were determined by each method ten times. The data are shown in Table I.

Finally the NTMP and HEDPA (phosphonates) content of some intermediate samples determined by titrimetric methods and NMR spectrometry are summarized in Table II.

To determine the phosphonates content, two titrimetric methods were developed. The data of Table II show good agreement between the titrimetric methods and the results of NMR spectrometry as a control method.

REFERENCES

[1] King, T. M., Malic, E. I.: Special Report 7158, Monsanto Industrial Chemicals Company, St. Louis 1968
[2] King, T. I., Mitchell, R. S.: Special Report 7666, Monsanto Industrial Chemicals Company, St. Louis 1970
[3] Spink, G. C.: Special Report of 7917, Monsanto Industrial Chemicals Company, St. Louis 1972
[4] Kindell, L. E.: Special Report 7823, Monsanto Industrial Chemicals Company, St. Louis 1972
[5] Harris, H. P.: Monsanto Industrial Chemicals Company, private communication 1978 (from ref. [6])
[6] Sloat, S. S., Buck, M.: Proc. International Water Conf. Eng. Soc. West Pa., **39,** 442 (1978)
[7] Sajó, I.: Komplexometria. Műszaki Könyvkiadó, Budapest 1974
[8] Moedritzer, K., Irani, R. R.: J. Org. Chem., **31,** 1603 (1966)
[9] Kosolapoff, G. M., Maier, L.: Organic Phosphorus Compounds, Vol. **VII** p. 14. John Wiley Co. Sons New York—London—Sydney—Toronto 1976

BOOK REVIEWS

Structure and Bonding, Vol. 50

Springer Verlag, Berlin, Heidelberg, New York, 1982

Vol. **50** of the fascinating series presents four reviews:

— J. A. Ibers, L. J. Pace, J. Martinsen, B. M. Hoffman: Stacked Metal Complexes: Structures and Properties (pp. 1—55)

— M. J. Clarke, P. H. Fackler: The Chemistry of Technetium: Toward Improved Diagnostic Agents pp. (57—78).

— R. J. P. Williams: The chemistry of Lanthanide Ions in Solution and in Biological Systems pp. (79—119).

— C. K. Jørgensen, R. Reisfeld: Uranyl Photophysics (pp. 121—171).

(1) In the review the authors discuss the structural aspects of crystals that contain molecular stacks and are comprised of two components, at least one of which is a planar transition-metal chelate complex. In an integrated stack crystal the metal-ligand complex is either neutral or ionic; in a segregated stack crystal it either has an integral oxidation state or a non-integral oxidation state. The non-integral oxidation state is sometimes referred to as "partial oxidation", "mixed valence", or "incomplete charge transfer". Some compounds are primarily of structural interest, while others have unusual magnetic properties. Still others, particularly those involving metallomacrocycles, exhibit high or unusual electrical conductivities. The authors anticipate a successful correlation of structures with physical properties that will accelerate the synthesis and utilization of these materials.

(2) From 1937, when technetium was explored as the first man-made element, until the ready availability of ^{99m}Tc for medical purposes, the chemistry of this element was regarded largely as an academic curiosity. Technetium is formed in good yield in fission reactors fueled by ^{235}U and it has found practical application in nuclear medicine. Owing to the development of the "technetium generator" almost two decades ago, ^{99m}Tc is now the preferred isotope for many diagnostic studies involving the imaging of internal organs by radioscintigraphic techniques. Subtle chemical differences often control the relative stabilities of the various oxidation states and each oxidation state exhibits more than one geometry. Coordination compounds involving Tc(III), Tc(IV) and Tc(V) tend to predominate in preparations used for diagnosis. The new synthetic methods for technetium compounds in the oxidation states I, II and V with well-described chemistry will play an important role in the development of improved radioscintigraphic agents.

(3) There are two outstanding reasons for the study of the Ln(III) ions as probes of biological action: (a) they are the simplest cations which have useful physical properties and a chemistry closely allied to that of Ca(II); (b) together they form a series which allows a knowledge of the interaction, of a (purely) electrostatic nature, between cations and water or organic ligands. In this review there is an examination of the structure of the Ln(III)-ion complexes in solution using NMR methods carried out in considerable detail. The importance of hydration in both the inner and outher spheres is stressed and the structural data are used in an attempt to understand the stability constants and the rates of exchange of bound ligands. Closely to the former, the importance of the structures, the stability constants and the kinetic properties are related to the effects of lanthanide(III) ions in biological systems.

(4) Among the elements known before transuranium elements started to be synthetized in 1940, uranium has a unique characteristic, namely the extreme stability of the triatomic uranyl ion, UO_2^{2+}. The electron transfer bands of the ion are due to a complicated manifold of excited levels described by relativistic effects in linear symmetry. The lowest of these energy levels can live for longer than 1 millisecond and has its own chemistry, reacting with many anions, univalent silver and thallium, in a way entirely different from the ground state. It is nearly as oxidizing as fluorine, forms exciplexes, and abstracts hydrogen atoms from organic

substances and from water. The spectroscopic and luminescent properties are compared with the hexafluorides and the dioxo complexes of quinquevalent and sexivalent uranium, neptunium, plutonium and americium, and with roughly octahedral species, and tungstates. Uranyl glasses are useful for energy transfer to lanthanides and converting solar energy via photovoltaics. All these show, how inorganic chemistry still seems to reveal endless supplies of surprises.

S. PAPP

Department of General and Inorganic Chemistry,
Veszprém University of Chemical Engineering,
Veszprém

B. Magyar: *Guide-lines to planning atomic spectrometric analysis*

Akadémiai Kiadó, 273 pages

The series "Studies in analytical chemistry" is published by Akadémiai Kiadó: Vol. 4 is written by B. Magyar for specialists in atomic absorption spectrometry. "Atomic absorption spectrophotometry" by W. I. Price, which appeared in 1977, and the book of Magyar complement each other, as the work of Price discusses mainly the problems of the analysis, sample preparation, and suggests instrumental parameters to be used, while the book of Magyar deals in detail with basic physicochemical knowledge needed for practical work.

The book consists of six chapters and two appendices.

In the introductory first chapter the place of atomic absorption spectrometry is outlined in comparison with other microanalytical methods. The concentration ranges which can be studied by the individual methods are also given.

In the second and third chapters the principles of spectrochemical methods using electromagnetic radiations are discussed. Radiation sources of the older and most modern types are treated (hollow cathode lamp, electrodeless discharge lamp, X-ray lamp, laser). The reasons for the splitting of spectral lines emitted by the hollow cathode lamp (line broadening due impact, Doppler and Lorentz effect) are dealt with in detail, as well as their influence on the initial slope of the linear part of the calibration curves which, in turn, determines the sensitivity of the analysis.

In Chapter *4* the correlation between the electron structure of atoms and the atomic spectra is described, what is missing in the literature until now, and what can give useful directions in the recognition and interpretation of interfering effects.

The description of the behaviour of atoms in magnetic fields is also provided in this chapter. This is the theoretical foundation for Zeeman atomic spectroscopy, which started to expand recently. This is very rarely found in the literature, therefore, this description is extraordinarily timely.

Chapter *5* discusses the characteristics of atomizing equipments and their influence on the sensitivity of atomic absorption and emission methods. This chapter lists and interprets physicochemical processes determining the local thermodynamic equilibrium (dissociation, ionization, atomization). A survey of physical and chemical phenomena occurring in the flame, plasma, graphite cuvette and other units not using flame, serves the purpose of estimating the expectable sensitivity of the analysis.

It deals in detail with processes of solution vaporization upon applying various atomizer designs. A comparison is made between pneumatic and ultrasonic vaporization, and the problems of non-continuous sample introduction into the graphite cuvette are also treated.

The subjects of chapter *5.5* and *5.6* are especially important. In chapter *5.5* the factors influencing the sensitivity of atomic absorption analysis are discussed, concerning both the instrument and the nature of the element to be determined. Chapter *5.6* compares the applicability and performance of ICP (plasma lamp) atomic absorption spectrophotometry with those of other, "traditional" methods.

Chapter *6* deals with the causes and elimination of background radiation measured in atomic absorption spectrometers. In this chapter a clear and detailed introduction of Zeeman atomic absorption spectrophotometers and ICP spectrophotometers is also included.

Summarizing, the book is written for specialists dealing with this subject already for a longer time: a beginner would not understand it. It is new and fortunate in the treatment

that everything is discussed from the point of view of the key problem of atomic spectroscopy, i.e. sensitivity. It is among the first books dealing with the functioning and applicability of Zeeman and ICP spectroscopy. In each chapter the advantages and disadvantages of the individual methods are compared.

The language of the book is clear, simple and comprehensive. At the end of the book the physical constants are given in CGS and SI units, and the transition probabilities measured on the different resonance lines of the elements (*gf* values) are summarized in a table. All these are useful aids for the specialist. The publication of the attainable sensitivity, and the resonance lines suggested for methods with solution-flame, graphite cuvette and for the ICP techniques is also valuable.

The work is supplying a great want. Its up-to-date subject and clear language make it suitable for the extension training of research and practical analysts.

L. LÁNG

Institute of Physics,
Technical University,
Budapest

K. SZÍVÓS

Department of Chemical Technolgy,
Technical University,
Budapest

Ernst Schmitz: *Organische Zwischenprodukte* (Organic intermediates)

Akademie Verlag Berlin 1980. WTB Series

The author says that one of the objects of this monograph was the following: as concerns chemical industry, today's chemist and non-chemist public opinion is aware mainly of heavy organic basic material industry, petrochemical industry and of giant factories belonging to them. As compared to this, intermediate products, indispensable in modern chemical industry play a minor role, or rather their importance is underestimated. These intermediates are the building stones of modern pharmaceutical, pesticide and plastics industries, branches of industry in rapid development in the last 20—30 years, both with respect to capacity and product assortment. According to the author, this work aims at directing attention to this field.

With respect to contents, the book can be divided into three parts.

1. Intermediates on petroleum, acetylene, coal tar and synthesis gas basis.

2. Industrial production of intermediates, production capacities, and mechanism of the most important reactions of intermediate chemistry.

3. Intermediates as building materials of various end-products; families of compounds based on identical intermediates.

The single chapters are of a depth possible for the extent of pocket-books, with a scientific popularizing character. The first 30 pages, dealing with definitions, raw material basis and development problems of intermediates, are particularly interesting.

The book (179 pages) is divided into the following chapters: *1.* Definitions and classification of intermediates. *2.* Aliphatic intermediates. *3.* Aromatic intermediates. *4.* Intermediates of plastics and synthetic fibres. *5.* Literature. *6.* Subject index.

J. PETRÓ

Department of Organic Chemical Technology,
Technical University,
Budapest

H. J. Fischbeck, K. H. Fischbeck: *Formulas, Facts and Constants for Students and Professionals in Engineering, Chemistry and Physics*

Berlin—Heidelberg—New York: Springer Verlag, 1982, 251 pages

The aim of the authors is to provide a handy collection of formulas, conversion factors and constants for every day practice. Formulas serving for practical purposes are complemented also with examples in cases where they are not clear enough by themselves. In many cases,

the book can substitute the use of huge tables. Part 1 provides basic mathematical knowledge needed in the fields of physical sciences. In Part 2 the SI units are summarized, conversion factors and accurate values of constants are given. In Parts 3 and 4 fundamental knowledge is included concerning spectroscopy, atomic structure and wave mechanics. Part 5 is meant for laboratory use. Formulas for often used instrumentation are given, such as e.g. vacuum systems and electronic instruments. Some material constants applicable for them are also provided.

The book is reproduced by rotaprint technique from a text written on an IBM typewriter, thus disadvantages owing to printing methods seldom appear. There are, however, more misprints by this technique due to e.g. the fact that the numbers in the main line and in the indices have the same size. However, the number of mistakes is small, though — if they occur in formulas — they are always distoring the sense.

The book contains 250 pages with a large number of tables and text illustrations. Corresponding to the nature of the book, they are not numbered.

The contents of the individual chapters are the following:

1. Basic mathematical facts and figures
1.1. Signs and symbols
1.2. Numerical constants
1.3. Exponentials and roots
1.4. Logarithm
1.5. Complex numbers
1.6. Factorial
1.7. Mensuration formulas
1.8. Solid angle
1.9. Trigonometric functions
1.10. Relations between sides and angles of a triangle
1.11. Hyperbolic functions
1.12. Algebraic equations and solutions
1.13. Calculus (differential and integral)
1.14. Series
1.15. Polynomials
1.16. Special functions (error function, Bessel, Gamma and Beta function)
1.17. Fourier transformation
1.18. Vectors and vector analysis
1.19. Solution of important differential equations
2. Units, conversion factors and constants
2.1. The international system of units (SI)
2.2. Conversion factors listed by physical quantity
2.3. Conversion factors in alphabetical order
2.4. Atomic units
2.5. X-ray units
2.6. Electrical units maintained by the Bureau International des Poids et Mesures (BIPM)
2.7. Relations between fundamental constants
2.8. Values of fundamental constants
2.9. Index of refraction of air
3. Spectroscopy and atomic structure
3.1. The electromagnetic spectrum
3.2. Energy-level diagram
3.3. Spectral lines for transitions between Rydberg terms
3.4. Quantum numbers specifying states of an atomic electron
3.5. Angular momentum
3.6. Term designation
3.7. Selection rules for electric dipole transitions
3.8. Schematic diagram of X-ray lines and terms
3.9. Wavelength of prominent spectral lines
3.10. Resonance lines of noble gas atoms
3.11. Atomic data
4. Basic wave mechanics
4.1. Schrödinger equation
4.2. Hydrogenic state functions
4.3. Expectation values for the radial distance
4.4. Expectation value for the root mean square velocity

4.5. Dipole moments
4.6. Values of hydrogenic radial transition integrals in units of the Bohr radius
5. Facts, figures and data useful in the laboratory
5.1. Fundamental relations of vacuum practice
5.2. Electronics
5.3. Digital electronics
5.4. Electrons
5.5. Radiation
5.6. Calibration sources frequently used in nuclear spectroscopy
5.7. Count loss correction
5.8. Material constants and other data (normal melting and boiling points, values for thermal expansion and conductivity, permittivity and dielectric strength, work function, characteristics of various thermocouples, composition and density of common alloys, terrestrial data)

Part I comprises 109, Part 2 36, Part 3 40, Part 4 10 and Part 5 57 pages. Especially valuable is the chapter dealing with mathematics, which provides fast aid for the practice in very different fields. The content of Parts 3 and 4 is very specialized, as well as that of Part 5, with a treatment of high standard. An appropriate justification of the choice of subjects is not given, but this book may serve as an example for the collection of material in other fields not treated here.

Concerning the usage of units, the book does not differentiate between the legal and illegal units outside the SI system. So beside the use of minute, hour, day, angular degree, minute and second of arc, litre, ton, bar, kilowatt-hour as equally usable are enumerated the angtröm, micron, barn, dyn, erg, stokes, poise, maxwell, gauss, inch, fermi, pound (as power- and mass units), powerkilogram, atmosphere, torr, Hg-mm, thermochemical and international calory, Rankine degree and curie. However, among the derived SI units the following cannot be found: gray, becquerel and sievert. Unfortunately, in Part 5 the majority of formulas does not relate to legal units, thus confirming the ingrained habits, instead of providing the conversion of the formulas into ones given in SI units.

It is sure that the book will be a useful and favourite aid of scientists and professionals due to its hand size.

G. VARSÁNYI

Department of Physical Chemistry,
Technical University,
Budapest

Metal ions in biological systems, Vol. 14

Inorganic drugs in deficiency and disease

Edited by Helmut Siegel, Marcel Dekker, Inc., New York and Basel, 1982, pp. 360.

This book is volume 14 of a continuing series dealing with the role of metal ions in biological systems, a field ingeniously called "bioinorganic chemistry" by the editor. Topics selected for this volume are mainly concernced with the pharmacological use of metals and are presented in nine chapters. These topics are at different stages of development, varying from such long-established fields like iron therapy of iron-deficiency anaemia to the rather speculative idea on the role of metal complexes in the action of hallucinogenic drugs.

Chapter *1* describes *drug-metal ion interactions in the gut* with special emphasis on metal-containing antacids. We learn that extrapolation of in vitro studies and animal experiments to the clinical scene has resulted in an overestimation of drug interactions of this type.

Chapters *2* and *3* deal with the ***biological use of zinc***. Causes, clinical manifestations, laboratory diagnosis and therapy of zinc deficiency are enumerated and rational of zinc administration in diseases other than zinc deficiency (sickle cell anaemia and rheumatoid arthritis) is described.

Chapter *4* reviews normal and pathological physiology of *copper complexes*, their pharmacological activities, possible mode of action and clinical use as anti-inflammatory agents.

Chapter 5 gives a comprehensive survey on iron chemistry, biochemistry and deficiency an goldand on the therapeutic use of *iron-containing drugs.*

Chapter *6* encompasses the use of *gold-complexes* in the treatment of arthritis, data on gold poisoning, pharmacokinetic properties of gold and its detection in biological materials.

Chapter 7 discusses the controversial perspectives of using chelating agents and *metal ions in antiviral chemotherapy.* The role of *drug-metal complexes in the hallucinogenic effect*, a likewise disputable idea, is presented in Chapter *8.*

Chapter *9* guides the reader back to firm ground reviewing the *clinical use of lithium* in manic-depressive psychoses and outlining the relevant chemical, biochemical and pharmacological aspects of lithium.

The book is completed with a comprehensive author and subject index helping orientation in these rather heterogeneous topics of "bioinorganic chemistry".

K. KELEMEN

Institute of Pharmacology,
Semmelweis Medical University,
Budapest

Juhász A. Zoltán—Opoczky Ludmilla: *Szilikátok mechanikai aktiválása finomőrléssel (Mechanical activation of silicates by fine grinding)*

Akadémiai Kiadó, Budapest, 1982

This handsomely printed and illustrated, well-edited 21-sheet book covers much wider territory than is suggested by its title: the general theory and practice of fine comminution and the structural-chemical effects taking place during this process. The majority of examples however deal with silicates.

In the general part of the book the characteristics of mechanical activation, mechanically-induced structural changes (including amorphization) and the basic principles of dispersing are discussed. An important part of this chapter describes the characterization of mechanically dispersed systems: this includes particle- and pore-size determination methods, with special emphasis to very fine particles, mathematical approximation of particle size distribution curves, investigation of external and internal surface areas, etc. The *PTH* (porosity-density-discontinuity) state diagram, elaborated by the authors can be well used for the characterization of internal morphology of various structural materials.

Another chapter of the book deals with mechanochemical reactions, i.e. with chemical reactions which normally take place at high temperatures only, but proceed with considerable speed at ambient temperatures when mechanically activated. The utilization of such phenomena might be of industrial use too, by activating otherwise nonreactive materials.

The final chapter of the book gives a brief description of various laboratory-scale and industrial machinery for superfine grinding, their advantages and disadvantages, energy-efficiency, etc.

The 635 references include classical and up-to-date papers and textbooks, selected from all around the world.

In the reviewer's opinion this book is particularly important for chemists, physicists, mineralogists and other scientists dealing with small-size morphology problems; however its perusal is recommended for engineers, griding technologists and similar experts too, struggling with the problems of their everyday activity, as it gives new and challenging vistas on some now possibilities.

F. D. TAMÁS

University of Veszprém,
Department of Silicate Chemistry,
Veszprém

Journal of Carbohydrate Chemistry

Editor: Donald E. Kiely (University of Alabama)

Publisher: Marcel Dekker Inc., New York, N.Y. 10016

The aims and scope, of this newly launched journal — as outlined in its first number (Volume **1**, Number 1, 1982, 120 pages) is to serve as an international forum for novel synthetic methods for carbohydrates; mechanistic carbohydrate chemistry; uses of carbohydrates in natural product, drug, carbohydrate antibiotic, saccharide, and oligosaccharide synthesis saccharide interconversions; carbohydrates as synthetic reagents; separation methods as applied to carbohydrate reactions and synthesis; and spectroscopic and crystallographic structure studies of carbohydrates.

Accordingly, this journal is in some respect similar to Carbohydrate Research, the well known international journal, which was founded two decades ago — but it differs from it in focusing on a limited, but highly significant area of the entire research domain of carbohydrates — excluding the huge field of polysaccharides and glycoconjugates. The other significant difference is its short production time, which is achieved by direct photography of the manuscripts. This means that special typing and format instructions, including special demands for the drawing of formulas, graphs, figures or schemes must be strictly followed.

Manuscripts may be papers, communications (2 to 6 pages) or reviews, and will be published in English, French or German. Contributions are published free of charge and the author(s) will be provided with twenty free reprints.

Three volumes are planned for 1982, and six for the next year. The regional editors, to whom manuscripts can be sent are D. C. Baker (Alabama), G. Descotes (Lyon), R. W. Binkley (Ohio), A. Hasegawa (Gifu, Japan) and J. Thiem (Hamburg). The editorial board of the new journal includes 29 well established scientists, representing the different European and oversea coutries.

The new journal can be strongly recommended to all organic chemists, especially to those dealing with the aspects of the chemistry of carbohydrates.

J. KUSZMANN

Institute for Drug Research,
Budapest

G. W. Gokel, S. H. Korzeniowski: *Macrocyclic Polyether Syntheses*

(Reactivity and Structure, Volume 13)

Springer-Verlag, Berlin, Heidelberg, New York, 1982, 89 tables, 410 pages

This volume of the series is devoted to one of the most rapidly growing fields of heterocyclic chemistry, polyheteroatom-containing macrocycles:

Oxygen Macrocycles, Azacrowns, Miscellaneous Macrocycles, Open-chain Equivalents of Crown Ethers, Cryptands and Related Polycyclic Systems.

The authors excellently managed to compress a survey of all the most important branches of macroheterocycles into a volume, without making it diffuse. The book purposefully is written without any experimental detail of syntheses. Some readers might feel that giving the details of a few, but just really a few, characteristic and most typical methods would not have enlarged the length to much.

On the other hand, the chapters are full of tabular data, well illustrated and thoroughly referenced. So it is easy to find the experimental procedures in the original papers. The chapters are divided according to heteroatoms:

Chapter *3*: Compounds containing oxygen in the macroring. Certain heterocyclic subunits are included even if a nonoxygen heteroatom is turned inward and may participate in binding.

Chapter *4*: Compounds containing one or more nitrogen atoms in the macroring, whether or not the nitrogen is part of another heterocyclic subunit. Certain pyridine and pyrimidine compounds have been included in Chapter *3* as well.

Chapter *5*: Compounds which contain either an ester or an amide likage in a single macrocyclic ring. This comprises lactones, lactams, carbonates, carbamates, ureas, phosphates, etc., including sulfur, nitrogen and other atoms in the ring.

Chapter *6*: Miscellaneous crown-type compounds, including acetals, and compounds containing sulfur, phosphorus, arsenic, etc. Polymer species are included here and in Chapter *3*.

Chapter *7*: Open-chain substances of all descriptions, including nitrogen, sulfur, ester, etc.

Chapter *8*: Macrobicyclic, macrotricyclic, or polycyclic compounds, including cryptands, spherands, etc.

Besides this grouping, the introductory chapters, an author index and a subject index make extremely easy the locating of data.

This book is essential for chemical libraries and will be found useful as a daily reference by synthetic organic chemists working in this field. Its purchase is highly recommended.

K. HIDEG

Central Laboratory, Chemistry,
Medical University of Pécs,
Pécs

PRINTED IN HUNGARY

Akadémiai Nyomda, Budapest

Text

The text of the paper should be concise. The description of new compounds (in the Experimental) must include the complete analytical data. Special attention must be paid to structural formulas given within the text. Complicated (non-linear) formulas should be drawn on separate sheets of paper and their position in the text should be clearly marked. The numbering of formulas and equations (in parentheses on the right-hand side) is only needed if they are referred to in the text. Units should conform to the International System of Units (SI). In nomenclature the rules of the I.U.P.A.C. are accepted as standard. Symbols for physical quantities are printed in italic type and should, therefore, be underlined in the manuscript.

References

References should be numbered in order of appearance in the text (where the reference number appears in brackets) and listed at the end of the paper. The reference list, too, should be typed double-spaced. Journal titles are to be abbreviated as defined by the Chemical Abstracts Service Source Index.

Examples:

[1] Brossi, A., Lindlar, H., Walter, M., Schneider, O.: Helv. Chim. Acta, **41**, 119 (1958)
[2] Parr, R. G.: Quantum Theory of Molecular Electronic Structure. Benjamin, New York 1964
[3] Warshel, A.: in Modern Theoretical Chemistry, Vol. **7**, Part A (Ed. G. A. Segal), Plenum Press, New York 1977

Tables

Each table should be given a Roman number and a brief informative title. Structural formulas should not be used in column headings or in the body of tables.

Figures

Figures should be numbered consecutively with Arabic numerals. Their approximate place should be indicated in the text on the margin. All figures must be identified on the back by the author's name and the figure number in pencil. Standard symbols (such as circles, triangles, squares) are to be used on line-drawings to denote the points determined experimentally. Line-drawings must not contain structural formulas and comments. Spectra or relevant segments thereof, chromatograms, and X-ray diffraction patterns will be reproduced only if concise numerical summaries are inadequate to replace them. Drawings and graphs should be prepared in black ink on good-quality white or tracing paper. Photographs should be submitted on glossy paper as high-contrast copies. Xerox or similar copies are not suitable for reproduction, but may be used for duplicate copies.

Redrawn illustrations will be sent to the authors for checking. No corrections of figures will, therefore, be accepted in the proofs.

Submission of manuscript

After having completed the corrections suggested by the referees and editors, the final manuscript should be submitted in duplicate, in a form ready for publication. If the corrected manuscript is not returned to the editors *within six weeks*, the intended publication of the paper will be regarded as withdrawn by the authors.

Page charge will not be assessed for the publication, however, authors from overseas countries must contribute to the postage of correspondence by sending, together with the manuscript, international postal coupons to the value of U.S. $ 10.—

Proofs and reprints

A set of proofs will be sent to the submitting author. The proofs must be returned within 48 hours of receipt. Late return may cause a delay in the publication of the paper. 100 reprints will be supplied to the authors free of charge.

Periodicals of the Hungarian Academy of Sciences are obtainable at the following addresses:

AUSTRALIA
C.B.D. LIBRARY AND SUBSCRIPTION SERVICE
Box 4886, G.P.O., *Sydney N.S.W. 2001*
COSMOS BOOKSHOP, 145 Ackland Street
St. Kilda (Melbourne), Victoria 3182

AUSTRIA
GLOBUS, Höchstädtplatz 3, *1206 Wien XX*

BELGIUM
OFFICE INTERNATIONAL DE LIBRAIRIE
30 Avenue Marnix, *1050 Bruxelles*
LIBRAIRIE DU MONDE ENTIER
162 rue du Midi, *1000 Bruxelles*

BULGARIA
HEMUS, Bulvar Ruszki 6, *Sofia*

CANADA
PANNONIA BOOKS, P.O. Box 1017
Postal Station "B", *Toronto, Ontario M5T 2T8*

CHINA
CNPICOR, Periodical Department, P.O. Box 50
Peking

CZECHOSLOVAKIA
MAD'ARSKÁ KULTURA, Národní třida 22
115 66 Praha
PNS DOVOZ TISKU, Vinohradská 46, *Praha 2*
PNS DOVOZ TLAČE, *Bratislava 2*

DENMARK
EJNAR MUNKSGAARD, Norregade 6
1165 Copenhagen K

FEDERAL REPUBLIC OF GERMANY
KUNST UND WISSEN ERICH BIEBER
Postfach 46, *7000 Stuttgart 1*

FINLAND
AKATEEMINEN KIRJAKAUPPA, P.O. Box 128
SF-00101 Helsinki 10

FRANCE
DAWSON-FRANCE S. A., B. P. 40, *91121 Palaiseau*
EUROPÉRIODIQUES S. A., 31 Avenue de Versailles, *78170 La Celle St. Cloud*
OFFICE INTERNATIONAL DE DOCUMENTATION ET LIBRAIRIE, 48 rue Gay-Lussac
75240 Paris Cedex 05

GERMAN DEMOCRATIC REPUBLIC
HAUS DER UNGARISCHEN KULTUR
Karl Liebknecht-Straße 9, *DDR-102 Berlin*
DEUTSCHE POST ZEITUNGSVERTRIEBSAMT
Sraße der Pariser Kommüne 3–4, *DDR-104 Berlin*

GREAT BRITAIN
BLACKWELL'S PERIODICALS DIVISION
Hythe Bridge Street, *Oxford OX1 2ET*
BUMPUS, HALDANE AND MAXWELL LTD.
Cowper Works, *Olney, Bucks MK46 4BN*
COLLET'S HOLDINGS LTD., Denington Estate
Wellingborough, Northants NN8 2QT
WM. DAWSON AND SONS LTD., Cannon House
Folkstone, Kent CT19 5EE
H. K. LEWIS AND CO., 136 Gower Street
London WC1E 6BS

GREECE
KOSTARAKIS BROTHERS INTERNATIONAL BOOKSELLERS, 2 Hippokratous Street, *Athens-143*

HOLLAND
MEULENHOFF-BRUNA B.V., Beulingstraat 2,
Amsterdam
MARTINUS NIJHOFF B.V.
Lange Voorhout 9–11, *Den Haag*

SWETS SUBSCRIPTION SERVICE
347b Heereweg, *Lisse*

INDIA
ALLIED PUBLISHING PRIVATE LTD., 13/14
Asaf Ali Road, *New Delhi 110001*
150 B-6 Mount Road, *Madras 600002*
INTERNATIONAL BOOK HOUSE PVT. LTD.
Madame Cama Road, *Bombay 400039*
THE STATE TRADING CORPORATION OF INDIA LTD., Books Import Division, Chandralok
36 Janpath, *New Delhi 110001*

ITALY
INTERSCIENTIA, Via Mazzé 28, *10149 Torino*
LIBRERIA COMMISSIONARIA SANSONI, Via Lamarmora 45, *50121 Firenze*
SANTO VANASIA, Via M. Macchi 58
20124 Milano
D. E. A., Via Lima 28, *00198 Roma*

JAPAN
KINOKUNIYA BOOK-STORE CO. LTD.
17-7 Shinjuku 3 chome, Shinjuku-ku, *Tokyo 160-91*
MARUZEN COMPANY LTD., Book Department,
P.O. Box 5050 Tokyo International, *Tokyo 100-31*
NAUKA LTD. IMPORT DEPARTMENT
2-30-19 Minami Ikebukuro, Toshima-ku, *Tokyo 171*

KOREA
CHULPANMUL, *Phenjan*

NORWAY
TANUM-TIDSKRIFT-SENTRALEN A.S., Karl Johansgatan 41–43, *1000 Oslo*

POLAND
WĘGIERSKI INSTYTUT KULTURY, Marszałkowska 80, *00-517 Warszawa*
CKP I W, ul. Towarowa 28, *00-958 Warszawa*

ROUMANIA
D. E. P., *Bucureşti*
ILEXIM, Calea Grivitei 64–66, *Bucureşti*

SOVIET UNION
SOJUZPECHAT — IMPORT, *Moscow*
and the post offices in each town
MEZHDUNARODNAYA KNIGA, *Moscow G-200*

SPAIN
DIAZ DE SANTOS, Lagasca 95, *Madrid 6*

SWEDEN
ALMQVIST AND WIKSELL, Gamla Brogatan 26
101 20 Stockholm
GUMPERTS UNIVERSITETSBOKHANDEL AB
Box 346, *401 25 Göteborg 1*

SWITZERLAND
KARGER LIBRI AG, Petersgraben 31, *4011 Basel*

USA
EBSCO SUBSCRIPTION SERVICES
P.O. Box 1943, *Birmingham, Alabama 35201*
F. W. FAXON COMPANY, INC.
15 Southwest Park, *Westwood Mass. 02090*
THE MOORE-COTTRELL SUBSCRIPTION AGENCIES, *North Cohocton, N. Y. 14868*
READ-MORE PUBLICATIONS, INC.
140 Cedar Street, *New York, N. Y. 10006*
STECHERT-MACMILLAN, INC.
7250 Westfield Avenue, *Pennsauken N. J. 08110*

YUGOSLAVIA
JUGOSLOVENSKA KNJIGA, Terazije 27, *Beograd*
FORUM, Vojvode Mišića 1, *21000 Novi Sad*

Index: 26.007

FORMERLY ACTA CHIMICA ACADEMIAE SCIENTIARUM HUNGARICAE

Acta Chimica Hungarica

VOLUME 114, NUMBER 2, OCTOBER 1983

EDITOR-IN-CHIEF
F. MÁRTA

MANAGING EDITOR
GY. DEÁK

ASSISTANT EDITOR
L. HAZAI

EDITORIAL BOARD
M. T. BECK, R. BOGNÁR, GY. HARDY, K. LEMPERT,
B. LENGYEL, K. POLINSZKY, E. PUNGOR, G. SCHAY,
Z. G. SZABÓ, P. TÉTÉNYI

Akadémiai Kiadó, Budapest
ACTA CHIM. HUNG. ACASA2 114 (2) 103–216 (1983) HU ISSN 0231-3146

ACTA CHIMICA HUNGARICA

A JOURNAL OF THE HUNGARIAN ACADEMY OF SCIENCES

Acta Chimica publishes original reports on all aspects of chemistry in English.

Acta Chimica is published in three volumes per year, each volume consisting of four issues, by

AKADÉMIAI KIADÓ

Publishing House of the Hungarian Academy of Sciences
H-1054 Budapest, Alkotmány u. 21.

Manuscripts and editorial correspondence should be addressed to

Acta Chimica
H-1450 Budapest P.O. Box 67

Subscription information

Orders should be addressed to

KULTURA Foreign Trading Company
H-1389 Budapest P.O. Box 149

or to its representatives abroad

Acta Chimica is indexed in Current Contents.

NOTICE TO AUTHORS

Acta Chimica publishes original papers on all aspects of chemistry in English. Before preparing a manuscript for submission to this journal authors are advised to consult recent issues.

Form of manuscript

Manuscripts, tables and illustrations should be submitted in triplicate. Manuscripts should be typewritten double spaced (25 lines, 50 characters per line including spaces). The *title page* should include (1) the title of the paper, (2) the full names of the author(s) in the sequence to be published; apply an asterisk to designate the name of the author to whom correspondence should be addressed, (3) name and address of the institution where the work was done. If the paper is part of a series, reference to the previous communication must be given as a footnote.

Abstract

A summary is printed at the head of each paper. This should not exceed 200 words and should state briefly the principal results and major conclusions of the work. It should be suitable for use by abstracting services.

CONTENTS

PHYSICAL AND INORGANIC CHEMISTRY

Excess volumes of binary mixtures of di-*n*-butylamine with normal alcohols at 303.15 K, **G. S. Sastry, M. Ramamurthy, P. R. Naidu** 113
Polarographic study of mixed ligand complexes of Pb(II) with some diamines and malonic acid, **J. K. Garg, D. S. Jain, P. S. Verma** 125
Deuterium vapour pressure isotope effect in bromoform, **Gy. Jákli, P. Juhász, G. Jancsó** 133
Theoretical interpretation of the vibrational spectra of *trans*- and *cis*-penta-1,3-dienes and 2,3-dimethylbutadiene, **Yu. N. Panchenko, V. I. Mochalov, P. Császár, F. Török, F. Benedetti, M. Aglietto** 149
On the C—S bond length variations and d-orbital participation in some sulphonyl chloride derivatives, **I. Mayer, M. Révész, I. Hargittai** 159
pH-Dependence of the catalytic effect of thiourea and *N,N'*-dimethylthiourea on hydrogen overvoltage at the dropping gallium electrode, **K. Szabó, É. M. Csobod** 173
Changing of the catalytic effect of thiourea with temperature at the dropping gallium electrode, **K. Szabó, É. M. Csobod, M. Takács** 187
Chemical reaction of substances under mechanical load, **Z. A. Juhász** 199

ORGANIC CHEMISTRY

Reactions of 4-thionochromones and 4-thionoisoflavones with hydroxylamine, **J. Borda, V. Szabó, J. Borbély** 103
Synthesis of some 3,5-diarylimino-2-phenyl-1,2,4-thiadiazolidines. Oxidative debenzylation and cyclization of 1-(*N,N'*-diarylamidino)-3-aryl-2-benzylisothioureas, **A. K. Pandey, R. Singh, V. K. Verma** 107
Acid-catalyzed condensation of isoprene and 2-methylbut-3-en-2-ol with phloroacetophenone, new synthesis of alloevodionol and franklinone, **V. K. Ahluwalia, K. K. Arora, R. S. Jolly** 117
Reaction of lead(IV) acetate with steroidal nitroolefins (Short communication), **Shafiullah, S. Husain, D. M. Basha** 121

PRINTED IN HUNGARY

Akadémiai Nyomda, Budapest

Acta Chimica Hungarica 114 (2), pp. 103—106 (1983)

REACTIONS OF 4-THIONOCHROMONES AND 4-THIONOISOFLAVONES WITH HYDROXYLAMINE

(PRELIMINARY COMMUNICATION)

J. BORDA, V. SZABÓ* and J. BORBÉLY

(Institute of Applied Chemistry, Kossuth Lajos University, H-4010 Debrecen, P. O. Box 10.)

Received October 28, 1982
In final form April 13, 1983
Accepted for publication May 4, 1983

In our previous papers it has been reported [1, 2] that the reaction of 4-thionoisoflavone (**Id**) with hydroxylamine, either in aqueous ethanol buffered with sodium acetate at 80 °C, or in aqueous ethanol at pH 11 and room temperature, results in a mixture of **II** and **IV** as the major products.

In a recent series of experiments the 4-thiones shown in Table I were allowed to react with hydroxylamine in two markedly different reaction media.

In the first case dry hydroxylamine hydrochloride was buffered with anhydrous sodium acetate in dry methanol, while in the second case a 1 : 1 mixture of ethanol and Britton—Robinson buffer was used as the solvent, and the solution was adjusted to about pH 14 with alkali. Both experiments were made at room temperature.

In the course of these reactions the formation of five products (**II—VI**) could be detected; their presence and ratio were dependent upon the substituents and the reaction conditions. The formation and the structures of compounds **II**, **V** and **VI** have been reported earlier [1—4].

On the basis of our previous and recent results, the reaction of 4-thiones with hydroxylamine can be represented by the sequence of formulas shown in Fig. 1.

In the case of the 4-thiones investigated, compounds **II** and **III** were the major products in abs. methanolic medium, whereas in alkaline medium of pH 14 the reaction gave mainly compound **IV**, formed by the cleavage of the γ-thionopyrone ring.

The formation of neither oxime, nor isothiazole derivative was observed from **Ia**.

* To whom correspondence should be addressed

Table I

Structures and physical characteristics of the synthesized compounds

	R	R_1	R_2	R_3	III			IV				
					M. p., °C	N, %		M. p., °C	N, %		S, %	
						Calcd.	Found		Calcd.	Found	Calcd.	Found
Ia	H	H	H	H	—	—	—	—	—	—	—	—
b	H	CH_3	H	H	143—4	8.00	7.88	116—8	7.33	7.13	16.75	16.49
c	H	CH_3	Cl	H	132—3	6.69	6.52	163—4	6.25	6.08	14.22	13.98
d	H	Ph	H	H	—	—	—	129—30	5.53	5.50	12.64	12.29
e	CH_3	Ph	H	H	188—9	5.77	5.66	167—8	5.24	5.07	11.98	11.72
f	H	Ph	CH_3	H	162—3	5.77	5.61	105—7	5.24	5.09	11.98	11.85
g	H	Ph	H	CH_3O	—	—	—	162—3	4.94	4.86	11.30	11.08

In the case of **Id** and **Ig** the isolation of product **III** is very difficult due to conversion into **II**.

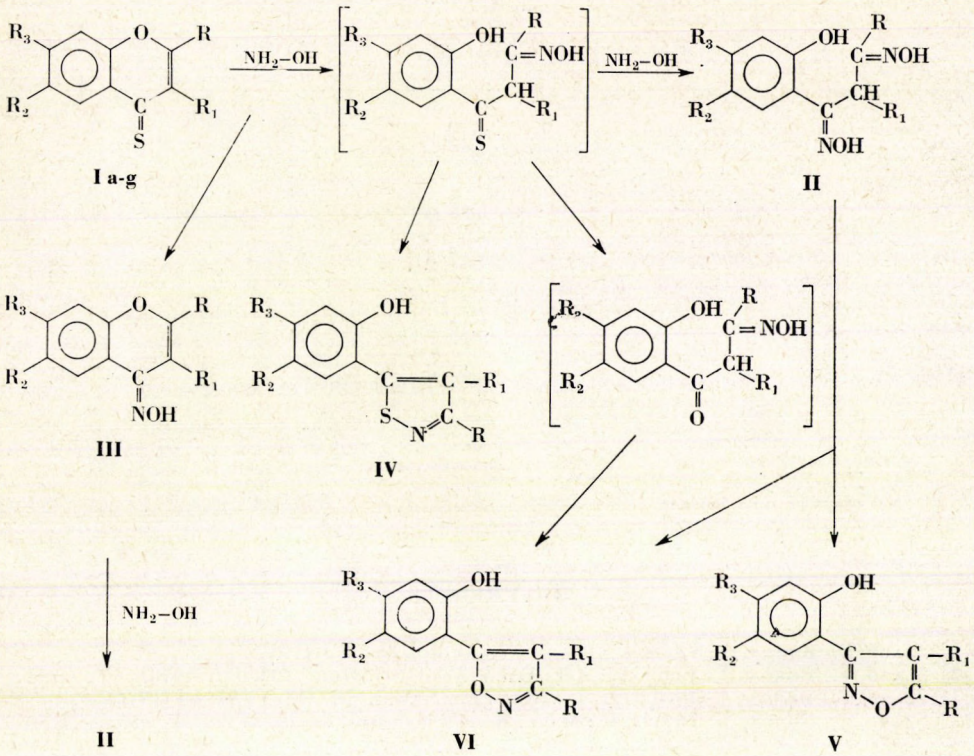

Fig. 1

The oximes and isothiazoles prepared from compounds **Ib—g** had not been reported in the literature, therefore their structure were confirmed various ways.

Contrary to **VI**, the isothiazoles **IV** are stable in dilute (0.1*M*) alkaline medium and their structures were confirmed by elemental analyses and UV, IR, NMR and mass spectroscopic methods.

In addition to the elemental analytical and ^{1}H—NMR spectroscopic evidence, decisive proof for the oxime structure of **IIIb—g** is afforded by the acid hydrolysis which gives chromone (**I**), and by the treatment with hydroxylamine, whereupon **II** is obtained. The ^{1}H—NMR data suggest the presence of the mixture of *syn* and *anti* isomers.

The characteristic ^{1}H—NMR parameters are shown for the case of 3-methyl-4-thionochromone (**Ib**).

Table II

^{1}H—NMR *spectral data*

Compound	H-2 (H-3)	CH_3-3 (CH_3-4)	OH	H-5 (H-6')
Ib	8.24 q	2.28 d	—	8.61 dd
		J^4_{H,CH_3} = 1.0 Hz		
IIIb	*S:* 7.09 q	*S:* 1.82 d	*S:* 9.45 s	*S:* 9.13 dd
	A: 6.88 q	*A:* 1.90 d	*A:* 8.85 s	*A:* 7.95 dd
		J^4_{H,CH_3} = 1.4 Hz		
VIb	8.27 q	2.10 d	10.8 s	7.37 dd
		J^4_{H,CH_3} = 0.45 Hz		
IVb	8.32 q	2.18 d	9.7 s	7.35 dd
		J^4_{H,CH_3} = 0.44 Hz		

Solvent: acetone-d_6
Instrument: Bruker WP-200 SY
S: syn, *A: anti* isomer

REFERENCES

[1] Szabó, V., Borda, J., Végh, V.: Magy. Kém. Foly., **83,** 433 (1977)
[2] Szabó, V., Borda, J., Végh, V.: Acta Chim. Acad. Sci. Hung., **98,** 457 (1978)
[3] Szabó, V., Borda, J., Losonczi, L.: Acta Chim. Acad. Sci. Hung., **97,** 69 (1978)
[4] Szabó, V., Borda, J., Theisz, E.: Magy. Kém. Foly., **84,** 134 (1978)

Acta Chimica Hungarica, 114 (2), pp. 107—111 (1983)

SYNTHESIS OF SOME 3,5-DIARYLIMINO--2-PHENYL-1,2,4-THIADIAZOLIDINES

OXIDATIVE DEBENZYLATION AND CYCLIZATION OF 1-(*N*,*N*'-DIARYLAMIDINO)-3-ARYL-2-BENZYLISOTHIOUREAS

A. K. PANDEY, R. SINGH and V. K. VERMA*

(Applied Chemistry Section, School of Applied Sciences, Institute of Technology, Banaras Hindu University, Varanasi-221005, India)

Received April 30, 1982
In revised form August 18, 1982
Accepted for publication September 28, 1982**

5-Arylimino-3-phenylimino-2-phenyl-1,2,4-thiadiazolidines have been prepared by the oxidative debenzylation and cyclization of the corresponding 1-(*N*,*N*'-diarylamidino)-3-aryl-2-benzylisothioureas.

The oxidation of 1(*N*,*N*'-diarylamidino)-3-arylthioureas has been a well known method for the synthesis of 3,5-diarylimino-2-aryl-1,2,4-thiadiazolidines [1, 2]. However, in view of our earlier studies in the oxidative debenzylation and cyclization of some *S*-benzylformamidinoisothiourea systems [3], it was thought of sufficient interest to test the feasibility of extending this reaction to the alternative synthesis of certain 3,5-diarylimino-2-phenyl-1,2,4--thiadiazolidines.

The present communication reports the successful conclusion of oxidative debenzylation and cyclization reaction as an alternative route to the synthesis of 3,5-diarylimino-2-phenyl-1,2,4-thiadiazolidines from the corresponding 1-(*N*,*N*'-diarylamidino)-3-aryl-2-benzylisothioureas.

N,*N*'-Diphenylguanidine was condensed with the appropriate arylisothiocyanate. The expected 1-(*N*,*N*'-diarylamidino)-3-arylthioureas (**II**), so obtained were benzylated with benzylchloride. The 1-(*N*,*N*'-diarylamidino)-3-aryl-2--benzylisothiourea bases (**III**), obtained, on oxidation with bromine in chloroform afforded the related 5-arylimino-3-phenylimino-2-phenyl-1,2,4-thiadiazolidines (**IV**). The structures were finally confirmed as the compounds were also obtained by the direct oxidation of the related 1-(*N*,*N*'-diarylamidino)--3-arylthioureas (**II**). The products were further characterized by the mixed melting point technique and by identical IR spectra.

* To whom correspondence should be addressed
** In final form accepted February 17, 1983

The scheme of the reactions can be depicted as follows:

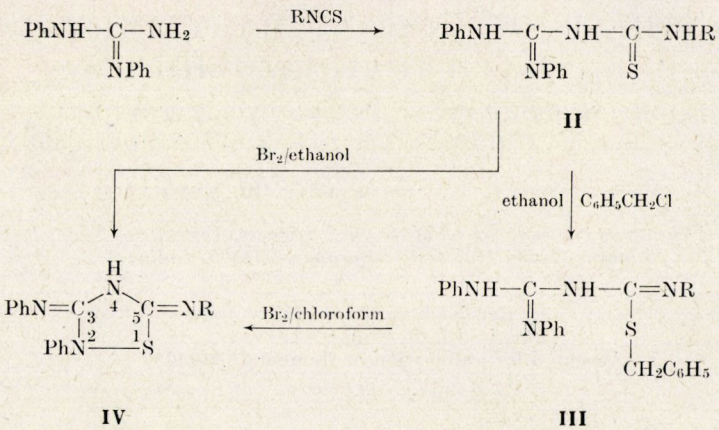

Ph = phenyl group

R = 4-tolyl, 4-chlorophenyl, 4-methoxyphenyl, 4-ethoxyphenyl or benzyl group

The following mechanism is suggested:

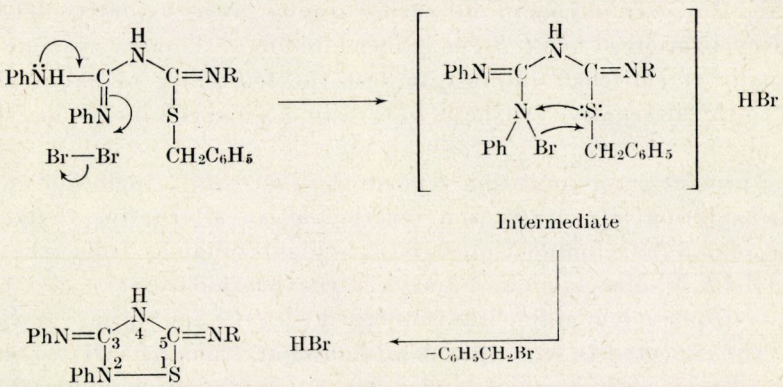

Experimental

M.p.'s were determined on a Kofler hot stage apparatus and are uncorrected; IR spectra were recorded in Nujol on a Perkin Elmer spectrophotometer Model 720.

1-(*N*,*N*'-Diphenylamidino)-3-arylthioureas (II)

The details of a representative experiment are as follows:

1,3-Diphenylguanidine (5 g) and 4-chlorophenyl isothiocyanate (2.9 g) were refluxed in ethanol (40 mL) for 2 h. The recation mixture was filtered. On cooling the expected formamidinothiourea separated and was filtered off (yield 3.5 g; 75%). It was recrystallized from ethanol; m.p. 146 °C. The results of these experiments are summarized in Table I.

Table I

1-(N,N'-Diphenylamidino)-3-arylsubstituted thioureas **(II)**

R	M.p. °C	Yield %	Molecular formula	Analysis	
				Found	Calcd
4-Tolyl	142	80	$C_{21}H_{20}N_4S$	C: 70.30 H: 5.55	C: 69.97 H: 5.59
4-Chlorophenyl	146	75	$C_{20}H_{17}ClN_4S$	C: 63.28 H: 4.48	C: 63.06 H: 4.49
4-Ethoxyphenyl	124	70	$C_{22}H_{22}N_4SO$	C: 68.00 H: 5.66	C: 67.66 H: 5.67
4-Methoxyphenyl	134	72	$C_{21}H_{20}N_4SO$	C: 67.37 H: 5.34	C: 66.99 H: 5.36
Benzyl	115	68	$C_{21}H_{20}N_4S$	C: 70.50 H: 5.20	C: 69.97 H : 5.59

Typical IR frequencies (cm^{-1}) of 1-(*N,N'*-diphenylamidino)-3-(4-chlorophenyl)-thiourea are: 3400w, 3250w, NH stretching (*lit.* [4], 3400 – 3100); 1320w, C=S stretching (*lit.* [4] 1400—1100); 1565w, N—C=N grouping (*lit.* [5] 1825—1582).

1-(*N,N'*-Diphenylamidino)-3-aryl-2-benzylisothioureas (III)

The details of a typical experiment are as follows:

A mixture of 1-(*N,N'*-diphenylamidino)-3-(4-chlorophenyl)-thiourea (5 g), benzyl chloride (2.8 mL) and ethanol (25 mL) was refluxed for about 1 $^1/_2$ h. On evaporation of the excess of solvent and basification, a semisolid mass was obtained, which on addition of a little ethanol afforded the expected 1-(*N,N'*-diphenylamidino)-3-(4-chlorophenyl)-2-benzylisothiourea. It was recrystallized from ethanol, m.p. 130 °C (yield 3 g, 70%). The results of these experiments are summarized in Table II.

Table II

1-(N,N'-Diphenylamidino)-3-arylsubstituted-2-benzylisothioureas **(III)**

R	M.p. °C	Yield %	Molecular formula	Analysis	
				Found	Calcd
4-Tolyl	112	72	$C_{28}H_{26}N_4S$	C: 74.60 H: 5.78	C: 74.63 H: 5.82
4-Chlorophenyl	130	70	$C_{27}H_{23}ClN_4S$	C: 68.86 H: 4.89	C: 68.85 H: 4.92
4-Ethoxyphenyl	liquid	70	—	—	—
4-Methoxyphenyl	110	65	$C_{28}H_{26}N_4SO$	C: 72.00 H: 5.56	C: 72.07 H: 5.62
Benzyl	liquid	68	—	—	—

In a few cases semisolid or liquid products were obtained, which could not be crystallized. The identity of these compounds **(III)** was confirmed by their quick reduction to the corresponding 1-(*N,N'*-diphenylamidino)-3-arylthioureas **(II)** with hydrogen sulfide in ethanolic ammoniacal solution.

5-Arylimino-3-phenylimino-2-phenyl-1,2,4-thiadiazolidines (IV)

These compounds were prepared by the oxidative debenzylation and cyclization of 1-(*N*,*N*'-diarylamidino)-3-aryl-2-benzylisothioureas with bromine in chloroform.

The details of a typical experiment are as follows:

1-(*N*,*N*'-Diphenylamidino)-3-(4-chlorophenyl)-2-benzylisothiourea (3 g) was moistened with a little chloroform (2mL) and bromine (1 mL) was added to it in small portions with vigorous stirring. Debenzylation was evident from the evolution of the lachrymatory fumes of benzyl bromide. The reaction mixture was allowed to stand for 30 min at room temperature and the product was washed with ether. Treatment of the resulting mass with ethanol afforded the desired 5-(4-chlorophenyl)-imino-3-phenylimino-2-phenyl-1,2,4-thiadiazolidine hydrobromide, which was crystallized from ethanol; m.p. 280 °C, yield 58%. On basification with ammonia, the base was obtained, which was crystallized from ethanol, m.p. 120 °C.

The results of these experiments are summarized in Table III.

Table III

5-Arylimino-3-phenylimino-2-phenyl-1,2,4-thiadiazolidines (IV)*

R	M.p. °C	Yield %	Molecular formula	Analysis of base		M.p. of Hydrobromide
				Found	Calcd	
4-Tolyl	129	55	$C_{21}H_{18}N_4S$	C: 70.37 H: 5.00	C: 70.36 H: 5.06	240
4-Chlorophenyl	120	58	$C_{20}H_{15}ClN_4S$	C: 63.40 H: 3.39	C: 63.40 H: 3.99	280
4-Ethoxyphenyl	145	52	$C_{22}H_{20}N_4SO$	C: 68.00 H: 5.15	C: 68.01 H: 5.10	218
4-Methoxyphenyl	140	55	$C_{21}H_{18}N_4SO$	C: 67.30 H: 4.80	C: 67.35 H: 4.84	215
Benzyl	134	50	$C_{21}H_{18}N_4S$	C: 70.58 H: 4.76	C: 70.36 H: 5.06	210

* Prepared from compounds **III**. Typical IR frequencies (cm^{-1}) of 5-(4-chlorophenyl)-imino-3-phenylimino-2-phenyl-1,2,4-thiadiazolidine: 3200w, NH stretching (*lit.* [4] 3400—3100); 1565w, N—C=N grouping (*lit.* [5] 1685—1582)

The thiadiazolidines (**IV**) thus obtained showed no depression in m.p. determination with authentic samples obtained by the oxidation of the corresponding 1(*N*,*N*'-diphenylamidino)-3-arylthioureas (**II**). The compounds were further characterized by the superimposable IR spectra.

Oxidation of 1-(*N*,*N*'-diphenylamidino)-3-arylthioureas (II) with bromine in ethanol

1-(*N*,*N*'-Diphenylamidino)-3-arylthioureas were dissolved in ethanol and a solution of bromine in dilute ethanol was added until a permanent colour of bromine persisted. After keeping the resulting mass at room temperature for 1 h, the expected 5-arylimino-3-arylimino-2-aryl-1,2,4-thiadiazolidines precipitated. The hydrobromides on basification with ammonia afforded the corresponding bases which were crystallized from ethanol. These were found to be identical with the corresponding compounds mentioned in Table III.

*

The authors are thankful to B. H. U. Varanasi, Director, Institute of Technology for the necessary facilities.

REFERENCES

[1] Kurzer, F., Sanderson, P. M.: J. Chem. Soc., **1960**, 3240
[2] Joshua, C. P., Rajasekharan, K. N.: Indian J. Chem., **14B**, 967 (1976)
[3] Pandey, A. K., Singh, R., Verma, V. K.: J. Indian Chem. Soc. (Accepted for publication)
[4] Katritzky, A. R.: Physical Methods in Hetrocyclic Chemistry, p. 325 Academic Press, New York 1963
[5] Colthop, N. B., Daly, L. H., Wiberly, S. E.: Introduction to Infrared and Raman Spectroscopy pp. 284, 322. Academic Press, New York 1963

Acta Chimica Hungarica, 114 (2), pp. 113–116 (1983)

EXCESS VOLUMES OF BINARY MIXTURES OF DI-*n*-BUTYLAMINE WITH NORMAL ALCOHOLS AT 303.15 K

G. S. SASTRY, M. RAMAMURTHY and P. R. NAIDU*

(Chemical Laboratories, College of Engineering, Sri Venkateswara University, Tirupati 517 502 India)

Received July 8, 1982
In revised form September 14, 1982
Accepted for publication September 30, 1982**

Excess volumes for binary mixtures of di-*n*-butylamine with *n*-butanol, *n*-pentanol, *n*-hexanol and *n*-heptanol have been determined at 303.15 K. The values of V^E are negative over the whole range of composition in the four mixtures. The results point out that hydrogen bond interactions between molecules of unlike components is dominant.

Introduction

Excess volumes for binary mixtures of *n*-butylamine with *n*-propanol, *n*-butanol, *n*-pentanol and *n*-hexanol have been reported by Krishnaiah and Naidu [1]. Excess volumes for the four mixtures were negative over the whole range of composition. The results were used to point out that hydrogen bond interaction between unlike molecules is stronger than that between like molecules of the components. Introduction of an additional butyl group into the amino function may modify the degree of interaction between unlike molecules and like molecules of the amine. These will in turn influence the excess volume. With a view to study the aforesaid influence, new excess volume data for mixtures of di-*n*-butylamine with the four alcohols were determined at 303.15 K.

Experimental

Di-*n*-butylamine (B. D. H. Poole-England) was used without purification. *n*-Butanol (B. D. H.), *n*-pentanol (B. D. H.) *n*-hexanol (B. D. H.) were purified as already described [2]. Analytical grade *n*-heptanol (Koch – Light Laboratories Ltd., England) was fractionally distilled. The purity of the samples were checked by comparing the measured densities of the compounds with those reported in the literature [3]. Densities were determined using a bi-capillary type pycnometer which afforded an accuracy of ± 5 parts in 10^5 g cm^{-3}. The densities of the present work are given along with the literature values in Table I.

* To whom correspondence should be addressed
** In final form accepted February 10, 1983

Table I

Densities of pure component liquids at 303.15 K

Component	Density ϱ/g cm^{-3}	
	experimental	literature
Di-*n*-butylamine	0.75519	—
n-Butanol	0.80202	0.80206
n-Pentanol	0.80769	0.80764
n-Hexanol	0.81209	0.81201
n-Heptanol	0.81571	—

The dilatometer used for measuring excess volumes was similar to that described by Rao and Naidu [4]. The mixing cell contained two bulbs of different capacites that were connected by a 'U' tube filled with mercury to separate the two components. One end of the first bulb was fitted with a capillary tube and the other end of the second bulb was closed with a ground glass stopper. Five dilatometers with different capacities were used to cover the entire composition range. Composition of each mixture was determined directly by weighing. Weights were corrected for buoyancy. The dilatometers were kept in a thermostat controlled to ± 0.01 K. The excess volumes were reproducible to ± 0.003 cm^3 mol^{-1}.

Results and Discussion

Excess volumes at 303.15 K are presented in Table II. The data at 303.15 K are presented graphically along with those reported by Krishnaiah

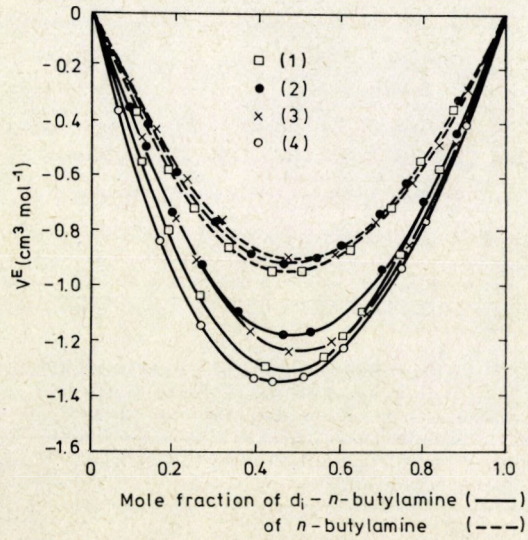

Fig. 1. Excess volumes V^E for di-*n*-butylamine (χ) (——) and *n*-butylamine (χ) (------) with *n*-alcohols:(1) *n*-butanol ($1 - \chi$), (2) *n*-pentanol ($1 - \chi$), (3) *n*-hexanol ($1 - \chi$), (4) *n*-heptanol ($1 - \chi$)

Table II

Experimental excess volumes V^E for four binary mixtures at 303.15 K

χ	V^E (cm³/mol)	χ	V^E (cm³/mol)	χ	V^E (cm³/mol)
		di-*n*-butylamine + *n*-butanol			
0.1182	−0.560	0.4248	−1.304	0.6642	−1.102
0.1860	−0.810	0.5577	−1.270	0.7419	−0.892
0.2657	−1.048	0.6156	−1.190	0.8412	−0.575
		di-*n*-butylamine + *n*-pentanol			
0.0867	−0.350	0.2695	−0.926	0.5344	−1.176
0.1288	−0.498	0.3550	−1.090	0.7077	−0.940
0.2024	−0.740	0.4626	−1.185	0.8031	−0.692
				0.8834	−0.441
		di-*n*-butylamine + *n*-hexanol			
0.1193	−0.474	0.3884	−1.171	0.6635	−1.112
0.2026	−0.762	0.4889	−1.252	0.7730	−0.860
0.2563	−0.925	0.5838	−1.220	0.8820	−0.494
		di-*n*-butylamine + *n*-heptanol			
0.0615	−0.365	0.4027	−1.340	0.6095	−1.224
0.1669	−0.835	0.4546	−1.350	0.7482	−0.928
0.2687	−1.145	0.5177	−1.330	0.8063	−0.761
				0.9061	−0.412

and Naidu in Fig. 1. The values of V^E may be expressed by an empirical equation of the form

$$V^E/\text{cm}^3\ \text{mol}^{-1} = \chi(1-\chi)[a_0 + a_1(2\chi - 1) + a_2(2\chi - 1)^2] \qquad (1)$$

where a_0, a_1 and a_2 are the adjustable parameters and χ in Eq. (1) represents the mole fraction of di-*n*-butylamine. The values of parameters obtained by a least squares analysis are given in Table III along with the standard deviation $\sigma(V^E)$.

Excess volumes for the four mixtures containing di-*n*-butylamine are negative over the entire range of composition. The negative excess volumes suggest that hydrogen bond interaction between unlike molecules is more dominant in these mixtures. This observation is similar to that made by Krishnaiah and Naidu [1]. However, the curves in Fig. 1 show that the mixtures

Table III

Standard deviation σ (V^E) and values of the parameters in Eq. (1) *at* 303.15 K

System	a_0 (cm³/mol)	a_1 (cm³/mol)	a_2 (cm³/mol)	$\sigma(V^E)$ (cm³/mol)
di-*n*-butylamine + *n*-butanol	−5.241	0.763	0.855	0.006
di-*n*-butylamine + *n*-pentanol	−4.751	0.144	0.684	0.005
di-*n*-butylamine + *n*-hexanol	−5.020	−0.133	0.652	0.005
di-*n*-butylamine + *n*-heptanol	−5.347	0.884	−0.252	0.006

containing di-*n*-butylamine have larger negative excess volumes. The larger negative excess volumes may be ascribed to enhancement of electron density on nitrogen in the amino function due to electron releasing effect of the additional butyl group. The negative excess volumes for the four mixtures fall in the order *n*-heptanol > *n*-butanol > *n*-hexanol > *n*-pentanol. The order shows that there is no simple correlation between excess volumes and chain length of the alcohols.

REFERENCES

[1] Krishnaiah, A., Naidu, P. R.: Acta Chim. Acad. Sci., Hung. **104,** 295 (1980)
[2] Riddick, J. A., Bunger, W. B.: Organic Solvents. Wiley-Interscience, New York 1970
[3] Timmermans, J.: Physico-chemical Constants of Pure Organic Compounds. Elsevier, New York 1950
[4] Rao, M. V. P., Naidu, P. R.: Can. J. Chem., **52,** 788 (1974)

Acta Chimica Hungarica, 114 (2), pp. 117–119 (1983)

ACID-CATALYZED CONDENSATION OF ISOPRENE AND 2-METHYLBUT-3-EN-2-OL WITH PHLOROACETOPHENONE, NEW SYNTHESIS OF ALLOEVODIONOL AND FRANKLINONE

V. K. AHLUWALIA*, K. K. ARORA and R. S. JOLLY

(Department of Chemistry, University of Delhi, Delhi-110007, India)

Received June 9, 1982
In revised form September 29, 1982
Accepted for publication November 4, 1982

The naturally occurring acetylchromenes, alloevodionol (**1**) and franklinone (**2**) have been synthesized by the nuclear isoprenylation of phloroacetophenone followed by the partial methylation and dehydrogenation of the chromans thus obtained.

Recently we have developed two new methods for nuclear isoprenylation [1, 2], leading to the one-step synthesis of acetylchromans. These methods involve the direct condensation of isoprene or 2-methylbut-3-en-2-ol with polyhydroxyacetophenones. The usefulness of acetylchromans has already been shown by the synthesis of naturally occurring acetylchromenes [1]. We wish to report here the convenient synthesis of two natural acetylchromenes, viz., alloevodionol (**1**) and franklinone (**2**) by carrying out the nuclear isoprenylation of phloroacetophenone with the two mentioned reagents.

Alloevodionol was isolated [3] from the leaves of *Medicosma cunninghamii* Hook f., whereas franklinone was found [4] in *Acrandenia franklinii*. Both compounds have been synthesized [5] by the dehydrogenation, with DDQ, of the corresponding chromans, **3** and **4**, respectively. Alloevodionol has also been obtained in very low yield by the direct condensation of 2,6-dihydroxy-4-methoxyacetophenone with 2-methylbut-3-yn-2-ol in the presence of zinc chloride.

In the present work, the condensation of isoprene with phloroacetophenone in the presence of 85% phosphoric acid yielded a mixture of three major products (overall yield 70%), which were separated by column chromatography over silica gel. Two of the products were identical with the known compounds [6, 7] **5** and **6**, while the third was found to be an isomer of **5**. Since it did not give a colour reaction with ferric chloride, it was assigned the linear dipyran structure **7**, which was in agreement with the ^{1}H-NMR spectral data.

* To whom correspondence should be addressed.

When the condensation of phloroacetophenone was carried out with 2-methylbut-3-en-2-ol under identical conditions, a mixture of same three products (**5**, **6** and **7**) was obtained in similar ratio as above.

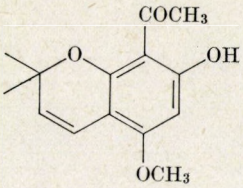

1

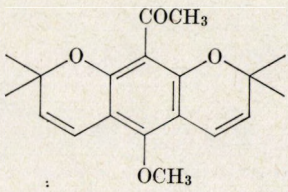

2

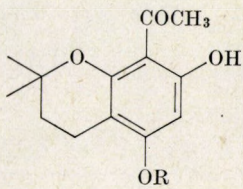

3 R = CH_3

6 R = H

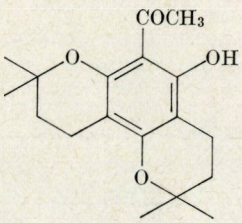

5

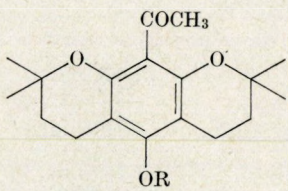

4 R = CH_3

7 R = H

The acetylchromans **6** and **7** on partial methylation gave the monomethyl ethers **3** and **4**, respectively. Dehydrogenation of **3** and **4** with DDQ to afford alloevodionol (**1**) and franklinone (**2**) has already been reported [5].

Experimental

M.p.'s are uncorrected. ^{1}H-NMR spectra were recorded on a Perkin-Elmer R-32 spectrometer with TMS as internal standard.

Condensation of isoprene with phloroacetophenone.

A solution of isoprene (1 mL) in petroleum ether (5 mL) was added to a suspension of 2,4,6-trihydroxyacetophenone (1 g) in 85% phosphoric acid (1 mL) and petroleum ether (5 mL), with constant stirring, during a period of 8 h, maintaining the temperature at 30—35 °C. Stirring was continued for further 12 h and then ether (25 mL) was added. The solution was washed successively with sodium bicarbonate (5% aqueous solution) and water, dried (Na_2SO_4), the solvent evaporated, and the residue was chromatographed on silica gel. The column was eluted successively with (i) petroleum ether, (ii) benzene : petroleum ether (1 : 9) and (iii) benzene : petroleum ether (1 : 4) giving the following three fractions.

Fraction I, crystallized from benzene : petroleum ether yielding **5** as colourless prisms (0.3 g; 26%), m.p. 118—119 °C (*lit.* [6] m.p. 117—118 °C).

^{1}H-NMR ($CDCl_3$): δ 1.36 (s, 12H, 2×CMe_2), 1.75 (t, J = 7 Hz 4H, H-3 andH- 9), 2.54 (t, J = 7 Hz, 4H, H-4 and H-10), 2.60 (s, 3H, $COCH_3$) and 13.76 (s, 1H, exchanged with D_2O, 5-OH).

Fraction II, crystallized from benzene : petroleum ether yielding **6** as colourless prisms (0.55 g; 48%), m.p. 148—149 °C (*lit.* [7] m.p. 150 °C).

^{1}H-NMR ($CDCl_3$): δ 1.32 (s, 6H, CMe_2), 1.85 (t, $J = 7$ Hz, 2H, H-3), 2.60 (triplet superimposed with a singlet, 5H, H-4 and $COCH_3$), 5.89 (s, 1H, H-6) and 13.72 (s, 1H, exchanged with D_2O, 7-OH).

Fraction III, crystallized from aqueous ethanol yielding **7** as colourless plates (0.3 g; 26%), m.p. 158—159 °C.

$C_{18}H_{24}O_4$. Calcd. C 71.1; H 7.9. Found C 71.0; H 8.1%.

^{1}H-NMR ($CDCl_3$): δ 1.28 (s, 12H, $2\times CMe_2$), 1.76 (t, $J = 7$ Hz, 4H, H-3 and H-7), 2.41 (s, 3H, $COCH_3$) and 2.52 (t, $J = 7$ Hz, 4H, H-4 and H-6).

8-Acetyl-3,4-dihydro-7-hydroxy-5-methoxy-2,2-dimethyl-2*H*-1-benzopyran (3)

Compound **6** (0.5 g) was refluxed for 6 h with dimethylsulfate (0.25 mL) in dry acetone (50 mL) in the presence of anhydrous potassium carbonate (1.5 g). The solution was filtered, the inorganic salts were washed with hot acetone and the combined filtrate was evaporated. The solid product obtained after the addition of crushed ice was filtered off and washed successively with 5% sodium carbonate solution and water. It was crystallized from benzene : petroleum ether to give **3** as colourless needles (0.5 g), m.p. 82—83 °C (*lit.* [5] m.p. 78 °C).

^{1}H-NMR ($CDCl_3$): δ 1.38 (s, 6H, CMe_2); 1.79 and 2.58 (each t, $J = 7$ Hz, each 2H, H-3 and H-4, respectively), 2.60 (s, 3H, $COCH_3$), 3.89 (s, 3H, OCH_3), 6.01 (s, 1H, H-6) and 13.72 (s, 1H, exchanged with D_2O, 7-OH).

10-Acetyl-3,4,6,7-tetrahydro-5-methoxy-2,2,8,8-tetra-methyl--2*H*,8*H*-benzo[1,2-*b*:5,4-*b*']dipyran (4)

Methylation of **7** (0.2 g), as described for **6**, grave **4**, which crystallized from petroleum ether as colourless prisms (0.2 g), m.p. 140—141 °C, (*lit.* [6] m.p. 141.5—142 °C).

^{1}H-NMR ($CDCl_3$): δ 1.27 (s, 12H, $2\times CMe_2$); 1.70 (t, $J = 7$ Hz, 4H, H-3 and H-7); 2.36 (s, 3H, $COCH_3$), 2.64 (t, $J = 7$ Hz, 4H, H-4 and H-6) and 3.67 (s, 3H, OCH_3).

*

The authors are thankful to CSIR, New Delhi, India, for financial assistance.

REFERENCES

[1] Ahluwalia, V. K., Arora, K. K.: Tetrahedron, **37,** 1437 (1981)
[2] Ahluwalia, V. K., Arora, K. K., Jolly, R. S.: Hetrocycles, **16,** 2155 (1981)
[3] Kirby, K. D., Sutherland, R. D.: Aust. J. Chem., **9,** 411 (1956)
[4] Baldwin, M. E., Bick, I. R. C., Komzak, A. A., Price, J. R.: Tetrahedron, **16,** 206 (1961)
[5] Cardillo, G., Cricchio, R., Merlini, L.: Tetrahedon, **24,** 4825 (1968)
[6] Brown, P. M., Burton, J. S., Stevans, R.: Tetrahedron Lett., **1963,** 289
[7] Backouse, T., Robertson, A.: J. Chem. Soc., **1939,** 1257

Acta Chimica Hungarica, 114 (2), pp. 121—123 (1983)

REACTION OF LEAD(IV) ACETATE WITH STEROIDAL NITROOLEFINS

(SHORT COMMUNICATION)

SHAFIULLAH*, S. HUSAIN and D. M. BASHA

(Steroidal Research Laboratory, Department of Chemistry, Aligarh Muslim University, Aligarh-202001, India)

Received September 19, 1982
Accepted for publication November 4, 1982

In recent years great interest has been attached to the reactions of lead(IV) acetate, particularly with olefins [1] and oximes [2, 3, 4]. No significant work has been done however with steroidal nitroolefins. This prompted us to study the reaction with lead(IV) acetate of 3-β-chloro-6-nitrocholest-5--ene (**1**), which afforded 3-β-chloro-7-α-acetoxy-6-nitrocholest-5-ene (**2**), 3-β--chloro-5,6-α-diacetoxy-6-nitro-5-α-cholestane (**3**) and 3-α-chloro-4-β-7-α-diacetoxy-6-nitrocholest-5-ene (4).

Compound **2** had correct analysis for $C_{29}H_{46}NO_4Cl$ and positive Beilstein test. The molecular composition indicated the addition of one acetoxy group

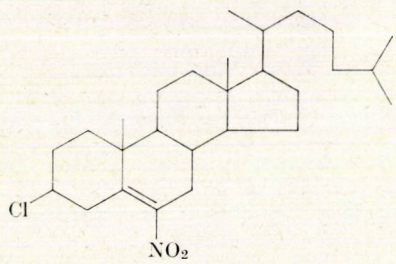

1

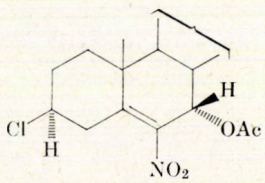

2

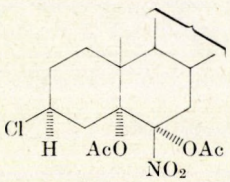

3

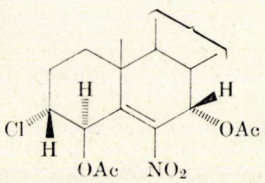

4

* To whom correspondence should be addressed

to the substrate **1**. The strong bands at 1745, 1270—1210 cm^{-1} [5] in the IR spectrum further signified the presence of the acetoxy group. The ^{1}H-NMR spectrum displayed a singlet at δ 2.1 (CH_3—C(=O)—O), and a broad singlet at δ 5.65, integrating for one proton, was assigned to the C-7-β proton. The Dreiding model of **2** showed the dihedral angle between the C-7-β and C-8-β protons to be almost 90° which accounts for the non split signal of the C-7-β proton. The acetoxy group at C-7 is *axial* (α) oriented.

Compound **3** analyzed for $C_{31}H_{50}NO_6Cl$. The molecular composition suggested the addition of two acetoxy groups to the parent compound **1**. The IR spectrum had strong peaks at 1730, 1280—1220 cm^{-1} (CH_3—C(=O)—O) [5] and 1510, 1365 cm^{-1} (C—NO_2) [6]. The ^{1}H-NMR spectrum showed a strong singlet at δ 1.96 with two notches at δ 2.0 and 1.93, integrating for six protons of the two acetoxy groups at C-5 and C-6. The configuration of the C-5 acetoxy group has been considered *axial* on the basis of the C-3 proton multiplet which appeared at δ 3.55 having a half bandwidth of 18 Hz. Evidently, the C-3 proton is *axial* (α) and the A/B ring junction is *trans* [7], rendering the acetoxy group α-oriented.

The analysis of compound **4**, $C_{31}H_{48}NO_6Cl$, confirmed the presence of two acetoxy groups. The ^{1}H-NMR spectrum exhibited two broad singlets at δ 4.50 and 4.26 for C-7-β-*H* ($W1/2 = 3$ Hz; *equitorial*) and C-3-α-*H* ($W1/2 = 8$ Hz; *equitorial*) [7] respectively, suggesting *axial* configuration for the C-7-acetoxy group and C-3 chlorine. A doublet which appeared at δ 7.56 integrating for one proton, was assigned to C4-α-*H* ($J = 3$ Hz; *equitorial*) [7]; a singlet found at δ 2.03 with two notches at δ 1.96 and 2.10, integrating for six protons, corresponds to the two acetoxy groups at C-4 and C-7.

Experimental

The IR spectrum was recorded in Nujol with a Perkin-Elmer 237B spectrophotometer. The NMR spectrum was obtained in $CDCl_3$ on a Varian A60 instrument with Me_4Si as the internal standard. TLC plates were coated with silica gel. A 20% aqueous solution of perchloric acid was used as spraying agent. Anhydrous sodium sulfate served as drying agent. NMR values are given in ppm.

Reaction of 3-β-chloro-6-nitrocholest-5-ene (1) with lead(IV) acetate

3-β-Chloro-6-nitrocholest-5-ene (**1**) [8] (2 g), lead(IV) acetate (4 g), anhydrous potassium acetate (1 g) were refluxed in glacial acetic acid (150 mL) for 12 h. The reaction mixture was cooled to room temperature, diluted with ice-cold water, and extracted with ether. The ethereal solution was washed with sodium hydrogen carbonate solution (10%) and water and dried. Evaporation of the solvent gave a residue which was chromatographed on silica gel (40 g). Elution with light petroleum ether : ether (20 : 1) furnished an oil (**2**) (600 mg).

$C_{29}H_{46}NO_4Cl$. Calcd. C 78.45; H 10.41; N 3.28. Found C 78.35; H 10.30; N 3.38%.
Continued elution with light petroleum ether : ether (18 : 1) gave an oil (**3**) (700 mg).
$C_{31}H_{50}NO_6Cl$. Calcd. C 65.49; H 8.79; N 2.46. Found C 65.40; H 8.70; N 2.43%.
Further elution with light petroleum ether : ether (16 : 1) gave an oil (**4**) (500 mg).
$C_{31}H_{48}NO_6Cl$. Calcd. C 65.54; H 8.45; N 2.46. Found C 65.50; H 8.43; N 2.43%.

*

The authors are grateful to Prof. W. Rahman, Head, Department of Chemistry for providing necessary facilities, to Prof. M. S. Ahmad for encouragement, and to UGC (New Delhi) for financial assistance (to S. H. and D. M. B.).

REFERENCES

[1] Mihailovic, M. Lj., Stefanovic, M., Jockic, A., Maksimovic, Z., Lorenc, Lj.: Helv. Chim. Acta, **53**, 1895 (1970)
[2] Shafiullah, Ali, H., Shamsuzzaman: J. Ind. Chem. Soc., **57**, 859 (1980)
[3] Shafiullah, Ali, H.: Synthesis, **1979**, 124
[4] Kaufmann, S., Tokes, L., Murphy, J. W., Crabbs, P.: J. Org. Chem., **34**, 1618 (1969)
[5] Fieser, L. F., Fieser, M.: Steroids, p. 171, 1959
[6] Silverstein, R. M., Bassler, G. C., Morrill, T. C.: Spectrometric identification of Organic Compounds p. 130, 1981
[7] Bhacca, N. S., Williams, D. H.: Application of N.M.R. Spectroscopy in Organic Chemistry, Holden-Day, Sanfrancisco, 1964, p. 135
[8] Blau, N. F., Stuckwisch, C. G.: J. Org. Chem., **27**, 370 (1962)

Acta Chimica Hungarica, 114 (2), pp. 125–131 (1983)

POLAROGRAPHIC STUDY OF MIXED LIGAND COMPLEXES OF Pb(II) WITH SOME DIAMINES AND MALONIC ACID

J. K. GARG[1]*, D. S. JAIN[2] and P. S. VERMA[2]

([1]Postgraduate Department of Chemistry, Government College, 32/1230 Dada Bhai Quarters, Ajmer-305001, India and [2]Department of Chemistry, University of Rajasthan, Jaipur-302004, India)

Received April 2, 1982
Accepted for publication November 23, 1982

Ternary complexes of Pb(II) with malonic acid as primary ligand and diamines as secondary ligands have been studied polarographically. The free ligand concentration is calculated from pH and total amount present using appropriate pk values. Pb(II) forms three mixed ligand species viz. $[Pb(X)(Y)]$, $[Pb(X)(Y)_2]^{2-}$ and $[Pb(X)_2(Y)]$ where X = ethylenediamine or propylenediamine and Y = malonate anion. The overall stability constants have been evaluated at 298 $\pm$0.5 °K and ionic strength of 1.50 (KNO_3), using the method of Schaap and McMasters [1]. The value of formation constants are correlated and discussed in term of statistical consideration and charge neutralization.

Numerous references are available in the literature on the polarographic study of single ligand complexes. However, polarographic method has been rarely applied to mixed ligand complexes. The mixed complexes of Pb(II) with various organic ligands have been studied recently by many workers [2—6]. Studies on the formation of mixed ligand complexes by Pb(II) with malonic acid as primary ligand and ethylenediamine or propylenediamine as secondary ligand are reported in this paper It was observed that Pb(II) forms 1 : 3 complexes with en, pn and malo.

Experimental

All the reagents used were of A. R. grade. The polarograms of all the solutions were obtained with a manual polarograph. Capillary characteristics for the open circuits were $m = 1.89$ mg/sec and $t = 3.5$ sec. pH of solution was maintained at the required value by adding nitric acid solution. The ionic strength of all the solutions were maintained at 1.50 by adding required amount of potassium nitrate. All the measurements were carried out at 298 $\pm$ 0.5 °K, which was maintained by a Haake type ultra thermostat. The solution was placed in an H-type cell coupled with saturated calomel electrode through a KCl saturated agar-agar salt bridge. Prior to reduction at d.m.e. purified nitrogen gas was streamed through the test solution for twenty minutes to expel dissolved oxygen. pK values of the ligands were measured by generally accepted procedure and were found to be as follows:

* To whom correspondence should be addressed

Ligands	pK_1	pK_2
1. Ethylenediamine	6.50	9.48
2. Propylenediamine	7.00	9.78
3. Malonic acid	2.85	5.69

Results and Discussion

The simple systems

The overall formation constants of simple complexes have been evaluated by DeFord and Humes [7] and Mihailov [8] methods and the results are reported in Table I. The reduction of Pb(II) in all these systems were found

Table I

Overall stability constants of Pb(II) complexes

System	De Ford and Hume method			Mihailov method		
	$\log \beta_1$	$\log \beta_2$	$\log \beta_3$	$\log \beta_1$	$\log \beta_2$	$\log \beta_3$
Pb-en	4.08	7.24	10.10	4.12	7.20	10.11
Pb-pn	5.06	8.20	10.96	5.10	8.14	11.00
Pb-malo	2.86	3.66	4.27	2.86	3.66	4.28

reversible involving two electrons and diffusion controlled as revealed by the linear plots of i_d vs. $h_{ef}^{1/2}$ of mecury column passing through the origin. The plots of $\log \frac{i}{i_d - i}$ vs. $E_{d.e.}$, were linear with a slope of 31 ± 2 mV. No maximum suppressor was needed in these systems. The concentration of free ligands was calculated from the pH and the total amount present using the appropriate pK values.

Mixed systems

Three different mixed complexes of Pb(II) are possible with two bidentate ligands. These are [Pb(en)(malo)], $[Pb(en)(malo_2)]^{2-}$ and $[Pb(en)_2(malo)]$ for ethylenediamine malonate systems and [Pb(pn)(malo)], $[Pb(pn)(malo)_2]^{2-}$ and $[Pb(pn)_2(malo)]$ for propylenediamine malonate systems.

Polarograms were taken with solution containing 0.5 m*M* Pb(II), KNO_3 ($\mu = 1.50$), two fixed concentrations of malonate (0.20 *M* and 0.25 *M*) and varying concentrations of ethylenediamine or propylenediamine at pH =

$= 7.7$. A shift in $E_{1/2}$ to more cathodic potentials with increasing en or pn concentration was observed in all the cases. This shift is greater in the presence of weaker ligand (malo) than in its absence. It signifies mixed complex formation. The Schaap and McMasters [1] treatment was applied to the half wave potential data and F_{i0} functions evaluated. Leeden's [9] graphical extrapolation method was applied to calculate A, B, C and D (Table II). The F_{00} functions may be written as:

$$F_{00} = A + B[\mathrm{X}] + C[\mathrm{X}]^2 + D[\mathrm{X}]^3$$

Where, [X] = en or pn

Table II

Mixed ligand stability constants parameters at 298 ± 0.5° K *and* $\mu = 1.50$ (KNO_3)

System	Concentration	A Calculated	B	C	D	log D_{av}
Pb-en-malo	[malo]=0.20M	4.77×10^2	64.0×10^4	7.5×10^7	10.98×10^9	10.04
	[malo]=0.25M	7.59×10^2	86.0×10^4	8.9×10^7	11.38×10^9	10.06
Pb-pn-malo	[malo]=0.20M	4.77×10^2	160.0×10^4	38.0×10^7	85.5×10^9	10.93
	[malo]=0.25M	7.59×10^2	208.0×10^4	43.5×10^7	88.8×10^9	10.94

$$A = 1 + \beta_{01}[\mathrm{malo}] + \beta_{02}[\mathrm{malo}]^2 + \beta_{03}[\mathrm{malo}]^3$$
$$B = \beta_{10} + \beta_{11}[\mathrm{malo}] + \beta_{12}[\mathrm{malo}]^2$$
$$C = \beta_{20} + \beta_{21}[\mathrm{malo}]$$
$$D = \beta_{30}$$

The values of A and D are known from the studies of the simple systems. However, values of B must be evaluated at least at two appropriate malonate ion concentrations, so that mixed constants β_{11} and β_{12} can be calculated.

Values for A for all the series were calculated using constants from the simple systems and each of them can be shown to agree well with the intercepts of the plots of the F_{00} values vs en or pn concentrations. The average values of log D from both series, in case of the en-malo system were found to be 10.04, 10.06. This agrees reasonably well with the value of log $\beta_{30} = 10.10$ while in the case of the pn-malo system, the values of log D were 10.93, 10.94, which are also in good agreement with the corresponding value of log $\beta_{30} =$ $= 10.96$.

The log of the overall formation constants (log β_{11}, log β_{12}, and log β_{21}) evaluated for the mixed complexes present in the system and for the equilibria between them are summarized in the Schemes 1 and 2.

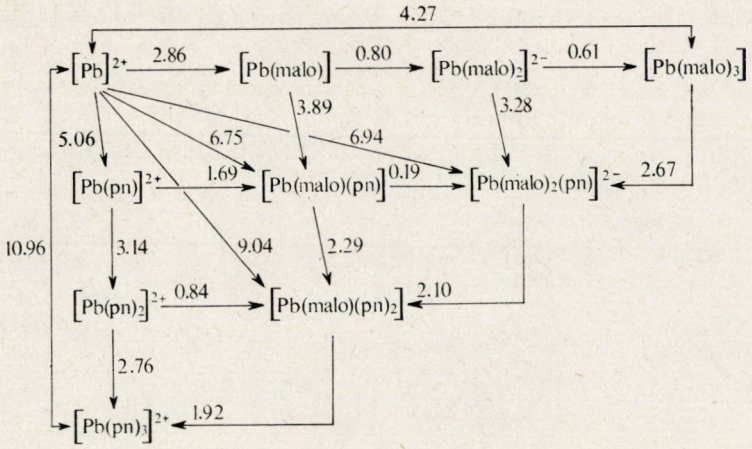

Scheme 1

Various interesting observations can be made. The tendency of [Pb(malo)] and $[Pb(en)]^{2+}$ to add a second ligand can be compared. For the addition of a malonate anion, the log K values are 0.80 and 2.25. Again the difference is much larger than the statistical factor of 2 would predict showing the effect of charge neutralization. In a similar way for the addition of malonate anions to [Pb(malo)] and $[Pb(pn)]^{2+}$, the log values are 0.80 and 1.69. This observation also shows that mixed complex formation is favoured. Addition of uncharged ethylenediamine ligand to each of the above complexes gives rise to log K values of 3.47 and 3.16, in a similar way the addition of an uncharged propylenediamine to each of the above complexes give rise to log K values of 3.89 and 3.14. These observations further show that the formation of mixed complex is favoured.

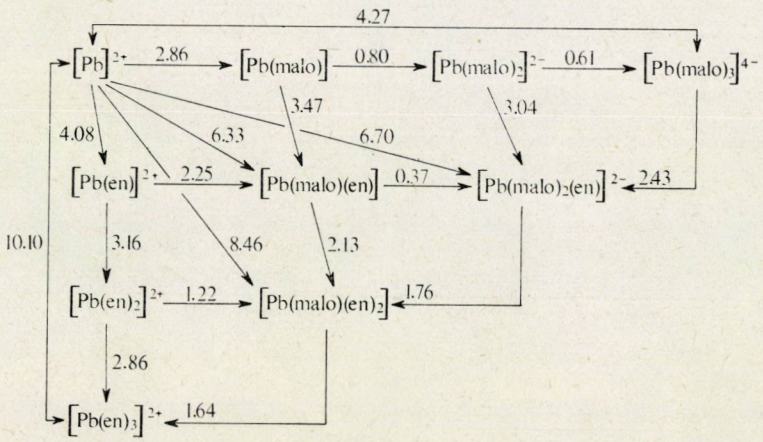

Scheme 2

The log K values for the additions of an uncharged ethylenediamine as third ligand to $[Pb(malo)_2]^{2-}$, [Pb(en)(malo)], and $[Pb(en)_2]^{2+}$ are 3.04, 2.13, 2.86 which shows that addition of a stronger ligand viz. en is preferred to a weaker ligand viz. malo. Similarly, the log K values for the additions of uncharged propylenediamine to $[Pb(malo)_2]^{2-}$, [Pb(pn)(malo)] and $[Pb(pn)_2]^{2+}$ are 3.28, 2.29 and 2.76. The log K values for the addition to malonate anion as third ligand to $[Pb(malo)_2]^{2-}$ [Pb(en)(malo)] and $[Pb(en)_2]^{2+}$ are 0.61, 0.37, 1.22 which shows that the addition of malonate anion is preferred to $[Pb(malo)_2]^{2-}$ and $[Pb(en)_2]^{2+}$ as compared to [Pb(en)(malo)]. In a similar way, the log K values for addition of malonate anion as third ligand to $[Pb(malo)_2]^{2-}$, [Pb(pn)(malo)] and $[Pb(pn)_2]^{2+}$ are 0.61, 0.19, 0.84.

These trends may be understood if it is assumed, in accord with much evidence which need not be cited here, that the N → metal bond is appreciably more covalent than the O → metal bond with these ligands. The ethylenediamine or propylenediamine complexes would then be more strongly influenced by the stereochemistry of the hybridized sp^3 orbitals of lead than would the more ionic malonate complexes and would have a correspondingly greater tendency to be tetrahedral. Addition of either ethylenediamine/propylenediamine molecule or malonate ion to $[Pb(en)_2]^{2+}$ / $[Pb(pn)_2]^{2+}$ would be hindered despite the opposite charges of the latter two species, while addition of either ligand to $[Pb(malo)_2]^{2-}$ would proceed more readily, off setting the repulsion of the like charges in the case of malonate addition.

For the reactions

$$[Pb(X)_2]^{2+} + [Pb(Y)_2]^{2-} \rightleftharpoons 2[Pb(X)(Y)]$$

(X) = en or pn

(Y) = malo.

We have $\log X_{11} = 2 \log \beta_{11} - (\log \beta_{20} + \log \beta_{02})$

while, for

$$[Pb(X)_3]^{2+} + 2[Pb(Y)_3]^{4-} \rightleftharpoons 3[Pb(X)(Y)_2]^{2-}$$

We have

$$\log X_{12} = 3 \log \beta_{12} - (\log \beta_{30} + 2 \log \beta_{03})$$

Similarly for,

$$2[Pb(X)_3]^{2+} + [Pb(Y)_3]^{4-} \rightleftharpoons 3[Pb(X)_2(Y)]$$

We have

$$\log X_{21} = 3 \log \beta_{21} - (2 \log \beta_{30} + \log \beta_{03})$$

The values of $\log X_{11}$, $\log X_{12}$ and $\log X_{21}$ for en-malo, and pn-malo systems are as below:

System	log X_{11}	log X_{12}	log X_{21}
Pb(II)-en-malo	1.76	1.46	0.91
Pb(II)-pn-malo	1.64	1.32	0.93

In each system under investigation, the value of log X_{11} is higher than the statistical value of log X, which for all geometries of the coordination sphere of metal ion is the same viz. 0.6. The log X_{12} and log X_{21} values are also higher than the expected statistical value. These observations further suggest that all these ternary complexes are considerably more stable than would be expected on purely statistical grounds.

The mixing constant (equilibrium constant) K_M for the reaction

$$1/2[\mathrm{Pb\,X_2}]^{2+} + 1/2[\mathrm{Pb\,Y_2}]^{2-} \rightleftharpoons [\mathrm{Pb\,XY}]$$

indicates the relative stability of the mixed complex in solution as compared to parent binary complex. K_M is given by the relation

$$K_M = \frac{\beta_{11}}{\sqrt{\beta_{02}\,\beta_{20}}} .$$

The statistical value of log K_M is 0.3 [10—12]. Alternatively, the stabilization constant K_S [13] for the ligand of equal denticity is expressed in the form

$$\log K_S = \log \beta_{11} - 1/2(\log \beta_{20} + \log \beta_{02} + \log 4)$$

The observed values are

$$[\mathrm{Pb - en - malo}];\ \log K_M = 0.88,\ \log K_S = 0.58$$
$$[\mathrm{Pb - pn - malo}];\ \log K_M = 0.82,\ \log K_S = 0.52$$

The positive values of stabilization constants show that the ternary complexes are more stable than binary complexes. The positive values of stabilization constants have been observed by Jain et al. [14], Brookes and Pettit [15], Gergely and Sovago [16] and Ting and Nancollas [10].

Many workers [17—19] have observed that charge neutralization favours formation of mixed ligand complexes. The results of our investigations are also in agreement with this postulation.

*

Thanks are due to Sri G. S. Kachhawha, Senior Lecturer in Chemistry, for helpful discussions.

REFERENCES

[1] Schaap, W. B., McMasters, D. L.: J. Am. Chem. Soc., **83,** 4699 (1961)
[2] Gupta, K. C., K. Tajendra: Electrochim. Acta, **24,** 1133 (1979)
[3] Yadav, R. D., Verma, P. S., Zutshi, K.: J. Electrochem. Soc. India, **293**, 145 (1980)
[4] Agarwal, L. K.: Ph. D. Thesis, Univ. of Rajasthan, Jaipur, India 1979
[5] Garg, J. K., Verma, P. S., Jain, D. S.: Monatsh. Chem. (Submitted)
[6] Garg, J. K., Verma, P. S., Jain, D. S.: Symposium on Polarography and Allied Technique, Indian Institute of Science, Bangalore, India, Abstract, Pg. 20 (1982)
[7] DeFord, D. D., Hume, D. N.: J. Am. Chem. Soc., **73,** 5321 (1951)
[8] Mihailov, M. H.: J. Inorg. Nucl. Chem., **36,** 107, 114 (1974)
[9] Leeden, I.: Z. Phys. Chem., **188A,** 160 (1941)
[10] Ting, P. I., Nancollas, G. H.: Inorg. Chem., **11,** 2414 (1972)
[11] Marcus, Y., Eliezer, I.: Coord. Chem. Rev., **4,** 273 (1969)
[12] Bianco, P., Heladjian, J., Pillard, R.: J. Electroanal. Chem., **72,** 341 (1976)
[13] Gergely, A., Nagyapal, I., Markas, S.: J. Inorg. Nucl. Chem., **37,** 551 (1975)
[14] Jain, S. L., Kishan, J., Kapoor, R. C.: Indian J. Chem., **18A,** 133 (1979)
[15] Brookes, G., Pettit, L. D.: J. Chem. Soc. (Dalton), **1977,** 1918
[16] Gergely, A., Sovago, I.: J. Inorg. Nucl. Chem., **35,** 4355 (1973)
[17] Sigel, H., Huber, P. R., Posternack, R. F.: Inorg. Chem., **10,** 226 (1971)
[18] Griesser, R., Sigel, H.: Inorg. Chem., **9,** 1238 (1970)
[19] Condike, G. F., Martell, A. E.: J. Inorg. Nucl. Chem., **31,** 2445 (1969)

Acta Chimica Hungarica, 114 (2), pp 133–148 (1983)

DEUTERIUM VAPOUR PRESSURE ISOTOPE EFFECT IN BROMOFORM

GY. JÁKLI*, P. JUHÁSZ and G. JANCSÓ

(Central Research Institute for Physics, H-1525 Budapest, P.O. Box 49.)

Received July 21, 1982
In revised form October 13, 1982
Accepted for publication November 23, 1982

The vapour pressure difference between $CHBr_3$ and $CDBr_3$ was determined by differential capacitance manometry in the temperature ranges of −25 to +8.5 °C (solid phase) and +8.5 to 64 °C (liquid phase). The vapour pressure of $CHBr_3$ between −53.4 and +70 °C has also been determined. The experimentally observed H/D vapour pressure isotope effect in the liquid phase was interpreted within the framework of the statistical theory of condensed phase isotope effects. The dielectric corrections to the vapour–liquid shifts of the vibrational frequencies of $CHBr_3$ have been evaluated. The anharmonicity constant of the CH stretching vibration has been found to increase by about 4.6% on the vapour–liquid transition at room temperature.

Introduction

The difference in the vapour pressure of isotopically substituted molecules (vapour pressure isotope effect, VPIE) is closely connencted to the intermolecular forces acting between the molecules in the condensed phase [1]. Recent experimental determinations of the VPIE's of different compounds and their subsequent interpretation within the framework of the statistical mechanical theory of condensed phase isotope effects [1, 2] have given information concerning the temperature dependence of the CH stretching force constant of acetonitrile [3] and benzene [4], the kinetic energy coupling between internal vibrations and molecular translations and/or rotations in the case of fluoroform [5] and benzene [4] and have shown that the deviation of isotopic mixtures from the ideal behaviour can be explained by considering the differences in the molar volumes of isotopic species [6]. It has been pointed out [7] that in the theoretical calculation of the VPIE that part of the spectroscopically observed vapour–liquid shift of vibrational frequencies should be employed which can be attributed to the intermolecular interactions, thus the observed liquid phase frequencies must first be corrected for the difference between the effective field of the light wave acting on the molecule in a condensed medium and the average field in this medium ("dielectric correction")

* To whom correspondence should be addressed.

[8—10]. In favourable cases VPIE studies may also provide information on the anharmonicity change of the molecular vibrations on condensation [11, 12].

Ishida et al. [5] measured the vapour pressures of $^{12}CHF_3$, $^{13}CHF_3$ and $^{12}CDF_3$ and the interpretation of the experimental data supported the spectroscopically observed blue shift ($\sim$26 cm^{-1}) of the CH stretching frequency on condensation which is assumed to be due to the kinetic energy coupling between the CH stretching and the molecular translation in the direction of the symmetry axis. Jancsó et al. [13] determined the vapour pressure difference between $CHCl_3$ and $CDCl_3$ and the interpretation of the results together with the literature data on $^{12}C/^{13}C$ and $^{35}Cl/^{37}Cl$ vapour pressure isotope effects have shown that the anharmonicity constant of the CH stretching vibration decreases by about 4% on the vapour–liquid transition. This should be compared with a 0.95% decrease in the CH stretching force constant, corresponding to a red shift of 14 cm^{-1} of this vibration on condensation. The CH stretching vibration of the third member of the haloforms, $CHBr_3$, undergoes an even larger red shift (28 cm^{-1}), therefore, a considerably higher inverse H/D VPIE can be expected in comparison with that of chloroform. The question arises whether this larger vapour–liquid shift is accompanied by a further decrease in the vibrational anharmonicity.

In the present paper the results of the experimental determination of the vapour pressure differences between $CHBr_3$ and $CDBr_3$ will be reported and discussed in terms of the theory of isotope effects in the condensed phase. The liquid phase frequencies employed in the calculations will be corrected for dielectric effect and an attempt will be made at estimating the effect of condensation on the anharmonicity constant of the CH stretching vibration from the VPIE results.

Experimental

Gas chromatographic analysis of $CHBr_3$ (Reanal, analytical reagent) showed that it contains about 2—3% impurities of low volatility. The sample was subjected to purification by preparative gas chromatography. The column was packed with celite-supported DC 550 silicon oil (10 wt. %). A sample of $CDBr_3$ (Isocommerz) with a deuterium content of 99.7 atom % was purified in the same fashion. Before measurement the protio and deutero compounds were dried in a vacuum apparatus over phosphorus pentoxide and distilled to the degassing bulb, where they were submitted to many freeze-pump-thaw cycles.

The vapour pressure measurements utilized apparatus and techniques which have been described previously in considerable detail [14]. A differential capacitance manometer was calibrated against the vapour pressure of water [15, 16] and the temperature was measured by a platinum resistance thermometer. Both the absolute vapour pressure of the protio compound and the vapour pressure difference between the isotopic molecules were determined to an accuracy of four figures. The uncertainty in the temperature can be estimated as being $\pm$0.03 °C.

Results

The measurement of the absolute vapour pressure of bromoform extended from —53.4 to +8.5 °C and from +8.5 to 70 °C in the solid and liquid phase,

respectively. The experimental data (113 in the solid and 164 in the liquid phase are available from the authors on request) have been fitted by a non-linear least squares technique to the Antoine equation giving

$$\log_{10}(p/\text{Pa}) = 15.839 - 4802.02/(349.55 + t/°\text{C}) \qquad (-53.4 < t < +8.5) \quad (1)$$

for the solid phase and

$$\log_{10}(p/\text{Pa}) = 9.1080 - 1486.03/(213.22 + t/°\text{C}) \qquad (+8.5 < t < 70) \quad (2)$$

for the liquid phase, giving a standard deviation of the calculated $\log_{10} p$ values about $\pm 2 \times 10^{-3}$ and $\pm 2 \times 10^{-4}$, respectively. No vapour pressure data for the solid phase are available in the literature for comparison with the present data. The agreement between the vapour pressures of liquid $CHBr_3$ measured in different laboratories is rather poor. Our value at room temperature lies 6% below the tabulated value of Stull [17] and 3% higher than that of Kireev and Simnikov [18]. At the highest temperature of our measurement (70 °C) the differences become smaller, our vapour pressure is 1% lower than that of Kireev and Simnikov [18] and 2% higher than the more recent value obtained by Boublik and Aim [19], whereas Stull's value [17] is 3% lower than ours.

The isotopic vapour pressure difference data for the liquid phase — grouped separately for the different runs — are presented in Table I (the list of the solid phase data is available from the authors on request). The VPIE values — which are given as $\ln(p_H/p_D)$ where p_H and p_D are the vapour pressures of $CHBr_3$ and $CDBr_3$ — were calculated from the observed isotopic vapour pressure differences and from the vapour pressure of $CHBr_3$ obtained from Eqs (1) and (2). The VPIE data in the liquid phase can adequately be described by the equation

$$\ln(p_H/p_D) = 1.486 \times 10^{-2} - 11.628/(T/\text{K}) \qquad (282 < T < 337) \quad (3)$$

The standard deviation of the calculated $\ln(p_H/p_D)$ values is about $\pm 7 \times 10^{-5}$. The solid phase data cover a narrow temperature range (−25 to +8.5 °C) with an intermediate phase transition at about −5 °C [20] and since their precision is poor in comparison with that of liquid phase data, therefore, we decided not to fit them to any equation. It is appropriate to emphasize that the VPIE is definitely normal in the solid phase (it amounts to about 5% in the β phase) and becomes inverse in the liquid phase (its magnitude is around 2%).

From the solid and liquid phase vapour pressure data it is possible to estimate the difference in the triple points of the isotopic molecules; the triple point of $CDBr_3$ was found to be 0.30 ± 0.05 °C higher than that of $CHBr_3$ (8.5 °C [17]).

Table I

Vapour pressure isotope effect of liquid bromoform
($\Delta P_{\text{measured}} = p_D - p_H$)

t (°C)	Δp/Pa	$\ln(p_H/p_D)$	t (°C)	Δp/Pa	$\ln(p_H/p_D)$
10.91	7.942	−0.0261	40.60	38.89	−0.0215
11.42	8.079	−0.0256	41.63	40.81	−0.0213
11.67	8.353	−0.0261	42.40	42.58	−0.0214
12.44	8.627	−0.0255	43.17	44.37	−0.0214
13.46	9.038	−0.0250	44.20	46.97	−0.0215
13.97	9.311	−0.0249	44.97	48.20	−0.0212
14.48	9.722	−0.0252	45.75	50.39	−0.0213
14.99	9.859	−0.0247	46.78	52.86	−0.0212
15.49	10.27	−0.0248	47.55	55.05	−0.0212
16.01	10.41	−0.0244	48.48	57.10	−0.0210
16.52	10.95	−0.0248	49.35	59.70	−0.0210
17.03	11.36	−0.0249	51.26	65.32	−0.0209
17.97	11.91	−0.0246	51.85	67.37	−0.0210
18.56	12.32	−0.0245	54.25	75.18	−0.0208
19.51	13.01	−0.0243	55.29	79.15	−0.0209
20.86	14.24	−0.0245	56.06	83.25	−0.0212
22.22	15.34	−0.0242			
23.29	16.29	−0.0241	10.01	7.394	−0.0258
25.77	18.62	−0.0237	10.45	7.394	−0.0251
27.00	19.72	−0.0233	11.03	7.805	−0.0254
28.33	20.81	−0.0227	11.29	7.805	−0.0250
29.66	22.32	−0.0266	11.92	8.079	−0.0248
30.84	22.59	−0.0214	12.18	8.216	−0.0248
31.36	24.65	−0.0226	12.69	8.490	−0.0247
31.92	25.47	−0.0226	13.46	8.764	−0.0243
35.46	29.98	−0.0219	14.09	9.174	−0.0243
36.39	31.49	−0.0218	14.35	9.448	−0.0247
37.00	32.59	−0.0218	14.73	9.585	−0.0244
39.57	37.11	−0.0216	14.99	9.859	−0.0247
15.75	10.41	−0.0248	38.54	35.33	−0.0218
16.01	10.54	−0.0247	39.05	36.42	−0.0218
16.52	10.95	−0.0248	39.83	37.93	−0.0218
17.28	11.36	−0.0245	40.60	39.03	−0.0215
18.56	12.05	−0.0239	41.63	40.81	−0.0213
19.84	13.14	−0.0241	43.17	44.37	−0.0214
20.35	13.55	−0.0240	44.20	47.24	−0.0216

Table I (continued)

t (°C)	Δp/Pa	$\ln(p_H/p_D)$	t (°C)	Δp/Pa	$\ln(p_H/p_D)$
21.12	14.10	−0.0238	44.97	48.61	−0.0214
21.63	14.65	−0.0240	45.75	51.07	−0.0216
22.14	15.06	−0.0239	46.78	53.13	−0.0213
22.65	15.47	−0.0238	47.55	55.46	−0.0214
23.16	16.43	−0.0245	48.06	56.96	−0.0214
23.67	17.25	−0.0249	48.84	59.02	−0.0213
24.19	17.53	−0.0245	49.35	59.43	−0.0209
24.70	17.66	−0.0240	50.13	62.03	−0.0210
25.21	17.94	−0.0236	50.90	64.77	−0.0211
25.72	18.48	−0.0236	51.93	68.74	−0.0213
26.24	19.03	−0.0236	52.71	70.93	−0.0212
26.74	19.58	−0.0235	53.74	73.40	−0.0209
27.77	20.67	−0.0234	54.51	76.68	−0.0210
28.28	21.77	−0.0239	55.29	80.24	−0.0212
28.79	22.32	−0.0237	56.06	83.39	−0.0212
29.56	22.59	−0.0230	56.58	85.72	−0.0213
30.33	23.41	−0.0228	57.09	86.54	−0.0210
31.36	24.78	−0.0227	57.61	88.18	−0.0209
32.13	25.74	−0.0226			
32.89	27.25	−0.0229	8.97	6.710	−0.0252
33.92	28.07	−0.0223	9.07	6.847	−0.0255
34.69	29.17	−0.0222	9.12	7.531	−0.0279
35.46	30.40	−0.0222	9.38	7.805	−0.0284
35.98	31.36	−0.0222	9.51	7.668	−0.0277
36.49	32.32	−0.0222	9.63	7.531	−0.0270
38.03	34.23	−0.0217	9.79	7.531	−0.0267
9.89	7.668	−0.0270	31.23	25.19	−0.0233
10.04	7.805	−0.0272	31.87	26.02	−0.0232
10.14	7.668	−0.0265	33.41	28.62	−0.0234
10.30	7.805	−0.0267	35.21	30.40	−0.0225
10.40	7.805	−0.0265	36.23	32.04	−0.0224
10.65	7.942	−0.0265	37.13	33.68	−0.0224
10.91	8.079	−0.0265	37.26	33.82	−0.0223
11.16	8.216	−0.0265	38.03	35.88	−0.0227
11.42	8.353	−0.0265	39.06	37.11	−0.0222
11.67	8.490	−0.0265	39.83	38.20	−0.0220
11.93	8.627	−0.0265	40.60	39.57	−0.0218
12.18	8.764	−0.0264	41.63	42.45	−0.0222

Table I (continued)

t (°C)	Δp/Pa	$\ln(p_H/p_D)$	t (°C)	Δp/Pa	$\ln(p_H/p_D)$
12.44	8.764	−0.0260	42.40	43.41	−0.0218
12.69	9.038	−0.0263	43.17	44.50	−0.0215
13.20	9.311	−0.0262	44.20	46.83	−0.0214
13.46	9.311	−0.0258	44.97	48.88	−0.0215
14.22	9.859	−0.0260	45.23	49.71	−0.0215
14.99	10.13	−0.0253	45.49	50.80	−0.0217
16.01	10.82	−0.0253	46.78	53.27	−0.0213
17.28	11.64	−0.0251	48.58	58.74	−0.0215
18.56	12.60	−0.0250	48.83	59.84	−0.0216
20.09	13.83	−0.0249	49.61	60.80	−0.0211
21.12	14.65	−0.0248	50.26	63.13	−0.0213
22.39	15.75	−0.0246	50.64	64.49	−0.0213
23.67	17.66	−0.0255	51.16	66.41	−0.0214
24.44	18.07	−0.0249	51.41	67.37	−0.0214
25.21	18.48	−0.0243	51.67	68.60	−0.0216
26.23	19.72	−0.0244	51.93	69.70	−0.0216
27.00	20.40	−0.0241	52.19	70.66	−0.0216
27.77	21.09	−0.0238	52.45	71.89	−0.0217
28.79	23.00	−0.0245	52.70	72.30	−0.0216
29.56	23.14	−0.0235	52.96	72.44	−0.0214
30.33	23.96	−0.0233	53.74	75.86	−0.0216
54.00	76.82	−0.0216	9.17	7.805	−0.0288
54.25	78.05	−0.0216	9.28	7.805	−0.0286
54.64	78.32	−0.0213	9.38	7.805	−0.0284
55.03	79.01	−0.0211	9.43	7.942	−0.0288
55.54	80.51	−0.0210	9.53	7.668	−0.0277
56.06	81.74	−0.0208	9.63	7.942	−0.0284
56.99	84 21	−0.0205	9.79	7.942	−0.0281
57.35	85.17	−0.0204	9.89	7.942	−0.0279
57.77	86.68	−0.0204	10.04	7.942	−0.0277
58.13	88.46	−0.0204	10.14	7.942	−0.0275
58.64	92.15	−0.0208	10.40	8.079	−0.0275
59.42	93.80	−0.0204	10.65	8.216	−0.0274
59.68	94.62	−0.0203	10.91	8.216	−0.0270
59.94	96.26	−0.0205	13.46	9.448	−0.0261
60.20	97.91	−0.0206	14.73	10.13	−0.0258
64.46	99.55	−0.0207	16.31	11.09	−0.0254
60.71	99.68	−0.0205	17.28	11.78	−0.0254

Table I (continued)

t (°C)	Δp/Pa	$\ln(p_H/p_D)$	t (°C)	Δp/pa	$\ln(p_H/p_D)$
60.97	100.4	−0.0204	19.07	13.14	−0.0253
61.23	103.5	−0.0207	21.37	15.06	−0.0250
61.49	103.1	−0.0204	22.39	15.88	−0.0248
61.75	103.6	−0.0203	23.16	16.43	−0.0245
62.00	104.6	−0.0202	23.93	17.2 5	−0.0245
62.27	104.9	−0.0202	24.95	18.35	−0.0245
62.78	107.8	−0.0201	25.98	19.31	−0.0243
63.30	110.5	−0.0202	26.23	19.85	−0.0246
			27.51	21.63	−0.0248
			28.79	22.73	−0.0241

For theoretical analysis the ratio of the reduced partition function ratios of the liquid and gas phase (f_c/f_g) is the important quantity obtainable from the experimentally observed VPIE using the equation [1, 2]

$$\ln(f_c/f_g) = \ln(p_H/p_D) - \frac{p_H V_H - p_D V_D}{RT} - \left(B_0 p + \frac{1}{2} C_0 p^2 + \cdots\right)_D + \left(B_0 p + \frac{1}{2} C_0 p^2 + \cdots\right)_H \quad (4)$$

where f_c and f_g are the reduced partition function ratios for the condensed and gaseous phase; V_H and V_D molar volumes in the liquid phase of $CHBr_3$ and $CDBr_3$; B_0 and C_0 are virial coefficients. A detailed knowledge of the virial coefficients and condensed phase molar volumes is necessary to make the corrections which are usually small (a few per cent of the measured effects) [1, 12]. Molar volume isotope effect data are not available therefore the approximation $V_H = V_D$ was used; the liquid density data were taken from [21]. The $V_H(p_H - p_D)/RT$ correction term was found to amount to 6×10^{-5} at room temperature which is less than the experimental precision of the VPIE measurements, thus it can be neglected. In the calculation of the real gas correction term the third virial coefficients (C_0) were taken as zero, and $B_{0H} = B_{0D}$ was assumed. The second virial coefficient of bromoform was obtained from the Berthelot equation of state using values of critical constants ($T_c = 698$ K and $p_c = 6.0 \times 10^6$ Pa) estimated by the methods of Lydersen and Riedel [22]. The magnitude of the correction was less than 0.5% of the logarithm of the vapour pressure ratios in the entire temperature range of investigation. The experimental reduced partition function ratio (f_c/f_g) for

$CHBr_3/CDBr_3$, which can be taken to be equal to $\ln p_H/p_D$, is shown against the temperature in Fig. 1.

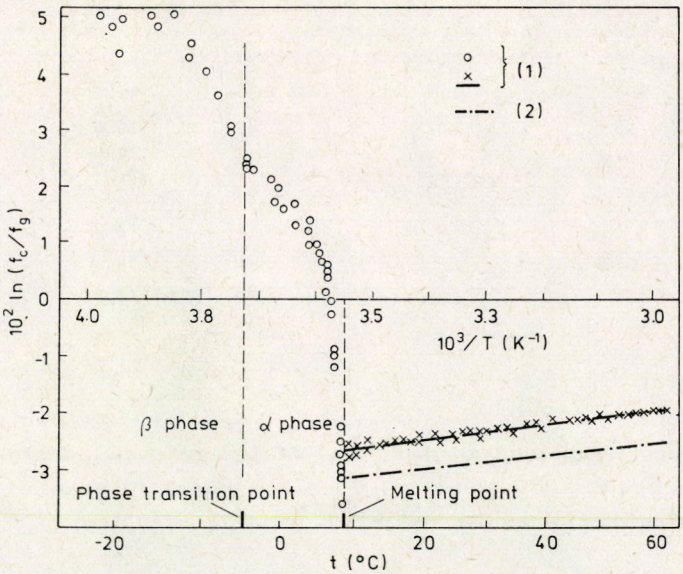

Fig. 1. Comparison of calculated and experimental reduced partition function ratios (f_c/f_g) for $CHBr_3$. (1): experimental; (2): calculated with force fields given in Table III. (To avoid clutter only every second experimental data point has been plotted for the solid and every fifth for the liquid phase)

Discussion

In the harmonic oscillator approximation using a simplified cell model for the liquid phase, the reduced partition function ratio can be calculated by using the expression [1, 23]

$$\frac{f_c}{f_g} = \prod_{\text{int. freq.}}^{3N-6} \frac{(u_i/u_i')_c \exp\left((u_i' - u_i)_c/2\right)(1 - \exp(-u_i')_c)/(1 - \exp(-u_i)_c)}{(u_i/u_i')_g \exp\left((u_i' - u_i)_g/2\right)(1 - \exp(-u_i')_g)/(1 - \exp(-u_i)_g)} \times$$

$$\times \prod_{\text{ext. freq.}}^{6} \frac{u_i}{u_i'} \left[\exp\left(\frac{u_i' - u_i}{2}\right)\right]\left[\frac{1 - \exp(-u_i')}{1 - \exp(-u_i)}\right], \qquad (5)$$

where $u_i = hcv_i/kT$; c and g refer to the condensed and gaseous phases; N is the number of atoms in the molecule; v_i is the i-th normal mode frequency in cm^{-1}; the prime refers to the lighter isotopic species. The model assumes an average condensed phase molecule with $3N$-6 internal and 6 external degrees of freedom. In the gas phase the six external translations and rotations are taken as zero frequencies but in the condensed phase they are assumed to be

subject to harmonic restoring forces. The frequencies are calculated from an isotope independent force constant (**F**) matrix and an isotope dependent kinetic energy (**G**) matrix which is obtained from the molecular structure, mass, and mass distribution by standard methods [23, 24]. The most important contribution to the VPIE of bromoform can be expected to be determined by the changes in the internal force constants of the F matrix on condensation which can be obtained from spectroscopic data on phase frequency shifts.

The calculation of the vapour phase frequencies was carried out in terms of the internal valence coordinates which are shown in Fig. 2; they consist of one CH bond stretch (D), three CBr bond stretches (d), three HCBr angle

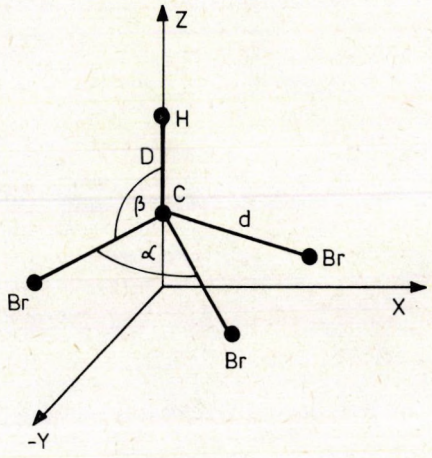

Fig. 2. Coordinate system and internal valence coordinates of bromoform

bends (β) and three BrCBr angle bends (α). The values of the molecular parameters used are shown in Table II. The gas phase force constants were determined from the available infrared and Raman data of $CHBr_3$ and $CDBr_3$ 20, 25—33] and from the force field of Galasso et al. [36] as an initial estimate.

Table II

Molecular parameters of $CHBr_3$

r_{CH}	106.8	pm	
r_{CBr}	193.0	pm	[34]
∢BrCBr	110.8°		
m_H	1.0078246	u.	
m_D	2.0141002	u.	[35]
$m_{^{12}C}$	12.0000	u.	
$m_{^{79}Br}$	78.918390	u.	

Table III

Gas and liquid phase force fields in internal valence coordinates for bromoform[a]

	Gas phase		Liquid phase (25 °C)
f_D	4.94520[b]		4.84579[d]
f_d	3.10859		3.02355
f_{dd}	0.78245		0.76479
f_{Dd}		0.06000	
$f_{d\alpha}$		0.10518	
$f_{D\beta}$	−0.45598		−0.47972
$f_{d\alpha}$		0.19926	
$f_{d\alpha'}$[c]		−0.12350	
$f_{d\beta}$		0.06104	
$f_{d\beta'}$	−0.18376		−0.18761
f_α		0.79198	
$f_{\alpha\alpha}$		−0.17900	
f_β	0.59540		0.58873
$f_{\beta\beta}$		0.02914	
$f_{\alpha\beta}$		−0.12926	
$f_{\alpha\beta'}$	−0.05405		−0.06360
$f_{T_x} = f_{T_y} = f_{T_z}$			1.47138
$f_{R_x} = f_{R_y}$			0.34470
f_{R_z}			free rotation

[a] Bond stretching, bond–bond interaction and translational constants are in 10^2 N/m, bond–angle interaction constants are in 10^{-8} N, angle bending, angle–angle interaction and rotational constants are in aNm.

[b] Values of the force constants are given to more significant figures than justified by the precision of the spectroscopic data used in order to permit replication of the computed results.

[c] The prime refers to the interaction between two coordinates which do not share a common C – Br bond.

[d] This force constant is temperature dependent: 1.79×10^{-3} Nm^{-1} $(°C)^{-1}$.

The elements of the final gas phase **F** matrix are shown in Table III and the calculated frequencies obtained by using this force field are compared with the observed ones in Table IV.

In order to obtain the liquid phase force constants, it is necessary to correct the observed vapour-liquid frequency shifts for the dielectric effect [7] brought about by the dielectric properties of the liquid medium sorrounding the absorbing molecule. The corrected liquid phase frequency, which is always higher than the observed absorption maximum, is given by the maximum of the imaginary part of the local susceptibility (this is different from the macroscopic susceptibility) vs. frequency function [10]. To construct such a plot

Table IV

Calculated and observed gas phase frequencies (in cm^{-1})

	$CHBr_3$			$CDBr_3$		
	obs.		calc.	obs.		calc.
ν_1 CH(CD) stretch	3049.2 3048 3048.3 3042	[25] [26] [27] [28]	3048.024	2270	[28]	2270.114
ν_2 sym. CBr_3 stretch	548	[26]	548.023	....		526.576
ν_3 sym. CBr_3 bend[a]	222 222.3	[29, 20] [30]	223.407	222 221.6	[32] [33]	221.276
ν_4 HCBr(DCBr) bend	1149 1147.7	[26, 31] [25]	1149.038	856	[32]	856.225
ν_5 antisym. CBr_3 stretch	669	[26, 31]	669.064	644	[32]	638.952
ν_6 antisym. CBr_3 bend[a]	155 153.8 153	[29] [30] [20]	153.431	155 153.4	[32] [33]	153.325

[a] No vapour phase frequencies were available for these low frequency fundamentals therefore, they were assumed to be equal to the observed frequencies in the liquid phase.

one needs to know — in addition to the absorption coefficient — the refractive index (n) as a function of frequency in the infrared region of liquid bromoform. This function is available for the ν_1, ν_4 and ν_5 vibrations [31, 37], although the precision of the refractive index data especially in the neighbourhood of the ν_4 and ν_5 bands can be considered as being rather poor, therefore, in these cases the $n(\nu)$ function in the region of the absorption band was determined from the absorption spectra [38] through the Kramers—Kronig relation [39]. To illustrate how the dielectric correction was calculated, the absorption coefficient, refractive index and the imaginary part of the local susceptibility vs. frequency plots for the ν_5 (655 cm^{-1}) band are shown in Fig. 3. The frequency which gives the maximum value of local susceptibility is seen to be slightly different from the absorption band center and this difference corresponds to a dielectric correction of 4 cm^{-1}. For the ν_4 band the correction is less than 0.5 cm^{-1} and also in the case of the ν_1 vibration (the absorption coefficients and refractive index data were taken from [26] and [37], respectively) it has

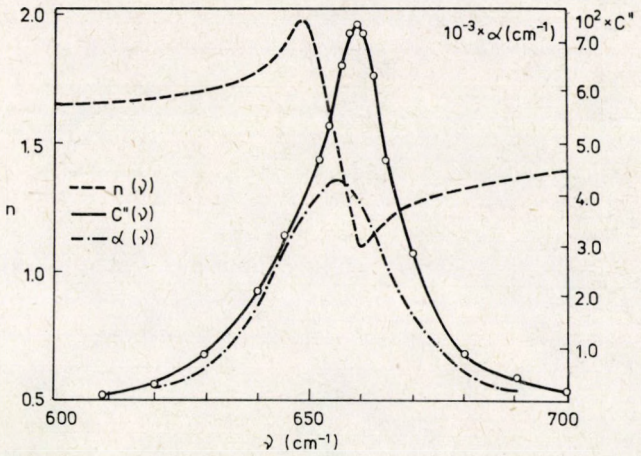

Fig. 3. Optical constants and local susceptibilities for the ν_5 (655 cm^{-1}) band of liquid bromoform. $n(\nu)$ — refractive index; $\alpha(\nu)$ — absorption coefficient; $C''(\nu)$ — imaginary part of the local susceptibility. The filled circles represent calculated points

been found to be negligible (less than 0.1 cm^{-1}). The ν_2 infrared band is very weak [26], therefore, in this case no correction can be expected. For the ν_3 and ν_6 fundamentals only the liquid phase frequencies have been determined, but as these show no measurable H/D isotope shift they do not contribute to the VPIE, in view of which we have not dealt with the calculation of the dielectric corrections for these frequencies.

The liquid phase force constants obtained from the gas force field by applying the corrected vapour–liquid frequency shifts are listed in Table III and the calculated and observed frequency shifts are compared in Table V. Spectroscopic measurements show that the frequency of the CH stretching vibration of $CHBr_3$ increases by about 0.0054 $cm^{-1}/°C$ with increasing temperature [38]. The consideration of this temperature dependence has little effect on the calculated H/D VPIE (at most 1.1×10^{-4} in $\ln(p_H/p_D)$) in contrast with the $CHCl_3/CDCl_3$ system [13]. The contribution of the external frequencies to the vapour pressure differences between $CHBr_3$ and $CDBr_3$ can be expected to be small (less than 1% of the overall VPIE): the rotation around the C_3 axis — which is presumably free in the liquid phase [42] — does not contribute to the VPIE since the isotopic substitution occurs on this axis, the hindered rotational frequency around the axis perpendicular to the symmetry axis was taken as 38 cm^{-1} [20] and the hindered translational frequency was estimated as being not larger than 100 cm^{-1}. Figure 1 shows the comparison between the experimental VPIE and that calculated with the force fields given in Table III; the calculated VPIE is more inverse than the observed one and the difference — e.g. 21% at room temperature — is larger than the experimental error. As in the case of the $CHCl_3/CDCl_3$ system [13] it is of interest

Table V

Frequency shifts on condensation ($\nu_{gas} - \nu_{liq}$) *for* $CHBr_3$ *and* $CDBr_3$ *in* cm^{-1} *(at room temperature)*

	$CHBr_3$				$CDBr_3$[b]	
	observed		dielectric correction	calculated	observed	calculated
ν_1	28[a] 36.8 [25] 18 [41] 23 [28]		<0.1	28.0	19 [28]	19.1
ν_2	8 [26]		0	8.0		8.0
ν_3	....[c]			0.8		0.8
ν_4	7 [26, 41] 5.3 [25]		<0.5	7.0	8 [32]	6.5
ν_5	14[d]		4	10.0	10 [32]	8.6
ν_6	....[c]			0.1		0.1

[a] This value is obtained from the gas phase (3048 cm^{-1} [26], 3048.3 cm^{-1} [27]) and liquid phase (3020 cm^{-1} [20, 26, 30,40] frequencies.

[b] For $CDBr_3$ dielectric corrections have not been calculated due to the lack of the necessary data.

[c] No gas phase frequency is available for this vibration.

[d] This value is obtained from the gas phase (669 [26, 31]) and liquid phase (655 cm^{-1} [29, 20]) frequencies.

to consider the change in the anharmonicity constant of the CH stretching vibration on condensation as a possible cause for the discrepancy. The substantial justification for this is that the most significant contribution to the calculated VPIE (about 70%) comes from the zero-point energy shift of the ν_1 vibration on condensation. This vibration has a high anharmonicity (the anharmonicity constant is —65.9 cm^{-1} [27] in the vapour phase) compared with those of the other normal modes of bromoform and it can be treated as a diatomic oscillator [43].

The contribution of a CH/CD harmonic oscillator to the VPIE calculated on the basis of Eq. (5) by using fundamental frequencies is given in the zero-point energy approximation [1] as

$$\ln (f_c/f_g)_{CH/CD} = \frac{1}{2} \frac{hc}{kT} \left[(\nu_{H/c} - \nu_{D,c}) - (\nu_{H,g} - \nu_{D,g}) \right] \qquad (6)$$

On the other hand the zero-point energy contribution of an anharmonic CH/CD oscillator [44] to the VPIE can be written as

$$\ln (f_c/f_g)_{CH/CD,anh} = \frac{hc}{kT}\left[\frac{1}{2}(\omega_{H,c} - \omega_{D,c}) - \frac{1}{2}(\omega_{H,g} - \omega_{D,g}) + \right.$$
$$\left. + \frac{1}{4}(X_{H,c} - X_{D,c}) - \frac{1}{4}(X_{H,g} - X_{D,g})\right] \quad (7)$$

where ω is the harmonic frequency (in cm^{-1}) and X is the anharmonicity constant [45].

By taking into account that $\nu = \omega + 2X$ [45] and $X_H/X_D = \mu_D/\mu_H$ [45, 46] one obtains for the difference between Eq. (7) and Eq. (6)

$$\Delta \ln (f_c/f_g) = \frac{3}{4}\frac{hc}{kT}\left(1 - \frac{\mu_H}{\mu_D}\right)\Delta X_H$$

where $\Delta \ln (f_c/f_g)$ is taken to be equal to the difference between the observed VPIE and that calculated by Eq. (5), μ_H and μ_D are the reduced masses of the CH and CD oscillators and $\Delta X_H = X_{H,g} - X_{H,c}$. The values for ΔX_H and ΔX_D obtained from Eq. (8) are shown in Table VI. It can be seen that

Table VI

The vapour–liquid shift of the anharmonicity constant of CH(CD) *stretching vibration of bromoform and deuterobromoform* (in cm^{-1})

Temperature (°C)	ΔX_H[a]	ΔX_D[a,b]
8.5	2.7_0	1.4_6
25.0	-0.4 ± 1.5[c] $3.0_6 \pm 0.8$[d]	1.6_5
40.0	3.3_9	1.8_3
63.3	3.8_8	2.0_9

[a] $\Delta X = X_{vapour} - X_{liquid}$

[b] $X_D = (\mu_H/\mu_D)\Delta X_H$

[c] This is calculated from $X_{vap} = -65.9$ cm^{-1} [27] and $X_{liq} = -65.5$ cm^{-1} [40].

[d] The error limit of ± 0.8 cm^{-1} was estimated on the basis of uncertainties in the spectroscopically observed fundamentals used in the calculations.

the anharmonicity increases by about 4.6% on vapour–liquid transition at room temperature and its magnitude increases with increasing temperature whereas within the precision of spectroscopic investigations the anharmonicity constant does not change (-65.9 ± 0.2 [27] in the vapour and $-65.5 \pm \pm 1.3$ [40] in the liquid phase). The present result is in contrast with the findings for chloroform where the anharmonicity constant was found to decrease by 4%. As was noted earlier, the shift of the ν_1 vibration on condensation is twice as large for bromoform as that observed for chloroform, but from this

no conclusion can be drawn on the magnitude of the change in the anharmonicity constant, since no simple relationship between these two quantities has been found so far [43, 47]. The haloform molecules may provide a good system for investigations of this kind, however, a theoretical analysis must wait until more spectroscopic information on $CHBr_3$ (and mainly on CHF_3) molecules becomes available.

Finally a few words are in order about the change in the VPIE on solid–liquid transition. Crystalline bromoform undergoes a phase transition at —5 °C [20] and with our present experimental technique it is difficult to obtain highly precise VPIE values in the neighbourhood of the melting and the phase transition region. However, the sign of the VPIE can be considered as definitely established and the magnitude of the observed normal isotope effect in the β phase (below —5 °C) seems to be surprisingly large. Measurements should be carried out with improved low temperature thermostating before detailed interpretation of this large change in isotope effect on melting can be attempted in terms of the difference between the liquid and solid phase frequencies of $CHBr_3$ and $CDBr_3$.

*

We wish to thank Dr. J. Mink and Dr. S. Dobos, Institute of Isotopes of the Hungarian Academy of Sciences, for carrying out IR measurements on the bromoform samples.

REFERENCES

[1] Jancsó, G., Van Hook, W. A.: Chem. Rev., **74,** 689 (1974)
[2] Bigeleisen, J.: J. Chem. Phys., **34,** 1485 (1961)
[3] Jákli, Gy., Koritsánszky, T., Jancsó, G.: Ber. Bunseges. Phys. Chem., **85,** 773 (1981); Proc. 4th Int. Conf. Stable Isotopes, Eds. Schmidt, H. L., Förstel, H., Heinzinger, K., Elsevier, Amsterdam, 1982, p. 15.
[4] Jákli, Gy., Tzias, P., Van Hook, W. A.: J. Chem. Phys., **68,** 3177 (1978); Jancsó, G., Van Hook, W. A.: J. Chem. Phys., **68,** 3191 (1978)
[5] Popowicz, A., Oi. T., Shulman, J., Ishida, T.: J. Chem. Phys., **76,** 3732 (1982)
[6] Jancsó, G., Van Hook, W. A.: Physica, **A91,** 619 (1978)
[7] Jancsó, G., Van Hook, W. A.: Can. J. Chem., **55,** 3371 (1977); Chem. Phys. Lett., **48,** 481 (1977)
[8] Akopyan, S. Kh., Girin, O. P., Bakhshiev, N. G.: Opt. Spektrosk., **36,** 185 (1974) and references cited therein
[9] Lefranc, B., Jacob, J., Vincent-Geisse, J.: Spectrochim. Acta, **22,** 1057 (1966)
[10] Clifford, A. A., Crawford, B., Jr.: J. Phys. Chem., **70,** 1536 (1966)
[11] Jancsó, G., Van Hook, W. A.: J. Mol. Struct., **48,** 107 (1978); ibid.: **74,** 360 (1981)
[12] Jancsó, G., Van Hook, W. A.: Acta Chim. Acad. Sci. Hung., **98,** 183 (1978)
[13] Jancsó, G., Jákli, Gy., Fetzer, Cs.: Z. Naturforsch., **38a,** 184 (1983)
[14] Jákli, Gy., Illy, H.: KFKI Report 80—15 (1980); Jancsó, G., Jákli, Gy.: Aust. J. Chem., **33,** 2357 (1980)
[15] Jancsó, G., Pupezin, J., Van Hook, W. A.: J. Phys. Chem., **74,** 2984 (1970)
[16] Goff, J. A.: in Humidity and Moisture, Vol. **3,** p. 289. Ed. Wexler, A., Reinhold, New York 1963
[17] Stull, D. R.: Ind. Eng. Chem., **39,** 517 (1947)
[18] Kireev, V. A., Simnikov, I. P.: Zh. Obshch. Khim., **14,** 483 (1941)
[19] Boublik, I., Aim, K.: Coll. Czech. Chem. Commun., **37,** 3513 (1972)
[20] Burgos, E., Halac, E., Bonadeo, H.: J. Chem. Phys., **74,** 1546 (1981)

[21] Int. Critical Tables, Vol. **III,** p. 146. McGraw Hill, New York 1928
[22] Reid, R. C., Sherwood, T. K.: The Properties of Gases and Liquids, McGraw Hill, New York 1966
[23] Stern, M. J., Van Hook, W. A., Wolfsberg, M.: J. Chem. Phys., **39,** 3179 (1973)
[24] Wilson, E. B. Jr., Decius, J. C., Corss, P. C.: Molecular Vibrations, McGraw Hill, New York 1955
[25] Jenkins, G. L., Straley, J. W.: Phys. Rev., **68,** 99 (1945)
[26] The IR measurements were carried out on DIGILAB FTS-20C spectrometer by Drs. J. Mink and S. Dobos of the Institute of Isotopes of the Hungarian Academy of Sciences
[27] Rossi, I., Nguyen-Van-Thanh, Haeusler, C.: Can. J. Chem., **47,** 3319 (1969)
[28] Forel, M. T., Leicknam, J. P., Josien, M. L.: J. Chim. Phys., **57,** 1103 (1960)
[29] Meister, A. G., Rosser, S. E., Cleveland, F. F.: J. Chem. Phys., **18,** 346 (1950)
[30] Redlich, O., Stricks, W.: Monatsh. Chem., **67,** 328 (1936)
[31] Lindsay, L. P., Schatz, P. N.: Spectrochim. Acta, **20,** 1421 (1964)
[32] Ferigle, S. M., Cleveland, F. F., Boyer, W. M., Bernstein, R. B.: J. Chem. Phys., **18,** 1073 (1950)
[33] Redlich, O., Stricks, W.: Sitz. Akad. Wiss. Wien IIb, **145,** 192 (1936)
[34] Harmony, M. D., et al.: J. Phys. Chem. Ref. Data, **8,** 619 (1979)
[35] Beynon, J. H., Saunders, R. A., Williams, A. E.: The Mass Spectra of Organic Molecules, Elsevier, Amsterdam 1968 p. 476.
[36] Galasso, V., deAlti, G., Costa, G.: Spectrochim. Acta, **21,** 669 (1965)
[37] Pittman, M. A.: J. Opt. Soc. Am., **29,** 358 (1938)
[38] Lisitsa, M. P., Tsyashchenko, Yu. P.: Opt. Spektrosk., **9,** 188 (1960)
[39] Crawford, B., Jr., Goplen, T. G., Swanson, D.: in Advances in Infrared and Raman Spectroscopy, Vol. **4,** p. 97. Eds. Clark, R. J. H., Hester, R. E., Heyden, London 1978
[40] Soussen-Jacon, J., Dervil, E., Vincent-Geisse, J.: Mol. Phys., **28, 935** (1974)
[41] Plyler, E. K., Benedict, W. S.: J. Res. Natl. Bur. Stand., **47,** 202 (1951)
[42] Pleshkov A. V., Brutan, E. G.: Izv. Vyssh. Uchebn. Zaved. Fiz., **5,** 140 (1972)
[43] Durocher, G., Sandorfy, C.: J. Mol. Spectrosc., **22,** 347 (1967)
[44] Bron, J., Chang, C. F., Wolfsberg, M.: Z. Naturforsch., **28a,** 129 (1972)
[45] Herzberg, G.: Molecular Spectra and Molecular Structure, Vol. **I**, Van Nostrand, Princeton 1950
[46] Johansen, H.: Z. Phys. Chem., **231,** 419 (1966)
[47] Kolomiitsova, T. D., Melikova, S. M., Tsepkin, D. N.: Opt. Spektrosk., **39,** 602 (1975)

Acta Chimica Hungarica, 114 (2), pp. 149–157 (1983)

THEORETICAL INTERPRETATION OF THE VIBRATIONAL SPECTRA OF *TRANS*- AND *CIS*-PENTA-1,3-DIENES AND 2,3-DIMETHYLBUTADIENE

YU. N. PANCHENKO,[1] V. I. MOCHALOV,[1] P. CSÁSZÁR,[2]* F. TÖRÖK,[2]+
E. BENEDETTI[3] and M. AGLIETTO[3]

([1]Molecular Spectroscopy Laboratory, Department of Chemistry M. V. Lomonosov Moscow State University, SU-11-117234 Moscow, U.S.S.R., [2]Department of General and Inorganic Chemistry, Eötvös L. University, H-1088 Budapest, Múzeum krt. 6–8., Hungary, [3] Centro di Studio del C.N.R. per le Macromolecole Stereoordinate ed Otticamente Attive, Instituto di Chimica Oranica e Istituto di Chimica Organica Industriale dell' Universita di Pisa, Pisa, Italy)

Received July 16, 1982
In revised form November 9, 1982
Accepted for publication November 25, 1982

Force constants and theoretical vibrational frequencies of *trans*- and *cis*-penta-1,3-dienes and 2,3-dimethylbuta-1,3-diene were calculated by CNDO/2 force method adopting the *s-trans* molecular conformation. The results lead to refinements in vibrational assignments and to frequencies assumed to be characteristic of the *trans* and *cis* structural isomers of penta-1,3-dienes and of buta-1,3-diene methyl substituted in positions 2 and 3.

Introduction

Detailed study of the vibrational spectra of *trans*- and *cis*-penta-1,3-dienes in different phases has become available recently [1]. Variable temperature studies of infrared and Raman bands in liquid phase and those of IR bands in the gas and solid phases showed that these molecules exist in the *trans* conformation [1]. This conclusion is in agreement with the microwave data on the structure of these molecules [2] which showed the predominance of the *s-trans* conformer. A critical discussion of the results obtained by variable temperature NMR study [3] is also reported [1]. Recent NMR investigations [4] confirm the planarity of these molecules.

The structure of 2,3-dimethylbuta-1,3-diene has been determined from the vibrational spectra [5], by gas electron diffraction [6], and by microwave spectroscopy [7]. The experimental value of dipole moment [8], the NMR spectrum [9], the vibrational spectra [5, 10, 11], the temperature dependence of band positions and shapes in the vibrational spectra [12] and analysis of

* To whom correspondence should be addressed
+ We are deeply saddened to report the untimely death of Prof. F. Török on September 3, 1981

the steric effects by a mechanical model [13] support that the molecule considered exsists predominantly in the planar *trans* form.

The calculation of the vibrational frequencies of *trans*- and *cis*-penta--1,3-dienes and 2,3-dimethylbuta-1,3-diene in the *s-trans* conformation was performed earlier by the trial-and-error method [14, 15]. In a first approximation the force field of buta-1,3-diene [16] was used, but it proved to be derived from an erroneous assignment of certain vibrational frequencies [17]. It was therefore necessary to perform independent quatum chemical calculations for the molecules considered in order to obtain unambiguous assignments of the vibrational frequencies.

Computational details

The force constants of *trans*- and *cis*-pentadiene-1,3 and 2,3-dimethylbuta-1,3-diene molecules were calculated by the gradient method [18, 19] in the CNDO/2 approximation [20].

Geometry parameters were taken from related molecules of similar structure [21, 6] as follows: r(C—C) = 1.491 Å, r(C=C) = 1.349 Å, r(C—C, sp^3) = 1.511 Å ,r(C—H) = 1.093 Å, r(C—H, sp^3) = 1.123 Å, $\sphericalangle$(C=C—C) = = 122°, $\sphericalangle$(H—C=C) = 120.4° and $\sphericalangle$(C=C—CH_3) = 120.4°. The bond angles in the CH_3 group were assumed to be tetrahedral. Optimization of geometries was not performed.

The systematic deviations in the force constants were corrected by using the following scaling factors; 0.377 for the carbon–carbon stretchings: 0.393 for the C—H stretchings; 1.136 for the in plane deformations of the C=C—C angles; 0.812 for the deformations of the H—C=C and H—C—H angles and for waggings of the C—CH_3 bonds out of the molecular plane; 0.692 for the twisting around the C=C bonds, for the out-of-plane waggings of carbon atoms and for the torsions of the methyl groups; 0.598 for the waggings of the C—H bonds out from the molecular plane and 1.302 for the torsions around the central C—C bond. These values of scaling factors were obtained correcting the force constants of well examined small molecules like glyoxal, acrolein and butadiene-1,3. Note that the force constants of propylene obtained by the CNDO/2 method and scaled by these factors are quite close to those determined by the ab initio method [22].

The methyl torsions in both the *trans* and *cis* forms were described by the same force constants calculated for the *trans* conformer. The numerical value obtained for the *cis* form was too small indicating that the geometry chosen may not reflect the actual structure of this molecule. This discrepancy is also detected in the high value of the ν_{10} frequency. The same reason is

Table I

Experimental and calculated vibrational frequencies of trans-pentadiene-1,3 (in cm^{-1})

ν_i	Description*	Symmetry	Experiment [1]		Calculated
			Raman	IR	
1	$\nu(CH_2)$ *as.* str.	A'	—	3098	3081
2	ν(C—H) *as.* str.	A'	—	3050	3041
3	$\nu(CCH_3—H)$ str.	A'	—	3018	3038
4	ν(C—H) *s.* str.	A'	—	3018	3035
5	$\nu(=CH_3)$ *s.* str.	A'	2997	—	3012
6	$\nu(CH_3)$ *as.* str.	A'	—	2973	2887
7	$\nu(CH_3)$ *s.* str.	A'	—	2937	2838
8	ν(C=C) *s.* str.	A'	—	1660	1638
9	ν(C=C) *as.* str.	A'	—	1608	1583
10	$\delta(CH_3)$ *as.* def.	A'	—	1449	1471
11	$\delta(=CH_2)$ sciss.	A'	—	1420	1439
12	$\delta(CH_3)$ *s.* def.	A'	—	1376	1408
13	δ(C—H) bend.	A'	—	1306	1328
14	δ(C—H) bend.	A'	1292	—	1306
15	$\delta(CCH_3—H)$ bend.	A'	1262	—	1271
16	ν(C—C) str.	A'	1180	—	1165
17	$\nu(C—CH_3)$ str.	A'	1082	—	1090
18	$\varrho(=CH_2)$ rock.	A'	977	—	968
19	$\varrho(CH_3)$ rock.	A'	—	948.5	912
20	$\delta(C=C—CH_3)$ bend.	A'	479	—	473
21	δ(C=C—C) *s.* bend.	A'	—	454	458
22	δ(C=C—C) *as.* bend.	A'	—	196	216
23	$\nu(CH_3)$ *as.* str.	A''	—	2973	2884
24	$\delta(CH_3)$ *as.* str.	A''	—	1449	1460
25	χ(C—H) wag.	A''	1037	—	1034
26	χ(C—H) wag.	A''	—	1003	993
27	$\varrho(CH_3)$ rock.	A''	—	973	974
28	$\chi(=CH_2)$ wag.	A''	—	899	921
29	$\chi(CCH_3—H)$ wag.	A''	—	818	794
30	τ(C=C) twist.	A''	—	630	621
31	$\tau(CCH_3=C)$ twist.	A''	—	250	259
32	$\tau(CH_3)$ tors.	A''	—	205	182
33	τ(C—C) tors.	A''	150	—	125

* Description of the vibrations is based on the calculated total energy distribution, Abbreviations used: *s.* = symmetric, *as.* = asymmetric, str. = stretching, bend. = bending, def. = deformation, twist. = twisting, wag. = wagging, rock. = rocking, tors. = torsion, sciss. = scissoring

Table II

Experimental and calculated vibrational frequencies of cis-penta-1,3-diene (in cm^{-1})

ν_i	Description*	Symmetry	Experiment [1]		Calculated
			Raman	IR	
1	$\nu(=CH_2)$ *as.* str.	A'	—	3097	3081
2	$\nu(CCH_3-H)$ str.	A'	—	3068	3046
3	$\nu(C-H)$ *as.* str.	A'	—	3033	3034
4	$\nu(C-H)$ *s.* str.	A'	—	3033	3030
5	$\nu(=CH_2)$ *s.* str.	A'	3010	—	3012
6	$\nu(CH_3)$ *as.* str.	A'	—	2970	2883
7	$\nu(CH_3)$ *s.* str.	A'	—	2928	2837
8	$\nu(C=C)$ *s.* str.	A'	1645	—	1630
9	$\nu(C=C)$ *as.* str.	A'	—	1592	1575
10	$\delta(CH_3)$ *as.* def.	A'	1453	—	1504
11	$\delta(=CH_2)$ sciss.	A'	—	1437	1461
12	$\delta(CH_3)$ *s.* def.	A'	—	1390	1429
13	$\delta(C-H)$ *s.* bend.	A'	—	1361	1376
14	$\delta(C-H)$ *as.* bend.	A'	1297	—	1325
15	$\delta(CCH_3-H)$ bend.	A'	1252	—	1225
16	$\nu(C-C)$ str.	A'	1166	—	1150
17	$\varrho(CH_3)$ rock.	A'	1043	—	1064
18	$\nu(C-CH_3)$ str.	A'	—	955	935
19	$\varrho(=CH_2)$ rock.	A'	886	—	918
20	$\delta(C=C-C)$ *s.* bend.	A'	—	610	598
21	$\delta(C=C-CH_3)$ bend.	A'	390	—	433
22	$\delta(C=C-C)$ *as.* bend.	A'	—	353	318
23	$\nu(CH_3)$ *as.* str.	A''	—	2970	2884
24	$\delta(CH_3)$ *as.* def.	A''	—	1390	1438
25	$\chi(C-H)$ wag.	A''	1035	—	1035
26	$\chi(C-H)$ wag.	A''	—	997	973
27	$\varrho(CH_3)$ rock.	A''	—	—	966
28	$\chi(=CH_2)$ wag.	A''	—	905	929
29	$\chi(CCH_3-H)$ wag.	A''	—	777	784
30	$\tau(C=C)$ twist.	A''	—	621	623
31	$\tau(CCH_3=C)$ twist.	A''	—	228	265
32	$\tau(CH_3)$ tors.	A''	214	—	155
33	$\tau(C-C)$ tors.	A''	140	—	130

* See footnotes to Table I

Table III

Experimental and calculated vibrational frequencies of 2,3-dimethylbuta-1,3-diene (in cm^{-1})

ν_i	Description*	Symmetry	Experiment [1]		Calculated
			Raman	IR	
1	$\nu(=CH_2)$ *as.* str.	A_g	3109	....	3078
2	$\nu(=CH_2)$ *s.* str.	A_g	3011	....	3011
3	$\nu(CH_3)$ *as.* str.	A_g	2983	....	2887
4	$\nu(CH_3)$ *s.* str.	A_g	2930	....	2838
5	$\nu(C=C)$ *s.* str.	A_g	1633	....	1655
6	$\nu(CH_3)$ *as.* def.	A_g	1471	....	1491
7	$\nu(=CH_2)$ *s.* sciss.	A_g	1414	....	1442
8	$\nu(CH_3)$ *s.* def.	A_g	1385	....	1462
9	$\nu(C-C)$ str.	A_g	1341	....	1363
10	$\varrho(CH_3)$ *s.* rock.	A_g	1025	....	1026
11	$\varrho(=CH_2)$ *s.* rock.	A_g	970	....	990
12	$\nu(C-CH_3)$ *s.* str.	A_g	726	....	748
13	$\delta(C=C-C)$ *s.* bend.	A_g	491	....	458
14	$\delta(C=C-CH_3)$ *s.* bend.	A_g	392	....	361
15	$\nu(CH_3)$ *as.* str.	A_u	....	2961	2886
16	$\delta(CH_3)$ *as.* def.	A_u	....	1447	1469
17	$\varrho(CH_3)$ *as.* rock.	A_u	....	1036	1018
18	$\chi(=CH_2)$ *as.* wag.	A_u	....	894	912
19	$\tau(=CH_2)$ *as.* twist.	A_u	....	657	679
20	$\chi(C-CH_3)$ *as.* wag.	A_u	....	327	348
21	$\tau(CH_3)$ *as.* tors.	A_u	....	215	235
22	$\tau(C-C)$ tors.	A_u	....	73	51
23	$\nu(CH_3)$ *as.* str.	B_g	2968	....	2886
24	$\delta(CH_3)$ *as.* def.	B_g	1447	....	1470
25	$\varrho(CH_3)$ *as.* rock.	B_g	....	....	1038
26	$\chi(=CH_2)$ *s.* wag.	B_g	895	....	905
27	$\tau(=CH_2)$ *s.* twist.	B_g	....	....	793
28	$\chi(C-CH_3)$ *s.* wag.	B_g	551	....	585
29	$\tau(CH_3)$ *s.* tors.	B_g	247	....	217
30	$\nu(=CH_2)$ *as.* str.	B_u	....	3104	3078
31	$\nu(=CH_2)$ *s.* str.	B_u	....	3011	3010
32	$\nu(CH_3)$ *as.* str.	B_u	....	2984	2887
33	$\nu(CH_3)$ *s.* str.	B_u	....	2932	2838
34	$\nu(C=C)$ *as.* str.	B_u	....	1605	1595
35	$\delta(CH_3)$ *as.* def.	B_u	....	1457	1473
36	$\delta(=CH_2)$ *as.* sciss.	B_u	....	1386	1413
37	$\delta(CH_3)$ *s.* def.	B_u	....	1377	1440
38	$\varrho(CH_3)$ *as.* rock.	B_u	....	1183	1202
39	$\varrho(=CH_2)$ *as.* roc.	B_u	....	998	1011
40	$\nu(C-CH_3)$ *as.* str.	B_u	....	920+	936
41	$\delta(C=C-CH_3)$ *as.* bend.	B_u	....	470+	433
42	$\delta(C=C-C)$ *as.* bend.	B_u	....	272	258

* See footnotes to Table I

+ These wave numbers are taken from crystal spectra of ref. [5]

responsibile, obviously, for the calculated high values of the ν_8 and ν_{37} frequencies of the 2,3-dimethylbuta-1,3-diene.

The calculated and experimental frequencies together with the assignments based on the total energy distribution [23] are given in Tables I—III.

The differences between the calculated and experimental frequencies of the C—H stretchings in the methyl groups may be due to the scaling factors fitted for small molecules without methyl groups. However, the assignmens of these frequencies are unambiguous.

Results and Discussions

Trans- and cis-penta-1,3-*dienes*

The vibrational assignments obtained here are, in general, in good agreement with those given in ref. [1]. From the experimental fundamentals we excluded the bands at 1170, 383 and 1048 cm^{-1} for the *trans* conformer, and those at 1127 and 484 cm^{-1} for the *cis* form. These low intensity bands can be assigned to overtones or combinations. For similar reasons we excluded from the fundamentals the bands at 456 and 361 cm^{-1} given in ref. [14] and reassigned a series of vibrational frequencies reported as fundamentals [1, 14] (cf. Tables I and II).

The vibrational spectra of the two conformers of penta-1,3-diene molecule should differ, first of all, in the region of the skeleton vibrations. Indeed, considerable difference, up to 150 cm^{-1} in magnitude, are predicted by the calculations for the δ(C=C—C) and δ(C=C—CH_3) bendings. In principle, this supported the novel assignments given in Tables I and II. Unfortunately, among this group of bands only that assigned to the δ(C=C—CH_3) vibrations are intense in the Raman spectra. The frequencies of the ν(C—CH_3) stretching modes are also different for the *trans* and *cis* forms: they are situated at 1082 cm^{-1} and 955 cm^{-1}, respectively. The intensity of these bands in the Raman spectra are quite low, but they are markedly polarized. Appreciable differences are also observed for the ϱ(=CH_2) and ϱ(CH_3) modes. Unfortunately, the corresponding bands are, in general, of low intensity thus cannot be used for identification of the conformers. It is of interest that the frequencies of the C—H out-of-plane modes of the methylene groups, ν_{29}, differ from each ofther in the two conformers: 818 and 777 cm^{-1} for the *trans* and *cis* forms, respectively. These bands are sufficiently intense and possess well defined type-C contours.

The spectral regions not mentioned above are practically insensitive of the actual conformation of the molecule. The basic features of the conjugated diene systems, e.g. the intense bands of the ν(C=C) stretching vibrations, are present in both spectra.

2,3-*dimethylbuta*-1,3-*diene*

The assignment obtained coincides almost completely with the description given in ref. [5], therefore, we discuss only the features that differ from those reported there.

The differences are mainly connected with two modes, ν_9 and ν_{10}. These modes are described as rocking of the methyl groups and stretching of the central C—C bond, respectively, on the basis of their relative intensities [5]. It is also claimed that the assignments might be interchanged. Our calculations showed that the bands related to the ν(C—C) and $\varrho(CH_3)$ vibrations must be at 1341 cm^{-1} and 1025 cm^{-1}, respectively. It is worth noting that the stretching frequency of the central C—C bond increases on passing from buta-1,3-diene (1205 cm^{-1}) to isoprene (1303 cm^{-1}) and then to 2,3-dimethylbuta--1,3-diene (1341 cm^{-1}) [17, 24]. In addition, a decrease in the intensities of these band is also observed.

As for the other frequencies of A_g symmetry it should be noted that only the splitting of the 1414 cm^{-1} band in the crystalline phase may be due to the davydov effect, but not the presence of the close bands ν_7 and ν_{24}, as suggested in ref. [5]. The calculations also showed that the depolarized band at 392 cm^{-1} should be ascribed to the symmetric deformation $\delta(C{=}C{-}CH_3)$, ν_{14}. The assignment proposed here is in agreement to the description of this mode in isoprene [24]. Our results for vibrations of symmetry A_u completely confirm the assignments of Durig and Compton [5].

In the symmetry species B_g the calculated frequency of the asymmetric rocking mode $\varrho(CH_3)$, ν_{25}, is 1038 cm^{-1}, that of the symmetric rocking of A_g species is 1025 cm^{-1}. The single band at 1025 cm^{-1} in the experimental spectrum was earlier assigned to ν_{10} [5]. Accidental degeneracy of these rocking modes may explain the presence of only one strong band in this region of the observed spectra.

Another ambiguous assignment in ref. [5] is concerning the ν_{27} mode, the symmetric twist around the C=C bond. The calculated value of this frequency is 793 cm^{-1}. The respective experimental band that would have been ascribed to this mode was not found in the Raman spectrum [5]. Note that the intensity of Raman lines of this kind are always very low.

In the assignments of the vibrational frequencies of B_u symmetry the only refinement proposed is the choice of the frequency for the asymmetric vibration $\varrho(CH_3)$, ν_{38}. According to our results the band at 1183 cm^{-1} should be assigned to this mode instead of the weak band at 1075 cm^{-1} suggested in ref. [5]. This choice is supported also by the remark in that paper saying that "the contour of this band (i.e. that of at 1183 cm^{-1}) is better described as of *A* type".

Assignments of all the remaining vibrations agree with the description

given in ref. [5] and are corroborated by experimental data such as the depolarization ratios, the type of band contours and the band intensities.

The interpretation of the experimental spectra as given above is slightly different from the descriptions in ref. [15], too. As it was discussed in ref. [17] the calculations reported in ref. [15] are based on the force field of buta-1,3-diene fitted to vibrational frequencies assigned incorrectly.

Conclusions

The performed calculations made it possible to refine the assignments of the vibrational frequencies of the *trans*- and *cis*-penta-1,3-dienes and to select characteristic bands for identification of the two structural isomers. The intense bands at 479 cm^{-1} (Raman) and 818 cm^{-1} (IR) characterize the *trans* form and those at 390 cm^{-1} (Raman) and 777 cm^{-1} (IR) characterize the *cis* isomer.

The present calculation carried out for 2,3-dimethylbuta-1,3-diene corroborates almost completely the assignments reported in ref. [5]. Theoretical results, however, show the need to refine the interpretations of certain experimental bands. All the experimental frequencies observed could be described adopting a planar molecular model of C_{2h} symmetry.

REFERENCES

[1] Compton, D. A. C., George, W. O., Maddams, W. F.: J. Chem. Soc., Perkin II, **1977,** 1311
[2] Hsu, S. L., Flygare, W. H.: J. Chem. Phys., **52,** 1053 (1970)
[3] Segre, A. L., Zetta, L.: Di Corato, A.: J. Mol. Spectr., **32,** 296 (1969)
[4] Albriksten, P., Cunliffe, A. V., Harris, R. K.: J. Magn. Resonance, **2,** 150 (1970)
[5] Durig, J. R., Compton, D. A. C.: J. Phys. Chem., **83,** 2879 (1979)
[6] Aten, C. F., Hedberg, L., Hedberg, K.: J. Am. Chem. Soc., **90,** 2463 (1968)
[7] Lide, D. R., Jen, M.: J. Chem. Phys., **40,** 252 (1964); Lide, D. R.: Trans. Amer. Crystallogr., **27,** 106 (1966)
[8] Atshuller, A. P.: J. Phys. Chem., **57,** 538 (1953)
[9] Hobgood, R. T., Goldstein, J. H.: J. Mol. Spectr., **12,** 76 (1964)
[10] Treshchova, E. G., Tatevskii, V. M., Levina, R. Ya., Faizil'berg, A. A., Viktorova, E. A.: Russian J. Phys. Chem., **26,** 1266 (1952)
[11] Szasz, G. J., Sheppard, N.: Trans. Faraday Soc.. **49,** 350 (1953)
[12] Batuev, M. I., Onishchenko, A. S., Matveeva. A. D., Aronova, N. I.: Dokl. Akad. Nauk SSSR, **132,** 581 (1960)
[13] Dodziuk, H.: J. Mol. Struct., **12,** 161 (1972)
[14] Tarasova, N. V., Sverdlov, L. M.: Opt. Spektrosk., **3,** 140 (1967); Sverdlov, L. M., Kovner, M. A., Krainov, E. P.: Vibrational Spectra of Polyatomic Molecules, Wiley, New York, 1974, Chapter 5
[15] Tarasova, N. V., Sverdlov, L. M.: Russian J. Phys. Chem., **52,** 1606 (1968); Sverdlov, L. M., Kovner, M. A., Krainov, E. P.: Vibrational Spectra of Polyatomic Molecules, Wiley, New York, 1974 Chapter 5
[16] Sverdlov, L. M., Tarasova, N. V.: Opt. Spektrosk., **9,** 159 (1960); Tarasova, N. V., Sverdlov, L. M.: Opt. Spektrosk., **18,** 336 (1965)
]17] Panchenko, Yu. N.: Spectrochim. Acta, **31A,** 1201 (1975); Panchenko, Yu. N., Pulay, P., Török, F.: J. Mol. Struct., **34,** 283 (1976)
[18] Pulay, P.: Mol. Phys., **17,** 197 (1969)

[19] Pulay, P., Török, F.: Mol. Phys., **25,** 1153 (1973)
[20] Pople, J. A., Beveridge, D. L.: Approximate Molecular Orbital Theory, McGraw-Hill, New York 1970
[21] Vilkov, L. V., Sadova, N. I.: Zh. Strukt, Khim., **8,** 398 (1967)
[22] Panchenko, Yu. N., Mochalov, V. I., Pupyshev, V. I., Stepanov, N. F., Török, F., Pulay, P., Fogarasi, G., Pongor, G.: Moscow Univ. Chem. Bull., **35,** 453 (1980)
[23] Pulay, P., Török, F.: Acta Chim. Acad. Sci. Hung., **47,** 273 (1966)
[24] Panchenko, Yu. N., Mochalov, V. I.: to be published

Acta Chimica Hungarica, 114 (2), pp. 159–172 (1983)

ON THE C–S BOND LENGTH VARIATIONS AND d-ORBITAL PARTICIPATION IN SOME SULPHONYL CHLORIDE DERIVATIVES

I. MAYER[1]*, M. RÉVÉSZ[2] and I. HARGITTAI[2]

([1]Central Research Institute of Chemistry, Hungarian Academy of Sciences, H-1525 Budapest, P.O. Box 17, [2]Department of Structural Studies, Research Laboratory for Inorganic Chemistry, Hungarian Academy of Sciences, H-1431 Budapest, P.O. Box 117)

Received August 17, 1982
Accepted for publication November 25, 1982

Ab initio and semiempirical (CNDO/2) calculations on methane sulphony chloride, vinyl sulphonyl chloride, benzene sulphonyl chloride, and 2-thiophene sulphonyl chloride were performed to interpret the experimentally observed variations of the C–S bond lengths in these molecules. The inclusion of sulphur d-orbitals in the basis is imperative to account for the sulphur–oxygen double bonds, while the sulphur d-orbital participation in the C–S bonding is relatively small. It is predicted, however, that even minor changes in the d-orbital involvement may considerably change the length of the C–S bond.

Introduction

In a recent paper [1] we have discussed the large difference found in the C—S bond lengths of methane sulphonyl chloride (1.763 ± 0.005 Å) and trifluoromethyl sulphonyl chloride (1.856 ± 0.006 Å) as determined by electron diffraction [2, 3]. The CNDO/2 calculations reproduced qualitatively this change and permitted to interpret its origin in simple terms related to the electron releasing ability of the CH_3 group and the electron withdrawing ability of the CF_3 one: the large electronegativity of the fluorine atoms makes the attached carbon rather positive and this results in a C—S bond being poor of electrons and out of balance in the electrostatic sense. The changes in different quantities as two-center energy contribution terms and Wiberg indices supported well this interpretation.

In the meantime a rather short C—S distance (1.73 ± 0.02 Å)** was measured [4] in 2-thiophene sulphonyl chloride, C_4SH_3—SO_2Cl; another short and more accurate C—S bond length (1.744 ± 0.005 Å) was reported for vinyl sulphonyl chloride, C_2H_3—SO_2Cl [5]. At the same time, the C—S distance in

* To whom correspondence should be addressed

** The estimated error limit of 0.02 Å for C_4SH_3—SO_2Cl is perhaps too pessimistic. All the sulphonyl chloride molecules mentioned have been investigated in the same laboratory under similar experimental conditions. When considering bond length differences and their uncertainties, perhaps important systematic errors cancel, so the observed differences are more meaningful than the error limits would indicate.

benzene sulphonyl chloride, C_6H_5—SO_2Cl, does not differ from that in methane sulphonyl chloride, CH_3—SO_2Cl (1.764 ± 0.009 Å [6] and 1.763 ± 0.005 Å [3], respectively). Although there are no such drastic differences as that caused by the CH_3/CF_3 substitution, it seemed reasonable to attempt a systematic theoretical study for comparing the C—S bond lengths in these four molecules CH_3—SO_2Cl, C_2H_3—SO_2Cl, C_6H_5—SO_2Cl and C_4SH_3—SO_2Cl. These systems (together with CF_3SO_2Cl mentioned above) cover all the sulphonyl chloride molecules in which C—S distances have already been determined. The only exception is CCl_3—SO_2Cl [7] for which, however, the C—S bond length is similar to that of CF_3—SO_2Cl but determined with large uncertainty (1.86 ± ± 0.03 Å).

The role of d-orbitals

As ab initio calculations, even with minimal basis sets, are accessible only for the simplest sulphonyl chloride derivatives, we were forced to perform the comparison of the molecules in question at the semiempirical CNDO/2 level. However, by checking some principal features against ab initio calculations for CH_3—SO_2Cl (and CF_3—SO_2Cl), we hoped that some useful qualitative information may be gained concerning the bonding situation in the molecules considered, in spite of the approximate character of the CNDO method.

A promising feature of the previous CNDO calculations [1] was the finding that for methane sulphonyl cloride the C—S bond lenght was reproduced within the experimental error by the standard CNDO/2 method including d-orbitals on S and Cl ("spd basis"). At the same time the rotational isomer found to be most stable in calculations for benzene sulphonyl chloride was consistent with the electron diffraction results [6] only when the d-orbitals were excluded ("sp basis") [8]. Therefore, as a first step, we investigated the importance of the inclusion of the d-orbitals for the electronic structure and the influence of their inclusion on the calculated C—S bond lengths.

We shall note here that the recent detailed ab initio study [9] of some related small molecules emphasised the importance of d-orbitals (used as polarization functions) both with respect to the character of the localized orbitals corresponding to the S=O bonds and to the values of the optimized geometrical parameters obtained. A drastic S—O bond lengthening was found for the SOH_2, SO_2H_2 and SO_2 molecules in the "sp" basis calculations as compared with the "spd" results. The latter was in agreement with the usual S=O distances. The results of [9] are important for us also because the SO_2H_2 molecule may be considered to some extent as a prototype of the systems studied here.

Figure 1 shows the potential curves obtained for CH_3—SO_2Cl by performing ab initio SCF calculations using three different basis sets and the approach

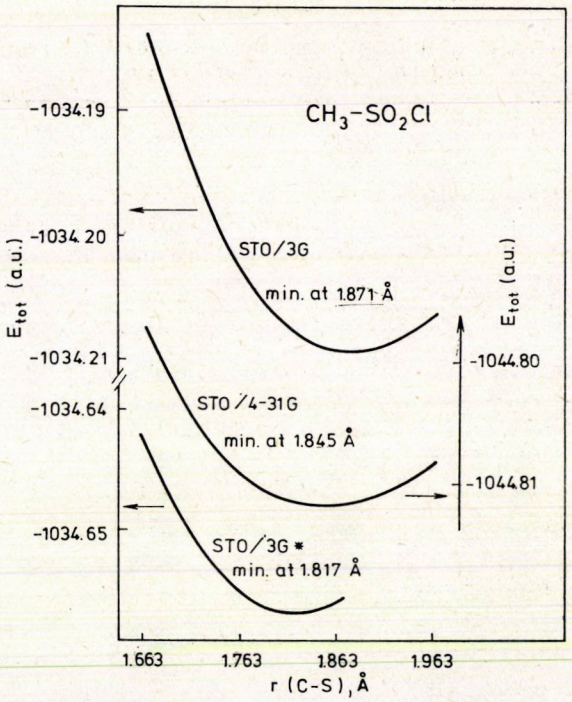

Fig. 1. C—S potential curves of CH_3-SO_2Cl for three different ab initio basis sets. (The arrows indicate the energy scale to be applied)

already employed in [1]: only the C—S bond length was varied, while all the other geometrical parameters were fixed at their experimental values determined by electron diffraction [3]*.

It can be seen that the results obtained in the minimal "sp" basis (STO/3G) give a C—S bond length which is too long by 0.108 Å. (The minimum on the potential curve is at 1.871 Å while the experimental C—S bond length is 1.763 Å). The extended "sp" basis (STO/4-31G) reduces this difference only by some 24% (the minimum is moved to 1.845 Å) although the total energy is lowered drastically, by more than 11 a.u.** At the same time just the half of the difference between the STO/3G and experimental results is accounted for by the "spd" basis, STO/3G*, in which polarization functions of *d*-symmetry on S and Cl are added to the STO/3G basis. (Only a single set of primitive *d*-type Gaussians is used on each S and Cl with the same exponent of 0.39.) Although this basis leads only to a quite moderate (~0.4 a.u.) energy lowering

* The molecules in question are relatively rigid so no considerable differences are expected between the geometrical parameters referring to the equilibrium and vibrationally average structures determined in the experiment.

** 1 a.u. (Hartree) = 2625.5 kJ/mol

Table I

Some results of Mulliken population analysis for $CH_3—SO_2Cl$ *molecule in three different basis sets*

Basis set	STO/3G	STO/4-31G	STO/3G*
Gross atomic populations			
S_1	14.716	14.452	15.493
Cl_2	17.337	17.104	17.223
$O_{3,4}$	8.503	8.791	8.223
C_5	6.292	6.677	6.168
H_6	0.885	0.718	0.889
$H_{7,8}$	0.882	0.733	0.891
Overlap populations			
S—Cl	0.035	0.170	0.237
S—O	0.173	—0.058	0.533
S—C	0.218	0.064	0.341
C—H_6	0.378	0.340	0.377
C—$H_{7,8}$	0.377	0.327	0.378

with respect to the STO/3G results, not only the C—S potential curve becomes much better, but the mere fact that orbitals of *d*-type on sulphur are present in the basis permits a qualitatively improved description of the electronic structure of the $CH_3—SO_2Cl$ molecule. In Table I some results of Mulliken population analysis are compared for $CH_3—SO_2Cl$ at the experimental geometry. As may be seen, both "sp" bases are unable to account for the fact that the sulphur atom is bonded to each of its four neighbours: one or more of its overlap populations are very small or even negative. The resulting positive and negative charges on S and O atoms, respectively, are extremely large, too. At the same time the STO/3G* "spd" results exhibit much more realistic gross atomic charges and overlap populations reflecting correctly the bonds formed by the sulphur atom. Moreover, the large values of the S—O overlap populations are in good agreement with the classical chemical assumption of sulphur–oxygen *double* bonds in this system.

It may be of interest to note that the STO/3G results for $CF_3—SO_2Cl$ are qualitatively very similar to those for $CH_3—SO_2Cl$. The minimum on the C—S potential curve appears at 2.017 Å which is again considerably larger than the experimental value (1.856 Å) and also reflects correctly the fact that the CF_3/CH_3 substitution leads to C—S bond lengthening. The results of Mulliken population analysis are also quite similar to the case of $CH_3—SO_2Cl$, except that the fluorine atoms bear a net negative charge (—0.12) while, in

Table II

Experimental and calculated C—S *bond lengths in some sulphonyl chloride molecules*

Molecule	r(C—S)Å		
	Experimental	CNDO/2[a]	
		"spd" basis	"sp" basis
$CH_3—SO_2Cl$	1.763(5)	1.759	1.897
$C_6H_5—SO_2Cl$[b]	1.764(9)	1.754	1.908
$C_2H_3—SO_2Cl$	1.744(5)	1.740	—
$C_4SH_3—SO_2Cl$	1.73(2)	1.722	—

[a] C—S distance corresponding to the energy minimum when all the other geometrical parameters are fixed at their experimental values.

[b] Rotational form with the S—Cl bond in the plane orthogonal to that of the phenyl ring ($\tau = 90°$). None of the calculated quantities discussed in this paper exhibits a significant dependence on the rotational angle τ.

agreement with the CNDO/2 results of [1], the carbon atom is rather positive ($q_C = 0.38$).

The foregoing discussion demonstrated that the ab initio results for $CH_3—SO_2Cl$ are of some interest although we were not able to use sufficiently large bases as to obtain such good agreement with the experiment as was provided by the CNDO/2 calculations described in [1] for $CH_3—SO_2Cl$ (also see below for the other molecules in question).

In discussing the CNDO/2 calculations performed for $CH_3—SO_2Cl$, $C_6H_5—SO_2Cl$, $C_4SH_3—SO_2Cl$ and $C_2H_3—SO_2Cl$, we shall first consider the importance of including the d-orbitals in the basis also at the CNDO/2 level. Table II shows the calculated C—S bond lengths obtained in the manner discussed above (only the C—S distances are varied) and using standard CNDO/2 parametrization. It can be seen that the C—S distances obtained by using the "spd" basis are in agreement with the observed values within experimental error for all four molecules. At the same time using the "sp" basis, the C—S distances are too long by 0.14—0.16 Å. (The same difference was obtained for the $CF_3—SO_2Cl$ molecule.) One may conclude, therefore, that the inclusion of the sulphur d-orbitals in the basis is inevitable for the description of the sulphonyl chloride derivatives at the CNDO/2 level as well.

As the ab initio results also show, this conclusion reflects some important aspects of the real bonding situation around the "hypervalent" sulphur atom: the formal valency of the sulphur in the molecules studied is six. In other words, it seems rather probable that the formation of the S=O *double* bonds cannot be imagined without involving the sulphur d-orbitals.

Besides the C—S bond lengths, the following CNDO/2 results (see Tables III and IV) may be mentioned as supporting the idea of the qualitative importance of the sulphur d-orbitals in these molecules:

Table III

Net atomic charges and d-electron populations calculated by the CNDO/2

Molecule	"sp" basis			
	Net atomic charges			
	S	Cl	C	O
$CH_3—SO_2Cl$	1.041	—0.205	—0.121	—0.448
$C_6H_3—SO_2Cl$[a]	1.019	—0.227	—0.055	—0.459
$C_2H_5—SO_2Cl$	—	—	—	—
$C_4SH_3—SO_2Cl$	—	—	—	—

[a] $\tau = 90°$

Table III summarizes the net atomic charges (see later) and the d-electron populations. The very large (1.95—2.0) numerical values of the electron population on the sulphur d-orbitals may be, to some extent, exaggerated by the approximations involved in the CNDO method and the "standard" CNDO/2 parameters applied. Nevertheless, it is noteworthy that the d-electron population ($\approx$0.14) of the chlorine atoms is less by an order of magnitude than that of sulphur. This result is in agreement with the assumption that there is no need in d-orbitals to describe the qualitative features of the single bond formed by Cl, but they are of utmost importance for the "hypervalent" sulphur. Similarly, the d-electron population (0.53) on the sulphur atom in the tiophene ring of C_4SH_3—Cl is significantly smaller than that on the sulphur atoms in the —SO_2Cl groups, in agreement with the difference in their bonding situation.

As is known, Wiberg's bond indices [10] are useful quantitative measures of the bond orders at the CNDO level. It seems, therefore, instructive to compare their values obtained for the case of the "sp" and "spd" bases, respectively (Table IV). It can be seen that in the "sp" CNDO basis we have *weak single bonds* between the sulphur atom and each of its neighbours, including also the S—O bonds. At the same time the values for the Wiberg indices obtained in the "spd" basis are much more realistic: they are close to the bond orders predicted by the classical valence concepts.

In order to analyse the importance of the d-orbitals on the resulting bond indices, we propose to introduce the "partial Wiberg indices", connected with the sulphur d-orbitals: this partial Wiberg index that may also be called

the "*d*-component" of a Wiberg index, is obtained if the summation defining the corresponding Wiberg index via the density matrix elements is extended only over the d-orbitals of the sulphur atom in question instead of all the

method at the experimental geometries of some sulphonyl chloride molecules

"spd" basis					
Net atomic charges				d-electron population	
S	Cl	C	O	S	Cl
0.377	−0.060	−0.079	−0.224	1.963	0.136
0.347	−0.084	−0.001	−0.227	1.973	0.137
0.375	−0.071	−0.037	−0.219	1.979	0.145
0.373	−0.080	−0.048	−0.226, −0.232 [b]	1.999	0.140

[b] The two oxygens are not strictly equivalent

sulphur orbitals. It seems to us that these "partial" Wiberg indices may give information which is not only similar to that obtained from a localized orbital analysis but is also free from the arbitraryness inherent in the selection of the localization criterion.

Table IV shows that the sulphur d-orbitals give a contribution cca. 1.1 to the values of the resulting S=O Wiberg indices (about 2.2). This confirms that the formation of the S=O double bonds is directly related to the sulphur

Table IV

Wiberg indices and their d-components calculated by the CNDO/2 method at the experimental geometries of some sulphonyl chlroide molecules

Molecule	Wiberg indices								
	"sp" basis			"spd" basis					
				C—S		S—O		S—Cl	
	C—S	S—O	S—Cl	total	S(d) comp.	total	S(d) comp.	total	S(d) comp.
$CH_3—SO_2Cl$	0.948	0.894	0.802	1.089	0.294	2.199	1.091	1.191	0.470
$C_6H_5—SO_2Cl$ [a]	0.871	0.911	0.784	1.040	0.287	2.208	1.097	1.177	0.473
$C_2H_3—SO_2Cl$	—	—	—	1.066	0.300	2.205	1.097	1.196	0.473
$C_4SH_3—SO_2Cl$	—	—	—	1.091	0.327	2.195, 2.109 [b]	1.092, 1.086 [b]	1.176	0.468

[a] $\tau = 90°$
[b] The two oxygens are not strictly equivalent

d-orbitals. The sulphur d-orbitals give only a small (0.2—0.3) contribution to the C—S Wiberg indices which are quite close to unity: the relatively high (about 1.2) S—Cl. Wiberg indices contain a significant ($\approx$0.5) contribution from the sulphur d-orbitals. The values of the S—Cl Wiberg indices may be related to other problems of the S—Cl bonds; we shall briefly discuss them below.

The results of the comparison of the "sp" and "spd" bases may be well interpreted also in terms of a simple picture of localized bonding electron pairs occupying their relevant localized orbitals.*

In the "sp" basis one can form only four hybrid valence orbitals of the sulphur. These four orbitals can form four bonding orbitals, each corresponding to a single bond; these four bonding orbitals altogether can accommodate eight electrons. As the number of the electrons in the valence shell of a free sulphur atom is six, in such a bonding scheme the sulphur would bear an atomic charge of the value +2, assuming that the bonds are not polarized. However, the large positive charge on S leads, of course, to a considerable polarization of the bonds, which in turn reduces the charge on the sulphur. This compensation cannot be complete, however, owing especially to the large electronegativities of the adjacent oxygen and chlorine atoms. Accordingly, in "sp" basis the sulphur remains strikingly positive, having an atomic charge of $\approx$1.0 (Table III), which is, of course, quite irrealistic.

If the d-orbitals of the sulphur are also included in the basis, all the six valence electrons of the sulphur can immediately participate in the bonding, as the formation of additional bonding orbitals becomes possible. This permits the adequate description of the S=O double bonds. In the "spd" basis the great electronegativity differences lead to a significant but more or less realistic positive atomic charge (0.35—0.4) on the sulphur (see Table III) that compares well with the ab initio "spd" results.

An important, though seemingly trivial, conclusion of the above discussions is that the problem of participation of the d-orbitals in the bonding of the third row elements may not be properly considered without taking into account the details of the real bonding situation in every case.

We have performed also a complete geometry optimization for CH_3—SO_2Cl, CF_3—SO_2Cl, C_2H_3—SO_2Cl and C_6H_5—SO_2Cl at the CNDO/2 level. The conclusions may be summarized as follows. The C—S bond lengths remain unchanged with respect to the calculated values in Table II within 0.01 Å, except C_2H_3—SO_2Cl, for which the change is greater. The extremely short ($\sim$1.85 Å) S—Cl distances and the remarkably long ($\sim$1.55 Å) S—O ones

* The sulphonyl chlorides represent hypervalent molecules of the second kind in Musher's classification [11]. For this type of molecules no predictions concerning the geometrical arrangement of atoms follow from that theory, and we think that most probably the whole concept of the three-center bonds is not applicable at all for the molecules studied here.

are in full agreement with the other results obtained in the literature [11,12] at the CNDO/2 level. Meaningless bond angles are obtained for the sulphonyl chloride group; this is especially the case for the C—S—Cl angle which is obtained acute. These results can unequivocally be attributed to the shortcomings of the standard CNDO/2 method and parametrization. Obviously the parametrization used for chlorine represents the most serious problem; it is enough to recall here that the standard CNDO/2 method gives a Cl—C—Cl angle of 69° in the CH_2Cl_2 molecule, instead of 112° [11]. This is confirmed also by the fact that performing the geometry optimization, in a somewhat arbitrary manner, by using d-orbitals only on the sulphur but not on the chlorine atom we obtained quite reasonable sulphonyl chloride bond angles. Finally, the changes in other parameters like Wiberg indices are in accordance with those in the bond distances: the S—O Wiberg indices fall to $\approx$1.9 (with *d*-component about 0.9); the S—Cl Wiberg indices become too high ($\approx$1.5, from which the contribution of the sulphur d-orbitals is $\approx$0.6; the S—C Wiberg indices change little. A decrease of the sulphur *d*-population to about 1.8 may be connected with that in the S—O bond indices; at the same time there is a slight increase of the *d*-population on the Cl atoms (to about 0.2) which may be attributed to the spurious S—Cl bond strengthening.

From our point of view it is especially important that the changes in the side-group geometries practically do not influences the parameters (bond lengths, Wiberg indices) related to the C—S bond. So one may hope to extract useful information from the CNDO/2 calculations for this particular bond, assuming that one uses experimental values for the other geometric parameters and does not try to optimize them at the CNDO/2 level. It is possible that the very good description of the C—S bond given by the standard CNDO/2 method may be related to the very small electronegativity difference between the C and S atoms: they both have an electronegativity of 2.5 on Pauling's scale, while the difference on the Mulliken's one is also negligible: the electronegativities are 2.23 and 2.21 for C and S, respectively.

Other structural considerations

As the results obtained for the C—S bond lengths reproduce well the experimental trends we may try to extract from the CNDO/2 results some qualitative information about the factors influencing this particular bond length in the sulphonyl chloride derivatives. However, in the series of CH_3—SO_2Cl, C_6H_5—SO_2Cl, C_2H_3—SO_2Cl and C_4SH_3—SO_2Cl there are no such drastic electronegativity effects as was the case when CH_3—SO_2Cl and CF_3—SO_2Cl were compared [1]. The differences in the C—S bond lengths are also much smaller. Accordingly, the analysis based on the CNDO/2 calcula-

tions may be only tentative and any of its results must be considered with care because of the approximate and semiempirical character of this method, even if the agreement with experimental C—S bond lengths is excellent. The importance of this caution is shown e.g. by the fact that no good correlation was obtained for the molecules in question either between the group charges q_R calculated at the CNDO/2 level and the group electronegativities χ_R determined empirically from the structural data of the R—SO_2Cl series [4, 13], or between the CNDO/2 charges on the chlorine atoms and the empirical χ_{R-SO_2} group electronegativities [14]. Similarly, the different charge-type quantities (q_C q_S, q_{SO_2Cl}) obtained for C_4SH_3—SO_2Cl having the shortest C—S bond are, between those for CH_3—SO_2Cl and C_6H_5—SO_2Cl, while the C—S bond lengths for the latter two are practically equal.*

Figure 2 shows the bond-length dependence on the C—S Wiberg bond indices. While the bond loosening in CF_3—SO_2Cl as compared with CH_3—SO_2Cl was well reflected also by the values of the Wiberg indices [1], the order of the curves in Fig. 2 does not correspond to that of the equilibrium bond lengths. However, if one compares only those three molecules, in which the sulphur is bonded to a π-electron system (or rather, to a carbon atom in an approximate sp^2 hybridization state) then the values of the Wiberg indices correlate well with the C—S bond lengths. This fact shows that if one is interested in rather subtle effects, as are the small changes in the bond strengths for the four sulphonyl chloride molecules in question, then the Wiberg indices are sufficiently sensitive measures only if one compares structurally similar enough

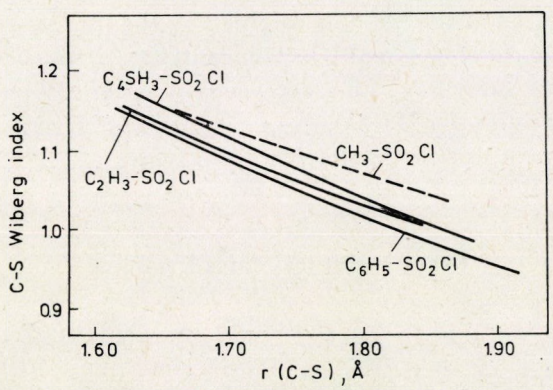

Fig. 2. Sulphur-carbon CNDO/2 Wiberg indices of some sulphonyl chloride molecules as functions of the C—S distance

* One may, however, observe, that the population of the sulphur d-orbitals is the highest in C_4SH_3—SO_2Cl. We shall return later to the discussion of the possible importance of the d-electron populations for the C—S bond lengths.

systems. As we shall see, analogous conclusion may be drawn concerning other quantities extracted from the CNDO/2 calculations.

In order to get a deeper insight into this problem, we performed also the partitioning [15, 16] of the CNDO/2 total energies into the one-center and two-center energy contributions. The ε_{C-S} two-center energy term may be considered as an immediate (though static, i.e. corresponding to a given geometry) measure of the C—S bond strength at the CNDO/2 level. Figure 3 displays the changes of the ε_{C-S} energy contributions when the C—S bond lengths are varied. It may be seen that the order of the curves in the interval of the bond distances interesting for us, again corresponds to that of the equilibrium bond lengths only for the three molecules with sp^2 carbon bonded to the sulphur. So, these curves do not reflect that the C—S bond length in CH_3—SO_2Cl and C_6H_5—SO_2Cl are practically equal and significantly longer than those in C_4SH_3—SO_2Cl and C_2H_3—SO_2Cl: the $\varepsilon_{S-C}(r_{S-C})$ curve for CH_3—SO_2Cl is close to that for C_2H_3—SO_2Cl and not to that for C_6H_5—SO_2Cl. Furthermore as usual, the C—S two-center energy components become monotonically more negative as the C—S bond length decreases, thus one expects a minimum on these curves only at the very short internuclear separations. Both these facts indicate that one must take into account different other factors as well in order to account for the variations in the C—S bond lengths.

Similarly to the case discussed [1], an effect of central importance is the changes in the one-center energy terms corresponding to the carbon and, especially, sulphur atoms. Figure 4 shows how the sum of the one-center terms

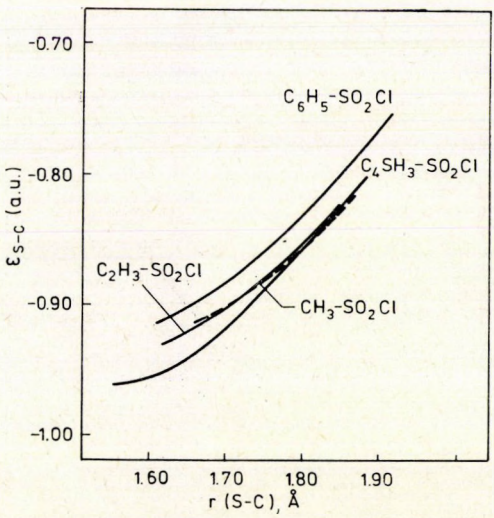

Fig. 3. The sulphur-carbon two-center CNDO/2 energy component for some sulphonyl chloride molecules as function of the C—S distance

ε_S, ε_C and two-center contribution ε_{C-S} varies with the internuclear distance. One observes that the minimum on these curves appears at C—S distances which are yet shorter by $\sim$0.1 Å than the equilibrium ones. Furthermore, the order of the curves exhibits similar features as we have seen in Fig. 2, but the curve for C_6H_5—SO_2Cl is going much above the other three. We did not find any explanations for this. Accordingly, we have to look for some additional factors having an influence on the C—S bond lengths. These factors may be connected both with the different non-bonded interactions as well as with the changes in the strengths, i.e. in the corresponding two-center energy terms, of bonds other than the C—S one.

There is only a relatively small number of different energy terms which change appreciably when the C—S distances are varied. By considering them we found that for C_4SH_3—SO_2Cl a minimum may be obtained practically at the experimental bond length if one takes into account a few other terms in addition to the sum of $\varepsilon_S + \varepsilon_C + \varepsilon_{C-S}$ discussed above. These are the energy terms corresponding to the non-bonded interactions of the "first sphere" i.e. the interactions between the sulphur atom and the first neighbours of the carbon and vice versa, and the terms reflecting those bond interactions which depend significantly on the C—S distance. At the smaller r(C—S) values the C—S bond is "stronger" (in the sense that ε_{C-S} is more negative) but the other bonds of the carbon and sulphur atoms become slightly "weaker". The strength of the next bonds in the rings increases again to some, although much smaller extent. The minor changes in the other energy component for C_6H_5—

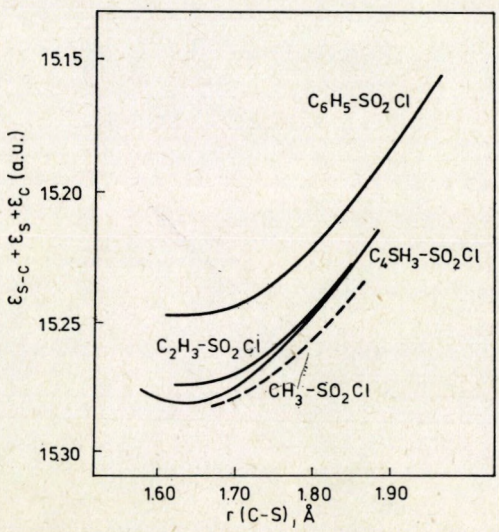

Fig. 4. The sum of the sulphur and carbon one-center and sulphur-carbon two-center CNDO/2 energy components for some sulphonyl chloride molecules as function of the C—S distance

—SO_2Cl and C_4SH_3—SO_2Cl compensate each other. In the case of CH_3—SO_2Cl and C_2H_5—SO_2Cl, however, the sum of the above energy components would give a minimum at a slightly (by ~0.02—0.03 Å) longer C—S distance than the equilibrium one. This discrepancy shows that it is rather difficult to select reliably those factors which influence a given bond length up to the finest details. Thus it is either quite fortuitous that the sum of a few particular energy terms discussed above describes so well the C—S bond length in C_6H_5—SO_2Cl and C_4SH_3—SO_2Cl,* or it is not quite correct to compare the details of energy partitioning for the methyl and vinyl derivatives and the aromatic ones is question. Nevertheless, we think that the alternating character exhibited by the bond strengths of the sulphonyl chloride molecules at the CNDO/2 level reflects some real physical tendencies of more general validity.

The above discussion shows that the consideration of the different energy components reveals some interesting features of the molecules studied but does not necessarily give a realistic answer to the question *why* the C—S bond is somewhat (by 0.02—0.03 Å) shorter in C_4SH_3—SO_2Cl and C_2H_3—SO_2Cl than in the other two molecules. The slightly more negataive value of the ε_{S-C} energy component and the somewhat greater slope (cf. Figs 3 and 4) of the ε_{S-C} and $\varepsilon_S + \varepsilon_C + \varepsilon_{S-C}$ curves *only reflect* but do not explain the fact that the C—S bond is the shortest in C_4SH_3—SO_2Cl. A tentative interpretation may be, however, given by observing that the sulphur d-electron population and, especially, the sulphur d-electron component of the C—S Wiberg index are significantly greater in C_4SH_3—SO_2Cl than in the other molecules considered. Figure 5 shows that there is a good empirical correlation between the

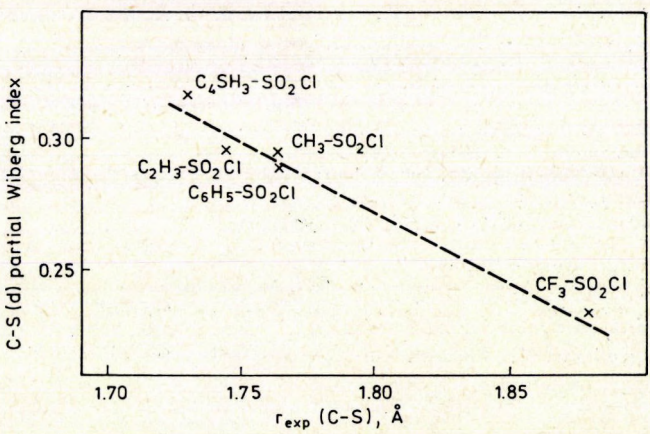

Fig. 5. Correlation between the sulphur d-electron components of the C—S Wiberg indices calculated at r(C—S) = 1.763 Å for some sulphonyl chloride molecules and their *experimental* C—S bond lengths

* E.g. there are further energy contributions as the non-bonded interactions of the "second sphere", whose changes are comparable with those in some terms taken into account in the above discussion.

experimental C—S bond lengths and the S(d)—C partial Wiberg indices calculated at the standard CNDO/2 level for the five sulphonyl chloride molecules already studied.* This result suggests that the sulphur d-orbitals are of importance not only for the S=O double bonds, but they make it also possible that a partial (hyper)conjugative $d_\pi - p_\pi$ bonding is added to the usual single C—S σ-bond, influencing the equilibrium bond length.

From this point of view the short C—S distance in C_4SH_3—SO_2Cl may be connected also with the relatively large interaction between the two sulphur atoms: the S...S Wiberg index is 0.086, with the dominating contribution from the d-orbitals. This sulphur–sulphur interaction enhances somewhat the d-orbital population. The increased d-population, in turn, leads to a greater conjugation with the thiophene ring and thus favours the shortening of the C—S bond.

The main conclusions of the present calculations may be summarized as follows. The consideration of the d-orbitals is inevitable to describe the bonding of the "hypervalent" sulphur atoms in the sulphonyl chloride molecules. The d-orbitals are of utmost importance for the formation of the S=O double bonds. Furthermore, even minor changes in the sulphur d-electron population may be connected with appreciable changes in the geometrical parameters.

REFERENCES

[1] Mayer, I., Hargittai, I.: Z. Naturforsch., **34a,** 911 (1979)
[2] Brunvoll, J., Hargittai, I., Kolonits, M.: Z. Naturforsch., **33a,** 1236 (1978)
[3] Hargittai, M., Hargittai, I.: J. Chem. Phys., **59,** 2513 (1973)
[4] Brunvoll, J., Hargittai, I., Székely, T., Pappalardo, G. C.: J. Mol. Struct., **66,** 173 (1980)
[5] Brunvoll, J., Hargittai, I.: Acta Chim. Acad. Sci., Hung., **94,** 333 (1977)
[6] Brunvoll, J., Hargittai, I.: J. Mol. Struct., **30,** 361 (1976)
[7] Brunvoll, J., Hargittai, I., Seip, R.: Z. Naturforsch., **33a,** 222 (1978)
[8] Van Eijck, B. P., Hargittai, I., Mayer, I.: J. Moll. Struct., **69,** 301 (1980)
[9] Schmiedekamp, A., Cruickshank, D. W. J., Skaarup, S., Pulay, P., Hargittai, I., Boggs, J. E.: J. Am. Chem. Soc., **101,** 2002 (1979)
[10] Wiberg, K. A.: Tetrahedron, **24,** 1083 (1968)
[11] Musher, J. I.: Angew. Chem., **81,** 68 (1969)
[12] Marsh, F. J., Gordon, M. S.: J. Mol. Struct., **31,** 345 (1976)
[13] Scharfenberg, P.: Theoret. Chim. Acta (Berlin), **49,** 115 (1978)
[14] Hargittai, I.: Z. Naturforsch., **34a,** 755 (1979)
[15] Hargittai, I., Bliefert, C.: Z. Naturforsch., **35b,** 1053 (1980)
[16] Pople, J. A., Beveridge, D. L.: Approximate Molecular Orbital Theory. McGraw-Hill, New York 1970
[17] Fischer, H., Kollmar, H.: Theoret. Chim. Acta (Berlin), **16,** 163 (1970)

* The partial Wiberg indices shown in Fig. 4 were calculated at the same $r(S-C) = 1.763$ Å, i.e. the experimental value for CH_3-SO_2Cl. A similar curve was obtained for the partial Wiberg indices calculated at the experimental bond lengths (c.f. Table IV). For $C_2H_5-SO_2Cl$ the sulphur d-electron population as a function of the C—S distance gives a curve which practically coincides with that for $C_6H_5-SO_2Cl$, but the S(d)—C partial Wiberg indices are significantly greater for $C_2H_5-SO_2Cl$ than for $C_6H_5-SO_2Cl$. CH_3-SO_2Cl exhibits again a somewhat different behaviour of both these quantities.

Acta Chimica Hungarica, 114 (2), pp. 173—186 (1983)

pH-DEPENDENCE OF THE CATALYTIC EFFECT OF THIOUREA AND *N,N'*-DIMETHYLTHIOUREA ON HYDROGEN OVERVOLTAGE AT THE DROPPING GALLIUM ELECTRODE

K. SZABÓ* and É. M. CSOBOD

(Department of Physical Chemistry and Radiology, Eötvös Loránd University, H-1088 Budapest, Puskin u. 11—13.)

Received October 16, 1982
Accepted for publication November 25, 1982

The effect of thiourea (TU) and dimethylthiourea (DMTU) on the rate of hydrogen evolution at the dropping gallium electrode was investigated in solutions of different pH (pH=0.9—12.3). It was found that the rate of electrolytic hydrogen evolution increases with increasing additive concentration. In acid medium the catalytic effect of DMTU is stronger than that of TU, while in alkaline medium TU is a more efficient catalyst than DMTU. The additives accelerate to a larger extent the rate of hydrogen evolution in acid media, than is alkaline media. This difference in catalytic action can be explained by a different catalysis mechanism in acid and in alkaline media.

Thiourea and its derivatives in perchloric acid solution increase the rate of electrolytic hydrogen evolution at the dropping gallium electrode, and this catalytic action increases with increasing thiourea or thiourea derivative concentration [1]. It has been presumed on the basis of our investigations that the given additives are adsorbed at the electrode surface and by the participation of H_3O^+ ions a surface complex is formed, the discharge of which requires lower activation energy, than the discharge of the H_3O^+ ion [1].

The interpretation of the catalytic effect of thiourea is different in the case of different systems [2, 3]. In cadmium deposition the catalytic action of thiourea was attributed to the formation of a Cd^{2+}–thiourea complex in the electric double layer,which increases the rate of electron transition. This surface complex is formed by the interaction of thiourea molecules adsorbed at the electrode surface and the Cd^{2+} ions [2]. Similarly, the reduction of Ni^{2+} ions at the mercury electrode is accelerated by thiourea, however, in this case the Ni^{2+}–thiourea complex is formed in a medium in which nickel aquacomplexes are dehydrated in the bulk of the solution [3].

For the further elucidation of the effect of thiourea and its derivatives in the case of hydrogen evolution at the gallium electrode, important informations can be obtained by the investigation of the pH-dependence of the catalytic recation. Therefore, the dependence of the catalytic effect of thiourea and

* To whom correspondence should be addressed

dimethylthiourea on the pH of the solution was investigated in the given system, which is all the more of interest, as in the alkaline solutions hydrogen is evolved from the H_2O molecules, and not from the H_3O^+ ions. Owing to the different reaction mechanism of hydrogen evolution, it is to be expected that in this case the mechanism of the catalytic action will also be different.

Experimental

Measurements were carried out with the experimental and evaluation methods described in [4], at the dropping electrode prepared from galium of 99.9999% purity, at 305 ± 0.2 K, in solutions of different hydrogen ion concentration, in the pH range from 0.9 to 12. In the measurements the total concentration of the base solutions investigated was 1 *M*.

Solutions were prepared with bidistilled water, using the following chemicals: 70% $HClO_4$, anal. grade, product Merck; twice recrystallized thiourea (TU), product Reanal; twice recrystallized *N*,*N*'-dimethylthiourea (DMTU), product Merck; twice recrystallized potassium dihydrogen phosphate, product Reanal; NaOH, product Reanal; 80% H_3PO_4 anal. grade, product Merck.

Before the investigation of the catalytic effect of thiourea and dimethylthiourea the η — log **j** polarization curves were plotted (where η is the overvoltage in V, and **j** the current density in A/cm²) in solutions of different pH, containing no additive. The slope of the η — log **j** curve obtained $\left(\frac{\partial \eta}{\partial \ln \mathbf{j}} = b\right)$ varies in the overvoltage interval investigated (—0.6 to 1.1 V) in the 0.9 to 6.4 pH range between 0.120 and 0.150 V, while in alkaline solution the value of b is 0.120 V. In the acid and neutral range overvoltage increases with increasing pH; $\left(\frac{\partial \eta}{\partial \ln}\right)_{\mathbf{j}\,c} =$ $= 0.042$ V; in alkaline solution η diminishes with increasing pH: $\left(\frac{\partial \eta}{\partial \mathrm{pH}}\right)_{\mathbf{j},\,c} = -0.052$ V. These changes in overvoltage are in good agreement with values published in the literature [5].

First the catalytic effect of thiourea was investigated at diffreent pH values and thiourea concentrations (C_{TU}). Polarization curves plotted from current density and overvoltage values measured are shown in Figs 1—7. It will be noted from these figures that in

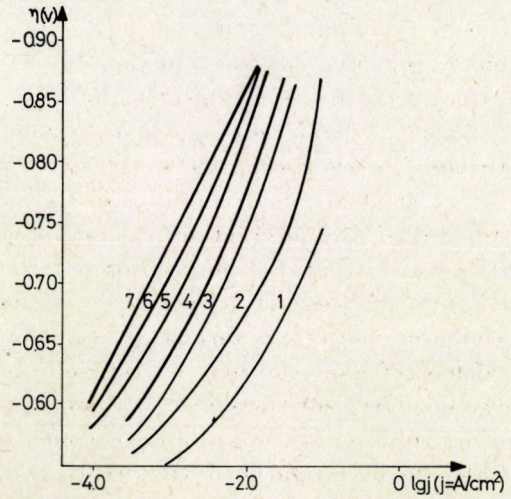

Fig. 1. η — lg **j** curves at the dropping gallium electrode at pH = 0.9, in a base solution of $(1-x)M$ $HClO_4 + xM$ $NaClO_4$, of 1 *M* total concentration + TU solutions of the following concentrations: ① 10^{-2}; ② 10^{-3}; ③ $3.1 \cdot 10^{-4}$; ④ 10^{-4}; ⑤ $3.1 \cdot 10^{-5}$; ⑥ 10^{-5}; ⑦ 0 (base solution) *M*

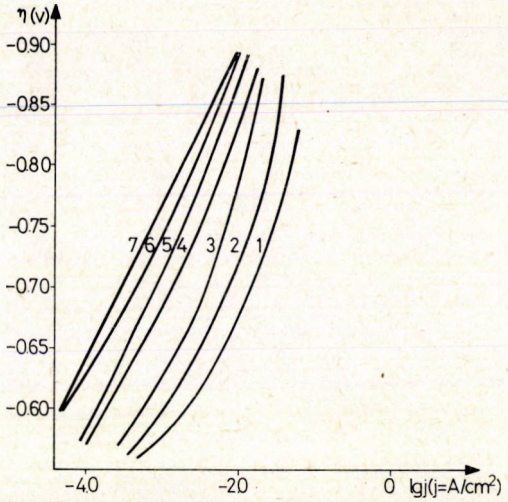

Fig. 2. η — lg **j** curves at the dropping gallium electrode at pH = 1.6, in a base solution of $(1 - x)$ *M* $HClO_4$ + x*M* $NaClO_4$, of 1 *M* total concentration + TU solutions of the following concentrations: ① 10^{-2}; ② 10^{-3}; ③ $3.1 \cdot 10^{-4}$; ④ 10^{-4}; ⑤ $3.1 \cdot 10^{-5}$; ⑥ 10^{-5}; ⑦ 0 (base solution) *M*

acid and neutral, further in alkaline solutions the rate of hydrogen evolution increases with increasing TU concentration in the potential interval investigated. On the η — log **j** curves obtained for solutions of pH = 0.9 (Fig. 1) and of pH = 1.6 (Fig. 2) in the presence of thiourea two sections can be distinguished in the overvoltage range more positive than —0.65 to —0.70 V, the lower section of the curve runs almost parallel with curves measured in a solution containing no thiourea. The slope of the lower section is 0.10—0.11 V.

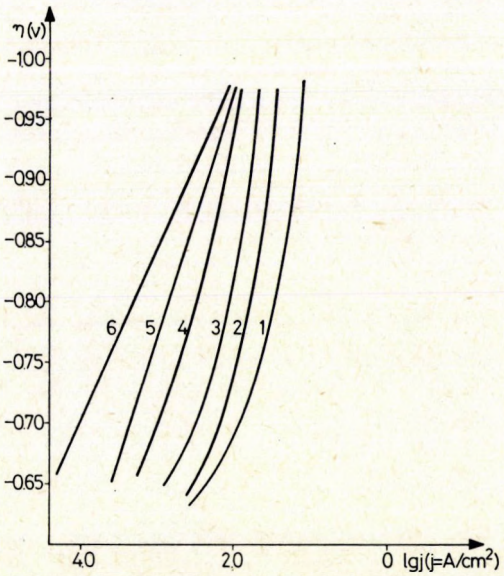

Fig. 3. η — lg **j** curves at the dropping gallium electrode at pH = 3.5, in 1 *M* KH_2PO_4 ground solution + TU solutions of the following concentrations: ① 10^{-1}; ② 10^{-2}; ③ $5 \cdot 10^{-2}$; ④ 10^{-3}; ⑤ 10^{-4}; ⑥ 0 (base solution) *M*

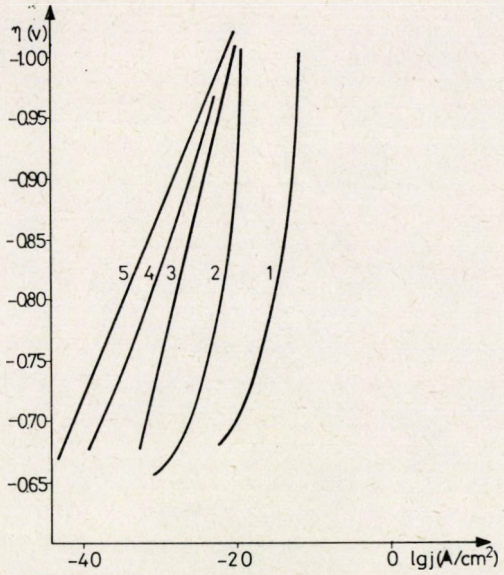

Fig. 4. η — lg j curves at the dropping gallium electrode at pH = 4.5, in a base solution of $(1 - x)$ *M* $KH_2PO_4 + x$*M* H_3PO_4, of 1 *M* total concentration + TU solutions of the following concentrations: ① 10^{-1}; ② 10^{-2}; ③ 10^{-3}; ④ 10^{-4}; ⑤ 0 (base solution) *M*

In a more negative range than the said overvoltage, curves deflect and approach the values measured for solutions containing no catalyst, i.e. in an overvoltage range more negative than —0.65 to 0.70 V the catalytic action of thiourea diminishes. Also in the case of solutions of higher pH (pH = 3.5 and 4.5) polarization curves measured in the presence of

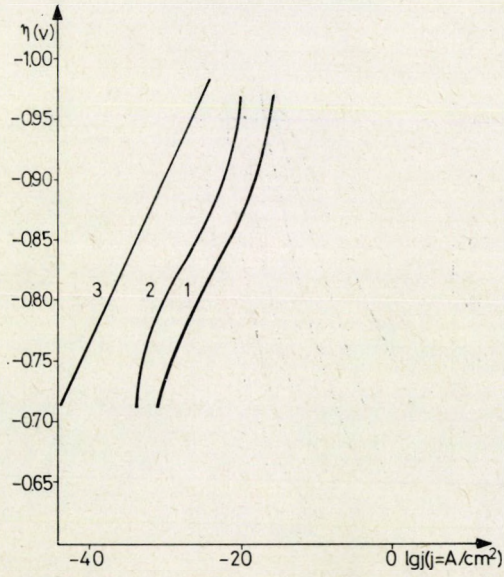

Fig. 5. η — lg j curves at the dropping gallium electrode, at pH = 6.4, in a base solution of $(1 - x)$ *M* $KH_2PO_4 + x$ *M* H_3PO_4 total concentration + TU solutions of the following concentrations: ① 10^{-1}; ② 10^{-2}; ③ 0 (base solution) *M*

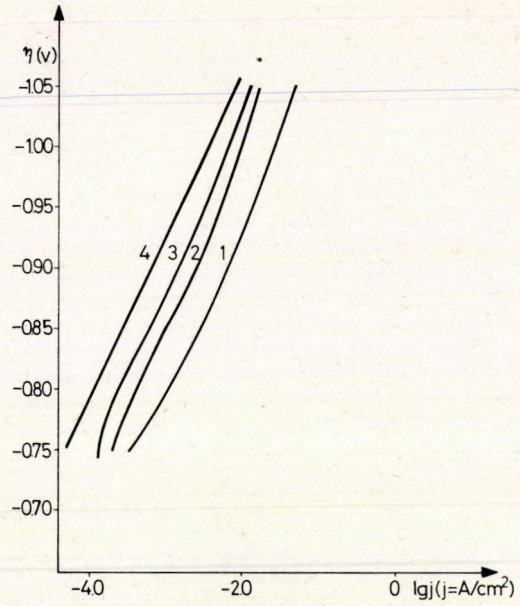

Fig. 6. η — lg j curves at the dropping gallium electrode, at pH = 10.9, in base solution of $(1 - x)$ *M* NaOH + x *M* $NaClO_4$, of 1 *M* total concentration + TU solutions of the following concentrations: ① 10^{-1}; ② 10^{-2}; ③ 10^{-3}; ④ 0 (base solution) *M*

TU can be divided into two parts: in the overvoltage range $\eta > -0.72 - -0.78$ V, η — lg j curves can be approximated by a straight line of a slope of 0.18—0.22 V, in a more negative range than the said overvoltage an ascent of the curves can be observed (Figs 3 and 4).

It may be seen from Fig. 5 that in solutions of pH 6.4 containing TU the course of the polarization curves recorded is more complicated than those measured in more acid solutions. At more positive overvoltage values, in the interval from —0.68 to —0.78 V, curves rise sharply and after a section of more moderate rise, a section of sharp rise follows again at an overvoltage of $\eta = -0.88 - -0.90$ V. Curves of more complicated course are obtained also in the alkaline range, at pH = 10.9 (Fig. 6) and pH = 12.3 (Fig. 7) in solutions containing TU, than in acid medium. It can be seen from Fig. 6 that η — log j curves measured in solutions of pH = 10.9 in the presence of TU have a similar course as curves measured in neutral solutions of pH 6.4. In this case too, three sections of different slopes can be distinguished, those in the range of $\eta < -0.88$ to —0.90 V can be best approximated with a straight line, with a slope of 0.13—0.15 V. In a more positive overvoltage range than this, a section of a slope of 0.10—0.11 V can be observed, and at overvoltages more positive than —0.75 V a section with a sharp drop follows. Figure 7 shows the curves measured in a medium of pH = 12.3 in the presence of TU. These curves have a simpler course than those shown in Fig. 6, and are more similar to those measured in acid medium: in the interval $\eta > -0.80$ to —0.90 V they can be approximated with a slope of 0.08—0.130 V, and in a range more negative than the said overvoltage a slow rising of the curve can be observed. It can be established on the basis of the aforesaid that polarization curves measured in the presence of TU can be divided, particularly in acid medium, into two sections: in the more positive overvoltage range they can be approximated with a straight section, then, in a more negative range than the pH-dependent overvoltage, the curves decline from the straight line, and values measured in the presence of TU approach values measured in solutions in absence of the additive, indicating the fact that the catalytic action of TU diminishes in the more negative potential range. Decrease in catalytic action may be attributed to the desorption of thiourea [1]. Apart from the more complicated course of the η — lg j curves, the rising section of the curve, indicative of thiourea desorption, can also be observed in neutral (pH = 6.4) and alkaline solutions.

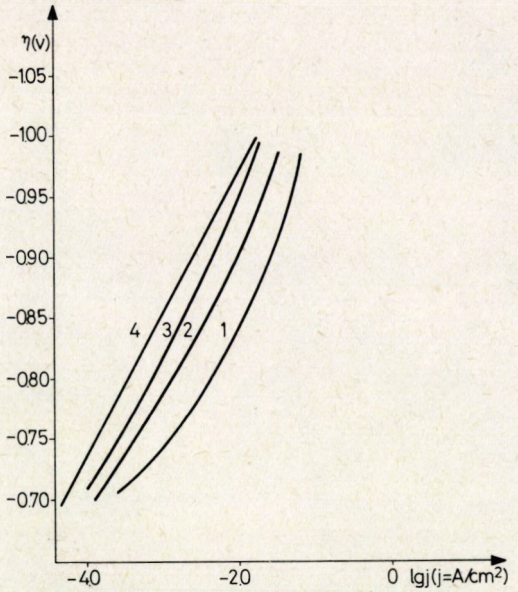

Fig. 7. η — lg j curves at the dropping gallium electrode, at pH = 12.3, in base solution of $(1 - x)$ *M* NaOH + x *M* $NaClO_4$, of 1 *M* total concentration + TU solutions of the following concentrations: ① 10^{-1}; ② 10^{-2}; ③ 10^{-3}; ④ 0 (base solution) *M*

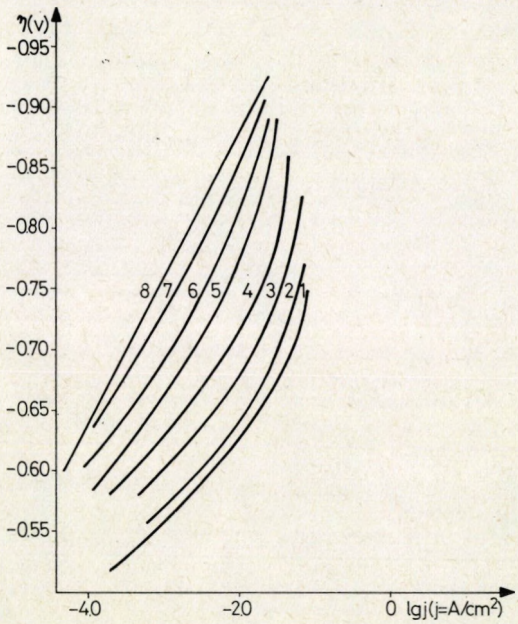

Fig. 8. η — lg j curves at the dropping gallium electrode, at pH = 0.9, in base solutions of $(1 - x)$ *M* $HClO_4$ + x *M* $NaClO_4$, of 1 *M* total concentration + DMTU solutions of the following concentrations: ① 10^{-2}; ② 10^{-3}; ③ 10^{-4}; ④ $3.1 \cdot 10^{-5}$; ⑤ 10^{-5}; ⑥ $3.1 \cdot 10^{-6}$; ⑦ 10^{-6}; ⑧ 0 (base solution) *M*

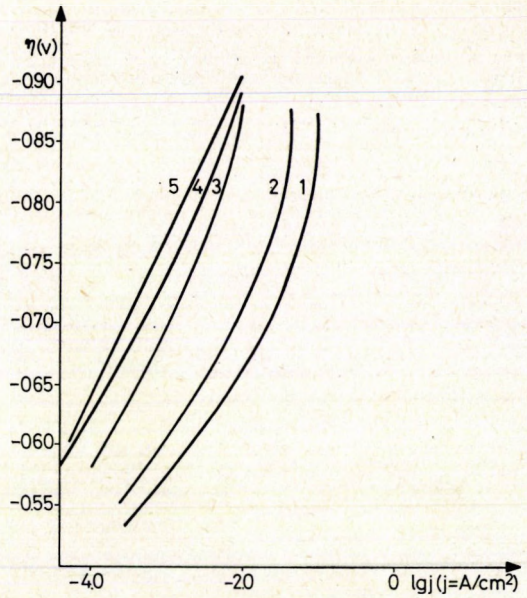

Fig. 9. η — lg j curves at the dropping gallium electrode, at pH = 1.6, in base solution of $(1-x)$ *M* $HClO_4 + x$ *M* $NaClO_4$, of 1 *M* total concentration + DMTU solutions of the following concentrations: ① 10^{-3}; ② 10^{-4}; ③ 10^{-5}; ④ 10^{-6}; ⑤ 0 (base solution) *M*

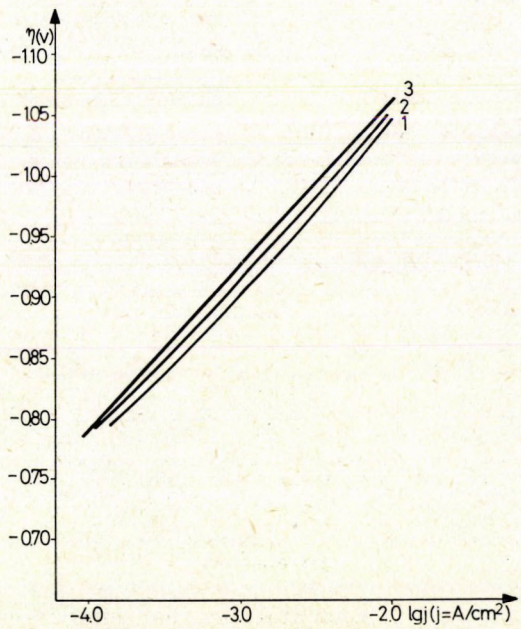

Fig. 10. η — log j curves at the dropping gallium electrode, at pH = 10.8, in base solutions of $(1-x)$ *M* $NaOH + x$ *M* $NaClO_4$, of 1 *M* total concentration + DMTU solutions of the following concentrations: ① 10^{-2}; ② 10^{-3}; ③ 0 (base solution) *M*

In further work the catalytic effect of dimethylthiourea on electrolytic hydrogen evolution at the dropping gallium electrode was investigated in the pH range from 0.9 to 12.0. Data measured are plotted in Figs 8—11. It will be noted from the figures that polarization curves obtained in acid media (pH = 0.9—1.6) in solutions containing DMTU reveal a similar course as in the case of TU. In the acid region two sections can be readily distinguished on the curves also in this case. At an overvoltage more positive than —0.66 to —0.74, the slope of the near linear curve section is 0.084 V, in a solution of pH = 0.9, while 0.11 V in a solution of pH = 1.6 (Figs 8, 9). In a more negative range than the said overvoltages, the curve is rising, indicating that at more negative potentials DMTU, similarly as TU, is presumably desorbed. The slope of the curve shown in Fig. 10, measured for the solution of pH = 10.8, is somewhat larger ($b \geq 0.132$ V) and at an overvoltage of $\eta \approx -1.10$ V the two curves melt together. Figure 11 shows the $\eta - \lg \mathbf{j}$ curves measured in a solution of pH = 12.0, and as may be seen from the figure, in this solution the catalytic effect of DMTU is the highest at $\eta \approx$ ≈ -0.85 to -0.90 V. A comparison of Figs 1—11 and Table I shows that in acid solutions, at given pH overvoltage and catalyst concentration, the catalytic ($\Delta \lg \mathbf{j}$) effect of DMTU is higher than that of TU, while in the alkaline range the catalytic effect of DMTU is lower than that of thiourea. This range in catalytic efficiency with pH may arise from the circumstance that due to the different reaction mechanism of hydrogen evolution, the mode of action of the additives investigated is different in alkaline and in neutral media.

According to the UV photometric investigation of additive-containing solutions of different hydrogen ion concentration, location and intensity of absorption maxima do not change even after standing for several days, which supports the assumption that the molecular state of thiourea and of dimethylthiourea does not change in the solutions.

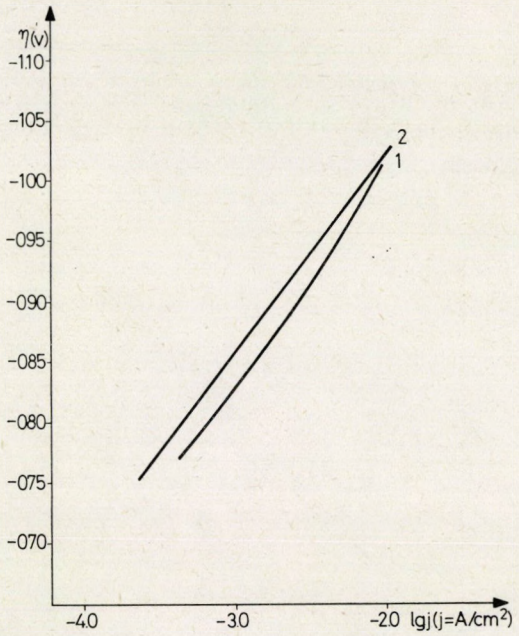

Fig. 11. η — lg **j** curves at the dropping gallium electrode, at pH = 12, in base solutions of $(1 - x)$ *M* NaOH + x *M* $NaClO_4$, of 1 *M* total concentration + DMTU solution of the following concentration: ① 10^{-2}; ② 0 (base solution) *M*

Discussion

It was shown in the experimental part that polarization curves measured in the presence of the additives investigated can be divided, particularly in acid medium, into two sections. The section falling into the more positive over-

voltage interval ($\eta > -0.65$ to -0.80 V) can be approximated with a straight line, the slope of which does not substantially differ from the slope of the curve, measured at the given hydrogen ion concentration in a solution containing no additive. Thus, presumably the rate-determining step of the hydrogen evolution reaction is also in the presence of the additive charge transition. According to our earlier assumption [1] TU and derivatives (A) exert their catalytic action by adsorption at the electrode surface and by the formation of a surface complex under participation of the H_3O^+ ions and the gallium atoms at the electrode surface ($Me.A.H_3O^+$). The discharge of this complex requires less activation energy, than the discharge of the H_3O^+ ion. It is to be presumed that similar complex is formed also in alkaline solution under participation of the gallium atoms at the electrode surface, the adsorbed additive and the H_2O molecules. According to the abovesaid, charge transition in acid and neutral solutions proceeds as follows:

$$Me \cdot A \cdot H_3O^+ + e \rightarrow A + H_2O + H + Me, \qquad (1)$$

in alkaline solutions the reaction is given by (2):

$$Me \cdot A \cdot H_2O + e \rightarrow A + OH^- + H + Me. \qquad (2)$$

Catalytic processes (1) and (2) proceed at these parts of the surface which are covered with the molecules of the additive. The current density measured ($\mathbf{j}$) is the sum of the partial current densities of the catalytic step (1) or (2) and of the processes without catalyst $H_3O^+ + e \rightarrow$ and $H_2O + e \rightarrow$, respectively. The partial current density of the catalyzed process, is $\mathbf{j}_k\,\theta$, where θ is the coverage of the electrode surface with the catalyst (the partial current density is $\mathbf{j}_k$ when $\theta = 1$), the rate of the uncatalyzed process at the uncovered parts of the surface is $\mathbf{j}_0(1 - \theta)$, ($\mathbf{j}_0$ is the partial current density when $\theta = 0$). $\mathbf{j}_0$ and $\mathbf{j}_k$ depend on hydrogen ion concentration and electrode potential, but are independent of catalyst concentration.

Current density measured is given by the following equation:

$$\mathbf{j} = \mathbf{j}_0(1 - \theta) + \mathbf{j}_k\,\theta, \qquad (3)$$

which formally agrees with equation (4) is Ref. [1].

Assuming that a simple catalytic process is involved in the case of the systems investigated, then current densities $\mathbf{j}_0$ and $\mathbf{j}_k$ can be written in the following form;

$$\mathbf{j}_0 = k_0(H^+), \qquad \text{and} \qquad (4)$$

$$\mathbf{j}_k = k_k(H^+), \qquad (5)$$

where y_0 is the rate coefficient of the discharge process from H_3O^+, and k_k that of the discharge process from the transition complex. k_0 and k_k depend on the electrode potential and on the nature of the catalyst. From Eqs (3), (4) and (5) the following expression is obtained:

$$\mathbf{j} = k_0(H^+) + k_k(H^+)\theta - k_0(H^+)\theta. \tag{6}$$

This gives after rearrangement and logarithming

$$\log \mathbf{j} = \lg (k_0 + k_k - k_0\theta) + \lg (H^+) \tag{7}$$

On reducing terms independent of hydrogen ion concentration, and introducing the notation $\lg K = \lg (k_0 + k_k\theta - k_0\theta)$, at some constant potential and catalyst concentration, the equation

$$-\lg \mathbf{j} = -\lg K + \mathrm{pH} \tag{8}$$

is obtained.

If our assumption made in the deduction of Eqs (3)—(8) is correct, then plotting lg **j** values measured at a given TU concentration as a function of pH a straight line will be obtained.

The correctness of our assumption is supported by Fig. 12, showing that the plotting of lg **j** as function of pH gives a straight line, i.e. TU exerts a simple catalytic effect on the charge transition process investigated.

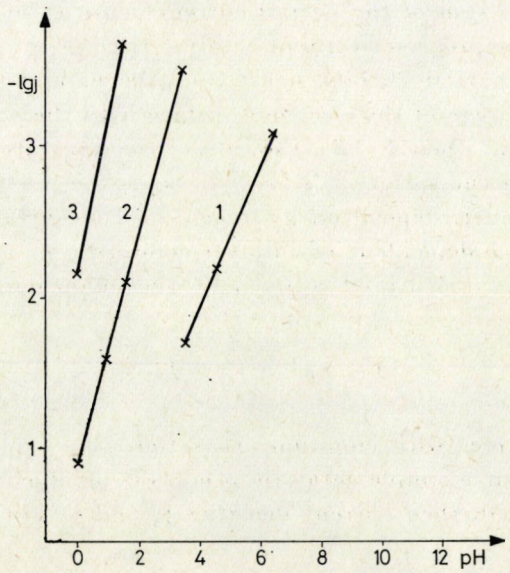

Fig. 12. lg **j** — pH curves plotted on the basis of data in Figs 1—7 at different potential (φ) and TU concentrations (C_{TU}): ① $\varphi = -0.115$ V and $C_{TU} = 10^{-2}$ *M*; ② $\varphi = -0.900$ V and $C_{TU} = 10^{-4}$ *M*; ③ $\varphi = -0.700$ V and $C_{TU} = 10^{-4}$ *M*

The relationship between the concentration and the catalytic effect of the additives for solutions of different pH can be given only, when the relationship between the coverage of the electrode surface with additive, θ, and the concentration of the additive, C_A, is known. It has been assumed in our earlier communication [1] that the Langmuir isotherm is unsuitable for the description of the relationship between the concentration of TU (or its derivatives) and its surface coverage. Frumkin's isotherm, taking also into consideration interactions between the particles of the adsorbate, was though to be more convenient:

$$BC_A = \frac{\theta}{1-\theta} \exp(-2a\theta), \tag{9}$$

where B is the equilibrium constant characteristic of the adsorption process and a takes into account the interaction between the particles (see Eq. (7) in [1]).

Presuming that coverage is low; $\theta \approx 0$, expressing θ from Eq. (3), substituting it into Eq. (9), and taking into consideration that $\mathbf{j}_k \gg \mathbf{j}_0$ [1], the relationship

$$\lg(\mathbf{j} - \mathbf{j}_0) \approx \lg \mathbf{j}_k B + \lg C_A \tag{10}$$

is obtained. For a given additive, at constant electrode potential and pH, the values $\mathbf{j}_0$, $\mathbf{j}_k$ and B are constant, therefore, under the simplifying assumptions made, according to Eq. (10) it is to be expected that $\lg(\mathbf{j} - \mathbf{j}_0)$ will change linearly with $\lg C_A$ in solutions of different pH (similarly as described in [1]).

To check the correctness of the presumed relationship between the catalytic effect of the additives, in the present case TU, and their concentration, the values pairs $\lg(\mathbf{j} - \mathbf{j}_0) - \lg C_A$ belonging together, calculated from data measured in solutions of different pH, were plotted. These curves are shown in Figs 13—15. It can be seen from the figures that at low additive concentra-

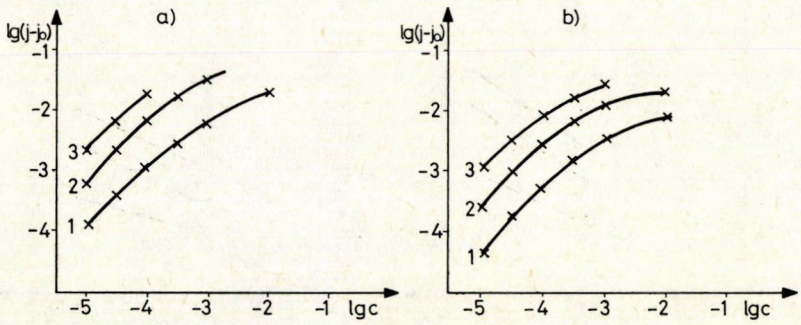

Fig. 13. $\lg(\mathbf{j} - \mathbf{j}_0) - \lg C_{TU}$ curves a) in a solution of 0.9 pH (plotted on the basis of data in Fig. 1), b) in a solution of pH = 1.6 (plotted on the basis of data in Fig. 2), at various ① $\eta = 0.660$ V; ② $\eta = -0.760$ V; ② $\eta = -0.860$ V overvoltages

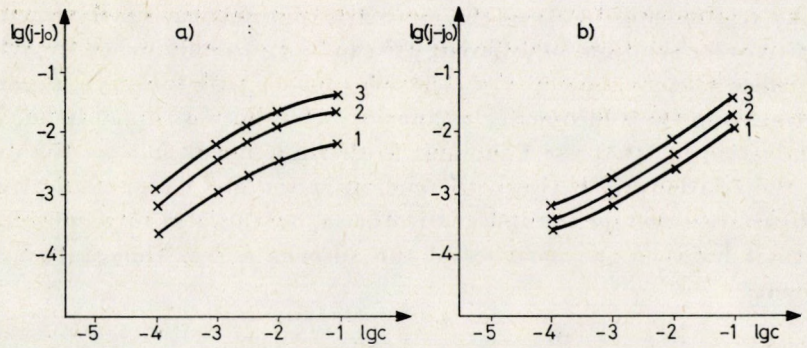

Fig. 14. lg ($\mathbf{j} - \mathbf{j}_0$) — lg C_{TU} curves a) in a solution of pH = 3.5 (on the basis of data in Fig. 3), b) in a solution of pH = 4.5 (on the basis of data in Fig. 4) at overvoltages of ① $\eta = -0.660$ V; ② $\eta = -0.760$ V; ③$\eta = -0.860$ V

tions lg ($\mathbf{j} - \mathbf{j}_0$) changes linearly with lg C_A, whereas at higher concentrations curves depart from the straight line, similarly as was found for solutions of pH = 0 [1]. At higher additive concentrations the terms $(1 - \theta)$ and exp $(-2a\theta)$ in Eq. (9) cannot be neglected anymore. $(1 - \theta)$ takes into consideration the number of free sites, while exp $(-2a\theta)$ the interactions between the adsorbed molecules at the interface.

As will be noted from Figs 13—15, the TU concentration up to which the approximating relationship (9) is valid (the point at which the curve lg ($\mathbf{j} - \mathbf{j}_0$) — lg C_A deviates from the straight line), depends on the pH of the solution. In acid and neutral solutions the deflection of the curve is to be observed at TU concentrations of $10^{-3} - 10^{-2}$ M, while in alkaline solutions a straight line is obtained up to a concentration of 10^{-1} M (Fig. 15). It is interesting to mention that in the solution of pH = 4.5 the lg ($\mathbf{j} - \mathbf{j}_0$) — — lg C_A curve deflects upwards in the TU concentration interval 10^{-3}—10^{-2} M as contrary to the behaviour found in more acid solutions. This means that

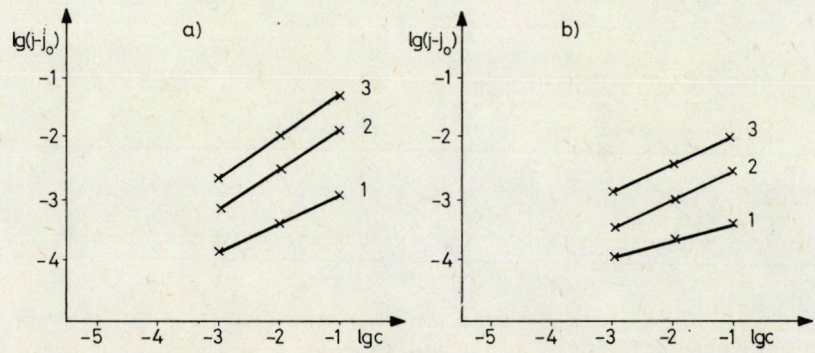

Fig. 15. lg ($\mathbf{j} - \mathbf{j}_0$) — lg C_{TU} curves, a) in a solution of pH = 10.9 (plotted on the basis of data in Fig. 6), b) in a solution of pH = 12.3 (plotted on the basis of data in Fig. 7) at various overvoltages of ① $\eta = -0.760$ V; ② $\eta = -0.860$ V; ③$\eta = -0.960$ V

in the given case the catalytic effect increases in this interval to a larger extent with increasing TU concentration, than would be expected on the basis of the linear relationship (10). This phenomenon indicates that in solutions of pH = = 4.5 the interaction between the adsorbed particles is of opposite sign than in acid solutions. Downwards deviation of the curve from the straight line indicates that there is a repulsion between the adsorbed particles, whereas an upwards deviation of the curve means an attraction between the adsorbly-particles. It should be mentioned that an increase of θ results independented of the interaction a downwards deviation of the curve, because of the dim inish ing of $(1 - \theta)$. The change of the shape of $\lg (\mathbf{j} - \mathbf{j}_0) - \lg C_A$ is possibly due to the fact that there is an important interaction between H_3O^+ ions and TU molecules, while the interaction between H_2O molecules and TU molecules may be of lesser extent and of different character. According to our investigations carried out so far [1] and data in the literature [7], it seems very similar that during the adsorption of TU of DMTU molecules a donor–acceptor complex is formed at the surface by the interaction of the unoccupied d orbitals of the gallium atom and the free electron orbitals of the sulfur atom in S=C bond, and the H_3O^+ ion interacts with this Ga ↔ S = C species, and due to this, the activation energy of discharge decreases. Probably, in the assumed complex the H_3O^+ ion is oriented in a position favourable for discharge, and is bound at the same time to the electrode surface and to the TU molecule. This donor — acceptor bond depends on the polarizability of the catalyst molecule, it is to be expected that at higher polarizability [4] the Ga ↔ S = C interaction will be stronger. This seems to be supported by that experimental result that under identical conditions the catalytic effect of DMTU of higher electron polarizability is stronger than that found for TU (see Table I). In alkaline medium, where hydrogen is evolved from water molecules [see Eq. (2)], conceivably this catalytic effect is achieved on account of the Ga ↔ S = C interaction by the TU molecules with their negative part directed towards

Table I

pH	TU		DMTU	
	$\Delta \lg \mathbf{j}$	$\alpha \cdot 10^{24}$ cm^3	$\Delta \lg \mathbf{j}$	$\alpha \cdot 10^{24}$ cm^3
0.9	1.29		1.48	
1.6	1.12	8.44	1.52	12.05
10.9	0.41		0.06	

$\Delta \lg \mathbf{j}$ is the difference of $\lg \mathbf{j}$ obtained in the additive-containing solution and of $\lg \mathbf{j}_0$ measured in the additive-free solution at an overvoltage of −0.80 V and at a TU or DMTU concentration of 10^{-3} *M*.

Values were calculated from the refractive indices by the Lorenz–Lorenz method [6]. Refractivity was measured on a Pulfrich PR II refractometer.

the surface, while the H_2O molecule, adjacent to the TU dipole, is oriented with its positive part, towards the surface. This means from the aspect of discharge a favourable orientation, so that discharge can proceed with a higher rate. Water dipoles are bound at the gallium electrode, a surface with positive or not too large negative charge, with their negative end [8], and presumably this orientation is changed by the TU molecules, by turning most of the H_2O molecules with their positive end towards the gallium surface, and thus fixing the H_2O molecules. The experimental observation that the catalytic effect of DMTU is weaker in alkaline solutions than that of TU, can be presumably attributed to the steric effect of the two CH_3 groups.

REFERENCES

[1] Szabó, K., Takács, M.: Magy. Kém. Folyóirat, **87,** 111 (1981)
[2] Vargalyuk, V. G., Loskarev, Ju. M., Ivanko, V. Sz.: Elektrohimija, **15,** 1840 (1977)
[3] Babkin, G. N., Dimitrovskaya, T. A., Iskakova, A. H., Lebedev, L. N.: Elektrohimija, **18,** 454 (1982)
[4] Szabó, K., Takács, M.: Magy. Kém. Folyóirat, **86,** 498 (1980)
[5] Bagockaya, I. A., Genkina, N. M., Boycov, V. G.: Elektrohimija, **5,** 132 (1969); Bagockaya, I. A., Potapova, E. N.: Elektrohimija, **5,** 1465 (1969); Elektrohimija, **6,** 855 (1970); Elektrohimija, **7,** 1849 (1971)
[6] Katz, M., Lobo, P. W., Minano, A. S.: J. Chim. Phys., **66,** 1045 (1969)
[7] Donelly, B., Dowine, T. C., Grzeskowiek, R., Hamburg, H., Short, D.: Corr. Sci., **14,** 597 (1974)
[8] Frumkin, A. N., Polianovskaya, N. I., Grigoryev, N. B., Bagotskaya, I. A.: Electrochim. Acta, **10,** 793 (1965); Trasatti, S.: J. Electroanal. Chem., **33,** 351 (1971)

Acta Chimica Hungarica, 114 (2), pp. 187—198 (1983)

CHANGING OF THE CATALYTIC EFFECT OF THIOUREA WITH TEMPERATURE AT THE DROPPING GALLIUM ELECTRODE

K. SZABÓ*, É. M. CSOBOD and M. TAKÁCS

(Department of Physical Chemistry and Radiology, Eötvös Loránd University, H-1088 Budapest, Puskin u. 11—13.)

Received September 16, 1982
In revised form October 13, 1982
Accepted for publication November 25, 1982

The effect of thiourea on the temperature-dependence of the rate of hydrogen evolution was investigated in acid and alkaline solutions. It was found that the rate of the hydrogen evolution reaction increases with increasing temperature both in alkaline and acid solutions. The values of activation energy (E) and pre-exponential factor (A) are lower in the presence of thiourea, than in acid and alkaline base solutions. The change in activation energy is higher in acid solution (26.7 kJ/mol) than in alkaline solution (13.5 kJ/mol).

In the interpretation of the catalytic effect of thiourea it was assumed that it is adsorbed at the electrode surface and forms with H_3O^+ a transition complex, the discharge of which requires less activation energy, than the $H_3O^+ + e \rightarrow$ process without catalyst [1].

As is well known, activation energy may be determined on the basis of the temperature-dependence of overvoltage. When the quantity of species adsorbed at the electrode surface changes with changing temperature, and the species affect the rate and mechanism of the electrode process, the interpretation of the energetic parameters becomes more complicated, than in the case of simple systems [2, 3, 4].

For the determination of the activation parameters the reaction rate of hydrogen evolution was measured at four different temperatures in acid and alkaline solutions containing thiourea (TU).

Experimental

Measurements were carried out at the dropping electrode made of gallium of 99.9999% purity, with the experimental and evaluation methods described in [5], in the 305—318 K temperature interval, in solutions containing 1 M $HClO_4$, and 0 and 10^{-3} M of TU, and in solutions of a total concentration of 1 M, of pH = 11.5, containing $(1 - x)M$ NaOH + xM $NaClO_4$, and 0 and 10^{-2} M of TU. The purity of the substances used was the same as given in [1].

Experiments were carried out at 305, 308, 313 and 318 K ± 0.2 K.

* To whom correspondence should be addressed

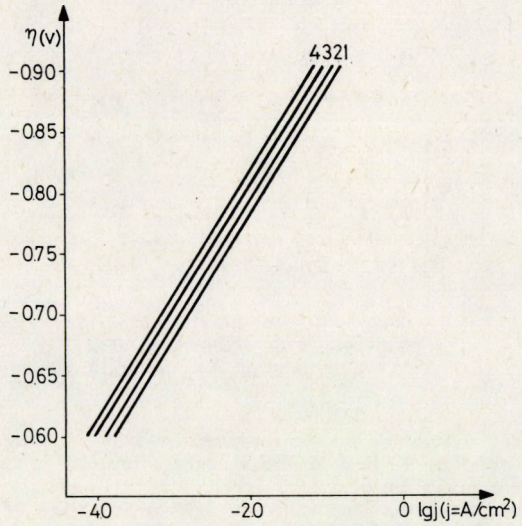

Fig. 1a. η — lg **j** curves at the dropping gallium electrode in 1 *M* $HClO_4$ solution at different temperatures: ① 318; ② 313; ③ 308; ④ 305 K

From the overvoltage (η) and current density (**j**) values the η — lg **j** polarization curves were plotted.

Polarization curves obtained in 1 *M* $HClO_4$ solution at different temperatures are shown in Fig. 1a, those measured in 1 *M* $HClO_4 + 10^{-3}$ *M* TU in Fig. 1b. It can be seen from the figures that the reaction rate of hydrogen evolution increases in both systems with increasing temperature. The slope of the η — lg **j** curve, (*b*), (according to relationship

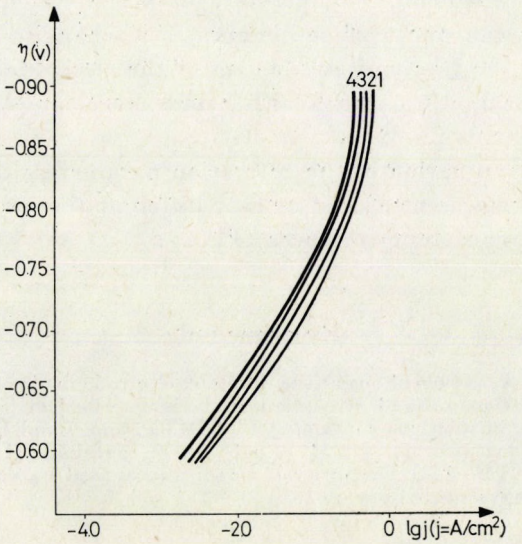

Fig. 1b. η — lg **j** curves at the dropping gallium electrode in 1 *M* $HClO_4 + 10^{-3}$ *M* TU solution at different temperatures: ① 318; ② 313; ③ 308; ④ 305 K

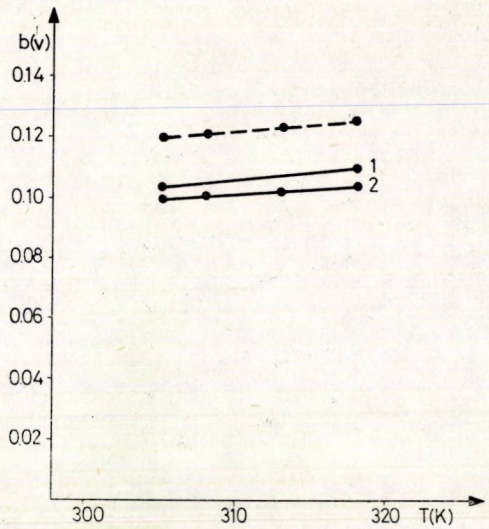

Fig. 2b. — T curves in ① 1 M $HClO_4$ solution (plotted from data in Fig. 1a); ② in 1 M $HClO_4 + 10^{-3}$ M TU solution (plotted from the linear sections of the curves in Fig. 1b). The curve drawn with dotted line was calculated with the value $\beta = 0.5$

Table I

Acid solution, pH = 0

T (K)	$\Delta \lg j$		
	$\eta = -0.70$ V	$\eta = -0.75$ V	$\eta = -0.80$ V
305	1.77	1.66	1.45
308	1.84	1.80	1.64
313	1.40	1.32	1.20
318	1.35	1.28	1.13

Concentration of thiourea: $c_{TU} = 10^{-3}$ M

Alkaline solution, pH = 11.5

T (K)	$\Delta \lg j$		
	$\eta = -0.85$ V	$\eta = -0.90$ V	$\eta = -0.95$ V
305	0.96	0.92	0.85
313	0.65	0.60	0.56
318	0.62	0.56	0.51

Concentration of thiourea: $c_{TU} = 10^{-2}$ M

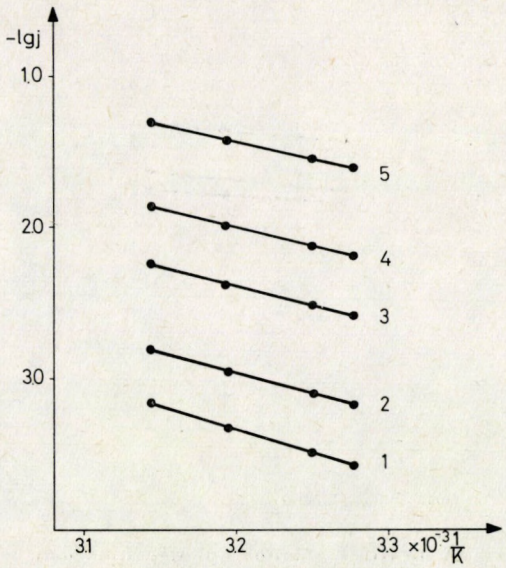

Fig. 3a. lg j — $1/T$ curves in 1 M $HClO_4$ solution (plotted on the basis of data in Fig. 1a), at diffreent overvoltages: ① $\eta = -0.66$ V; ② $\eta = -0.70$ V; ③ $\eta = -0.76$ V; ④ $\eta = -0.80$ V; ⑤ $\eta = -0.86$ V

$b = 2.3 \frac{RT}{\beta F}$) changes linearly with temperature (Fig. 2). It will be noted from a comparison of Figs 1a and 1b and from data in Table I that the catalytic effect of TU, the value Δ lg j characteristic of it (which is the difference of lg j_0 measured in perchloric acid solution and lg j measured in perchloric acid solution containing TU at the same η and temperature) dimin-

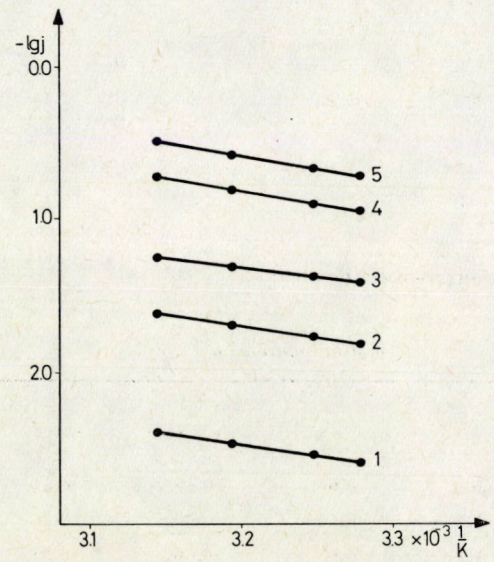

Fig. 3b. lg j — $1/T$ curves in 1 M $HClO_4 + 10^{-3}$ M TU solution (plotted on the basis of data in Fig. 1b) at different overvoltages: ① $\eta = -0.60$; ② $\eta = -0.66$ V; ③ $\eta = -0.70$ V; ④ $\eta = -0.76$ V; ⑤ $\eta = -0.80$ V

ishes with increasing temperature, which may be attributed to the fact that thiourea adsorption at the gallium electrode surface decreases with increasing temperature.

The straight line $b - T$ (in Fig. 2, curve 1, marked with a continuous line) plotted with data obtained in the solution without additive, differs only slightly from the straight line plotted with the value $\beta = 0.5$ (marked with a dotted line), and a straight line similar to these is obtained in perchloric acid solution containing TU (curve 2, marked with a continuous line in Fig. 2). It will be noted from data in Fig. 2 that in the case of the systems investigated β is independent of temperature, so that the activation parameters of the hydrogen evolution reaction can be calculated in the systems by equation $\lg j = \lg A - 2.3\,RT$, where A is the pre-exponential factor, E the activation energy at $\beta =$ constant overvoltage, the other quantities having the usual meaning.

The values of the apparent activation energy, E were calculated in the usual way, by plotting the $\lg j - 1/T$ curves with $\lg j - T$ value pairs, read off from $\eta - \lg j$ curves in Fig. 1b at an overvoltage $\eta =$ constant (Figs 3a—b). From the slopes of the straight lines obtained in this way E values belonging to a given overvoltage were calculated, and knowing these, the respective pre-exponential factor and the $\lg A$ values were calculated. The $\lg j - 1/T$ curves were fitted with the least squares method. The value of apparent activation energy (E_0) at overvoltage $\eta = 0$ was determined by extrapolating the straight line $E = E_0 + \beta F\eta$ to $\eta = 0$ (Fig. 4, curve 1). E_0 was 75.38 kJ/mol, and this value agreed well with data in the literature [3, 4]. Activation parameters calculated from data in Figs 3a—b (E and $\lg A$ values) are summarized in Table II. It can be seen from the data of the table that E values obtained at identical overvoltage in solutions containing TU are always lower, than values obtained in pure perchloric acid solution. Moreover, Fig. 4 shows that value pairs $E - \eta$

Table II

	Acid medium,* pH = 0				Alkaline medium,** pH = 11.5			
	Base solution		Base solution + TU		Base solution		Base solution + TU	
$-\eta$ [V]	E [kJ/mol]	$\lg A$ [A: A/cm²]	E [kJ/mol]	$\lg A$ [A: A/cm²]	E [kJ/mol]	$\lg A$ [A: A/cm²]	E [kJ/mol]	$\lg A$ [A: A/cm²]
1.100					44.95	8.2		
1.050					46.10	8.8		
1.000					50.00	9.4	33.80	3.8
0.950					51.50	10.2	35.05	3.5
0.900					52.50	9.3	39.00	3.3
0.850							41.50	4.2
0.800	46.04	5.68	20.72	2.87			43.40	5.1
0.780			18.80	2.42				
0.760	46.17	5.32	22.60	2.91				
0.740			22.60	2.76				
0.720			22.59	2.59				
0.700	48.48	5.18	22.61	2.42				
0.680			24.50	2.52				
0.660	49.63	4.94	28.00	2.92				

* Base solution: 1 M $HClO_4$
Base solution + TU: 1 M $HClO_4$ + 10^{-3} M TU; in the base solution $E_0 = 75.38$ (kJ/mol)

** Base solution: $(1 - x)M$ NaOH + $x\,M$ $NaClO_4$
Base solution + TU: $(1 - x)$ M NaOH + $x\,M$ $NaClO_4$ + 10^{-2} M TU; in the base solution $E_0 = 78.00$ (kJ/mol)

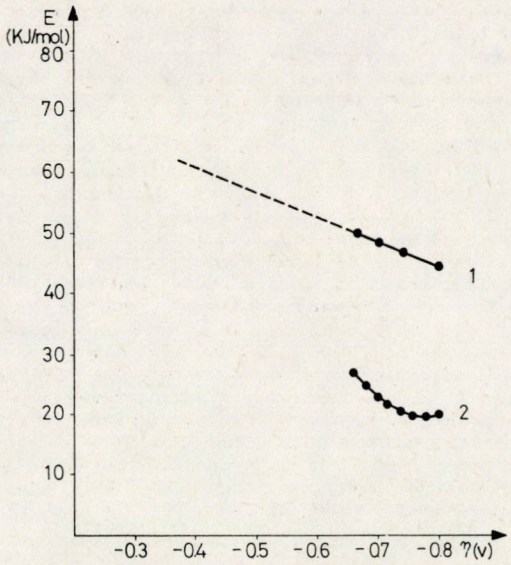

Fig. 4. $E - \eta$ curves plotted on the basis of values measured in ① 1 M $HClO_4$ solution; ② in 1 M $HClO_4 + 10^{-3}$ M TU solution, using data in Fig. 3a and 3b, respectively

measured in perchloric acid solution give a straight line, while $E - \eta$ values obtained in perchloric acid solution containing TU do not lie on a straight line but give a curve with a minimum in the $\eta = -0.66$ to -0.88 V potential range. At the η value corresponding to the minimum, the value of the activation energy is 41—49 kJ/mol (see Table II). Table II shows also that the value of lg A in perchloric acid containing TU is lower, than in the ground solu-

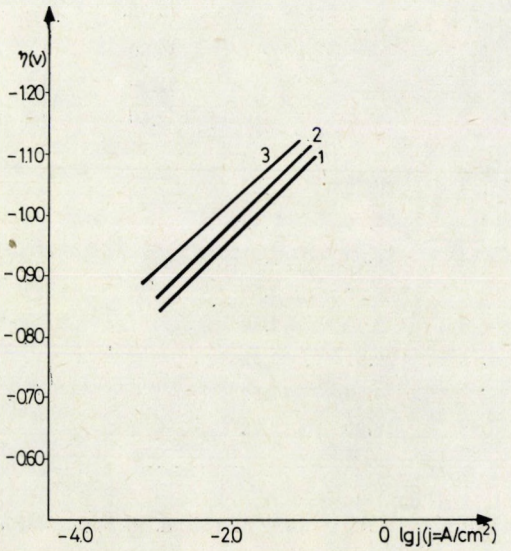

Fig. 5a. $\eta = \lg \mathbf{j}$ curves at the dropping gallium electrode in $(1 - x)M$ NaOH + x M $NaClO_4$ solution of 1 M total concentration and pH 11.5, at different temperatures ① 318; ② 313; ③ 305 K

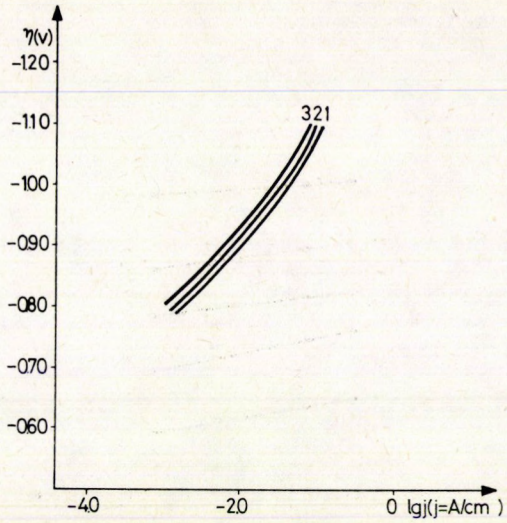

Fig. 5b $\eta = \lg \mathbf{j}$ curves at the dropping gallium electrode in $(1 - x)$ *M* NaOH + x *M* $NaClO_4$ + + 10^{-2} *M* TU solution of 1 *M* total concentration, of pH = 11.5 at various temperatures: ① 318; ② 313; ③ 305 K

tion. With the shift of overvoltage in the negative direction, the value of lg *A* increases in pure perchloric acid solution, whereas in perchloric acid containing TU, similarly to the value of *E*, lg *A* changes also along a minimum curve.

The temperature dependence of overvoltage in alkaline solution was measured in a base solution of 1 *M* total concentration of the composition $(1 - x)M$ NaOH + xM $NaClO_4$ (pH = 11.5), and in the base solution + 10^{-2} *M* of thiourea. $\eta - \lg \mathbf{j}$ curves plotted from

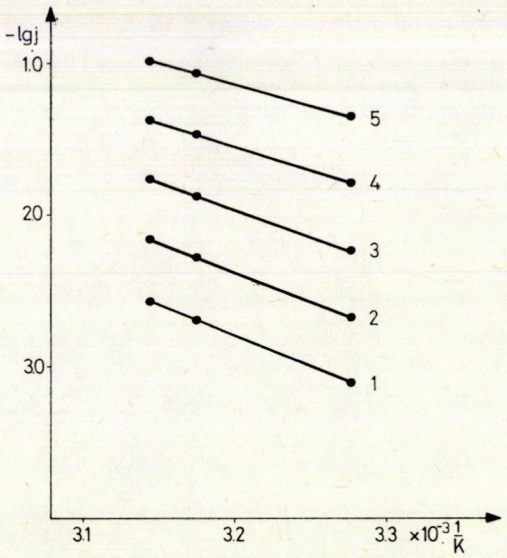

Fig. 6a. $\lg \mathbf{j} - 1/T$ curves in $(1 - x)$ *M* NaOH + x *M* $NaClO_4$ solution of 1 *M* total concentration and of pH = 11.5 (plotted on the basis of data in Fig. 5a) at different overvoltages: ① $\eta = -0.90$ V; ② $\eta = -0.95$ V; ③ $\eta = -1.00$ V; ④ $\eta = -1.5$ V; ⑤ $\eta = -1.10$ V

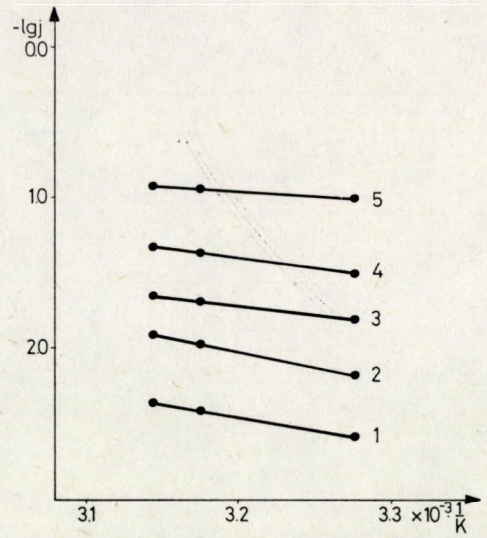

Fig. 6b. lg j — $1/T$ curves in $(1 - x)$ *M* NaOH + x *M* $NaClO_4$ + 10^{-2} *M* solution of 1 *M* total concentration and of pH = 11.5 (plotted on the basis of data in Fig. 5b) at various overvoltages: ① $\eta = -0.86$ V; ② $\eta = -0.90$ V; ③ $\eta = -0.95$ V; ④ $\eta = -1.00$ V; ⑤ $\eta = -1.10$V

data measured are shown in Figs 5a and 5b, and the lg j — $1/T$ straight lines plotted on the basis of data calculated from these curves in Figs 6a and 6b. The temperature- dependence of the slope of the polarization curves is shown in Fig. 7. Activation energy and pre-exponential factor values calculated from data in Figs 6a—b are summarized in Table II. Calculations were carried out similarly as described for the evaluation of measurements in acid medium. Data in Table II show that in the case of both base solutions and solutions containing thiourea activation energy decreases with increasing overvoltage, but as can be seen in Fig. 8 (curve 1), in the case of the base solution the activation energy of the hydrogen evolving reaction changes

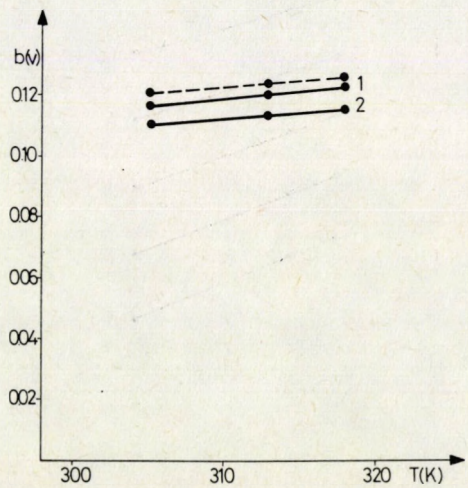

Fig. 7b. T curves plotted on the basis of data pertinent to the straight sections ① in Fig. 5a; ② in Fig. 5b. The curve drawn with an interrupted line was calculated with a value of $\beta = 0.5$

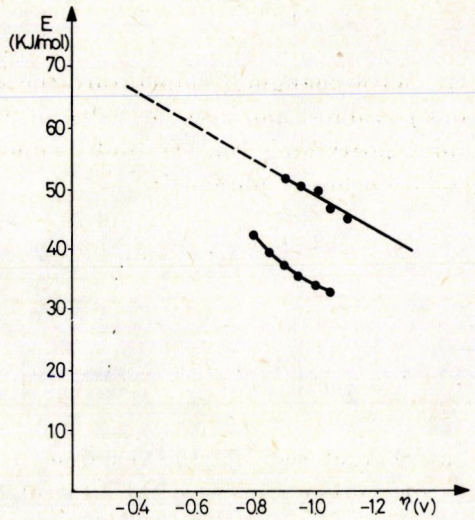

Fig. 8. $E - \eta$ curves plotted on the basis of data measured in ① base solution of pH = 11.5; ② in base solution of pH = 11.5 + 10^{-2} *M* TU, using data of Fig. 6a and 6b, respectively

linearly with overvoltage, while in the case of a solution containing also thiourea the value pairs $E - \eta$ do not lie on a straight line (curve 2).

Data in Fig. 8 and Table II show that activation energies measured in the presence of thiourea at a given overvoltage are also in the alkaline region lower, than those measured in the base solution. Moreover, it will be noted from data in Table II that in thiourea-free acid and alkaline base solutions the values of the activation energy at $\eta = 0$ are near identical (75 and 78 kJ/mol), while in solutions containing also thiourea, at an overvoltage of $\eta = -0.80$ V (where values are comparable) the activation energy is lower in acid solution than in alkaline medium (20 and 43 kJ/mol). Activation energy measured in alkaline medium in the presence of TU differs less from the value measured in the base solution, i.e. the change in activation energy (ΔE) produced by thiourea is greater in acid medium, than in alkaline solutions: $\Delta E_{acid} > \Delta E_{alkaline}$.

These latter values are conform with the experimental results that the catalytic activity of thiourea is lower in alkaline than in acid solutions. It should be mentioned in connection with data in Table II that E and lg A values measured in pure perchloric acid solution agree well with data in the literature [3], while of the activation parameters measured by us in alkaline medium only the values of activation energy were comparable with data in [3], while considerably higher lg A values were obtained. Data published in [3] were calculated from measurements carried out in NaOH + NaCl solutions of 1 *M* total concentration, while in our case the composition of the solution was NaOH + $NaClO_4$. This difference in solution composition does not motivate the difference in lg A found by us.

Discussion

As shown in the experimental part (Table II), the value of activation energy measured in acid solutions containing thiourea (E_{TU}) is lower than the value measured in the base solution at given overvoltage, $E_{TU} < E$. In the examination of the change with temperature of the given electrode process, at the condition η = const., we start from equation (1)

$$\mathbf{j} = \mathbf{j}_0(1 - \theta) + \mathbf{j}_k\,\theta \tag{1}$$

(see Ref. [1], Eq. (4)). With changing temperature the rate of reaction (the corresponding $\mathbf{j}$, $\mathbf{j}_k$ and $\mathbf{j}_0$ values) and also the value of θ are changing.

Rearranging and logarithming Eq. (1) and assuming that $\mathbf{j}_k \gg \mathbf{j}_0$ and $\theta \approx 0$,the following relationship is obtained:

$$\ln(\mathbf{j} - \mathbf{j}_0) = \ln \mathbf{j}_k\,\theta. \tag{2}$$

Substituting in (2)

$$\mathbf{j}_k = k \exp\left[-\frac{E}{RT}\right] \text{ and } \theta = B_0\, c_{TU} \exp\left[\frac{-q}{RT}\right],$$

(where k is a constant characteristic of the reaction investigated, B_0 is the coefficient of the TU adsorption process, q the heat of adsorption,* c_{TU} the concentration of thiourea in the bulk of the solution, the above quantities being independent of temperature) and differentiating this expression with respect to temperature, the following equation is obtained;

$$\frac{\partial \ln(\mathbf{j} - \mathbf{j}_0)}{\partial T} = \frac{E' + q}{RT^2} = \frac{E_m}{RT^2}\,. \tag{3}$$

In Eq. (3) $E' + q = E_m$, where E_m is the activation energy of the catalytic process, which is the lower, the higher is the value of the heat of adsorption. It follows from this that one cause of the decrease in activation energy may be the adsorption of thiourea at the electrode surface. E_m, the activation energy of the catalytic process at given overvoltage, can be calculated from the slope of the $\lg(\mathbf{j} - \mathbf{j}_0) - 1/T$ curve. E_m is not identical with E_{TU} in the experimental part, calculated from relationship $\lg \mathbf{j} - 1/T$. The two kinds of activation energies can be considered as near identical only if $\mathbf{j} \gg \mathbf{j}_0$ (Eq. 3).

Nevertheless, under consideration of the abovesaid, the qualitative conclusion may be drawn that in acid solutions, where the change in activation energy is considerable, one of its reasons is the adsorption of thiourea, leading to the formation of the complex Me—TU—H_3O^+, because due to this adsorption, the activation energy of the discharge process decreases according to $E_m = E' + q$. Where E' is the activation energy of the catalytic process if $q = 0$, including the change in energy of the interaction TU—H_3O^+ and the change in ptoential Ψ'. In alkaline solutions ΔE is lower, which can be explained by the circumstance that there is no considerable interaction between H_2O and TU molecules, and catalytic action presumably consists in an orientation

* $q < 0$.

into more favourable position and in the fixing at the electrode surface of the H_2O molecules by the thiourea molecules. If the charge of the electrode is not too negative, the water molecules are turned with the oxygen atom towards to metal at the gallium electrode [6]. Electron transition, $H_2O + e \rightarrow$ is more favourable, if the water molecule is turned with the hydrogen atom towards the surface, the electron donor. Presumably, between the TU molecules bound with their negative end, with the S atom, at the surface, an orientation of the water molecule with its positive part, i.e. with the hydrogen atom, towards the metal surface is more favourable, creating energetically more favourable conditions for discharge, and thus, results in a diminishing of the activation energy.

As seen in the experimental part, $E - \eta$ value pairs obtained for solutions containing TU do not lie along a straight line (Figs 4 and 8). The $E - \eta$ curve reveals in acid medium in the potential interval —0.66 to 0.88 V a minimum. This is probably due to the fact that the coverage of the electrode surface with thiourea is the highest in the said potential range, because the zero point charge potential of gallium falls into this range. In alkaline solutions the $E - \eta$ curve has no distinct minimum.

It has been shown in the experimental part that besides the activation energy the value of the pre-exponential factor is also changing. $\lg A$ is decreased both in acid and alkaline media by thiourea (Table II). $\lg A$ obtained for solutions containing thiourea, similarly to the activation energy, is composite, because it comprises also the change in entropy of thiourea during adsorption. $\lg A$ measured can be identified only when $\mathbf{j} \gg \mathbf{j}_0$ with the value derived from Eq. (3).

According to general reaction kinetic theory, $A \sim \exp \frac{\Delta S^*}{R}$, where ΔS^* — is the activation entropy of the rate determining step of the reaction, which is in the case of acid base solution the activation entropy of the step $H_3O + e \rightarrow$, ΔS_0^*; and in thiourea-containing solution the activation entropy of the step $(Me—TU—H_3O^+) + e \rightarrow$, ΔS_{TU}^*.

With a view to the fact that the pre-exponential factor (A_{TU}) obtained for solutions containing thiourea is a composite, quantity, from its comparison with the pre-exponential factor measured in the base solution (A_0) (from the fact that $\lg A_{TU} < \lg A_0$) no conclusions can be drawn on the relationship of the activation entropies (ΔS_{TU}^* and ΔS_0^*).

It should be mentioned that the zero point charge potential of gallium, and thus the Ψ' potential, are shifted during the adsorption of TU, and this cannot be left out of consideration from the aspect of the change in reaction rate. In our case the change of Ψ' is included in E'.

REFERENCES

[1] Szabó, K., Takács, M.: Magy. Kém. Folyóirat, **97,** 111 (1981)
[2] Conwey, B. E., Mac Kinnon, D. I., Tilak, B. V.: Trans. Faraday Soc., **66,** 1203 (1970)
[3] Potapova, E. N., Kristalik, L. I., Bogockaya, I. A.: Elektrohimiya, **10,** 49 (1974)
[4] Szabó, K., Mika, J.: Magy. Kém. Folyóirat, **78,** 352 (1972); Szabó K., Mika, J., Hangos, K.: Magy Kém. Folyóirat, **81,** 21 (1975)
[5] Szabó, K., Takács, M.: Magy. Kém. Folyóirat, **86,** 498 (1980)
[6] Frumkin, A. N., Polianovskaja, N. I., Grigoryev, N. B., Bagotskaya, I. A.: Electrochim. Acta, **10,** 793 (1965); Trasatti, S.: J. Electroanal. Chem., **33,** 351 (1971)

Acta Chimica Hungarica, 114 (2), pp. 199–216 (1983)

CHEMICAL REACTION OF SUBSTANCES UNDER MECHANICAL LOAD

Z. A. JUHÁSZ

(Department of Building Materials, Technical University, Budapest H-1111 Budapest, Műegyetem rkp. 3.)

Received September 1, 1982
Accepted for publication December 9, 1982

Changes of the chemical reactivity of some inorganic building materials, due to the action of mechanical forces, are discussed. Some electrochemical properties, viz. electrode potential and solubility of reinforcing steel wire change in function of the load to which this wire is exposed; the changes of crystal structure and of the binding force of magnesium oxide in function of the duration of milling the polymorphism of limestone in function of exposure to milling forces in a mill are explored. Reference is made to experiments being carried out in order to elucidate the chemical and structural changes in a piece of set cement subjected to mechanical load. Maximum chemical reactivity can be attained at a critical degree of load, this is characterized by the yield point.

Discussions of chemistry with respect to the various kinds of energy released by chemical processes or with respect to the types of energy consumed in chemical processes justify an autonomous chapter on "Mechanochemistry" [1] (for a summary, cf. [2, 3, 4]). Alterations in material structure, as well as chemical reactions which proceed while, or because, the substances involved are subject to mechanical load can be subsumed under this title. A mechanically loaded state can be the common result of pressure, tension, banding, etc. and of electricity magnetism, heat, etc. The free energy of a substance exposed to these effects increases, therefore the operations that produce this loaded state are justly described as "mechanical activation" [5].

In connexion with this theme in its wider sense, we have worked towards the understanding of correlations between the chemical reactivity of metal and certain inorganic solid substances and the mechanically loaded state these exist in, and used some definite building materials important in practice test substances in this study. We think the phenomena observed are specially important when considered from the point of view of the production, and the general properties like ageing, dilapidation, erosion, corrosion etc. of the several building materials. The experimental method applied consists of the activation of the test material by subjecting it to tensile loads of various force or by milling it at various degrees of intensity, and the determination of the correlation between loaded state and chemical reactivity on the basis of data directly recorded, or in some indirect way.

1) Chemical reactivity of metals in a mechanically loaded state

Several authors [6—11] have drawn attention to the change of chemical activity of metals in a mechanically loaded (strained, stretched, rolled etc.) state. In what follows we present results of experiments carried out in order to determine a "critical loaded state".

The experiment consisted essentially of two parts.

The first was to plot tension vs. elongation in a tensile test with reinforcing steel wire, in an experimental arrangement schematically shown in Fig. 1. The test bar was clamped into the test machine and kept immersed there in a saturated solution of $Ca(OH)_2$. Alongside the test bar under tension another test bar of the same material and dimensions was placed and not subjected to tension. The voltage between the two bars was conducted on to a voltmeter provided with a recorder. Elongation ε due to increasing tensile load and voltage were simultaneously and continuously recorded. Between points σ_A and σ_B the load was cut and then applied again till rupture occurred.

A notable feature shown in Fig. 1 is the very small voltage between the two test bars in the (Hooke) domain of elastic deformation. Electric potential

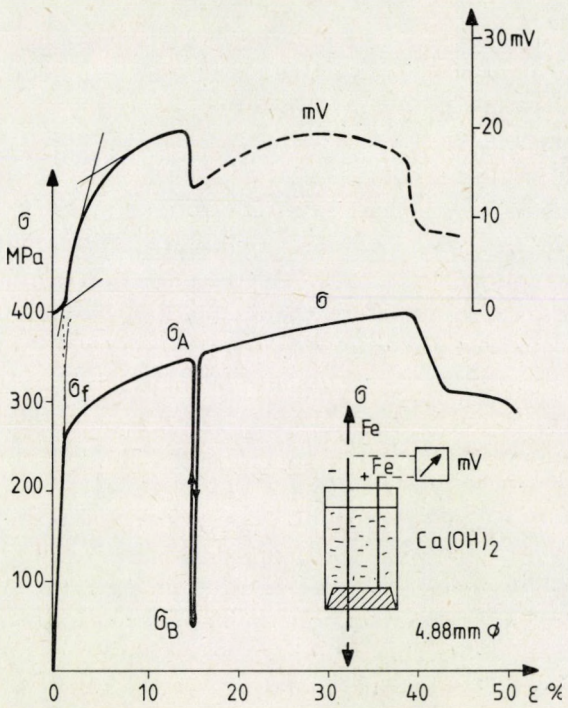

Fig. 1. Tensile strength diagram of a steel wire: potential difference between a test rod under load and one in the unloaded state

increases significantly near the yield point, i.e. in the boundary region between elastic and elastic-plastic deformation. At load-relief within the elastic section voltage between the two metal bars becomes zero, within the section subsequent to the yield point voltage diminishes but does not disappear completely. At reloading, a smaller voltage is generated at the same loaded state, then the voltage again increases with deformation, suddenly falls at rupture and assumes a constant lower value after rupture.

In the experimental arrangement just mentioned, the best bar in the loaded state is always the negative pole of the cell.

The voltage generated during elastic deformation is very much a function of the rate at which the load is being applied.

The scheme in Fig. 2 shows the second experiment. Prismatic test pieces were made from the reinforcing steel and their surfaces were polished to high gloss. A glass sphere was pressed with various force on to various points of

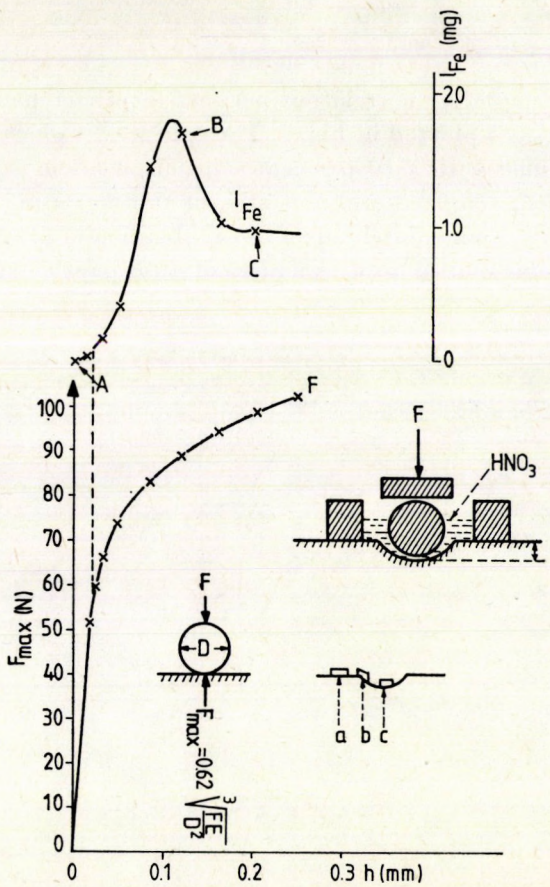

Fig. 2. **Solubility of the surface of a steel rod under tension**

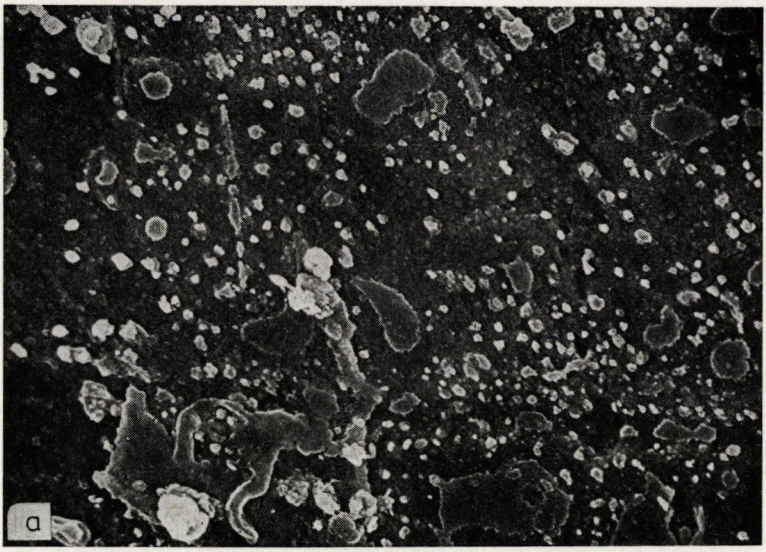

the polished surfaces. The correlation between depth of penetration, h, and force applied, F_{max}, is plotted in Fig. 2. The sphere was placed inside a plastic ring which was filled with a 10 per cent solution of nitric acid. The duration of pressure applied, temperature, and area of the metal in contact with the acid were constants. Immediately after the application of pressure was stopped the acid solution was soaked up with a piece of filter paper and its iron content,

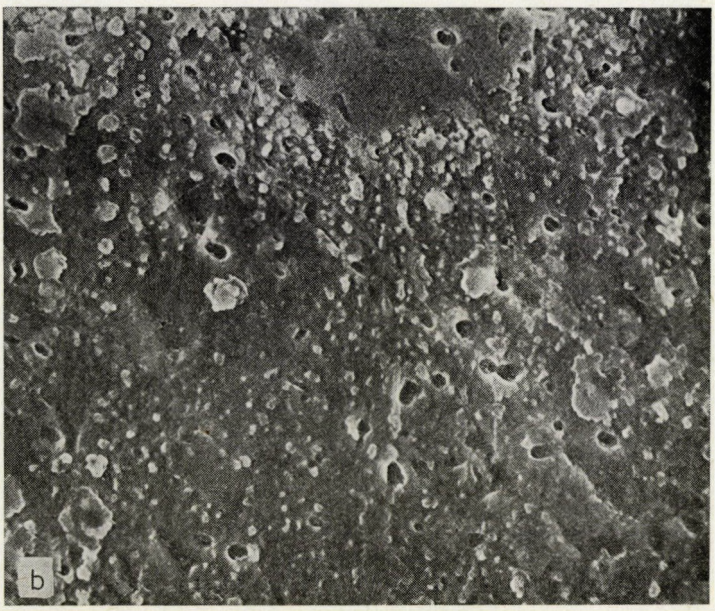

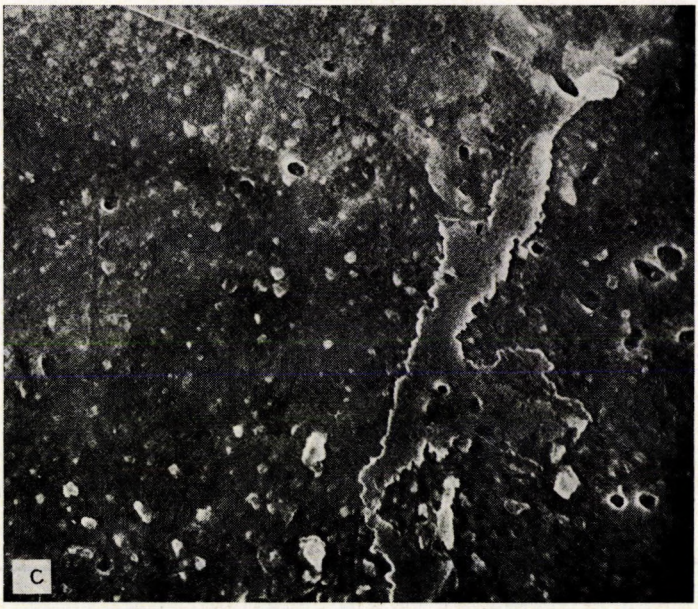

Fig. 3. Photographs taken in a scanning electron microscope, of an etched steel surface. Etching was carried out at the degree of load noted in Fig. 1 ($n = 3300\times$)

l_{Fe}, was determined. The impression made by the glass sphere was inspected with the help of a scanning electron microscope. Three points (marked *a*, *b*, and *c* in the Figure) of an impression were photographed. Generally, at point *a* the original texture was observable, at point *b* an intermediary (disturbed) structure was seen, while the most visible change occurred at point *c*, that is at the deepest point of the impression, where glass sphere and metal surface were in direct contact. Some characteristic photographs of points *c* are those in Fig. 3.

Experimental results tally with those from tensile tests. Solubility increases but slightly in the region of elastic deformation. It increases, however, during the initial period of plastic deformation (in proximity of the yield point), then it decreases somewhat when plastic deformation proceeds.

The emergence of etch holes near the yield point, especially along the slip surface (Fig. B) is to be seen quite clearly on the photographs taken in the electron microscope (Fig. 3). Here also solubility is the greatest. Photograph C, that of the zone of plastic deformation, reveals a diminution of the number of etch holes. Corrosion holes are scarce when the pressure applied is not great (Fig. A).

It must be noted that solubility is less when etching is carried out not during relief from loading but after it. E.g. 1.4 mg Fe was dissolved from around the glass sphere pressed with a force of 8.95 N. 0.6 mg Fe was dissolved

from around the pressure point after pressure had been brought to an end, and only a few corrosion holes were revealed by photography.

The conclusion [11, 12] to be drawn from the results of these two tests is that chemical potential (respectively Nernst potential, which is proportional to it) of metals while subjected to a mechanical load is greater than the increase of potential after the state of mechanical load. The tendency to corrode is much more significant while metals are under strain than after the relief of it; chemical activity after permanent deformation or after rupture is more pronounced than at the initial state. To all this we must add, however, that maximum activity coincides with the critical state due to mechanical loading; this state is characterized by the yield point.

2) Mechanical activation of crystalline building materials by means of fine-milling

Mechanical activation of various solid substances can be realized by fine-milling for a considerable time with the help of mills that are capable of exerting great force [4].

In what follows, two experimental results are described which allow to draw conclusions pertinent to changes of material structure and of chemical reactivity in a state due to mechanical load. It must be noted, however, that here we meet the difficulty caused by the fact that only the permanent changes in material structure, brought about during the state of load, can be determined from the data found for the milling product, and this is only part of the overall change in material structure characteristic of the loaded state.

The test substances were milled in a KEFAMA-type laboratory vibration mill (frequency 1400 min^{-1}, amplitude 2 mm, capcity of the vessel 0.8 litre). The duration of milling, and the quality of the crushers were changed from case to case.

The milling product was subjected to X-ray diffraction analysis; besides phase partition, dimensions of the crsytallites, A, and crystal-lattice deformation $\frac{\delta a}{a_0}$ were calculated from the width of reflexions [13, 14]; crystallinity K was calculated on the basis of line intensity [15]. Specific surface was calculated according to the BET method [16] for water vapour adsorption isotherms.

The first experiment was the activation of sintered technical magnesium oxide for various periods of time τ_A in the vibration mill.

Experimental results were, in general, like those noted by Schrader, and Kneschke [17] for pure MgO. From among these we may point out (cf. Figure 4) the following.

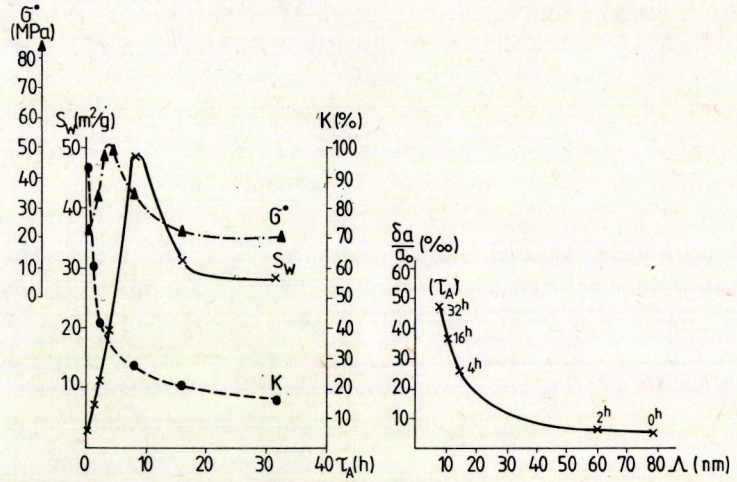

Fig. 4. Activation of magnesium oxide in a vibration mill. On the left: Changes of resistance to rupture σ^0, specific surface S_W, and crystallinity K, as functions of the duration of milling τ_A. On the right: Deformation of crystal lattice $\delta a/a_0$ as a function of crystallite dimension Λ

Also in the case of this test substance the diminution of particle size, respectively the increase of specific surface, is evident as one of the most frequent processes which occur during milling. Milling, however, consists of two phases: the initial period, from 0 to 8 hours, is characterized by the monotonous increase of specific surface with duration of milling, the characteristic of the second, i.e. milling continued after the first 8 hours of it, is "overmilling", when specific surface tends to decrease.

Formally, the Rittinger formula [18] is valid for the initial period:

$$W_z = \text{const}_1 \, \Delta S_W$$

where W_z stands for milling energy. In this case $\tau_A = \text{const}_2 \, W_z$, i.e. the energy put to use in milling seems to have been consumed by the ΔS_W increase of the surface of the test substance.

In fact, however, already in this phase of milling a significant decrease of crystallinity K can be observed, this is ascribable primarily to the diminution of crystallite size Λ and in a lesser degree to deformation of crystal lattices $\frac{\delta a}{a_0}$.

During the overmilling phase a high degree of surface activation occurs and, due to this: aggregation and agglomeration proceed [19]. This leads to the adhesion of particles to each other, and to the growing together of particles. Though crystallinity K seemingly changes at a smaller rate in this section of overmilling, within this section only the rate of the diminution of crystallite

dimensions decreases and, in reference to this, the permanent deformation of crystal lattices occurs much frequently, i.e. the density of dislocations increases.

This latter phenomenon is felt to be primarily important when considered from mechanochemical point of view. It can be stated — in accord with experimental results relevant to many other substances — that the permanent deformation of crystal structures that is concomitant with the diminution of crystallite dimensions during milling occurs chiefly below a critical crystallite dimensions. Considered with a view to the cohesive power of Sorel cement made with magnesium oxide (the compressing strength of a test piece), the increase of the specific surface of the magnesium oxide is favourable, but the breakdown of its crystal structure (overactivation) is detrimental [20].

The second experiment was a study of the conversion of calcite into aragonite.

The polymorphic change from calcite into aragonite occurs during the milling of either substance (Figure 5). According to Schrader, and Hoffman [21], this process is characterized by a definite ratio of calcite to aragonite, and proceeds till a mechanochemical equilibrium, function, of the method of milling, is attained.

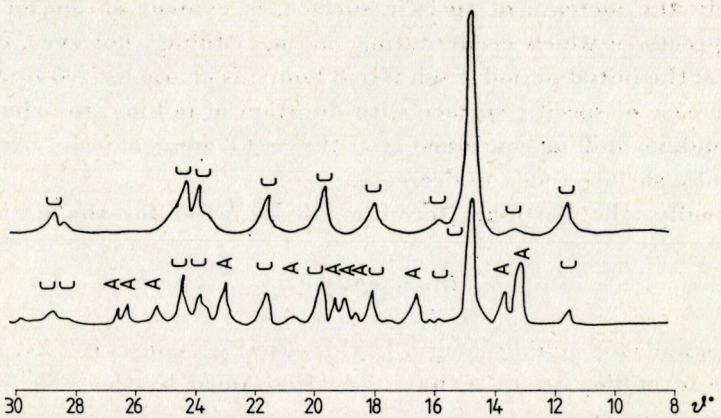

Fig. 5. Refractogram of limestone before milling (upper line) and after milling for 19 hours in a vibration mill (lower line); C = calcite; A = aragonite

The above authors have studied this phenomenon by plotting kinetical curves [21]: the carbonates were milled for various times, the milled part was subjected to phase-analysis. In the present work this method was altered in so far as not the duration of milling was varied (this was kept constant, i.e. 19 hours) but the crushers were changed (density, and dimensions of these were different), so the conversion calcite → aragonite could be observed as a function of the mechnical force applied to the test substance.

In these experiments the spherical crushers were made of steel, porcelain, or corundum, their size was from 2 to 10 mm.

The simple expression

$$F_z = \frac{mg}{A}$$

was used for the characterization of the force exerted by the spherical crushers, where mg = weight of one sphere, and A = surface of one sphere.

As shown in Fig. 6, an increase of force applied is accompanied by a steady decrease of the amount of calcite, together with a parallel increase of that of aragonite (polymorphic mechanochemical transformation). The change of the dimensions of the crystallites is the greatest at the application of medium force: then will the crystals be comminuted most. When changes of crystal structure are considered as a function of crystallite dimension (cf. the drawing on the right hand side in the Figure) then the following changes can be observed.

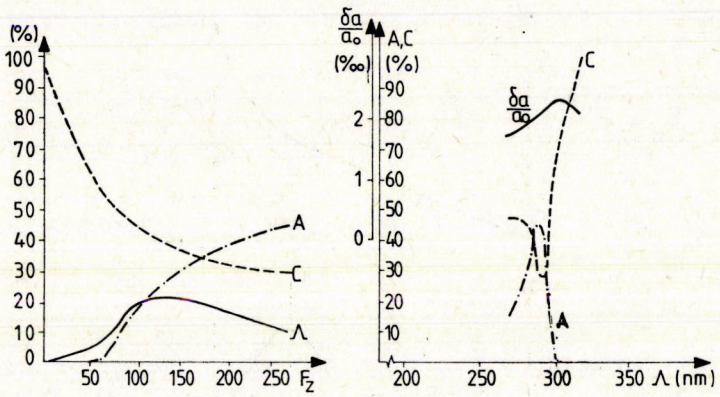

Fig. 6. Activation of limestone in a vibration mill. On the left: Amounts of C = calcite, A = aragonite; Λ = dimension of crystallite as a function of mechanical impact force F_z transmitted by crusher spheres. On the right: Amount of aragonite (A) and of calcite (C), and lattice deformation $\delta a/a_0$ as functions of crystallite dimension Λ

At the increase of force applied, lattice deformation (dislocation density) increases first: this may be regarded as the introductory phase of the polymorph transformation. This is followed by a calcite → aragonite conversion, it involves a significant proportion of the material. Finally, due to still greater force applied, the density of dislocations decreases and with this a partial desactivation of the system occurs, probably due to a translation of crystal planes, respectively to plastic deformation.

These two experiments suggest that the effect of forces applied during milling consists not only of the increase of the degree of dispersion but also

of the deep structural change of the substance that affects crystal structure (decrease of the size of crystallites and of crystallinity, polymorph transformations, amorphization; for a summary cf. [4]).

To all this we must add that transformations are greatest after the attainment of a critical (low) particle size [22] at the exertion of a critical (medium) force. The supposition is perhaps justifiable that, here also, this critical state of load can be characterized with the yield point. This supposition can be supported by the following argument.

Let the start be an ideal, unimpaired crystalline body of which the load vs. deformation (σ, ε) diagram is drawn as the upper scheme in Figure 7. When a sufficiently great force is applied, a body of ideal behaviour can be brought to plastic deformation at above the yield point σ_f, up to the break point σ_T^0. Permanent lattice deformation $\frac{\delta a}{a_0}$ occurs in the domain of plastic deformation and, at the beginning, increases together with deformation, then decreases as dislocations are relieved.

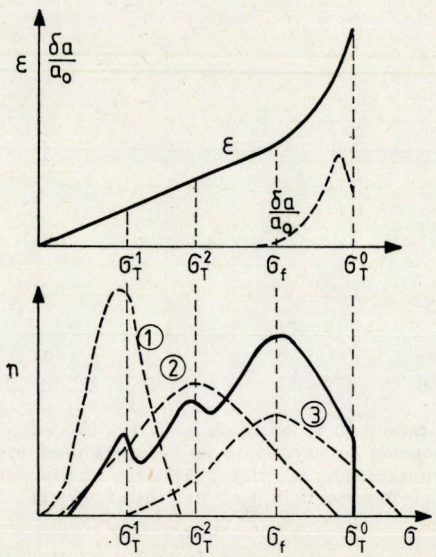

Fig. 7. Diagram for the interpretation of milling experiments

If there is a weak point (e.g. micro fissure) characterized by strength σ_T^1 in this ideal body then it will break at this σ_T^1 when steadily increasing load is applied, consequently (in a rough approximation) no plastic deformation will ensue.

If there is present also a σ_T^2 weak point in the ideal test piece then a repeatedly applied load allows only the tension state σ_T^2 to be reached, and so on. In such cases a break "protects", so to speak, this ideal test substance

against plastic deformation, respectively against deformation of crystal structure.

Obviously, in the course of repeated application of loading force the yield point will be attained in simplified case is that the crystalline pieces should contain no weak, defective points in the domain below the yield point.

The lower drawing in Figure 7 represents (also schematically) the frequency of possible strength values (unbroken line) in the particles of the milling product of this ideal material (a schematic picture, in the manner of Hüttig's bonding-spectrum [23]); and the partition (broken lines) of the forces exerted by the crusher spheres. These two curves show that there is a high grade of probability of breakings at the weak points of the particles to occur in the initial phase of milling when very weak bonds are abundant (therefore the cpecific surface of a milled real substance increases in the initial period of milling). When milling is continued over a more extended period, weak points become scarce and plastic deformation comes to the fore. This is why experience shows that, generally, deformation of crystal st. .ctures begins to increase below a critical dimension of the crystallites when no weak bonds are present in the particles. The specific surface area changes at a lower rate in this phase of milling, it even decreases sometimes because of aggregation.

Finally, it seems to be quite plausible that it is the effect of the force exerted by the crusher spheres that determines in what measure simple milling, by the exposure of weak point (scheme 1) will occur, with plastic deformation of lattice structures added (scheme 2) or even accompanied by disruption of chemical bonds due to mechanical force (scheme 3). According to calculations carried out by Schrader, and Tetzner [24], the phenomenon mentioned last can occur when vibration milling is used.

3) Mechanochemical processes in pieces of set cement

The solidification of aqueous cement paste is explained [25] as the formation of calcium-aluminium-silicate-hydrates of various compositions, which are formed in the course of rather complicated chemical processes, and can occasionally convert one into another. Hydration at ambient temperature is a slow process. In a piece of set cement at an intermediary state of its formation, solidification, which attained e.g. on the 28th day, 70 to 80 per cent of its final strength, the residues of the initial clinker minerals can still be found, when several end-products of hydratation are present already together with intermediary reaction products.

The question has been raised whether mechanical loads to which cement pieces not yet completely set are exposed affect the process of further hydratation, in other words, can structural transformations like those that occur in other hydro-silicates (kaolin, bentonite, talc) be observed also here?

In the attempt at finding an answer to this question, a test by means of vibration milling was carried out. The test substance was a paste of portland 450 cement made with 30 per cent of water; this paste was cast into test pieces and allowed to harden under water for 28 days, then the pieces were pre-milled to a fineness better than 0.1 mm and dried at 105 °C.

This test substance was activated by milling for 8 hours in a vibration mill. The original and the activated samples were studied by thermoanalytical methods using a MOM-type derivatograph.

Though the overall loss of mass of the cement piece did change but very slightly after activation, the height of the several TG-steps, and the pattern of the pertinent DTA-curves, underwent significant alterations. The most important of these were (Fig. 8):

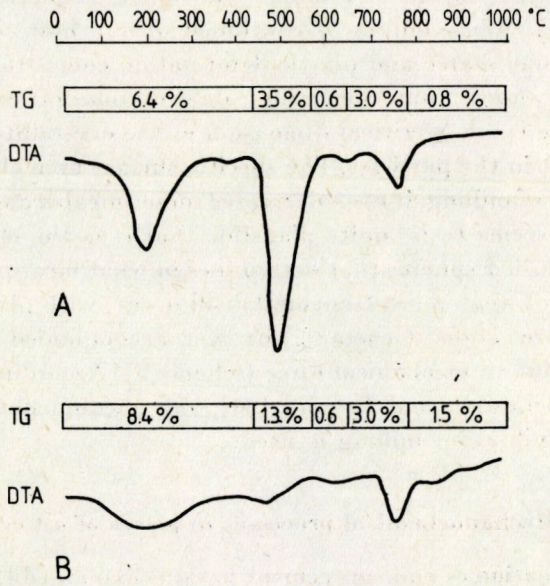

Fig. 8. DTA curves, and losses of mass, of a piece of set cement before (upper line) and after (lower line) milling

a) The amount of "gel-water" bound by comparatively lower energy in the hydratation product increased (uniformly calculated from loss of mass between 25 and 440 °C).

b) The amount of water removed between 440 and 580 °C, set free in the course of the thermal dissociation of portlandite $Ca(OH)_2$, was significantly smaller.

c) Loss of mass between 580 and 650 °C (water strongly bonded in tobermorite) did not change, neither did the amount of CO_2 formed in the decomposition of $CaCO_3$ present in the form of dispersed, very fine particles.

d) CO_2 escaping above 780 °C increased, i.e. the amount of $CaCO_3$ in the form of particles larger than the preceding ones.

When it is supposed that the changes just mentioned can be characterized first of all by the variations of the mass of portlandite then a material balance can be calculated as follows: an about 9.1 per cent of $Ca(OH)_2$ present in the original cement piece (63 per cent of the calcium hydroxide total) was transformed in the course of milling, of this 1.2 per cent yielded carbonate and 7.9 per cent became involved in a chemical conversion in the product of which water and OH-groups were held by bonds of a force lesser than that of the Ca—OH bonds in the original portlandite.

The chemical processes, however, that occur when the cement piece is subjected to mechanical load are not confined to one component, i.e. portlandite, alone: also other crystalline, and amorphous, components of the cement piece take part in them. The details of these very intricate processes are being studied, and the few phenomena noted up to now are mentioned here by way of giving examples.

a) *Mechanochemical dissociation of portlandite*

In a first approximation the process is reversible within the cycle of load — relief. Deeper investigation shows that the stability of the $Ca(OH)_2$ due to secondary formation is smaller than that of which it originates, so that this secondary $Ca(OH)_2$ decomposes at a lower temperature (around 380 °C) and is more easily converted into carbonate.

b) *Chemical reactions in water condensed in capillaries*

Water produced within the submicroscopic capillaries of gel structures and in the course of the mechanochemical dissociation of portlandite, and that which enters the gas phase, will condense after relief from the loaded state and will dissolve various components of the cement piece. In the solution so produced further chemical reactions will occur, partly to yield calcium-aluminium hydrates, partly to form calcium carbonate by means of binding the carbon dioxide present in the atmosphere.

c) *Chemical reactions in the aqueous phase present in the capillary system*

When in the state under load, hydration products liberate water (water is pressed out) in which further chemical reactions occur.

d) *Change of the way water is bonded*

There exists the possibility that gel-water bonded by medium level energy will change into bonded states partly of greater, partly of lesser energy

when in a state under load. This is especially important from the point of view of the change of strength (ageing, fatigue).

e) *Reactions in the solid state*

These are connected to diffusion processes.

f) *Reactions between solid and gaseous phases*

The concentrated solution of $Ca(OH)_2$ present in the capillary system in the loaded state or at release, absorbs CO_2, SO_2, SO_3 etc. gases at an exceptionally high rate: this is especially important from the point of view of carbonate formation on the hand, and from that of sulphate corrosion on the other. The phenomena just mentioned will be discussed in detail in a later publication. Here we point out that the changes found to occur are functions of the degree of the mechanical load to which cement pieces are exposed, chiefly to repeated dynamic effects in the nature of blows, abrasion, and to great loads. It is felt, though evidence for it is not forthcoming yet, that these transformations are most pronounced at the critical state of load.

4) Discussion

The decrease of bond energy in a material system is concomitant [5] with the deformation, or breaking, of a solid body, due to mechanical forces that act on it. H e r e bond energy means that amount of energy that must be applied in order to remove the atoms of a given system from the position they occupy in a given state of the system and in order to separate them beyond the sphere in which they can interact.

The more important cases of the changes of bond energy which occur at deformation or at breaking are easily explained according to the argument which follows.

The atoms of an ideal solid are differentiated as inner atoms and surface atoms; the number of atoms is $n = n_i + n_s$. If the removal of one single inner atom out of its co-ordination sphere requires, on the average, e_i energy and that of a surface atom e_s energy then the bond energy is

$$\begin{aligned} E_B &= n_i \cdot e_i + n_s \cdot e_s \\ &= (n - n_s)\, e_i + n_s \cdot e_s \\ &= n \cdot e_i - n_s)e_i - e_s). \end{aligned} \tag{1}$$

In this equation (and referred to a mass of 1 g)

$n \cdot e_i = E_L$ lattice energy
$n_s (e_i - e_s) = E_S$ surface free energy;

where, based upon specific surface S and specific surface potential E_γ

$$E_S = S \cdot E_\gamma.$$

After substitutions,

$$E_B = E_L - S \cdot E_\gamma \tag{2}$$

When the body is subjected to mechanical work dW_z, and this work brings about, at an effectivity η_z, the change of bond energy is

$$\eta_z \, dW_z = dE_B = dE_L - d(S \cdot E_\gamma) > 0 \tag{3}$$

Processes that bring about the decrease of bond energy (increase of free energy) and are caused by mechanical forces are called primary mechanochemical processes. These occur when mechanical energy is adsorbed, i.e. when material is put in a state of load. Primary processes the following: increase of surface due to deformation or breaking accompanied, perhaps, by the generation of active, fresh fissure surface (surface activation), further the destruction of stable crystal structures, the increase of the density of lattice defects, the decrease of crystallinity till a completely amorphous structure is arrived at (structural activation).

Material that is activated by the application to it of mechanical energy acquires the tendency to enter into processes that decrease the free energy or increase the bond energy. These are secondary mechanochemical processes which in part take place when in the state of load or, incidentally, when relieved if, after the load — relief cycle, free energy remains greater than it was initially. Secondary mechanochemical processes are: relaxation phenomena, recrystallization, adhesion, aggregation, agglomeration [19], adsorption, adhesion and chemisorption phenomena, chemical reactions inside a phase or between phases, etc.

In a load — relief cycle the crystal structure and the surface of the body either regain their original state (reversible cycles, including perfectly elastic deformations) or shape, dimensions, internal and surface structures of the body change (irreversible cycles, including plastic deformation). In the latter case there is a difference between the bond energy at the initial state I and that at the final state II:

$$E_{B_I} - E_{B_{II}} = \Delta E_B = \Delta E_L - \Delta(S \cdot E_\gamma) \tag{4}$$

When $\Delta E_B > 0$ (i.e. $E_{B_I} > E_{B_{II}}$) the material will have become permanently active in the course of mechanical treatment. Fundamentally, also here two cases can be distinguished:

— surface activation ($\Delta E_L = 0$) comprising deformation and comminution, $\Delta E_B = -E_\gamma \Delta S$, or concomitant changes of the surface, $\Delta E_B = -\Delta(E_\gamma S)$;

— mechanochemical activation comprising changes in the structure of the material, $\Delta E_B = \Delta E_L$ or also surface-activation contomitant with these changes, $\Delta E_B = \Delta E_L - \Delta(E_\gamma S)$.

Mechanical (surface, structural, and mechanochemical) activation of materials can be realized by means of a load — relief cycle.

The experiments discussed in this paper offer direct evidence for the fact that chemical reactivity is generally greater during a state of load that after this state ceased to exist. Maximum activity is in evidence during the state of load characterized by the yield point because here secondary processes responsible for a decrease of free energy (recrystallization, disappearance of dislocations during the flow of them) play a subordinate role in comparison with the role of primary mechanochemical processes, viz. of crystal lattice deformation, generation of dislocations. Secondary processes cause desactivation (passivation), according to the terminology used by Naeser, and Scholz [10] with plastic (permanent) deformation, therefore structural activation is driven back though "surface activation" due to the increase of the surface, principally because fresh surfaces appear, has begun already.

In the case of load — relief cycles surface activity is very important from the point of view of mechanochemical activation since the reactivity of broken, but chiefly of finely milled, material can be enhanced through the increase of the specific surface, especially through the production of surfaces that show greater activity. The same degree of importance must be attributed to the permanent deformation of crystal structure since also a defective, perhaps amorphous, consequently labile inner structure enhances the chemical reactivity.

Milling products that are active when considered from this point of view can be produced by exposure of the particles to a load up to the critical state of load which also means milling up to critical particle size [4]. Obviously, mechanochemical activation, i.e. production of milled material that is active as to particle-surface and crystal structure, requires various technologies severally in accord with the quality of the material, the type of the mill used, respectively with limit particle size.

Symbols

e_i = energy for the removal of an inner atom
e_s = energy for the removal of a surface atom
h = depth of penetration
n_i = number of inner atoms
n_s = number of surface atoms
D = diameter of glass sphere
E_B = bond energy
E_L = lattice energy
E_S = surface free energy
E = specific surface potential
F = force of pressure
F_z = force exerted by a crusher sphere
K = crystallinity
S_W = specific surface
W_z = milling energy
ε = elongation
Λ = dimension or size of a crystallite
σ = load force, tensile strain
σ_f = yield point
σ_T° = break point
τ_A = duration of milling
$\frac{\delta_0}{a_0}$ = lattice deformation

REFERENCES

[1] Oswald, W.: Handbuch der allg. Chemie, I., Leipzig 1919
[2] Thissen, P. A., Meyer, K., Heinicke, G.: Grundlagen der Tribochemie, Berlin, Akad. Vol. 1967
[3] Juhász, Z.: The Position of Mechanochemistry in the Literature (in Hungarian), Communication No. 33 of the Department of Building Materials, University of Technical Sciences, Budapest 1980
[4] Juhász, Z., Opoczky, L.: Mechanical Activation of Silicates by means of Fine Milling (in Hungarian) Budapest, Akadémiai Kiadó 1982
[5] Juhász, Z.: Aufbereitungstechnik, **10,** 558 (1974)
[6] Shaw, M. C.: J. Appl. Mechan., **15,** 37 (1948)
[7] Fink, M., Hofmann, V.: Z. Metallkunde, **24,** 276 (1968)
[8] Grohn, H., Friedrich, H., Paudert, R.: Z. Chem., **2,** 24 (1962)
[9] Paudert, R. et al.: Chem. Techn., **20,** 276 (1968)
[10] Naeser, G.: Scholz, W.: Ber. der DKG, **39,** 106 (1962)
[11] Kovács, K.: Fundamentals of Corrosion (in Hungarian) Budapest, Műszaki Kiadó 1965
[12] Gerischer, H.: Werkstoffe u. Korrosion, **8,** 394 (1957)
[13] Kochendorfer, A.: Z. Krist., **105,** 393 (1944)
[14] Fricke, R., Gwinner, E.: Z. Phys. Chem., **A 183,** 165 (1938)
[15] Toth, M.: Acta Geol. Acad. Sci. Hung., **19,** 197 (1977)
[16] Juhász, Z.: Építőanyag, **XXXIV** (1982) 161, XX
[17] Schrader, R., Kneschke, G.: Silikattechnik, **18,** 239 (1967)

[18] Beke, B.: Theory of Comminution (in Hungarian) Budapest, Akadémia Kiadó 1963
[19] Opoczky, L.: Power Technology, **17,** 1 (1977)
[20] Juhász, Z.: Periodica Polytechnica, **17,** 211 (1973)
[21] Schrader, R., Hofmann, B.: Z. Anorg. Allg. Chem., **39,** 41 (1969)
[22] Rumpf, H.: Chem. Ing. Technik, **34,** 731 (1962)
[23] Hüttig, G. F.: Zement-Kalk-Gips, **7,** 151 (1954)
[24] Schrader, R., Tetzner, G.: Freiberger Forschungshefte, **A-292,** 5 (1964)
[25] Bogue, R. H.: The Chemistry of Portland Cement New York 1947
[26] Kelley, W. P., Jenney, M.: Soil Science, **41,** 367 (1936)
[27] Juhász, Z.: Kémiai Közlemények (in Hungarian), **31,** 227 (1969)

Text

The text of the paper should be concise. The description of new compounds (in the Experimental) must include the complete analytical data. Special attention must be paid to structural formulas given within the text. Complicated (non-linear) formulas should be drawn on separate sheets of paper and their position in the text should be clearly marked. The numbering of formulas and equations (in parentheses on the right-hand side) is only needed if they are referred to in the text. Units should conform to the International System of Units (SI). In nomenclature the rules of the I.U.P.A.C. are accepted as standard. Symbols for physical quantities are printed in italic type and should, therefore, be underlined in the manuscript.

References

References should be numbered in order of appearance in the text (where the reference number appears in brackets) and listed at the end of the paper. The reference list, too, should be typed double-spaced. Journal titles are to be abbreviated as defined by the Chemical Abstracts Service Source Index.

Examples:

[1] Brossi, A., Lindlar, H., Walter, M., Schneider, O.: Helv. Chim. Acta. **41**, 119 (1958)
[2] Parr, R. G.: Quantum Theory of Molecular Electronic Structure. Benjamin, New York 1964
[3] Warshel, A.: in Modern Theoretical Chemistry, Vol. 7, Part A (Ed. G. A. Segal), Plenum Press, New York 1977

Tables

Each table should be given a Roman number and a brief informative title. Structural formulas should not be used in column headings or in the body of tables.

Figures

Figures should be numbered consecutively with Arabic numerals. Their approximate place should be indicated in the text on the margin. All figures must be identified on the back by the author's name and the figure number in pencil. Standard symbols (such as circles, triangles, squares) are to be used on line-drawings to denote the points determined experimentally. Line-drawings must not contain structural formulas and comments. Spectra or relevant segments thereof, chromatograms, and X-ray diffraction patterns will be reproduced only if concise numerical summaries are inadequate to replace them. Drawings and graphs should be prepared in black ink on good-quality white or tracing paper. Photographs should be submitted on glossy paper as high-contrast copies. Xerox or similar copies are not suitable for reproduction, but may be used for duplicate copies.

Redrawn illustrations will be sent to the authors for checking. No corrections of figures will, therefore, be accepted in the proofs.

Submission of manuscript

After having completed the corrections suggested by the referees and editors, the final manuscript should be submitted in duplicate, in a form ready for publication. If the corrected manuscript is not returned to the editors *within six weeks*, the intended publication of the paper will be regarded as withdrawn by the authors.

Page charge will not be assessed for the publication, however, authors from overseas countries must contribute to the postage of correspondence by sending, together with the manuscript, international postal coupons to the value of U.S. $ 10.—

Proofs and reprints

A set of proofs will be sent to the submitting author. The proofs must be returned within 48 hours of receipt. Late return may cause a delay in the publication of the paper. 100 reprints will be supplied to the authors free of charge.

Periodicals of the Hungarian Academy of Sciences are obtainable at the following addresses:

AUSTRALIA
C.B.D. LIBRARY AND SUBSCRIPTION SERVICE
Box 4886, G.P.O., *Sydney N.S.W. 2001*
COSMOS BOOKSHOP, 145 Ackland Street
St. Kilda (Melbourne), Victoria 3182

AUSTRIA
GLOBUS, Höchstädtplatz 3, *1206 Wien XX*

BELGIUM
OFFICE INTERNATIONAL DE LIBRAIRIE
30 Avenue Marnix, *1050 Bruxelles*
LIBRAIRIE DU MONDE ENTIER
162 rue du Midi, *1000 Bruxelles*

BULGARIA
HEMUS, Bulvar Ruszki 6, *Sofia*

CANADA
PANNONIA BOOKS, P.O. Box 1017
Postal Station "B", *Toronto, Ontario M5T 2T8*

CHINA
CNPICOR, Periodical Department, P.O. Box 50
Peking

CZECHOSLOVAKIA
MAD'ARSKÁ KULTURA, Národní třida 22
115 66 Praha
PNS DOVOZ TISKU, Vinohradská 46, *Praha 2*
PNS DOVOZ TLAČE, *Bratislava 2*

DENMARK
EJNAR MUNKSGAARD, Norregade 6
1165 Copenhagen K

FEDERAL REPUBLIC OF GERMANY
KUNST UND WISSEN ERICH BIEBER
Postfach 46, *7000 Stuttgart 1*

FINLAND
AKATEEMINEN KIRJAKAUPPA, P.O. Box 128
SF-00101 Helsinki 10

FRANCE
DAWSON-FRANCE S. A., B. P. 40, *91121 Palaiseau*
EUROPÉRIODIQUES S. A., 31 Avenue de Versailles, *78170 La Celle St. Cloud*
OFFICE INTERNATIONAL DE DOCUMENTATION ET LIBRAIRIE, 48 rue Gay-Lussac
75240 Paris Cedex 05

GERMAN DEMOCRATIC REPUBLIC
HAUS DER UNGARISCHEN KULTUR
Karl Liebknecht-Straße 9, *DDR-102 Berlin*
DEUTSCHE POST ZEITUNGSVERTRIEBSAMT
Sraße der Pariser Kommüne 3–4, *DDR-104 Berlin*

GREAT BRITAIN
BLACKWELL'S PERIODICALS DIVISION
Hythe Bridge Street, *Oxford OX1 2ET*
BUMPUS, HALDANE AND MAXWELL LTD.
Cowper Works, *Olney, Bucks MK46 4BN*
COLLET'S HOLDINGS LTD., Denington Estate
Wellingborough, Northants NN8 2QT
WM. DAWSON AND SONS LTD., Cannon House
Folkstone, Kent CT19 5EE
H. K. LEWIS AND CO., 136 Gower Street
London WC1E 6BS

GREECE
KOSTARAKIS BROTHERS INTERNATIONAL BOOKSELLERS, 2 Hippokratous Street, *Athens-143*

HOLLAND
MEULENHOFF-BRUNA B.V., Beulingstraat 2,
Amsterdam
MARTINUS NIJHOFF B.V.
Lange Voorhout 9–11, *Den Haag*
SWETS SUBSCRIPTION SERVICE
347b Heereweg, *Lisse*

INDIA
ALLIED PUBLISHING PRIVATE LTD., 13/14
Asaf Ali Road, *New Delhi 110001*
150 B-6 Mount Road, *Madras 600002*
INTERNATIONAL BOOK HOUSE PVT. LTD.
Madame Cama Road, *Bombay 400039*
THE STATE TRADING CORPORATION OF INDIA LTD., Books Import Division, Chandralok
36 Janpath, *New Delhi 110001*

ITALY
INTERSCIENTIA, Via Mazzé 28, *10149 Torino*
LIBRERIA COMMISSIONARIA SANSONI, Via Lamarmora 45, *50121 Firenze*
SANTO VANASIA, Via M. Macchi 58
20124 Milano
D. E. A., Via Lima 28, *00198 Roma*

JAPAN
KINOKUNIYA BOOK-STORE CO. LTD.
17-7 Shinjuku 3 chome, Shinjuku-ku, *Tokyo 160-91*
MARUZEN COMPANY LTD., Book Department, P.O. Box 5050 Tokyo International, *Tokyo 100-31*
NAUKA LTD. IMPORT DEPARTMENT
2-30-19 Minami Ikebukuro, Toshima-ku, *Tokyo 171*

KOREA
CHULPANMUL, *Phenjan*

NORWAY
TANUM-TIDSKRIFT-SENTRALEN A.S., Karl Johansgatan 41–43, *1000 Oslo*

POLAND
WĘGIERSKI INSTYTUT KULTURY, Marszałkowska 80, *00-517 Warszawa*
CKP I W, ul. Towarowa 28, *00-958 Warszawa*

ROUMANIA
D. E. P., *Bucureşti*
ILEXIM, Calea Grivitei 64–66, *Bucureşti*

SOVIET UNION
SOJUZPECHAT — IMPORT, *Moscow*
and the post offices in each town
MEZHDUNARODNAYA KNIGA, *Moscow G-200*

SPAIN
DIAZ DE SANTOS, Lagasca 95, *Madrid 6*

SWEDEN
ALMQVIST AND WIKSELL, Gamla Brogatan 26
101 20 Stockholm
GUMPERTS UNIVERSITETSBOKHANDEL AB
Box 346, *401 25 Göteborg 1*

SWITZERLAND
KARGER LIBRI AG, Petersgraben 31, *4011 Basel*

USA
EBSCO SUBSCRIPTION SERVICES
P.O. Box 1943, *Birmingham, Alabama 35201*
F. W. FAXON COMPANY, INC.
15 Southwest Park, *Westwood Mass. 02090*
THE MOORE-COTTRELL SUBSCRIPTION AGENCIES, *North Cohocton, N. Y. 14868*
READ-MORE PUBLICATIONS, INC.
140 Cedar Street, *New York, N. Y. 10006*
STECHERT-MACMILLAN, INC.
7250 Westfield Avenue, *Pennsauken N. J. 08110*

YUGOSLAVIA
JUGOSLOVENSKA KNJIGA, Terazije 27, *Beograd*
FORUM, Vojvode Mišića 1, *21000 Novi Sad*

Index: 26.007

FORMERLY ACTA CHIMICA ACADEMIAE SCIENTIARUM HUNGARICAE

Acta Chimica Hungarica

VOLUME 114, NUMBERS 3—4 NOV/DEC 1983

EDITOR-IN-CHIEF
F. MÁRTA

MANAGING EDITOR
GY. DEÁK

ASSISTANT EDITOR
L. HAZAI

EDITORIAL BOARD
M. T. BECK, R. BOGNÁR, GY. HARDY, K. LEMPERT,
B. LENGYEL, K. POLINSZKY, E. PUNGOR, G. SCHAY,
Z. G. SZABÓ, P. TÉTÉNYI

Akadémiai Kiadó, Budapest
ACTA CHIM. HUNG. ACASA2 114 (3—4) 217—385 (1983) HU ISSN 0231-3146

ACTA CHIMICA HUNGARICA

A JOURNAL OF THE HUNGARIAN ACADEMY OF SCIENCES

Acta Chimica publishes original reports on all aspects of chemistry in English.

Acta Chimica is published in three volumes per year, each volume consisting of four issues, by

AKADÉMIAI KIADÓ

Publishing House of the Hungarian Academy of Sciences
H-1054 Budapest, Alkotmány u. 21.

Manuscripts and editorial correspondence should be addressed to

Acta Chimica
H-1450 Budapest P.O.Box 67

Subscription information

Orders should be addressed to

KULTURA Foreign Trading Company
H-1389 Budapest P.O. Box 149

or to its representatives abroad

Acta Chimica is indexed in Current Contents

NOTICE TO AUTHORS

Acta Chimica publishes original papers on all aspects of chemistry in English. Before preparing a manuscript for submission to this journal authors are advised to consult recent issues.

Form of manuscript

Manuscripts, tables and illustrations should be submitted in triplicate. Manuscripts should be typewritten double spaced (25 lines, 50 characters per line including spaces). The *title page* should include (1) the title of the paper, (2) the full names of the author(s) in the sequence to be published; apply an asterisk to designate the name of the author to whom correspondence should be addressed, (3) name and address of the institution where the work was done. If the paper is part of a series, reference to the previous communication must be given as a footnote.

Abstract

A summary is printed at the head of each paper. This should not exceed 200 words and should state briefly the principal results and major conclusions of the work. It should be suitable for use by abstracting services.

CONTENTS

PHYSICAL AND INORGANIC CHEMISTRY

Polymetallic complexes, II. Schiff base complexes of cobalt(II), nickel(II), copper(II), zinc(II), cadmium(II) and mercury(II), **B. B. Mahapatra, B. Patel, D. Satyanarayana, S. K. Pujari** 217

Copolymerization of cholesterol-based mesogenic monomers, **K. Nyitrai, F. Cser, L. Parragh, Gy. Hardy** 223

Studies on copolymerization of hexadecyl acrylamide, **A. Cherneva, F. Cser, K. Nyitrai, K. Kiss, Gy. Hardy** 235

Complexes of 3,4-dihydroxyphenyl derivatives, V. Ambidentate character of L-dopa in manganese(II) and cobalt(II) complexes, **T. Kiss, A. Gergely** 249

Catalytic activity of the Al_2O_3—AlF_3 system for the Claus reaction, **S. Kowalak, I. Bresińska** 255

Comparative study of polymer gels based on theories of critical phenomena and classical thermodynamics, **F. Horkay, M. Zrinyi** 261

Effect of surface modification on immersional wetting of organophilic kaolinite and illite derivatives, **I. Dékány, F. Szántó, W. Rudzinski** 283

Preparation and characterization of complexes of uranium(VI), vanadium(IV), titanium(IV), zirconium(IV) and hafnium(IV) with mercapto triazoles, **S. K. Sengupta** 323

Dithiocarbamate anions as salts of oxinate chelates of zirconium(IV), **G. S. Sodhi, S. Kumar, N. K. Kaushik** 329

Characterization of Cu(II), Ni(II), Co(II), Pd(II) and Fe(III) complexes of anilic acids, **C. L. Sharma, S. S. Narvi, R. S. Arya** 349

H_2O—D_2O solvent isotope effects on apparent and partial molar volumes of $CaCl_2$ and $BaCl_2$ solutions, **Gy. Jákli, S. Cooper, R. S. Hutchings, W. A. Van Hook** 365

ORGANIC CHEMISTRY

Heterocyclic compounds, IV. Structure of the salts of 1-(3,4-dimethoxyphenyl)-7,8-dimethoxy-5-ethyl-4-methyl-5*H*-2,3-benzodiazepine, **A. Neszmélyi, T. Láng, J. Kőrösi** 293

Heterocyclic compounds, V. The preparation and characterization of 1-(3,4-dimethoxyphenyl)-6,7-dimethoxy-4-ethyl-3-methyl-isoquinoline-*N*-imine salts, **J. Kőrösi, T. Láng, A. Neszmélyi, Gy. Horváth** 301

Synthesis of (1 → 1)-bonded rhamnopyranosyl-rhamnopyranosides containing L,L and L,D building-stones. High-field ^1H- and ^{13}C-NMR spectroscopic studies on the conformation of the interglycosidic bonds, **A. Lipták, M. Göndör** 309

Azachalcones, III. Reactions of azachalcones with amines and hydrazines, **A. Attia, M. Michael** 337

(Hydroxyimino)-3(2*H*)-isoquinolinones, III. Determination of the structure of phenyl-substituted 1,4-dihydro-3(2*H*)-isoquinolinone obtained in the cyclization reaction of 3-biphenyl-*N*-methylacetamide by ^1H-NMR spectroscopic study of the 4-(hydroxyimino)-derivative, **I. Tikk, G. Tóth, Gy. Deák** 355

Synthesis of Agecorynin-A, **V. K. Sharma, S. R. Gupta** 361

Decomposition of carbonate esters of 1,3-diols. The chemistry of 1,3-bifunctional systems, XXVI., **M. Bartók, A. Molnár, G. Bartók-Bozóki** 375

BOOK REVIEW 381

Acta Chimica Hungarica 114 (3—4), pp. 217—221 (1983)

POLYMETALLIC COMPLEXES, II

SCHIFF BASE COMPLEXES OF COBALT(II), NICKEL(II), COPPER(II), ZINC(II), CADMIUM(II) AND MERCURY(II)

B. B. MAHAPATRA*, B. PATEL, D. SATYANARAYANA and S. K. PUJARI

(Department of Chemistry, G. M. College, Sambalpur — 786 004, Orissa, India)

Received September 17, 1982
Accepted for publication November 25, 1982

Twelve binuclear metal complexes have been synthesised of the composition $M_2L_2 4H_2O$, $M_2L'_2 4H_2O$ [M = Co(II), Ni(II)], M_2L_2, $M_2L'_2$ [M = Cu(II), Zn, Cd and Hg(II)], LH_2 and $L'H_2$ are the tridentate Schiff bases derived from benzoin with 2-amino-2-methyl-1-propanol, and 1-amino-2-propanol. The complexes of the first two categories are bimetallic octahedral and a dinuclear square planar or tetrahedral structures have been assigned to the later categories on the basis of analysis, conductance, magnetic susceptibility, IR and electronic spectral data.

Introduction

Complexation behaviour of a number of tridentate dibasic ligands with a variety of metal ions have been reported in recent years [1—6]. These ligands force the metal ions to form polymetallic complexes with uncommon structural and magnetic properties. Therefore, it was thought worthwhile to synthesise two new tridentate Schiff bases and the complexing ability of these ligands with divalent metal ions like Co(II), Ni(II), Cu(II), Zn, Cd and Hg(II) have been studied.

Experimental

All chemicals were of AR grade.

Preparation of the Schiff base [$BnAMPH_2$]

Benzoin (2.12 g) in ethanol was mixed with 2-amino-2-methyl-1-propanol (0.89 mL) and refluxed on a water bath for 2 hrs. On cooling, white coloured Schiff base separated. It was then filtered, washed with ethanol, dried and recrystallized from ethanol (95%). M.p., 130 °C. Yield, 70%.

C, 76.32%, H, 7.42%, N, 4.94% for $C_{18}H_{21}O_2N$ found C, 75.47%, H, 7.38%, N, 4.91%.

The other Schiff base [$BnAPH_2$] was synthesized by reacting benzoin with 1-amino-2-propanol in ethanolic medium. M.p., 120 °C. Yield, 80%.

C, 75.83%, H, 7.06%, N, 5.2% for $C_{17}H_{19}O_2N$, found C, 74.26%, H, 6.95%, N, 5.18%. The structure of these two ligands are shown below:

* To whom correspondence should be addressed

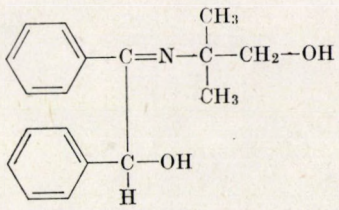

(A)

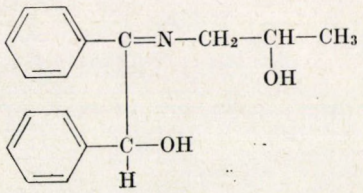

(B)

Preparation of the complexes

Ethanolic solution of the metal chlorides were reacted with an ethanolic solution of the Schiff bases separately and the mixture was refluxed for $1 - 1\frac{1}{2}$ hrs on a water bath. Then it was allowed to cool and the pH of the solution was adjusted to about 7 by adding *conc.* NH_4OH drop by drop. The metal chelates were separated, which were filtered, washed with ethanol and ether, and dried in vacuum.

Metal contents and nitrogen in the complexes were estimated by standard methods. Conductance was measured in 10^{-3} *M* dimethylformamide solution of the complexes, using a Toshniwal conductivity bridge. Magnetic moment measurements were made on solid specimens at room temperature by the Gouy method. IR spectra were recorded in KBr phase using a Perkin-Elmer-389 spectrphotometer. Electronic spectra were recorded on a Hilger—Watt uvispeck spectrophotometer by preparing a mull of the complexes with nujol. Analytical, conductance and magnetic susceptibility data are given in Table I and the IR and electronic spectral data in Table II.

Table I

Analysis, m.p., conductance and magnetic susceptibility data

Compound	M.p. °C	Colour	% Metal		% Nitrogen		Λ_M mhos Cm²	μ_{eff} B.M
			Found	Reqd.	Found	Reqd.		
LH_2	130	White	—	—	4.91	4.94	—	—
$L'H_2$	120	White	—	—	5.18	5.20	—	—
$Co_2L_2 \cdot 4H_2O$	>250	Black	15.48	15.66	3.69	3.71	2.5	2.90
$Co_2L_2' \cdot 4H_2O$	>250	Violet	16.19	16.27	3.81	3.86	2.0	2.75
$Ni_2L_2 \cdot 4H_2O$	>250	Blue	15.57	15.62	3.68	3.72	3.8	2.80
$Ni_2L_2' \cdot 4H_2O$	>250	Blue	16.19	16.22	3.77	3.87	3.2	2.85
Cu_2L_2	>250	Green	18.41	18.43	3.98	4.06	2.2	1.32
Cu_2L_2'	>250	Green	19.15	19.21	4.18	4.23	1.5	1.25
Zn_2L_2	>250	White	18.74	18.87	4.01	4.04	3.7	—
Zn_2L_2'	>250	White	19.61	19.67	4.15	4.21	2.4	—
Cd_2L_2	>250	White	28.50	28.57	3.50	3.55	2.8	—
Cd_2L_2'	>250	White	29.58	29.62	3.58	3.69	3.5	—
Hg_2L_2	205	White	41 54	41.65	2.85	2.90	4.7	—
Hg_2L_2'	160	White	42.71	42.89	2.90	2.90	3.8	—

LH_2 and $L'H_2$ are the tridentate Schiff bases derived from benzoin with 2-amino-2-methyl-1-propanol and 2-amino-1-propanol, respectively.

Table II

Infrared and electronic spectral data

Compound	ν(C—O)	ν(C=N)	ν(M—O)	ν(M—N)	ν_{max} (cm^{-1})
LH_2	1195	1670			
$L'H_2$	1220	1620			
$Co_2L_2 \cdot 4H_2O$	1210	1620	450	510	8 500, 18 000, 19 500, 26 000
$Co_2L'_2 \cdot 4H_2O$	1230	1600	460	515	8 200, 18 500, 19 700, 26 300
$Ni_2L_2 \cdot 4H_2O$	1215	1610	440	510	9 000, 18 500, 26 500, 27 000
$Ni_2L'_2 \cdot 4H_2O$	1235	1600	450	505	9 500, 19 000, 26 000, 27 100
Cu_2L_2	1210	1620	445	510	15 400, 22 800
$Cu_2L'_2$	1230	1595	450	515	15 200, 24 300
Zn_2L_2	1210	1610	440	510	
$Zn_2L'_2$	1240	1605	440	505	
Cd_2L_2	1215	1610	445	510	
$Cd_2L'_2$	1230	1610	450	510	
Hg_2L_2	1210	1620	440	505	
$Hg_2L'_2$	1230	1605	445	510	

Results and Discussion

Complexes reported in the present investigation have the composition $M_2L_24H_2O$, $M_2L'_2 \cdot 4H_2O$ (M = Co(II), Ni(II)], M_2L_2, $M_2L'_2$ [M = Cu(II), Zn, Cd and Hg(II)], LH_2 and $L'H_2$ are the tridentate biprotic Schiff bases derived from benzoin with 2-amino-2-methyl-1-propanol and 1-amino-2-propanol, respectively. The cobalt(II) complexes are black and violet, the nickel(II) complexes are blue, the copper(II) complexes are green, and the zinc, cadmium and mercury(II) complexes are white in colour. All complexes are amorphous, have high melting point, and are insoluble in common organic solvents, but slightly soluble in DMF. Low conductance values in dimethylformamide indicate the non-electrolytic nature of the complexes (Table I). The analytical data (Table I) indicate a 1 : 1 (metal : ligand) stoichiometry and hence the Schiff bases act as dibasic tridentate ligands. In the IR spectra of the ligands, a band of medium intensity around 2750 cm^{-1} may be assigned to intramolecular hydrogen bond (νO—H). In the spectra of the complexes, absence of this band indicates the deprotonation of the alcoholic groups and the consequent dibasic behaviour of the Schiff bases. The structure of the ligands show that the bridging must take place through any one of the alcoholic oxygen atom. The ν(C—O) vibration appears at 1195 cm^{-1} in the ligand [$BnAMPH_2$] and at 1220 cm^{-1} in [$BnAPH_2$], and it undergoes a positive shift

of 10—20 cm^{-1} and this is due to the formation of the 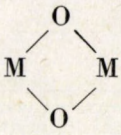 bridge in

conformity with earlier observation [7]. In the spectra of the ligands, bands at 1670 cm^{-1} [$BnAMPH_2$] and 1620 cm^{-1} [$BnAPH_2$] can be assigned to ν(C=N) vibration. In the metal complexes these bands are observed around 1620 cm^{-1} and 1600 cm^{-1}, respectively. This lowering of ν(C=N) frequency in the complexes in comparison to the free ligand values indicates co-ordination of azomethine group of the Schiff bases through the nitrogen atom [8—12]. In case of cobalt(II) and nickel(II) complexes, the presence of coordinated water molecule is ascertained by the observation of a broad double hump around 3400 cm^{-1}. This is further confirmed by an additional peak $\sim$820 cm^{-1} in these complexes. However, the conclusive evidence regarding the bonding of the potential donor atoms of the Schiff bases with the metal ions have been provided by the bands $\sim$450 cm^{-1} and $\sim$510 cm^{-1} attributable [14] to ν(M—O) and ν(M—N) vibrations, respectively.

The magnetic moment of the cobalt(II) complexes at room temperature lies between 2.80 and 2.85 B.M. Figgis and Nyholm have reported [15] that low-spin octahedral complexes possess magnetic moments in the range 1.8—2.9 B.M. Electronic spectra of the complexes exhibit bands at 8500 (10), 18 000 (25), 19 500 (30) and 26 000 cm^{-1} and at 8200 (8), 18 500 (27), 19 700 (35) and 26 300 cm^{-1}, respectively. The positions and intensities of the first three bands in case of two complexes suggest some amount of tetragonal distortion and can be attributed [16] to the transitions $^4T_{1g}(F) \rightarrow {}^4T_{2g}(F)$, $^4T_{1g}(F) \rightarrow {}^4A_{2g}(F)$ and $^4T_{1g}(F) \rightarrow {}^4T_{1g}(P)$, respectively, for an approximately octahedral field around low-spin cobalt(II) ion. The band around 26 000 cm^{-1} most probably results from either intra-ligand or charge-transfer transitions.

The visible electronic spectrum of nickel(II) complexes shows bands at 9000 (5.0), 18 500 (9.0) and 26 500 (16.5) cm^{-1} followed by a strong band at $\sim$27 000 cm^{-1}. On the basis of these values, the bands can be assigned to $^3A_{2g} \rightarrow {}^3T_{2g}(F)$, $^3A_{2g} \rightarrow {}^3T_{1g}(F)$ and $^3A_{2g} \rightarrow {}^3T_{1g}(P)$ transitions in a tetragonally distorted octahedral field. The magnetic moments at room temperature are around 2.5 B.M. which can be attributed to partial quenching of paramagnetism due to spin-spin interaction.

The mull absorption band of copper(II) complexes, located around 17 350 (broad) can be assigned to $^2B_{1g} \rightarrow {}^2B_{2g}$ transition in planar geometry [17—20]. The very weak bands observed around 12 800 cm^{-1} are attributed to the tetragonal distortion of the planar structure [21—24]. The complexes display another strong band in the range 22 800—24 300 cm^{-1}. This band is due to symmetry-forbidden ligand $\rightarrow$ metal charge-transfer transition rather than due to dimetallic species [25, 26]. The absence of any absorption below

10 000 cm^{-1} eliminates the possibility of tetrahedral stereochemistry of the complexes [27]. The two copper(II) complexes show sub-normal magnetic moments, μ_{eff} ~1.2 B.M. indicating spin-spin interactions between Cu(II) ions present in a polymeric structure.

Subnormal magnetic moments, spectral positions, high melting points and slight solubility in common organic solvents support binuclear structure of the Co(II), Ni(II), and Cu(II) complexes. The zinc, cadmium and mercury(II) complexes are also presumed to be polymeric as inferred from their analytical, melting point, solubility tests and spectral data. Therefore we propose dimetallic structures with alcoholic oxygen bridges.

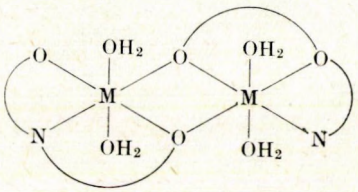

M = Co(II), Ni(II)

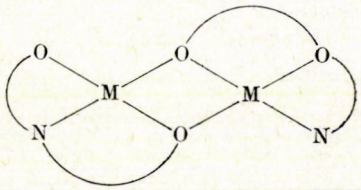

M = Cu(II), Zn, Cd and Hg(II)

REFERENCES

[1] Hatfield, W. E., Whyman, R.: Transition Met. Chem., **5,** 47 (1969)
[2] Bertrand, J. A., Breece, J. I., Kalyanaraman, A. R., Long, G. J., Baker, W. A.: J. Am Chem. Soc., **92,** 5233 (1970)
[3] Bertrand, J. A., Eller, P. G.: Inorg. Chem., **13,** 928 (1974)
[4] Hodgson, D. J.: Prog. Inorg. Chem., **19,** 173 (1975)
[5] Ginsberg, A. P., Sherwood, R. C., Koubeck, E.: J. Inorg. Nucl. Chem., **29,** 353 (1967)
[6] Syamal, A., Kale, K. S.: Transition Met. Chem., **4,** 298 (1979)
[7] Syamal, A., Kale, K. S.: Indian J. Chem. **16A,** 46 (1978)
[8] Covasis, J. E.: Spectrochim. Acta, **23A,** 183 (1967)
[9] Teyssi, P., Charrettee, J. J.: Spectrochim. Acta, **19,** 1407 (1963)
[10] Freedman, H. H.: J. Am. Chem. Soc., **83,** 2900 (1961)
[11] Kubo, M., Kimura, M., Kuroda, Y., Yamamato, O.: Bull. Chem. Soc., Japan, **34,** 1081 (1961)
[12] Kimura, M., Kuroda, Y.: Bull Chem. Soc., Japan, **36,** 464 (1963)
[13] Gamo, I.: Bull. Chem. Soc. Japan, **34,** 760 (1961)
[14] Ferraro, J. R.: Low Frequency Vibrations of Inorganic and Co-ordination Compounds. Plenum Press, New York 1971
[15] Figgis, B. N., Nyholm, R. S.: J. Chem. Soc., **1954,** 12
[16] Lever, A. B. P.: Inorganic Electronic Spectroscopy. Elsevier, Amsterdam 1968
[17] Rao, C. D., Mahapatra, B. K., Guru, S.: J. Inorg. Nucl. Chem., **42,** 1195 (1980)
[18] Gopalakrishnan, K., Uma, Ch. Bhattacharya, P. K.: J. Ind. Chem. Soc., **56,** 752 (1979)
[19] Doraswamy, U., Bhattacharya, P. K.: J. Inorg. Nucl. Chem., **37,** 1665 (1975)
[20] Wallies, W. N.: Inorg. Chem., **13,** 991 (1974)
[21] Banister, E., Cotton, F. A.: J. Chem. Soc., **1960,** 2276
[22] Jørgensen, C. K.: Acta. Chem. Scand., **8,** 1282 (1954)
[23] Bjerrum, J., Ballhausen, C. J., Jørgensen, C. K.: Acta. Chem. Scand., **8,** 1275 (1954)
[24] Byers, W., Lever, A. B. P., Parish, R. V.: Inorg., Chem., **7,** 1835 (1968)
[25] Dubicki, L., Martin, R. L.: Inorg. Chem., **5,** 2203 (1966)
[26] Gregson, A. K., Martin, R. L., Mitra, S.: Proc. R. Soc. London, Ser. A., **320,** 473 (1971)
[27] Laue, L. W., Taylor, L. T.: J. Coord. Chem., **2,** 295 (1973)

Acta Chimica Hungarica 114 (3—4), pp. 223—234 (1983)

COPOLYMERIZATION OF CHOLESTEROL-BASED MESOGENIC MONOMERS*

K. NYITRAI, F. CSER, L. PARRAGH and GY. HARDY**

(Research Institute for Plastic, H-1950 Budapest, Hungária krt. 114.)

Received October 11, 1982
Accepted for publication December 9, 1982

Copolymerization of phenyl-*p*-acryloyloxy-benzoate (PAB) with cholesteryl acrylate (CA), cholesteryl-vinyl succinate (CVS), cholesteryl-succinyl-glycoyl acrylate (CSGA) and methyl methacrylate (MMA) as well as of CA with styrene (St) were carried out in solution. The composition and the transition temperatures of the copolymers were investigated. The relative constants of reactivity, $r_{PAB} = 0.62$, $r_{CA} = 0.58$, $r_{PAB} = 2.36$, $r_{CVS} = 0.01$, $r_{PAB} = 1.26$, $r_{CSGA} = 0.20$, $r_{PAB} = 1.04$, $r_{MMA} = 0.30$, $r_{CA} = 0.53$, $r_{St} = 0.26$, differ from those expected on the basis of chemically similar monomers without mesogenic group with the exception of the system PAB/CA. The PAB and CA/St systems are isomorphous, the other copolymers have transition temperatures characteristic for non-isomorphous solid systems. The least difference between the measured an the estimated ratio of reactivities was found in isomorphous systems.

Introduction

Investigation on copolymerization of two methacrylic monomers (containing a *p*-methoxyphenyl benzoate group) reacting with each other or with cholesteryl acrylate, showed copolymerization constants differing considerably from those expected on the basis of data of other related monomers of similar structure [1]. The higher the difference between the molecular mass of the monomers the greater was the observed difference. By modification of the chemical structure, enhanced incorporation of the monomers with greater molecular mass was demonstrated.

In the present paper, copolymerization reactions of high-molecular-mass monomers were studies. One of the four investigated mesogenic monomers was an aromatic acrylic of relatively low molecular mass (phenyl *p*-acryloyloxybenzoate, PAB). Previous studies on structure [2—4] and miscibility characteristics [4, 5] of poly-PAB demonstrated that the "primary globules" observed both in solution and in bulk consisted of rods of individual macromolecules and their anisotropy caused the optical anisotropy of the homopolymer. The polymer had an aperiodic helical structure.

* Polymerization in Liquid Crystals, XV, Part XIV: Acta Chim. Acad. Sci. Hung. (to be published in the 1st issue of Vol. **115**).

** To whom correspondence should be addressed.

The other monomer was cholesteryl acrylate (CA), already frequently studied in copolymerization reactions [1, 6, 7]. In the polymer the cholesteryl group is directly bonded to the polyacrylate chain.

In the cholesteryl vinyl succinate (CVS) polymer, the mesogenic group is separated from the poly(vinyl ester) main chain by a short alkyl insertion. CVS has also been used as a comonomer in copolymerizations [8, 9]; some kinetic constants of its homopolymerization have been determined [10].

In the polymer of cholesterylsuccinylglycoyl acrylate (CSGA), the cholesteryl group is separated from the polyacrylate chain by a longer flexible chain. This compound was used as comonomer for the first time. Structure of poly-CA was classified as an aperiodic helix [11]. Structure of pCVS [11—13] and pCSGA [13] was smectic. In the present paper, as previously [1], the fitting of these monomers into the *Q—e* scheme introduced by Alfrey and Price [14] was attempted. For this purpose, two standard monomers, methyl methacrylate (MMA) and styrene (St) were used as a copolymerization partner for PAB and for the aliphatic monomers, respectively. The copolymer compositions were determined by UV spectroscopy.

Experimental

Monomers

CA [15] PAB [2] and CVS 10] monomers were prepared according to previous descriptions in indentical grades.

CSGA was synthesized through the following reaction:

$$\text{Chol}-\text{OH} \xrightarrow[(CH_3CH_2)_3N]{(CH_3CO)_2O} \text{Chol}-\text{O}-\text{CO}-\text{CH}_2\text{CH}_2-\text{COOH} \rightarrow$$

$$\xrightarrow[(CH_3)_2N\,CHO]{SOCl_2} \text{Chol}-\text{O}-\text{CO}-\text{CH}_2-\text{CH}_2-\text{CO}-\text{Cl} \xrightarrow{\text{HO}-\text{CH}_2-\text{CH}_2-\text{O}-\text{CO}-\text{CH}=\text{CH}_2}$$

$$\longrightarrow \text{Chol}-\text{O}-\text{CO}-\text{CH}_2-\text{CH}_2-\text{CO}-\text{O}-\text{CH}_2-\text{CH}_2-\text{O}-\text{CO}-\text{CH}=\text{CH}_2$$

where Chol designates the cholesteryl group.

0.025 mol (13 g) of cholesterylsuccinyl chloride (**I**) prepared according to ref. [15] was dissolved in 20 cm^3 chloroform in an Erlenmeyer flask. In another Erlenmayer flask, 0.05 mol (6 g) of 2-hydroxyethyl acrylate (purum, Polyscience) was dissolved in 10 cm^3 of chloroform. Both solutions were cooled in ice-water bath to 0 °C then the latter was added to the solution of **I** with continuous stirring. The reaction mixture was stored below 5 °C for 24^h, then poured into 200 cm^3 icy water containing 5 cm^3 hydrochloric acid, stirred by a rapid stirrer for half an hour, keeping the temperature below 5 °C. The chloroform layer was separated and dried over Na_2SO_4. The solvent was evaporated in vacuum and the crude product was crystallized from ethanol. Yield was 8.2 g (65%) with m.p. of 79—81 °C. Both styrene and methyl methacrylate were purified as follows. Inhibitor was washed three times with a 5% solution of Na_2CO_3 then again three times with distilled water. The monomers were dried over Na_2SO_4 in the dark then distilled in vacuum. Purified monomers were stored for a maximum of 72^h in the dark at −18 °C until use.

Polymerization

Polymerizations were carried out in chloroform solution initiated by 1% AIBN referred to the monomer mixture (1 g in 2 cm^3 solvent). After a preliminary study of the reaction time vs. conversion relation, the reaction mixture was immersed into a thermostat at 60 °C

for a period that conversion should not exceed 10%. The reaction rate was found to depend on the composition of the monomer mixture.

After the reaction period (20 min to 3^h), the copolymers were precipitated from their homogeneous clear solutions by a 4 : 1 mixture of acetone and methanol for CA and CSGA products and by methanol for CVS and MMA copolymers. The products were purified by redissolution and precipitation. The samples were dried to constant mass. Their compositions were determined by UV spectroscopy.

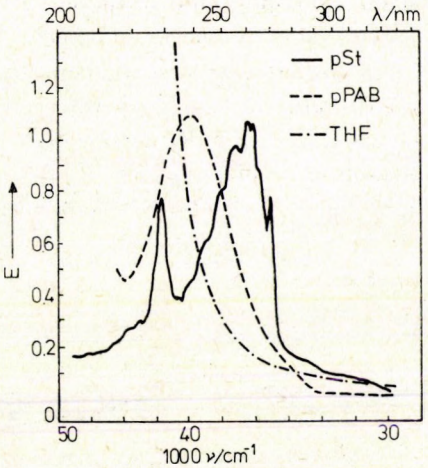

Fig. 1. UV spectra of poly(phenyl-*p*-acryloxyloxybenzote) and polystyrene (in tetrahydrofuran)

UV spectroscopy

Copolymers were dissolved in freshly purified tetrahydrofuran (THF) (16 cg in 25 cm^3) and their absorbances were read on a Zeiss Specord UV VIS spectrograph. Absorbances of PAB-containing samples at their absorption maximum of 230 nm were calibrated by mixtures of solutions of poly-PAB and homopolymer of its comonomer at identical concentration. The homopolymers were prepared in the same way as the copolymers. For styrene-containing systems, the absorption maximum of polystyrene at 267 nm was used, calibrating in the same way as for PAB samples. Absorbance data were processed for copolymer compositions and for the relative reactivity ratios by the Tüdős—Kelen—Turcsányi [16] method on a HP 67 computer.

Especially the determination of compositions of PAB-containing copolymers was strongly disturbed by the peroxide content of THF. Reproducible data could only be obtained with solvents purified within 48^h before use. Spectra of poly-PAB and poly-St are shown in Fig. 1.

Polarization microscopy

Copolymers were anisotropic. Their transition temperatures were determined by a Zeiss Polmi A polarization microscope equipped with a Boetzius-type heated plate.

Results and Discussion

Correlation between reaction time, conversion, and composition were studied in detail for PAB/CA systems. The result obtained with PAB/CA composition of 1 : 9 is presented in Fig. 2. The figure shows that the time dependence of conversion is linear up to high conversions ($\xi > 50\%$) while

the PAB content of the copolymer decreases. Initial monomer composition, copolymer compositions and conversions are collected in Table I. Since the incorporation of PAB is higher than that of CA in this composition, the changes in the composition as a function of conversion are consistent with the composition diagram Fig. 3.

In Fig. 3, compositions of copolymers obtained from the five copolymerization systems up to 5—10% conversions are plotted against the compositions of the initial monomer mixture. It can be established that the aromatic acrylate is more active than the aliphatic or cycloaliphatic acrylate and styrene is also more active than CA. MMA is more active than PAB.

Compositions of copolymers of the three PAB-containing systems produced up to 20—50% conversion are plotted against those of the initial mo-

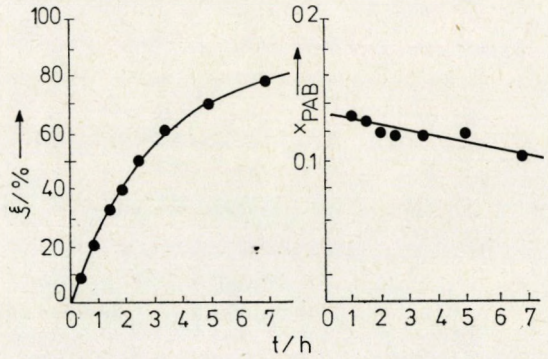

Fig. 2. Copolymerization conversion of a phenyl *p*-acryloyloxybenzoate/cholesteryl acrylate mixture of 1 : 9 molar ratio and PAB content of the copolymer plotted against the reaction time

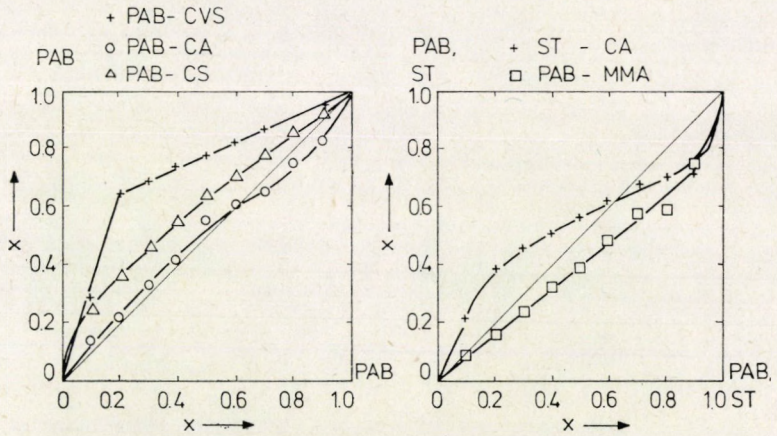

Fig. 3. Composition of the copolymers vs. initial monomer mixtures

Table I

Characteristic data for copolymers of PAB *with* CA, CVS, CSGA *and* MMA, *and* CA *with* ST

Mole fraction of PAB in monomer	Mole fraction of PAB in copolymer	Conversion (%)	Mole fraction of PAB in monomer	Mole fraction of PAB in copolymer	Conversion (%)
Comonomer: CA			Comonomer: CVS		
0.10	0.138	5.8	0.10	0.289	8.6
0.20	0.215	5.2	0.20	0.640	6.9
0.30	0.332	5.7	0.30	0.682	8.1
0.40	0.408	2.7	0.40	0.732	4.6
0.50	0.551	1.9	0.50	0.771	6.1
0.60	0.605	9.4	0.60	0.819	5.8
0.70	0.650	1.2	0.70	0.864	8.2
0.80	0.750	5.0	0.80	—	11.7
0.90	0.825	4.1	0.90	0.934	11.9
Comonomer: CSGA			Comonomer: MMA		
0.10	0.243	6.9	0.10	0.087	8.5
0.20	0.345	7.7	0.20	0.167	4.8
0.30	0.443	7.6	0.30	0.241	9.0
0.40	0.530	8.0	0.40	0.331	10.9
0.50	0.625	8.4	0.50	0.396	9.1
0.60	0.683	8.3	0.60	0.488	4.9
0.70	0.773	10.6	0.70	0.583	6.7
0.80	0.843	10.5	0.80	0.595	7.3
0.90	0.914	8.0	0.90	0.754	8.6

Mole fraction of ST in monomer	Mole fraction of ST in copolymer	Conversion (%)
Comonomer: CA		
0.10	0.212	8.2
0.20	0.390	9.2
0.30	0.456	6.2
0.40	0.503	6.1
0.50	0.562	2.2
0.60	0.623	5.4
0.70	0.678	4.8
0.80	0.800	5.4
0.90	0.825	3.3

nomer mixtures in Fig. 4. The measured points fit relatively well to the Tüdős—Kelen [16] representation of linearity for the systems PAB/CA and PAB/CA and PAB/CSGA (Fig. 5). The low activity of CVS in the PAB/CVS system is well observable (at $\eta = 0$ the linear section tend to $\xi = 0$) but the points in the range of $\eta = 0.5$ may be fitted to another straight line. In this case, however, negative r values are obtained.

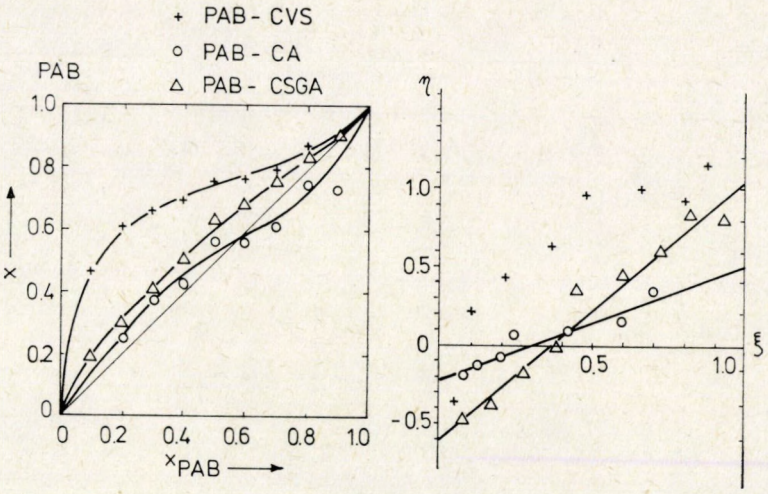

Fig. 4. Composition of copolymers produced up to conversions of 20—50% plotted against that of the initial monomer mixtures in the Tüdős—Kelen—Turcsányi representation for three systems

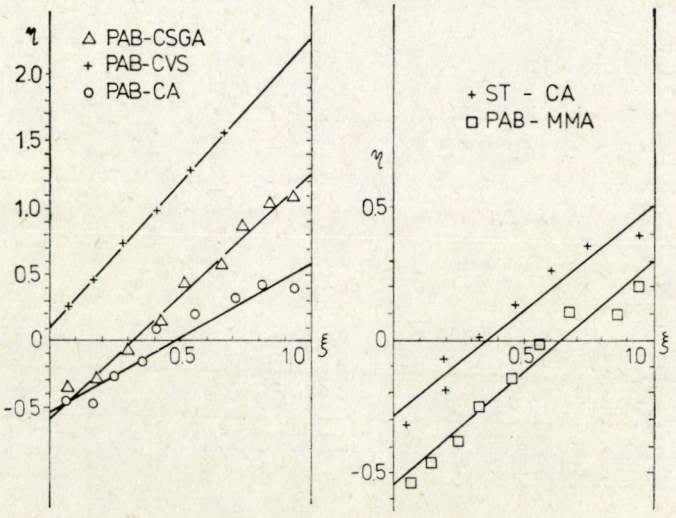

Fig. 5. Composition of copolymers produced up to low conversions in the Tüdős—Kelen—Turcsányi representation

Table II

Copolymerization reactivity ratios (r) of the monomers
Table A: measured values; *Table B:* values estimated by using Q and e parameters of non-mesogenic related compounds
Table A: measured values

	MMA	St	PAB	CA	CVS	CSGA
MMA	1	0.48[a]	1.04	0[b]	—	—
St	0.49	1	—	0.26	—	—
PAB	0.31	—	1	0.62	2.36	1.26
CA	$\geqslant 1$[b]	0.53	0.58	1	—	—
CVS	—	—	−0.04	—	1	—
CSGA	—	—	0.20	—	—	—

[a] From ref. [17]
[b] From ref. [1]

Table B: estimated values

	MMA	St	PAB	*s*BuA	VAc	2-AEA
MMA	1	0.48	1.04	1.82	17.98	1.74
St	0.49	1	0.14	0.99	38.45	0.55
PAB	0.31	0.04	1	0.54	1.41	0.80
*s*BuA	0.54	0.28	0.52	1	1.04	0.91
VAc	0.01	0.03	0.03	0.02	1	0.01
2-AEA	0.50	0.16	0.77	0.91	5.01	1

In the systems copolymerized up to low conversions, scattering of measured points is lower than for those of higher conversions. In Table II, r values determined based on the linearized formula are summarized. Rows of the Table refer to r values of the monomer, columns to the r values of the comonomer. In the lower half of the Table, copolymerization constants for chemically related but not mesogenic monomers are presented from tables of Bandrup and Immergut [17]. CA and *sec* butyl acrylate [1], CVS and vinyl acetate, CSGA and 2-acetoxyethyl acrylate were compared. The non-mesogenic analogue of PAB would be phenyl acrylate; since no data for this monomer could be acquired even from indirect sources, Q and e values derived from copolymerization constants of MMA/PAB systems were used ($Q = 1.16$, $e = 1.47$). Comparing data of identically substituted methacrylates and acrylates, these values seemed acceptable. *Sec*-butyl acrylate is an acrylate bonded to a secondary C atom. For this structure, Q and e values were taken

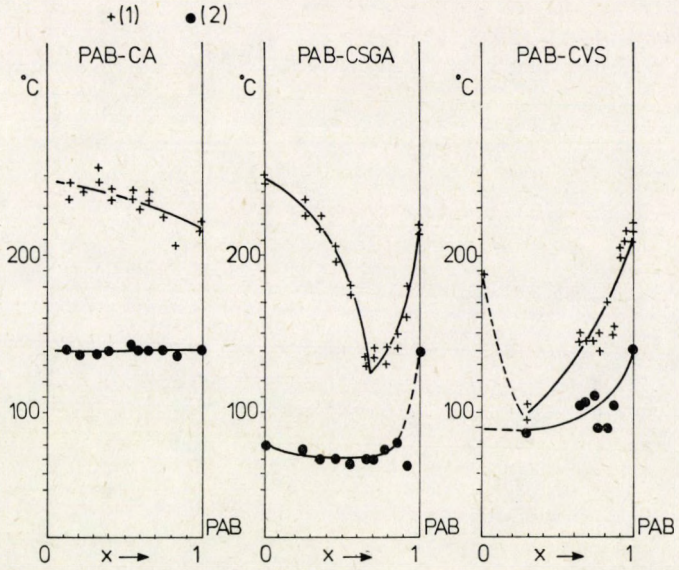

Fig. 6. Clearing temperature of copolymers containing two mesogenic monomers plotted against their composition. (1) = clearing point, (2) = starting point of decrease in birefringence

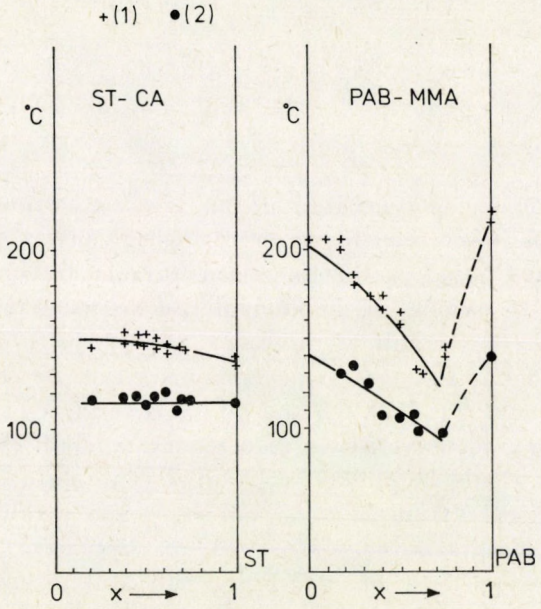

Fig. 7. Transition temperature vs. composition functions of copolymers containing one mesogenic monomer. (1) = fusion point, (2) = softening point

from tables of Brandrup and Immergut [17] (0.41 and 0.34), respectively. Data of the exact analogue, cyclohexyl acrylate, are missing. CVS and CSGA were represented by the Q and e values of vinyl acetate (0.026, —0.88) and 2-acetoxyethyl acrylate (0.52, 0.77), respectively. These data were taken from the recent tables of Greeley [18].

Only some tendencies can be established by comparing the two halves of the two tables since the monomers containing cholesteryl group have not been copolymerized with one another, due to the problems reluted to the determination of the composition. In the system St/CA, the r value of St was one third of the expected, that of CA was identical with the value of PAB. It can be established by the comparison of PAB/CA and PAB/CSGA systems that incorporation of PAB is enhanced as the flexible chain length increases.

Transition temperatures of copolymers are plotted against the composition in Figs 6 and 7. For samples containing PAB, an unequivocal determination of the clearing point was only possible when the comonomer was mesogenic itself. Among the samples containing St or MMA, only the CA/St system was slightly birefringent; its cessation, however, could not be determined unambiguously. For this reason, only softening and fusion points of the copolymers are presented in Fig. 7. Both values should be regarded as upper limits, since warming of the small bubble-containing heterogeneous samples previously cooled under pressure the temperature at which these bubbles start (moving) was regarded as the softening point. The temperature values were reproduced within 5—8 °C provided that the heating rate was identical. At the fusion point, the amples got into molten state. In Fig. 6 the initial and final temperatures of the change (decrease) in birefringence are demonstrated by measuring the depolarization current proportional to birefringence.



Fig. 8. Polarization micrograph of poly(cholesterylsuccinylgylcoylacrylate). Magnification: 360×

In two systems of the five, viz. in PAB/CA and CA/St systems, properties change continuously as the composition changes; these properties resemble those of the homopolymers. In the other cases, a minimal transition temperature is observed at intermediate composition. PAB and CA have aperiodic helical structure which corresponds to that of atactic polystyrene, thus the continuous composition dependence of isomorphic character is justified. As mentioned in the Introduction, poly-CVS and poly-CSGA are smectic polymers, therefore, they are not isomorphic with aperiodic helical polymers. This results in a reduction of transition temperatures with increas-

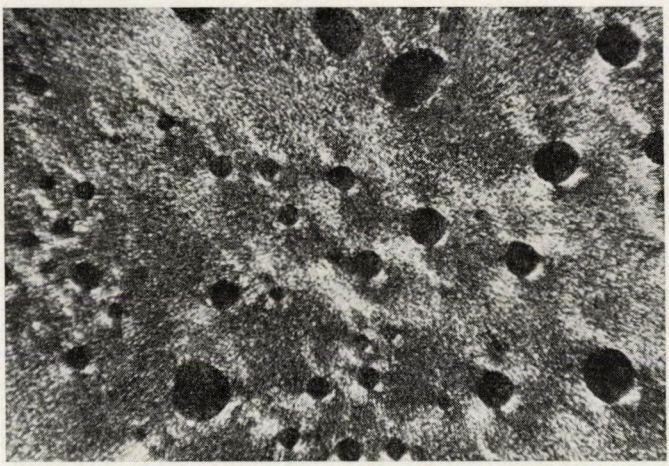

Fig. 9. Polarization micrograph of the equimolar copolymer of phenyl-*p*-acryloyloxybenzoate with cholesteryl succinylglycoylacrylate. Magnification: 360×

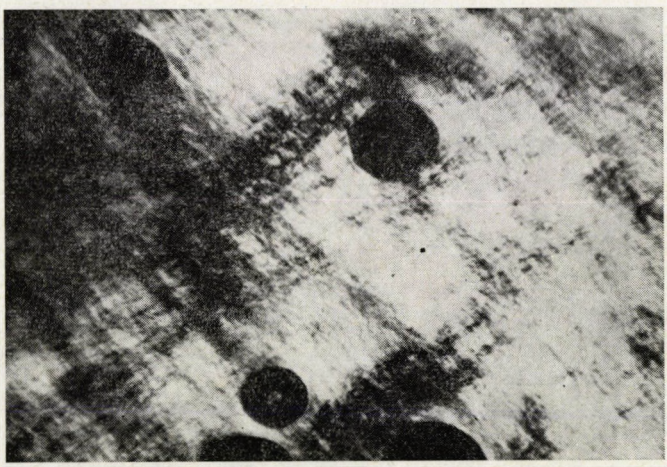

Fig. 10. Polarization micrograph of the copolymer of cholesteryl succinylglycoylacrylate with 0.9 mole fraction of phenyl *p*-acryloyloxybenzoate. Magnification: 360×

ing comonomer content. Behaviour of the PAB/CVS system is similar to that of *p*-methoxyphenyl *p*-acryloyloxy azoxybenzene/CVS copolymers studied previously [9].

Structural modifications can be followed clearly in Figs 8, 9 and 10 by the polarization micrographs of poly-CSGA, equimolar PAB/CSGA copolymer, and a copolymer containing 0.2 mole fraction of CSGA, respectively. Copolymers of low PAB content have similar texture to the broken fan configuration of doly-CSGA. Around the melting point minimum, a characterless texture appears (Fig. 9) then, with increasing PAB content, the characteristic texture of poly-PAB appears [2, 4]. The structural change was well observable in *N*-acryloyl piperidine/PAB systems [7] by both polarization microscopy and wide-angle X-ray diffractometry.

Conclusion

Data presented in this paper repeatedly indicate that mesogenic monomers cannot be unequivocally fitted into the *Q—e* scheme. Composition of copolymers containing mesogenic monomers differs from the expected. On the other hand, structural and thermodynamic features of the copolymers depend on the structure of homopolymers obtained from the mesogenic monomer. The structure is isomorphic when both homopolymers belong to the same structural type. Minimal transition temperatures are observed when the two homopolymers are not isomorphic. These structures are formally analogous to solid solutions or eutectics. Such structural features can be well interpreted by the previously published model [2—4] in which an aperiodic helical macromolecule itself forms a thermodynamic system, i.e. no interchange occurs with the segments of adjacent molecules. This is not the case in smectic structures, where the neighbouring molecular segments mix. As the amount of segments linked to the main chain through a flexible chain increases, rigidity and collective character of aperiodic helices is reduced; consequently, the decomposition temperature and also the clearing point is decreased. With increasing number of segments bonded directly to the main chain, i.e. sticking out of the smectic plane, the smectic layers become gradually disoriented (increasing entropy content, decreasing melting enthalpy), consequently, the melting point of the layer decreases.

Aperiodic helical structures actually remain also in solutions. This is indicated by the fact that inhomogeneity distribution measured by X-ray diffractometry in bulk is in fair agreement with the distribution measured by GPC in solution [19, 20]. It can, therefore, be assumed that this structure, as a topochemical factor, may modify the reactivity of the monomers. This assumption is supported by the fact that the least difference between the expected

and measured reactivity ratios was found in the isomorphic structure. In this case, the molecular mass of CA is not substantially different from that of CSGA, however, their reactivities differ basically.

REFERENCES

[1] Hardy, G., Cser, F., Nyitrai, K., Bartha, É.: Ind. Eng. Chem. Prod. Res. Dev., **21,** 321 (1982)
[2] Hardy, G., Cser, F., Nyitrai, K., Samay, G., Kalló, A.: J. Cryst. Growth, **48,** 191 (1980)
[3] Cser, F., Nyitrai, K., Pocsik, I., Tompa, K., Hardy, G.: Mol. Cryst. Liqu. Cryst. (in press)
[4] Cser, F.: J. Phys., **40,** C3-459 (1979)
[5] Cser, F., Nyitrai, K., Hardy, G., Menczel, J., Varga, J.: J. Polym. Sci. Polym. Symp., **69,** 91 (1981)
[6] Nyitrai, K., Cser, F., Hardy, G.: Polym. J., **13,** 1085 (1981)
[7] Nyitrai, K., Cser, F., Babaev, T. M., Hardy, G.: Eur. Polym. J., **17,** 871 (1981)
[8] Nyitrai, K., Cser, F., Seyfried, É., Lengyel, M., Hardy, G.: Eur. Polym. J., **13,** 673 (1977)
[9] Cser, F., Nyitrai, K., Kocsis, I., Hardy, G.: Eur. Polym. J., **17,** 865 (1981)
[10] Nyitrai, K., Cser, F., Csermely, G., Bui Doc Ngoc, Füzes, L., Samay, G., Hardy, G.: Eur. Polym. J., **14.,** 467 (1978)
[11] Cser, F., Nyitrai, K., Hardy, G.: Acta Chim. Acad. Sci. Hung., **100,** 463 (1979)
[12] Hardy, G., Cser, F., Nyitrai, K., Fedorova, N.: Proc. IV-Tihany Symp. Rad. Chem. Akadémiai Kiadó, Budapest 1977
[13] Cser, F., Nyitrai, K., Kiss, K. Á., Hardy, G.: in "Liquid Crystals and Ordered Fluids" Vol. IV, (accepted for publication)
[14] Alfrey, K., Price, G. C.: J. Polym. Sci., **2,** 101 (1974)
[15] Hardy, G., Cser, F., Kalló, A., Nyitrai, K., Bodor, G., Lengyel, M.: Acta Chim. Acad. Sci. Hung., **65,** 287 (1970)
[16] Kelen, T., Tüdős, F.: J. Macromol. Sci. Chem., **A9,** 1 (1975)
[17] Brandrup, J., Immergut, E. H.: Polymer Handbook 2nd Ed. Interscience, New York
[18] Greenley, R. Z.: J. Macromol. Chem., **A14,** 427 (1980)
[19] Samay, G., Füzes, L., Cser, F., Bodor, G.: J. Chromatogr., **218,** 473 (1981)
[20] Cser, F., Nyitrai, K., Samay, G., Bodor, G., Hardy, G.: Macro Mainz, 1979, Preprints Vol. II, p. 930

Acta Chimica Hungarica 114 (3—4), pp. 235—247 (1983)

STUDIES ON COPOLYMERIZATIONS OF HEXADECYL ACRYLAMIDE*

A. CHERNEVA+, F. CSER, K. NYITRAI, K. KISS and GY. HARDY**

(Research Institute for Plastics, H-1950 Budapest, Hungária krt. 114.)

Received October 11, 1982
Accepted for publication December 9, 1982

Hexadecyl acrylamide (HAA) was copolymerized with cholesteryl acrylate (CA), cholesterylsuccinyl glycoyl acrylate (CSGA), styrene (St), and methyl methacrylate (MMA). Reactivity ratios were as follows:

$r_{HAA} = 0.48$ $\quad$ $r_{CA} = 1.39$
$r_{HAA} = 0.75$ $\quad$ $r_{CSGA} = 0.72$
$r_{HAA} = 0.34$ $\quad$ $r_{St} = 1.97$
$r_{HAA} = 0.49$ $\quad$ $r_{MMA} = 3.05$

Q and e values for HAA could not be determined on the basis of the four copolymerization partners since the results were controversial.

Clearing points of the copolymers if birefringent (CA, CSGA) have minimum values at an intermediate composition. The structure of homopolymers, poly-HAA and poly-CSGA was sudied by X-ray diffractometry and by their phase diagrams with terephthaloyl bis-butylaniline (TBBA) and *p*-butoxyphenyl-*p*-propionyloxybenzoate (BPPB). Smectic B structure of poly-HAA and smectic C structure of poly-CSGA were rendered probable or verified. Poly-CA is not isomorphic with the nematic BPPB. The three homopolymers are not isomorphic with each other as reflected by the heteromorphic structure of the copolymers.

Introduction

In studies on the solid-state polymerization of hexadecyl acrylamide (HAA) [1] formation of a smectic polymer with hexagonal lamellar structure was observed. It was found [2—4] that the structure of copolymers from monomers containing mesogenic groups would be isomorphic with the homopolymers if both homopolymers of the comonomers were isomorphic. In the present paper, it was investigated whether the above observation would be valid even when the monomer contained a long elastic side chain. The further aim of our work was to determine Q—e parameters of HAA [5] and to examine whether the copolymerization constants would deviate [4] from those expected on the basis of the chemical structure even if the monomer contained a large elastic carbon chain.

* Polymerization in Liquid Crystals, XVI, Part XV. cf. ref. [2]
** To whom correspondence should be addressed
+ Present address: Technological Institute for Chemistry, Sofia, Bulgaria

Experimental

Hexadecyl acrylamide (HAA), cholesteryl acrylate (CA) and cholesterylsuccinyl glycoyl-acrylate (CSGA) [2] were prepared and purified according to our previous reports [1, 6]. Styrene (St) and methyl methacrylate (MMA) were washed three times with Na_2CO_3 solution then three times with distilled water, dried over Na_2SO_3, and distilled in vacuum. Until use for a maximum of 48 hours, they were stored at −18 °C in the dark.

Polymerization were carried out in 50% *m/m* chloroform solution at 60 °C. 0.5% *m/m* azobisisobutyronitrile initiator was used in terms of the monomer. Reaction times were empirically selected so that conversions should remain in the range of 8 to 15%. Polymeric products were precipitated by methanol then purified by repeated dissolution and precipitation.

Copolymers were dried to constant mass then their compositions were determined by microanalysis for N. Melting and clearing temperatures were measured by polarization microscopy [7].

Phase conditions of the two mesogenic monomers and of HAA homopolymers were estimated by X-ray diffractometry and by means of their phase diagrams produced with terephthaloyl bis-butylaniline (TBBA). The phase diagrams were recorded by DSC, by polarization microscopic, and thermomechanical investigations of melting characteristics of polymer-TBBA systems at different compositions.

DSC thermograms were recorded by a Perkin-Elmer DSC-2/b instrument at a scanning rate of 10 K/min. For the determination of miscibility diagrams, master blends of different compositions were prepared by heating the finely disintegrated and blended polymer — TBBA powder above its clearing point then chilling it at a rate of 10—15 K/min. The cooled blends were stored for 10—30 days before starting the investigations. During this period, the possible separation of TBBA could proceed; a longer storage caused no change in transition heats and in the feature of thermograms as demonstrated by some repeated DSC recordings. Transition temperatures were characterized by two limit values. The lower one was defined by the section point of the ascending wing of the endothermic peak with the base line while the upper one was considered as the top of the enthalpy peak. When these limits encompassed a wide range, two overlapping peaks could often be distinguished indicating that dissolution and phase transition of TBBA were relatively well separated. These lower and upper limits indicated in the thermograms were in good agreement with the initial and final points of changes in the depolarization current measured by polarization microscopic as a function of temperature.

Glass transition temperatures (T_g) of blends were also determined by thermomechanical measurements by elevating the temperature by 5-K steps. A force of 50 *N* was used for the cylindrical specimens of 1 cm diameter and 1 cm height. Size changes measured in 10 sec were plotted against temperature. The temperature at which the changes in Hook deformation of the specimen elevated abruptly was considered as T_g. At this point, generally the plastic deformation of the specimen started. Around T_g, a step was found in the base line of thermograms. Temperature of this step was plotted in the miscibility diagrams.

X-ray diffractometry was performed in the Sect. Chem. laboratory of Martin-Luther University, Halle, Wittenberg (GDR), in Guinier and small-angle chambers. Specimens could be thermostated at an accuracy of 1—2 K. Cu—Kα radiation was used: intensities were recorded by a proportional scaler.

Results

Initial monomer and copolymer compositions are collected in Table I. In Figs 1 and 2 compositions of HAA-containing copolymers are plotted against the composition of the initial monomer mixtures. Reactivity ratios (r) were determined from the composition by the linearization method of Tüdős et al. [8]. Auxiliary diagrams for this calculation are shown in Figs 3 and 4. Three copolymerizations fit fairly well to the preconditions of linearization while the sytem HAA/MMA cannot be evaluated by the above method

Table I

Characteristic data for copolymer of HAA *with* CA, CSGA, MMA *and* St

Mole fraction of HAA in monomer	Mole fraction of HAA in copolymer	Conversion (%)	Mole fraction of HAA in monomer	Mole fraction of HAA in copolymer	Conversion (%)
Comonomer: CSGA			Comonomer: MMA		
0.10	0.068	4.3	0.10	0.033	3.1
0.20	0.132	5.4	0.20	0.079	5.6
0.30	0.230	4.7	0.30	0.140	4.8
0.40	0.387	6.7	0.40	0.189	7.2
0.50	0.377	5.2	0.50	0.273	6.7
0.60	0.513	8.1	0.60	0.348	5.3
0.70	0.582	7.6	0.70	0.550	6.9
0.80	0.700	3.7	0.80	0.643	3.5
0.90	0.789	4.6	0.90	0.769	3.5
Comonomer: CSGA			Comonomer: St		
0.10	0.140	6.2	0.10	0.051	4.6
0.20	0.216	4.8	0.20	0.111	5.2
0.30	0.314	5.6	0.30	0.174	5.4
0.40	0.363	7.7	0.40	0.240	4.8
0.50	0.502	6.3	0.50	0.303	6.2
0.60	0.595	8.2	0.60	0.389	8.1
0.70	0.635	4.2	0.70	0.502	3.9
0.80	0.707	4.7	0.80	0.588	4.6
0.90	0.873	4.1	0.90	0.704	5.9

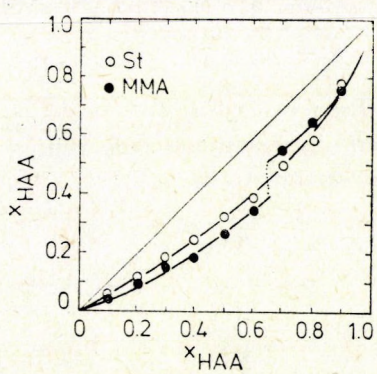

Fig. 1. Composition of HAA/St and HAA/MMA copolymers ploted against that of the initial monomer mixture

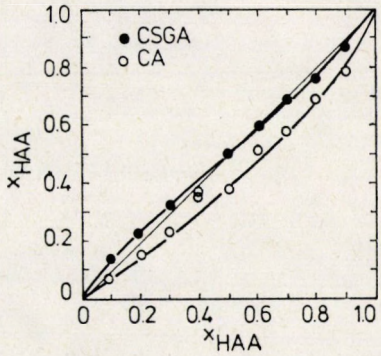

Fig. 2. Composition of HAA/CA and HAA/CSGA copolymers plotted against that of the initial monomer mixture

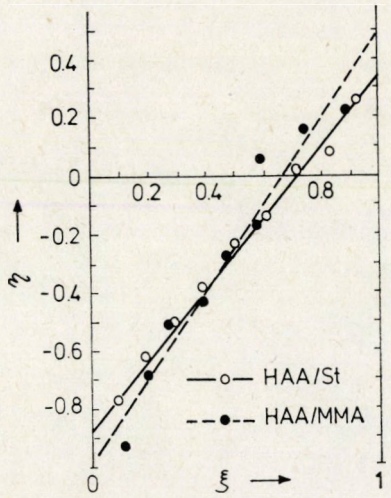

Fig. 3. Kelen—Tüdős—Turcsányi diagrams of HAA/St and HAA/MMA copolymers

nor by the Finemann—Ross procedure. In Table II, r constants calculated by the auxiliary diagrams are summarized, supplemented by r values of octadecyl acrylamide in relation to St and MMA from the date of Greenley [9, 10]. On the basis of the Figures, all monomers except CSGA should be regarded more active than HAA. The composition function of MMA-containing copolymers has to be divided into two parts since the product $r_1 r_2$ exceeds unity when all the points are considered. The product will be lower than one if only the results from three systems of the lowest MMA content are taken into account. This, however, makes the acceptability of these results doubtful. Similarly unreasonable r values were obtained for a carbon chain longer than

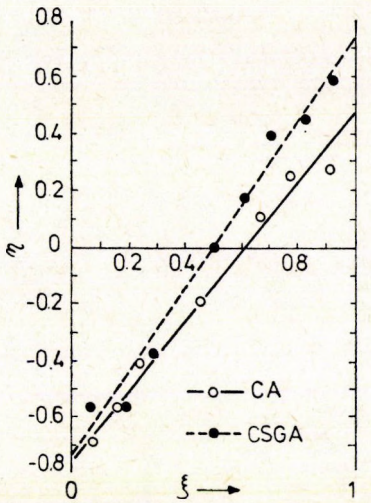

Fig. 4. Kelen—Tüdős—Turcsányi diagrams of HAA/CA and HAA/CSGA copolymers

Table II

Copolymerization reactivity ratios of hexadecyl acrylamide

Comonomer	r_{HAA}	r_2	Correlation coeff.
CA	0.48	1.39	0.97
CSGA	0.75	0.72	0.98
St	0.34	1.97	0.99
OAA/St	0.54	2.09	
MMA	0.49	3.05	0.95
OAA/MMA	0.42	4.13	

OAA = Based on the data for octadecyl acrylamide

HAA, octadecyl acrylamide, in association with St and MMA; their product is higher then 1. Our measured values, therefore, are experimental errors.

Q and e values calculated from the constants of HAA are shown in Table III together with those of non-mesogenic analogues of CA and CSGA [9—11] and with the Q and e values calculated from the measured r values.

In Figs 5 and 6, melting (1) and clearing (2) points of HAA/CA and HAA/CSGA copolymers are plotted against the composition. Copolymers containing St or MMA are not birefringent, thus, in these cases, no clearing point can be specified.

Table III

Q and e values of hexadecyl acrylamide

Comonomer	Q_{HAA}	e_{HAA}	Q_2	e_2	Ref.
CA	1.33	1.25	1.25	0.61	[2]
	0.61	−0.03			
CSGA	0.26	1.08	0.15	0.29	[2]
	0.17	−0.50			
St	0.31	−0.17	1.00	0.80	[10]
	0.84	−1.43			
MMA	—	—	0.74	0.40	[10]
SBUA	0.33	0.97	0.37	0.33	[11]
	0.22	−0.31			
2-AE-A	1.33	1.56	0.52	0.77	[10]
	0.39	−0.03			

SBUA = *sec* Butyl acrylate
2-AE-A = 2-Acetoxyethyl acrylate

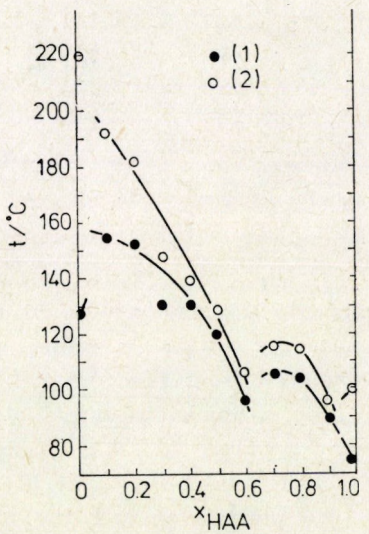

Fig. 5. Melting (1) and clearing (2) points of HAA/CSGA copolymers plotted against the composition of copolymers

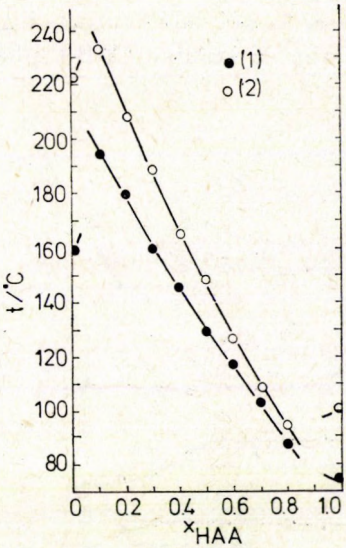

Fig. 6. Melting (1) and clearing (2) points of HAA/CA copolymers plotted against the composition of copolymers

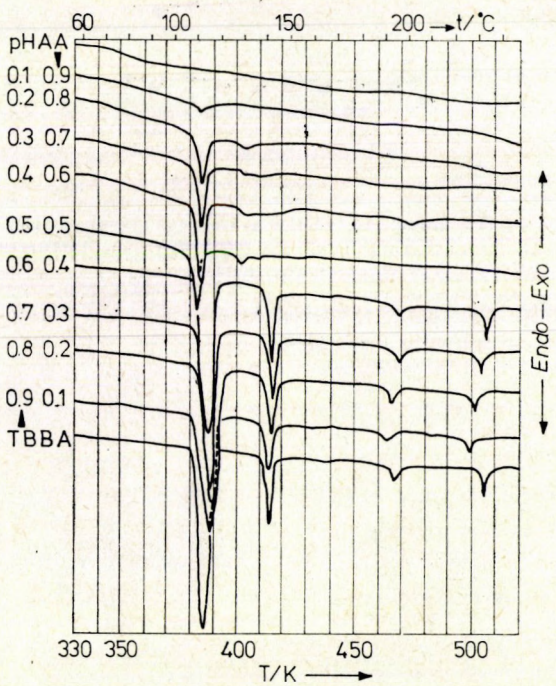

Fig. 7. DSC thermograms of poly-HAA/TBBA system (On the left side, the volume fraction of the composition is indicated)

transitions of TBBA decrease. At polymer contents higher than the 1 : 1 ratio, only the melting peak of the crystalline TBBA phase shows the presence of a second phase.

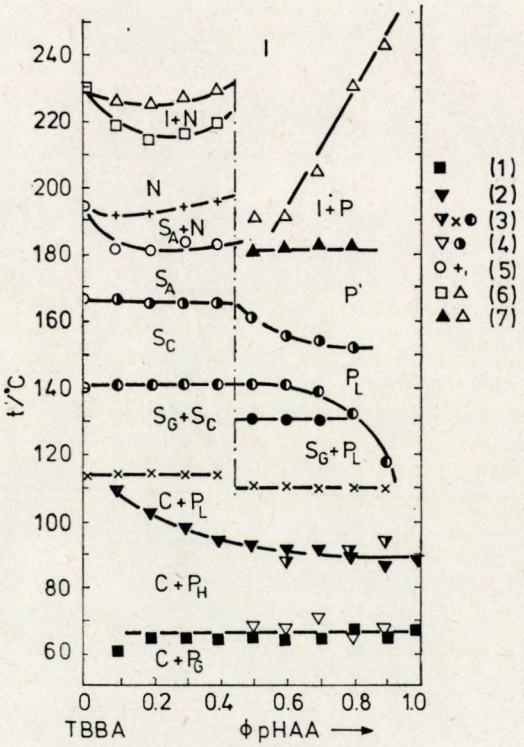

Fig. 8. Phase diagram of the poly-HAA/TBBA system; (1) = glass transition temperature, (2) = fusion temperature (from thermomechanical curves), (3) = starting and terminating of the first and 2nd DSC peaks, (4) = steps on the thermogram, (5) = starting and terminating of 3rd DSC peak, (6) = starting and terminating of 4th DSC peak, (7) = starting and terminating of the broad diffuse DSC peak. C = crystalline TBBA, I = isotropic poly-HAA, P = polyHAA, G, H and L in subscript mean glassy, high elastic and liquid states. S = smectic (type is indicated in subscript). N = nematic, P' = unidentified structure

Melting point, clearing point, and their difference decrease with increasing HAA content of the copolymers in both systems involved. Copolymers with HAA content higher than the mole fraction of 0.8—0.9 are not birefringent. In the HAA/CA system, a break point is observed in the melting and clearing point functions at $x_{HAA} = 0.6$. This composition is similar to the azeotropic point of the composition diagram.

DSC thermograms of poly-HAA/TBBA systems are presented in Fig. 7. With increasing poly-HAA content, sizes of melting peaks reflecting the phase

A similar series of thermograms were obtained for poly-CA/BPPB and poly-CSGA/TBBA systems. The miscibility diagram of the three systems (Figs 8, 9 and 10) were designed by collation of the thermograms with polarization microscopic and thermomechanical results.

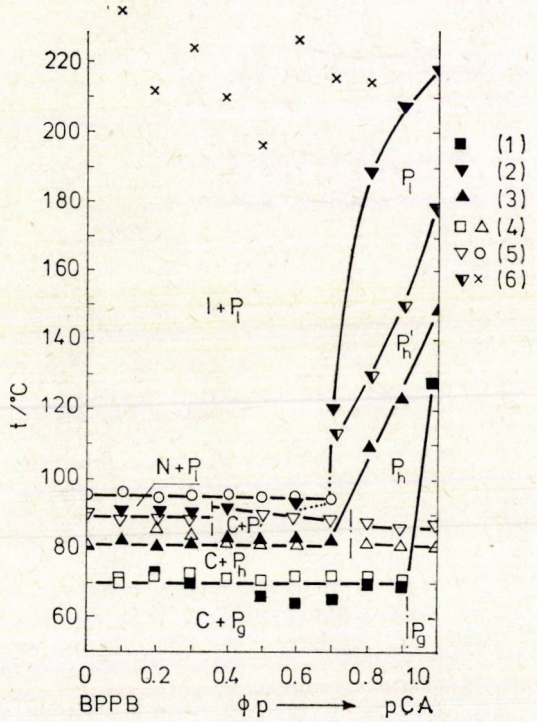

Fig. 9. Phase diagram of the poly-CA/BPPB system; (1) = glass transition temperature (2) = fusion point (from thermomechanical curves), (3) = break point on the thermomechanical curve, (4) = starting and terminating of the first DSC peak, (5) = starting and terminating of the 2nd DSC peak, (6) = starting and terminating of diffuse DSC peak. C = crystalline BPPB, P = poly-CA (in subscript, g = glassy state, h = highly state, l = liquid state), P'_h = gelous state, N = nematic BPPB, I = isotropic

For two homopolymers, poly-CA and poly-HAA, no phase completely miscible with the reference material is detected. Poly-CSGA has unrestricted miscibility with the smectic C phase of TBBA. It was previously supposed on the basis of polarization micrographs that poly-CSGA revealed a smectic C phase. Above the glass transition temperature of poly-CA, two thermally indicated transitions were observed. The lower transition represents a gelation followed by an inflation at the upper transition point. The latter is presumably caused by the fact that gases collected on the surface of particles during sample

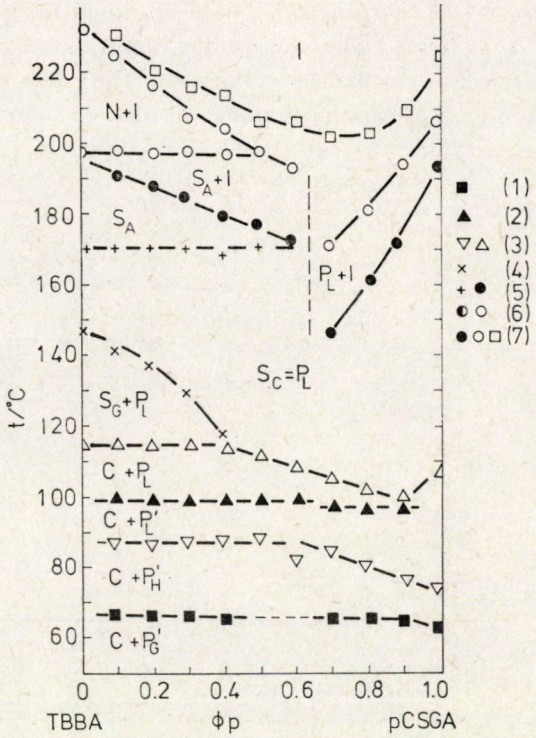

Fig. 10. Phase diagram of the poly-CSGA/TBBA system; (1) = glass transition temperature, (2) = fusion point (from thermomechanical curves), (3) = starting and terminating of the first DSC peak, (4) = terminating of the 2nd DSC peak, (5) = starting and terminating of the 3rd DSC peak, (6) = starting and terminating of the 4th DSC peak ($\Phi_P < 0.6$), (7) = starting, top, and returning point of the diffuse DSC (peak ($\Phi_P < 0.6$). C = crystalline TBBA, P = polymer (in subscript, G = glassy state, H = highly elastic state, L = liquid state), S = smectic state (type of lamellae is indicated in subscript), N = nematic, I = isotropic

preparation could not escape due to the strong film-forming nature of the polymer. In the so-called formed gel state, the expansion indicates changes in mobility within the matrix. After recooling, the specimen can be compacted with difficulty when compressed below this temperature.

Discussion

Copolymerization

In Table III, extremely scattered data are presented for calculations of Q and e values. e value of acrylamide is positive, thus, in these cases, positive values are expected. This was found, however, only for CA and CSGA. Their corresponding Q values ewre very different. If Q—e values of CA and CSGA are replaced by those of *sec* butyl acrylate (SBUA) and 2-acetoxyethyl acrylate

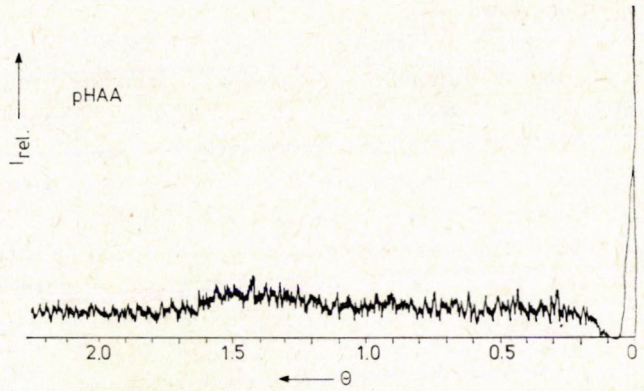

Fig. 11. Small-angle X-ray diffractograms of poly-HAA at different temperatures (Cu—K_α, $\lambda = 154.1$ pm)

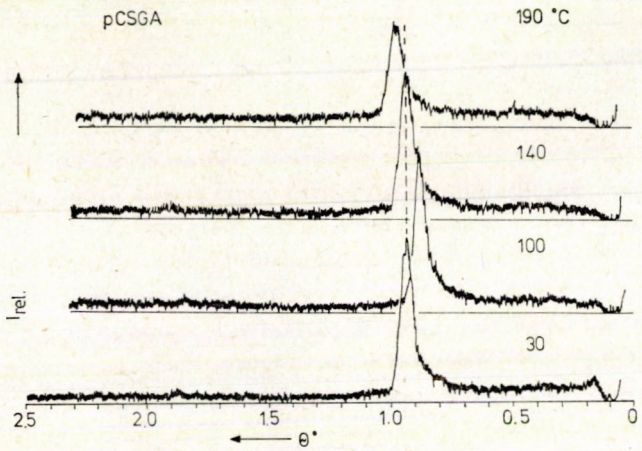

Fig. 12. Small-angle X-ray diffractograms of poly-CSGA at different temperatures (Cu—K_α, $\lambda = 154.1$ pm)

(2-AE-A), respectively [11], the situation remains the same. The long carbon chain causes the same anomaly in Q and e values as the mesogenic groups with rigid core. It is almost impossible that the long carbon chain would change Q and e values which are considered as molecular parameters; it has an effect much rather in the reaction zone as a topochemical factor. A detailed derivatographic analysis [12] of HAA/CA and HAA/CSGA copolymers and homopolymer blends revealed significant differences in the decomposition kinetics between the homopolymer blends and the copolymers of identical composition. It can be assumed reasonably on this basis that the copolymers are statistical ones.

Structure of the Polymers

Poly-HAA prepared in solution by radical initiation is much less ordered than that initiated by irradiation in the solid state. Though the reflexion representing a periodicity commensurable with the length of the side chain is detectable in its X-ray diffractogram, it is a diffuse band with extremely low intensity. The disordered structure is also reflected by the low birefringence of the polymer. In TBBA-containing blends, an induced smectic and nematic state can still exist. The "clearing point" (DSC peak) of poly-HAA decreases rapidly with increasing TBBA content (with simultaneous reduction in melting heat). The clearing process is of eutectic character, i.e. in the virtual S_A state no homogeneous mixed phase is possible. The clearing point has a minimum at mass fraction 0.5; at higher TBBA contents homogeneous mixtures are formed. Since the temperature of $S_G \rightarrow S_C$ transition is constant, the dissolution of poly-HAA may presumably take place rather in the S_A than in the S_C state of TBBA. At higher polymer contents, TBBA of S_G and S_C states is dissolved in poly-HAA. For this reason, poly-HAA seems to have actually an S_A state with perpendicular lamellae. As the S_B state is not birefringent from view perpendicular to the lamellae, the slight birefringence may be caused by the close parallelism of S_A lamellae with the glass plate. This appears in a small angle X-ray diffractogram as a broad peak (Figure 11).

According to the experimental data, poly-CSGA is inevitably in the S_C state. Its layer period (4.8 nm) is considerably longer than the estimated length of side chains (3.0 nm) but lower than its doubled value. It refers to a double smectic structure with tilted lamellae. Below 90 °C the polymer is transformed into the glassy state (see Figure 12).

Structure of poly-CA is not smectic on the basis of the miscibility diagram, there is no reason to deny the previous judgement for the structure of this polymer as an aperiodic helix.

Minima of melting and clearing points of the copolymers appear at compositions near to poly-HAA. This repeatedly confirmed the previous observations that the structure of copolymers resembled eutectic crystal mixtures if the homopolymers had different structures.

Summarizing the experimental results, it can be established that the HAA monomer elastic side chains shows identical feature in the copolymerization reaction and in the copolymer product as the mesogenic monomers with rigid side groups. It is reasonable, therefore, to assume that the particular properties of mesomorphic polymers are associated primarily with the anisometric arrangement of side-chains rather than with their rigidity or dipolar character.

REFERENCES

[1] Cser, F., Nyitrai, K., Dévényi, V., Hardy, H.: Acta Chim. Acad. Sci. Hung., **96,** 235 (1978)
[2] Nyitrai, K., Cser, F., Parragh, L., Hardy, G.: Acta Chim. Hung., **114,** 223 (1983)
[3] Nyitrai, K., Babaev, T. M., Cser, F., Hardy, G.: Europ. Polym. J., **17,** 871 (1981)
[4] Nyitrai, K., Cser, F., Bartha, É., Hardy, G.: Ind. Eng. Ehem. Prod. Res. Dev., **21,** 321 (1982)
[5] Alfrey, T., Price, C. C.: J. Polym. Sci., **2,** 101 (1974)
[6] Hardy, G., Cser, F., Kalló, A., Nyitrai, K., Bodor, G., Lengyel, M.: Acta Chim. Acad. Sci. Hung., **65,** 287 (1970)
[7] Cser, F., Nyitrai, K., Hardy, G.: Acta Chim. Acad. Sci. Hung., **100,** 463 (1979)
[8] Tüdős, F., Kelen, T., Turcsányi, B.: Kém. Közl., **43,** 87 (1975)
[9] Greenley, R. Z.: J. Macromol. Sci. Chem., **A14,** 445 (1980)
[10] Greenley, R. Z.: J. Macromol. Sci. Chem., **A14,** 427 (1980)
[11] Brandrup, J., Immergut, E. H.: Polymer Handbook, 2nd Ed. J. Wiley, New York 1975
[12] Cherneva, A., Adonyi, Z., Cser, F., Hardy, G.: Proc. Sec. Eur. Symp. on Thermal Anal., p. 272. Ed. D. Dollimore. Heyden, London 1982

Acta Chimica Hungarica 114 (3—4), pp. 249—253 (1983)

COMPLEXES OF 3,4-DIHYDROXYPHENYL DERIVATIVES, V*

AMBIDENTATE CHARACTER OF L-DOPA IN MANGANESE(II) AND COBALT(II) COMPLEXES

T. KISS and A. GERGELY**

(Institute of Inorganic and Analytical Chemistry, Lajos Kossuth University, H-4010 Debrecen, P.O.B. 21)

Received October 25, 1982
Accepted for publication December 9, 1982

The stoichiometry and stability constants of the complexes formed in manganese(II)- and cobalt(II)-L-dopa systems have been determined by pH-metric titration. On the basis of visible spectral studies, conclusions have been drawn about the metal ion binding sites in the complexes. It has been found that amino acid (N, O) and catechol (O, O)-type complexes are formed with both metal ions. Furthermore, in the case of some complexes more than one arrangement of the donor atoms belongs to the same stoichiometric composition.

Introduction

The L-3,4-dihydroxyphenylalanine (L-dopa) molecule contains two separate chelate-forming donor group pairs and is therefore capable of (N, O) coordination via the amino acid side-chain and of (O, O) coordination via the phenolic hydroxy groups in the ortho position. The possibility exists for the simultaneous coordination of both binding sites and, as a consequence, monomeric and dimeric species with mixed bonding mode may also be formed.

Earlier publications dealt in detail with the dependence of the coordination of the different binding sites of L-dopa on the pH of the solution and on the metal ion in the cases of nickel(II), copper(II) and zinc(II) [1—5]. Apart from the qualitative observation of complex formation [6], our knowledge concerning other transition metal-L-dopa systems is rather scanty.

The aim of the present work was to determine the stoichiometric compositions, the stability constants and the bonding modes of the complexes formed in the cobalt(II)- and manganese(II)-L-dopa systems. A study was also made of the metal ion — alanine — *o*-catechol model systems, where the potential donor groups of L-dopa are to be found in separate ligands.

* Part IV: ref. [7]
** To whom correspondence should be addressed

Experimental

Chemicals

Reanal and Fluka products were used. The purification of the ligands and the checking of the concentrations of the metal chloride solutions were performed as described previously [5, 7].

pH-metric measurements

The stability constants of the parent and mixed ligand complexes were determined by pH-metric titration of 25 cm^3 samples. In every solution the ionic strength was adjusted to 0.2 mol/dm^3 with KCl. The compositions of the samples, the performance of the measurements and the evaluation of the titration data corresponded to those reported earlier [7—9].

Spectral studies

In the spectrophotometric studies in the visible region, the spectra were recorded of the parent and mixed ligand complexes of alanine and tiron (the disodium salt of *o*-catechol-3,5-disulfonic acid) and also of the cobalt(II)-L-dopa system at various pH values at metal ion/ligand ratios of 1 : 2 and 1 : 4. These studies were carried out on a Beckman ACTA MIV double-beam recording spectrophotometer, with the careful exclusion of air.

Results and Discussion

The stability constants of the complexes formed in the metal ion — alanine, metal ion — *o*-catechol and metal ion — alanine — *o*-catechol model systems are listed in Table I.

These data reveal that for both metal ions the formation of the mixed ligand complexes of composition MAB is favoured ($\Delta \log \beta_{MAB} \sim 0.4$—$1.0$).

Table I

Stability constants for the manganese(II) and cobalt(II) complexes of alanine (A) *and o-catechol* (B)
$t = 25$ °C; $I = 0.2$ mol/dnm^3 KCl

		Mn(II)	Co(II)
A = alanine	$\log K_{MA}$	2.27 ± 0.02	4.24 ± 0.02
	$\log \beta_{MA_2}$	4.17 ± 0.06	7.65 ± 0.03
	$\log \beta_{MA_3}$	—	9.91 ± 0.08
	$\log K_{MA}/K_{MA_2}$	0.37	0.84
B = *o*-catechol	$\log K_{MB}$	7.53 ± 0.01	8.60 ± 0.01
	$\log \beta_{MB_2}$	11.95 ± 0.03	14.94 ± 0.02
	$\log \beta_{MAB}$	9.35 ± 0.1	11.98 ± 0.05
	$\Delta \log \beta_{MAB}$*	0.99	0.38
	$\Delta \log K_{MAB}$**	0.45	0.90

* $\Delta \log \beta_{MAB} = \log \beta_{MAB} - 1/2(\log \beta_{MA_2} + \log \beta_{MB_2} + \log 4)$
** $-\Delta \log K = \log K_{MA} + \log K_{MB} - \log \beta_{MAB}$

However, the $\Delta \log K$ values expressing the ratios of the stepwise constants for the mixed ligand complexes [10] are approximately the same as the log K_1/K_2 values relating to the alanine parent complexes. It may be assumed, therefore, that the formation of the mixed ligand complexes is favoured because of the differences characteristic of the parent complexes and expressed in their constants and not as a consequence of special effects due to the ligand pair in question.

On the basis of data for the model systems and the results relating to other transition metal-L-dopa complexes [1—5], attempts were made to evaluate the titration data by asuming various (N, O), (O, O) and mixed bonding mode complexes. In the process of the combined treatment of the titration curves recorded at the different metal ion/ligand ratios, the best agreement between the measured and the calculated titration curves was obtained with the species with the compositions and stability data given in Table II.

To clarify the binding sites of the complexes formed in the cobalt(II)--L-dopa system, comparisons were made of the spectral properties of the alanine and *o*-catechol parent complexes CoA_2 and their mixed complexes CoAB, and also of the cobalt(II)-L-dopa system at various pH values. The spectra obtained are presented in Fig. 1.

The present experimental data, together with our earlier results on other transition metal-L-dopa systems [4, 5], permit the following conclusions concerning the binding sites in the cobalt(II)- and the manganese(II)-L-dopa complexes:

1. As a consequence of its stoichiometric composition, only (N, O) coordination is possible in the species CoH_2A. In the complexes MHA, however, an (O, O) bound is presumably formed in the case of both metal ions, while the amino group of the side-chain is protonated. This is supported by the good

Table II

Stability data on manganese(II)- and cobalt(II)-dopa complexes
$t = 25$ °C; $I = 0.2$ mol/dm³ KCl

	Mn(II)	Co(II)
MH_2A	—	26.84 ± 0.02
MHA	17.76 ± 0.01	19.10 ± 0.02
MA	8.14 ± 0.05	10.01 ± 0.10
MH_3A_2	—	45.10 ± 0.03
MH_2A_2	33.43 ± 0.08	36.14 ± 0.06
MHA_2	23.75 ± 0.07	26.41 ± 0.05
MA_2	12.43 ± 0.03	15.41 ± 0.03

agreement of these stability constants with the corresponding values of the dopamine species [7], dopamine being capable only of (O, O) coordination. The species MA is probably formed by the deprotonation of the chain-terminal

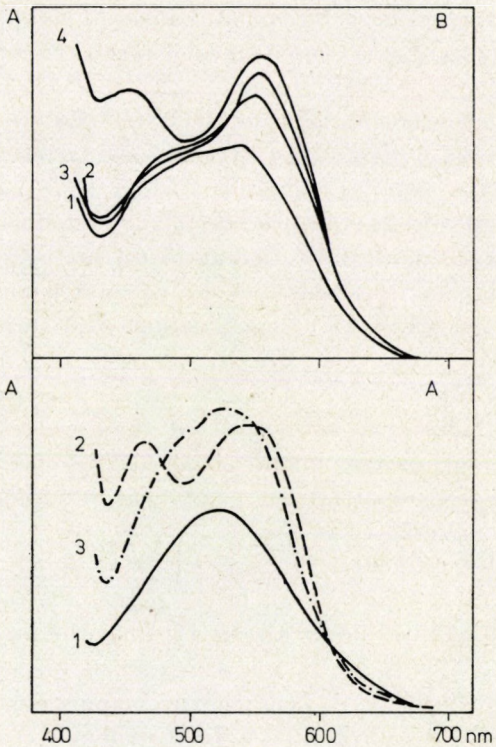

Fig. 1. Visible spectra of the following systems: A: (1) Co(II)-alanine at a 1 : 2 metal/ligand ratio at pH 8.5; (2) Co(II)-*o*-catechol at a 1 : 2 ratio at pH 8.9; (3) Co(II)-alanine-*o*-catechol at a 1 : 1 : 1 ratio at pH 9.5; B: Co(II)-dopa at a 1 : 2 ratio: (1) at pH 9.3; (2) at pH 10.5; (3) at pH 11.3; (4) at a 1 : 4 ratio at pH 11.6

ammonium group of the (O, O)-coordinated ligand, though parallel hydroxo complex formation cannot be excluded in the case of cobalt(II).

2. In the complex CoH_3A_2 a mixed bonding mode involving both (N, O) and (O, O) bonds is probable. This is suggested above all by the fact that mixed ligand complex formation is favoured in the model systems too. Another indication is that the spectral behaviour of the cobalt(II)-L-dopa system at pH $\sim$9.3 (where this species is formed in maximum concentration) is reminescent of the spectral properties of the mixed ligand complex cobalt(II)-alanine-tiron (see Fig. 1). As part B of this Figure shows, the spectra of the cobalt(II)--L-dopa system in the pH interval 10—11.3 cannot be ascribed to a species with one definite bonding mode. With the increase of the pH, however, i.e.

with the stepwise deprotonation of the complex CoH_3A_2, the shape of the spectrum changes; this is indicative of a continuous rearrangement from the mixed bonding mode to the complex CoA_2 containing only (O, O) bonds. This rearrangement is completed only at a greater ligand excess and at high pH. The characteristics of the spectrum (see spectrum 4, Fig. 1) then exhibit good agreement with those of Co(*o*-catecholate)$_2$. (A similar rearrangement was observed in the zinc(II)-L-dopa system [5].)

Such a rearrangement does not take place to an appreciable extent in the manganese(II)-L-dopa system. This is indicated by the fact that the (O, O)-bonded complex Mn(*o*-catecholate)$_2$ is present only in negligible concentration in the manganese(II) — alanine — *o*-catechol model system, even in the pH range of 10—11. Similarly as for the behaviour of the nickel(II)-L-dopa system [5], therefore, it is highly probable that the species MnH_2A_2, $MnHA_2$ and MnA_2 all remain of mixed bonding mode. Accordingly, their deprotonation constants can be ascribed to the ionization processes of the phenolic hydroxy and ammonium groups not coordinated to the metal ion, and those of the water molecule to be found in the coordination sphere.

Since the rearrangement processes observed in the cobalt(II)-L-dopa system and the deprotonation processes of the donor groups not bonded to the metal ion take place in the same pH range, these processes may proceed via different pathways. One given stoichiometric composition may therefore involve different species with different arrangements of the donor groups [5]. Formation of the (O, O) bonded species can be followed separately by means of the UV spectrum of the phenolate group of the ligand. Thus, the joint evaluation of the pH and spectral data may provide a possibility for the determination of the microconstants of complex formation. Such investigations will be reported in a forthcoming publication.

*

The authors are grateful to Mr. L. Kabai for technical assistance in the experimental work.

REFERENCES

[1] Gorton, J. E., Jameson, R. F.: J. Chem. Soc. (A), **1968,** 2615
[2] Gorton, J. E., Jameson, R. F.: J. Chem. Soc. (A), **1972,** 304
[3] Bogges, R. K., Martin, R. B.: J. Am. Chem. Soc., **97,** 3076 (1975)
[4] Gergely, A., Kiss., T.: Inorg. Chim. Acta, **16,** 51 (1976)
[5] Gergely, A., Kiss, T., Deák, Gy.: Inorg. Chim. Acta, **36,** 113 (1979)
[6] Rajan, K. S., Mainer, S., Davis, J. M.: Bioinorg. Chem., **9,** 187 (1978)
[7] Gergely, A., Kiss. T., Deák, Gy., Sóvágó, I.: Inorg. Chim. Acta, **56,** 35 (1981)
[8] Nagypál, I.: Acta Chim. Acad. Sci. Hung., **82,** 29 (1974)
[9] Gergely, A., Nagypál, I., Farkas, E.: Acta Chim. Acad. Sci. Hung., **82,** 43 (1974)
[10] Sóvágó, I., Gergely, A.: Inorg. Chim. Acta, **37,** 233 (1979)



Acta Chimica Hungarica 114 (3—4), pp. 255—259 (1983)

CATALYTIC ACTIVITY OF THE Al_2O_3—AlF_3 SYSTEM FOR THE CLAUS REACTION*

S. KOWALAK** and I. BRESIŃSKA

(Institute of Chemistry, A. Mickiewicz University, Grunwaldzka 6, 60—78 Poznań, Poland)

Received May 7, 1982
In revised form December 10, 1982
Accepted for publication January 4, 1983

Al_2O_3—AlF_3 catalysts containing 0—100% β-AlF_3 have been studied in the Claus reaction. A maximum in specific activity has been found at 50% ALF_3.

Changes in activity are discussed in terms of one-electron donating centres such as OH^-, O^{2-} and F_2^- anions.

Preparation and properties of the Al_2O_3—AlF_3 binary system [1] and its catalytic activity for acid-catalyzed reactions such as cumene cracking and n-butene isomerization [2] have been reported in our previous papers. We have found that the catalytic activity for the mentioned reactions strongly depends on the chemical composition of the binary system under study. Catalysts containing AlF_3 of about 10 and 30 wt.% were of highest activity. A good correlation between catalytic activity for the above reactions and acidity of the samples has been observed [1, 2]. On the other hand, redox properties of fluorided aluminas were determined by Flockhart et al. for iodine reduction [3], and formation of ion-radicals of perylene and tetracyanoethylene [4], where one-electron transfer is involved.

Alumina is well-known as an effective catalyst for the Claus reaction which proceeds, most likely, on one-electron-donor centres of the catalyst surface [6—8]. According to the authors cited [6—8], SO_2 molecules adsorb on the above centres and then convert into SO_2^- anion-radicals which are supposed to be the reaction intermediates. The present study is aimed at determining the effect of fluorine introduction to alumina on its catalytic behaviour in the Claus reaction in order to explain changes occurring in one-electron-donor properties of the Al_2O_3—AlF_3 system in a wide range of chemical compositions.

Experimental

The same Al_2O_3—AlF_3 samples as described in our earlier papers [1, 2] were used in this study. They were calcined at 500 °C and contained catalytically active modification of aluminium fluoride, i.e. β-AlF_3. The Claus reaction has been carried out for 5 h at 180 °C

* For previous papers of the series, see Ref. [1, 2].
** To whom correspondence should be addressed.

under the same conditions as those described in our previous paper [9], in a flow-type reactor connected to a gas chromatograph. Catalyst samples of 0.5 g (fraction of 0.5—1.0 mm) were activated prior to the reaction in a stream of oxygen-free nitrogen for 1 h at 500 °C. The reaction mixture consisted of 3 vol. % SO_2, 6 vol.% H_2S (both Fluka, Switzerland) and 91 vol.% nitrogen.

Main reaction products (water and sulphur) condensed before reaching the chromatograph. Conversion was determined by the change in SO_2 and H_2S contents in gas mixture before and after the reaction. In addition to unreacted H_2S and SO_2, some otker sulphur-containing compounds, namely volatile hydrogen polysulphides were present in the gas leaving the reactor. The concentration of the polysulphides was estimated only roughly.

Results and Discussion

Figures 1 and 2 show conversions of H_2S and SO_2 during the Claus reaction, catalyzed by the samples under study, as a function of time.

In some cases the conversion of H_2S is higher then that of SO_2, which can be contributed to the side-reaction occurring in the Claus process, viz.:

$$S_n + H_2S \rightarrow H_2S_{(n+1)}.$$

In the beginning of the process, the activity of Al_2O_3—AlF_3 samples decreases rapidly, but it stabilizes after about 30 min. During the stationary activity period (i.e. after 150 min), conversions on samples "10" and "30" are above 30% and about 30%, respectively, in the case of SO_2 and about 50% and 38%, respectively, in the case of H_2S. Conversions on other Al_2O_3–AlF_3 samples are considerably lower and range about 10%. It follows from the figures that the

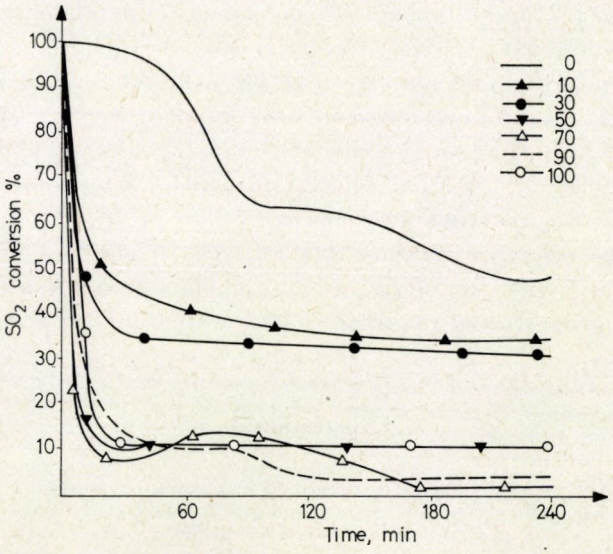

Fig. 1. Dependence of hydrogen sulphide conversion on time on stream. Note: Numbers 0, 10, 30 etc. stand for AlF_3 content (wt.%) in respective catalysts

most effective catalyst tested is alumina. Conversion of H_2S on this catalyst is almost complete during the first hour on stream and then diminishes to the level of about 75%. After 150 min, conversion of H_2S decreases again and is maintained at about 55% after 200 min on stream. The curve representing conversion of SO_2 shows a shape similar to that of H_2S but the conversion levels are only about 55% after 60 min and about 45% after 200 min.

Figure 3 shows the dependence of conversion during stationary activity period (after 150 min) on the chemical composition of catalysts studied. It follows from the above figure that an increase in fluorine content results in a decrease in activity for the Claus reaction. The reduction in activity is the highest for the catalysts containing up to 50% AlF_3. Further rise in fluorine content causes a considerably smaller drop in activity and, in the case of sample "100", even some increase in activity is observed. As concerns hydrogen polysulphide content in the reaction products, which has been plotted in the same figure as a function of catalyst composition, it appears that changes in polysulphide content follows those in conversions of the main products of the Claus process. One can suppose that high conversions observed in the case of samples containing none or small amounts of fluorine result from their large surface area [1] rather than from high population of active centres per unit surface area. Therefore, conversions of H_2S and SO_2 per 1 m^2 were plotted in Fig. 4 versus AlF_3 content. The course of curves shown in the latter figure differs significantly from that given in Fig. 3. Figure 4 shows that catalytic activity of the samples studied increases almost linearly with AlF_3 content

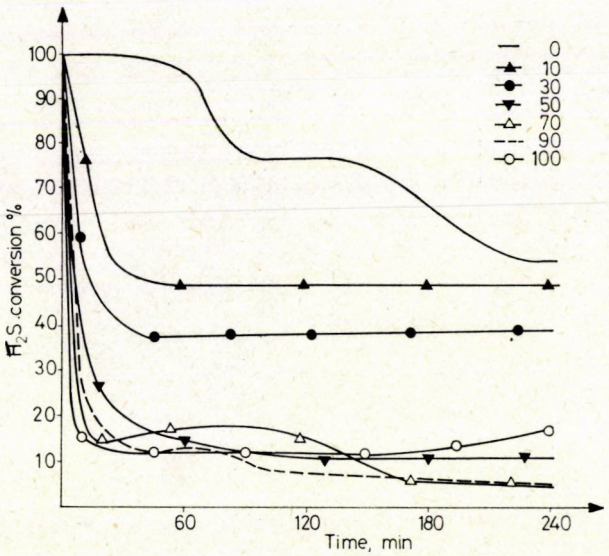

Fig. 2. Sulphur dioxide conversion as a function of time on stream. For the note concerning symbols on curves-see Fig. 1

up to 50%. After reaching this value, a nearly linear decrease in specific activity (conversion/surface area) occurs up to 90% AlF_3. With sample "100" a marked increase in conversion can be observed again.

How to explain the catalytic behaviour of catalysts investigated? If OH^- and O^{2-} anions on the alumina surface are the electron-donor centres

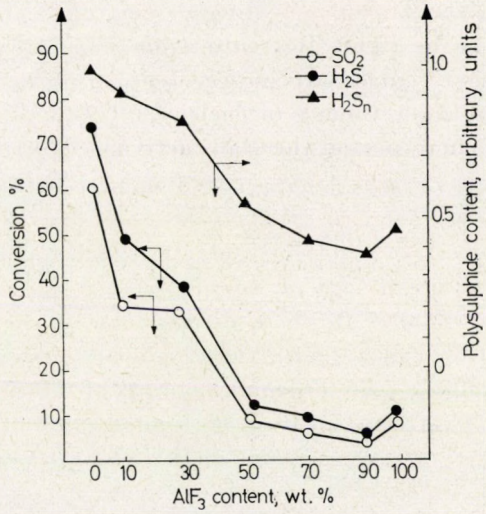

Fig. 3. Conversion during stationary activity period and polysulphide content versus AlF_3 content

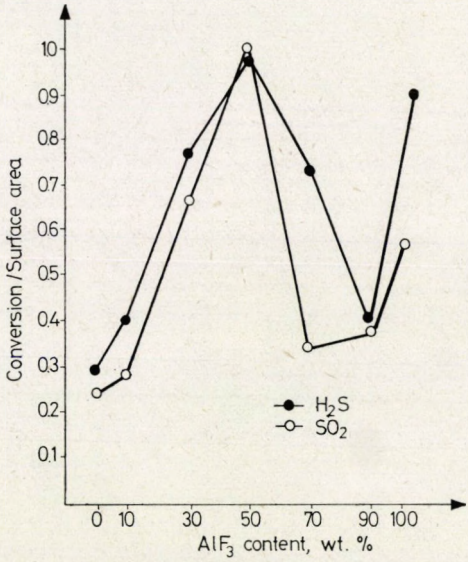

Fig. 4. Specific activity (conversion/surface area) as a function of catalyst composition

[5] reponsible for SO_2^- anion radical formation [6—8], then high conversion (per 1 g of catalyst) observed for pure alumina and low-fluorine catalysts are an obvious result of an abundance of hydroxide and oxide anions, since total number of these electron donating centres must be high due to large surface area of the above samples. If, however, conversion is related to unit surface area as presented in Fig. 4, then our supposition that the number of active centres per 1 m^2 for the Claus reaction is on fluorine-rich samples higher than on alumina, seems to be right. It results from Fig. 4 that surfaces densely populated with active centres are obtained at some optimal concentration of fluorine in the catalyst, though in each case fluorine-containing aluminas surpass pure alumina in respect of the Claus activity. Thus, we interpret specific activity maxima seen in Fig. 4 in a similar way as proposed by Flockhart et al. [4] and in our earlier paper [9], i.e. by the development of relatively high number of new one-electron-donor centres (F_2^- ions) for some ranges of fluorine content. This effect is clearly seen only after relating the conversion to unit surface area, because the increase in Claus activity due to new centre formation does not compensate the activity decrease resulting from a strong reduction in surface area, when fluorine-containing samples are compared with pure alumina. ESR study on the formation of tetracyanoethylene radicals on Al_2O_3—AlF_3 catalysts is under way in order to confirm the above interpretation.

REFERENCES

[1] Kowalak, S.: Acta Chim. Acad. Sci. Hung., **107,** 19 (1981)
[2] Kowalak, S.: Acta Chim. Acad. Sci. Hung., **107,** 27 (1981)
[3] Flockhart, B. D., Liew, K. Y., Pink, R. C.: J. Catal., **32,** 20 (1974)
[4] Flockhart, B. D., Liew, K. Y., Pink, R. C.: J.C.S. Faraday I, **76,** 2026 (1980)
[5] Flockhart, B. D., Leith, J. R., Pink, R. C.: Trans. Faraday Soc., **65,** 542 (1969)
[6] Dudzik, Z., George, Z. M.: J. Catal., **63,** 72 (1980)
[7] Karge, H., Tower, R. W., Dudzik, Z. George, Z. M.: Proc. 7th Intern. Congr. Catal., Kodansha, Tokyo—Elsevier, Amsterdam 1981, p. 643.
[8] Khulbe, K. C., Mann. R. S.: J. Catal., **51**, 364 (1978)
[9] Kowalak, S., Bresińska, I.: React. Kinet. Catal. Lett., **19,** 249 (1982)

Acta Chimica Hungarica 114 (3—4), pp. 261—281 (1983)

COMPARATIVE STUDY OF POLYMER GELS BASED ON THEORIES OF CRITICAL PHENOMENA AND CLASSICAL THERMODYNAMICS

F. HORKAY[1]* and M. ZRÍNYI[2]

([1]National Institute of Occupational Health, H-1096 Budapest, Nagyvárad t. 2. and [2]Department of Colloid Science, Loránd Eötvös University, H-1088 Budapest, Puskin u. 11—13.)

Received August 6, 1982
In revised form October 5, 1982
Accepted for publication January 4, 1983

In the first part of the present paper some principles of the classical and scaling theories of polymer solutions and gels are discussed.

Following this, scaling relations describing the swelling and mechanical behaviour of polymer gels are compared with equations obtained on the basis of the classical approach.

Finally, in order to check the validity of the proposed relationships, some experimental results relevant to chemically cross-linked poly(vinyl acetate) gels are presented.

Introduction

In recent years remarkable advances has been achieved in the field of polymer physics. Previously the discussion of the conformation properties of macromolecular systems (solutions and gels) was mainly based on the Flory-Huggins treatment. From the first half of the 1970s, a new approach appeared, owing to results achieved in other fields of physics, particularly in that of critical phenomena.

In the first part of this paper some fundamental relationships referring to polymer solutions and gels, derived on the basis of the classical thermodynamic theory, which was developed in the 1940s, will be presented. It will be followed by a brief sketch of the main results of the scaling theory based on the analogies found between phase transitions of second order and the conformation-dependent properties of polymer systems.

In the second part mechanical and swelling properties of gels will be discussed. The concentration dependenc of elastic moduli and swelling pressure of cross-linked swollen networks will be analysed in order to compare experimental data with relationships obtained by classical and scaling theories.

* To whom correspondence should be addressed

Systems consisting of ideal chains

The classical theory of polymer solutions and gels [1, 2] is a mean-field theory, i.e. the potential (produced in polymer solutions by the interaction of the monomer with the solvent molecules, or of the monomer and solvent molecules with their own kind) acting on the constituents of the system is substituted by an average potential. The consequence of this approach is that there is no possibility to take into consideration long-range interactions, as e.g. the interaction between monomers located far from one another along the same or different polymer chains.

The classical theory (Flory-Huggins' theory), using the so-called lattice model of solutions, results the entropy of mixing. Taking into consideration the changes of molecular energetic interactions by introduction the Huggins' interaction parameter (χ), the following equations can be derived:
for the change in free enthalpy per lattice site

$$\frac{\Delta G_{\text{mix}}}{kT} = \frac{\varphi}{N} \ln \varphi + (1 - \varphi) \ln (1 - \varphi) + \chi \varphi (1 - \varphi), \tag{1}$$

for the osmotic pressure (π) of the polymer solution

$$\frac{\Pi d^3}{kT} = \frac{\varphi}{N} + \ln \frac{1}{1 - \varphi} - \varphi - \chi \varphi^2, \tag{2}$$

and for the change in chemical potential in conjunction with mixing [$(\Delta \mu_1)_{\text{mix}} = -\pi d^3$]

$$\frac{(\Delta \mu_1)_{\text{mix}}}{kT} = \ln (1 - \varphi) + \left(1 - \frac{1}{N}\right) \varphi + \chi \varphi^2, \tag{3}$$

where φ is the volume fraction of the polymer, N the degree of polymerization, d the lattice constant, T the temperature and k Boltzmann's constant.

In polymer gels macromolecules are not independent of one another: the free diffusion of chains is hindered by the chemical, physical, or possibly both types of cross-links. In good solvent condition, i.e. when the energy of the interaction between polymer chains and solvent molecules is higher than that of the monomer-monomer interaction, monomers tend to get as far away from one another, as possible. In the case of networks, due to the permanent cross-links between the chains, this tendency is manifested in the macroscopic swelling of the system. The swelling of a network is limited, because neighbouring network chains must remain linked also in the swollen state. The limit of swelling is set by the fact that the number of conformation possibilities of the network chains, and in conjunction with this, the entropy

of the network, diminish with increasing end-to-end distance, i.e. at given temperature and pressure further swelling would cause an increase in free enthalpy of the system. Thus, a swollen polymer network may be in equilibrium with the diluent (which may be either liquid or vapour). The composition of the polymer gel is primarily determined by the interactions of the polymer — solvent system and the network structure. It is assumed that deformation of network chains due to swelling produces only conformation changes one gets for the change in free enthalpy [3, 4]:

$$\Delta G_{\text{net}} = -kT \ln \frac{\Omega(\lambda_x, \lambda_y, \lambda_z)}{\Omega(1, 1, 1)} , \tag{4}$$

where $\Omega(\lambda_x, \lambda_y, \lambda_z)$ and $\Omega(1, 1, 1)$ are the number of conformation states in the deformed and undeformed network, respectively, λ_x, λ_y, and λ_z are the deformation ratios referred to the unperturbed dimensions of the chains. In the case of affine deformation (the components of the end-to-end distance vector of single network chains change according to the macroscopic deformation ratios) of ideal networks (the end-to-end distance of the network chains has an a priori Gaussian distribution) the following equation can be obtained:

$$\Delta G_{\text{net}} = \frac{K_1 nkT}{2}(\lambda_x^2 + \lambda_y^2 + \lambda_z^2 - 3) + K_2 nkT(\lambda_x \lambda_y \lambda_z) \tag{5}$$

where n is the number of the elastically active network chains, and K_1 and K_2 are numerical quantities depending on the structure of the gel. According to the Flory—Wall—Hermans theory [5—7], $K_1 = 1$ and $K_2 = \frac{2}{z}$ (z is the functionality of the junction point), while according to the James—Guth theory [8—10] $K_1 = 1$ and $K_2 = 0$. The difference in K_2 values in the theories can be attributed to the difference of the model systems used for the calculations. According to the opinion of the present authors, the James—Guth theory seems to be more reliable in the case of permanent networks [11, 12].

From relationship (5) the following equation can be obtained for the network-dependent component of the chemical potential change, accompanying swelling:

$$(\Delta\mu_1)_{\text{net}} = K_1 nkT q_0^{-2/3} \frac{d^3}{V_g} - K_2 nkT \frac{d^3}{V_g} \tag{6}$$

where V_g is the volume of the dry gel and q_0 is the so-called reference degree of swelling (the volume degree of swelling belonging to the unperturbed state of the network chains).

From Eqs (3) and (6) the swelling pressure (ω) of the gel can be expressed by the following relationship:

$$-\omega = K_1 n^* q_0^{-2/3} \varphi^{1/3} RT - K_2 n^* \varphi RT + \frac{RT\left[\ln(1-\varphi) + \varphi + \chi\varphi^2\right]}{\overline{V}_1} \quad (7)$$

In Eq. (7) n^* is the concentration of the elastically active network chains in the dry network, and $\overline{V}_1$ is the partial molar volume of the swelling agent.

As may be concluded from this brief survey, on the basis of classical theory explicit relationships can be deduced for the chemical potential functions, though the meaning of several parameters, depending on the model system (K_1, K_2, q_0) are not satisfactorily elucidated.

Discussion of polymer systems based on critical phenomena

In 1972 de Gennes recognized that in the exact consideration of the excluded volume effect similar problems arise as in phase transitions of the second order, or more generally, as in critical phenomena [15].

Owing to the excluded volume effect, the polymer chain can be considered as a correlated region, in which the end-to-end distance of chains corresponds to the correlation length, and the degree of polymerization to the reciprocal of the reduced temperature [17]. The close relation found between polymers and critical phenomena is based on the recognition that exponents pertinent to the polymer problem agree with the exponents of a non-existing phase transition in which the order parameter has zero component [16]. The well established theoretical concepts, e.g. scaling concept [19], renormalization [18] etc. developed to treat critical phenomena have proved to be particularly powerful in describing problems in polymer statistics.

For the end-to-end distance renormalization procedure results:

$$R \propto N^{\nu} \quad (8)$$

where ν is the so-called excluded volume exponent, which has universal properties. In the excluded volume limit $\nu = 0.588 \pm 0.0015$ was obtained [20]. (Further on for the sake of simplicity we use the value $\nu = 3/5$.) It should be mentioned that in absence of long range interactions (ideal case, Θ-conditions), $\nu = 1/2$.

A further substantial result of renormalization group method is the verification of the scaling hypothesis, according to which, thermodynamic quantities are generalized homogeneous function of their variables [19]. Thus, applying the dimensional analysis deduction of several scaling relation-

ships (scaling laws) become possible. It is sufficient to determine only two exponents, since the exponents referring to all other properties are interrelated by scaling laws.

Instead of the quantities characteristic of polymers, often their magnetic equivalents are used. For example the excluded volume theory of polymer solutions developed by des Cloiseaux [21], is based on the following correspondances found between the excess free enthalpy of the magnetic system and polymer properties:

$$\varphi = \frac{\partial G}{\partial \tau} \tag{9}$$

$$\frac{\varphi}{N} = \frac{1}{2} M \frac{\partial G}{\partial M} \tag{10}$$

$$\frac{\Pi}{kT} = -G + M \frac{\partial G}{\partial M} \tag{11}$$

where G is the magnetic free enthalpy, τ the reduced temperature and M the magnetization. Using the Widom form [19] of G and Eqs (9)—(11) the osmotic pressure of polymer solutions can be given:

$$\Pi = kT \frac{\varphi}{N} f(x) \tag{12}$$

where $f(x)$ is the universal function of the variable $x = \varphi N^{3\nu-1}$: in the case of $x < 1$ $f(x) = 1 + x + x^2 + \ldots$, and in the case of $x \geq 1$ $f(x) = x^m$, where m is another exponent. The relationship between m and ν can be expressed by a scaling law

$$m = \frac{1}{3\nu - 1} . \tag{13}$$

Transition between the two kinds of behaviour of the $f(x)$ function occurs at the value $x = \varphi N^{3\nu-1} = 1$. The concentration $\varphi = \varphi^*$, belonging to the transition, has a descriptive meaning: it is proportional to the average concentration of the individual coils, ie.

$$\varphi^* \cong \frac{Nd^3}{R^3} \cong \frac{Nd^3}{d^3 N^{3\nu}} \cong N^{1-3\nu} \tag{14}$$

The polymer solution is dilute if $\varphi < \varphi^*$, i.e. $x < 1$, and semi-dilute if $1 \geqslant \varphi > \varphi^*$, i.e. $x > 1$.

In the dilute regime, the known relationship for dilute polymer solutions

$$\Pi = kT \left[\frac{\varphi}{N} + \left(\frac{\varphi}{N} \right)^2 R^3 + \ldots \right] \tag{15}$$

is obtained, where the terms in brackets are in their order of succession the first, second, etc. virial coefficients.

In the semi-dilute regime

$$\Pi = kT \frac{\varphi}{N} \left(\frac{\varphi}{\varphi^*} \right)^m . \tag{16}$$

As may be seen, the relationship derived for the osmotic pressure in the semi-dilute regime substantially differs from that obtained on the basis of the Flory-Huggins theory. According to Eqs (13) and (16) in good solvents ($\nu = 3/5$) the osmotic pressure of semi-dilute polymer solutions increases according to the 9/4th power of concentration, while in the Θ-state ($\nu = 1/2$) according to the third power of concentration.

As has been already shown, in polymer gels being in swelling equilibrium, two effects of opposite direction, the mixing of the chains and of the solvent molecules, and the force acting against deformation compensate one another. A gel in equilibrium with pure diluent can be considered as a semi-dilute polymer system, the φ_e concentration of which is proportional to the φ^* concentration of the solution of a polymer having the same molecular mass as the network chains (φ^* theory [17]).

$$\varphi_e = k(z)\, \varphi^* \cong k(z) \left(\frac{1}{2} - \chi \right)^{-3/5} N^{1-3\nu}, \tag{17}$$

where $k(z)$ is a numerical constant depending on the functionality of the cross-links. Eq. (17) indicates that the extent of swelling is in close correlation with parameters characteristic of gel structure [$k(z)$, N], and depends also on the solvent power (χ).

Comparison of the theories of polymer gels based on classical thermodynamics and on critical phenomena

In the further discussion we focus on the comparison of the results of the two different approaches described earlier. Only the character of the functions obtained will be compared, as there is no possibility for absolute comparison due to the unknown numerical values of parameters involved in equations.

Shear modulus of swollen gels

According to the classical Flory-Huggins theory, the shear modulus of gels (E_G) is equal to the product [2]

$$E_G = K_1 n^* q_0^{-2/3} \varphi^{1/3} RT. \tag{18}$$

If gel homologues (gels differing from one another only with respect to the degree of cross-linking) are investigated, then the concentration dependence of 1/3 predicted by Eq. (7) cannot be fulfilled, because the individual values of the terms included in $K_1 n^* q_0^{-2/3}$ change.

If the elastic modulus is determined in swelling equilibrium with the pure solvent, then it follows from equilibrium conditions that

$$E_G \overline{V}_1 = -RT \left[\ln (1 - \varphi_e) + \varphi_e + \chi \varphi_e^2\right]. \tag{19}$$

It can be established from Eq. (19) that the shear modulus of gels is a quantity similar to the osmotic pressure of a solution of infinite molecular mass [see Eq. (3)]. Since in a good solvent the value of φ_e is considerably lower than 1, no substantial error is committed if the logarithmic term in Eq. (19) is expanded to the third order term [23]:

$$\frac{E_G \overline{V}_1}{RT} \cong \left(\frac{1}{2} - \chi\right) \varphi_e^2 + \frac{1}{3} \varphi_e^3. \tag{20}$$

It depends on Huggins' interaction parameter and on φ_e which of the two terms predominates. The first term of Eq. (20) is dominant, if $3\left(\frac{1}{2} - \chi\right) \gg \varphi_e$, i.e. if $\chi \ll \frac{1}{2}$, and if the cross-linking density is not too high:

$$E_G \cong \frac{RT\left(\frac{1}{2} - \chi\right)}{\overline{V}_1} \varphi_e^2. \tag{21}$$

An increase in Huggins' interaction parameter or in cross-linking density (increase in φ_e) makes the second term of Eq. (20) predominant

$$\left[\left(\frac{1}{2} - \chi\right) \ll \frac{1}{3} \varphi_e\right],$$

that is

$$E_G \cong \frac{RT}{3\overline{V}_1} \varphi_e^3. \tag{22}$$

The same concentration dependence of E_G can also be expected, independently of cross-linking density, if the swelling agent is a Θ-solvent of the polymer $\left(\chi = \frac{1}{2}\right)$.

Thus, it may be seen that for gels in swelling equilibrium with a good solvent the shear modulus is proportional to the second power of concentration, while in Θ-solvent to the third power.

On the basis of scaling arguments, the concentration dependence of the modulus can be calculated from relationship (16) utilizing the analogy between shear modulus and osmotic pressure [22]. For gel homologues in swelling equilibrium the elastic modulus can be expressed

$$E_G \cong kT \frac{\varphi_e}{N} \left(\frac{\varphi_e}{\varphi^*}\right)^m . \tag{23}$$

Taking into consideration that $\varphi_e \propto \varphi^*$, one gets [17]:

$$E_{G_i}' \cong \varphi_e^{\frac{3\nu}{3\nu-1}} . \tag{24}$$

It should be emphasized, that relationship (24) is valid only for gels in equilibrium with the pure diluent. On comparing Eqs (21) and (24), it can be established that the exponent of the concentration dependence of the shear modulus in a good solvent (similarly to the osmotic pressure) differs from that obtained on the basis of classical theory. Under Θ-conditions the exponent agrees in both theories.

Eq. (16) exhibits also a possibility to determine the concentration dependence of the elastic modulus of gel homologues in equilibrium with a swelling agent of arbitrary activity, a_1. It can be shown on the basis of general continuum-rheological considerations that for a given gel the modulus is proportional to the 1/3rd power of concentration [23]. Under consideration of this, we can write [24]

$$E_G = kT \frac{\varphi}{N} \left(\frac{\varphi}{\varphi_e}\right)^{-2/3} . \tag{25}$$

It may be seen from Eq. (25) that at fixed $\frac{\varphi}{\varphi_e}$, similarly to (24), the exponent of the concentration dependence of the shear modulus is $\frac{3\nu}{3\nu-1}$, while at fixed φ the exponent for gel homologues is $-\frac{6\nu+1}{9\nu-3}$.

Swelling pressure of gels

The swelling pressure of gels in equilibrium with a swelling agent of given activity has been defined with Eq. (7), and the dependence of ω on the parameters characteristic of gel structure and on composition was shown. If $K_2 = 0$ is assumed (James–Guth theory), the relationship between the

shear modulus, the osmotic pressure of the network chains (π_n) and the swelling pressure, can be expressed as follows:

$$\omega(\varphi) = \pi_n(\varphi) - E_G(\varphi). \tag{26}$$

(We note, that π_n is not identical with the osmotic pressure of the solution of the polymer, equivalent to the network chains.) Remaining within the frame of classical theory, further important relationships can be obtained by the series expansion of Eq. (2). This process is similar to what has been done in the previous section.

If the first term of equation

$$\frac{\Pi_n}{RT} \cong \frac{\frac{1}{2} - \chi}{\bar{V}_1} \varphi^2 + \frac{1}{3\bar{V}_1} \varphi^3 \tag{27}$$

predominates, using Eqs (18) and (26) one obtains:

$$\frac{\omega}{E_G} = \frac{\left(\frac{1}{2} - \chi\right) \varphi^2}{K_1 n^* q_0^{-2/3} \varphi^{1/3} \bar{V}_1} - 1. \tag{28}$$

For a gel in equilibrium ($\omega = 0$) with the pure swelling agent ($a_1 = 1$) we get

$$\frac{\frac{1}{2} - \chi}{K_1 n^* q_0^{-2/3} \bar{V}_1} = \frac{\varphi_e^{1/3}}{\varphi_e^2} = \varphi_e^{-5/3} \ . \tag{29}$$

Under consideration of Eqs (28) and (29), the following expression

$$\frac{\omega}{E_G} = \left(\frac{\varphi}{\varphi_e}\right)^{5/3} - 1 \tag{30}$$

can be derived.

If the second term of expression (27) predominates, on the basis of completely similar considerations one obtains

$$\frac{\omega}{E_G} = \left(\frac{\varphi}{\varphi_e}\right)^{8/3} - 1. \tag{31}$$

On the basis of scaling arguments [22], using Eqs (16), (17) and (25), and taking into consideration that in the case of $a_1 = 1$, $\omega = 0$, the following

equation can be written for the swelling pressure:

$$\omega = kT\frac{\varphi}{N}\left[\left(\frac{\varphi}{\varphi_e}\right)^{\frac{1}{3\nu-1}} - \left(\frac{\varphi}{\varphi_e}\right)^{-\frac{2}{3}}\right]. \tag{32}$$

Rearrangement of Eq. (32) gives

$$\frac{\omega}{E_G} = \left(\frac{\varphi}{\varphi_e}\right)^{\frac{6\nu+1}{9\nu-3}} - 1. \tag{33}$$

Under consideration of the excluded volume effect, ($\nu = 3/5$) the value of the exponent is $\frac{23}{12}$, while for systems consisting of Gaussian chains ($\nu = 1/2$), in accordance with Eq. (31), $\frac{8}{3}$.

It should be mentioned that relationships deduced for $\frac{\omega}{E_G}$ do not contain quantities depending on the individual characteristics of studied gel systems.

Compressibility of gels and the microscopic Poisson ratio

Using Eq. (7), the osmotic compressibility $\left(\frac{\partial\varphi}{\partial\omega}\right)$ of gels is, according to the classical theory [25], given by the relationship

$$\left(\frac{\partial\varphi}{\partial\omega}\right) = \frac{3}{5\,RT\,\bar{V}_1^{-1}\left(\frac{1}{2} - \chi\right)\varphi + \omega\varphi^{-1}}. \tag{34}$$

For gel homologues in equilibrium with the pure diluent ($\omega = 0$), Eq. (34) gives

$$\left(\frac{\partial\varphi}{\partial\omega}\right)\Big|_{\omega=0} = \frac{3}{5\,RT\,\bar{V}_1^{-1}\left(\frac{1}{2} - \chi\right)\varphi} = \text{const.}\,\varphi^{-1}, \tag{35}$$

i.e. the osmotic compressibility of gels changes proportionally to the reciprocal concentration.

For systems in Θ-state (the second term of series expansion of Eq. (20) predominates) we have

$$\left(\frac{\partial\varphi}{\partial\omega}\right) = \frac{3}{\frac{8}{3}RT\bar{V}_1^{-1}\varphi^2 + \omega\varphi^{-1}} \tag{36}$$

from which the following relationship can be deduced for the equilibrium with the pure solvent ($\omega = 0$):

$$\left(\frac{\partial\varphi}{\partial\omega}\right)_{\omega=0} = \frac{9}{8\,RT\bar{V}_1^{-1}\varphi^2} = \text{const.}\,\varphi^{-2}\,. \tag{37}$$

On the basis of scaling arguments, Eq. (32) gives for compressibility

$$\left(\frac{\partial\varphi}{\partial\omega}\right) = \frac{3}{\frac{kT}{N}\frac{6\nu+1}{3\nu-1}\left(\frac{\varphi}{\varphi_e}\right)^{\frac{1}{3\nu-1}} + \omega\varphi^{-1}} \tag{38}$$

from which we have for $\omega = 0$ [25]

$$\left(\frac{\partial\varphi}{\partial\omega}\right)\Big|_{\omega=0} = \frac{3}{\frac{kT}{N}\frac{6\nu+1}{3\nu-1}\left(\frac{\varphi}{\varphi_e}\right)^{\frac{1}{3\nu-1}}} = \text{const.}\,\varphi^{-\frac{1}{3\nu-1}}\,. \tag{39}$$

It may be seen that in good solvent conditions ($\nu = 3/5$) the exponent of concentration dependence is —5/4, while in Θ-conditions, in accordance with Eq. (37), —2.

It should be mentioned here, that there is a close correlation between the osmotic compressibility and the microscopic characteristics of the gel system. The ratio of the compressional modulus $\left[K = \varphi\left(\frac{\partial\omega}{\partial\varphi}\right)\right]$, obtainable from compressibility to the shear modulus can be expressed for gels in equilibrium with the pure solvent by microscopic Poisson ratio (p):

$$\frac{K(\varphi_e)}{E_G(\varphi_e)} = \frac{2(1+p)}{3(1-2p)} \tag{40}$$

The microscopic Poisson ratio exhibits the ratio of the deformations of the network chains in the transverse ($\Delta R_\perp$) and in the longitudinal ($\Delta R_{||}$) directions [26, 27]:

$$p = -\frac{\Delta R_\perp}{\Delta R_{||}}\,. \tag{41}$$

The microscopic Poisson ratio of ideal chains (Gaussian coils) is zero, because the projection of the coil along the three orthogonal directions are independent of one another. Thus, $K(\varphi_e) = \frac{2}{3}E_G(\varphi_e)$. Owing to the excluded volume effect, for real chains $p = \frac{1}{4}$ and $K(\varphi_e) = \frac{5}{3}E_G(\varphi_e)$.

Materials, gel preparation

Investigations were carried out on poly(vinyl acetate) (PVAc) gels. PVAc gels were prepared from poly(vinyl alcohol) (PVA) gels by complete acetylation in the gel phase [28, 29].

PVA of trade mark Kuraray Poval 420 (Kuraray Co. Japan) was used for the preparation of the gels. The acetate content of the commercial product was removed by hydrolysis with a mixture of 20 *v/v* % of methanol and 80 *v/v* % of water in the presence of excess sodium hydroxide, and the polymer was fractionated with *n*-propanol [30]. Thus, four fractions were prepared, which were dissolved again, and first their components of low, then of high relative molecular mass were removed. For further investigations the fractions of medium relative molecular mass were used. For the characterization of the fractions their viscosities were measured at 303 K. The concentration of the polymer solution was varied between 0.2 and 0.9 g/100 cm^3; the $\frac{\eta_{sp}}{c} - c$ function was found to be linear for all fractions. Table I contains the intrinsic viscosities of the fractions and the relative molecular masses calculated by equation [31]:

$$[\eta]_{303K} = 4.28 \times 10^{-4} \overline{M}_w^{0.64} \tag{42}$$

PVA gels were prepared by the cross-linking of solutions of 6, 9 and 12 m% concentration. Glutaric aldehyde (GDA, Merck, GFR) was used as cross-linking agent. From each of the three polymer concentrations, four gels characterized by different degree of cross-linking values were prepared. (Degree of cross-linking means the ratio of the quantities in mole of the monomer of the polymer and of the cross-linking agent.) Cross-linking reaction was

Table I

Intrinsic viscosity and relative molecular mass of the PVA fractions

Marking of fraction	$[\eta]_{303K}$ [100 cm^3/g]	$\overline{M}_w$
*I	0.26	22 300
II	0.45	52 600
III	0.70	102 700
IV	0.84	139 600
V	1.50	345 500

* Since Poval 420 practically did not contain polymers of $\overline{M}_w < 50\,000$ relative molecular mass, the fraction marked I was prepared in the same way as fractions II—V from a sample of trade mark Mowiol 4—88 (Hoechts, GFR)

carried out under isotermal conditions, at 298 ± 0.1 K, in a frame, suitable for the preparation of cylindrical specimens.

PVAc gels were prepared from PVA gels by complete acetylation in a mixture of pyridine—acetic acid—acetic anhydride. During this procedure, gels were kept in spherical flasks under reflux for 8 h at 363 K, using a fresh acetylating mixture each hour. In order to shift the equilibrium in the direction of acetate formation as far as possible, in the last three hours the acetic acid was omitted from the fresh mixtures. After completion of the acetylation the media of the gels was exchanged for acetone, toluene and isopropanol, respectively. The degree of conversion was checked by mass measurement. The solid content of PVAc gels was compared with that calculated from stoichiometry. An agreement was found within 1—2%. Moreover, the saponification number of PVAc gels was determined, which supported our previous results, i.e. that the acetate content of the gels is about 98—99%.

Methods

On all the systems mechanical (unidirectional compression) and equilibrium deswelling tests were carried out.

For the mechanical measurement an apparatus of own construction, described in detail in a previous paper [32] was used. In the case of unidirectional compression, the apparatus is suitable for the determination of force and deformation with an accuracy of ±0.1 mN and ±6 μm, respectively, in a wide range (from 0.1 mN to 2.0 N, and from 6 μm to 3.333 mm, resp.). The appratus is equipped with a thermostated sample holder, providing the study of mechanical properties of gels, under isothermal conditions. Investigations were carried out on cylindrical network specimens prepared in the gel pouring frame, in equilibrium with toluene, acetone and isopropanol, respectively. Mechanical measurements were evaluated by the Mooney–Rivlin equation [33, 34]:

$$\sigma = 2C_1(\Lambda_x - \Lambda_x^{-2}) + 2C_2(\Lambda_x - \Lambda_x^{-2})\,\Lambda_x^{-1}, \qquad (43)$$

where σ is the nominal stress (referring to the undeformed cross-section), C_1 and C_2 are constants characteristic of the system, and Λ_x is the macroscopic deformation ratio measured in the direction of the stress (e.g. in the case of compression in the direction of the x-axis $\Lambda_x = L_x/L_{Vx}$, where L_x is the length of the deformed sample, and L_{Vx} the length of the undeformed sample of volume V). During the deformation of the gels, the absence of volume change and barrel distortion, which would have been indicative of anisotropic stress distribution, was established.

Moreover, it became evident from the tests that for all the systems studied C_2 equals zero within the experimental error [29, 32].

The value of the constant $2C_1$ in Eq. (43) is equal to the numerical value of the shear modulus, because in the limiting case of $\Lambda_x = 1$, the relationship

$$E^\circ = \lim_{\Lambda_x \to 1} \left(\frac{\partial \sigma}{\partial \Lambda_x} \right) = \lim_{\Lambda_x \to 1} \frac{\partial}{\partial \Lambda_x} \left[2C_1 (\Lambda_x - \Lambda_x^{-2}) \right] = 6C_1 \qquad (44)$$

can be written for initial Young's modulus (E°). As by definition, $E^\circ = 3E_G$, the above statement directly follows from Eqs (43) and (44).

Mechanical tests were performed in each case on 3 gel cylinders prepared in an identical way, and the arithmetic mean of the 3 parallel measurements was used for evaluation. Reproducibility, including gel preparation, was found to be within 4—5%.

By the equilibrium deswelling method, the activity of the swelling agent within the gel was changed [35]. The method differs from deswelling techniques realized earlier as the gel and the liquid phase of known solvent activity is separated by a semipermeable membrane. The semipermeable membrane prevents the permeation of molecules used for lowering the activity of the swelling agent into the gel. Since at swelling equilibrium the activity of the diluent is identical in the gel and in the solution (or vapour) phase, this method makes possible the investigation of the characteristics of gel systems as a function of solvent activity. The adjustment of solvent activity was done by dissolving a polymer in the liquid phase, for which the relationship polymer concentration vs. solvent activity was known from independent measurements (e.g. from measurement of osmotic pressure). The fundamental condition of the applicability of the equilibrium deswelling method is that the molecules of the polymer should not diffuse through the semipermeable membrane. For the adjustment of activity, polystyrene (PS) was used in PVAc--toluene systems, and poly(vinyl acetate) in PVAc-acetone systems. The polymer solutions were dialyzed to remove the fraction of low relative molecular mass. Some characteristics of the dialyzed samples are summarized in Table II. The activity of the solvent was calculated from high-precision ($\pm 0.1\%$) osmotic pressure data [36], obtained for toluene and acetone solutions of similar polymer samples.

Table II

Some characteristics of the polymers used for the adjustment of the activity of the swelling agent

Marking of the sample	d_2 [gcm^{-3}]	$\bar{M}_n$	$\bar{M}_w$
PS	1.05	33 000	37 000
PVAc	1.17	122 000	130 000

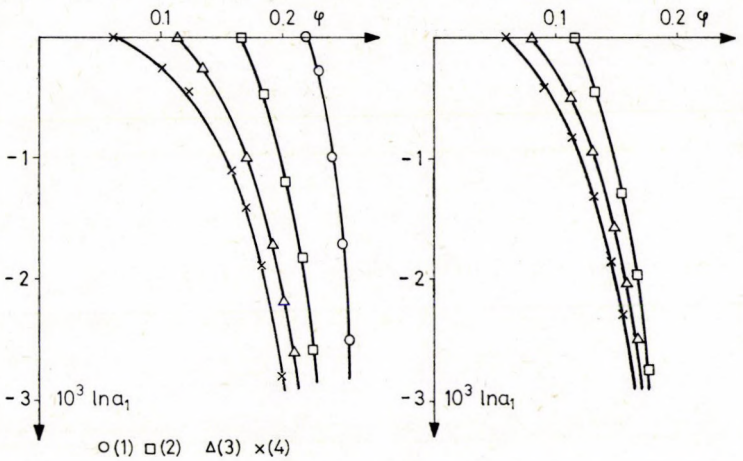

Fig. 1. $\ln a_1$ vs φ functions of PVAc — toluene (a) and PVAc — acetone (b) gels. Symbol of system: fraction V, degree of crosslinking: (1) 50; (2) 100; (3) 200; (4) 400

For $\ln a_1$ vs. φ functions determined by the equilibrium deswelling method some examples are shown in Fig. 1. Swelling pressure can be calculated from the $\ln a_1$ values by the following relationship:

$$-\omega\bar{V}_1 = RT \ln a_1 \tag{45}$$

It has been established that the swelling process is revertible for the systems investigated [35]. The reproducibility of these measurements was found to be within 2—3%.

On the PVAc—toluene and PVAc—acetone systems all the measurements were carried out at 298 ± 0.1 K. The force vs. deformation relation for PVAc—isopropanol gels was determined at 323 ± 0.1 K and at 343 ± 0.1 K.

Results and Discussion

The scaled form of the elastic modulus

It was indicated earlier that the thermodynamic properties of polymer solutions depend on the $\varphi N^{3\nu-1}$ universal quantity in a unique way. Furthermore it was shown that the shear modulus of the gels is analogous to the osmotic pressure of the solutions.

Using Eqs (12) and (19), scaled equation of state of des Cloiseaux can be written in the following general form:

$$EN^{3\nu} = f(\varphi N^{3\nu-1}) \tag{46}$$

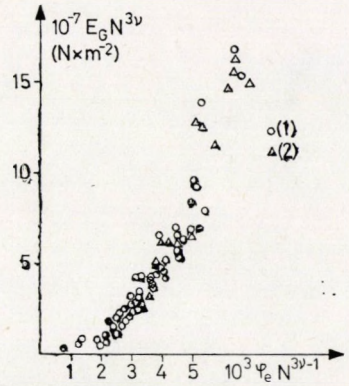

Fig. 2. Application of des Cloiseaux's equation to gel systems of various types in equilibrium with the pure solvent; (1) PVAc — toluene; (2) PS — benzene [37]

In Eq. (46) N means the degree of polymerization of the network chains connecting either chemical or physical cross-links. If only network chains connecting chemical cross-links are considered, then $\varphi_e > \varphi^*$, and the scaling function can be written in the form

$$f(\varphi N^{3\nu-1}) = (\varphi N^{3\nu-1})^{\frac{3\nu}{3\nu-1}} = \left(\frac{\varphi}{\varphi^*}\right)^{\frac{3\nu}{3\nu-1}}. \tag{47}$$

From Eqs (14) and (47) for the concentration dependence of the shear modulus of gels in equilibrium with the pure swelling agent one gets

$$E_G \cong \varphi_e^{\frac{3\nu}{3\nu-1}}. \tag{48}$$

Taking into consideration all the junction points in the system (both chemical and physical cross-links) $\varphi_e \cong \varphi^*$, and the argument of the scaling function become equal to 1, i.e.

$$E_G N^{3\nu} = f(1) = \text{const.} \tag{49}$$

From Eq. (49), using Eq. (14), we get Eq. (48) again. In Fig. 2, $E_G N^{3\nu}$ values of PVAc—toluene and PS—benzene gel homologues [37] are plotted as a function of $\varphi_e N^{3\nu-1}$. It can be seen that $\varphi_e N^{3\nu-1}$ is different for different gels, while scaling function (46) seems to be actually a universal power function [38].

Shear modulus of gels

Figure 3 shows, for PVAc gels in equilibrium with pure isopropanol ($a_1 = 1$), log E_G values as a function of log φ at 323 and 343 K. At 323 K isopropanol is nearly a Θ-solvent for PVAc, and at 343 K a good solvent. It can be seen that experimental points scatter at both temperatures along straight lines with slopes of 3.1 and 2.3, respectively. Exponents found experi-

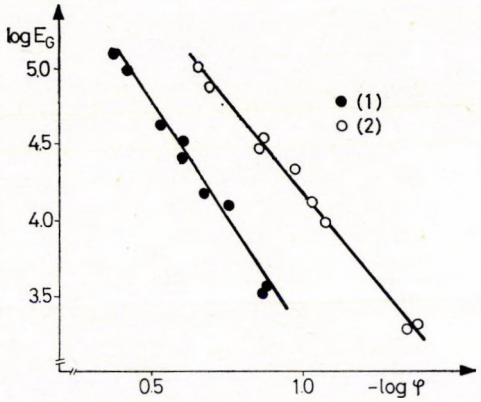

Fig. 3. Dependence of log E_G on log φ in PVAc — isopropanol gels [T: 323 K (1); 343 K (2)]

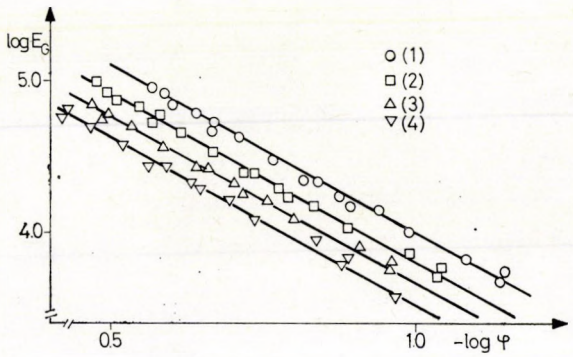

*Fig. 4.** log E_G vs. log φ functions of PVAc — toluene gels at fixed $\frac{\varphi}{\varphi_e}$ values $\left[\frac{\varphi}{\varphi_e}\right.$: 1.00 (1); 1.25 (2); 1.50 (3); 1.75 (4)]

mentally are in good agreement both with theoretical values relative to gels in Θ-state, and with Eq. (24) deduced for good solvent condition.

To investigate the validity of Eq. (25) derived for the concentration dependence of the shear modulus of gels in equilibrium with a swelling agent of arbitrary activity, in Fig. 4 the log E_G — log φ functions are plotted at fixed $\frac{\varphi}{\varphi_e}$ values, and in Fig. 5 the log E_G — log $\frac{\varphi}{\varphi_e}$ relations at fixed φ values. The slope of the straight lines is 2.38 and —1.89, close to the respective exponents (9/4 and —23/12), obtained for a good solvent on the basis of Eq. (25). The dashed lines in Fig. 4 connect points determined at different $\frac{\varphi}{\varphi_e}$ values for identical gel samples. The slope of the parallel lines is 0.34, in accordance with

* This figure has been redrawn erroneously. The correct figure will be published in the next issue as an errata.

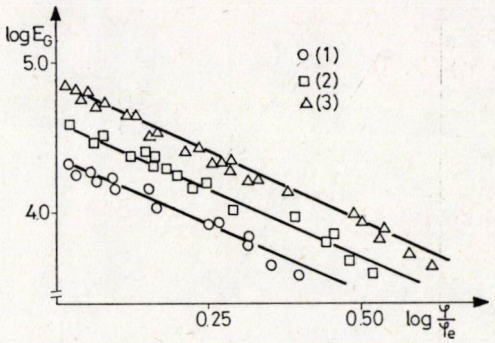

Fig. 5. log E_G vs. log $\frac{\varphi}{\varphi_e}$ functions of PVAc — toluene gels at fixed φ values [φ: 0.15 (1); 0.20 (2), 0,25 (3)]

relationship (18). Moreover, it can be established that experimental points lie along the same straight line, independently of the concentration of the initial polymer solution, of the degree of cross-linking and of the relative molecular mass of the polymer. This result supports that the exponent is really independent of the network topology in conformity with theory [22, 38].

Swelling pressure of gels

To decide whether Eq. (26) is suitable for the description of the properties of swollen gels, in Fig. 6 the log $(E_G + \omega)$ values of PVAc gels are plotted as a function of log φ. Experimental points pertinent to various gels scatter along the same straigth line, independently of the $\frac{\varphi}{\varphi_e}$ values. The slope of the straight line is 2.46, which is close to the exponent 9/4 predicted, that is to say, the concentration dependence of the osmotic pressure of the network

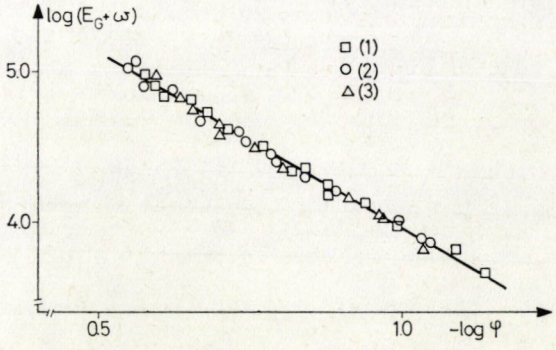

Fig. 6. log $(E_G + \omega)$ vs. log φ functions of PVAc — toluene gels $\left[\frac{\varphi}{\varphi_e}\right.$: 1.00 (1); 1.25 (2); 1.50 (3)$\left.\right]$

chains in the gel is the same as that of semi-dilute polymer solutions. The finding, that experimental points lie independently of $\frac{\varphi}{\varphi_e}$ along the same straight line, proves that in the case of swelling equilibrium only the quantities contained in Eq. (26) should be taken into consideration [22]. This result supports that $K_2 = 0$ in Eq. (7).

To establish the validity of Eq. (33) the $\frac{\omega}{E_G}$ values of various PVAc—toluene and PVAc—acetone gels are plotted in Fig. 7 as a function of $\frac{\varphi}{\varphi_e}$. The figure shows also the curves calculated on the basis of Eq. (33) using $\nu = 1/2$ and $\nu = 3/5$ values. It can be seen that experimental points scatter along the curve calculated with $\nu = 3/5$, systematic deviation cannot be observed for any type of systems. This experimental result proves that, independently of the chemical nature of the gel system studied, Eq. (33) expresses

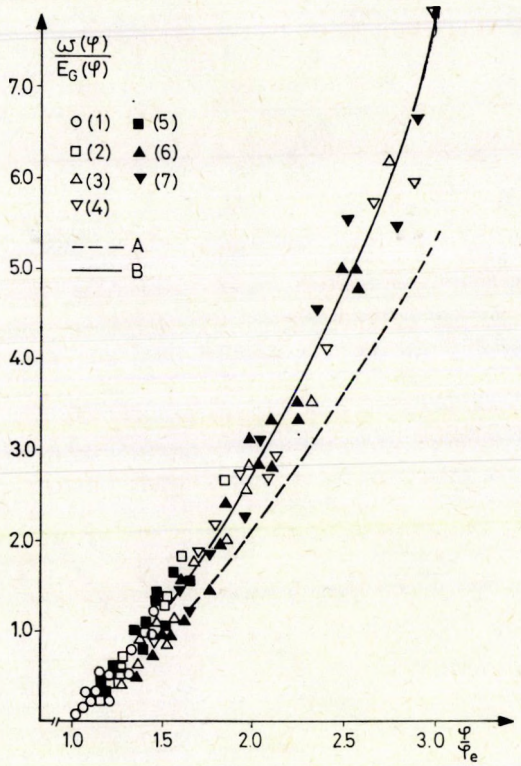

Fig. 7. $\frac{\omega}{E_G}$ vs. $\frac{\varphi}{\varphi_e}$ functions for various gel systems [PVAc — toluene: 50 (1); 100 (2); 200 (3), 400 (4) PVAc — acetone: 100 (5); 200 (6); 400 (7)]. The figure shows functions calculated on the basis of Eq. (30) (A) and (33) (B)

the relationship between polymer concentration and the most important macroscopic measurable quantities characteristic of gels: swelling pressure and shear modulus [22].

Compressibility of gels and the microscopic Poisson ratio

In Fig. 8 the osmotic compressibility of PVAc—toluene and PVAc—acetone gels, determined in equilibrium with the pure swelling agent ($a_1 = 1$) is plotted as a function of the volume fraction. $\left(\frac{\partial \varphi}{\partial \omega}\right)\Big|_{\omega=0}$ values were determined under consideration of Eq. (45) by the graphical differentiation of the experimental ln a_1 vs. φ functions (see Fig. 1). It can be seen from the figure that the exponent of concentration dependence is —1.4 for PVAc—toluene gels, and —1.1 for PVAc—acetone gels [25]. The exponent obtained experimentally approaches the value of —5/4, obtained for good solvent condition from Eq. (39). [According to the classical theory the exponent is —1, see Eq. (35).]

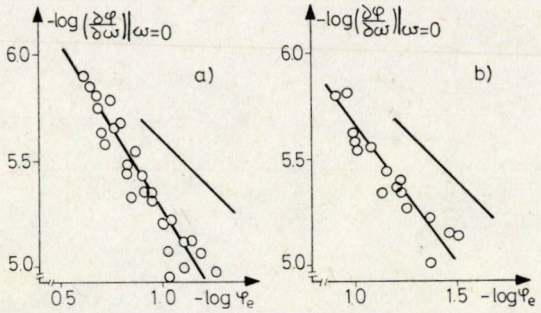

Fig. 8. Osmotic compressibility of PVAc gels as a function of equilibrium volume fractions ($\varphi = \varphi_e$, $\omega = 0$). a. PVAc — toluene; b. PVAc — acetone. The straight line of slope 1 in the figure is given by Eq. (35)

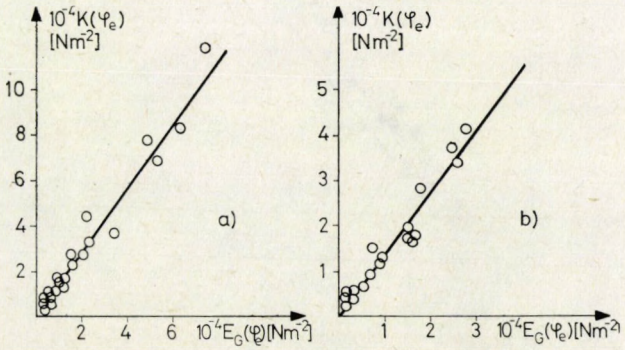

Fig. 9. Compressional moduli of PVAc gels as a function of shear moduli ($\varphi = \varphi_e$, $\omega = 0$); a. PVAc — toluene, b. PVAc — acetone

Figure 9 shows the compressional modulus of PVAc—toluene and PVAc—acetone gels as a function of shear modulus. It is noted that in both swelling agents there is a linear relationship between the moduli of two kinds. The slope of the straight line is 1.4, independently of the swelling agent. For the microscopic Poisson ratio 0.2 is obtained [25].

REFERENCES

[1] Flory, P. J.: Principles of Polymer Chemistry. Cornell University Press, Ithaca, New York 1953
[2] Dušek, K., Prins, W.: Fortschr. Hochpolym. Forschung, **6,** 1 (1969)
[3] James, H. M., Guth, E.: J. Polym. Sci., **4,** 153 (1949)
[4] Prins, W.: Physics of Noncrystalline Solids. J. A. Prins Ed., North-Holland 1965
[5] Wall, F. T.: J. Chem. Phys., **10,** 132 (1942)
[6] Hermans, J. J.: J. Polym. Sci., **59,** 191 (1962)
[7] Flory, P. J.: Proc. Roy. Soc. London, **A 351,** 351 (1976)
[8] James, H. M., Guth, E.: J. Chem. Phys., **11,** 455 (1943)
[9] James, H. M.: J. Chem. Phys., **15,** 651 (1947)
[10] Guth, E.: J. Polym. Sci. Pt. C, **12,** 89 (1966)
[11] Horkay, F., Nagy, M.: Acta Chim. Acad. Sci. Hung. (in press)
[12] Horkay, F., Nagy, M., Zrinyi, M.: 9th Europhysics Conference on Macromolecular Physics, Jablonna, Vol. **3C,** 125 (1979)
[13] Yamakawa, H.: Modern Theory of Polymer Solutions. Harper and Row, New York 1971
[14] de Gennes, P. G.: Rep. Progr. Phys., **32,** 187 (1969)
[15] de Gennes, P. G.: Phys. Lett., **38 A,** 339 (1972)
[16] Ma, S.: Modern Theory of Critical Phenomena, W. A. Benjamin Inc., London 1976
[17] de Gennes, P. G.: Scaling Concepts in Polymer Physics. Cornell University Press, Ithaca and London 1979
[18] Pfeuty, P., Toulouse, G.: Introduction to the Renormalization Group and to Critical Phenomena. John Wiley and Sons, London—New York—Sydney—Toronto 1977
[19] Stanley, H. E.: Introduction to Phase Transition and Critical Phenomena. Clarendon Press, Oxford 1971
[20] Le Guillon, J. C., Zinn-Justin, J.: J. Phys. Rev. Lett., **39,** 95 (1977)
[21] des Cloiseaux, J.: Phys. (Paris), **36,** 281 (1975)
[22] Horkay, F., Zrinyi, M.: 27th International Symposium on Macromolecules, Strasbourg, Vol. II. 714 (1981); Macromolecules, **15,** 1306 (1982)
[23] Treloar, L. R. G.: The Physics of Rubber Elasticity. Clarendon Press, Oxford 1975
[24] Zrínyi, M., Horkay, F.: Kémiai Közlemények (in press)
[25] Zrínyi, M., Horkay, F.: J. Polym. Sci., Polym. Phys. Ed., **20,** 815 (1982)
[26] Landau, L. D., Lifsic, E. M.: Elméleti fizika VII. Rugalmasságtan (Theoretical Physics VII, Elasticity) Tankönyvkiadó, Budapest 1974
[27] Geissler, E., Hecht, A. M.: Macromolecules, **13,** 1276 (1980)
[28] Horkay, F., Nagy, M.: Polymer Bulletin, **3,** 457 (1980)
[29] Horkay, F., Nagy, M., Zrínyi, M.: Acta Chim. Acad. Sci. Hung., **108,** 287 (1981)
[30] Horkay, F., Nagy, M.: Acta Chim. Acad. Sci. Hung., **108,** 111 (1981)
[31] Matsumoto, M., Ohyanagi, Y.: Kobunshi Kagaku, **17,** 17 (1960)
[32] Horkay, F., Nagy, M., Zrínyi, M.: Acta Chim. Acad. Sci. Hung., **103,** 387 (1980)
[33] Mooney, M.: J. Appl. Phis., **11,** 582 (1940)
[34] Rivlin, R. S.: Phil. Trans. Roy. Soc., **A 241,** 379 (1948)
[35] Nagy, M., Horkay, F.: Acta Chim. Acad. Sci. Hung., **104,** 49 (1980)
[36] Vink, H.: Europ. Polym. J., **10,** 149 (1973)
[37] Munch, J. P., Candau, S., Herz, J., Hild, G.: J. Phys. (Paris), **38,** 971 (1977)
[38] Zrínyi, M., Horkay, F.: Polymer Bulletin, **3,** 665 (1980)
[39] Horkay, F., Zrinyi, M.: Polymer Bulletin, **4,** 361 (1981)

Acta Chimica Hungarica 114 (3—4), pp. 283—292 (1983)

EFFECT OF SURFACE MODIFICATION ON IMMERSIONAL WETTING OF ORGANOPHILIC KAOLINITE AND ILLITE DERIVATIVES

I. DÉKÁNY[1]*, F. SZÁNTÓ[1] and W. RUDZINSKI[2]

([1]Department of Colloid Chemistry, Attila József University, H-6720 Szeged, Aradi Vértanúk tere 1. and [2]Department of Theoretical Chemistry, Institute of Chemistry UMCS, 20—031 Lublin, Nowotki 12, Poland)

Received November 22, 1982
Accepted for publication January 4, 1983

Heats of immersion of various kaolinite and illite derivatives in benzene and methanol are reported. The derivatives were obtained from appropriate pure materials organophilized to a systematically increasing extent with hexadecylpyridinium chloride. The immersional data were analyzed next quantitatively, using a simple adsorption model involving the concept of energetic heterogeneity of the unmodified adsorption sites. Our analysis shows, that the measurements of heats of immersion may provide a very valuable information about the nature of solid surfaces.

Introduction

In our previous papers [1—4], we have described the preparation of vaious organophilic adsorbents from the pure Na-kaolinite, and the pure Na-illite. These organocomplexes were prepared from appropriate pure materials organophilized to a systematically increasing extent with hexadecylpyridinium chloride (HDPCl). Then, we have investigated their adsorptive properties with respect to various binary liquid mixtures. To this purpose, their excess adsorption isotherms have been measured, and then analyzed in terms of the adsorption theories developed by Schay and Nagy [5—7].

A simple adsorption model has been proposed, assuming that the organophilized samples contain two types of adsorption sites, their mutual proportion being dependent upon the degree of the chemical modification by HDPCl [8—10]. These adsorption sites were assumed to be distributed randomly on the modified surfaces, leading to what we have called — the "mosaic structure", of the organophilized surfaces.

We have thought, however, that this simple model needed further investigation and refinement. To this purpose, we have performed additional calorimetric studies showing how the degree of surface modification influences the heats of immersion in various pure solvents.

* To whom correspondence should be addressed

Having these experimental data measured, we have refined our original adsorption model by introducing the concept of a surface heterogeneity of the originally existing, unmodified adsorption sites. On the ground of the refined model, we are able of explain quantitatively the dependence of the heat of immersion of a modified sample, on the degree of its surface modification by HDPCl.

Theory

The heat of wetting of a solid surface Q_w into a single liquid is composed of two terms: A work term W associated with the formation of a semi-infinite liquid bulk phase, and a potential term ε associated with the external potential field created by the semi-infinite solid phase, and imposed on the surface molecules of the immersional liquid.

$$Q_w = W + \varepsilon \tag{1}$$

The term ε can, to a good approximation, be identified with the "adsorption energy" [11]. This adsorption energy is composed from the negative value of a local minimum of the solid-liquid interaction potential $(-U_0)$ and the lowest quantum-mechanical vibrational energy level in the surface phase E_v°. Usually, the contribution from $(-U_0)$ is much bigger than that given by E_v°.

The term W can be interpreted using lattice models of the liquid phase [11]. The potential field created by the solid phase, in general, causes some perturbation in the structure of the surface liquid, compared with its bulk structure. These perturbations obviously depend on the strength of this potential field, and therefore on the value of the adsorption energy ε. Therefore, the term W is also slightly dependent on the adsorption energy value ε. However, we neglect this small effect, in comparison to another much more important one.

This is the dispersion of the adsorption energy ε on various adsorption sites, due to the well-known structural defects, and local variations, in the chemical composition. This effect is known in literature as the "effect of surface heterogeneity" in the physical adsorption on the really existing solid surfaces. The generally accepted, quantitative measure of this dispersion, is the so-called "adsorption energy distribution". Strictly speaking, it is the differential distribution of the adsorption sites among various values of the adsorption energy $\chi(\varepsilon)$. This energy distribution function is used usually in its form normalized to unity.

$$\int_\Omega \chi(\varepsilon)\, d\varepsilon = 1 \tag{2}$$

where Ω is the domain of the variable ε. For some obvious physical reasons it should be a closed interval or a set of such intervals. However, for the purpose of mathematical convenience it is often accepted that Ω is the interval $(0, +\infty)$ [12]. The correct choice of the upper integration limit ε_{max} has no great effect on the results of a theoretical analysis of adsorption data, except for the region of very low surface concentrations of adsorbate [13]. At the same time, a correct choice of the lower integration limit ε_{min} is essential for both the region of very high and moderate surface concentrations. Therefore, for the purpose of our present work, we will accept $(\varepsilon_{min}, +\infty)$ as the domain of the variable ε.

The formation of the really existing solid surfaces is influenced by many independent physical factors, acting during the preparation of an adsorbent. It seems, therefore, reasonable to assume that the distribution of the adsorption energy $\chi(\varepsilon)$ should be a gaussian-like one. We approximate it here by the following gaussian-like function

$$\chi(\varepsilon) = \frac{C_N \frac{1}{c} \exp\left(\frac{\varepsilon - \varepsilon_0}{c}\right)}{\left[1 + \exp\left(\frac{\varepsilon - \varepsilon_0}{c}\right)\right]^2} \tag{3}$$

where ε_0 is the most probable value of the adsorption energy ε, c is the heterogeneity parameter describing the spread of this energy distribution, whereas C_N is the normalization factor,

$$C_N = 1 + \exp\left(\frac{\varepsilon_{min} - \varepsilon_0}{c}\right). \tag{4}$$

When $c \to 0$, the function (3) degenerates into the Dirac delta distribution $\delta(\varepsilon - \varepsilon_0)$, describing the energy distribution on a hypothetical homogeneous surface characterized by the adsorption energy $\varepsilon = \varepsilon_0$.

Thus, in the case of immersion of a real solid sample into a single liquid, the heat of immersion Q_w is given by the following average Q_{wt},

$$Q_{wt} = W + N_0^s \int_{\varepsilon_{min}}^{\infty} \varepsilon\chi(\varepsilon)\, d\varepsilon \tag{5}$$

where N_0^s is the capacity of the adsorbed phase. Now, let us consider the case of a partially modified surface.

This is the case when a part of the originally existing adsorption sites is modified by the chemically adsorbed organic modifier. We refer further to the originally existing adsorption sites as OS (Original Sites), and to the chemically modified ones as MS (Modified Sites).

We assume yet that the chemisorption of the organic modified (HDPCl) is running in an ideally stepwise fashion. We mean, the OS sites are modified in the sequence of decreasing chemisorption energies of the organic modifier. Assuming, in addition, that the difference of the adsorption energy ε, and the chemisorption energy of the organic modified is the same on all the sites, the chemisorption process can be depicted as shown in Figure 1.

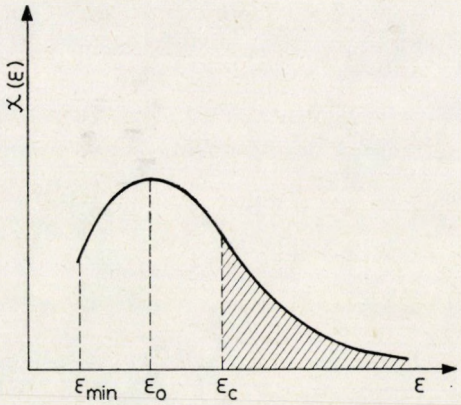

Fig. 1. A schematic representation for the process of the chemical modification of kaolinite and illite — surfaces by HDPCl. The shadowed area corresponds to the modified surface Θ_2

It means, at a given chemisorbed amount of HDPCl, the adsorption sites having an adsorption energy ε greater than ε_c (a certain "critical" value) are totally modified, whereas the other ones are free, i.e., uncovered by the molecules of the chemical modifier. This picture of adsorption is known for a long time in adsorption literature as "Condensation Approximation".

Let Θ_2 be the fraction of the chemically modified surface, i.e., the fraction of the MS sites. It is given by the following equation,

$$\Theta_2 = \int_{\varepsilon}^{\infty} \chi(\varepsilon)\, \mathrm{d}\varepsilon = C_N \left[1 + \exp\left(\frac{\varepsilon_c - \varepsilon_0}{c}\right)\right]^{-1}. \tag{6}$$

The chemically modified sites should exhibit a fairly identical interaction with the molecules of the immersional liquid. This modification process, like silanisation, esterification and similar processes are used for a long time to obtain homogeneous surfaces.

Let ε_{MS} denote the adsorption energy on the MS sites. Then, the heat of immersion of a partially modified surface will be given by,

$$Q_{wt} = W + N_0^s \Theta_2 \varepsilon_{MS} + N_0^s \int_{\varepsilon_{min}}^{\varepsilon_c} \varepsilon \chi(\varepsilon)\, \mathrm{d}\varepsilon \tag{7}$$

After performing the integration, we obtain:

$$Q_{wt} = W + \Theta_2 N_0^s \varepsilon_{MS} + \\ + N_0^s C_N \left\{ \frac{\varepsilon_{min}}{1 + \exp\left(\frac{\varepsilon_{min} - \varepsilon_0}{c}\right)} - \frac{\varepsilon_c}{1 + \exp\left(\frac{\varepsilon_c - \varepsilon_0}{c}\right)} + \right. \\ \left. + c \ln\left[1 + \exp\left(\frac{\varepsilon_c - \varepsilon_{min}}{c}\right)\right] - c \ln\left[1 + \exp\left(\frac{\varepsilon_0 - \varepsilon_c}{c}\right)\right] \right\}. \quad (8)$$

Let us remark, that according to eqn. (6),

$$\varepsilon_c = \varepsilon_0 + c \ln\left(\frac{C_N}{\Theta_2} - 1\right) \quad (9)$$

and, therefore, eqn. (8) can be rewritten to the following simple form,

$$Q_{wt} = Q_{w0} + \Theta_2 N_0^s (\varepsilon_{MS} - \varepsilon_0) + Q_{wh} \quad (10)$$

where Q_{w0} is the heat of immersion of an original unmodified sample,

$$Q_{w0} = W + N_0^s C_N \left\{ \frac{\varepsilon_{min}}{1 + \exp\left(\frac{\varepsilon_{min} - \varepsilon_c}{c}\right)} + \right. \\ \left. + c \ln\left[1 + \exp\left(\frac{\varepsilon_0 - \varepsilon_{min}}{c}\right)\right] \right\} \quad (11)$$

and Q_{wh} is the contribution to Q_{wt} due to the energetic heterogeneity of the originally existing adsorption sites.

$$Q_{wh} = cN_0^s \left[(C_N - \Theta_2) \ln (C_N - \Theta_2) - C_N \ln C_N + \Theta_2 \ln \Theta_2\right]. \quad (12)$$

When the surface of the original sample is homogeneous (i.e. $c \to 0$), this heterogeneity contribution vanishes. The second term in eqn. (10) represents the heat of immersion of a homogeneous sample characterized by the adsorption energy ε_0, and modified chemically up to the relative coverage Θ_2.

Experimental

In our experimental work the $d \leq 2$ μm fine fraction of Na-kaolinite and Na-illite was used in the sorption measurements. According to X-ray diffraction measurements these samples show the characteristic reflections of pure minerals.

The organocomplexes of clay minerals were produced by the ion-exchange reaction with hexadecylpyridinium chloride (HDPCl). The amounts of surfactant bound on the surface of kaolinite and illite are shown in Table I. In our earlier studies we have already described the methods for the production of these organocomplexes [1—3]. The HDP-kaolinite III and the HDP-illite IV organocomplexes were further modified by anionic surfactant adsorption in order to get total organophilicity (maximal surface modification), because the anionic surfactants bound on the edge of layer silicates [4]. In this way entirely organophilic HDP—DS-kaolinite and HDP—DS-illite organocomplexes were produced by sodium-dodecylsulfate NaDS (Table I). The determination of the adsorption capacity of the adsorbents (N_0^s) was carried out in pure methanol and benzene from the methanol-benzene excess isotherms according to Schay and Nagy [5—7].

The specific enthalpy of immersion (q_w) was determined in methanol and benzene using an LKB 2107 sorption microcalorimeter at 298 $\pm$ 0.02 K. In Table I the molar enthalpies of immersion (Q_{wt}) are given where $Q_w = q_w/N_0^s$, where N_0^s is the adsorption capacity for pure component. The term (Θ_2) has already been introduced by us to denote the fraction of the surface modified by HDP-cation [8, 9, 10]. In our previous works it has already been established that in the case of the adsorption of methanol(1)-benzene(2)mixture the methanol is adsorbed preferentially on the free silicate surface, while the preferential adsorption of benzene can be noticed on the apolar surface parts covered with the surfactant. There is a wide concentration range, and therefore the adsorption capacities n_1^s and n_2^s can be determined from the adsorption excess isotherms using a graphical extrapolation method. Knowing these

Table I

The heat of immersion on kaolinite and illite organocomplexes in methanol and benzene

Adsorbent	HDP+ -cation mmol/g	Θ_2	Q_{wt} (in methanol) J/mmol	Q_{wt} (in benzene) J/mmol
kaolinite	0	0	9.09	3.09
kaolinite (extracted with methanol)	0	0.39	3.30	3.20
HDP-kaolinite I.	0.024	0.64	1.24	3.30
HDP-kaolinite II.	0.035	0.68	1.09	3.35
HDP-kaolinite III.	0.044	0.72	0.95	3.39
HDP-DS-kaolinite	0.044	0.95	0.64	3.52
	0.014*			
illite	0	0	12.26	3.57
illite (extracted with methanol)	0	0.23	7.53	3.75
HDP-illite I.	0.097	0.57	2.87	4.64
HDP-illite II.	0.139	0.66	2.33	4.70
HDP-illite III.	0.171	0.73	2.28	4.95
HDP-illite IV.	0.233	0.78	2.16	5.29
HDP-DS-illite	0.233	0.81	1.91	5.25
	0.016*			

* DS-anion

capacities the Θ_2 value can easily be calculated according to the equation [10]:

$$\Theta_2 = \frac{n_2^s a_{m,2}}{n_1^s a_{m,1} + n_2^s a_{m,2}}$$

where $a_{m,1}$ and $a_{m,2}$ are the cross-sectional areas of component 1 and 2, respectively.

Results and Discussion

From eqn. (10), it is obvious that the following three parameters determine the shape of the function $Q_{wt}(\Theta_2) : N_0^s(\varepsilon_{MS} - \varepsilon_0)$, cN_0^s and C_N. Thus, we treated these parameters as best fit parameters, while fitting eqn. (10) to the experimental data for Q_{wt} presented in Table I. Appropriate numerical calculation yields the values of these parameters which are compiled in Table II. Since the value of N_0^s was known from the independent adsorption experiment, we were able to list the values: $(\varepsilon_{MS} - \varepsilon_0)$, c, and C_N.

Using these best-fit parameters, we have evaluated next the theoretical curves $Q_{wt}(\Theta_2)$ for all four immersional systems investigated by us. In Figs 2 and 3 the agreement is shown between the theoretical curves and the related experimental data. We are ready to believe that this agreement provides a good support for the adsorption model accepted in our theoretical analysis. In Figs 4 and 5, the heterogeneity contribution Q_{wh} is shown separately for all the immersional systems. Now, we are going to consider the reported results in more detail:

Let us consider first the systems kaolinite derivatives/benzene. The positive value of $(\varepsilon_{MS} - \varepsilon_0)$ indicates that most of the originally existing sites show weaker interactions with benzene molecules than the chemically modified sites. Further, the small value of c suggests that the original adsorption

Table II

Immersional liquid	N_0^s mmol/g	C_N	c J/mmol	$(\varepsilon_{MS} - \varepsilon_0)$ J/mmol
	Kaolinite derivatives			
Benzene	0.97	2.25	0.056	0.51
Methanol	1.83	2.00	3.01	−0.55
	Illite derivatives			
Benzene	0.97	2.25	0.135	2.26
Methanol	1.85	2.50	3.36	−0.82

sites exhibit very similar features when interacting with benzene molecules. Therefore, the heterogeneity contribution Q_{wh} is very small in these systems.

The situation becomes dramatically different when the kaolinite derivatives are immersed in methanol. There, the originally existing sites show a variety of interactions with methanol molecules, but most of them exhibit stronger interactions with methanol molecules than the modified sites.

Similar observations can be made in the case of illite derivatives immersed in benzene and methanol. Here, however, the original sites exhibit much weaker

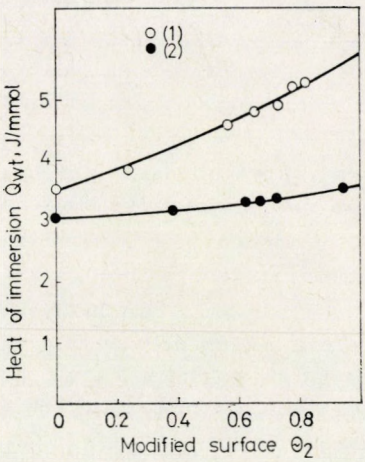

Fig. 2. The change of the heat of immersion Q_{wt} in benzene, with the degree of the chemically modified surface Θ_2; (1) — illite derivatives, (2) — kaolinite derivatives

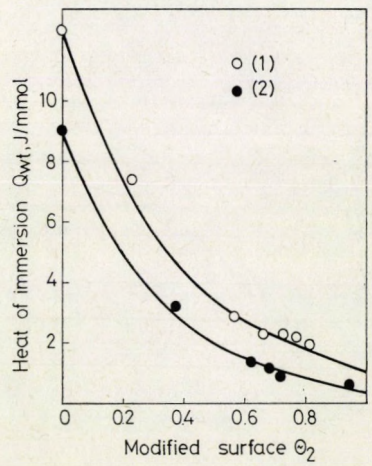

Fig. 3. The change of the heat of immersion Q_{wt} in methanol, with the degree of the chemically modified surface Θ_2: (1) — illite derivatives, (2) — kaolinite derivatives

interactions with benzene molecules, and somewhat stronger interactions with methanol molecules, compared to kaolinite derivatives. Further, the scatter of adsorption energy ε on the original sites is here much greater for both benzene and methanol molecules.

We feel, that drawing more detailed conclusions would be risky at the present stage of our experimental and theoretical investigation. However,

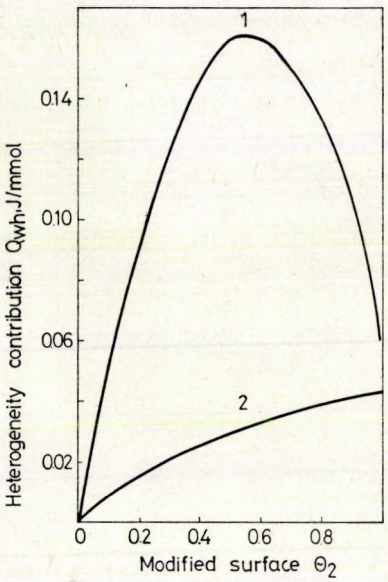

Fig. 4. The heterogeneity contribution Q_{wh} in the case of immersion in benzene: (1) — illite derivatives, (2) — kaolinite derivatives

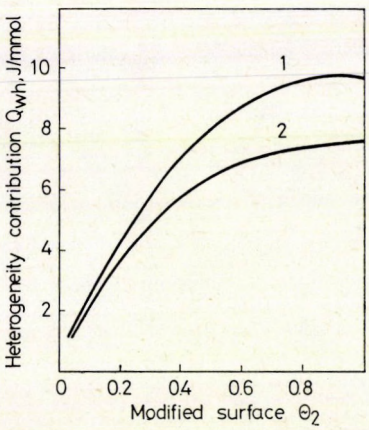

Fig. 5. The heterogeneity contribution Q_{wh} in the case of immersion in methanol: (1) — illite derivatives, (2) — kaolinite derivatives

even the already obtained results show, that measurement of the heats of immersion and the sorption data may be a very valuable source of information about the nature of adsorption systems.

REFERENCES

[1] Dékány, I., Szántó, F., Nagy, L. Gy.: Magyar Kémiai Folyóirat, **82,** 491 (1976)
[2] Dékány, I., Szántó, F., Nagy, L. Gy.: Colloid and Polymer Sci., **256,** 150 (1978)
[3] Dékány, I., Szántó, F., Nagy, L. Gy.: Progr. Colloid and Polymer Sci., **65,** 125 (1978)
[4] Dékány, I., Szántó, F., Nagy, L. Gy.: Magyar Kémiai Folyóirat (in press)
[5] Schay, G.: in "Surface Area Determination", Proc. Int. Symp. 1969, p. 273, London 1970
[6] Nagy, L. Gy., Schay, G.: Acta Chim. Acad. Sci. Hung., **39,** 365 (1963)
[7] Schay, G., Nagy, L. Gy.: J. Colloid and Interface Sci., **38,** 302 (1972)
[8] Dékány, I., Nagy, L. Gy., Schay, G.: Magyar Kémiai Folyóirat, **84,** 333 (1978)
[9] Dékány, I., Nagy, L. Gy.: Acta Phys. et Chem. Szeged Hung., **23,** 485 (1977)
[10] Dékány, I., Nagy, L. Gy., Schay, G.: J. Coll. Interface Sci., **66,** 197 (1978)
[11] Lane, J. E.: Aust. J. Chem., **21,** 827 (1968)
[12] Sips, R.: J. Chem. Phys., **16,** 490 (1948); **18,** 1024 (1950)
[13] Rudzinski, W., Jagiello, J.: J. Low. Temp. Physics, **45,** 1 (1981)

Acta Chimica Hungarica 114 (3—4), pp. 293—300 (1983)

HETEROCYCLIC COMPOUNDS, IV*

STRUCTURE OF THE SALTS OF 1-(3,4-DIMETHOXYPHENYL)-7,8-DIMETHOXY-5-ETHYL-4-METHYL-5*H*-2,3-BENZODIAZEPINE

A. NESZMÉLYI[1], T. LÁNG[2]** and J. KŐRÖSI[2]

([1]Central Research Institute for Chemistry, Hungarian Academy of Sciences, H-1025 Budapest, Pusztaszeri u. 59—67 and [2]Institute for Drug Research, H-1045 Budapest, Szabadságharcosok u. 47—49.)

Received July 26, 1982
Accepted for publication January 18, 1983

1-(3,4-Dimethoxyphenyl)-7,8-dimethoxy-5-ethyl-4-methyl-5*H*-2,3-benzodiazepine (**1**), a representative of 1-aryl-5*H*-2,3-benzodiazepines, is a weak base and — even from an excess of strong protonic acids — can only bind one proton, notably on the N-3 atom. In contrast with the free base, the equilibrium concentrations of the conformers of the salts are attained immediately after dissolution.

Two of the present authors have reported earlier [1] that the first representative of the 5*H*-2,3-benzodiazepine group synthesized by them, 1-(3,4-dimethoxyphenyl)-7,8-dimethoxy-5-ethyl-4-methyl-5*H*-2,3-benzodiazepine (**1**), is only monoprotonated by inorganic acids, even if the latter are present in excess;*** no salt is formed with acetic acid, and the only aliphatic alcohol giving an adduct is methanol.

To decide which of the two N-atoms binds the proton, we prepared a series of **1**-salts (**2a—e**) and studied them by ^{1}H- and ^{13}C-NMR spectroscopy. Comparison of the chemical shifts of the proton multiplets in the spectra of **2a** and **2e** with that of **1** [2] has shown that both the multiplicities of the line groups and the chemical shifts are closely similar, and there is only a single new signal appearing. This broad signal corresponding to one proton in intensity, adsorbs at δ 13.2 and can be assigned to a $\overset{\oplus}{\text{N}}\text{H}$ function.

The two conformers of **1**, studied in detail [2], can also be detected in the salts of **1**; however, in the latter cases the equilibrium concentrations of the conformers are less different and the difference in the conformational energy is also less, about 0.5 kcal/mol. While -- owing to the higher potential barrier — one must wait for 10—12 hours at 25 °C until the steady-state equilibrium of **1** is established, equilibrium is reached immediately after dissolution in the case of the salts.

* Part III: G. Zólyomi et al.: Chem. Ber., **107**, 3904 (1974)
** To whom correspondence should be addressed
*** The same was experienced with numerous 1-aryl-5*H*-2,3-benzodiazepines synthesized recently

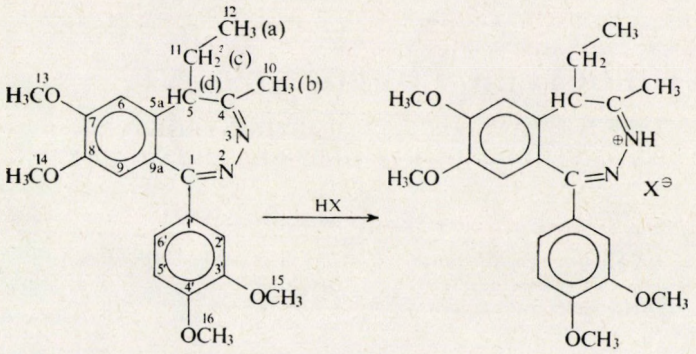

2	X
a	Cl
b	Br
c	HSO_4
d	SCN
e	ClO_4

1 2a-e

According to the literature [3], chemical shifts of adjacents protons and —C— atoms of quaternary N-atoms exhibit paramagnetic shifts. Based on the data in Table I one can conclude that in **2a—e** the proton should be assigned to the N-3 atom.

The same conclusion can be drawn from determining the structure of the compounds obtained by quaternization with methyl iodide. From the methiodide **3** one obtains with aqueous NaOH [4], through water addition to the

Table I

^{1}H and ^{13}C chemical shifts in the vicinity of the N*-atoms in* **1** *(cf. Part* II [2]*),* **2a** *and* **2e** *in* $CDCl_3$; *internal standard* TMS

Mark of H atom	1		2a		2e	
Number of C atom	δ[ppm][a)]	δ[ppm][b)]	δ[ppm][a)]	δ[ppm][b)]	δ[ppm][a)]	δ[ppm][b)]
a	1.10 (t)	0.85	1.15	0.90	1.18	0.92
b	1.97 (s)[e)]	2.15	2.35[e)]	2.65	2.22	2.48
c	2.13 (qui)	1.57	2.30	1.70	2.35	1.60
d	2.79 (t)	3.40	2.88	3.50	3.00	3.65
12	12.40	12.87	12.17	12.31	121.12	12.12
10	17.53	25.56	17.45	24.87	17.89	25.45
11	19.88	18.68	19.54	19.67	19.64	20.62
5	46.21	54.50	47.18	53.75	48.34	53.96
4	156.2[d)]	156.4	171.0[d)]	173.3	173.3	175.9
1	156.9[c)]	157.3	166.3[c)]	167.5	166.8	167.7

[a)] Prevalent conformer [b)] Minor conformer. [c)] $\delta_{2a} - \delta_1 = 0.38$ ppm. [d)] $\delta_{2a} - \delta_1 = 14.8$ ppm. [e)] $\delta_{2a} - \delta_1 = 9.4$ ppm

non-isolable compound **4**, the compounds **5** $\rightleftharpoons$ **5'**. In solution (^{1}H-NMR spectrum) the tautomers **5** and **5'** appear in the ration 1 : 1; in the mass spectrum the strongest peak corresponds to the ion $m/z = 369$, formed by loss of $\cdot NH—NH—CH_3$.

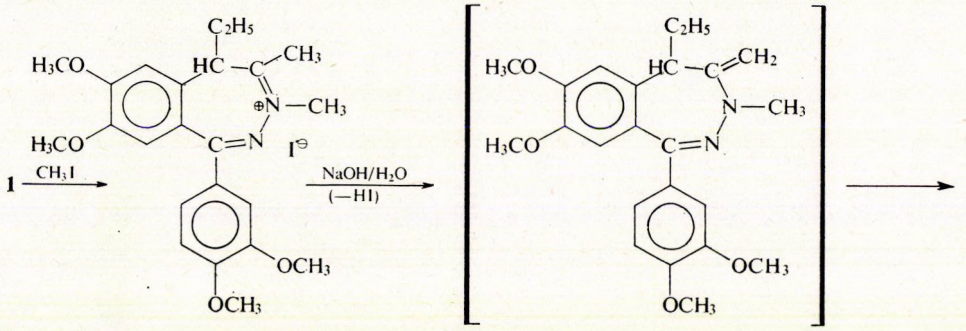

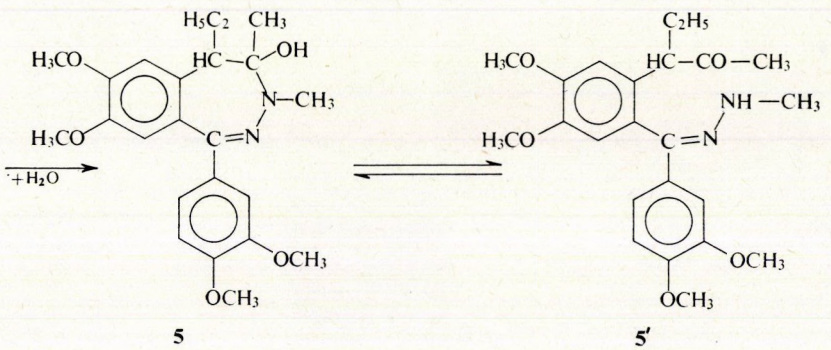

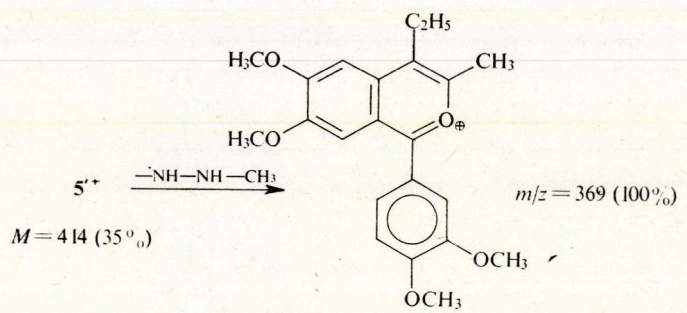

To elucidate the structure of **2a—e**, we used the well-known 3,5,7--triphenyl-4*H*-1,2-diazepine **6** [5—8] as a model compound for salt formation. As expected, it was found that no hydrochloride could be prepared from **6**

owing to the phenyl groups on the C atom adjacent to the N atom, while the perchlorate **7** was readily obtainable.

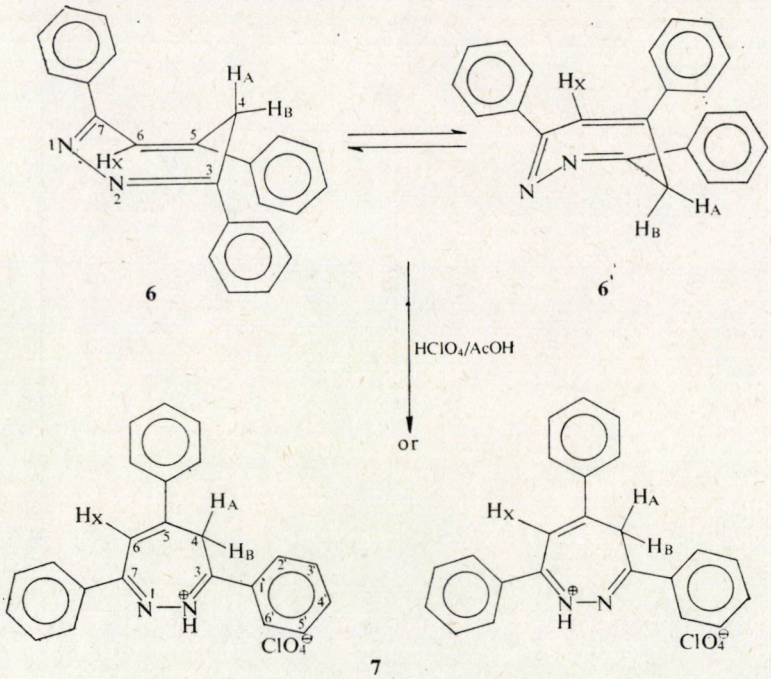

In **6**, there are two protons in the $\delta = 2$—5 ppm range, both firmly coupled and giving an AB quartet ($J = 12.4$ Hz); this can be assigned to the protons geminally coupled with the sp^3-hybridized C-atom, while the differing chemical shifts indicate the non-equivalent positions of these protons *(endo-exo* positions), evidencing the presence of the **6**⇌**6'** conformers [6—8]. The energy barrier $\Delta G^{\ddagger}$ of the inversion of the seven-membered rings in **6**⇌**6'** is about 17.5 kcal/mol [7, 8]; the corresponding value for 2,5,6,7--tetrasubstituted 4*H*-1 2-diazepines exceeds 22 kcal/mol [9], for cycloheptatriene it is around 6.1 kcal/mol [9], for 2-anilino-3*H*-azepine 10.2 ± 0.4 kcal/mol [10], and for 2-R-4-R'-3*H*-1,5-benzodiazepines it is about 11—13 kcal/mol [10].

A broad signal is observed at $\delta = 4.1$ ppm in the ^{1}H-NMR spectrum of compound **7**; its intensity corresponds to that of a two-proton signal, and it becomes sharper with rising temperature. In terms of conformational analysis this implies the presence of a coalescence phenomenon. At lower temperatures the chemical shifts of these protons differ *(exo-endo)*. Salt formation — similarly to salt formation from **1** — results in increased flexibility of the seven-membered ring and, accordingly, the potential barrier between the

Table II

^{1}H and ^{13}C chemical shifts of **6** *(in* $CDCl_3$*) and* **7** *(in* DMSO-d_6*); internal standard* TMS

Mark of H atom	**6**[a]	**7**	$\delta_7-\delta_6$
Number of C atom	δ[ppm]	δ[ppm]	Δδ[ppm]
H_B *(endo)*	2.63 (d, d)	4.1[b] (d)	
H_A *(exo)*	4.42 (d, d)		
H_X (vinyl proton)	6.68 (t)	7.25	0.57
Ar—H	7.17—8.17 (m)	7.30—8.17	∅
⊕ NH	—	9.7[b] (s)	—
4	32.59	34.02	1.43
6	116.50	117.94	1.44
2', 3', 5', 6'	127.08—128.65	128.81—129.21	~1.6
4'	129.12, 129.27, 129.61	131.44, 131.95, 131.95	~2.3
1'	134.83, 136.67, 138.06	132.70, 134.19, 135.50	~2.4
3,5,7	144.42, 147.70, 155.33[c]	149.66, 154.10, 160.25[c]	2—10

[a] ^{1}H-NMR data from [7]. [b] Concentration dependent. [c] Not assigned

two conformers becomes significantly lower. In the spectrum of **7**, the third proton of the heterocycle (H_X) also appear at $\delta = 7.25$ ppm, being readily discernible from the aromatic signal. The signals structure of the aromatic protons is less expressed in **7** than in **6**, indicating that conformational transitions are faster. The compound 1-acetyl-3,5,7-triphenyl-1*H*-1,2-diazepine, obtained by acetylation of **6** [11], evidently provides no possibility to decide to which N-atom the proton is bound in **7**.

The chemical shifts of **6** and **7** measured in ^{1}H-NMR and ^{13}C-NMR are presented in Table II.

Experimental

M.p.'s are uncorrected. The instruments used were Unicam SP 800 for UV spectra; Perkin-Elmer 577 for IR spectra (in KBr pellets); Varian A-60D and Jeol-C-60 spectrometers for ^{1}H-NMR, Varian-XL-100-15-FT spectrometer for 100 MHz-^{1}H-NMR and 25 MHz-^{13}C-NMR spectra. Chemicals shifts are given relative to TMS internal standard ($\delta = 0$ ppm). Varian MAT-SM-1 was used for mass spectrometry.

1-(3,4-Dimethoxyphenyl)-7,8-dimethoxy-5-ethyl-4-methyl-5*H*-2,3-benzodiazepine · HCl (2a)

(*a*) To a solution of **1** (20 g; 52 mmol) [1, 2] in hot methanol (105 mL) *conc.* hydrochloric acid (5.5 mL; 68 mmol) was dropwise added. When the orange-coloured solution cooled, yellowish crystals separated (15.1 g; 70%); m.p. 220—221 °C (decomp.), unchanged after recrystallization from methanol.

^{1}H-NMR (60 MHz, in $CDCl_3$, data of the prevalent conformer, cf. also Table I): δ 6.82—7.21 ppm (5 arom. H), 3.75—4.1 (4 OCH_3), 2.88 (5-H), 2.35 (4-CH_3), 2.30 (ethyl-CH_2), 1.15 (ethyl-CH_3).

^{13}C-NMR (25.16 MHz, in $CDCl_3$, off-resonance decoupling experiment 42.000 pulses, broadband proton decoupling 4000 pulses, concentration 0.8 mol/litre, data of the prevalent conformer, cf. also Table I): δ 12.17 ppm (C-12), 17.45 (C-10), 19.54 (C-11), 47.18 (C-5), 56.28—56.86 (C-13-16), 105.51 (C-5'), 110.84 (C-6), 113.91 (C-2'), 114.66 (C-9), 120.77 (C-5a), 124.65 (C-6'), 127.48 (C-1'), 134.63 (C-9a), 148.94 (C-7), 149.62 (C-8), 154.20 (C-3') 156.59 (C-4'), 166.28 (C-1), 171.05 (C-4).

$[C_{22}H_{27}N_2O_4]Cl$ (418.9). Calcd. C 63.08; H 6.45; Cl 8.46; N 6.69. Found C 63.15; H 6.62; Cl 8.33; N 6.56%.

(*b*) A yellow suspension was made from **1** (20 g; 52 mmol) with water (100 mL) and *conc.* hydrochloric acid (8.1 mL, 0.1 mol). The major part of **1** dissolved as a result of salt formation, and on standing **2a** precipitated. It was filtered off, washed with 5×5 mL of water and dried at 60 °C. Yield: 20.4 g (93.5%) of yellowish crystals, m.p. 217—218 °C (decomp.).

(*c*) Dry gaseous HCl was passed into a solution of **1** (1.0 g; 2.6 mmol) in ether (450 mL). Yellow flakes of **2a** separated in nearly quantitative yield; m.p. 220—221 °C (decomp.). No depression was observed in m.p. determination with the products prepared by methods (*a*) and (*b*).

Hydrobromide (2b)

M.p. 218—219 °C (decomp.) (recrystallized from 95% isopropyl alcohol).
$[C_{22}H_{27}N_2O_4]Br$ (463.4). Calcd. Br 17.23. Found: Br 17.17%.

Hydrogen sulfate dihydrate (2c · $2H_2O$)

To a solution of **1** (3.82 g; 10 mmol) in glacial acetic acid (20 mL) *conc.* sulfuric acid (0.55 mL; 10 mmol) was added. The pale yellow solutions was evaporated to dryness in vacuum and the residue recrystallized from water (10 mL). The crystals were washed with 2×2 mL of ice-cold water (the product is fairly soluble in water). Yield: 3.58 g (69%) of yellow crystals, m.p. 95—98 °C. Recrystallization from 6 mL of water raised the m.p. to 98—101 °C (loss of water).

IR:3430 cm^{-1} (OH); 2800—1850 ($\overset{\oplus}{N}H$, broad); 1060, 590 (SO_4).

^{1}H-NMR ($CDCl_3$): δ 7.4 ppm ($\overset{\oplus}{N}H$ + $2H_2O$ + HO(S), disappears on addition of D_2O).

^{1}H-NMR (DMSO-d_6): δ 5.2 ppm ($\overset{\oplus}{N}H$ + $2H_2O$ + HO(S), disappears on the addition of D_2O). The other signals in both spectra were similar to those listed for **2c**.

$[C_{22}H_{27}N_2O_4]HSO_4 \cdot 2H_2O$ (516.6). Calcd. C 51.15; H 6.24; N 5.42; S 6.21. Found C 51.23; H 6.15; N 5.44; S 6.04.

Hydrogen sulfate (2c)

Recrystallization from isopropyl alcohol removed the water of crystallization from **2c.2H$_2$O**. Colourless crystals were obtained, m.p. 189—191 °C (slight decomp.).

^{1}H-NMR ($CDCl_3$; 60 MHz; data in italics correspond to the prevalent conformer): $\overset{\oplus}{N}H$, HSO_4^-, disappears on addition of D_2O); 6.74—7.55 (5 arom. H); 3.60—4.15 (4 OCH_3); 3.05, 3.65 (5-H); 2.4, 1.60 (ethyl-CH_2); 2.25, 2.55 (4-CH_3); 1.10, 0.82 (ethyl-CH_3).

^{1}H-NMR (DMSO-d_6, 60 MHz): data similar to those recorded in $CDCl_3$, but δ_{NH, HSO_4} 8.12 ppm.

$[C_{22}H_{27}N_2O_4]HSO_4$ (480.55). Calcd. C 54.99; H 5.87; N.5.83; S 6.67. Found C 54.68; H 6.03; N 5.62; S 6.46%.

Thiocyanate (2d)

To a solution of **2a** (2.1 g; 5 mmol) in hot dimethylformamide (120 °C; 10 mL) ammonium thiocyanate (0.42 g; 5.5 mmol) was added. The yellow solution was evaporated to dryness in vacuum and the residue recrystallized from abs. ethanol (3.5 mL) to yield 1.7 g (77.5%) of yellow crystals, m.p. 180—182 °C (slight decomp)..

IR: 2800—2100 ($\overset{\oplus}{N}H$), 2040 cm^{-1} (ν_{as} SCN).
$[C_{22}N_{27}N_2O_4]SCN$ (441.56). Calcd. N 9.52; S 7.26. Found N 9.68; S 7.25%.

Perchlorate (2e) [1]

M.p. 200—202 °C (decomp.) (crystallized from a mixture of glacial acetic acid and isopropyl alcohol). Yellow crystals. For UV data, see [1].

^{1}H-NMR ($CDCl_3$, 100 MHz, cf. also Table I): practically identical with the data recorded for **2a**.

$[C_{22}H_{27}N_2O_4]ClO_4$ (482.9). Calcd. C 54.72; H 5.64; N 5.80. Found C 54.54; H 5.34; N 5.74%.

Perchlorate hydrate (2e · H_2O)

M.p. 151—153 °C (decomp.), (from **2e**, by recrystallzation from 10% acetic acid). Colourless crystals. The UV and ^{1}H-NMR data are identical with those of **2e**.

$[C_{22}H_{27}N_2O_4]ClO_4 \cdot H_2O$ (500.95). Calcd. C 52.75; H 5.84; N. 5.59. Found C 52.77; H 5.93; N 5.44%.

1-(3,4-Dimethoxyphenyl)-7,8-dimethoxy-3,4-dimethyl-5-ethyl--5*H*-2,3-benzodiazepin-3-ium iodide · H_2O (3)

Compound **1** (11.46 g; 0.03 mol) was dissolved in acetone (100 mL) and refluxed for 1 h with excess methyl iodide. Concentration of the solution yielded anhydrous **3** (15.5 g) in the form of a yellow foam that crystallized from water (100 mL) in pale yellow needles; m.p. 150—152 °C (slight decomp.). The compound is sensitive to light.

UV (in ethanol): λ 216 nm (ε = 45 000), 312 (13 750).

^{1}H-NMR (in $CDCl_3$, 60 MHz): δ 6.5—7.5 ppm (5 arom. H); 3.85—4.15 (4 OCH_3); 3.62 ($\overset{\oplus}{N}-CH_3$); 3.19 (5-H); 2.39 (ethyl-CH_2); 2.17 (4-CH_3); 1.18 (ethyl-CH_3) (data of the prevalent conformer).

$[C_{23}H_{29}N_2O_4]I \cdot H_2O$ (542.43). Calcd. C 50.93; H 5.76; N 5.16; I 23.40; H_2O 3.32. Found C 51.09; H 5.74; N 5.26; I 23.32; H_2O (KF) 3.15%.

***N*-{α-(3,4-Dimethoxyphenyl)-[2-(1-ethylacetonyl)-4,5-dimethoxybenzal]}--*N*'-methylhydrazine (5')**

Compound **3** (5.42 g; 0.01 mol) was dissolved in water (50 mL) and stirred with 10% NaOH (11 mL) for 1 h. After filtration, repeated washings with small amounts of iodide-free water and drying at 25 °C, 3.5 g of crude **5** was obtained. Recrystallization from isopropyl alcohol-petroleum ether yielded honey-coloured, granular crystals of **5**; m.p. 92—94 °C.

IR (in KBr): νNH 3270, νC=O 1705 cm^{-1}.

^{1}H-NMR ($CDCl_3$, 60 MHz): δ 6.55—7.50 ppm (arom. H); 3.83—4.08 (OCH_3), ~3.50, 3.80 (**CH**—CH_2—CH_3); 3.02—3.10 (NH—**CH_3**, N—CH_3); 2.18 ($COCH_3$); ~1.95, ~1.45 (ethyl--CH_2); 1.75 (C(OH)—CH_3), 0.83, 0.63 (ethyl-CH_3).

MS (*m*/*z*): 414 (35%), 369 (100).

3,5,7-Ttriphenyl-4*H*-1,2-diazepine · $HClO_4$ (7)

A mixture of **6** (3.22 g; 10 mmol) [5—8], glacial acetic acid (7 mL) and 70% perchloric acid (1 mL; 11.5 mmol) was heated until complete dissolution was achieved and then the solution was cooled. The yellow crystals which separated were filtered off by suction, washed with 4×5 mL of abs. ethanol and dried to obtain 3.5 g (83%) of **7**, m.p. 210—212 °C. After recrystallization from 13 parts of methanol the m.p. rose to 212—214 °C.

UV (in abs. ethanol): λ = 293 nm (ε = 20650), 258 (28250); in glacial acetic acid: 344 (12700).

IR:1100 and 620 cm^{-1} (ClO_4).

^{1}H- and ^{13}C-NMR: cf. Table II.

$[C_{23}H_{19}N_2]ClO_4$ (422.9). Calcd. C 65.32; H 4.53; N 6.62; Cl. 8.38. Found C 65.16; H 4.67; N 6.80; Cl 8.52.

*

The authors' thanks are due to Mrs. G. Szabó—Czibula for performing the experiments, to Dr. P. Sohár and Dr. Zs. Méhesfalvi-Vajna for recording the UV, IR and ^{1}H-NMR spectra (**2c**, **2d**).

REFERENCES

[1] Kőrösi, J., Láng, T.: Chem. Ber., **107,** 3882 (1974)
[2] Neszmélyi, A., Gács-Baitz, E., Horváth, Gy., Láng, T., Kőrösi, J.: Chem. Ber., **107,** 3894 (1974)
[3] Cf. e.g. Staab, H. A., Vögtle, F.: Chem. Ber., **98,** 2701 (1965); Solladié-Cavallo, A., Solladié, G.: Org. Magn. Reson., **7,** 18 (1975); Christl, M.: ibid., **7,** 349 (1975)
[4] For similar HI eliminations, see Vongerichten, E., Höfchen, C.: Ber. Dtsch. Chem. Ges., **41,** 3054 (1908); Hamer, F. C., Rathbone, R. J., Winton, B. S.: J. Chem. Soc., **1947,** 954; King, L. C., Abramo, S. V.: J. Org. Chem., **23,** 1609 (1958)
[5] Klingsberg, E.: Abstr. Am. Chem. Soc. Meeting, Sept. 1965, p. 668; cf. also Popp, F. D., Noble, A. V.: Adv. Heterocycl. Chem., **8,** 24 (1967); Harris, D. J., Kan, G. Y.-P., Snieckus, V., Klingsberg, E.: Can. J. Chem., **52,** 2798 (1974)
[6] Balaban, A. T.: Tetrahedron, **24,** 5059 (1968)
[7] Buchardt, O., Christian, L., Svanholm, U., Duffield, A. M., Balaban, A. T.: Acta Chem. Scand., **23,** 3125 (1969)
[8] Svanholm, U.: Acta Chem. Scand., **25,** 640 (1971)
[9] Anet, F. A.: J. Am. Chem. Soc., **86,** 458 (1954)
[10] Hannschreck, A., Rissmann, G., Vögtle, F., Wild, D.: Chem. Ber., **100,** 335 (1967)
[11] Harris, D. J., Kan, G. Y.-P., Snieckus, V., Buchardt, O.: Synthesis, **1975,** 603

Acta Chimica Hungarica 114 (3—4), pp. 301—307 (1983)

HETEROCYCLIC COMPOUNDS, V*

THE PREPARATION AND CHARACTERIZATION OF 1-(3,4-DIMETHOXYPHENYL)-6,7-DIMETHOXY-4--ETHYL-3-METHYLISOQUINOLINE-*N*-IMINE SALTS

J. KŐRÖSI[1], T. LÁNG[1]**, A. NESZMÉLYI[2] and GY. HORVÁTH[1]

([1]Institute for Drug Research, H-1045 Budapest, Szabadságharcosok u. 47—49. and [2]Central Research Institute for Chemistry, Hungarian Academy of Sciences, H-1025 Budapest, Pusztaszeri u. 59—67.)

Received July 26, 1982
Accepted for publication January 18, 1983

No *N*-imine salts **3** can be obtained by *N*-aminating agents from the known compound 1-(3,4-dimethoxyphenyl)-6,7-dimethoxy-4-ethyl-3-methyl isoquinoline (**4**). A novel process is described allowing the convenient synthesis of the salts of 1-aryl-2--iminoisoquinolinium-*N*-ylides, starting in the present case from the monohydrazone **1**.

Both our own experiences and reports of other authors [1] have demonstrated that no isoquinolinium-*N*-ylide salts of type **3** can be prepared from the known compound **4** [2] by treatment with *N*-aminating agents, such as chloramine [3], hydroxylamine-*O*-sulfonic acid [4], sulfonazide [5] or *O*-(2,4,6--trimethylphenylsulfonyl)-hydroxylamine [6].

In this work we describe a novel, simple process developed for preparing the salts of 1-aryl-2-iminoisoquinolinium-*N*-ylides from the corresponding 1,5-diketone monohydrazones, in the present case from **1**.

Dehydrating cyclization experiments with 2-(1-ethyl-2-hydrazonopropyl)-4,5,3',4';tetramethoxybenzophenone (**1**) [7] resulted in the following reactions: treatment with mineral acids gave 1-(3,4-dimethoxyphenyl)-7,8--dimethoxy-5-ethyl-4-methyl-5*H*-2,3-benzodiazepine salts (**2a—d**) [7—9], while carboxylic acids or other weak protonic acids, such as sulfuric acid monoesters, react to afferd the corresponding isoquinoline-*N*-imine salts (2-iminoisoquinolinium-*N*-ylide salts) (**3a—c**).

Compounds **3d—l** can then be prepared from the salts **3a—c** by allowing them to react with the corresponding acid or salt; e.g., **3d** · $3H_2O$ can be obtained from an aqueous solution of **3a** by adding NaCl. The water of crystallization can be removed from **3d** · $3H_2O$ in vacuum at 110 °C or, preferably, by partial evaporation of a suspension in xylene. In the experimental part of this paper a process will be described by which **3h—l** are readily accessible from **3a** and/or **3d**.

* Part IV: Ref. [9], preceding paper
** To whom correspondence should be addressed

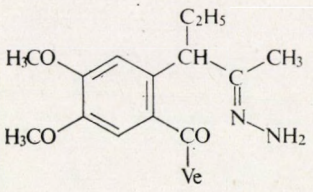

1

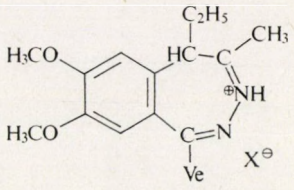

2a-d

2	X
a	Cl
b	Br
c	HSO_4
d	ClO_4

Ve = 3,4-Dimethoxyphenyl

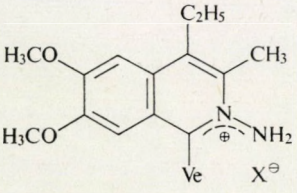

3a-l

3	X
a	$CH_3COO \cdot 2CH_3COOH$
b	$C_4H_5O_6$(*d*-H-tartrate)$\cdot H_2O$
c	$OSO_2OCH(CH_3)_2$
d	Cl(and $\cdot H_2O$ or $\cdot 3H_2O$)
e	$Br \cdot 3H_2O$
f	HSO_4

3	X
g	ClO_4
h	SCN
i	HCO_3
j	N_3
k	$HCrO_4 \cdot H_2O$
l	$FeCl_4$

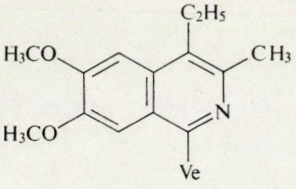

4

The compounds synthesized were characterized by their UV, IR, ^{1}H-NMR and ^{13}C-NMR spectra (see Experimental). For comparison, the ^{13}C-NMR spectra of **3d** and **4** · HCl are presented in Fig. 1; as expected, they are closely similar.

In the mass spectra of the salts **3** fragment ions are also found, originating from the products of the preceding thermolysis. If, e.g., **3d** · $3H_2O$ is submitted to electronolysis at 150, 170 and 190 °C, the products will include **4** and methyl chloride; the main fragmentation proceeds analogously to the well-known reaction of 2-phenylquinoline-*N*-oxide [10]: cyclization with the elimination of H ($m/z = 381$) (Fig. 2).

Experimental

M.p.'s are uncorrected. The instruments used were Unicam SP 800 for the UV spectra; Perkin-Elmer 577 for IR (KBr pellets); Jeol-C-60 and Varian A-60D for ^{1}H-NMR; Varian--XL-100-15-FT for 100 MHz ^{1}H-NMR and 25 MHz ^{13}C-NMR (internal standard TMS, $\delta =$ 0 ppm); Varian MAT-SM-1 for mass spectroscopy; and derivatograph Orion-GYEM 676 for thermal analysis [11] (sample mass 200 mg, heating rate 3 °C/min, nitrogen atmosphere).

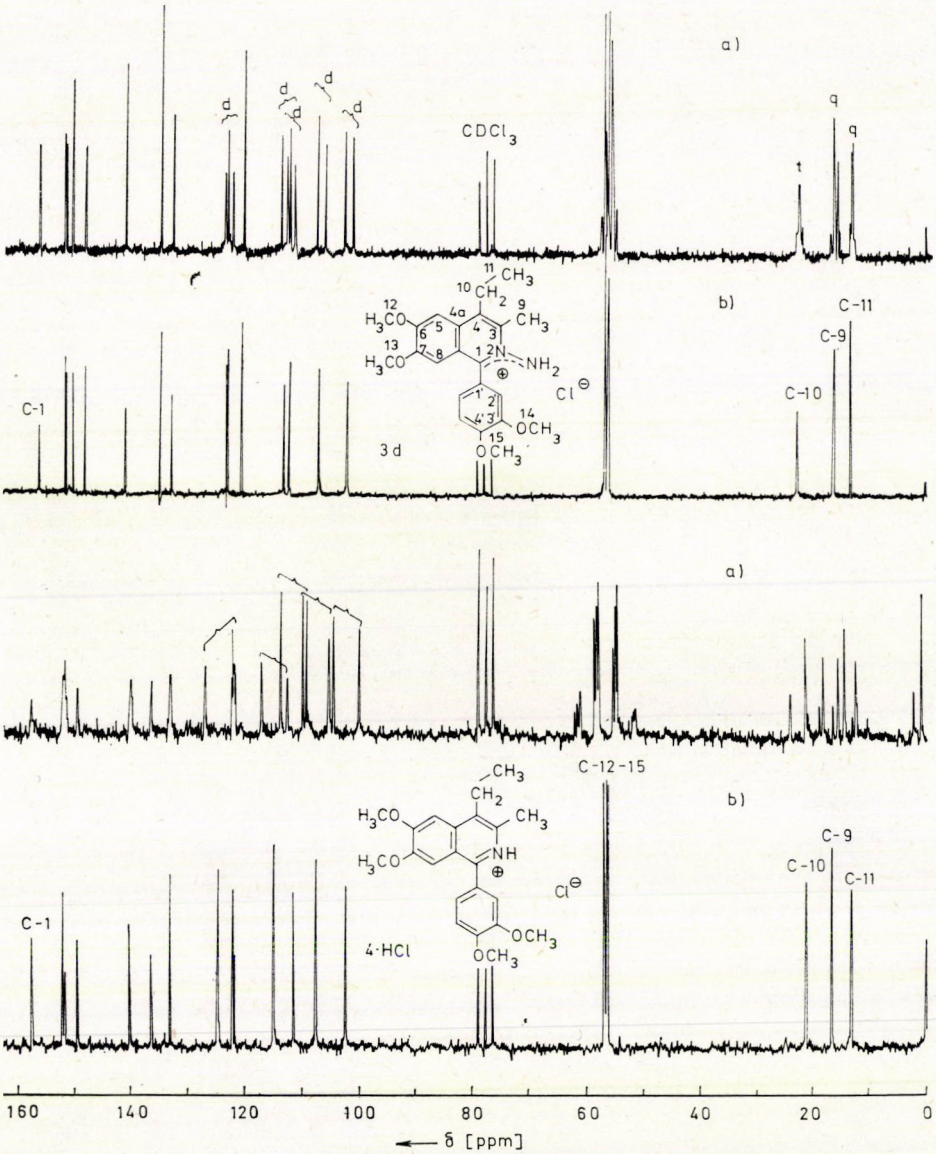

Fig. 1. Pulse-Fourier transform ^{13}C-NMR spectra of the compounds *3***d** and *4* · **HCl** at 25 °C. Recording frequency 25.16 MHz concentration 0.35 mol/litre in $CDCl_3$; internal standard tetramethylsilane. a) off-resonance decoupling experiment, 48000 pulses; b) broad band decoupled spectra, 4000 pulses

2-Amino-1-(3,4-dimethoxyphenyl)-6,7-dimethoxy-4-ethyl-3-methylisoquinolinium acetate (3a) · $2CH_3COOH$

A solution of **1** [7] (15.0 g; 37.4 mmol) in glacial acetic acid (100 mL) was stirred for 1 h at 100 °C. The reddish solution was evaporated to dryness in vacuum, the resinous residue (22.2 g) was recrystallized from benzene (30 mL), filtered with suction and washed with benzene

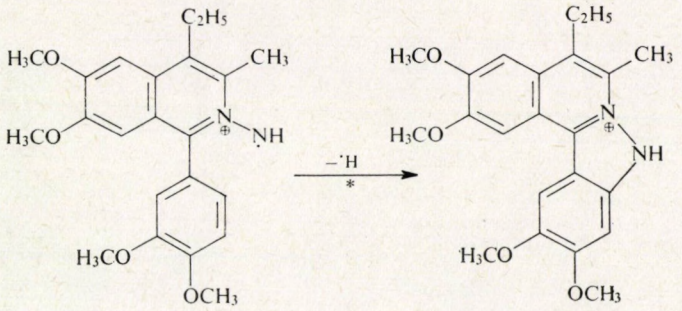

$M = 382$ (45%) $m/z = 381$ (100%)

Fig. 2. MS reaction of the salts **3**

(4×5 mL) at 10 °C. Yield: 11.98 g (57%) of transparet yellowish crystals, m.p. 87—89 °C.
UV (EtOH): $\lambda = 261$ nm ($E^{1\%}_{1cm}$1150), 323 (218).

IR: 3310, 3195 cm^{-1} (NH_2), 1630 (shoulder, C⋯$\overset{\oplus}{N}$⋯).
^{1}H-NMR ($CDCl_3$): δ 7.05—7.65 (5 arom. H); 6.88 (NH_2); 3.81, 397, 4.07, 4.21 (4 OCH_3); 3 20 (ethyl-CH_2); 2.97 (3-CH_3); 1.81 (CH_3COO); 1.40 (ethyl-CH_3).
$[C_{22}H_{27}N_2O_4]CH_3COO \cdot 2\ CH_3COOH$ (562.6). Calcd. C 59.77; H 6.81: N 4.98. Found C 59.65; H 6.84; N 5.01%.

On drying in vacuum over KOH at 80 °C **3a** loses 11.8% of its mass; a yellow compound containing 1 mol combined acetic acid is formed, m.p. 126—128 °C. Complete elimination of the combined acetic acid is only feasible by evaporation of a solution in xylene, and subsequent crystallization from isopropanol to obtain a cream-coloured crystalline powder, m.p. 222—223 °C.

2-Amino-1-(3,4-dimethoxyphenyl)-6,7-dimethoxy-4-ethyl-3--methylisoquinolinium-(*R*,*R*)-hydrogen tartrate (3b) · H_2O

Compound **1** (4.0 g; 10 mmol) was added to a hot solution of L-tartaric acid)1.65 g: 11 mmol) in ethanol (30 mL) and refluxed for 1 h. On cooling almost colourless crystals (4.8 g: 89%) separated, m.p. 174—175 °C; recrystallized from 90% ethanol (30 mL) gave pure **3b** (4.44 g), m.p. 175—176 °C; $[\alpha]_D^{25}$ +7.23° ($c = 2$, in water).
UV (EtOH): $\lambda = 207$ nm ($\varepsilon = 33480$), 261 (53060), 326 (11260).
$[C_{22}H_{27}N_2O_4]C_4H_5O_6 \cdot H_2O$ (550.6). Calcd. C 56.72; H 6.22; N 5.51. Found C 56.38; H 6.27; N 5.37%.

2-Amino-1-(3,4-dimethoxyphenyl)-6,7-dimethoxy-4-ethyl-3--methylisoquinolinium isopropyl sulfate (3c)

A mixture of isopropanol (30 mL) and *conc.* sulfuric acid (0.66 mL; 12 mmol) was refluxed for 1 h, then compound **1** (4.0 g; 10 mmol) was added, and the mixture was heated for further 30 min. After evaporation to dryness the residue was recrystallized from water (12 mL) to yield 3.8 g (73%), of almost colourless crystals, m.p. 182—184 °C. Recrystallization from isopropanol (11 mL) gave a cream-coloured crystalline powder (3.24 g), m.p. 183—185 °C.

IR: 3350 (NH_2), 1610 cm^{-1} (C⋯$\overset{\oplus}{N}$⋯).
^{1}H-NMR ($CDCl_3$): δ 6.62—7.50 ppm (5 arom. H); 6.86 (NH_2, exchangeable with D_2O); 4.41 (isopropyl-CH); 3.75, 3.96, 3.98, 4.11 (4 OCH_3), 3.17 (ethyl-CH_2); 2.95 (3-CH_2), 1.39 (ethyl-CH_3), 1.12 (isopropyl-CH_3).
MS: the main product of fragmentation was **4** ($M = 367$).
$[C_{22}H_{27}N_2O_4]C_3H_7O_4S$ (522.6). Calcd. C 57.45; H 6.56; N 5.36; S 6.14. Found C 57.38; H 6.72; N 5.40; S 5.96%.

2-Amino-1-(3,4-dimethoxyphenyl)-6,7-dimethoxy-4-ethyl-3-methylisoquinolinium chloride (3d, 3d · H_2O, and 3d · $3H_2O$)

Compound **1** (120 g; 0.3 mol) was stirred in glacial acetic acid (240 mL) for 1 h at 92—95 °C and evaporated to dryness in vacuum. The resinous residue (crude **3a**, 184 g) was dissolved in water (240 mL) and mixed with a 25% NaCl solution (200 mL) whereupon **3d** · $3H_2O$ separated immediately. After cooling for several hours the mixture was covered with benzene (150 mL), filtered with suction and dried to give 120.15 g of light cream-coloured crystals still containing some NaCl; m.p. 22—24°C (decomp.). For purification, the crude product was dissolved in hot water (105 mL), and cooled. A dense crystal mass formed, which — after filtration with suction, washing with ice-cold water (2×20 mL) and drying in vacuum — yielded almost colourless crystals (100.4 g; 71%), m.p. 226–227 °C (decomp.), sintering accompanied by loss of water at 92—100 °C.

Thermogravimetry: 11—12% mass loss occurred between 50 and 100 °C (H_2O) in two stages. The mass of the residue remained constants up to 180 °C. Between 180 and 225 °C a further mass loss of 14% was observed in a separate endothermic stage (CH_3Cl and NH_2Cl). (*Note:* the error of thermogravimetry, as known, is 2—10%.)

$[C_{22}H_{27}N_2O_4]Cl \cdot 3\ H_2O$ (472.98). Calcd. C 55.86; H 7.03; N 5.92; Cl 7.50; H_2O 11.43. Found C 55.57; H 7.26; N 5.66; Cl 7.58; H_2O (KF) 11.40%.

Removal of the water of crystallization

(*a*) Compound **3d** · $3H_2O$ (12 g) was dissolved in $CHCl_3$ (25 mL), and the water droplets were removed over Na_2SO_4. From the clear solution, after adding ethyl acetate (125 mL), a light cream-coloured crystalline powder, **3d** · H_2O, separated; yield: 11 g, m.p. 226—227 °C (decomp.).

(*b*) Pulverized **3d** · $3H_2O$ (14.3 g; 30 mmol) was suspended in xylene (100 mL) and the suspension was refluxed for 3 h using a Dean-Stark trapi it was then evaporated in vacuum and dried to constant mass at 100 °C in vacuum. Yield: 12.6 g (100%) of cream-coloured **3d**; m.p. 226—227 °C (decomp.).

UV (EtOH): $\lambda = 206$ nm ($\varepsilon = 43020$), 261 (54910), 324 (11230).

IR: 3340, 3190 (NH_2), 1625 cm^{-1} (shoulder, $C{\cdots}\overset{\oplus}{N}{\cdots}$).

^{1}H-NMR ($CDCl_3$): δ 7.1—7.8 ppm (5 arom. H); 6.85 (NH_2, disappears on the addition of D_2O); 3.82, 4.00, 4.03, 4.20 (4 OCH_3); 3.25 (ethyl-CH_2); 3.04 (3-CH_3); 1.40 (ethyl-CH_3).

^{13}C-NMR: see Fig. 1.

MS is described in the text.

$[C_{22}H_{27}N_2O_4]Cl$ (418.9). Calcd. C 63.08; H 6.45; N 6.69; Cl 8.46. Found C 62.90; H 6.58; N 6.60; Cl 8.34%.

2-Amino-1-(3,4-dimethoxyphenyl)-6,7-dimethoxy-4-ethyl-3-methylisoquinolinium bromide (3e) · $3H_2O$

From a hot solution of **3a** (1.0 g; 1.8 mmol) and NaBr (0.3 g) in water (6 mL) cream-coloured, glittering crystals separated on cooling. Yield: 0.62 g (67%), m.p. 215—217 °C (decomp.).

$[C_{22}H_{27}N_2O_4]Br \cdot 3\ H_2O$ (517.4). Calcd. Br 15.44. Found Br 15.31%.

2-Amino-1-(3,4-dimethoxyphenyl)-6,7-dimethoxy-4-ethyl-3-methylisoquinolinium hydrogen sulfate (3f)

Compound **3d** (2.1 g; 5 mmol) was heated to the boiling point in a mixture of isopropyl alcohol (15 mL) and *conc.* sulfuric acid (0.36 mL; 6.5 mmol). On cooling a white crystalline powder separated from the yellow solution; yield: 2.05 g (85%), m.p. 202—204 °C (sintering from 199 °C on).

IR: 3345, 3260 (NH_2); 1150, 585 cm^{-1} (HSO_4).

^{1}H-NMR ($CDCl_3$): as for **3d**.

$[C_{22}H_{27}N_2O_4]HSO_4$ (480.55). Calcd. C 54.99; H 5.66; S 6.67. Found C 54.71; H 5.73; S 6.50%.

2-Amino-1-(3,4-dimethoxyphenyl)-6,7-dimethoxy-4-ethyl-3-methylisoquinolinium perchlorate (3g)

To a solution of **3d** · **3 H_2O** (1.0 g; 2.1 mmol) in hot isopropanol (20 mL) 70% perchloric acid (0.25 mL; 2.85 mmol) was added. On cooling **3g** (0.96 g; 94%) separated as yellow crystals, m.p. 237—238 °C.

IR: 3260, 3360 (NH_2), 1110, 630 cm^{-1} (ClO_4).

$[C_{22}H_{27}N_2O_4]ClO_4$ (482.9). Calcd. C 54.72; H 5.64; N 5.80. Found C 54.66; H 5.78; N 5.83%.

2-Amino-1-(3,4-dimethoxyphenyl)-6,7-dimethoxy-4-ethyl-3-methylisoquinolinium thiocyanate (3h)

To a solution of **3d** · **$3H_2O$** (4.73 g; 10 mmol) in water (30 mL) ammonium thiocyanate (1.0 g; 14.5 mmol) was added at 50 °C. The flakes that separated were filtered off after cooling. Yield: 4.37 g (99%), m.p. 192—194 °C (decomp.). Recrystallization from aqueous 17% DMF (12 parts) gave glittering, colourless crystals (95%), m.p. 193—195 °C.

$[C_{22}H_{27}N_2O_4]SCN$ (441.56). Calcd. C 59.84; H 6.16; N 9.54; S 7.26. Found C 59.82; H 6.22; N 9.63; S 7.16%.

2-Amino-1-(3,4-dimethoxyphenyl)-6,7-dimethoxy-4-ethyl-3-methylisoquinolinium hydrogen carbonate (3i)

To a solution of **3d** (0.9 g; 2.15 mmol) or **3d** · **$3H_2O$** (1.02 g; 2.15 mmol) in water (5 mL), $NaHCO_3$ (0.3 g; 3.55 mmol) was added in portions at 5 °C. After 1 h an almost colourless powder began to separate from the yellow solution. On the next day the precipitate was filtered off, washed with water (5×1 mL) until free of chloride, and dried at 50 °C. Yield: 0.83 g (86%) of **3i**; m.p. 162—164 °C (decomp.; yellow coloration appears from 150 °C on).

IR: 3600—3130 (3380 broad band, OH and NH_2); 1635 (intense, HCO_3); 1620 cm^{-1} (shoulder, $C{=}\overset{\oplus}{N}{-}$).

^{1}NMR (TFA): δ 6.8—7.6 ppm (5 arom. H); 7.00 (NH_2, disappears on addition of D_2O); 3.80, 3.90, 4.00, 4.11 (4 OCH_3); 3.25 (ethyl-CH_2); 2.92 (3-CH_2); 1.41 (ethyl-CH_3).

MS: vigorous formation of CO_2 and **4** already below 501 °C. Fragmentation as with **3d**.

$[C_{22}H_{27}N_2O_4]HCO_3$ (444.5). Calcd. C 62.15; H 6.35; N 6.30. Found C 62.26; H 6.50; N 6.37%.

2-Amino-1-(3,4-dimethoxyphenyl)-6,7-dimethoxy-4-ethyl-3-methylisoquinolinium azide (3j)

From a solution of **3a** (5.63 g; 10 mmol), or **3d** · **$3H_2O$** (4.73 g; 10 mmol) and sodium azide (0.84 g; 12 mmol) in water (75 mL) of 70 °C, large, colourless, slightly yellowish crystals separated on cooling. These were filtered off by suction and washed with water (5×5 mL) and ethanol (2×10 mL), to yield 4.05 g (95%) of **3j**; the compound turns yellow from 195 °C on, and *decomposes at 202—204 °C explosion-like.*

IR: 3325 (NH_2); 2020 (N_3); 1620 cm^{-1} ($C{=}\overset{\oplus}{N}{-}$).

$[C_{22}H_{27}N_2O_4]N_3$ (425.5). Found C 62.10; H 6.40. Found C 61.92; H 6.35%.

2-Amino-1-(3,4-dimethoxyphenyl)-6,7-dimethoxy-4-ethyl-3-methylisoquinolinium chlorochromate and hydrogen chromate (3k) · H_2O

To a solution of **3d** · **$3H_2O$** (4.73 g; 10 mmol) in glacial acetic acid (25 mL) CrO_3 (1.0 g; 10 mmol) in water (3 mL) was adzdd. After 1 h crystallization started. After a few hours, the crystals were filtered off with suction, washed with 50% acetic acid (5×2 mL) and subsequently with water (3×3 mL), and dried over KOH in a vacuum desiccator. Yield: 4.09 g (79%), orange powder, m.p. 186—188 °C (decomp.).

$[C_{22}H_{27}N_2O_4]ClCrO_3$ (518.9). Calcd. C 50.92; H 5.24; N 5.40; Cl 6.83; Cr_2O_3 14.65. Found C 51.18; H 5.42; N 5.39; Cl 6.96; Cr_2O_3 14.50%.

A solution of the chlorochromate (3.0 g) in hot water (300 mL) was evaporated to half its volume and subsequently cooled; **3k** · H_2O was obtained as an orange-coloured, glittering crystal powder 2.24 g, m.p. 135—137 °C (decomp., sintering from 120 °C on).

$[C_{22}H_{27}N_2O_4]HCrO_4 \cdot H_2O$ (518.5). Calcd. C 50.96; H 5.83; N 5.40; CrO_3 14.66. Found C 50.70; H 5.53; N 5.42; Cr_2O_3 14.80%.

2-Amino-1-(3,4-dimethoxyphenyl)-6,7-dimethoxy-4-ethyl-3-methylisoquinolinium chloroferrate (31)

Compound **3d** · $3H_2O$ (5 g; 11.2 mmol) was heated in a 6% $FeCl_3$ solution (100 mL) to 95 °C. At 60 °C an orange-coloured solution was obtained from which dark-orange crystals separated at 95 °C. Yield: 2.56 g (38%); m.p. 200—201 °C (decomp.).

IR: 3290, 3370 (NH_2); 1625 ($C{=}\overset{\oplus}{N}{-}$); 383 cm^{-1} (intense, $FeCl_3$).

$[C_{22}H_{27}N_2O_4]FeCl_4$ (518.15). Calcd. C 45.47; H 4.68; N 4.82; Cl 24.40; Fe_2O_3 13.74. Found C 45.59; H 4.94; N 4.70; Cl 24.16; Fe_2O_3 13.50%.

*

The authors' thanks are due to Mrs. G. Szabó-Czibula for technical assistance, to Dr. P. Sohár and Mrs. M. Sóti-Tolvay for part of the ^{1}H-NMR spectra and to Dr. Gy. Liptay (Technical University, Budapest) for the thermogravimetric analyses.

REFERENCES

[1] Lempert-Sréter, M.: Acta Chim. Acad. Sci. Hung. **83,** 115 (1974)
[2] a) Doering, W. v. E., Berson, J. A.: J. Am. Chem. Soc., **72,** 1118 (1950); b) Müller, A., Lempert-Sréter, M., Karczag-Wilhelms, A.: J. Org. Chem., **19,** 1533 (1953)
[3] Omietanski, G. A., Sisler, H. H.: J. Am. Chem. Soc., **78,** 1211 (1956)
[4] Meuwsen, A., Gösl, R.: Angew. Chem., **69,** 754 (1957); Chem. Ber., **92,** 2521 (1959); Org. Synth. Coll. Vol. V., p. 43 (1973)
[5] Buchanan, G. L., Levine, R. M.: J. Chem. Soc., **1950,** 2248
[6] Tamura, Y., Minamikawa, J., Miki, Y., Matsugashita, S., Ikeda, M.: Tetrahedron Lett., **1972,** 4133; Tamura, Y., Minamikawa, J., Kita, Y., Kim, J. H., Ikeda, M.: Tetrahedron, **29,** 1063 (1973)
[7] Kőrösi, J., Láng, T.: Chem. Ber., **107,** 3883 (1974)
[8] Neszmélyi, A., Gács-Baitz, E., Horváth, Gy., Láng, T., Kőrösi, J.: Chem. Ber., **107,** 3894 (1974)
[9] Neszmélyi, A., Láng, T., Kőrösi, J.: Acta Chim. Hung. **114,** 293 (1983)
[10] Buchardt, D., Duffield, A. M., Shapiro, R. R.: Tetrahedron, **24,** 3139 (1968)
[11] Paulik, F., Paulik, J., Erdey, L.: Z. Anal. Chem., **160,** 241 (1958)

Acta Chimica Hungarica 114 (3—4), pp. 309—321 (1983)

SYNTHESIS OF (1 → 1)-BONDED RHAMNOPYRANOSYL-RHAMNOPYRANOSIDES CONTAINING L,L AND L,D BUILDING-STONES. HIGH-FIELD ^{1}H- AND ^{13}C-NMR SPECTROSCOPIC STUDIES ON THE CONFORMATION OF THE INTERGLYCOSIDIC BONDS

A. LIPTÁK* and M. GÖNDÖR

(Institute of Biochemistry, Kossuth Lajos University, H-4010 Debrecen, P.O.B. 55)

Received September 14, 1982
Accepted for publication January 18, 1983

Rhamnosylation of 2,3,4-tri-*O*-acetyl-L- (**1**) and 2,3,4-tri-*O*-benzyl-D-rhamnopyranose (**9**) with α-acetobromo-L-rhamnose resulted in fully protected α-L, α-L-, α-L,β-L-, α-D,α-L- and β-D,α-L-rhamnopyranosyl-rhamnopyranosides. The signals of the anomeric carbons of the α-L,α-L- and β-D,α-L- isomers appeared at high field, independently of the substitution patterns. By measuring of the $^{3}J_{C-1,H-1}$, values the existence of the *exo*-anomeric effect was concluded. In the case of the α-L,β-L- and α-D,α-L-isomers the anomeric carbons resonated in the low-field region, and the anomeric carbon atoms and the ring-oxygen atom were not in *syn-clinal* arrangement.

Introduction

Trehalose is a widespread sugar in nature, occurring in fungi, bacteria, the blood of insects, and the trehala manna. It was also found in certain algae and lichens as well as in higher plants [1]. The discovery of the cord factor in human tubercle bacillus [2] and the isolation of its amino derivatives possessing antibiotic activity [3, 4] have initiated several syntheses [5—13] of this sugar. The structure elucidation of apramycin [14], tunicamycin [15], everninomycins [16, 17], flambamycin [18] and avilomycin [19, 20] demonstrated the presence of trehalose-type oligosaccharides in these antibiotics. For organoleptic studies [21—23] and enzyme assay procedures [24] a large number of trehalose-type derivatives have been synthesized and precise conformational studies using ^{13}C-NMR parameters [25, 26] have been made. In this paper we wish to report on the synthesis and conformational analysis of L,L- and D,L-rhamnopyranosyl-rhamnopyranosides.

* To whom correspondence should be addressed

Results and Discussion

The syntheses of rhamnopyranosyl-rhamnopyranoside were achieved starting with suitably protected L- or D-rhamnopyranose derivatives having a free hydroxyl group only at position C-1. For the preparation of the L,L-isomers 2,3,4-tri-*O*-acetyl-L-rhamnopyranose (**1**) was selected. This compound was first synthesized by E. Fischer [27] from α-acetobromo-L-rhamnose, and most recently its formation was reported [28] by the treatment of 1,3,4-tri-*O*-acetyl-β-L-rhamnopyranose with pyridine in aqueous ethanol, but neither physical data nor the reaction conditions were given.

The readily accessible benzyl 2,3,4-tri-*O*-acetyl-α-L-rhamnopyranoside [29] was hydrogenated under neutral conditions to obtain **1**; in this way acetyl migration could be avoided. In the ^{13}C-NMR spectrum of **1** about 10% of the β-anomer could be detected as well, consequently during the glycosylation reaction the β-anomer content of the aglycone also had to be taken into account.

Reaction of **1** with α-acetobromo-L-rhamnose, using the Helferich procedure, required prolonged reaction time due to the diminished reactivity of the anomeric hydroxyl group [12]. After 20 h the aglycone disappeared, and two products were detected by TLC and GLC in a ratio of 3 : 1. The two reaction products were separated by column chromatography; the faster moving component (**2**) showed a considerably high negative value of optical rotation, whereas the other isomer (**3**), a crystalline compound, had low negative optical rotation. On the basis of these data it was assumed that **2** was the α-L,α-L- and **3** was the α-L,β-L-isomer. This assumption was clearly confirmed by the ^{1}H- and ^{13}C-NMR spectra. Although the ^{1}H-NMR spectra of **2** and **3** were of higher order and could not be directly assigned, it was clear that **2** was a symmetric compound since only one H-1 singlet and one C_5—CH_3 doublet could be detected. On the contrary, in the spectrum of compound **3** two singlets and two doublets belonging to the H-1 and to the —CH_3 protons, respectively, were observed.

The symmetric structure of **2** was also clearly demonstrated by its ^{13}C-NMR spectrum; only six skeleton carbon signals were detected, and according to the value of the $^1J_{C1-H1}$ coupling constant (174.1 Hz) an α-anomeric configuration was assigned. In the ^{13}C-NMR spectrum of **3** eleven skeletal carbon signals could be seen, however, — unfortunately — the C-1's had the same chemical shifts. At the same time, two doublets appeared in the proton-coupled spectrum and the coupling constants of 171.9 Hz and 158.1 Hz were assigned to the α- and the β-linked C-1 carbons, respectively.

Zemplén deacetylation of **2** resulted in crastalline **4**; the dihydrate of this disaccharide had been isolated by Birkofer and Hammes [30] as the by-product obtained in the Koenigs—Knorr reactions using α-acetobromo-L-

-rhamnose as glycosylation agent; the coupling partner, the 2,3,4-tri-*O*-acetyl--L-rhamnose derived from the decomposition of the α-acetobromo-L-rhamnose.

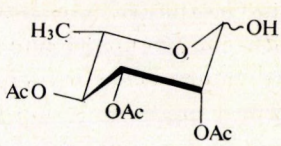

1

6 R=CH3; R′=Bn; R″=OH
7 R=CH3; R′=Bn; R″=OTs
8 R=CH3; R′=Bn; R″=H
9 R=R″=H; R′=Bn

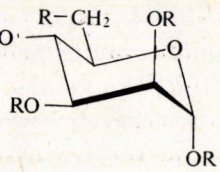

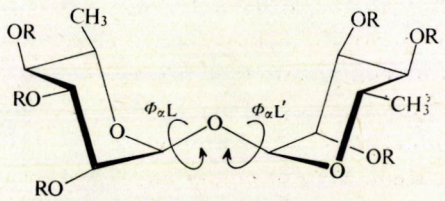

2 R=Ac
4 R=H

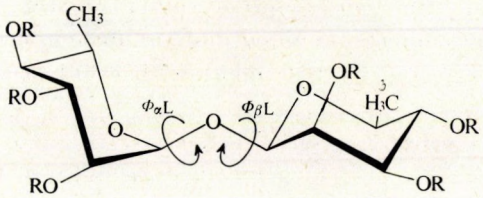

3 R=Ac
5 R=H

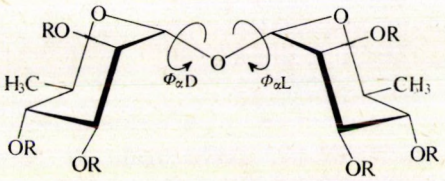

10 R=Ac; R′=Bn
12 R=H; R′=Bn
14 R=R′=H
16 R=R′=Ac

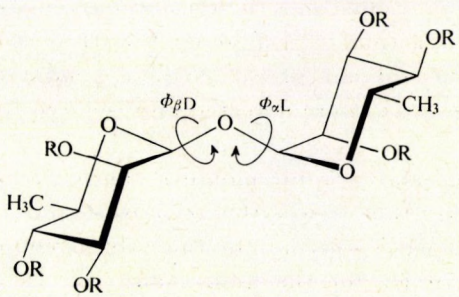

11 R=Ac; R′=Bn
13 R=H; R′=Bn
15 R=R′=H
17 R=R′=Ac

Similarly, deacetylation of 3 gave the syrupy disaccharide (5) with a very low $[\alpha]_D$ value.

The 400 MHz ^{1}H-NMR spectra of the two disaccharides (**4** and **5**) could be directly analyzed confirming the postulated symmetry properties.

From the values of the $^3J_{H,H}$ coupling constants the conformation of the pyranosyl rings could be estimated. These values shoved that the L-rhamnopyranoside units had the same conformation in both compounds (**4** and **5**), and thus the very different ^{13}C-NMR chemical shift values *(vide infra)* of the disaccharides were not to be attributed to a bond angle deformation.

For the synthesis of D-rhamnopyranosyl-L-rhamnopyranosides 2,3,4-tri-*O*-benzyl-D-rhamnopyranose (**9**) was chosen. Methyl 2,3-di-*O*-benzyl-4,6-*O*-benzylidene-α-D-mannopyranoside [31] was hydrogenolyzed by treatment with the $LiAlH_4$—$AlCl_3$ reagent to give methyl 2,3,4-tri-*O*-benzyl-α-D-mannopyranoside (**6**). For the preparation of compound **6** a procedure has been published via the 6-*O*-trityl derivative [32], but the detritylation was hampered [33, 34], and the resulting crude product was not characterized. Tosylation of **6** resulted in the crystalline **7** [32]. Reduction of compound **7** with $LiAlH_4$ in benzene-ether gave methyl 2,3,4-tri-*O*-benzyl-α-D-rhamnopyranoside (**8**). It is to be noted that by applying the benzene-ether solvent system, the formation of a very stable emulsion could be avoided and the decomposition of the excess of $LiAlH_4$ could be effected by treatment with ethyl acetate-water.

Recently, the hydrolysis of methyl 2,3,4-tri-*O*-benzyl-α-L-rhamnopyranoside was reported using dilute sulfuric acid in a 1,4-dioxane solution [35], but the yield was moderate (30%). Therefore, we tried to use the method of Koto et al. [36] described for the preparation of 2,3,4,6-tetra-*O*-benzyl-D-gluco-, -D-galacto- and -D-mannopyranoses. Also in the case of our compound this reaction proved to be very successful, and the crystalline compound **9** was isolated in 70% yield.

Compound **9** was rhamnosylated with α-acetobromo-L-rhamnose using the same reaction conditions as described for the preparation of the L,L-disaccharide peracetates (**2** and **3**). Unfortunately, this reaction gave the desired disaccharides only in very low yields and their isolation remained unsuccessful. However, the coupling reaction of compound **9** with α-acetobromo-L-rhamnose using acetonitrile as solvent proceeded in a good yield, and two disaccharide derivatives (**10** and **11**) were detected and isolated from the reaction mixture.

The component having higher chromatographic mobility showed a very low value of optical rotation suggesting that it was the α-L,α-D-isomer. This assumption was verified by its ^{13}C-NMR spectrum; in the proton coupled spectrum the $^1J_{C1-H1}$ values were 170 Hz for the L-form and 168 Hz for the D-form. The minor component with lower R_f-value had a high negative optical rotation, supporting the α-L,β-D configurations, confirmed by the measurement of the $^1J_{C1-H1}$ coupling constants (173.8 Hz and 159.3 Hz).

The exclusive formation of the α-L,α-L-, α-L,β-L- and the absence of the β-L,β-L-isomers observed in the reaction of 2,3,4-tri-*O*-acetyl-L-rhamnopyranose and α-acetobromo-L-rhamnose suggested that rhamnosylation proceeded with complete stereoselectivity resulting only in α-L-rhamnopyranosyl units. This assumption was unequivocally verified by the absence of β-L,α-D- or β-D,β-L-isomers in the coupling reaction of **9** with α-acetobromo-L-rhamnose. It is worth to note that the stereoselectivity of glycosylation reactions under the same conditions strongly depends on the character and nucleophilicity of the aglycone, as it has been demonstrated by the studies with α-acetobromo-L--rhamnose [37] and also with α-acetobromo-L-fucose [38]. These observations support Paulsen's scepticism that each oligosaccharide synthesis remains an independent problem, and there are no universal reaction conditions for oligosaccharide syntheses [39].

Saponification of compounds **10** and **11** resulted in the disaccharide derivatives **12** and **13**, respectively, having free hydroxyl groups only at the L-rhamnose part of the molecules. The $^1J_{C1-H1}$ coupling constants were especially very informative in the case of the α-L,β-D-isomer (**13**) where the assignment to the C-1 signals was straightforward (Table I). Namely, on the basis of the chemical shifts of the anomeric carbons in compound **11**, an α-D-Rhap--(OBn)$_3$-(1-1)-β-L-Rhap-(OAc)$_3$ structure could also be assumed. This structure could be excluded, however, on the basis of the $^1J_{C1-H1}$ coupling constant having a value of 171.8 Hz, and this large value could be unambiguously assigned to the C-1 (97.3 ppm) of the α-L-rhamnopyranosyl unit. Catalytic debenzylation of the above compounds gave the crystalline, optically inactive α-D,α-L-disaccharide (**14**) being the first "meso-disaccharide" in the literature, and the syrupy **15** possessing a high value of negative optical rotation. Acetylation of the free disaccharides resulted in the respective peracetates **16** and **17**.

From the ^{13}C-NMR chemical shift data of the C-1 atoms, listed in Table I, it can be concluded that the α-L,α-L- (**2** and **4**) and the β-D,α-L-compounds (**11**, **13**, **15** and **17**) show high-field signals, and the chemical shift differences are about 4—5 ppm, as compared with the α-L,β-L- (**3** and **5**) and α-D,α-L--compounds (**10**, **12**, **14** and **16**). These differences seem to appear regardless of the character of the substituents. This finding strongly suggests, that these chemical shift differences do not arise from a conformational change induced by the different substituents, or by inter-unit hydrogen bondings.

The anomaly of the C-1 chemical shifts can be ascribed to the conformational change of the glycosidic linkages; these latter can be characterized by the φ and ψ angles [40]. In oligosaccharides, $\varphi = 0°$ when H-1' and the aglycone carbon are eclipsed; $\psi = 0°$ when the anomeric carbon and the proton on the aglycone carbon are eclipsed (Figure 1). Theoretically, the value of these angles can be determined by measuring of the ^3J homo- or heteronuclear coupling constants which follow a Karplus-type relationship [41].

Table I

The C-1 *chemical shift,* $^1J_{C-1;H-1}$ *and* $^3J_{C,H}$ *values of* L,L- *and* D,L-*rhamnopyranosyl--rhamnopyranoside derivatives*

No.	Compound composition	δ	^1J	^3J
2	α-L-Rhap(OAc)$_3$- (1]	93.6	174.1	2.8
	α-L-Rhap(OAc)$_3$- (1]			
3	α-L-Rhap(OAc)$_3$- (1]	97.6	171.9	
	β-L-Rhap(OAc)$_3$- (1]	97.6	158.1	
4	α-L-Rhap- (1]	96.4	171.2	2.9
	α-L-Rhap- (1]			
5	α-L-Rhap- (1]	101.0	170.9	4.0
	β-L-Rhap- (1]	100.2	159.4	6.0
10	α-D-Rhap(OBn)$_3$-(1]	97.7	168.0	
	α-L-Rhap(OAc)$_3$- (1]	99.4	170.0	
11	β-D-Rhap(OBn)$_3$-(1]	95.9	159.3	
	α-L-Rhap(OAc)$_3$- (1]	94.2	173.8	
12	α-D-Rhap(OBn)$_3$-(1]	98.7	167.5	
	α-L-Rhap- (1]	100.3	169.0	
13	β-D-Rhap(OBn)$_3$-(1]	96.2	156.9	
	α-L-Rhap- (1]	97.3	171.8	
14	α-D-Rhap- (1]	101.3	169.4	3.8
	α-L-Rhap- (1]			
15	β-D-Rhap- (1]	95.8	159.4	
	α-L-Rhap- (1]	97.7	172.7	
16	α-D-Rhap(OAc)$_3$- (1]	97.4	170.0	
	α-L-Rhap(OAc)$_3$- (1]			
17	β-D-Rhap(OAc)$_3$-(1]	93.2	160.0	
	α-L-Rhap(OAc)$_3$- (1]	94.5	174.0	

In the case of the α-L,α-L- and the α-L,α-D-isomers the φ and ψ angles are the same owing to the symmetry elements (twofold symmetry axis and plane of symmetry, respectively). To determine the values of the $\varphi(=\psi)$ angles in the case of the above mentioned compounds one has to measure the $^3J_{C1-H1}$, $(=\ ^3J_{C1'-H1})$ couplings through the $C1_{\alpha L}$-*O*-$C1'_{\alpha L}$-$H1'_{\alpha L}$ $(=H1_{\alpha L}$-$C1_{\alpha L}$-*O*-$C1'_{\alpha L})$ and through the $C1_{\alpha L}$-*O*-$C1_{\alpha D}$-$H1_{\alpha D}$ $(=H1_{\alpha L}$-$C1_{\alpha L}$-*O*-$C1_{\alpha D})$ bonds, or the $^3J_{C1-C2'}$ $(=\ ^3J_{C1'-2C})$ couplings through the $C1_{\alpha L}$-*O*-$C1'_{\alpha L}$-$C2'_{\alpha L}$ $(=C2_{\alpha L}$-$C1_{\alpha L}$-*O*-$C1'_{\alpha L})$ and through the $C1_{\alpha L}$-*O*-$C1_{\alpha D}$-$C2_{\alpha D}$ $(=C2_{\alpha L}$-$C1_{\alpha L}$-*O*-$C1_{\alpha D})$ bonds.

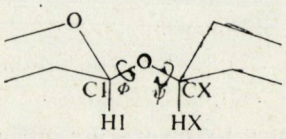

Fig. 1. The conformation about a glycosidic bond is specified by the angles φ and ψ

In the case of the α-L,β-L- and β-D,α-L-isomers two φ angles (φ_α and φ_β) can be taken into account; the first can be characterized by the $^3J_{H1_{\alpha L}-C1_{\beta L}}$ and $^3J_{H1_{\alpha L}-C1_{\beta D}}$ couplings through the $H1_{\alpha L}$-$C1_{\alpha L}$-*O*-$C1_{\beta L}$ and through the $H1_{\alpha L}$-$C1_{\alpha L}$-*O*-$C1_{\beta D}$ bonds or by the $^3J_{C2_{\alpha L}-C1_{\beta L}}$ and $^3J_{C2_{\alpha L}-C1_{\beta D}}$ couplings through the $C2_{\alpha L}$-$C1_{\alpha L}$-*O*-$C1_{\beta L}$ and through the $C2_{\alpha L}$-$C1_{\alpha L}$-*O*-$C1_{\beta D}$ bonds. The second angle (φ_β) can be described by the $^3J_{H1_{\beta L}-C1_{L\alpha}}$ and $^3J_{H1_{\beta D}-C1_{\alpha L}}$ couplings through the $H1_{\beta L}$-$C1_{\beta L}$-*O*-$C1_{\alpha L}$ and through the $H1_{\beta D}$-$C1_{\beta D}$-*O*-$C1_{\alpha L}$ bonds or by the $^3J_{C2_{\beta L}-C1_{\alpha L}}$ and $^3J_{C2_{\beta D}-C1_{\alpha L}}$ couplings through the $C2_{\beta L}$-*O*-$C1_{\beta L}$-$C1_{\alpha L}$ and through the $C2_{\beta D}$-$C1_{\beta D}$-*O*-$C1_{\alpha L}$ bonds.

The ^{13}C-^1H three-bond coupling can be obtained from the ^1H-coupled ^{13}C-NMR spectra, and its determination is rather easy in the case of anomeric carbons, as these signals are well-separated from the skeleton lines. In the case of reducing oligosaccharides the measurement of the ψ angle through the CX-*O*-C1′-H1′ bonds is more complicated [42].

The determination of the ^{13}C-^{13}C couplings from natural abundance ^{13}C-NMR spectra could be carried out only very recently [43, 44]. These measurements require large quantities of the samples and a very long time, additionally, the determination of the three-bond couplings is particularly difficult as these values are between 0—6 Hz. However, these couplings can be evaluated from the natural abundance portion of the spectrum using specifically ^{13}C-enriched oligosaccharides synthesized by chemical and biochemical methods [45—47]. In monosaccharides and simple glycosides, $^3J_{C-H}$ displays a Karplus dependence ranging from ~6 Hz when the dihedral angle is 180°, 0 Hz at 90°, 1.5—2.5 Hz at 60° or 120°, and ~5 Hz when the dihedral angle is 0° [48].

Based on these considerations, our approach was the determination of the $^3J_{C1-H1}$ coupling constants between the anomeric centers.

The work of Lemieux and Koto [49] attributes a preferred conformation to the glycosidic linkages; this assumption led to the formulation of the *exo*-anomeric effect which resulted in minimized nonbonding interactions. The meaning of the *exo*-anomeric effect may be summarized as follows. The *exo*-anomeric effect directs the torsional angle, φ ca. |55—60°|, and the torsional angle, ψ ca. |0—15°|. In this arrangement there are not any significant attractive or repulsive interactions, and in these energetically favoured conformations the protons of the anomeric and aglyconic carbons will be held in virtual VAN DER WAALS contact.

Using the concept of the *exo*-anomeric effect by measuring of the $^3J_{C-H}$ coupling constants and applying the hard-sphere *exo*-anomeric (HSEA) method, the conformations of different oligosaccharides in solution were predicted [50—54] and correlated with biological phenomena [50, 52 and 53].

On the basis of the chemical shifts of the C-1 carbons, our compounds were divided into two groups. Compounds **2**, **4**, **11**, **13**, **15** and **17** belong to

the first group in which the C-1's resonate at high field and the values of the $^3J_{C1-H1}$ coupling constants are between 2—3 Hz. In the light of the general *gauche* effect, introduced by Gorenstein [55], the presence of these high-field signals can be explained by specific spatial arrangement; the C-1 carbons

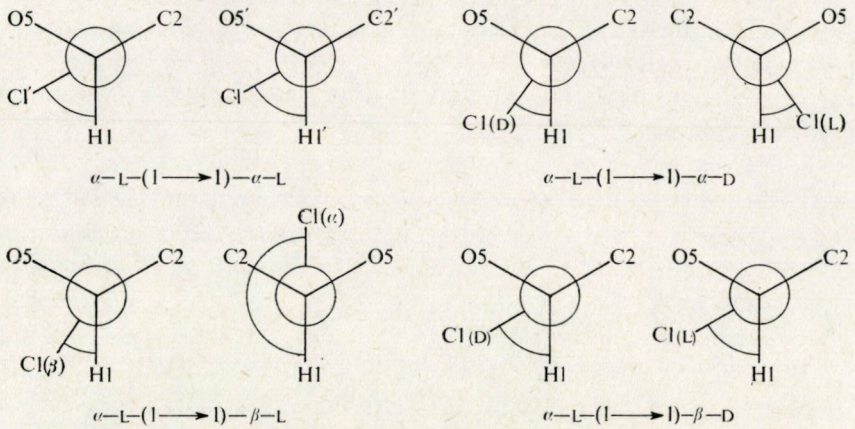

Fig. 2. Possible φ torsional angles about the Rhap-(1—1)-Rhap glycosidic linkages

Table II

^{13}C-NMR *chemical shifts of rhamnopyranosyl-rhamnopyranoside derivatives*

Carbons	Compounds							
α-Rhamnosyl	**2**	**16**	**3**	**17**	**4**	**14**	**5**	**15**
1	93.6	97.4	97.6	94.5	96.4	101.3	101.0	97.7
2	69.8	69.6	69.8	69.6	71.0	71.1	70.9	70.8
3	69.0	69.0	69.0	68.9	71.0	71.1	70.8	70.8
4	70.8	71.0	71.0	71.0	72.9	72.7	73.1	73.1
5	67.6	68.1	67.7	67.8	70.1	70.6	70.1	70.0
6	17.4	17.5	17.6	17.6	17.6	17.6	17.6	17.4
β-Rhamnosyl								
1			97.6	93.2			100.2	95.8
2			70.7	70.7			71.2	71.4
3			71.1	70.9			73.4	73.4
4			71.1	70.9			72.7	72.7
5			69.2	68.9			72.7	72.8
6			17.1	17.4			17.2	17.4

Compounds **2**, **3**, **16** and **17** measured in $CDCl_3$; the spectra of the free disaccharides (**4**, **5**, **14** and **15**) were taken in D_2O solution.

are *syn-clinal* to the ring oxygen. But this arrangement means that the *exo*-anomeric effect exists in these compounds, and the dihedral angles (φ) are near to 50—60°.

The second group involves compounds **3**, **5**, **10**, **12**, **14** and **16** with chemical shifts of the C-1 carbons at the low-field region. In the case of compound **5**, owing to the absence of symmetry elements, two different $^3J_{C1-H1}$ coupling constants could be determined; $^3J_{C1_{\alpha L}-H1_{\beta L}} = 4.0$ Hz and $^3J_{C1_{\beta L}-H1_{\alpha L}} = 6.0$ Hz. Dreiding model examinations showed that the very probable conformation was that in which $\varphi_{\alpha L}$ had a value of about 20°, and the $\varphi_{\beta L}$ angle was near to 160—170°, meaning that the *exo*-anomeric effect did not exist in this disaccharide. A similar arrangement can be proposed for the α-L,α-D--isomers (**10**, **12**, **14** and **16**), for example in the case of compound **14** to the 3.8 Hz coupling constant a $\varphi_{\alpha L}(= \varphi_{\alpha D})$ value of 20—30° is to be ordered. The ^{13}C chemical shifts of the completely assigned compounds are listed in Table II and the probable spatial arrangement of the substituents around the anomeric centers can be seen in Figure 2.

On the basis of these experiments it is concluded that the L,L- and D,L--forms of the trehalose-type oligosaccharides are very suitable models for conformational investigations, and the irregularities found in their ^{13}C-NMR spectra can be explained in terms of the conformation of their interglycosidic bonds.

Experimental

M.p.'s were determined on a Kofler hot-stage apparatus and are uncorrected. Optical rotations were measured with a Perkin-Elmer 241 automatic polarimeter. ^1H-NMR spectra were obtained on a Bruker WH-400 instrument operating in the Fourier-transform mode at 310 K unless otherwise specified, or on a Jeol MH-100 spectrometer, in solutions of D_2O or $CDCl_3$. Acetone (2.480 ppm) or TMS were used as the internal references. ^{13}C-NMR spectra were taken at the frequency of 25.16 MHz with a Varian XL-100-FT-15 using TMS or dioxan as the internal references. The $J_{C,H}$ values were measured by using the gated decoupling technique. TLC examination was carried out on DC-Alurolle Kieselgel 60 F (Merck), detection with 50% sulfuric acid. Kieselgel G (Reanal) was used for column chromatography.

2,3,4-Tri-*O*-acetyl-α-L-rhamnopyranose (1)

Benzyl 2,3,4-tri-*O*-acetyl-α-L-rhamnopyranoside (3.0 g) was hydrogenated in ethanol (100 mL) in the presence of 10% Pd—C (0.5 g). When the starting material had disappeared (monitored by TLC, dichloromethane-acetone, 9 : 1) the catalyst was filtered off, the filtrate was concentrated and the residue crystallized from ether to yield **1** (1.5 g; 66.1%), m.p. 92—94 °C, $[\alpha]_D$ +24.5° (*c* = 1.13, chloroform,) *lit.* [27] m.p. 96—98 °C, $[\alpha]_D$ +28.1° (ethanol). $C_{12}H_{18}O_8$ (290.20). Calcd. C 49.64; H 6.26. Found C 48.82; H 6.29%.

2,3,4-Tri-*O*-acetyl-α-L-rhamnopyranosyl 2,3,4-tri-*O*-acetyl-α-L-rhamnopyranoside (2) and 2,3,4-tri-*O*-acetyl-α-L-rhamnopyranosyl 2,3,4-tri-*O*-acetyl-β-L-rhamnopyranoside (3)

A 1 : 1 benzene-nitromethane mixture (200 mL) was concentrated to half its volume, in which 1.4 g of compound **1** had been dissolved. After the addition of $Hg(CN)_2$ (2.8 g) and α-acetobromo-L-rhamnopyranose (3.7 g), the mixture was stirred at 45 °C for 20 h. It was

then filtered, the filtrate concentrated, and the syrupy residue was dissolved in dichloromethane (300 mL). After filtration, the filtrate was washed with 5% potassium iodide solution (3×50 mL) and water (3×300 mL), dried over $MgSO_4$ and concentrated. The syrupy product was purified by short-column chromatography (dichloromethane-acetone, 9 : 1) to give pure **2**, which was crystallized from ether-hexane; yield 0.74 g (26.8%), m.p. 212 °C, $[\alpha]_D$ −91.1° (c = 0.814 chloroform), R_f 0.74; R_T 3.36 min (10% UCW-982, T: 250 °C, isothermal).

^{1}H-NMR (100 MHz, in $CDCl_3$): δ = 5.35−5.04 ppm (m, 6H, H-2,3,4); 4.98 (s, 2H, H-1); 3.91 (m, 2H, H-5); 2.16, 2.07 and 1.98 (3s, 18H, 6 OAc); 1.22 (d, 6H, C_5-CH_3, $J_{5,6}$ = = 6 Hz).

$C_{24}H_{34}O_{15}$ (562.51,. Calcd. C 51. 24; H 6.09. Found C 51.40; H 6.12%.

Continuing the elution, crystalline **3** (R_f 0.57) was obtained (0.31 g; 11.5%), m.p. 79−80 °C, $[\alpha]_D$ −11° (c = 0.36, chloroform), R_T 4.6 min.

^{1}H-NMR (100 MHz, in $CDCl_3$): δ = 5.48−5.00 ppm (m, 6H, H-2,2',3,3',4,4'); 4.98 (s, 1H, H-1); 4.78 (s, 1H, H-1'); 4.22 and 3.64 (2m, 2H, H-5,5'); 2.21, 2.14 (2s, 6H, 2 OAc); 2.03 (s, 6H, 2 OAc); 1.98 and 1.95 (2s, 6H, 2 OAc); 1.28 and 1.18 (2d, 6H, C_5-CH_3 and $C_{6'}-CH_3$).

$C_{24}H_{34}O_{15}$ (562.51). Calcd. C 51.24; H 6.09. Found C 51.28; H 6.12%.

α-L-Rhamnopyranosyl α-L-rhamnopyranoside (4)

A solution of **2** (300 mg) in abs. methanol (15 mL) was treated with 0.1 M sodium methoxide solution. The mixture was neutralized with Amberlite IR-120 (H^+) resin, concentrated, and the crystalline residue was recrystallized from ethanol (15 mL) to give 136 mg of **4** (82.4%), m.p. 133−134 °C, $[\alpha]_D$ −114.5° (c = 0.80, pyridine), R_f 0.60 (*n*-butanol-methanol-water, 2 : 1 : 1).

^{1}H-NMR (400 MHz, in D_2O): δ = 5.03 ppm (d, 1H, H-1, $J_{1,2}$ = 1.83 Hz); 3.95 (dd, 1H, H-2, $J_{2,3}$ = 3.48 Hz); 3.78 (dd, 1H, H-3, $J_{3,4}$ = 9.61 Hz); 3.70 (m, 1H, H-5); 3.48 (dd, 1H, H-4, $J_{4,5}$ = 9.57 Hz); 1.29 (d, 3H, C_5-CH_3, $J_{5,6}$ = 6.23 Hz).

$C_{12}H_{22}O_9$ (310.30). Calcd. C 46.44; H 7.14. Found C 46.58; H 7.21%.

α-L-Rhamnopyranosyl β-L-rhamnopyranoside (5)

A solution of **3** (150 mg) in abs. methanol (10 mL) was treated with 0.1 M sodium methoxide solution (0.05 mL). Working up of the reaction mixture as described for **4** yielded a solid foam which could not be crystallized; yield: 65 mg (78.7%), $[\alpha]_D$ −0.9° (c = 0.40, pyridine, R_f 0.50 (*n*-butanol-methanol-water 2 : 1 : 1).

^{1}H-NMR (400 MHz, in D_2O): δ = 5.03 ppm (d, 1H, H-1α, $J_{1,2}$ = 1.68 Hz); 4.77 (d, 1H, H-1β, $J_{1,2}$ = 1.07 Hz); 4.02 (dd, 1H, H-2β, $J_{2,3}$ = 3.36 Hz); 3.97 (dd, 1H, H-2α, $J_{2,3}$ = = 3.51 Hz); 3.90 (m, 1H, H-5α); 3.80 (dd, 1H, H-3α, $J_{3,4}$ = 9.76 Hz); 3.59 (dd, 1H, H-3β, $J_{3,4}$ = 9.46 Hz); 3.45 (dd, 1H, H-4α, $J_{4,5}$ = 9.68 Hz); 3.39 (m, 1H, H-5β); 3.36 (dd, 1H, H-4β, $J_{4,5}$ = 9.50 Hz); 1.30 (d, 3H, $C_{5\alpha}-CH_3$, $J_{5,6}$ = 5.80 Hz); 1.25 (d, 3H, $C_{5\alpha}-CH_3$, $J_{5,6}$ = 6.41 Hz).

$C_{12}H_{22}O_9$ (310.30). Calcd. C 46.44; H 7.14. Found C 46.62; H 7.24%.

Methyl 2,3,4-tri-*O*-benzyl-α-D-mannopyranoside (6)

To a solution of methyl 2,3-di-*O*-benzyl-4,6-*O*-benzylidene-α-D-mannopyranoside (3.6 g) in 1 : 1 dichloromethane-ether (120 mL) $LiAlH_4$ (1.2 g) and $AlCl_3$ (3.6 g) were added, and the stirred reaction mixture was boiled for 2 h. After cooling, the excess of $LiAlH_4$ was decomposed with 3 ml of ethyl acetate and $Al(OH)_3$ was precipitated with 6 mL of water. The organic layer was decanted and the residue washed with 2×30 mL of ether. The combined organic layer was extracted with water (3×20 mL), dried (Na_2SO_4) and concentrated under reduced pressure to give syrupy **6** (3.43 g; 94.7%) pure enough for the next step.

A portion (0.5 g) of the crude product was purified by column chromatography to give pure **6** $[\alpha]_D$ +35.2° (c = 1.2, chloroform), R_f 0.58 (dichloromethane-acetone, 85 : 15).

^{1}H-NMR (100 MHz, in $CDCl_3$): δ = 7.40−7.20 ppm (m, 15H, 3Ph); 4.62 (s, 1H, H-1); 3.34 (s, 3H, OCH_3); 2.30 (t, 1H, OH-6).

$C_{28}H_{32}O_6$ (464.53). Calcd. C 72.39; H 6.94. Found C 72.50; H 7.02%.

Methyl 2,3,4-tri-*O*-benzyl-6-*O*-(*p*-toluenesulfonyl)-α-D-mannopyranoside (7)

A solution of **6** (2.92 g) in 20 mL of abs. pyridine was chilled in ice-water and treated with 1.36 g (20% molar excess) of *p*-toluenesulfonyl chloride. The mixture was allowed to stand for 1 h in ice-water, then for 48 h at room temperature. The reaction mixture was poured into 150 g of ice-water and the solid obtained was recrystallized from 24 mL of hot ethanol to give 3.30 g (85%) of **7**, m.p. 111 °C; $[\alpha]_D$ +30.8° (c = 0.62, chloroform); R_f 0.55 (petroleum ether-ethyl acetate, 7 : 3). *Lit.* [32] m.p. 110–111 °C; $[\alpha]_D$ +34.4° (chloroform).

^{1}H-NMR (100 MHz, in $CDCl_3$): δ = 7.71 ppm (d, 2H); 7.40–7.20 (m, 17H, aromatic protons); 4.64 (s, 1H, H-1); 3.30 (s, 3H, OCH_3); 2.36 (s, 3H, C_5-CH_3).

$C_{35}H_{38}O_8S$ (618.40). Calcd. C 67.97; H 6.19. Found C 68.10; H 6.22%.

Methyl 2,3,4-tri-*O*-benzyl-α-D-rhamnopyranoside (Methyl 2,3,4-tri-*O*-benzyl-6-deoxy-α-D-mannopyranoside) (8)

A solution of **7** (1.50 g) in 1 : 1 dry benzene-ether (50 mL) was boiled under reflux with $LiAlH_4$ (0.50 g) for 30 min. TLC showed the complete disappearance of the starting material and the presence of only one product could be detected. After cooling, the excess of the reagent was decomposed with 3 mL of ethyl acetate and $Al(OH)_3$ was precipitated by the addition of 10 mL of water. The organic layer was decanted and the residue washed with 2×20 mL of ether. The combined organic layer was extracted with 3×20 mL of water, dried (Na_2SO_4) and concentrated. The syrupy residue (1.05 g; 96.7%) was purified on a Kieselgel G (80 g) column using petroleum ether-ethyl acetate 4 : 1 as eluant. $[\alpha]_D$ +27.1° (c = 1.45, chloroform), R_f 0.80, R_T 9.75 min (10% UCW-982, T: 275 °C, isothermal). *Lit.* [35] for the L-isomer, $[\alpha]_D$ −27.8° (chloroform).

^{1}H-NMR (100 MHz, in $CDCl_3$): δ = 7.40–7.20 ppm (m, 15H, 3 Ph); 4.64 (s, 1H, H-1); 3.27 (s, 3H, OCH_3) and 1.30 (d, 3H, C_5-CH_3).

$C_{28}H_{32}O_5$ (448.53). Calcd. C 74.91; H 7.19. Found C 75.06; H 7.13%.

2,3,4-Tri-*O*-benzyl-D-rhamnopyranose (9)

Compound **8** (2.5 g) was dissolved in acetic acid (25 mL) and 3*M* sulfuric acid (3 mL). The solution was stirred at 80–85 °C for min, when TLC examination showed the complete disappearance of the starting material. The cooled reaction mixture was diluted with water (30 mL) and extracted with dichloromethane (5×50 mL). The extract was washed with 5% aqueous $NaHCO_3$ solution (2×20 mL) and water (2×20 mL), dried (Na_2SO_4) and evaporated. The crystalline residue was recrystallized from cyclohexane to give **9** (1.57 g; 71.8%), m.p. 91–92 °C, $[\alpha]_D$ +16.6° equil. (c = 1.3, chloroform). *Lit.* [35] for the L-isomer: m.p. 90–92 °C, $[\alpha[_D$ −15.4° (c = 1.6, chloroform).

$C_{27}H_{30}O_5$ (434.51). Calcd. C 74.63; H 6.96. Found C 74.50; H 7.30%.

2,3,4-Tri-*O*-benzyl-α-D-rhamnopyranosyl 2,3,4-tri-*O*-acetyl-α-L-rhamnopyranoside (10) and 2,3,4-tri-*O*-benzyl-β-D-rhamnopyranosyl 2,3,4-tri-*O*-acetyl-α-L-rhamnopyranoside (11)

To a solution of 2,3,4-tri-*O*-benzyl-D-rhamnopyranose (**9**, 1.50 g) in dry acetonitrile (12 mL) $Hg(CN)_2$ (1.72 g) and α-acetobromo-L-rhamnose were added. After stirring for 20 h, TLC examination showed the complete disappearance of **9** and two disaccharide derivatives could be detected by UV-light or charring with sulfuric acid. The rection mixture was diluted with dichloromethane (50 mL), filtered, and the filtrate was evaporated. The residue of the evaporation was dissolved in dichloromethane (100 mL), the precipitated inorganic salts were filtered off and the filtrate was extracted with 5% aqueous potassium iodide (3×30 mL) and water (2×50 mL), dried (Na_2SO_4), and evaporated. The syrupy mixture (3.10 g) was eluted from Kieselgel G (300 g) with dichloromethane-acetone (98 : 2) to give first **10** (920 mg; 37.7%), $[\alpha]_D$ +3° (c = 1.15, chloroform), R_f 0.47.

$C_{39}H_{46}O_{12}$ (706.76). Calcd. C 66.27; H 6.56. Found C 67.01; H 6.48%.

The second compound eluted was **11** (390 mg; 16%); m.p. 118–119 °C (from 12 mL of cyclohexane); $[\alpha]_D$ −87.5° (c = 0.70, chloroform), R_f 0.34.

$C_{39}H_{46}O_{12}$ (706.76). Calcd. C 66.27; H 6.56. Found C 66.40; H 6.61%.

2,3,4-Tri-*O*-benzyl-α-D-rhamnopyranosyl α-L-rhamnopyranoside (12)

A solution of **10** 0.75 g) in abs. methanol (10 mL) was deacetylated with 0.5 mL of 0.1*M* $NaOCH_3$. After standing for 24 h at room temperature, the reaction mixture was neutralized with Amberlite IR-120 (H^+) ion-exchange resin, filtered and evaporated to give 487 mg (70.7%) of amorphous **12**, $[\alpha]_D$ =7.7° (*c* = 0.69, chloroform), R_f 0.78 (dichloromethane-methanol, *85 : 15*).

2,3,4-Tri-*O*-benzyl-β-D-rhamnopyranosyl α-L-rhamnopyranoside (13)

Compound **11** (0.16 g) was deacetylated in 3 mL of abs. methanol. The usual working-up resulted in 115 mg (87.8% of 13 as a solid foam, $[\alpha]_D$ −57.6° (*c* = 0.82, chloroform), R_f 0.72 (dichloromethane-methanol, 85 : 15).

α-D-Rhamnopyranosyl α-L-rhamnopyranoside (14)

A suspension of 10% Pd—C catalyst (50 mg) in a 9 : 1 mixture of ethanol-acetic acid (25 mL) was saturated with hydrogen for 1 h. After the addition of a solution of **12** (400 mg) in 25 mL of ethanol-acetic acid (*9 : 1*), the mixture was hydrogenated at room temperature for 48 h. The catalyst was filtered off and the filtrate concentrated to give 193 mg (90.1%) of **14**, which was crystallized from abs. ethanol to give pure 14, m.p. 213 °C, $[\alpha]_D$ 0° (*c* = 1.25, water), R_f 0.56 (*n*-butanol-methanol-water, 2 : 1 : 1*)*.

$C_{12}H_{22}O_9$ (310.30). Calcd. C 46.44; H 7.14. Found C 46.56; H 7.21%.

β-D-Rhamnopyranosyl α-L-rhamnopyranoside (15)

Compound **13** (160 mg) was hydrogenated as described for compound **14**. The resulting syrupy disaccharide (78 mg; 91.2%) was homogeneous by TLC and ^{13}C-NMR spectroscopic investigations. $[\alpha]_D$ −56.8° (*c* = 1.10, water), R_f 0.48 (*n*-butanol-methanol-water, 2 : 1 : 1).

$C_{12}H_{22}O_9$ (310.30). Calcd. C 46.44; H 7.14. Found C 46.81; H 7.03%.

2,3,4-Tri-*O*-acetyl-α-D-rhamnopyranosyl 2,3,4-tri-*O*-acetyl-α-L-rhamnopyranoside (16)

The free disaccharide **14** (100 mg) was caetylated in abs. pyridine (2 mL) and acetic anhydride (2 mL) at room temperature for 36 h. The usual working-up resulted in a crystalline product, which was recrystallized from ethanol (5 mL) to obtain **16** (130 mg; 71.8%), m.p. 202 °C, $[\alpha]_D$ 0° (*c* = 0.72, chloroform), R_f 0.60 (dichloromethane-acetone, 9 : 1).

$C_{24}H_{34}O_{15}$ (562.51). Calcd. C 51.24; H 6.09. Found C 51.40; H 6.03%.

2,3,4-Tri-*O*-acetyl-β-D-rhamnopyranosyl 2,3,4-tri-*O*-acetyl-α-L-rhamnopyranoside (17)

Compound **15** (96 mg) was acetylated in abs. pyridine (1 mL) with acetic anhydride (1 mL) to yield a syrupy crude product, which was purified on a Kieselgel G (10 g) column using dichloromethane-acetone (9 : 1) as eluant to give **17** (140 mg; 81.4%), $[\alpha]_D$ −60.3° (*c* = 0.65, chloroform), R_f 0.69.

$C_{24}H_{34}O_{15}$ (562.51). Calcd. C 51.24; H 6.09. Found C 51.01; H 5.88%.

*

The authors are grateful to Professor P. Nánási for his interest in this work and to Drs. E. Bartholdi, A. Neszmélyi and J. Harangi for recording of the ^{1}H- and ^{13}C-NMR spectra

REFERENCES

[1] Birch, G. G.: Adv. Carbohydr. Chem., **18,** 201 (1963)
[2] Noll, H., Bloch, H., Asselineau, J., Lederer, E.: Biochem. Biophys. Acta, **20,** 299 (1956)
[3] Arcamone, F., Bizioli, F.: Gazz. Chim. Ital., **87,** 896 (1957)

[4] Naganawa, H., Usui, N., Takita, T., Hamada, M., Maeda, K., Umezawa, H.: J. Antibiot., **27,** 145 (1974)
[5] Helferich, B., Zirner, J.: Chem. Ber., **95,** 2604 (1962)
[6] Lee, C. K.: Carbohydr., Res., **50,** 152 (1976)
[7] Polonsky, J., Soler, E., Varenne, J.: Carbohydr. Res., **65,** 295 (1978)
[8] Goren, M. B., Jiang, K.-S.: Chem. Phys. Lipids, **25,** 209 (1979)
[9] Liav, A., Goren, M. B.: Chem. Phys. Lipids, **27,** 345 (1980)
[10] Liav, A., Goren, M. B.: Carbohydr. Res., **84,** 171 (1980)
[11] Jezo. I.: Chem. Zvesti, **29,** 126 (1975)
[12] Paulsen, H., Sumfleth, B.: Chem. Ber., **112,** 3203 (1979)
[13] Liav, A., Goren, M. B.: Carbohydr. Res., **87,** 287 (1980)
[14] Oconnor, S., Lam, L. K. T., Jones, N. D., Chaney, M. O.: J. Org. Chem., **41,** 2087 (1970)
[15] Takatsuki, A , Kawamura, K., Okina, M., Kodama, Y., Ito, T., Tamura, G.: Agric. Biol. Chem., **41,** 2307 (1977)
[16] Ganguly, A. K., Sarre, O. Z., Greeves, D., Norton, J.: J. Am. Chem. Soc., **95,** 944 (1973)
[17] Ganguly, A. K., Saksena, A. K.: J. Chem. Soc., Chem. Commun., **1973,** 531
[18] Ollis, W. D., Smith., C., Wright, D. E.: J. Chem. Soc. Chem. Commun., **1974,** 881 and 882
[19] Ollis, W. D., Smith, C., Wright, D. E.: J. Chem. Soc. Chem.Commun., **1976,** 348
[20] Ollis, W. D., Smith, C., Sutherland, I. O., Wright, D. E.: J. Chem. Soc. Chem. Commun., **1976,** 350
[21] Birch, G. G., Lee, C. K., Rolfe, E. J.: J. Sci. Food Agric., **21,** 650 (1970)
[22] Birch, G. G., Cowell, N. D., Eyton, D.: J. Food Technol., **5,** 277 (1970)
[23] Birch, G. G., Lee, C.-K., Richardson, A. C.: Carbohydr. Res., **36,** 97 (1974)
[24] Defaye, J., Driguez, H., Henrissat, B., Bar-Guilloux, E.: Nouv. J. Chim., **4,** 59 (1980)
[25] Koto, S., Inada, S., Zen, S.: Chem. Letters, **1980,** 403
[26] Pavia, A. A., Ung-Chhun, S. N., Lacombe, J.-M.: Nouv. J. Chim., **5,** 101 (1971)
[27] Fischer, E., Bergmann, M., Rabe, A.: Chem. Ber., **53,** 2362 (1920)
[28] Pozsgay, V., Neszmélyi, A.: Carbohydr. Res., **80,** 196 (1980)
[29] Brimacombe, J. S., Cook, M. C., Tucker, L. C. N.: J. Chem. Soc., **1965,** 2292
[30] Birkofer, L., Hammes, B.: Justus Liebigs Ann. Chem., **1973,** 731
[31] Winnik, F. M., Brisson, J.-R., Carver, J. P., Krepinsky, J. J.: Carbohydr. Res., **103,** 15 (1982)
[32] Sondheimer, S. J., Eby, R., Schuerch, C.: Carbohydr. Res., **60,** 187 (1978)
[33] Wolfrom, M. L., Burke, W. J., Waisbrot, S. W.: J. Am. Chem. Soc., **61,** 1827 (1939)
[34] Helferich, B.: Adv. Carbohydr. Chem., **3,** 79 (1948)
[35] Fréchet, J. M. J., Baer, H. H.: Carbohydr., Res., **42,** 369 (1975)
[36] Koto, S., Morishima, N., Miyata, Y., Zen, S.: Bull. Chem. Soc. Jpn., **49,** 2639 (1976)
[37] Lipták, A., Szurmai, Z., Nánási, P., Neszmélyi, A.: Carbohydr. Res., **99,** 13 (1982)
[38] Dejter-Juszynski, M., Flowers, H. M.: Carbohydr. Res., **37,** 75 (1974)
[39] Paulsen, H.: Angew. Chem., **94,** 184 (1982)
[40] Rees, D. A., Skerrett, R. J.: J. Chem. Soc. B, **1970,** 189
[41] Lemieux, R. U., Nagabhushan, T. L., Paul, B.: Can. J. Chem., **50,** 773 (1972)
[42] Hayes, M. L., Serianni, A. S., Barker, R.: Carbohydr. Res., **100,** 87 (1982)
[43] Bax, A., Freeman, R., Kempsell, S. P.: J. Am. Chem. Soc., **102,** 4849 (1980)
[44] Pinto, A. C., Goncalves, M. A. L., Filho, R. B., Neszmélyi, A., Lukács, G.: J. Chem. Soc. Chem. Commun., **1982,** 293
[45] Serianni, A. S., Pierce, J., Barker, R.: Biochemistry, **18,** 1192 (1979)
[46] Nunez, H. A., Barker, R.: Biochemistry, **19,** 489 (1980)
[47] Rosevear, P., Nunez, H. A., Barker, R.: Biochemistry, **21,** 1421 (1982)
[48] Schwarcz, J. A., Perlin, A. S.: Can. J. Chem., **50,** 3667 (1972)
[49] Lemieux, R. U., Koto, S.: Tetrahedron, **30,** 1933 (1974)
[50] Lemieux, R. U., Bock, K.: J. Antibiot., XXXII Suppl. S-163 (1979)
[51] Lemieux, R. U., Bock, K., Delbaere, L. T. J., Koto, S., Rao, V. S.: Can. J. Chem., **58,** 631 (1980)
[52] Bock, K., Lemieux, R. U.: Carbohydr. Res., **100,** 63 (1982)
[53] Bock, K., Josephson, S., Bundle, D. R.: J. Chem. Soc., Perkin Trans. 2, **1982,** 59
[54] Bock, K., Vignon, M.: Nouv. J. Chim., **6,** 301 (1982)
[55] Gorenstein, D. G.: J. Am. Chem. Soc., **99,** 2254 (1977)

Acta Chimica Hungarica 114 (3—4), pp. 323—328 (1983)

PREPARATION AND CHARACTERIZATION OF COMPLEXES OF URANIUM(VI), VANADIUM(IV), TITANIUM(IV), ZIRCONIUM(IV) AND HAFNIUM(IV) WITH MERCAPTO TRIAZOLES

S. K. SENGUPTA

(Department of Chemistry, University of Gorakhpur, Gorakhpur-273001, India)

Received March, 26, 1982
In revised form January 6, 1983
Accepted for publication January 28, 1983

Complexes of UO_2(VI), VO(IV), TiO(IV), ZrO(IV) and HfO(IV) with 4-amino--5-mercapto-3-trifluoromethyl-1,2,4-triazole(HAFT), 4-benzylidene-amino-5-mercapto--3-trifluoromethyl-1,2,4-triazole (HBFT) 4-salicylidene-amino-5-mercapto-3-trifluoromethyl-1,2,4-triazole (H_2SFT) have been prepared and characterized on the basis of elemental analysis, electrical conductance, magnetic susceptibility and spectral (electronic and infrared) data. The ligands HAFT and HBFT act as NS^- bidentate chelating agents whereas H_2SFT acts as NS^-O^- tridentate chelating agent.

Introduction

In recent years, an increasing number of transition metal complexes of heterocyclic thiones have been studied on account of the striking structural features presented by this class of compounds [1—5]. These ligands, capable of undergoing thiol-thione (—N=C—SH⇌HN—C=S) tautomerism, can act as mono as well as polydentate ligands. However, there is hardly any known example of thione complexes of oxycations. In this paper the synthesis and characterization of dioxouranium(VI), oxovanadium(IV), oxotitanium(IV), oxozirconium(IV) and oxohafnium(IV) with 4-substituted-5-mercapto-3-trifluoromethyl-1,2,4-triazoles are reported .

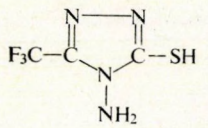

(HAFT)

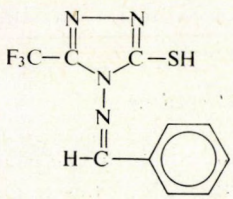

(HBFT)

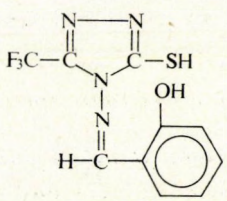

(H_2SFT)

Experimental

All the reagents used were of A.R. (B.D.H.) quality. The ligands were prepared by the reported method [6].

Preparation of the complexes

All complexes were prepared by a general method briefly described below. A warm ethanolic solution of the appropriate ligand (HAFT, HBFT or H_2SFT) was added to an aqueous methanolic solution of the appropriate metal salt (uranyl acetate, vanadyl sulphate, potassium titanyl oxalate, zirconyl chloride or hafnyl chloride) in 1 : 1 (in the case of H_2SFT) or 1 : 2 (in the case of HAFT or HBFT complexes) metal to ligand molar ratio. The solution was refluxed for about 3—4 hrs, and the precipitate obtained was filtered, thoroughly washed with ethanol and finally with ether, dried over anhydrous $CaCl_2$ in a vacuum desiccator.

Analyses

Metals were estimated by standard gravimetric methods after decomposing the complexes with conc. HNO_3. Sulphur was estimated as $BaSO_4$ and nitrogen by Kjeldahl's method.

Physical measurements

Magnetic measurements were carried out by Gouy's method using copper sulphate as a calibrant. Electrical conductance measurements were carried out in nitrobenzene on a Beckmann conductivity bridge Model RC-18A. The infrared spectra were recorded on a Perkin Elmer-621 instrument in KBr phase in the 4000—200 cm^{-1} range. The electronic spectra of the complexes were run on a Perkin Elmer-4000A and on a Cary-14 spectrophotometer in dimethylformamide.

Results and Discussion

The elemental analyses (Table I) show 1 : 2 metal to ligand stoichiometry for HAFT and HBFT complexes whereas it is 1 : 1 for H_2SFT complexes. These complexes, except HAFT and HBFT complexes of UO_2(VI), contain coordinated water molecule. The nature and number of water molecules in the complexes have been confirmed by thermogravimetric study which show weight loss at about 160—170 °C corresponding to one (HAFT and HBFT complexes of VO(IV), TiO(IV), ZrO(IV), HfO(IV) and H_2SFT complex of UO_2(VI)) or two (H_2SFT complexes of VO(IV), TiO(IV), ZeO(IV) and HfO(IV)) water molecules. All these complexes are soluble in dimethylformamide, dimethylsulphoxide, nitrobenzene and partially soluble in benzene, dichloromethane and tetrahydrofuran. The electrical conductance measurements in DMF indicate the non-electrolytic nature of the complexes.

Magnetic and electronic spectral studies

The room temperature magnetic moment of the oxovanadium(IV) complexes is between 1.71 and 1.80 B.M. These values are well within the range reported for vanadyl(IV) complexes with one unpaired electron [7]. All other complexes are found to be diamagnetic.

The electronic spectra of VO(IV) complexes show bands in the regions 12 000—12 8000, 16 000—17 000 and 22 000—23 200 cm^{-1}. The symmetry

Table I

*Analytical data of the complexes**

Compound	Calculated %			Found %		
	N	S	M	N	S	M
$UO_2(AFT)_2$	17.6	10.0	37.4	17.2	9.8	37.1
$UO_2(BFT)_2$	13.7	7.8	29.3	13.3	7.5	29.1
$UO_2(SFT) \cdot H_2O$	9.7	5.5	41.3	9.6	5.2	41.0
$VO(AFT)_2 \cdot H_2O$	24.8	14.1	11.2	24.6	14.0	11.2
$VO(BFT)_2 \cdot H_2O$	17.8	10.2	8.1	17.4	10.0	8.1
$VO(SFT) \cdot (H_2O)_2$	14.3	8.2	13.0	14.0	8.1	12.9
$TiO(AFT)_2 \cdot H_2O$	25.0	14.2	10.6	24.8	14.2	10.2
$TiO(BFT)_2 \cdot H_2O$	17.9	10.2	7.6	17.2	10.0	7.2
$TiO(SFT) \cdot (H_2O)_2$	14.4	8.2	12.3	14.1	8.0	12.1
$ZrO(BFT)_2 \cdot H_2O$	16.8	9.5	13.6	16.4	9.2	13.1
$ZrO(SFT) \cdot (H_2O)_2$	13.0	7.4	21.1	12.8	7.2	21.0
$HfO(AFT)_2 \cdot H_2O$	19.3	11.0	30.8	19.0	11.0	30.4
$HfO(BFT)_2 \cdot H_2O$	14.8	8.4	23.6	14.4	8.0	23.6
$HfO(SFT) \cdot (H_2O)_2$	10.8	6.1	34.4	10.6	6.0	34.2

* Where HAFT = $C_3H_3N_4SF_3$, HBFT = $C_{10}H_7N_4SF_3$, H_2SFT = $C_{10}H_7N_3SF_3O$

of the complexes is obviously not an idealised one. Several schemes have been advanced to interpret the electronic spectra of VO(IV) complexes [7, 8]. However, in spite of all these developments the energy level scheme developed by Ballhausen and Gray can account well for complexes conforming both to idealised and low symmetry systems [9]. The BG scheme predicts three d—d transitions for pseudo-octahedral complexes. Accordingly, the three bands observed in the present complexes may be assigned to $b_2 \rightarrow e^*$ ($^2B_2 \rightarrow E^*$), $b_2 \rightarrow b_1(^2B_2 \rightarrow {}^2B_1)$ and $b_2 \rightarrow a_1(^2B_2 \rightarrow {}^2A_1)$ transitions in an increasing order of energy. The absorption spectra of UO_2(IV) complexes exhibit three bands in the ultraviolet region at about 33 000—32 000, 34 000—33 800 and 40 000 cm^{-1}, all being charge-transfer bands from ligand to metal. No d—d transitions are expected in this case. The electronic spectra of TiO(IV), ZrO(IV) and HfO(IV) show a single band in the 24 800—24 000 cm^{-1} region which can be assigned to the charge transfer band and is in accord with their $(n-1)d^\circ, ns^\circ$ electronic configuration [10].

Infrared spectral studies

The assignments of infrared spectral bands of the ligands and the complexes are based on an earlier study [11] of similar ligands. The important i.r. bands and their tentative assignments are given in Table II. These ligands

Table II

Important infrared bands

Compound	νOH	νNH	νC=N	Thioamide Bands				νM=O	νM—N	νM—S
				—I	—II	—III	—IV			
$UO_2(AFT)_2$	—	3150s	—	1550m	1260s	1060m	740m	970s	460m	370w
$UO_2(BFT)_2$	—	—	1610s	1540m	1270s	1070m	750m	960s	450m	370w
$UO_2(SFT)H_2O$	3500mb	—	1600s	1545m	1270s	1065m	755m	960s	450m	365w
$VO(AFT)_2H_2O$	3500mb	3100s	—	1550m	1265s	1060m	740m	940s	440m	360w
$VO(BFT)_2H_2O$	3500mb	—	1605s	1540m	1260s	1060m	740m	940s	440m	365w
$VO(SFT)(H_2O)_2$	3480m	—	1600s	1540m	1270s	1070m	750m	935s	440m	360w
$TiO(AFT)_2H_2O$	3500m	3120s	—	1545m	1262s	1062m	745m	740s	420m	340w
$TiO(BFT)_2H_2O$	3490mb	—	1610s	1550m	1260s	1062m	740m	720s	420m	340w
$TiO(SFT)(H_2O)_2$	3480m	—	1605s	1540m	1270s	1070m	740m	720s	420m	335w
$ZrO(AFT)_2H_2O$	3500s	3100s	—	1540m	1265s	1065s	755m	780s	440m	350w
$ZrO(BFT)_2H_2O$	3500m	—	1610s	1540m	1260s	1065m	750m	770s	435m	350w
$ZrO(SFT)(H_2O)_2$	3480mb	—	1610s	1545m	1570s	1070m	745m	760s	440m	350w
$HfO(AFT)_2H_2O$	3500s	3100s	—	1550m	1270s	1065m	740m	910s	460m	370w
$HfO(BFT)_2H_2O$	3490m	—	1610s	1550m	1260m	1060m	750m	910s	460m	370w
$HfO(SFT)(H_2O)_2$	3480mb	—	1600s	1540m	1270s	1060m	750m	900s	460m	362w

s = strong, m = medium, mb = medium broad, w = weak.

contain the H—N—C=S group which can undergo thione⇌thiol tautomerism. The spectrum of the ligands show four bands at about 1560—1550, 1250, 1090—1080 and 790—780 cm^{-1} which are assigned [16] to thioamide-I, -II, -III and -IV vibrations, respectively. These bands are not pure and have contributions from δN—H, νC=N, νC=S and δC—H. The thioamide-IV band has been found to have maximum contribution from νC=S vibration. In the complexes, this band shifts to lower frequency (~50—40 cm^{-1}) suggesting [11, 12] a sulphur-metal coordination bond. A weak band at about 2550—2480 cm^{-1} in the spectra of the ligands suggest th presence of —SH group. However, the disappearance of this band in the spectra of all complexes suggests [13] the bonding through sulphur after deprotonation. This is further confirmed by the appearance of new bands in the far i.r. region in the spectra of the complexes at about 370—340 cm^{-1} which can be assigned to the ν(M—S) vibration.

Bands observed around 3250—3150 (in HAFT), 1630 (in HBFT and H_2SFT), 1580—1565 and 1500 cm^{-1} in the spectra of the ligands may be assigned [11] to νN—H, νC=H (—N—N=C—), νC=N(ring) and νC=C (phenyl) vibrations, respectively. Strong vibrations in the 1600—1550 cm^{-1} region are usually associated with phenyl and C=N groups and it is not usually possible to identify such bands with particular C=C or C=N linkage. However, a stringent assignment of C=N group can be made by comparing the spectrum of ligand HAFT containing N—NH_2 group with that of the ligands HBFT and H_2SFT in which it is replaced by the N—N=CH group. Following this method, strong bands observed around 1630 cm^{-1} are assigned to νC=N vibrations. However, the spectra of the complexes show the shift of this band to lower frequency (~20 cm^{-1}) indicating the coordination of the azomethine nitrogen to metal atom. The i.r. band in the region of 3250—3150 cm^{-1} in the ligand HAFT due to ν(N—H) of the primary amino group is shifted towards the lower wave number (~50 cm^{-1}) in the complexes which indicate the coordination of the amino nitrogen to the metal atom. The bands observed at about 460—420 cm^{-1} may be assigned to ν(M—N).

The ligand H_2SFT shows one band at about 3350 cm^{-1} which may be assigned to νOH of phenolic groups. However, in the spectra of complexes of H_2SFT, this band disappears indicating the coordination of the phenolic oxygen to the metal atom through deprotonation. The bands in the 500—480 cm^{-1} regions in the complexes can be assigned to ν(M—O).

Bands observed in the i.r. spectra of UO_2(VI), VO(IV), TiO(IV), ZrO(IV), and HfO(IV) complexes at about 970—960, 940—935, 740—720, 780—760 and 910—900 cm^{-1}, respectively, may be tentatively assigned to the presence of M—O multiple bonds. The conformation of the structures involving M=O bonds, specially for titanyl, zirconyl and hafnyl complexes, can only be possible by X-ray crystallography. All complexes, except HAFT and HBFT

complexes of UO_2(VI), show bands at about 3500—3480 and 880 cm^{-1} assignable to νOH and $\varrho(H_2O)$ vibrations, respectively, of coordinated water molecule [14].

REFERENCES

[1] Preti, C., Tosi, G.: Aust. J. Chem., **29**, 543 (1976); Can. J. Chem., **54**, 1558 (1976); J. Inorg. Nucl. Chem., **38**, 1125 (1976)
[2] Reedjik, J.: J. Inorg. Nucl. Chem., **35**, 239 (1973)
[3] Gupta, B. K., Gupta, D. S., Agarwala, U.: Bull. Chem. Soc. Japan, **51**, 2724 (1978)
[4] Sinha, B. K., Singh, R., Srivastava, J. P., Mishra, L. K.: J. Inorg. Nucl. Chem., **39**, 1797 (1977)
[5] Sengupta, S. K., Sahni, S. K., Kapoor, R. N.: Synth. React. Inorg. Met.-org. Chem., **10**, 269 (1980); Indian J. Chem., **20A**, 515 (1981)
[6] George, T., Thailramani, R., Dabholkar, D. A.: Indian J. Chem., **7**, 959 (1969)
[7] Selbin, J.: Coord. Chem. Rev., **1**, 293 (1966); Chem. Rev., **65**, 153 (1965)
[8] Syamal, A.: Coord. Chem. Rev., **21**, 209 (1975)
[9] Ballhausen, C. J., Gray, H. B.: Inorg. Chem., **1**, 111 (1962); Hallhausen, C. J., Djurinskij, B. F. Watson, K. H.: J. Am. Chem. Soc., **90**, 3305 (1968)
[10] Dorain, P. B., Patterson, H. H., Jordon, P. C.: J. Chem. Phys., **49**, 3845 (1968)
[11] Singh, B., Lakshmi, Agarwala, U.: Inorg. Chem., **8**, 2341 (1969); Singh, B., Agarwala, U.: J. Inorg. Nucl. Chem., **31**, 2575 (1969); Dwivedi, J. S., Agarwala, U.: Indian, J. Chem., **10**, 652 (1972)
[12] Rao, C. N. R.: Chemical Applications of Infrared Spectroscopy, Academic Press 1963
[13] Adams, D. M.: Metal Ligand and Related Vibrations, E. Arnold, London 1967
[14] Nakamoto, K.: Infrared Spectra of Inorganic and Coordination Compounds, Wiley, New York 1970

Acta Chimica Hungarica 114 (3—4), pp. 329—335 (1983)

DITHIOCARBAMATE ANIONS AS SALTS OF OXINATE CHELATES OF ZIRCONIUM(IV)[1,2]

G. S. SODHI, S. KUMAR[3] and N. K. KAUSHIK*

(Department of Chemistry, University of Delhi, Delhi-110007, India)

Received December 10, 1982
Accepted for publication January 25, 1983

(η^5-Cyclopentadienyl) (η^5-pyrrolyl) zirconium(IV) dichloride, (η^5-indenyl) (η^5-pyrrolyl) zirconium(IV) dichloride and (η^5-cyclopentadienyl) (η^5-indenyl) zirconium(IV) dichloride, when treated with 8-hydroxyquinoline (oxine) in aqueous medium form ionic derivatives of the type, $[(\eta^5\text{-R})(\eta^5\text{-R'})ZrL]^+Cl^-$ (R = C_5H_5, C_9H_7, R' = C_4H_4N; R = C_5H_5, R' = C_9H_7; L is the conjugate base of oxine). These react with dithiocarbamate anions in aqueous solution, giving ionic complexes of the type, $[(\eta^5\text{-R})(\eta^5\text{-R'})ZrL]^+X^-$ (X = Me_2NCS_2, Et_2NCS_2 and $i\text{-}Pr_2NCS_2$). IR and ^{1}H-NMR studies demonstrate that the ligand L is chelating in all the cases. Consequently there is tetrahedral coordination around the zirconium(IV) ion.

Introduction

During the course of our recent investigations [1, 2] we elucidated that the coordination of two oxygen and two nitrogen atoms around the (η^5-R)(η^5-R')M^{2+}(IV) moiety [R = C_5H_5, C_9H_7, R' = C_4H_4N; R = C_5H_5, R' = C_9H_7; M = Ti(IV), Zr(IV)] would lead to the weakening of the metal-ring bonds. In an extension of our earlier work, we report in this communication, the isolation and characterisation of some dithiocarbamate anions as salts of oxinate chelates of zirconium(IV). The interaction of (η^5-R)(η^5-R')$ZrCl_2$ with oxine in aqueous medium yielded ionic complexes of the type, $[(\eta^5\text{-R})(\eta^5\text{-R'})ZrL]^+Cl^-$, where L, the conjugate base of oxine is bidentate. Such ionic complexes possess low solvation energy, as evident from the ease of their preparation. This suggested that dithiocarbamate anions present in aqueous solution might be isolated as salts of these complexes. Thus a number of dithiocarbamate salts of the type, $[(\eta^5\text{-R})(\eta^5\text{-R'})ZrL]^+X^-$ (X = Me_2NCS_2, Et_2NCS_2, $i\text{-}Pr_2NCS_2$) were prepared and characterised.

[1] From Ph. D. Thesis of G.S.S.
[2] Presented before the Annual Convention of Chemists, Madras (India), Dec. 1981
[3] Present address: O.N.G.C., Bombay High, Bombay (India)
* To whom correspondence should be addressed

Results and Discussion

The method used for preparing and isolating $(\eta^5\text{-R})(\eta^5\text{-R'})ZrCl_2$ complexes yields materials of good purity as judged from elemental analyses and spectroscopic data. The complexes are soluble in acetone, THF, DMSO and slightly soluble in halogenated hydrocarbons. These are nonelectrolytes as evident from the conductance value of 0.5 $ohm^{-1}\,cm^2\,mole^{-1}$ for 0.5×10^{-3} *M* solution of the complexes in nitrobenzene. The electronic spectra of these compounds exhibit a single band in the 24 700—24 320 cm^{-1} region which may be assigned to the charge transfer band [3] in accordance with the electronic configuration, $(n-1)d^{\circ}ns^{\circ}$ of zirconium(IV) ion in each case. Magnetic susceptibility measurements at room temperature reveal that the complexes are diamagnetic.

Table I lists the analytical data and physical characteristics of the dithiocarbamate salts $[(\eta^5\text{-R})(\eta^5\text{-R'})ZrL]^+X^-$ ($X = Me_2NCS_2$, Et_2NCS_2, $i\text{-}Pr_2NCS_2$). The green coloured complexes are soluble in acetone, THF and partially soluble in chloroform and dichloromethane. Conductivity measurements reveal that all these complexes are 1 : 1 electrolytes in nitrobenzene.

Since the oxidation state of the metal ion in $(\eta^5\text{-R})(\eta^5\text{-R'})ZrCl_2$ and $[(\eta^5\text{-R})(\eta^5\text{-R'})ZrL]^+X^-$ is the same, the zirconium complex cation is useful for isolating anionic complexes because it is diamagnetic and does not absorb in much of the visible region of the spectrum. Hence the absorption in the UV region due to the presence of chromophoric groups in the dithiocarbamate moiety can be effectively studied. The intense band at ca. 256 nm ($\log \varepsilon \sim 4.5$) arises due to the intraligand $\pi \rightarrow \pi^*$ transitions of the N—C—S group [4—6]. The transitions of the S—C—S group are generally observed as a shoulder band [7]. Another absorption band is observed at ca. 375 nm ($\log \varepsilon \sim 4.8$). This band is considered to be a reliable indication for the presence of a chelated oxinate ligand [8]. The infrared spectra of the $[(\eta^5\text{-}C_5H_5)(\eta^5\text{-}C_9H_7)ZrL]^+X^-$ and $[(\eta^5\text{-}C_9H_7)(\eta^5\text{-}C_4H_4N)ZrL]^+X^-$ complexes show a doublet around 1470 ± 20 cm^{-1} region. This is attributed to the vibration of C—N bonds present in the pyrrolyl and dithiocarbamate groups [9, 10]. As the frequency of this band lies in between that for C—N and C=N, it is evident that C—N bond possesses some double bond character. The $[(\eta^5\text{-}C_5H_5)(\eta^5\text{-}C_9H_7)ZrL]^+X^-$ complexes show a single band in the 1480 cm^{-1} due to the stretching frequency of C—N bond in the dithiocarbamate group.

The C—N bond in the oxinate group shows a very intense absorption frequency at $\sim$1320 cm^{-1}. Since this bond too possesses partial double bond character, similar to the C—N bond in the pyrrolyl and dithiocarbamate groups, it is expected that its vibrational frequency should also occur in the 1450—1500 cm^{-1} range. In fact free oxine shows an intense absorption in this region. The occurrence of this band at lower energy in the present complexes

Table I

Analytical data and physical characteristics

Complex	M.P. °C (1)	Conductivity data $\Lambda(2)$ $(1.5\times10^{-3}M)$	Found (Calc.) %		
			Zr	S	N
$[(\eta^5\text{-R})(\eta^5\text{-R'})ZrL]^+[[Me_2NCS_2]^-$ [a]	56	29.6	17.12 (17.04)	11.81 (11.95)	5.32 (5.23)
$[(\eta^5\text{-R})(\eta^5\text{-R'})ZrL]^+[Et_2NCS_2]^-$ [a]	52	27.8	16.28 (16.19)	11.28 (11.36)	4.90 (4.97)
$[(\eta^5\text{-R})(\eta^5\text{-R'})ZrL]^+[i\text{-}Pr_2NCS_2]^-$ [a]	46	28.2	15.30 (15.42)	10.72 (10.82)	4.66 (4.73)
$[(\eta^5\text{-R})(\eta^5\text{-R'})ZrL]^+[Me_2NCS_2]^-$ [b]	72(d)	29.2	18.60 (18.75)	13.09 (13.16)	8.74 (8.63)
$[(\eta^5\text{-R})(\eta^5\text{-R'})ZrL]^+[Et_2NCS_2]^-$ [b]	65(d)	28.8	17.82 (17.73)	12.56 (12.44)	8.28 (8.16)
$](\eta^5\text{-R})(\eta^5\text{-R'})ZrL]^+[i\text{-}Pr_2NCS_2]^-$ [b]	96(d)	26.6	16.73 (16.82)	11.71 (11.80)	7.85 (7.74)
$[(\eta^5\text{-R})(\eta^5\text{-R'})ZrL]^+[Me_2NCS_2]^-$ [c]	136(d)	26.4	17.11 (17.00)	11.81 (11.93)	7.75 (7.83)
$[(\eta^5\text{-R})(\eta^5\text{-R'})ZrL]^+[Et_2NCS_2]^-$ [c]	58	28.6	16.26 (16.16)	11.44 (11.34)	7.52 (7.44)
$[(\eta^5\text{-R})(\eta^5\text{-R'})ZrL]^+[i\text{-}Pr_2NCS_2]^-$ [c]	95	27.6	15.32 (15.40)	10.72 (10.80)	7.01 (7.09)

[a] where R = C_5H_5, R' = C_9H_7; [b] where R = C_5H_5, R' = C_4H_4N; [c] where R = C_9H_7; R' = C_4H_4N
(1) Uncorrected values; (2) in ohm^{-1} cm^2 mole^{-1}; (d) with decomposition; L is the conjugate base of oxine (C_9H_6NO).

Table II

Relevant IR *data** (cm^{-1})

Complex	ν(C=N)	ν(C=S)	ν(C—O)	ν(C—H) in plane deformation	ν(C—H) out of plane deformation
$[(\eta^5\text{-R})(\eta^5\text{-R'})^{a}ZrL]^{+}[Me_2NCS_2]^{-a}$	1500(s) (1320)(s)	1000, 1020(s)	1115(s)	1070(w) (1215)(m)	810(w), 840(m) (870)(m)
$[(\eta^5\text{-R})(\eta^5\text{-R'})^{a}ZrL]^{+}[Et_2NCS_2]^{-a}$	1480(m) (1330)(s)	980, 1000(s)	1110(s)	1075(w) (1220)(m)	805(w), 815(m) 845(m) (775)(m)
$[(\eta^5\text{-R})(\eta^5\text{-R'})^{a}ZrL]^{+}[i\text{-}Pr_2NCS_2]^{-a}$	1490(m) (1325)(s)	990, 1020(s)	1110(s)	1075(w) (1225)(m)	800(w), 820(m) 850(w) (785)(m)
$[(\eta^5\text{-R})(\eta^5\text{-R'})^{b}ZrL]^{+}[Me_2NCS_2]^{-b}$	1500(m) 1450(m) (1320)(s)	970, 990(s)	1105(s)	1080(w) (1215)(m)	815(w), 840(m) (785)(m)
$[(\eta^5\text{-R})(\eta^5\text{-R'})^{b}ZrL]^{+}[Et_2NCS_2]^{-b}$	1495(s) 1455(m) (1320)(s)	980, 1005(s)	1110(s)	1085(w) (1200)(m)	800(w), 815(m) 850(m) (775)(m)
$[(\eta^5\text{-R})(\eta^5\text{-R'})^{b}ZrL]^{+}[i\text{-}Pr_2NCS_2]^{-b}$	1485(m) 1445(m) (1330)(s)	990, 1010(s)	1110(s)	1075(w) (1210)(s)	805(w), 850(m) (780)(m)
$[(\eta^5\text{-R})(\eta^5\text{-R'})^{c}ZrL]^{+}[Me_2NCS_2]^{-c}$	1480(s) 1450(m) (1330)(s)	1005, 1020(s)	1115(s)	1075(w) (1220)(s)	810(w), 825(m), 845(w) (770)(m)
$[(\eta^5\text{-R})(\eta^5\text{-R'})^{c}ZrL]^{+}[Et_2NCS_2]^{-c}$	1480(s) 1450(m)	980, 1005(s)	1105(s)	1080(w) (1230)(m)	810(w), 830(m) (775)(m)
$[(\eta^5\text{-R})(\eta^5\text{-R'})^{c}ZrL]^{+}[i\text{-}Pr_2NCS_2]^{-c}$	1490(m) 1445(m) (1325)(s)	980, 1000(s)	1110(s)	1075(w) (1225)(m)	800(w), 825(m) 850(m) (780)(m)

[a] Where R = C_5H_5, R' = C_9H_7; [b] where R = C_5H_5, R' = C_4H_4N; [c] where R = C_9H_7, R' = C_4H_4N

* The values in parenthesis are due to the oxinate group.

indicates considerably less double bond character of the (C=N) bond in the oxinate group. It may be assumed that the lone pair of electrons on nitrogen is involved in the formation of a coordinate bond with the metal ion, which causes a drift of ring electrons towards nitrogen, making the double bond formation of the C=N bond considerably less compared to that in free oxine. The presence of intense band at $\sim$1320 cm^{-1} thus indicates that the oxinate ligand is chelating in all the reported complexes. Magee and Gordan [11] studied the IR spectra of oxine and a number of metal oxinates. In the free oxine they attributed the peaks in the $\sim$1500 cm^{-1} region to the ν(C=C) and ν(C=N) stretching frequencies. No absorption frequency at $\sim$1320 cm^{-1} was observed in this case. The IR spectra of the metal oxinates showed a vibrational frequency which absorbed at $\sim$1320 cm^{-1}. However, these authors did not give any explanation of this fact. The absorption due to the ν(C=S) stretching frequency observed as a strong band at $\sim$1000 cm^{-1} [12]. A shoulder band is observed in some cases.

The oxinate group and η^5-ring systems show coupled C=H and C=C aromatic stretching at $\sim$3000 cm^{-1} and $\sim$1435 cm^{-1} respectively. The former absorption appears as a comparatively broad band. The C—H out of plane deformation due to the oxinate group occurs at $\sim$750 cm^{-1} [11] and that due to the η^5-ring system occur as weak to medium intensity bands in the range 800—850 cm^{-1} [2]. The C—H in plane deformations due to the η^5-ring systems absorb as a weak band at $\sim$1075 cm^{-1} and that due to the oxinate group occur at $\sim$1220 cm^{-1} [11]. The medium intensity band at $\sim$740 cm^{-1} is assigned to the in-plane oxine ring deformation [13]. The η^5--ring stretching frequencies result in an absorption band at $\sim$1370 cm^{-1} [2]. The strong band at $\sim$1110 cm^{-1} arises due to the C—O stretching frequency [11]. A doublet is observed at 500 $\pm$ 30 cm^{-1}. The peak at higher frequency is attributed to the C—O in-plane bending [13] and that at lower frequency to the M—O stretching frequency [2]. The relevant IR data are presented in Table II.

The ^{1}H-NMR spectra of the complexes show that the C2 proton resonance of oxinate group occurs at a lower field (δ 9.06, q, J = 4.0 Hz, 1.8 Hz) than reported for free oxine (δ 8.73). This supports the conclusion that the oxinate ligand is chelating. Hence from a structural viewpoint the C2 proton resonance signal of the oxinate group is most important. The signals due to the remaining protons of the oxinate group result in a complex multiplet in the range δ7.4—8.2. In case of the $[(\eta^5\text{-}C_9H_7)(\eta^5\text{-}C_4H_4N)ZrL]^+X^-$ derivatives, the resonance signal arising as a result of α protons of pyrrolyl group, overlaps with that of indenyl protons. There is a lack of evidence of splitting between the α and β protons of the pyrrole ring, similar to the pyrrolyl derivatives reported earlier [14]. The resonance signals of the alkyl groups in the dithiocarbamate moiety occur at almost the same frequency as for the free dithiocarbamate ligands.

The possibility of oxinate ligand bonding by simple hard sphere coulombic interactions to $(\eta^5\text{-R})(\eta^5\text{-R'})Zr(IV)^{2+}$ moiety is ruled out because in such a case a bis-oxinate complex, in contrast with the present observation, with two oxygen and two nitrogen atoms in the xy plane and parallel aromatic rings could be isolated. Such a structure would maximise the coordination number of the metal ion and simultaneously maximise the total metal-ring overlap. Since the η^5-clouds are used in the formation of metal-ring bonds and would exert less of a steric effect on the *equitorial* ligands, this configuration cannot be described as unstable on the basis of steric effects. However, applying Ballhausen and Dahl's theory [15] to the present complexes, it can be assumed that two strongly directed metal hybrids which are used in $(\eta^5\text{-R})(\eta^5\text{-R'})ZrCl_2$, are binding one oxinate ligand. Corodination of two oxygen and two nitrogen atoms in the *xy* plane by strong covalent bonds would result in the weakening of the metal ring bonds and would be energetically unfavourable. The Zr—O and Zr—N bonds have appreciable covalent character as only one oxinate ligand interacts.

Experimental

Nitrobenzene was purified for conductance measurements by the method described by Fay et al. [16]. Sodium salts of dithiocarbamic acid were prepared by the method of Gilman and Blatt [17]. Cyclopentadienyl thallium(I) [18], indenyl thallium(I) [19], sodium pyrrolyl [20] and $(\eta^5\text{-}C_5H_5)ZrCl_3$ [21] were prepared by standard methods. $(\eta^5\text{-}C_9H_7)ZrCl_3$ was prepared by the reaction of indenyl thallium(I) and zirconium tetrachloride by a method described by us elsewhere [22].

Conductance measurements were made at 30.00 $\pm$ 0.005 °C, using a Beckmann Conductivity Bridge (Model RC-18A). Magnetic susceptibilities at room temperatures were measured on a standard Gouy's balance. Mercury tetrathiocyanatocobaltate(II) ($\chi = 16.44 \times 10^{-6}$ cgs units) was used as a calibrant. Solid state IR spectra were recorded in KBr pellets in the 4000 — 200 cm^{-1} region using a Perkin-Elmer 621 grating spectrophotometer. Visible and UV spectra were recorded on a Perkin-Elmer UV-Vis. spectrophotometer model 554. Chemical shifts are expressed relative to an internal reference of TMS (1% by volume).

Preparation of $(\eta^5$-cyclopentadienyl)$(\eta^5$-pyrrolyl) zirconium(IV) dichloride

To a rapidly stirred solution of $(\eta^5\text{-}C_5H_5)ZrCl_3$ (2.62 g, 0.01 mol) in THF, a solution of freshly distilled sodium pyrrolyl (0.89 g, 0.01 mol) in THF was added dropwise. Stirring was continued for about 1 hr after the addition of sodium pyrrolyl was complete. Thereafter, the contents were refluxed for about 3 hrs. The solution was filtered through a G-4 filtration disc and upon addition of petroleum ether (60—80°), brown crystals were obtained. These were filtered, washed with petroleum ether and recrystallised from acetone solution by the addition of hexane. Yield 60%; dec. temp., 162 °C.

Anal. Found: Zr, 31.12; Cl, 24.31; N, 4.86%. Calc. for $C_9H_9NCl_2Zr$: Zr, 31.05; Cl, 24.23; N, 4.77%.

IR(KBr): ν(C—H), 3110; ν(C⋯N), 1450; ν(Zr—Cl), 360 cm^{-1}.

^{1}H-NMR ($CDCl_3$): δ 5.92 (s, 5H of cyclopentadienyl); δ 6.74 (s, 2H, Hα of pyrrolyl); δ 6.12 (s, 2H, Hβ of pyrrolyl).

Preparation of $(\eta^5$-indenyl)$(\eta^5$-pyrrolyl) zirconium(IV) dichloride

The reddish brown complex was obtained by the interaction of $(\eta^5\text{-}C_9H_7)ZrCl_3$ (3.12 g, 0.01 mol) and sodium pyrrolyl (0.89 g, 0.01 mol) in THF by following the sequence of operations given above. Yield, 65%; dec. temp., 194 °C.

Anal. Found: Zr, 26.63; Cl, 20.60; N, 4.16%. Calc. for $C_{13}H_{11}NCl_2Zr$: Zr, 26.53; Cl, 20.69; N, 4.08%.

IR(KBr): ν(C—H), 3110; ν(C⋯N), 1440; ν(Zr—Cl), 365 cm^{-1}.

^{1}H-NMR ($CDCl_3$): δ 6.18 (s, 2H, Hβ of pyrrolyl); δ 6.8—7.3 (m, 9H, Hα of pyrrolyl and 7H of indenyl).

Preparation of (η^5-cyclopentadienyl) (η^5-indenyl) zirconium(IV) dichloride

The reddish brown complex was obtained by a similar method by the reaction of (η^5-C_5H_5)$ZrCl_3$ (2.62 g; 0.01 mol) with indenyl thallium(I) (3.21 g, 0.01 mol) in THF. Yield, 60%; dec. temp., 178 °C.

Anal. Found: Zr, 26.71; Cl, 20.67%. Calc. for $C_{14}H_{12}Cl_2Zr$: Zr, 26.60; Cl, 20.76%.

IR(KBr): ν(C—H), 3000; ν(Zr—Cl), 370 cm^{-1}.

^{1}H-NMR ($CDCl_3$): δ 5.92 (s, 5H of cyclopentadienyl); δ 6.89—7.25 (m, 7H of indenyl).

Preparation of oxinate chelates and their dithiocarbamate salts

An aqueous solution of [(η^5-R)(η^5-R')ZrL]$^+Cl^-$ was obtained by stirring an aqueous solution of (η^5-R) (η^5-R')$ZrCl_2$ with an excess of solid oxine. After about 2 hrs, the contents were filtered and the aqueous solution was shaken with about 25 mL benzene. The aqueous phase was collected and added separately to an aqueous solution of sodium dithiocarbamates. Ionic complexes of the type [(η^5-R)(η^5-R')ZrL]$^+X^-$ (X = Me_2NCS_2, Et_2NCS_2, i-Pr_2NCS_2) were obtained as green precipitates. These were filtered and washed with petroleum ether. The complexes were reprecipitated from acetone by the addition of petroleum ether.

*

We take this opportunity to thank the Council of Scientific and Industrial Research for awarding a research fellowship to G.S.S.

REFERENCES

[1] Sodhi, G. S., Kaushik, N. K.: Inorg. Nucl. Chem. Lett., **17,** 211 (1981)
[2] Sodhi, G. S., Sharma, A. K., Kaushik, N. K.: J. Organomet. Chem., **238,** 177 (1982)
[3] Dorain, P. B., Patterson, H. H., Jordan, P. C.: J. Chem. Phys., **49,** 3845 (1968)
[4] Jorgensen, C. K.: J. Inorg. Nucl. Chem., **24,** 1571 (1962)
[5] Takami, F., Wakahara, S., Maeda, T.: Tetrahedron Lett., **28,** 2645 (1971)
[6] Tsipis, C. A., Manoussakis, G. E.: Inorg. Chim. Acta, **18,** 35 (1976)
[7] Jansen, M. L.: Recl. Trav. Chim., **79,** 1066 (1960)
[8] Melnema, H. A., Noltes, J. G.: J. Organomet. Chem., **25,** 139 (1970)
[9] Kaushik, N. K., Bhushan, B., Chhatwal, G. R.: Transition Met. Chem. **3,** 215 (1978)
[10] Chatt, J. A., Duncanson, L. A., Venanzi, L. M.: Suomen Kemi, **29B,** 75 (1956)
[11] Magee, R. J., Gordan, L.: Talanta, **10,** 851 (1963)
[12] Bonati, F., Ugo, R.: J. Organomet. Chem., **10,** 257 (1967)
[13] Tackett, J. E., Sawyer, D. T : Inorg. Chem., **6,** 392 (1964)
[14] King, R. B., Bisnette, M. B.: Inorg. Chem., **3,** 796 (1964)
[15] Ballhausen, C. J., Dahl, J. P.: Acta Chem. Scand., **15,** 1333 (1961)
[16] Fay, R. C., Lowry, B. N.: Inorg. Chem., **6,** 1512 (1967)
[17] Gilman, H., Blatt, A. H.: Organic Synthesis, Collective Vol. I., John Wiley, New York, 1958, 448. p.
[18] Meister, H.: Angew. Chem., **69,** 533 (1957)
[19] Chandra, K., Sharma, .R K., Garg, A. K., Garg, B. S.: Chem. Ind., **1980,** 537
[20] Joshi, K. K., Pauson, P. L., Qazi, A. B., Stubbs, W. H.: J. Organomet. Chem., **1,** 471 (1964)
[21] Jain, V. K., Garg, B. S., Singh, B. P.: Aust. J. Chem., **30,** 3545 (1977)
[22] Sodhi, G. S., Kaushik, N. K.: Bull. Soc. Chim. France, **1982,** 45

Acta Chimica Hungarica 114 (3—4), pp. 337—348 (1983)

AZACHALCONES, III

REACTIONS OF AZACHALCONES WITH AMINES AND HYDRAZINES‡

A. ATTIA* and M. MICHAEL

(Lab. of Applied Organic Chemistry, National Research Centre, Dokki, Cairo, Egypt)

Received March 11, 1982
In revised form January 4, 1983
Accepted for publication February 9, 1983

1-(X-Pyridyl)-3-(2-thienyl)-2-propen-1-ones (**1a—c**) react with hydroxylamine hydrochloride to give the corresponding oxime derivatives (**2**) which were further converted to the corresponding carbamates (**3**). The dibromo derivatives of **1** gave the isoxazoles **4**. Treatment of **1** with thiourea or hydrazines afforded the corresponding thiopyrimidines (**5**) and pyrazolines (**6**), respectively. The newly synthesized products have been screened for their antimicrobial activity against a number of microorganisms.

Various biological activities have been ascribed to several groups of compounds obtained from the reactions of α, β-unsaturated ketones [1—3]. These reports induced us to undertake the synthesis of some new compounds derived from the reactions of chalcone analogues bearing two heterocyclic moieties (azachalcones), for biological evaluation [4,5]. The present work reports the reaction of some amines and hydrazines with 1-(X-pyridyl)-3--(2-thienyl)-2-propen-1-ones (**1a—c**) [6] (Scheme 1).

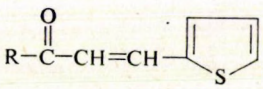

1a; R=4-pyridyl
b; R=3-pyridyl
c; R=2-pyridyl

It was found that the reaction of **1a—c** with hydroxylamine hydrochloride in boiling pyridine afforded the corresponding oxime derivatives (**2a—c**) in almost quantitative yield. The same products were obtained when the reaction was conducted in boiling ethanol in the presence of catalytic amounts of triethylamine. The IR spectra of the oximes **2** lack ν(C=O) bands and have a broad band in the 3200—2800 cm^{-1} region, characteristic of the oxime hydroxyl group, in addition to a ν(C=N) band at 1600 cm^{-1}. The UV spectra show two bands in the 265 and 305 nm regions (Table I).

+ Part II: A. Attila and M. Michael, Pharmazie, **37**, 551 (1982)
‡ Presented at the 8th International Congress of Heterocyclic Chemistry, Graz/Austria, 1981, p. 215.
* To whom correspondence should be addressed.

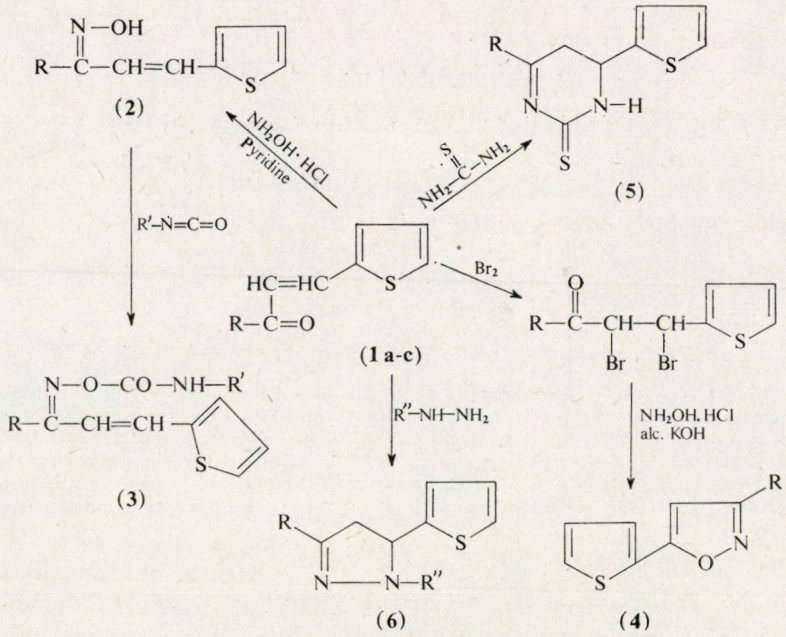

Scheme 1

The oxime derivatives (**2a** and **2b**) were further converted to the corresponding carbamates (**3a—h**) when allowed to react with methyl, isopropyl, *n*-butyl, phenyl and *p*-chlorophenyl isocyanates, respectively, in boiling dry benzene in the presence of triethylamine (Table II). The assigned structures of compounds **3** were confirmed by their spectral properties which exclude the possible formation of cyclized products. The ^{1}H-NMR spectrum of **3a** is devoid of signals corresponding to a CH_2 group and showed signals in the δ 7.1—8.9 ppm region (9H) due to the aromatic and the ethylenic protons, and a signal at 10.2 ppm (1H), assigned to the NH group, which disappeared upon deuteration. The IR spectra of **3** lack ν(OH) and include ν(NH) as a single band in the 3200 cm^{-1} region and ν(C=O, carbamate) in the 1700 cm^{-1} region. The presence of the carbonyl stretching vibration in these carbamates at such high frequencies implies that their ester tautomeric form predominates over the amide form. As expected, the UV spectra are mainly similar to those of the parent oximes (**2**). The mass spectrum of **3d** shows the molecular ion peak (M^+) at m/e 349. This peak is of very low intensity and can only be detected during the first stages of sample heating, which should be due to the thermal instability of the compound corresponding to the extremely easy fragmentation of the =N—O— and the —O—CO— bonds (Scheme 2).

It has been reported that isoxazoles; are formed in the reaction of hydroxylamine hydrochloride with propenone derivatives [7]. However, such prod-

Table I

Physical and spectral data of oximes **2**

Compound	R	Yield % (Method)	M.p., °C Solvent	Molecular formula (mol.wt)	Analysis Found/Calcd., %				UV (in MeOH)		IR (in KBr)	
					C	H	N	S	λ_{max} (nm)	ε_{max}	ν(OH) (cm^{-1})	ν(C=N) (cm^{-1})
2a	4-py	(*A*) 96 (*B*) 75	132—133 ethanol	$C_{12}H_{10}N_2OS$ (230.29)	62.60 62.58	4.34 4.38	12.17 12.17	14.14 13.92	265 305	15.800 10.150	3400—2800 (broad)	1600
2b	3-py	(*A*) 85 (*B*) 70	214—215 ethanol	$C_{12}H_{10}N_2OS$ (230.29)	62.63 62.58	4.30 4.38	12.20 12.17	13.80 13.92	265 305	13.950 14.050	3200—2700 (broad)	1600
2c	2-py	(*A*) 72 (*B*) 65	134—135 benzene	$C_{12}H_{10}N_2OS$ (230.29)	63.02 62.58	4.56 4.38	12.33 12.17	14.12 13.92	265 305	13.700 11.300	3300—2800 (broad)	1600

py = pyridyl

Table II

Physical and spectral data of carbamates **3**

Compound	R	R'	Yield %	M.p., °C solvent	Molecular formula (mol.wt.)	Analysis Found/Calcd., % C	H	N	UV (in MeOH) λ_{max}	ε_{max}	IR (in KBr) ν(NH)	ν(C=O)
3a	4-pyridyl	methyl	62	156–159 benzene	$C_{14}H_{13}N_3O_2S$ (227.33)	58.50 58.52	4.51 4.56	14.27 14.62	265 330	11.050 19.400	3190	1725
3b	4-pyridyl	isopropyl	53	141–412 benzene	$C_{16}H_{17}N_3O_2S$ (315.39)	61.23 60.93	5.33 5.43	13.56 13.32	265 335	15.400 22.050	3200	1700
3c	4-pyridyl	*n*-butyl	51	130–131 benzene	$C_{17}H_{19}N_3O_2S$ (329.41)	62.30 61.98	5.53 5.81	13.20 12.76	265 325	23.970 23.800	3200	1715
3d	4-pyridyl	phenyl	74	167–168 benzene	$C_{19}H_{15}N_3O_2S$ (349.40)	65.50 65.31	4.78 4.33	12.59 12.03	260 330	16.400 15.900	3200	1750
3e	4-pyridyl	*p*-Cl-phenyl	49	196–197 methanol	$C_{19}H_{14}ClN_3O_2S$ (383.84)	59.84 59.45	3.47 3.68	10.67 10.95	260 330	17.650 17.100	3300	1720
3f	3-pyridyl	methyl	43	134–135 ethanol	$C_{14}H_{13}N_3O_2S$ (227.33)	58.83 58.52	4.23 4.56	14.35 14.62	265 330	11.050 19.400	3225	1765
3g	3-pyridyl	phenyl	48	198–199 methanol	$C_{19}H_{15}N_3O_2S$ (349.40)	65.73 65.31	4.53 4.33	12.23 12.03	260 330	16.400 15.900	3200	1750
3h	3-pyridyl	*p*-Cl-phenyl	53	199–200 ethanol	$C_{19}H_{14}ClN_3O_2S$ (383.84)	59.33 59.45	3.52 3.68	10.88 10.95	260 330	16.900 15.800	3300	1720

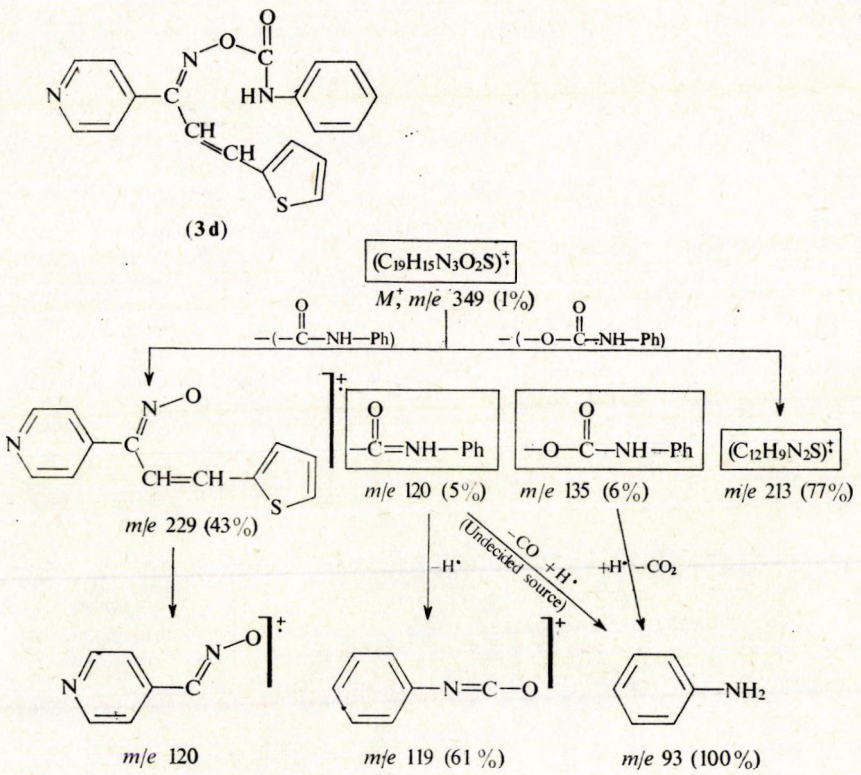

Scheme 2

ucts were not isolated when applying this reaction directly to **1a—c**. Bromination of **1a—c** in carbon tetrachloride gave the dibromo derivatives which were found to be highly unstable. The dibromo derivatives of **1a** and **1b** actually reacted with hydroxylamine hydrochloride in boiling ethanolic potassium hydroxide solution to give the corresponding isoxazoles **4a** and **4b**, respectively (Table III). The IR spectra of **4** are devoid of ν(C=O) and exhibit a ν(C=N) band at 1600 cm^{-1}. The UV spectra had two bands in the 240 and 290 nm regions, characteristic of 3,5-diarylisoxazoles.

The reactions of the propenone derivatives **1a—c** with urea and thiourea in boiling 20% alcoholic potassium hydroxide solution were also investigated. In the case of urea, no products were isolated, only tarry oils were obtained. By contrast, the reaction of thiourea with **1a** and **1b** afforded the corresponding pyrimidinethiones **5a** and **5b**, respectively. The structures of compounds **5** are based on analogy [8, 9], elemental analysis and IR spectral data. Their IR spectra revealed the presence of ν(NH) at 3320 cm^{-1}, ν(C=N) at 1600 cm^{-1} and ν(C=S) at 1230 cm^{-1} (Table III).

Table III

Physical and spectral data of compounds **4** *and* **5**

Compound	R	Yield %	M.p., °C solvent	Molecular formula (mol.wt.)	Analysis Found/Calcd., % C	H	N	S	UV (in MeOH) λ_{max}	ε_{max}	IR (in KBr), cm^{-1} ν(C=N)	ν(NH)	ν(C=S)
4a	4-py	62	135—136 methanol	$C_{12}H_8N_3OS$ (242.27)	63.25 63.14	3.37 3.53	12.29 12.27	13.99 14.05	240 290	10.850 12.170	1600	—	—
4b	3-py	60	105—106 ethanol	$C_{12}H_8N_3OS$ (242.27)	63.29 63.14	3.25 3.53	12.30 12.27	14.22 14.05	240 292	10.550 13.700	1600	—	—
5a	4-py	65	220—221 benzene	$C_{13}H_{10}N_3S_2$ (272.36)	57.45 57.32	3.50 3.70	15.12 15.42	23.65 23.54			1605	3400	1250
5b	3-py	66	184—185 methanol	$C_{13}H_{10}N_3S_2$ (272.36)	56.95 57.32	3.02 3.70	15.20 15.42	23.42 23.54			1600	3320	1250

Table IV

Physical and spectral data of pyrazolines **6**

Compound	R	R'	Yield %	M.p., °C solvent	Molecular formula (mol.wt.)	Analysis Found/Calcd., % C	H	N	UV (in MeOH) λ_{max}	ε_{max}	IR (in KBr), cm^{-1} ν(C=O)	ν(C=N)
6a	4-pyridyl	acetyl	44	134–135 pet. ether	$C_{14}H_{12}N_3OS$ (270.32)	62.23 62.20	4.38 4.47	15.50 15.54	300	21.450	1670	1600
6b	3-pyridyl	acetyl	43	115–116 cyclohexane	$C_{14}H_{12}N_3OS$ (270.32)	62.28 62.20	4.49 4.47	15.66 15.54	295	16.750	1660	1590
6c	2-pyridyl	acetyl	43	120–121 n-hexane	$C_{14}H_{12}N_3OS$ (270.32)	62.30 62.20	4.52 4.47	15.32 15.54	300	21.200	1650	1580
6d	4-pyridyl	phenyl	57	111–112 n-hexane	$C_{18}H_{14}N_3S$ (304.38)	70.85 71.02	4.52 4.64	14.02 13.80	245 305 380	22.800 3.350 20.800	—	1590
6e	3-pyridyl	phenyl	52	100–101 pet. ether	$C_{18}H_{14}N_3S$ (304.38)	70.98 71.02	4.32 4.64	13.93 13.80	250 305 375	20.700 4.200 19.600	—	1590
6f	2-pyridyl	phenyl	65	92–93 pet. ether	$C_{18}H_{14}N_3S$ (304.38)	71.33 71.02	4.72 4.64	13.65 13.80	240 305 370	18.500 4.710 19.500	—	1600
6g	4-pyridyl	*p*-tolyl	60	241–242 ethanol	$C_{19}H_{16}N_3S$ (318.40)	71.56 71.02	5.33 5.07	12.25 12.20	245 310 395	19.200 4.900 19.800	—	1605
6h	3-pyridyl	*p*-tolyl	63	108–109 pet. ether	$C_{19}H_{16}N_3S$ (318.40)	71.63 71.02	5.03 5.07	12.01 12.20	240 315 370	19.700 6.840 15.900	—	1600
6i	2-pyridyl	*p*-tolyl	65	104–105 methanol	$C_{19}H_{16}N_3S$ (318.40)	71.36 71.02	5.31 5.07	12.46 12.20	240 310 370	24.250 6.750 24.050	—	1600
6j	2-pyridyl	*p*-chlorophenyl	69	177–178 benzene	$C_{18}H_{13}ClN_3S$ (338.83)	63.50 63.80	4.03 3.87	12.44 12.40	255 285 370	22.330 6.200 20.300	—	1600

Table V

Antimicrobial activity of compounds **2 – 6**

Test organism	Minimum Inhibitory Concentration (ppm)														
	2a	**2b**	**2c**	**3a**	**3b**	**3c**	**3d**	**3e**	**3f**	**3g**	**3h**	**4a**	**4b**	**5a**	**5b**
Fusarium monoliforma	100	—	100	—	—	—	50	—	—	—	—	—	—	—	—
Fusarium oxysporum	—	100	50	—	—	—	—	—	—	—	—	100	100	50	25
Aspergillus flavus	—	—	25	—	—	—	—	—	—	—	—	—	—	100	100
Candida albicans	100	25	100	25	50	—	50	—	—	100	100	100	100	50	50
Pseudomonas aeroginosa	—	—	—	—	—	—	—	—	—	—	—	—	—	—	—
Staphylococcus aureus	100	25	—	—	100	—	—	—	—	—	25	100	100	—	—
Sarcina leutea	100	—	50	—	—	—	—	—	—	50	100	100	—	100	100
Bacillus cereus	—	—	100	25	50	—	—	—	—	—	100	100	100	25	50
Bacillus subtilis	—	—	—	—	—	—	100	—	12.5	—	25	25	25	25	25
Escherichia coli	—	—	—	—	—	—	50	—	12.5	—	50	—	—	—	—

(Table V continued)

Test organism	Minimum Inhibitory Concentration (ppm)									
	6a	6b	6c	6d	6e	6f	6g	6h	6i	6j
Fusarium moniliforma	25	25	100	100	25	100	100	50	—	50
Fusarium oxysporum	25	25	—	25	25	25	25	—	—	100
Aspergillus flavus	25	100	—	100	—	100	100	100	—	—
Candida albicans	25	—	—	25	—	100	—	—	—	50
Pseudomonas aeroginosa	—	—	—	—	—	—	—	—	—	—
Staphylococcus aureus	—	—	—	25	—	25	25	—	—	—
Sarcina leutea	—	100	—	25	—	25	50	—	—	—
Bacillus cereus	25	100	25	25	—	25	50	—	—	—
Bacillus subtilis	25	25	25	25	50	25	25	50	100	25
Escherichia coli	—	—	—	25	25	25	25	25	100	50

It was found that when **1a—c** were subjected to the action of hydrazine hydrate in boiling ethanol, a yellow product was obtained which decomposed on crystallization. Acetylation of the crude products or effecting the condensation in boiling acetic acid, yielded the stable colourless *N*-monoacetylpyrazoline derivatives **6a—c** in crystalline form. Treatment of **1a—c** with phenylhydrazine and *p*-tolylhydrazine hydrochloride in boiling ethanol in the presence of a few drops of triethylamine afforded readily the corresponding Δ^2-pyrazolines (**6d—f** and **6g—i**). Similar treatment of **1c** with *p*-chlorophenylhydrazine hydrochloride gave the Δ^2-pyrazoline **6j** (Table IV). The structures of the pyrazoline derivatives **6** are based on analogy [10], analytical, as well as spectral data. The UV spectra of the products showed absorption maxima characteristic of this class of compounds [11—13]. The IR spectra had bands at about 1390 cm^{-1} of medium or low intensity, attributed to the CH_2 deforming vibrations of the 2-pyrazoline ring [12, 14, 15]. In addition, the spectra included bands corresponding to ν(C=N), ν(Ar—N), ν(CH—N) and ν(C—H) vibrations which, according to numerous authors [12, 15, 16], prove the pyrazoline arrangement.

Antimicrobial activity

The newly synthesized compounds have been screened for their antimicrobial activity against ten microorganisms. The antimicrobial activity was measured as previously described [4]. The results are given in Table V.

Experimental

M.p.'s are uncorrected. Microanalyses were performed by the Central Services Laboratory, National Research Centre, Cairo. The IR spectra was recorded on a Beckman Spectrophotometer Model Acculab 8. The UV spectra were measured using a Carl Zeiss Spectrophotometer Type PMQ II. The mass spectra were obtained by the Danish Institute of Protein Chemistry Laboratories, Hørsholm, Denmark. Ionization by electron impact (EI) was effected on a Perkin Elmer 270 apparatus; acceleration voltage 2 kV; electron energy: 70 eV (100 μA); ion source temperature: 150 °C. The spectra were recorded during heating the sample from 90 to 140 °C. The NMR spectra were measured in $CDCl_3$ using a JEOL JWM-PMX 60 Spectrometer and obtained by the Chemistry Department, Odense University, Odense, Denmark.

Reaction of 1a—c with hydroxylamine hydrochloride

Method A: A solution of **1a—c** (0.01 mol) and hydroxylamine hydrochloride (0.015 mol) in dry pyridine (20 mL) was refluxed for 3 h. The reaction mixture was poured into icewater and the precipitated solid was filtered off and crystallized from an appropriate solvent to give the corresponding oxime derivatives **2a—c**, respectively (Table I).
Method B: A solution of **1a—c** (0.01 mol) and hydroxylamine hydrochloride (0.01 mol) in absolute alcohol (25 mL) and a few drops of triethylamine was refluxed for 4 h. The solution was filtered while hot, concentrated and cooled. The separated solid was filtered off and crystallized to give **2a—c** (Table I).

Preparation of the carbamates 3

A solution of **2a—c** (0.01 mol) and methyl, isopropyl, *n*-butyl, phenyl or *p*-chlorophenyl isocyanate (0.01 mol) and a few drops of triethylamine in dry benzene (25 mL) was refluxed for 3 h. The reaction mixture was concentrated and cooled. The separated solid was filtered off, washed with ether and crystallized from an appropriate solvent to give the corresponding oxime *N*-alkyl or *N*-aryl carbamate derivatives **3a—h** (Table II).

Bromination of 1

To a stirred solution of **1** (0.02 mol) in 25 mL of carbon tetrachloride, a solution of bromine (0.02 mol) in 10 mL of carbon tetrachloride was dropwise added at 0—5 °C. The reaction mixture was kept for 1 h in an ice-bath. The separated yellowish solid was filtered off, washed with carbon tetrachloride and directly used to prepare the isoxazole derivatives **4**.

Preparation of the isoxazole derivatives 4

A mixture of the bromo derivative of **1** (1.5 g) in 20 mL of ethanol and hydroxylamine hydrochloride (0.56 g; 0.008 mol) in 5 mL of water was treated at the boiling point of the solvent with an aqueous potassium hydroxide solution (2 g in 5 mL water). The resulting red solution was filtered and the filtrate was acidified with dilute acetic acid. The resulting solid was filtered off, washed with water, dried and crystallized from methanol to give the isoxazole derivatives **4** (Table III).

Reaction of 1a—c with thiourea

Equimolecular amounts of **1** and thiourea (0.01 mol) in 50 mL of 2% alcoholic potassium hydroxide solution was refluxed for 3 h. The separated solid was filtered off, dissolved in water and acidified with dilute hydrochloric acid. The precipitated solid was filtered off and crystallized from an appropriate solvent to give the corresponding 5,6-dihydro-4,6-disubstituted 2(1*H*)-pyramidinethiones **5a** and **5b** (Table III).

Reaction of 1a—c with hydrazine hydrate

A mixture of **1a—c** (0.01 mol) and hydrazine hydrate (0.02 mol) in 20 mL of glacial acetic acid was refluxed for 3 h. The reaction mixture was poured into ice-water. The oily product was extracted with chloroform and the extract was washed with water, dried and evaporated to dryness under reduced pressure. The oily residue was triturated with *n*-hexane and the obtained solid was crystallized to give the corresponding *N*-acetylpyrazoline derivative **5a—c** (Table IV).

Reaction of 1a—c with aryl hydrazines

Equimolecular amounts of **1** (0.01 mol) and phenyl-, *p*-tolyl- or *p*-chlorophenylhydrazine hydrochlorides in 25 mL of absolute alcohol and a few drops of triethylamine were refluxed for 3 h. The solvent was evaporated under reduced pressure. The oily residue was washed with water and treated with methanol. The solid product was filtered off and crystallized to give the corresponding 1,3,5-trisubstituted pyrazoline derivatives **6d—j** (Table V).

REFERENCES

[1] Fukuto, T. R., Metcalf, R. L., Jones, R. L., Meyers, R. O.: J. Agric. Food Chem., **17**, 923 (1969); Chem. Abstr., **71**, 90211n (1969)

[2] (a) Kost, A. N., Grandberg, I. I.: "Advances in Heterocyclic Chemistry", Vol. **6**, p. 347. Academic Press, New York, London 1966; (b) Kochetkov, N. K., Sokolov, S. D.: "Advances in Heterocyclic Chemistry", Vol. **2**, p. 465, Academic Press, New York, London 1963

[3] Thorn, G. D.: Phytopathology, **51,** 77 (1961); Chem. Abstr., **55,** 13750h (1961)
[4] Attia, A., Michael, M.: Acta Chim. Hung., **112,** 89 (1983)
[5] Attia, A., Michael, M.: Pharmazie, **37,** 551 (1982)
[6] Tsukerman, S. V., Nikitchenko, V. M., Bugai, A. I., Lavrushin, V. F.: Khim. Str. Sovistva Reactivnost Org. Soedin., **1969,** 53; Chem. Abstr., **73,** 45276t (1970)
[7] Albercht, A.: Monatsch. Chem., **35,** 1439 (1914); Chem. Abstr., **9,** 911 (1915)
[8] Sammour, A., Selim, M. I. B., Nour El-Din, M. M., Abd El-Halim, M.: U.A.R. J. Chem., **13,** 7 (1970)
[9] Sammour, A., Abdallah, M., Zoorob, H.: J. Prakt. Chem., **317,** 387 (1975)
[10] Latif, N., Mishriky, N., Girgis, N. S.: Chem. & Ind., **1976,** 28
[11] Wiley, R. H., Jarboe, C. H., Hayes, F. N., Hansbury, E., Nielsem, J. T., Callahan, P. X., Sellars, M. C.: J. Org. Chem., **23,** 732 (1958)
[12] Toi, Y. Kawai, M., Isagawa, K., Fushizaki, Y.: Nippon Kagaku Zasshi, **88,** 1095 (1967); Chem. Abstr., **69,** 36025a (1968)
[13] Korneeva, O. G., Kutsyna, L. M., Tishchenko, V. G.: Zh. Prikl. Spektrosk., **14,** 288 (1971); Chem. Abstr., **75,** 12821e (1971)
[14] Lavrushin, V. F., Tsukerman, S. V., Buryakovskaya, E. G.: Khim. Geterotsikl. Soedin., **1965,** 323; Chem. Abstr., **65,** 18067c (1965)
[15] Toi, Y., Kamai, M., Isagawa, K., Muruyama, T., Fushizaki, Y.: Nippon Kagaku Zasshi, **86,** 1322 (1965); Chem. Abstr., **65,** 13685g (1966)
[16] Tsukerman, S. V., Buryakovskaya, L. G., Rozum, Yu. S., Lavrushin, V. F.: Zh. Prikl. Spektrosk,. **8,** 453 (1968); Chem. Abstr., **68,** 118155m (1968)

Acta Chimica Hungarica 114 (3—4), pp. 349—354 (1983)

CHARACTERISATION OF Cu(II), Ni(II), Co(II), Pd(II) AND Fe(III) COMPLEXES OF ANILIC ACIDS

C. L. SHARMA*, S. S. NARVI and R. S. ARYA

(Chemical Laboratory, University of Roorkee, Roorkee-247667, India)

Received October 28, 1982
In revised form January 5, 1983
Accepted for publication February 9, 1983

Complexes of the type $[M(A-A)_2]$ where M = Cu(II), Pd(II) and A—A = =phthalanilic, 4-methyl phthalanilic and 4-nitrophthalanilic acids (deprotonated), $[M(A-A)_2(H_2O)_2]$ where M = Co(II), Ni(II) and $Na[Fe(A-A)_2(OH)_2]$ have been prepared and characterised on the basis of I.R., electronic spectra, conductance and magnetic measurements. Mössbauer studies of Fe(III) complexes have also been made. The complexes of Cu(II) and Pd(II) are square planer while others of octahedral structure.

Introduction

A survey of the existing literature reevals that the studies made on anilic acids are mainly concerned with their use in the gravimetric [1] and amperometric [2, 3] determinations of zirconium(IV) and thorium(IV). Nothing has so far been done on the preparation and characterisation of their metal complexes. The present communication deals with the preparation of copper(II), nickel(II), cobalt(II), palladium(II) and iron(III) complexes of phthalanilic, 4-methyl phthalanilic and 4-nitro phthalanilic acids and their characterisation on the basis of various physicochemical techniques. These complexes may also be of biological importance as the anilic acids have carboxylate and secondary amido groups as coordinating sites.

Experimental

Reagents and solutions

Physical measurements were performed as reported earlier [4, 5]. The solutions of hydrated metal chlorides and ferric nitrate of A.R. (B.D.H.) grade and of anilic acids, prepared in the laboratory by the method of Rao and Ratnam [6], were made in ethanol.

Preparation of the complexes

The freshly prepared metal hydroxides and anilic acids were mixed in the ratio of 1 : 2, 70% alcohol was then added to bring it into the suspended form and then the pH of the mixture was raised to ≈8.0 in the case of nickel(II), cobalt(II) and palladium(II) complexes and to ≈5.0 in the case of copper(II) and iron(III) complexes by the addition of sodium hydroxide. The mixture was then refluxed on water bath for about six hours. The precipitates

* Correspondence to be made at 134/3 Vikas Nagar, University of Roorkee, Roorkee U.P.), INDIA, 247667.

formed were filtered, washed several times with alcohol and then dried in a desiccator over anhydrous sulphuric acid.

The complexes are soluble in ethanol. The results of analysis for metal, carbon and hydrogen confirmed the formules of the complexes given in Tables I, II and III. Copper complexes were found to have the formula $[Cu(A)_2] \cdot 2\,H_2O$ where A = anilic acid. All the complexes were non-electrolytic in ethanol except that of iron(III) ($\Lambda_M = 85$ S cm^2 mole^{-1}). The reflectance spectra of the complexes gave the same bands as were obtained in their solution spectra indicating no dissociation.

Table I

Electronic spectral data of Ni(II) complexes

Complex	Observed bands and their assignments ($\times 10^{-23}$ J)			Calculated band positions ($\times 10^{-23}$ J)		$[(\nu_3-\nu_2)$ calc $-(\nu_3-\nu_2)$ obs]	$\frac{\nu_2}{\nu_1}$	B
	$^3A_{2g}(F) \rightarrow$							
	$^3T_{2g}(F)$	$^3T_{1g}(F)$	$^3T_{1g}(P)$	ν_2	ν_3			
1. $[Ni(PA)(H_2O)_2]$	21250.0	34755.0	56601.0	34387.5	56968.3	734.8	1.64	927
2. $[Ni(MPA)(H_2O)_2]$	20654.0	33762.0	55210.8	33452.0	55520.6	619.6	1.63	907
3. $[Ni(NPA)(H_2O)_2]$	21051.6	34953.6	56203.8	34179.0	56980.0	1551.0	1.66	940

PA, MPA and NPA are deprotonated Phthalanilic, 4-Methyl-Phthalanilic and 4-Nitro-Phthalanilic acids respectively.

Table II

Electronic spectral data of Co(II) complexes

Complex	Observed bands and their assignments ($\times 10^{-23}$ J)			Calculated band positions ($\times 10^{-23}$ J)		B	$10\,Dq$ ($\times 10^{-23}$ J)
	$^4T_{1g}(F) \rightarrow$						
	$^4T_{2g}(F)$ (ν_1)	$^4A_{2g}(F)$ (ν_2)	$^4T_{1g}(P)$ (ν_3)	ν_2	ν_3		
1. $[Co(PA)_2(H_2O)_2]$	16833	35350.8	39720.0	35958.5	39720.0	845	19125.0
2. $[Co(MPA)_2(H_2O)_2]$	17020	35748.0	40117.0	36355.7	40117.0	853	19335.7
3. $[Co(NPA)_2(H_2O)_2]$	17119	35946.6	39918.6	36546.0	39920.6	843	19429.0

Table III

Isomer shift (δ) and quadrupole splitting (ΔE) with respect to natural iron absorber

Complexes	δ(m sec^{-1}) ($\pm 0.03 \times 10^{-3}$)	ΔE(m sec^{-1}) ($\pm$ 0.04$\times 10^{-3}$)
1. $Na[Fe(PA)_2(OH)_2]$	0.38×10^{-3}	0.73×10^{-3}
2. $Na[Fe(MPA)_2(OH)_2]$	0.36×10^{-3}	0.80×10^{-3}
3. $Na[Fe(NPA)_2(OH)_2]$	0.36×10^{-3}	0.80×10^{-3}
4. $FeCl_3 \cdot 6H_2O$	0.65×10^{-3} (77.2 K)	0.50×10^{-3} (77.2 K)

Results and Discussion

I.R. studies

The main characteristic features of the I.R. spectra of the complexes were as follows:

The frequency of the N—H stretching vibrations occurs in the range 3100—3200 cm^{-1}. The carbonyl stretching frequency of the secondary amide in complexed form fall within the range 1660—1680 cm^{-1} which is well removed from the 1700 cm^{-1} band in free secondary amide. Although the C=O group does not take part in coordination, the shift to lower frequency may be due to the mass effect of heavy metal ions [7] linked to nitrogen, as well as to a possible weakening of C=O linkage [8]. The stretching frequency around 1470 cm^{-1} due to C—N in the spectra of anilic acids shifted to about 1480 cm^{-1} in the spectra of their complexes. The bands obtained in the region 1600—1620 cm^{-1} and 1365—1400 cm^{-1} indicate the coordination of carboxylate of anilic acids [9]. The stretching bands due to M—N and M—O were obtained at $\approx$410 and $\approx$350 cm^{-1}, respectively, in the spectra of all complexes [10]. The band at 810 cm^{-1} in the case of Ni(II) and Co(II) complexes indicate the presence of water molecules inside the coordination sphere [11] which remain unaffected on heating to $\approx$90 °C while the bands at 3480 and 1635 cm^{-1} in the case of Cu(II) complexes indicate the presence of water of crystallisation. The absence of these bands in the spectra of Pd(II) complexes indicated the absence of water molecules. An extra band at 1000 cm^{-1} was obtained only in the case of Fe(III) complexes due to the presence of coordinated OH group.

Magnetic and electronic spectral studies

The magnetic moment of copper(II) complexes was about 1.92 BM which indicated the complete quenching of the orbital contribution by the crystal field. The electronic spectra of the complexes in methanol gave three bands at 34755×10^{-23}, 39720×10^{-23} and 73482×10^{-23} J corresponding to the transitions $^2B_{1g}\rightarrow{}^2A_{1g}$, $^2B_{1g}\rightarrow{}^2E_g$ and charge transfer band respectively, and this is generally found in the compounds which belong to a square planer stereochemistry [12]. Secondly the ratio of the principal band of the copper(II) complexes and of the first spin allowed band of the high spin octahedral nickel(II) complex with the same ligands was found near 1.60 which also confirmed the square planer structure of these copper(II) complexes, the extreme case of tetragonal distortion [13].

The complexes of palladium(II) were found to be diamagnetic and square planer in structure. The electronic spectra in 50% alcohol gave three spin-allowed d—d transitions at 40713×10^{-23}, 52033×10^{-23} and 57197×10^{-23} J corresponding to $^1A_{1g}\rightarrow{}^1A_{2g}$, $^1A_{1g}\rightarrow{}^1B_{1g}$ and $^1A_{1g}\rightarrow{}^1E_g$, respectively, and

one charge-transfer band at 73482×10^{-23} J corresponding to $^1A_{1g} \rightarrow {}^1E_u$. Thus the three orbital energy parameters Δ_1, Δ_2 and Δ_3 for $C = 7B = 4866\times$ $\times10^{-23}$ J were found to be 45579×10^{-23}, 14101×10^{-23} and 4469×10^{-23} J, respectively. The separation Δ_1 for these complexes was the largest of the three orbital parameters which indicated the $d_{x^2-y^2}$ was much more strongly antibonding than any of the other d orbitals. Similarly the smaller value of Δ_3 indicated the greater stability of d_{z^2} than d_{xz} and d_{yz} in these palladium(II) complexes.

The magnetic moment of nickel(II) complexes was near to 3.10 B.M. which indicated an octahedral structure. The electronic spectra in alcohol gave three spin-allowed transitions (Table 1). The values of 'B' for these complexes were calculated using the diagonal sum rule [14], $15B = \nu_2 + \nu_3 -$ $- 3\nu_1$ and using the value of first spin allowed band (ν_1) as 10 Dq, the energies of the other bands (ν_2 and ν_3) were calculated from the standard equations [15]. The calculated values of ν_2 and ν_3 were checked against the observed values. The values of ν_2/ν_1 for these complexes were in the range 1.63—1.66, and were nearly the same as found for the octahedral complexes of nickel(II), i.e. around 1.65.

The magnetic moments of cobalt(II) complexes were in the range 4.80—5.10 B.M., characteristic for high spin octahedral complexes of cobalt(II). These three spin allowed d—d transitions obtained in their electronic spectra (alcoholic solutions) and the value of 10 Dq and B calculated from them are given in Table II. The calculated values were compared with the observed values which were found nearly the same, confirming their cubic symmetry. The values of ν_1 given in Table II were calculated assuming the transition ratio $\nu_2/\nu_1 = 2.10$. Lever [16] suggested that this ratio should be approx. 2.0 but not greater than 2.2. Ferguson et al. [17] and Holmes and McClure [18] calculated this ratio to be 1.97, 2.02 and 2.10 for the aqua, chloro and bromo complexes of Co(II), respectively.

Mössbauer and electronic spectra of the Fe(III) complexes

The electronic spectra of Fe(III) complexes in alcohol contained three bands at around 66035×10^{-23}, 75468×10^{-23} and 86391×10^{-23} J corresponding to the transitions $^6A_{1g} \rightarrow {}^4T_{1g}(P)$, $^6A_{1g} \rightarrow {}^4T_{1g}(F)$ and $^6A_{1g} \rightarrow {}^4T_{2g}(F)$, respectively. The values of magnetic moments indicated the formation of high spin complexes. The values of isomer shift δ(m sec^{-1}) and quadrupole splitting ΔE(m sec^{-1}) are given in Table III. There was a pronounced difference in the isomer shift value of $FeCl_3 \cdot 6H_2O$ and those of complexes under studies where four water molecules have been replaced by two molecules of anilic acids and two water molecules by two hydroxo groups. The values decreased to $0.38\times$ $\times10^{-23}$ indicated a greater electron density at the nucleus. Values of the same

order are reported for $[Fe(terpy)Cl_3]$ [19] the quadrupole splitting is caused by a non-zero electric field gradient at the iron nucleus. A ligand environment of lower than cubic symmetry will give an electric field gradient so that a complex containing more than one type of ligand will show a quadrupole splitting.

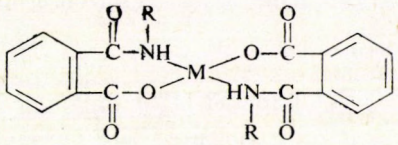

M=Pd(II), Cu(II), R=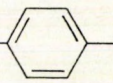 X where

X=H, CH_3, NO_2

Fig. 1

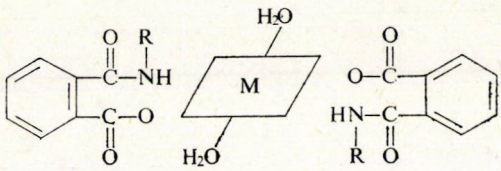

M=Ni(II), Co(II), Fe(III) containing OH in place of H_2O

Fig. 2

In our complexes this large value may be due to crystallographic distortions caused by the presence of different types of ligands inside the coordination sphere.

Thus the proposed structures of the complexes based on these studies are given below;

REFERENCES

[1] Datta, S. K.: Z. Anal. Chem., **23**, 174 (1960)
[2] Sharma, C. L., Arya, R. S.: Talanta, **26**, 577 (1979)
[3] Sharma, C. L., Arya, R. S.: Analytical Lett, **12**, A-9 (1979)
[4] Sharma, C. L., Singh, A. K., Devi, L.: J. Ind. Chem. Soc., **54**, 657 (1977)
[5] Sharma, C. L., Jain, P. K.: J. Inorg. Nucl. Chem., **41**, 805 (1979)
[6] Subba Rao, N. V., Ratnam, C. V.: J. Sci. Ind. Res., **21B**, 45 (1962)
[7] Narain, G.: J. Inorg. Nucl. Chem., **28**, 2403, 2703 (1966)

[8] Narain, G., Shukla, P., Srivastava, L. N.: J. Prakt. Chem., **31,** 123 (1966)
[9] Sharma, C. L., De, T. K., Jain, P. K.: Chemica Scripta, **18,** 79 (1981)
[10] Springer, M. P., Curran, C.: Inorg. Chem., **2,** 1270 (1963)
[11] Ueno, K., Martell, A. E.: J. Phys. Chem., **59,** 998 (1955)
[12] Figgis, B. N.: Introduction to Ligand Fields (Interscience, N. Y.), pp. 222, 316 (1967)
[13] Jorgenson, C. K.: Absorption Spectra and Chemical Bonding in Complexes (Pergamon Press, N. Y.), p. 125 (1962)
[14] Bostrup, O., Jorgenson, C. K.: Acta Chem. Scand., **11,** 1223 (1957)
[15] Nakamoto, K., McCarthy, P. J.: Spectroscopy and Structure of Metal Chelate Compounds (Wiley, N. Y.) p. 83 (1968)
[16] Lever, A. B. P.: J. Chem. Soc., A, **1967,** 2041
[17] Ferguson, J.: J. Chem. Phys., **39,** 116 (1963)
[18] Holmes, O. G., McClure, D. S.: J. Chem. Phys., **26,** 1686 (1957)
[19] Reiff, W. M., Baker, W. A., Frickson, W. E.: J. Am. Chem. Soc., **901,** 4794 (1968)

Acta Chimica Hungarica 114 (3—4), pp. 355—360 (1983)

(HYDROXYIMINO)-3(2*H*)-ISOQUINOLINONES, III[+]

DETERMINATION OF THE STRUCTURE OF PHENYL-SUBSTITUTED 1,4-DIHYDRO-3(2*H*)-ISOQUINOLINONE OBTAINED IN THE CYCLIZATION REACTION OF 3-BIPHENYL-*N*-METHYLACETAMIDE BY ^{1}H-NMR SPECTROSCOPIC STUDY OF THE 4-(HYDROXYIMINO)-DERIVATIVE

I. TIKK,[1] G. TÓTH[2] and GY. DEÁK[1]*

(*[1]Institute of Experimental Medicine, Hungarian Academy of Sciences, H-1083 Budapest, Szigony u. 43. and [2]General and Analytical Chemical Department, Technical University, H-1521 Budapest, Gellért tér 4.*)

Received November 26, 1982
Accepted for publication February 9, 1983

By means of ^{1}H-NMR spectroscopic investigations it has been established that the compound prepared from 3-methylbenzyl cyanide and benzaldehyde and described earlier as 8-methyl-1-phenyl-1,4-dihydro-3(2*H*)-isoquinolinone is actually the 6-methyl derivative. The isoquinolinone derivative carrying the substituent at position **6** was also obtained when the cyclization reaction took place between 3-biphenyl-*N*-methylacetamide and formaldehyde.

Earlier investigations on the cyclization reactions of arylacetonitriles with benzaldehyde indicated the probability that in polyphosphoric acid medium 3-methylbenzyl cyanide gave the 8-methyl derivatives of 1-phenyl--1,4-dihydro-3(2*H*)-isoquinolinone [2]. This conclusion was based on the IR spectra, since the spectrum of the 5-methyl derivative obtained from 2-methylbenzyl cyanide and that of the product prepared from 3-methylbenzyl cyanide were very similar and the bands characteristic of 1,2,3-trisubstituted benzene could be observed in them.

In the present work, the possibility of effecting the cyclization to *ortho* position, as against the sterically more favourable *para* position, was to be studied, starting from the appropriate 3-phenylacetic acid derivative. To eliminate any possible interfering effect of the phenyl group at C-1, the reaction was tried with formaldehyde instead of using an aromatic aldehyde. When starting from phenylacetamide, the 1,4-dihydro-3(2*H*)-isoquinolinone **1** was obtained in a very poor (8%) yield; however, the *N*-methyl (**2**) or *N*-ethyl (**3**) derivative gave the corresponding lactam in about 70% yield (Scheme 1). On the basis of these results, the reaction of 3-biphenyl-*N*-methylacetamide with formaldehyde was proposed. For this purpose, 3-biphenylacetic acid was prepared from 3-aminoacetophenon as described by Sam and Shafik [3]. In the next step, 3-biphenylacetic acid (**4**) was converted into the acid chloride **5** with thionyl chloride, then into the *N*-methyl acid amide **6**, by means of

[+] Part II: Ref. [1], part I: Ref. [4]
* To whom correspondence should be addressed.

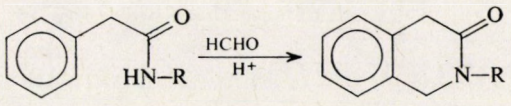

1; 2; 3

	R	%
1	H	8
2	Me	73
3	Et	70

Scheme 1

methylamine. Simultaneously, the biphenylacetamide **7** was prepared using thiourea [3]. In acetic acid medium, in the presence of acetic anhydride and sulfuric acid at 120 °C, 3-biphenyl-*N*-methylacetamide and formaldehyde yielded the isoquinolinone derivative **8**, whereas the similar reaction of 3-biphenylacetamide failed (Fig. 1). According to the IR spectrum of the product, it contained rather a 1,2,4-trisubstituted one, that is, the 6-phenyl derivative of 1,4-dihydro-3(2*H*)-isoquinolinone was apparently formed in the reaction. Since the IR investigations on the structures of the compounds obtained from the 3-methyl and 3-phenyl derivatives were contradictory, confirmation by NMR spectroscopy was necessary.

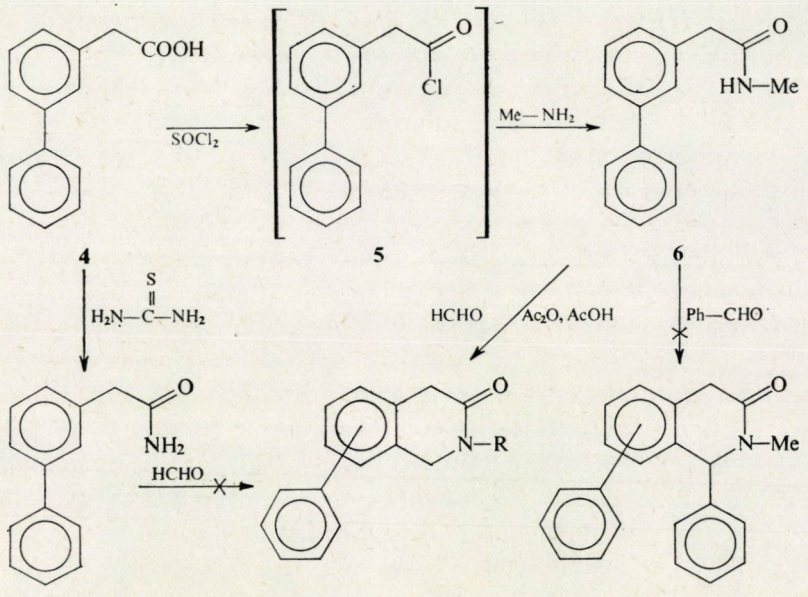

Fig. 1

In the ^{1}H-NMR spectrum of the product obtained in the reaction of 3-methylbenzyl cyanide and benzaldehyde, the protons of the aromatic ring are isochronic gicing a singlet at 6.81 ppm of 3H intensity. This does not allow direct conclusions to be drawn regarding the 1,2,3- or 1,2,4-type of substitution. In order to eliminate the above accidental isochronism of the aromatic protons, Eu(fod-d_{27})$_3$ shift reagent was employed. During earlier studies [5] it has been confirmed that in the 1,4-dihydro-3(2*H*)-isoquinolinone derivatives the reagent is attached to the oxygen atom. Since in this way the distance between the Eu atom and H-5, and the two other hydrogen atoms in the condensed ring and the Eu atom are different, the coincidence of the proton signals can be expected to disappear on increasing the amount of the reagent, and thus this part of the spectrum will be amenable to analysis. In accordance with the expectations, first the separation of the signal of H-5 could be observed. Its broad but singlet-like appearance (halfwidth: 4 Hz) indicated that no hydrogen atom can be attached to the C-6 atom, since in this case a coupling constant of about 8—9 Hz should appear (J_{ortho} spin-spin coupling). Further increase of the amount of the shift reagent resulted in the separation also of the H-7 and H-8 signals, producing an AB spectrum, with $J_{ortho} = 8$ Hz. The above experiments, besides supporting the 6-methyl-1--phenyl-1,4-dihydro-3(2*H*)-isoquinolinone structure, also led to the elucidation of another anomaly, the isochronism of the H_2-4 methylene protons. A rapid ring inversion could be responsible for the averaging of the H_{ax}-4 and H_{eq}-4 signals, but the high chemical shift (5.45 ppm) of H-1 unambiquously indicates, in view of our earlier studies, the predominating character of the conformer containing H-1 in *equatorial* position [5]. Thus the above isochronism is probably due to the fact that the anisotropic effects on the neighbouring groups affect the H_{ax}-4 and H_{eq}-4 chemical shifts differently. This is supported by the observation that the two signals separate on the effect of Eu(fod-d_{27})$_3$, and the AX coupling also yield the geminal coupling constant of 19 Hz.

The 1,2,4-type of substitution was also confirmed by the investigation of the ^{1}H-NMR spectrum of the 4-(hydroxyimino) derivative (**10**) prepared by nitrosation of the above compound according to the method developed by us earlier [4]; here the signal of the H-5 proton had a significant downfield shift (8.52 ppm), owing to the anisotropic effect of the oxime group. The coupling constant is 1.7 Hz, characteristic of a J_{meta} coupling. At the same time, the H-7 and H-8 signals also appear separately at 6.88 and 7.05 ppm ($J_{ortho} = 8.1$ Hz).

In the ^{1}H-NMR spectrum of compound **8**, the aromatic protons give a strongly overlapping signal between 7.05 and 7.55 ppm, allowing no conclusions as regards the substitution pattern. The 4-(hydroxyimino)derivative **9** was more informative in this respect; it proved to be a mixture of the *Z* and *E* isomers in 85 : 15 ratio. In accordance with our earlier investigations [4],

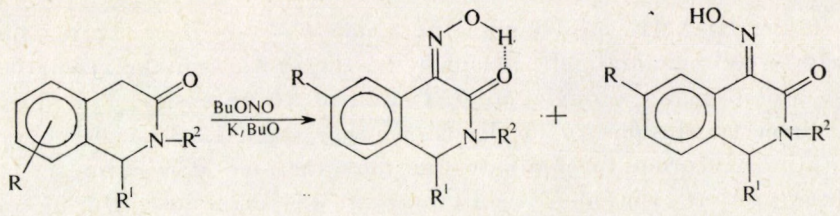

9

R=Ph; R^1=H; R^2=Me

Z/*E* = 85/15

10

R=Me; R^1=Ph; R^2=H

Fig. 2

the isomers can be distinguished and identified on the basis of the fact that in the *E* isomer the OH signal appears at an extreme low field (15.76 ppm) because of the presence of the intramolecular hydrogen bridge; also the chemical shifts of the H-5 signals differ significantly and characteristically in the *Z* and *E* isomers. In both isomers, however, the signal shows a $J_{meta} = 2$ Hz splitting which, as already discussed in connection with the analogous methyl derivative, is indicative of a C-6 substituted structure.

In compound **8**, the H_2-4 methylene protons give off a singlet signal, which is, in this case, the result of the rapid interconversion of the two boat conformers of identical energy. In 2-methyl-1,4-dihydro-3(2*H*)-isoquinolinone the above signal appears as a triplet with a splitting of $J = 1.8$ Hz. Double resonance experiments have proved that the coupling is produced by the H_2-4 methylene protons.

In continuation of our earlier work [5] on the ^{13}C-NMR investigation of 1,4-dihydro-3(2*H*)-isoquinolinone derivatives, the spectra of compounds **2** and **8** were recorded in order to determine what information the can provide in confirmation of the 6-phenyl-substituted isoquinolinone structure. In the assignment of the individual signals the known additivity rules [6] and the biphenyl signal assignment [7] were employed, in addition to the off-resonance spectra; furthermore, the spectrum of 3-biphenyl-*N*-methylacetamide (**6**) was recorded. In view of the chemical shifts of C-4a and C-8a in **2** (131.9 and 130.8 ppm) and the fact that the introduction of a phenyl group essentially does not affect the chemical shift at *meta* position while it produce an upfield shift at the C atom in *para* position, the C-4a and C-8a chemical shifts (132.6 and 129.8 ppm) in **8** are in agreement with the 6-phenyl structure. This can also be confirmed by comparing the C-3 chemical shift in 3-biphenyl-*N*-methylacetamide **6** (142.0 ppm) with the C-6 shift in **8**, where the 1.7 ppm upfield shift unambiguously indicates that cyclization took place at *para* position related to the phenyl group.

Experimental

M.p.'s were determined on a Büchi-Tottoli apparatus and are uncorrected. IR spectra were recorded in KBr pellets (Perkin Elmer Model 457). The ^{1}H- and ^{13}C-NMR spectra were obtained in the PFT mode (16K data points for the FID) at 99.6 and 25.0 MHz using a Jeol FX-100 spectrometer. The chemical shifts were determined on the δ scale using tetramethylsilane ($\delta_{TMS} = 0$) as internal standard.

1,4-Dihydro-3(2*H*)-isoquinolinone (1)

Phenylacetamide (3.7 g; 27 mmol) and paraformaldehyde (1.0 g; 33 mmol) were refluxed in a mixture of 96% acetic acid (50 mL) and *conc.* sulfuric acid (5 mL) for 50 min. The solution was poured onto ice, made alkaline (pH 8) with 25% NH_4OH, then extracted with chloroform. The organic phase was washed with water, dried over Na_2SO_4 and evaporated to dryness in vacuum. The yellow oil (2.75 g) was rubbed with ether and the yellow solid (1.0 g) obtained was recrystallized from ethyl acetate (yield: 0.32 g; 8%), m.p. 148—149 °C. (Ref. [9], m.p. 150 °C).

C_9H_9NO. (147.2) Calcd. C 73.45; H 6.16; N 9.52. Found C 73.15; H 6.23; N 9.75%.

IR: 3300, 3190 (NH), 1655 (C=O), 742 (=CH) cm^{-1}.

3-Biphenylacetyl chloride (5)

3-Biphenylacetic acid (4) 31.3 g; 136 mmol was dissolved in chloroform (800 mL) and thionyl chloride (18.3 mL; 250 mmol) was added at a slow rate. The solution was refluxed until the evolution of gas ceased (about 2 h), then the solvent was evaporated in vacuum and the acid obtained (29.3 g; 93%) was processed further without purification.

3-Biphenyl-*N*-methylacetamide (6)

Crude biphenylacetyl chloride (23.9 g; 120 mmol) was added to a mixture of 6*N* NaOH (83 mL) and 33.4% aqueous methylamine (75.6 mL) with cooling, to keep the temperature of the reaction mixture below 10 °C. The precipitate which separated was stirred for 3 h, filtered off and crystallized from ethyl acetate (17.3 g; 62%) m.p. 120—121 °C.

$C_{15}H_{15}NO$. (225.3) Calcd. C 79.97; H 6.71; N 6.21. Found C 80.20; H 6.84; N 6.15%.

IR: 3270, 3082 (NH), 1632 (C=O) cm^{-1}.

^{1}H-NMR ($CDCl_3$): 2.69 (N—Me), $J_{CH,NH} = 5$ Hz; 3.54 ($-CH_2-$); 5.56 (broad, NH); 7.05—7.55 (arom. protons) ppm.

^{13}C-NMR ($CDCl_3$): 26.5, 126.1, 127.1, 127.5, 128.3, 128.8, 129.4, 135.6, 140.7, 171.5 ppm.

2-Methyl-6-phenyl-1,4-dihydro-3(2*H*)-isoquinolinone (8)

3-Biphenyl-*N*-methylacetamide (1.0 g; 4.4 mmol) was dissolved in a mixture of acetic acid (10 mL) and acetic anhydride (5 mL). Formaldehyde (0.3 g; 10 mmol) was added to the solution, followed by sulfuric acid (0.6 mL) which was added dropwise, under vigorous stirring. The solution was heated to 120 °C; the reaction was complete in 2 h. After pouring onto ice, the product was isolated by extraction with ethyl acetate, the organic phase was washed with a saturated solution of Na_2CO_3 until neutral, dried over Na_2SO_4 and evaporated to dryness. The oily residue crystallized spontaneously (0.73 g; 75%), m.p. 130—132 °C. After recrystallization from ethanol, m.p. 136—139 °C.

IR: 3800, 2800 (broad), 1600 (broad), 1475, 1400, 1330, 1315, 1240, 818, 755, 705 cm^{-1}.

^{1}H-NMR ($CDCl_3$): 3.10 (N-Me), 3.64 (H_2-4), 4.48 (H_2-1), 7.05—7.55 (arom.H).

^{13}C-NMR ($CDCl_3$): 34.3, 36.9, 52.6, 125.4, 125.5, 125.9, 127.0, 127.5, 128.8, 129.8, 132.6, 140.3, 140.6, 168.6 ppm.

$C_{16}H_{15}NO$. (237.4) Calcd. C 80.99; H 6.37; N 5.90. Found C 80.66; H 6.20; N 5.60%.

(*Z*,*E*)-4-(hydroxyimino)-2-methyl-6-phenyl-1,4-dihydro-3(2*H*)-isoquinolinone (9)

Compound **8** (0.7 g; 2.0 mmol) was dissolved in anhydrous toluene (20 mL), butyl nitrite (1.0 mL; 8 mmol) and then potassium *t*-butoxide (0.7 g; 6.2 mmol) were added to the solution under cooling, stirring and introduction of N_2 gas, at a rate suitable to keep the temperature of the mixture below 5 °C. The toluene solution was then poured into ice-water, and the aqueous phase was acidified (pH 2) with 2*N* HCl. After extraction with chloroform, the organic phase was dried over Na_2SO_4 and evaporated to dryness in vacuum. The residual oil was crystallized by rubbing with ether; yield: 0.1 g (13%); m.p. 146—148 °C.

$C_{16}H_{14}N_2O_2$. (266.3). Calcd. C 72.17; H 5.29; N 10.51. Found C 71.88; H 5.12; N 10.30%.

IR: 3450, 3120, 2910, 1638, 1545, 1495, 1482, 1435, 1395, 1350, 1052, 1020, 972, 960, 842, 824, 765, 700 cm^{-1}.

^{1}H-NMR ($CDCl_3$): 3.12 (N—Me), 4.62 (NCH_2) 8.20 (H-5) for *Z*; 3.0 (NMe), 4.36 (NCH_2), 9.17 (H-5) for *E*; 7.1—7.7 (arom. H), 15.76 (OH) ppm. (*Z*/*E* = 85/15).

(*E*)-4-(Hydroxyimino)-6-methyl-1-phenyl-1,4-dihydro-3(2*H*)-isoquinolinone (10)

6-Methyl-1-phenyl-1,4-dihydro-3(2*H*)-isoquinolinone [2] (0.5 g; 1.5 mmol) was dissolved in benzene (15 mL) and butyl nitrite (6.4 mL) was added to it. The solution was cooled to 0 °C and mixed with potassium *t*-butoxide (0.65 g; 5.7 mmol), with stirring. The solution was poured into ice-water, the aqueous phase was acidified to pH 2 with 2*N* HCl, the precipitate which separated was filtered off (0.5 g) and recrystallized from methanol (30 mL); yield: 0.25 g (45%); m.p. 201 °C.

IR: 3150, 3030, 2920, 1685, 1598, 1492, 1472, 1325, 1298, 1185, 1095, 1060, 1012, 895, 832, 802, 780, 718, 700, 618 cm^{-1}.

^{1}H-NMR [$(CD_3)_2SO—CDCl_3$ = 1 : 1]: 2.34 (Ar—Me), 5.55 (H-1), 8.52 (H-5), J_{meta} = = 1.7 Hz, 6.88 (arom. H), J_{ortho} = 8.1 Hz, 7.05 (arom. H), 7.18 (arom. H), ppm.

2-Methyl-1,4-dihydro-3(2*H*)-isoquinolinone (2) [8]

^{1}H-NMR ($CDCl_3$): 3.00 (N—Me), 3.45 (H_2-4), 4.55 H_2-1 J = 1.8 Hz, 6.9—7.2 (arom. H), ppm.

^{13}C-NMR ($CDCl_3$): 34.1, 36.6, 52.5, 125.0, 126.4, 127.1, 127.2, 130.8, 131.9, 168.8 ppm.

REFERENCES

[1] Tikk, I., Deák, Gy., Tóth, G.: Acta Chim. Hung. (In the press)
[2] Csürös, Z., Deák, Gy., Hoffmann, I., Török-Kalmár, A.: Acta Chim. Scad. Sci. Hung., **60,** 177 (1969)
[3] Sam, J., Shafik, R. M.: J. Pharm. Sci., **58,** 952 (1969)
[4] Tikk, I., Deák, Gy., Tóth, G.: Acta Chim. Acad. Sci. Hung., **106,** 83 (1981)
[5] Tóth, G., Hazai, L., Deák, Gy., Duddeck, H.: Justus Liebigs Ann. Chem., **1978,** 1103
[6] Pretsch, E., Clerc., T., Seibl, J., Simon, W.: Tabellen zur Strukturaufklärung Organischer Verbindungen mit Spektroskopischen Methoden, Springer Verlag, Berlin 1981
[7] Alger, T. D., Grant, D. M., Paul, E. G.: J. Am. Chem. Soc., **88,** 5397 (1966)
[8] Jap. Pat. 54-138577; Chem. Abstr., **92,** 128757 (1980)
[9] Kim, Y. C.: Can. J. Chem., **47,** 3259 (1969)

Acta Chimica Hungarica 114 (3—4), pp. 361—363 (1983)

SYNTHESIS OF AGECORYNIN-A

V. K. SHARMA and S. R. GUPTA*

(Department of Chemistry, University of Delhi, Delhi-110 007, India)

Received January 7, 1983
Accepted for publication February 17, 1983

Synthesis of Agecorynin-A(**1**), a new methylenedioxyflavanone from *Ageratum corymbosum* Zucc. has been achieved to verify the proposed constitution.

Recently, a new methylenedioxyflavanone Agecorynin-A (**1**) has been isolated [1] from *Ageratum corymbosum* Zucc. The constitution of **1** has been assigned as 3',4'-methylenedioxy-5,6,7,5'-tetramethoxyflavanone on the basis of spectral (UV, IR, ^{1}H-NMR and MS) data and degradative studies. Only a few naturally occurring flavanones possessing methylenedioxy group as a substituent have been reported [1—3]. To provide synthetic confirmation of the proposed constitution for Agecorynin-A we now report the synthesis of **1**.

Condensation of 2-hydroxy-4,5,6-trimethoxyacetophenone [4] and 4,5--dibenzyloxy-3-methoxybenzaldehyde **2** in alkaline medium afforded the

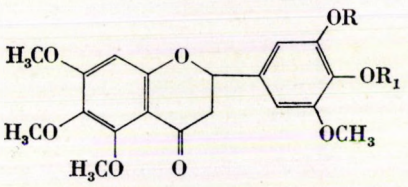

1 R + R_1 = $-CH_2-$
4 R = R_1 = H

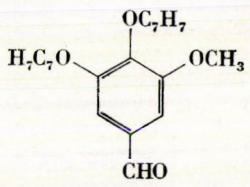

2

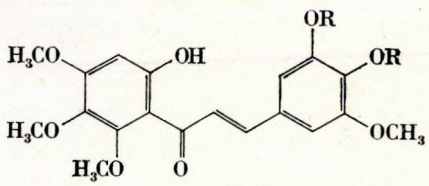

3 R = C_7H_7
5 R = H

* To whom correspondence should be addressed.

benzylated chalcone **3** ($C_7H_7 = CH_2C_6H_5$). Compound **2** was prepared by dibenzylation of 4,5-dihydroxy-3-methoxybenzaldehyde [5]. Compound **3** was then cyclised in 4% H_2SO_4 in methanol [6] to furnish tow major products, viz. the dihydroxyflavanone **4** and trihydroxychalcone **5**. The formation of **4** and **5** could be explained by cleavage of protecting groups by the acid [7]. Two more products were obtained in the above reaction which could not be identified due to paucity of the material. Methylenation of **4** using CH_2I_2 gave **1**. The spectral data of **1** were in complete agreement with those reported [1] for the natural product. Direct comparison could not be made as natural sample was not available with the authors [1].

Experimental

M.p.'s are uncorrected. IR spectra were recorded on a Perkin-Elmer IR spectrophotometer Model-621 (ν_{max} in cm^{-1}), UV spectra on a Beckmann DU-2 spectrophotometer (λ_{max} in nm) and ^{1}H-NMR spectra on a Perkin-Elmer R-32 (90 MHz) spectrometer using TMS as internal standard; chemical shifts were recorded in δ (ppm).

4,5-Dibenzyloxy-3-methoxybenzaldehyde (2)

4,5-Dihydroxy-3-methoxybenzaldehyde [5] (1 g) was dissolved in dimethyl formamide (50 mL) and refluxed with benzyl chloride (2.2 mL) and anhydrous potassium carbonate (5 g) for 20 h. The reaction mixture, after cooling, was poured on to crushed ice where upon an oily product was obtained. It was then extracted with ethyl acetate (5×30 mL). Removal of the solvent gave a product which was purified by column chromatography over silica gel. Elution with benzene-petroleum ether (1 : 1) gave **2** as a yellow oil (1.2 g).

^{1}H-NMR ($CDCl_3$): 3.75 (s, 3H, $-OCH_3$), 4.95 (s, 4H, 2× $-OCH_2C_6H_5$), 6.87 (m, 2H, H-2 and H-6), 6.95–7.30 (m, 10H, 2× $-OCH_2C_6H_5$), 9.40 (s, 1H, —CHO).

3,4-Dibenzyloxy-2'-hydroxy-4',5',6',5-tetramethoxychalcone (3)

To a stirred solution of 2-hydroxy-4,5,6-trimethoxyacetophenone [4] (500 mg) in ethanol (10 mL) was added at 0–5 °C a solution of potassium hydroxide (10 g in 25 mL of ethanol and 6 mL of H_2O) followed by the dropwise addition of a solution of **2** (450 mg in 5 mL of ethanol) in the course of 30 min. After 48 h stirring at room temperature, the deep-orange coloured solution was diluted with water, cooled and acidified with dilute acetic acid. The product was extracted from the reaction mixture with ethyl acetate (3×30 mL). After removal of the solvent, the crude chalcone was purified by preparative TLC (silica gel; benzene). Compound **3** was obtained as an orange yellow solid (600 mg), m.p. 93–94 °; it gave an orange-red colour with *conc.* H_2SO_4.

UV (MeOH): 370, 275.

IR (KBr): 3400 (br), 1680, 1605.

^{1}H-NMR ($CDCl_3$): 3.80 (s, 3H, $-OCH_3$), 3.85 (s, 9H, 3× $-OCH_3$), 5.07 (s, 2H, $-OCH_2C_6H_5$), 5.12 (s, 2H, $-OCH_2C_6H_5$), 6.27 (s, 1H, H-3'), 6.85 (m, 2H, H-2 and H-6), 7.20–7.50 (m, 11H, 2× $-OCH_2C_6H_5$ and α-H), 7.72 (d, 1H, β-H), 13.6 (s, 1H, D_2O exchangeable, —OH).

3',4'-Dihydroxy-5,6,7,5'-tetramethoxyflavanone (4)

Compound **3** (500 mg) was refluxed with methanolic sulphuric acid (4%, 60 mL) for 48 h. The reaction mixture was then concentrated to about 10 mL by evaporation under reduced pressure and crushed ice was added. The crude product was then extracted with

ethyl acetate (3×30 mL). After removal of the solvent the product was subjected to preparative TLC (silica gel; benzene : ethyl acetate, 20 : 1) to give **4** and **5** along with two minor components which have not been identified.

3',4'-Dihydroxy-5,6,7,5'-tetramethoxyflavanone (4)

Light yellow needles (250 mg) from methanol, m.p. 205—206 °C, the compound gave pink colour with conc. H_2SO_4.

UV (MeOH): 275, 320 (sh).

^{1}H-NMR ($CDCl_3$): 2.75 and 2.90 (two m, 2H, H-3), 3.80 (s, 3H, $-OCH_3$), 3.86 (s, 3H, $-OCH_3$), 3.90 (s, 6H, 2×$-OCH_3$), 5.20 (d, 1H, H-2), 6.30 (s, 1H, H-8), 6.65 (m, 2H, H-2' and H-6').

2',3,4-trihydroxy-4',5',6',5-tetramethoxychalcone (5)

Yellow needles (50 mg) from methanol, m.p. 144—145 °C; the compound gave orange-red colour with *conc.* H_2SO_4.

UV (MeOH): 375, 320, 260.

^{1}H-NMR ($CDCl_3$): 3.80 (s, 3H, $-OCH_3$), 3.85 (s 9H, 3×$-OCH_3$), 6.17 (s, 1H, H-3'), 6.85 (m, 2H, H-2 and H-6), 7.35 (d, 1H, α-H), 7.95 (d, 1H, β-H).

3',4'-Methylenedioxy-5,6,7,5'-tetramethoxyflavanone (1)

Compound **4** (200 mg) was dissolved in a mixture of dimethyl formamide and acetone (30 mL, 1 : 3), and refluxed with methylene iodide (0.5 mL) and anhydrous K_2CO_3 (5 g), the progress of the reaction was monitored by TLC. After 50 h, the inorganic salts were filtered off and the filtrate concentrated. Crushed ice was added and the product extracted with ethyl acetate (5×20 mL) and dried (Na_2SO_4). Removal of the solvent yielded **1**, which crystallised from acetone — petroleum ether as cream coloured needles (30 mg), m.p. 175 °C, it gave a positive Labat test for the methylenedioxy function.

UV (EtOH): 275, 323.

IR (KBr): 1680, 1605, 1500.

^{1}H-NMR ($CDCl_3$): 2.70 and 2.98 (two dd, 2H, H-3); 3.80 (s, 3H, $-OCH_3$), 3.86 (s, 3H, $-OCH_3$), 3.92 (s, 6H, 2×$-OCH_3$), 5.26 (dd, 1H, H-2), 5.96 (s, 2H, $-O-CH_2-O-$), 6.3 (s, 1H, H-8), 7.02 (m, 2H, H-2' and H-6').

REFERENCES

[1] Quijano, L., Calderon, J. S., Gomez, G. F., Soria, I. E., Rios, T.: Phytochemistry, **19,** 2439 (1980)
[2] Geigert, J., Stenmitz, F. R., Johnson, G., Maag, D. D., Johnson, D. K.: Tetrahedron, **29,** 2703 (1973)
[3] Gupta, R. K., Krishnamurti, M.: Phytochemistry, **15,** 1795 (1976)
[4] Sastri, V. D. N., Seshadri, T. R.: Proc. Indian Acad. Sci., **23A,** 262 (1946)
[5] Bradley, W., Robinson, R., Schwarzenbach, G.: J. Chem. Soc., **16,** 793 (1930)
[6] Zemplen, G., Bognar, R.: Ber., **75,** 1043 (1942)
[7] Garg, S. K., Sharma, N. D., Gupta, S. R.: Indian J. Chem., **17B,** 394 (1979)
[8] Bhardwaj, D. K., Jain, S. C., Sharma, G. C., Singh, R.: Indian J. Chem., **18B,** 339 (1978)

Acta Chimica Hungarica 114 (3—4), pp. 365—373 (1983)

H_2O-D_2O SOLVENT ISOTOPE EFFECTS ON APPARENT AND PARTIAL MOLAR VOLUMES OF $CaCl_2$ AND $BaCl_2$ SOLUTIONS

GY. JÁKLI[1]*, S. COOPER[2], R. S. HUTCHINGS[2] and W. A. VAN HOOK[2]

([1]Central Research Institute for Physics, H-1525 Budapest, P.O.B. 49, and [2]Chemistry Department, University of Tennessee, Knoxville, TN 37996 USA)

Received February 2, 1983
Accepted for publication February 22, 1983

Densities of $CaCl_2$ and $BaCl_2$ solutions in H_2O and D_2O have been measured at 15 and 30 °C using a vibrating densitometer. Isotope effects on the apparent and partial molar volumes were calculated and are described with an equation of the form $\Delta\Phi_v = \Phi_v(H) - \Phi_v(D) = \Delta\Phi_v^0 + Gm^{1/2} + Em$, where G and E are parameters. Solvent isotope effects on the molar volumes of both solutes are large. They are discussed in the context of the theory of isotope effects in condensed phases.

Introduction

Partial and apparent molar volumes as obtained from density measurements are certainly one of the oldest and most extensively investigated properties of electrolyte solutions [1]. The data can be used to evaluate certain features of solute-solvent and solute-solute interactions in the solution by analyzing the concentration dependence of the effects. The popularity of this approach is partly due to the appeal of the relatively simple experimental techniques which are involved, and partly to the fact that comparisons of apparent or partial molar volume data at different concentrations, temperatures, or solvents can often be explained in terms of simple theories, sometimes ones based on straightforward geometric reasoning [2]. The study of transfer functions from H_2O to D_2O offers additional advantages because of the close similarity of the molecular and dielectric properties of the two solvents. The differences in the properties of the solvents are amenable to interpretation in terms of basic theory and it follows that the measured isotope effects will be useful in deducing the effect of solute-solvent interaction on the structural properties of solution. Finally excess transfer functions can be useful in testing ion-ion structural interaction models and to check different extended models for electrolyte solutions.

* To whom correspondence should be addressed

Experimental

Density data were taken in Knoxville and Budapest using Mettler-Paar DMA 601 HT and Anton-Paar DMA 02C vibrating tube densitometers, respectively. A detailed description of the apparatus and experimental procedures is given elsewhere [3]. Some modifications were necessary in the present case because of the very wide density range to be covered (1.0 to 1.5 kg/dm^3). In the Mettler-Parr instrument the parameter of experimental interest is the natural vibrational period of the tube, τ. The density is extracted using the relation

$$d_{\text{sample}} = A + k\tau^2 \tag{1}$$

where A and k are constants characterizing the spring and τ is the period. Measurements on two standard substances (usually water and air) allow an equation to be written for the density of an unknown in terms of a standard

$$d_{\text{unknown}} = d_{\text{stand}} + (\tau^2_{\text{unknown}} - \tau^2_{\text{stand}})\, k\,. \tag{2}$$

Using water as the standard with aqueous NaCl solutions we showed in an earlier investigation [3] that the linearity of equation (1) holds at $d = 1.2$ kg/dm^3 to within several parts in 10^5. This can be regarded as acceptable agreement between different laboratories. Comparison of our $BaCl_2$ and $CaCl_2$ densities in H_2O with literature values showed around $d = 1.3$ kg/dm^3 that the linearity no longer holds within the acceptable interlaboratory agreement ($\pm 1\times 10^{-4}$ kg/dm^3) and by $d = 1.5$ the deviation becomes significant ($\pm 2\times 10^{-4}$ kg/dm^3). Therefore we made up normal $BaCl_2/H_2O$ and $CaCl_2/H_2O$ solutions with concentrations very close to the heavy water solutions of interest and used these samples in equation (2) as standards. Densities of the reference solutions were obtained from a fit to selected literature values as discussed in the results section. With this procedure the maximum density differenc between our measured heavy water solution and the reference normal water solution was 0.11 kg/dm^3 in the case of $BaCl_2$ and 0.18 kg/dm^3 in the case of $CaCl_2$, i.e., well within the validity of equations (1) and (2).

Materials: The salts were Fisher reagent grade materials, dried in vacuum at 100 °C to constant weight. As solvent we used triply distilled tap water or 99.8% D_2O obtained from Merck and Co. Mother solutions were prepared by weight. Solutions of lower concentration were prepared by dilution. With a temperature control of 0.002, the reproducibility of the density measurement was several parts in 10^6. Because relatively small amounts of samples were prepared at each concentrations (5—6 g), the error in the calculated molar volumes is determined by the uncertainty in the concentration which is several parts in 10^5.

Results

To calculate the densities of our normal reference solutions, selected literature data [1, 4—8] were fitted to the Masson equation;

$$\Phi_v = \Phi_v^0 + S_v^* m^{1/2} + bm \tag{3}$$

where Φ_v^0 is the apparent molar volume at infinite dilution, m is molality, S_v^* and b are fitting parameters. Although there are many reports in the literature for densities of both $CaCl_2$ and $BaCl_2$ solutions (in references [7] for example, $CaCl_2$ data from 35 laboratories are summarized), the data are of very different quality. The ones we judged best were selected after studying large scale plots of the literature results. Least squares fitting parameters are summarized in Table I at both 15 and 30 °C.

Table I

Least squares parameters of equation (3) *for* $CaCl_2$ *and* $BaCl_2$ *normal water solutions*

	Temp. °C	φ_v^{0a} cm³/mol	S_v^*	b	Variance
$CaCl_2$	15	16.50	6.557 ± 0.075	-0.1705 ± 0.037	7.6×10^{-3}
	30	18.25	6.155 ± 0.045	-0.1357 ± 0.017	5.1×10^{-3}
$BaCl_2$	15	21.54	7.010 ± 0.28	0.643 ± 0.28	2.8×10^{-2}
	30	23.70	7.843 ± 0.31	-0.168 ± 0.31	3.3×10^{-2}

[a] From References [1, 4—6]

Table II

Solvent isotope effect on the apparent molar volume of $CaCl_2$[a]

Aquamol	15 °C			30		
	$10^3(d-d_0)_{D_2O}$ kg/m³	$\Phi_v(D_2O)$ cm³	$\Phi_v(H_2O)-\Phi_v(D_2O)$ cm³	$10^3(d-d_0)_{D_2O}$ kg/m³	$\Phi_v(D_2O)$ cm³	$\Phi_v(H_2O)-\Phi_v(D_2O)$ cm³
0.49934[b]	44.134	19.36	1.69	42.721	21.73	0.80
0.49934[b]	44.128	19.37	1.68	—	—	—
0.99856[b]	84.887	21.54	1.34	82.487	23.51	0.76
1.99993[b]	159.739	24.34	1.09	155.468	26.03	0.65
3.99978[b]	286.039	28.16	0.77	279.254	29.47	0.55
5.99933[b]	387.386	30.92	0.62	378.199	32.10	0.41
7.89745[b]	464.087	33.12	0.46	454.401	34.09	0.39
		15 °C			30 °C	
0.31605[c]	27.720	18.37	1.76	27.424	20.84	0.83
0.50005[c]	43.178	19.44	1.61	42.698	21.77	0.76
0.69986[c]	59.530	20.26	1.61	58.894	22.54	0.76
0.99980[c]	83.319	21.44	1.45	82.461	23.52	0.75
4.00020[c]	281.887	28.07	0.86	279.131	29.43	0.59

[a] d_0 (99.77% D_2O): 1.105786 and 1.103242 kg/dm³ at 15 and 30 °C, respectively
[b] Knoxville
[c] Budapest

Density and apparent molar volume of the solutions are connected with the defining equation

$$\Phi_v = \frac{55.5084\, M_w (d_0 - d)}{d\, d_0\, m} + \frac{M_s}{d} \,. \tag{4}$$

Here M_w the molar mass of normal or heavy water, d and d_0 are the densities of solution and pure solvent, M_s is the molar mass of the salt and m is aqua-

Table III

Solvent isotope-effect in the apparent molar volume of $BaCl_2$[a]

M Aquamol	15 °C $(10^3(d-d_0)_{D_2O}$ kg/m³	15 °C $\Phi_v^\circ(D_2O)$ cm³	15 °C $\Phi_v(H_2O)-\Phi_v(D_2O)$ cm³	30 °C $10^3(d-d_0)_{D_2O}$ kg/m³	30 °C $\Phi_v^\circ(D_2O)$ cm³	30 °C $\Phi_v^\circ(H_2O)-\Phi_v^\circ(D_2O)$ cm³
0.03844[b]	7.102	20.48	2.48	6.951	23.71	1.52
0.07670[b]	14.097	21.26	2.32	—	—	—
0.19127[b]	34.765	22.63	2.14	34.048	25.64	1.46
0.37883[b]	67.900	24.15	2.00	66.479	27.10	1.36
0.56193[b]	99.534	25.27	1.95	97.430	28.17	1.32
0.74158[b]	129.878	26.27	1.86	127.159	29.05	1.28
0.91787[b]	158.977	27.20	1.73	155.678	29.88	1.18
1.56372[b]	260.860	29.86	1.56	255.655	32.21	1.04
		15 °C			30 °D	
0.49000[c]	—	—	—	85.287	27.71	1.40
0.67200[c]	—	—	—	115.562	28.64	1.38
0.90300[c]	—	—	—	153.203	29.73	1.26
1.0610[c]	—	—	—	178.254	30.46	1.14
1.2100[c]	—	—	—	201.640	30.96	1.16
1.4160[c]	—	—	—	233.150	31.73	1.07
1.5380[c]	—	—	—	251.581	32.10	1.06

[a] d_0 (99.95% D_2O): 1.105978 and 1.103436 kg/dm³ at 15 and 30 °C, respectively
[b] Knoxville
[c] Budapest

Table IV

Fits of isotope effect on apparent molar volume data to eq. (5)

		$\Delta\Phi_v^\circ$ cm³/mol	G	H	Variance
$CaCl_2$	15 °C	2.282 ±0.07	−0.9658 ±0.11	0.1143 ±0.03	2.0×10^{-3}
	30 °C	0.9338 ±0.02	−0.1951 ±0.01	—	7.1×10^{-4}
$BaCl_2$	15 °C	2.659 ±0.06	−1.197 ±0.20	0.2607 ±0.14	1.8×10^{-3}
	30 °C	1.676 ±0.04	−0.4821 ±0.04	—	2.1×10^{-3}
NaCl[a]	15 °C	1.417 ±0.016	−0.394 ±0.03	0.0295 ±0.01	—
	30 °C	0.869 ±0.01	−.204 ±0.01	—	—
	45 °C	0.690 ±0.01	−.172 ±0.01	—	—

[a] From ref. [3], data at 15 °C were refitted to a 3-constant equation

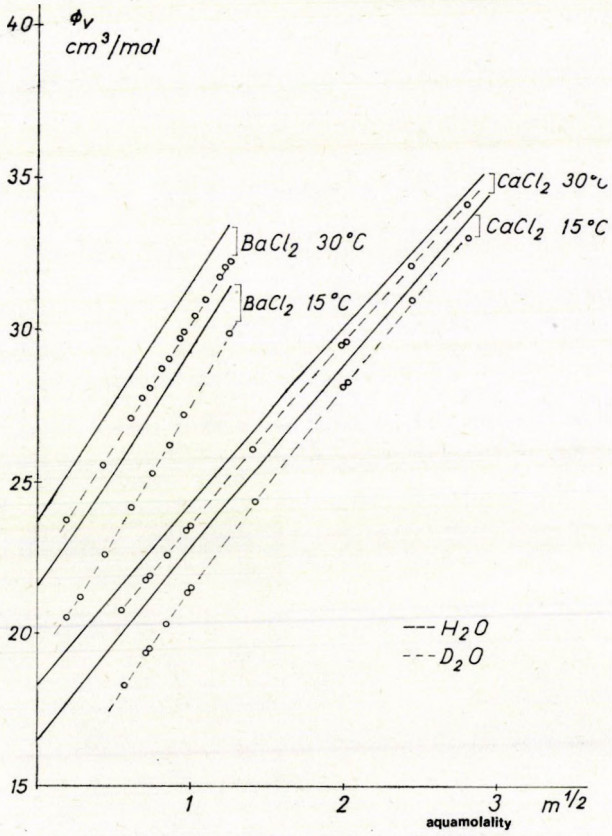

Fig. 1. Apparent molar volumes of $BaCl_2$ and $CaCl_2$ at 15 and 30 °C

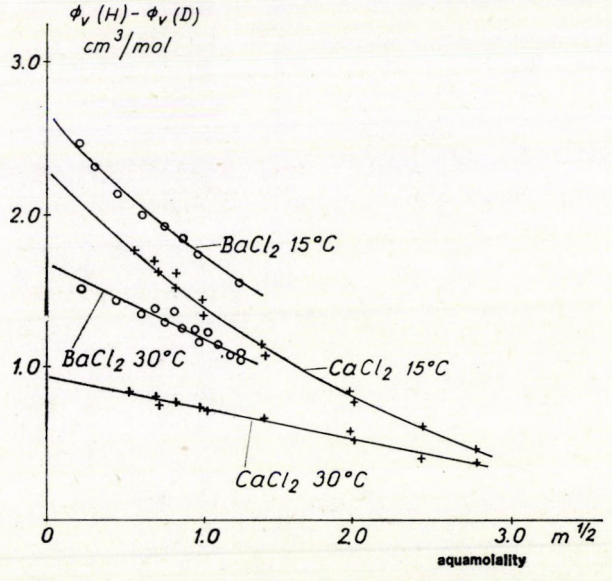

Fig. 2. Isotope effects on apparent molar volumes of $BaCl_2$ and $CaCl_2$ at 15 and 30 °C

Table V

Solvent isotope effect on apparent and partial molar volumes of $CaCl_2$ *and* $BaCl_2$

Aquamolality	$\Phi_v(H_2O)$ cm³/mol		$\Delta\Phi_v = \Phi_v(H) - \Phi_v(D)$ cm³/mol		$\overline{V}_2$ (salt) cm³/mol		$\Delta\overline{V}_2 = \overline{V}_2(H) - \overline{V}_2(D)$ cm³/mol		$\overline{V}_1$ (solvent) cm³/mol		$\Delta\overline{V}_1 = \overline{V}_1(H) - \overline{V}_1(D)$ cm³/mol	
	15 °C	30 °C	15 °C	30 °C	15 °C	30 °C	15 °C	30 °C	15 °C	30 °C	15 °C	30 °C
						$CaCl_2$						
0.0	16.50	18.25	2.28	0.93	16.50	18.25	2.28	0.93	18.032	18.094	−0.079	−0.059
1.0	22.89	24.27	1.43	0.74	25.99	27.21	1.06	0.64	17.976	18.041	−0.072	−0.057
2.0	25.43	26.68	1.15	0.66	29.73	30.76	0.69	0.52	17.877	17.947	−0.063	−0.054
3.0	27.34	28.50	0.95	0.60	32.51	33.43	0.46	0.43	17.752	17.828	−0.052	−0.050
4.0	28.93	30.02	0.81	0.54	34.81	35.63	0.30	0.35	17.608	17.690	−0.042	−0.045
5.0	30.31	31.33	0.69	0.50	36.79	37.54	0.19	0.28	17.448	17.535	−0.033	−0.039
6.0	31.54	32.51	0.60	0.46	38.54	39.24	0.11	0.22	17.274	17.367	−0.025	−0.033
7.0	32.65	33.58	0.53	0.42	40.13	40.78	0.05	0.16	17.088	17.187	−0.019	−0.026
8.0	33.68	34.57	0.47	0.38	41.59	42.19	0.01	0.11	16.892	16.996	−0.013	−0.019
						$BaCl_2$						
0.0	21.54	23.70	2.66	1.68	21.54	23.70	2.66	1.68	18.032	18.094	−0.079	−0.059
1.0	29.19	31.37	1.72	1.19	33.34	35.13	1.38	0.95	17.956	18.026	−0.073	−0.054
2.0	32.74	34.45	1.49	0.99	38.98	39.67	1.16	0.65	17.807	17.906	−0.067	−0.047

molality (moles of salt per 55.5084 mol of solvent). The Φ_v data for the heavy water $CaCl_2$ solutions, together with the isotope effects are reported in Table II, while those for $BaCl_2$ are given in Table III. The solvent isotope effects reported in Tables II and III were obtained by subtracting the raw $\Phi_v(D_2O)$ data points from smoothed values for $\Phi_v(H_2O)$ as calculated from equation (3) and Table I at the appropriate aquamolality.

Graphs of $\Phi_v(H_2O)$ or $\Phi_v(D_2O)$ against $m^{1/2}$ are shown in Figure 1, as are the isotopic differences in Figure 2. It is clear from Figure 2 that the Knoxville and Budapest data are in good agreement and that both sets of data can phenomenologically be described by equation (5).

$$\Delta\Phi_v = \Phi_v(H_2O) - \Phi_v(D_2O) = \Delta\Phi_v^0 + Gm^{1/2} + Hm. \tag{5}$$

Parameters of fit to equation (5) are presented in Table IV.

Discussion

Dessauges, Miljevic and Van Hook [3] have discussed molar volume isotope effects in the context of the extended Debye—Huckel and other formalisms. In common with isotope effects on other thermodynamic properties [9] the molar volume effects display a phenomonological $m^{1/2}$ concentration dependence, but with a slope significantly larger than calculated from the DH theory [ΔS_Φ in eq. (6), below]. However, precise experiments extending over a wide concentration range were previously available only for NaCl, so the present data are particularly useful to test the contribution of the electrostatic part of the potential to the isotope effects. Expressing the apparent molar volume and its isotope effect in the DH formalism gives

$$\Phi_v = \Phi_v^0 + S_\Phi I^{1/2} + B_2 I + B_3 I^2 + \ldots \tag{6}$$

$$\Delta\Phi_v = \Delta\Phi_v^0 + \Delta S_\Phi I^{1/2} + \Delta B_2 I + \ldots \tag{7}$$

with

$$\frac{\Delta S_\Phi}{S_\Phi} = \frac{\Delta\left(\frac{\mathrm{d}\ln D}{\mathrm{d}P} - \frac{\beta}{3}\right)}{\left(\frac{\mathrm{d}\ln D}{\mathrm{d}P} - \frac{\beta}{3}\right)} - \frac{3}{2}\frac{\Delta D}{D} - \frac{1}{2}\frac{\Delta V_1^0}{v_1^0} \tag{8}$$

where D is the dielectric constant of the solvent, β the expansivity, and Δ denotes isotopic differences, H—D. The Dessauges—Van Hook [10] formalism leads to a similar result but with a different power dependence for the higher

order terms

$$\Delta\Phi_v = \Delta\Phi_v^0 + \Delta S_\Phi I^{1/2} + 3/5\,\Delta E\, I^{2/3} + \frac{1}{2}\Delta F'\, I + \ldots \qquad (9)$$

In either case, the phenomenological observed (and approximate) limiting $m^{1/2}$ dependence leads to an initial analysis in which the higher oder terms (those containing ΔB_2 and ΔB_3 or ΔE and $\Delta F'$) are assumed small, in which case $Gm^{1/2}$ in equation (5) is identified with $\Delta S_\Phi m^{1/2}$ (for a 1 : 1 electrolyte) or $\sqrt{3}\, S_\Phi m^{1/2}$ (for a 2 : 1 electrolyte). Clearly the prediction $G_{1,2} = \sqrt{3}G_{1,1}$ is not met (Table IV) and we conclude, in agreement with the earlier authors [3], that the principal origin of the isotope effects is not electrostatic but is due to some other cause, for convenience one labelled "structural". Using the values of ΔS_Φ calculated earlier [3] we have plotted $\Delta\Phi_v - \Delta S_\Phi m^{1/2}$ vs. m (cf. eq. 7) and also vs. $m^{2/3}$ (eq. 9). In the first case significant curvature was observed at both temperatures and at least two higher order and compensating parameters would be required to fit the data to within experimental precision. In the second case good straight line fits were obtained for both salts at 30° but significant curvature was observed at the lower temperature, so once again at least two higher order parameters would be required for a proper description. Since the data are not of sufficient precision to define more than two parameters of fit (including the intercept, $\Delta\Phi_v^0$, terms) with useful accuracy we prefer the fits to the modified Masson equation earlier reported in Table IV. These show good linearity over a wide concentration range at both temperatures, even though the observed $m^{1/2}$ concentration dependence has not yet been properly rationalized in terms of the theory.

A brief discussion of the isotopic differences on the limiting apparent molar volumes, $\Delta\Phi_v^0$ (Table IV) is in order. As far as the data in Table IV is concerned a simple geometric interpretation is tempting chiefly because the order of IE's on limiting volumes correlates with the cation radii [13] at each of the two experimental temperatures. However, the correlation does not hold usefully for IE data of somewhat lower precision found [2, 11, 12] in the literature. Further experimental data of high precision are required before it will be useful to pursue this point. As a final remark we note the very large values for isotope effects on the partial molar expansivity which are implied by the present data. Again, this is clear evidence that the bulk of the partial molar volumetric properties are primarily structural rather than electrostatic in origin.

*

This work was supported by the National Science Foundation under grant 81-12965 and by the Central Research Institute for Physics, Budapest. We thank the Hungarian Bureau of Standards for use of their Anton-Par DMA-02 used in the collection of part of the data.

REFERENCES

[1] Millero, F. in Horne, R. A. Ed.: Water and Aqueous Solutions: Structure, Thermodynamics, and Transport Processes. p. 519, Wiley-Interscience, New York 1972
[2] Friedman, H. L., Krishnan, C. V. in Franks, F. Ed.: Water; A Comprehensive Treatise, V. 3p. 1. Plenum Press, New York 1973; Battino, R.: Chem. Reviews, **71,** 5 (1971); Leyendekkers, J. V.: J. Chem. Soc., Far. Trans. I., **78,** 357 (1982)
[3] Dessauges, G., Miljevic, N., Van Hook, W. A.: J. Phys. Chem., **84,** 2587 (1980)
[4] Dunn, L. A.: Trans. Far. Soc., **64,** 2951 (1968)
[5] Dunn, L. A.: Trans. Far. Soc., **62,** 2348 (1966)
[6] Perron, G., Desnoyers, J. E., Millero, F. J.: Can. J. Chem., **52,** 3738 (1974)
[7] Aksmanovic, M., Krey, J.: Chem. Ing. Techn., **42,** 1568 (1970)
[8] International Critical Tables, Vol. **3,** McGraw Hill, New York 1927
[9] Craft, Q. C., Van Hook, W. A.: J. Solution Chem., **4,** 923 (1975); ibid., **4,** 901 (1975); Dessauges, G., Miljevic, N., Van Hook, W. A.: J. Solution Chem., **9,** 81 (1980)
[10] Dessauges, G., Van Hook, W. A.: J. Inorg. Nucl. Chem., **43,** 1005 (1981)
[11] Conway, B. E., LaLiberte, L. H.: Trans. Faraday Soc., **66,** 3032 (1970); Mathieson, J. G., Conway, B. E.: Trans. Faraday Soc., **70,** 752 (1974)
[12] Choi, Y. S., Bonner, O. D.: J. Phys. Chem., **87,** 188 (1973)
[13] Pauling, L.: Nature of the Chemical Bond, Cornell Press, Ithaca N. Y. 1960 Ch. 13

Acta Chimica Hungarica 114 (3—4), pp. 375—379 (1983)

DECOMPOSITION OF CARBONATE ESTERS OF 1,3-DIOLS. THE CHEMISTRY OF 1,3-BIFUNCTIONAL SYSTEMS, XXVI*

M. BARTÓK**, Á. MOLNÁR and G. BARTÓK-BOZÓKI

(Department of Organic Chemistry, József Attila University, H-6720 Szeged, Dóm tér 8)

Received October 8, 1982
Accepted for publication March 1, 1983

The decomposition reactions of three cyclic carbonates and, in order to establish the reaction mechanisms, the corresponding diols were studied in the presence of KOH, KCN and LiCl. Besides the previously known transformations (fragmentation yielding oxo compounds; CO_2 elimination to give oxetanes; fragmentation to olefins), a new reaction of high selectivity has been found. On the action of a large excess of KOH, the carbonate esters of 1,3-diols are transformed into alcohols containing one carbon atom less than the corresponding diols.

Introduction

Three research groups have studied the decompositions of the cyclic carbonates of 1,3-diols, under various experimental conditions [1—3]. The reaction directions observed are illustrated in Scheme 1. In our experimental work on the preparation of oxetanes [4] some of our observations were in conflict with the above experimental findings, and we therefore considered it necessary to study the model compounds depicted in Scheme 2 (**1A**, **1B** and **1C**), together with the corresponding diols (**6A**, **6B** and **6C**), under identical experimental conditions. The results on the decomposition of 1,3-diols in the presence of strong bases [5], [6] may be of help towards an understanding of the mechanism of decomposition of the cyclic carbonates.

Experimental

Cyclic carbonates and diols

1C was made available by Chemische Werke Hüls; **1A** and **1B** were prepared by literature methods [1], [4]. Diols **6A**, **6B** and **6C** were provided by Chemische Werke Hüls. Before use, the examined substances were distilled and their purity was checked by GLC. Some of the physical constants are given in Table I.

Procedure

Pyrolysis was carried out as described in [1], with the difference that the temperature was raised to 320 °C during the reaction, and the experiments were performed with 5—30 g cyclic carbonate or diol. A 20% quantity of reagent was used in methods *A*, *C* and *D*, and

* Part XXV: Acta Phys. et Chem. Szeged, **26**, 177 (1980).
** To whom correspondence should be addressed.

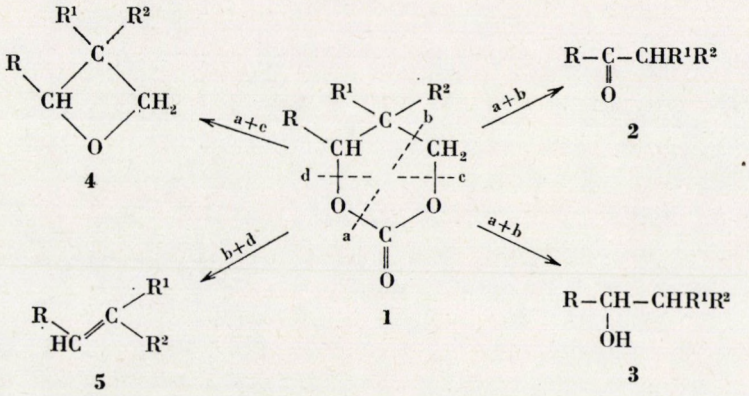

A R=Me, $R^1=R^2=H$
B R=H, $R^1=R^2=Et$

Scheme 1

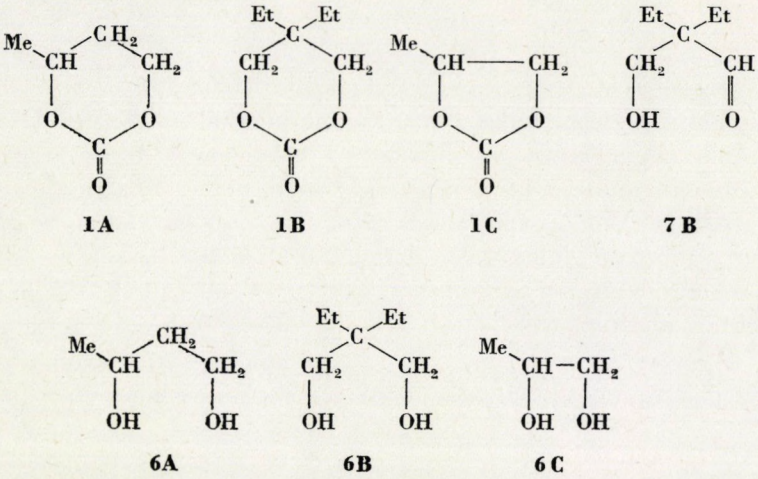

Scheme 2

a 10-fold molar excess of KOH or LiCl in methods *B* and *E*. In all cases 1–2 mL of water was also added to the mixture. The compositions of both the gaseous and the liquid products were analyzed by GC (Carlo Erba GV instrument, alumina column, 80 °C) and by GLC (15% PEG 20M on a 1.2 m Kieselguhr column, 40 mL H_2/min, 70–120 °C). The gaseous product was mainly CO_2, except in method *B*, where only CO was formed. For determination of the composition of the gaseous product, the pyrolysis was also carried out without the introduction of N_2. With KOH and LiCl as reagents, methanol could be detected among the products, while with KCN, formaldehyde and an organic compound containing the C≡N group were also detected. The potassium formate and potassium carbonate contents of the alkaline melt were also determined after the reaction products had been distilled off.

The selectivities of the pyrolyses of the cyclic carbonates and diols are listed in Table II, and the main physical constants of the products in Table I.

Table I

Physical constants of reactants and products

Compound	B.p.		n_D^{20}
	°C	Pa	
1A	110—115	0.13×10^3	1.4443
1B[a]	126—130	0.4×10^3	1.4512
1C	110—112	1.33×10^3	1.4212
2A	56	101×10^3	1.3592
2B	114—116	100×10^3	1.4042
3A	82	101×10^3	1.3771
3B	148—150	100×10^3	1.4220
4B	134—136	100×10^3	1.4235
5B	60—62	100×10^3	1.3963
6A	114—116	2.66×10^3	1.4417
6B[b]	125—130	1.6×10^3	—
6C	94—97	2.66×10^3	1.4306

[a] M.p. 45 °C. [b] M.p. 61 °C

Table II

Transformation of cyclic carbonates and diols

Compound	Reagent	Method	Conversion, %	Selectivity, mol-%			
				2	3	4	5
1A	KOH	*B*	100	6	92	0	0
1B	KOH	*A*	100	32	15	47	traces
1B	KOH	*B*	100	0	98	0	0
1B	KCN	*C*	100	20	traces	65	5
1B	LiCl	*D*	100	60	5	30	5
1B	LiCl	*E*	100	85	5	5	traces
1C[a]	KOH	*B*	50	0	0	0	0
6A	KOH	*B*	100	7	91	0	0
6B	KOH	*B*	100	0	97	0	0
6C[a]	KOH	*B*	50	0	0	0	0

[a] The products are acetone and 1-propanol (selectivities: 80% and 20%, respectively)

Results

The pyrolyses of the cyclic carbonates were studied either in the presence of KOH, KCN [1] and LiCl [2], or by using a nearly 10-fold molar excess of LiCl or KOH, in the latter case essentially under the conditions of alkali fusion

[7]. As an illustration of the experimental results, some typical data are given in Table II. The following main conclusions can be drawn from these data:

1. Under basic conditions the 6-membered cyclic carbonates decompose more quickly than the 5-membered ones. The differences in reaction rate can be explained by the diverse reaction directions.

2. The four reaction directions outlined in Scheme 1 can be observed during decomposition of the 6-membered cyclic carbonates. The extents to which the individual reactions take place are determined by the reagent used.

(a) On the action of LiCl, **1B** is transformed mainly to **2B**.

(b) On the action of KCN, **1B** is transformed mainly to **4B**, i.e. the method can be used for the preparation of oxetanes.

(c) On the action of KOH, the 6-membered cyclic carbonates are converted to **3** and **4**. In the presence of a 10-fold molar excess of KOH the decomposition is selective; two molecules of CO are eliminated, and alcohol **3** is formed.

(d) The formation of products **2**, **4** and **5** is accompanied by elimination of CO_2.

3. In the decomposition of the 5-membered cyclic carbonate **1C** in an excess of KOH, mainly acetone is formed; i.e. by contrast with the 6-membered cyclic carbonates, C—C bond splitting does not occur.

4. In an excess of KOH, the diols are transformed similarly to the corresponding cyclic carbonates.

Discussion

Our discussion of the experimental results will deal merely with the newly-recognized transformation of the carbonate esters of the 1,3-diols, taking place in the presence of a large excess of KOH. The reaction directions observed in the presence of LiCl and KCN have been interpreted satisfactorily on the basis of comprehensive investigations [1—3]. As supplementary evidence, our comparative examinations in the present work revealed that the use of a 10-fold molar excess of LiCl did not cause such an appreciable change in the reaction directions as was observed in the case of KOH.

On the basis of our experimental data and the earlier observations relating to the diols [5], [6] we consider that the action of KOH leads to the transformation of the carbonate esters of 1,3-diols to the alcohols **3** via the following steps (illustrated for compounds **1B**):

$$\mathbf{1B} \rightarrow \mathbf{6B} \rightarrow \mathbf{7B} \rightarrow CH_2O + \mathbf{2B} \rightarrow \mathbf{3B}$$

(In this system **6B** and **7B** are present mainly in the form of their potassium salts.) However, the experimental data obtained so far do not permit exclu-

sion of the direct decomposition of **1** to **3**, i.e. without involvement of the diol or the potassium salt.

The decarbonylation reaction **1** → **6** is in conformity not only with the elimination of CO, but also with the experimental results on the transformation of the diols under similar conditions. The base-catalyzed dehydrogenation **6** → **7** has been the subject of much study [6]. The retrograde aldol condensation of β-hydroxycarbonyl compounds is a well-known process (e.g. [8]).

A clear-cut explanation cannot be given for the transformation **2** → **3** under the given experimental conditions: the reduction may occur on the action of the formaldehyde formed, e.g. via a Cannizzaro-type reaction; a role may also be played by a base-catalyzed reaction of the Meerwein—Ponndorf type between **2** and **6**. However, intramolecular oxidation-reduction processes preceding the splitting-out of formaldehyde cannot be excluded either in the formation of **3**.

As regards the fate of the formaldehyde under basic conditions, a number of unanswered questions arise. One problem is that the behaviour of formaldehyde under basic conditions is not sufficiently well known. Contradictory literature data are found in this respect [1], [5—7]. Our informatory examinations indicate that the concentration of the aqueous alkaline solution determines the direction of formaldehyde transformation. Under the experimental conditions used in method *B*, formaldehyde decomposes to hydrogen and potassium formate, or to hydrogen and carbon monoxide, depending on the temperature. The experimental data suggest that because of this, the quantity of the KOH reagent has a determining role from the aspect of the high selectivity of the hydrogenation process.

A detailed investigation of the above chemical change, which is free from side-reactions, involved very many possibilities. We consider it to be of importance not only because it reveals the actual mechanism and elementary steps of this unusual process; it also permits study of the behaviour of different types of compounds under such extremely drastic experimental conditions as provided by a concentrated base at high temperature.

REFERENCES

[1] Searles, S., Hummel, D. G., Nukina, S., Throckmorton, P. E.: J. Am. Chem. Soc., **82**, 2928 (1960)
[2] Isard, A., Bennard, G., Weiss, E.: Bull. Soc. Chim. Fr., **1966**, 1151
[3] Halary, J. L., Yvernault, T., Casteignau, G.: Bull. Soc. Chim. Fr., **1972**, 4655
[4] Shuikin, N. I., Bartók, M., Kozma, B.: Izv. Akad. Nauk SSSR, Otdel. Khim., **1967**, 153
[5] Brannock, K. C., Lappin, G. R.: J. Am. Chem. Soc., **77**, 6052 (1955)
[6] Searles, S., Ives, E. K., Nukina, S.: J. Org. Chem., **24**, 1770 (1959)
[7] Weedon, B. C. L.: in "Technique of Organic Chemistry" (ed. A. Weissberger) Vol. **11**, p. 655. Interscience, New York—London 1963
[8] Szántay, Cs.: Elméleti szerves kémia, Műszaki Könyvkiadó, Budapest 1971

BOOK REVIEWS

J. Havas: *Ion and Molecule-Selective Electrodes in Biological Systems*

Akadémiai Kiadó, Budapest. 1980. 315 p. (in Hungarian)

The book, appeared in the "Recent Results in Chemistry" series (No. 49) is no doubt fills a gap in several aspects. Unfortunately, inspite of the increased interest in ion-selective electrodes no books appeared on the subject since 1973 (E. Pungor, K. Tóth, Zs. Fehér: Indicator Electrode as a Base for Automation in Chemical Industries. No. 13. in the series mentioned) in Hungarian. On the other hand, the field of application selected and reviewed by the author, i.e. the biological systems is one of the most attractive and promising areas, in which ion- and molecule-selective sensors can be used almost uniquely and successfully.

The book is divided into five chapters. The first chapter deals with the essential, most important equilibrium processes existing in human body fluids and the corresponding mathematical treatments, which are inevitable in respect of biological applications of these sensors. Following this the fundamentals and the analytically important parameters of potentiometric sensors useful for the practical analysts are compiled in a separate chapter. Finally, in the last three chapters the practical applicability of different ion- and molecule-selective electrodes and ISFET sensors are shown through a great number of practical examples.

The orientation in the immense literature data and different possible applications is helped to a great extent by comprehensive tables.

A further advantage is offered especially for the Hungarian readers by the fact that the author gives a special account on ion- and molecular-sensors as well as biological analysers and other corresponding measuring instruments developed in Hungary.

The book incorporates almost 600 literature references referring to the corresponding publications appeared in international and national periodicals and also a survey of books appeared on ion-selective electrodes.

In reading the book one can feel that it is written by an expert of ion- and molecule-selective electrodes' research.

The book is especially welcomed by researchers and analysts working in clinical laboratories and also by chemists facing the problems of working with biological samples.

General and Analytical Chemical Department,
Technical University,
Budapest

K. Tóth

W. E. Morf: *The Principle of Ion-Selective Electrodes and of Membrane Transport*

Akadémiai Kiadó, Budapest. 1981. 433 p. (in English)

There is no doubt a need for book dealing with the comprehensive survey of theory and principles of ion-selective membranes and membrane electrodes. W. E. Morf professor of the Swiss Federal Institute of Technology Zürich (Switzerland), one of the most outstanding researchers of the theory of ion-selective electrodes intents to fill up this gap by his book which appeared in the "Studies in Analytical Chemistry" series.

In the book the author presents a general unified membrane model and its mathematical formulation on the basis of earlier theories on membrane potential and membrane transport for the unified interpretation of the working mechanism of all types of ion-selective electrodes. However, Morf's work is more than a simple synthesis of the existing, earlier theories of membrane transports and membrane potentials; it is rather a new, unique attempt for the general and comprehensive treatment of the extremely complex problem.

The book is divided into two main parts. Part *A* gives a general discussion on membrane potentials and membrane transports. Within this the corresponding earlier theories (e.g. Donnan, Nernst, Planck, Teorell, Schlögl, etc.) and in several cases their extensions are dealt with. The different approaches used for the calculation of the liquid junction potentials are shown in a separate chapter and a comparison is given between different calculation procedures and experimental results. An excellent survey is presented on membrane transport; on the electrical and transport properties of bulk membranes, and on the passive and carrier mediated transports. The most important results and fundamental equations are summarised shortly at the end of Part *A*.

In Part *B* the theory of different types of ion-selective membrane electrodes i.e. solid-state-, liquid ion-exchange membrane-, neutral carrier membrane electrodes and glass electrodes, are discussed on the basis of the general membrane model formulated in Part *A*. Attention is paid to the interpretation of analytically important phenomena e.g. ion-selectivity, limit of detection. In a separate chapter the models derived for the elucidation of the dynamic response behaviour of ion-selective electrodes are dealt with. The author in short chapters discusses the so-called modified ion-selective electrodes, i.e. gas sensing probes and enzyme electrodes. A special merit of this part of the book is that it incorporates many up-to-date, still unpublished results of the author, e.g. the interpretation of the apparent selectivity of liquid ion-exchange membrane electrodes.

Summing-up W. E. Morf's work is of high value and it is no doubt an excellent gain for scientists dealing especially with the theory of ion-selective membrane, membrane electrodes. It helps to orientate in the corresponding extended literature and provides a theoretical background to those interested in analytical chemistry and membrane sciences.

General and Analytical Chemical Department,
Technical University,
Budapest

K. Tóth

Structure and Bonding, Vol. **52.**

Springer Verlag, Berlin, Heidelberg, New York, 1982

The present 52th volume of the excellent series Structure and Bonding contains compendious treatises which describe the present state of four, some rather diverse field of structural chemistry.

Part 1. R. G. Woolley: Natural Optical Activity and the Molecular Hypothesis (pp. 35, Refs. 70). In the last few years there seems to have been a renewed interest in theoretical aspects of optical activity, which, perhaps, is due to a greater awareness of the possibilities and relevance of quantum mechanics in chemistry. On the basis of quantum theory of the molecular hypothesis for chemical substances the author gives a critical discussion of the theory of natural optical activity. Chapter **2** contains a detailed discussion of the molecular hypothesis from the point of view of quantum field theory. Chapter **3** presents the linear response theory of natural optical activity, the definition of chirality and the summary of the mathematical treatment of the phenomena. Chapter **4** deals with the representation of the space-inversion operator, while in Chapter **5** there are critical remarks about the microscopic theories of optical activity based on some approximate models of the field theory.

The reader can state that R. G. Woolley gives in his work a concise, easy to survey picture about the recent situation of the theory of natural optical activity and about the quantum mechanical treatment of the phenomena.

Part 2. L. Banci, A. Bencini, C. Benelli, D. Gatteschi and C. Zanchini: Spectral-Structural Correlations in High-Spin Cobalt(II) Complexes (pp. 50, Refs. 227, Figs. 30, Tables 4). The spectral (electronic, EPR, MCD, NMR) and magnetic properties of a wide range of high-spin cobalt(II) complexes are discussd and interpreted with in the Angular Overlap (AO) approach. In Chapter **2** the energy levels and the electronic spectra were discussed using the

Angular Overlap formalism, on the basis of which it is easy to calculate the energy levels and that of several other parameters for low symmetry complexes, too. Energy level diagrams are published for octahedral, tetrahedral, square pyramidal, trigonal bipyramidal, and pseudo-tetrahedral (CoA_2B_2 and $CoAB_3$) symmetries, and the calculated ligand field parameters are also summarized. In Chapter **3** the dependence of the spectral and magnetic properties on the ground states is discussed in detail. Chapter **4** contains the survey of experimental data; the spectra and the magnetic properties of 56 octahedral, 62 tetrahedral and 42 trigonal bipyramidal and square-planar complexes have been interpreted.

Part **3**. A. Tressaud and J.-M. Dance: Relationships Between Structure and Low-Dimensional Magnetism in Fluorides (pp. 60, Refs. 274, Figs. 36, Tables 12). The authors discussed the relationship between crystallographic features and dimensionality of the magnetic interaction in fluorides. The crystallographic features of fluorides of d-transition elements can be deduced from the arrangement of MF_6 octahedra. Besides the three-dimensional (3-D) networks such as found in perovskite, in rutile types, e.g., fluorides crystallize in two-dimensional (2-D) layer, one-dimensional (1-D) chain structures and isolated unit arrangements. Part 1 of the article contains the theoretical approach (the Ising and the Heisenberg model, the dimensionality of interaction and structures, the theoretical calculations of magnetic functions). In Part **2** are discussed the experimental problems (magnetic measurements; high-applied field; neutron diffraction; Mössbauer resonance; NMR; EPR). Part **3** contains detailed discussion of the experimental data: the low-dimensional magnetism in 3-D crystallographic systems; magnetism in layer-type fluorides; magnetism in chain fluorides; magnetic clusters in fluorides; the field-induced transitions and the zero-point spin-reduction.

The fluorides provide examples for most of the different theoretical models of low dimensional magnetism and this review can contribute to a better understanding of this type of magnetism.

Part **4**. V. K. Jain, R. Bohra and R. C. Mehrotra: Structure and Bonding in Organic Derivatives of Antimony(V) (pp. 50, Refs. 407, Figs. 24, Tables 3). In this review the most important results of the last decade from the area of the chemistry of organic derivatives of antimony(V) are summarized. Attention is focussed on the structural and bonding aspects, but, when it is necessary and reasonable, the synthetic problems are also reviewed. The numerous antimony(V) derivatives are divided in nine Chapters. In Chapter **2** the alkyls, alkenyls and aryls; in Chapter **3** the halides, pseudohalides, oxides; in Chapter **4** the alkoxides, thiolates, glycolates and peroxy compounds; in Chapter **5** the carboxylates and thiocarboxylates; in Chapter **6** the β-diketonates; in Chapter **7** the Schiff base complexes; in Chapter **8** the oxinates; in Chapter **9** the oximates and in Chapter **10** some other compounds are discussed. The structure and bonding properties are discussed on the basis of data from infrared, Raman, ^{1}H-NMR, ^{13}C-NMR, X-ray, Mössbauer, dipole moment and mass-spectrometric investigations. In this review the readers receive the newest results from the field of chemistry of organoantimony(V) derivatives.

It can be stated that this volume of the series contains very valuable informations concerning four fields of the molecule structural investigations. All the works discuss first of all the theoretical aspects and can be regarded as an excellent comprehensive material for all readers interested in structural problems.

József Attila University,
Department of General and Physical Chemistry,
Szeged

J. CSÁSZÁR

The Modern Theory of Capillarity to the Centennial of Gibbs' Theory of Capillarity

Ed. by F. C. Goodrich and A. I. Rusanov

Akademie-Verlag, Berlin, 1981, 231 pages, 51 figures, 19 tables

The centennial of the publication of the book by Willard Gibbs: "On the Equilibrium of Heterogeneous Substances" was celebrated in 1978. Gibbs presented in this book the thermodynamic theory of surface phenomena, which had an immense influence on branches

of science dealing with interface phenomena. Famous scientists are engaged in elaborating and developing of certain details of the theory even up to the present.

The essence of the memorial volume is provided by lectures held on the centennial celebration in Leningrad (February 1978), other papers are written especially for this purpose by authors invited by the editors. The only connection between the 12 papers included is the use of Gibbs' theory, otherwise they show with a sparkling change of colours the varieties, results and problems of today's interface science.

Gibbs wrote: "One of the principal objects of theoretical research is to find the point of view from which the subject appears in its greatest simplicity". Such a point of view in Gibbs' theory of capillarity is the concept of dividing surfaces.

A. I. Rusanov gave a deeper insight into this theory discussing the new aspects of some well known rule.

F. C. Goodrich showed that the mathematical methods of Gibbs devised by him to handle problems in capillary thermodynamics are equally applicable to problems in capillary hydrodynamics.

Gibbs had studied only such liquid films whose medium parts possessed the phase proparties. B. V. Derjaguin treated colloid systems in which the approaching of two interfaces causes the overlapping of their surface zones and he showed a new world of phenomena which arises from the interaction of surfaces.

The rigorous, general theory of the excess interfacial energy and entropy for a binary, liquid-liquid system is developed by R. J. Good and F. P. Buff. With the choice of the pure liquids as reference states simple expressions were found, which were capable of being interpreted in terms of interfacial structure and intermolecular forces. The theory was applied to the benzene-water system and a qualitative interpretation of the results was presented.

The fundamental difference between the methods for calculating the volume and surface distribution of adsorbent pores lies in their theoretical basis. From a careful analysis of experimental data M. M. Dubinin concluded that a modified form of the Kelvin equation with additional inclusion of the change in surface tension with meniscus curvature leads to results which agree better with the data of independent methods in the case of mesopores.

On the surface of a bubble or a drop moving in a continuous phase the motion influences the formation of the adsorption layer, but there is also a reverse effect, in that the properties of the adsorption layer influences the bubble or drop motion. S. S. Dukhin presented a theory of the dynamic adsorption layer based upon the simultaneous solution of the diffusion and hydrodynamic equations.

The progress in understanding of thermodynamic (including capillary) phenomena was not possible without conc ete ideas on molecular interactions. F. M. Kuni and A. I. Rusanov presented a systematic review of the microscopic theory of dispersion interactions in capillary systems. A wide range of key problems in the theory of capillary systems in considered: the molecular structure of flat, slightly and strongly curved surface layers, the interaction of macroscopic particles; however, we have to know that this theory always refers to large distances and so it has asymptotic character.

The contribution of O. A. Petrii considers the main stages of the thermodynamic theory of electrocapillarity on the basis of 104 references. It gives the basic equations for ideally polarizable and reversible electrodes and an interesting discussion on the experimental data of Gorkhshtein illustrating the difference between the surface tension and the reversible surface work for solid metals.

Gibbs idea of line tension for a system with a three phase contact line is discussed by A. Scheludko, B. V. Thosev and D. Platikanov. It was shown, on the basis of Graetz's formula, that the work of nucleus formation was strongly influenced by the line tension. The various experiments for measurement of line tension is reviewed including the authors' work. The involvement of line tension in contact formation between a solid sphere and a liquid-liquid interface was examined in detail, because this phenomena served as the starting point of a recent capillary theory of flotation.

An extension of the Glansdorff—Prigogine thermodynamic stability criteria to charged surfaces separating two immiscible fluids is given by A. Steinchen and A. Sanfeld. The explicit form of the excess surface entropy production was developed and the new destabilizing terms were analysed mathematically.

Lipid bilayers are widely used as models for biomembranes and methods to measure the bilayer membrane tension have been devised. Thus interesting information concerning the thermodynamic properties of lipid bilayers can be reached. The purpose of J. Ch. Eriksson's article was to forward the development of a rigorous and complete thermodynamic formalism for bilayer lipid membranes.

The last article in this excellent series was written by J. A. Wingrave, R. S. Schechter and W. H. Wade. They measured the curvature dependence of surface tension.

I think that, after reviewing the content and listing the name of the authors, no appreciation seems to be necessary, since experts interested in the content of the book, are well acquainted with the activity of the authors. However, it is worth noting that the papers of this book give an overall picture of the intellectual efforts exerted both by theoreticians and experimentals to clarify the theoretical principles of this field and to try to narrow the gap between theory and practice.

Department of Physical Chemistry,
Technical University,
Budapest

GY. RÁCZ

PRINTED IN HUNGARY

Akadémiai Nyomda, Budapest

Text

The text of the paper should be concise. The description of new compounds (in the Experimental) must include the complete analytical data. Special attention must be paid to structural formulas given within the text. Complicated (non-linear) formulas should be drawn on separate sheets of paper and their position in the text should be clearly marked. The numbering of formulas and equations (in parentheses on the right-hand side) is only needed if they are referred to in the text. Units should conform to the International System of Units (SI). In nomenclature the rules of the I.U.P.A.C. are accepted as standard. Symbols for physical quantities are printed in italic type and should, therefore, be underlined in the manuscript.

References

References should be numbered in order of appearance in the text (where the reference number appears in brackets) and listed at the end of the paper. The reference list, too, should be typed double-spaced. Journal titles are to be abbreviated as defined by the Chemical Abstracts Service Source Index.

Examples:

[1] Brossi, A., Lindlar, H., Walter, M., Schneider, O.: Helv. Chim. Acta, **41**, 119 (1958)
[2] Parr, R. G.: Quantum Theory of Molecular Electronic Structure. Benjamin, New York 1964
[3] Warshel, A.: in Modern Theoretical Chemistry, Vol. 7[7] Part A (Ed. G. A. Segal), Plenum Press, New York 1977

Tables

Each table should be given a Roman number and a brief informative title. Structural formulas should not be used in column headings or in the body of tables.

Figures

Figures should be numbered consecutively with Arabic numerals. Their approximate place should be indicated in the text on the margin. All figures must be identified on the back by the author's name and the figure number in pencil. Standard symbols (such as circles, triangles, squares) are to be used on line-drawings to denote the points determined experimentally. Line-drawings must not containg structural formulas and comments. Spectra or relevant segments thereof, chromatograms, and X-ray diffraction patterns will be reproduced only if concise numerical summaries are inadequate to replace them. Drawings and graphs should be prepared in black ink on good-quality white or tracing paper. Photographs should be submitted on glossy paper as high-contrast copies. Xerox or similar copies are not suitable for reproduction, but may be used for duplicate copies.

Redrawn illustrations will be sent to the authors for checking. No corrections of figures will, therefore, be accepted in the proofs.

Submission of manuscript

After having completed the corrections suggested by the referees and editors, the final manuscript should be submitted in duplicate, in a form ready for publication. If the corrected manuscript is not returned to the editors *within six weeks*, the intended publication of the paper will be regarded as withdrawn by the authors.

Page charge will not be assessed for the publication, however, authors, from overseas countries must contribute to the postage of correspondence by sending, together with the manuscript, international postal coupons to the value of U.S. $ 10. –

Proofs and reprints

A set of proofs will be sent to the submitting author. The proofs must be returned within 48 hours of receipt. Late return may cause a delay in the publication of the paper. 100 reprints will be supplied to the authors free of charge.

Periodicals of the Hungarian Academy of Sciences are obtainable at the following addresses:

AUSTRALIA
C.B.D. LIBRARY AND SUBSCRIPTION SERVICE
Box 4886, G.P.O., *Sydney N.S.W. 2001*
COSMOS BOOKSHOP, 145 Ackland Street
St. Kilda (Melbourne), Victoria 3182

AUSTRIA
GLOBUS, Höchstädtplatz 3, *1206 Wien XX*

BELGIUM
OFFICE INTERNATIONAL DE LIBRAIRIE
30 Avenue Marnix, *1050 Bruxelles*
LIBRAIRIE DU MONDE ENTIER
162 rue du Midi, *1000 Bruxelles*

BULGARIA
HEMUS, Bulvar Ruszki 6, *Sofia*

CANADA
PANNONIA BOOKS, P.O. Box 1017
Postal Station "B", *Toronto, Ontario M5T 2T8*

CHINA
CNPICOR, Periodical Department, P.O. Box 50
Peking

CZECHOSLOVAKIA
MAD'ARSKÁ KULTURA, Národní třida 22
115 66 Praha
PNS DOVOZ TISKU, Vinohradská 46, *Praha 2*
PNS DOVOZ TLAČE, *Bratislava 2*

DENMARK
EJNAR MUNKSGAARD, Norregade 6
1165 Copenhagen K

FEDERAL REPUBLIC OF GERMANY
KUNST UND WISSEN ERICH BIEBER
Postfach 46, *7000 Stuttgart 1*

FINLAND
AKATEEMINEN KIRJAKAUPPA, P.O. Box 128
SF-00101 Helsinki 10

FRANCE
DAWSON-FRANCE S. A., B. P. 40, *91121 Palaiseau*
EUROPÉRIODIQUES S. A., 31 Avenue de Versailles, *78170 La Celle St. Cloud*
OFFICE INTERNATIONAL DE DOCUMENTATION ET LIBRAIRIE, 48 rue Gay-Lussac
75240 Paris Cedex 05

GERMAN DEMOCRATIC REPUBLIC
HAUS DER UNGARISCHEN KULTUR
Karl Liebknecht-Straße 9, *DDR-102 Berlin*
DEUTSCHE POST ZEITUNGSVERTRIEBSAMT
Sraße der Pariser Kommüne 3–4, *DDR-104 Berlin*

GREAT BRITAIN
BLACKWELL'S PERIODICALS DIVISION
Hythe Bridge Street, *Oxford OX1 2ET*
BUMPUS, HALDANE AND MAXWELL LTD.
Cowper Works, *Olney, Bucks MK46 4BN*
COLLET'S HOLDINGS LTD., Denington Estate
Wellingborough, Northants NN8 2QT
WM. DAWSON AND SONS LTD., Cannon House
Folkstone, Kent CT19 5EE
H. K. LEWIS AND CO., 136 Gower Street
London WC1E 6BS

GREECE
KOSTARAKIS BROTHERS INTERNATIONAL BOOKSELLERS, 2 Hippokratous Street, *Athens-143*

HOLLAND
MEULENHOFF-BRUNA B.V., Beulingstraat 2,
Amsterdam
MARTINUS NIJHOFF B.V.
Lange Voorhout 9–11, *Den Haag*
SWETS SUBSCRIPTION SERVICE
347b Heereweg, *Lisse*

INDIA
ALLIED PUBLISHING PRIVATE LTD., 13/14
Asaf Ali Road, *New Delhi 110001*
150 B-6 Mount Road, *Madras 600002*
INTERNATIONAL BOOK HOUSE PVT. LTD.
Madame Cama Road, *Bombay 400039*
THE STATE TRADING CORPORATION OF INDIA LTD., Books Import Division, Chandralok
36 Janpath, *New Delhi 110001*

ITALY
INTERSCIENTIA, Via Mazzé 28, *10149 Torino*
LIBRERIA COMMISSIONARIA SANSONI, Via Lamarmora 45, *50121 Firenze*
SANTO VANASIA, Via M. Macchi 58
20124 Milano
D. E. A., Via Lima 28, *00198 Roma*

JAPAN
KINOKUNIYA BOOK-STORE CO. LTD.
17-7 Shinjuku 3 chome, Shinjuku-ku, *Tokyo 160-91*
MARUZEN COMPANY LTD., Book Department, P.O. Box 5050 Tokyo International, *Tokyo 100-31*
NAUKA LTD. IMPORT DEPARTMENT
2-30-19 Minami Ikebukuro, Toshima-ku, *Tokyo 171*

KOREA
CHULPANMUL, *Phenjan*

NORWAY
TANUM-TIDSKRIFT-SENTRALEN A.S., Karl Johansgatan 41–43, *1000 Oslo*

POLAND
WĘGIERSKI INSTYTUT KULTURY, Marszałkowska 80, *00-517 Warszawa*
CKP I W, ul. Towarowa 28, *00-958 Warszawa*

ROUMANIA
D. E. P., *Bucureşti*
ILEXIM, Calea Grivitei 64–66, *Bucureşti*

SOVIET UNION
SOJUZPECHAT — IMPORT, *Moscow*
and the post offices in each town
MEZHDUNARODNAYA KNIGA, *Moscow G-200*

SPAIN
DIAZ DE SANTOS, Lagasca 95, *Madrid 6*

SWEDEN
ALMQVIST AND WIKSELL, Gamla Brogatan 26
101 20 Stockholm
GUMPERTS UNIVERSITETSBOKHANDEL AB
Box 346, *401 25 Göteborg 1*

SWITZERLAND
KARGER LIBRI AG, Petersgraben 31, *4011 Basel*

USA
EBSCO SUBSCRIPTION SERVICES
P.O. Box 1943, *Birmingham, Alabama 35201*
F. W. FAXON COMPANY, INC.
15 Southwest Park, *Westwood Mass. 02090*
THE MOORE-COTTRELL SUBSCRIPTION AGENCIES, *North Cohocton, N. Y. 14868*
READ-MORE PUBLICATIONS, INC.
140 Cedar Street, *New York, N. Y. 10006*
STECHERT-MACMILLAN, INC.
7250 Westfield Avenue, *Pennsauken N. J. 08110*

YUGOSLAVIA
JUGOSLOVENSKA KNJIGA, Terazije 27, *Beograd*
FORUM, Vojvode Mišića 1, *21000 Novi Sad*

Index: 26.007